BASIC, CLINICAL, AND SURGICAL NEPHROLOGY

DEVELOPMENTS IN NEPHROLOGY

Cheigh JS, Stenzel KH, Rubin AL: Manual of clinical nephrology of the Rogosin Kidney Center. 1981. ISBN 90-247-2397-3.

Nolph KD ed.: Peritoneal dialysis. 1981. ISBN 90-247-2477-5.

Gruskin AB, Norman ME eds: Pediatric nephrology. 1981.
ISBN 90-247-2514-3.

Schück O ed: Examination of the kidney function. 1981. ISBN 0-89838-565-2.

Strauss J ed: Hypertension, fluid-electrolytes and tubulopathies in pediatric nephrology. 1982. ISBN 90-247-2633-6.

Strauss J ed: Neonatal kidney and fluid-electrolytes. 1983.
ISBN 0-89838-575-X.

Strauss J ed: Acute renal disorders and renal emergencies. 1984.
ISBN 0-89838-663-2.

Didio LJA, Motta PM eds: Basic, clinical, and surgical nephrology. 1985.
ISBN 0-89838-698-5.

Friedman EA, Peterson CM eds: Diabetic nephropathy: Strategy for therapy. 1985. ISBN 0-89838-735-3.

Dzúrik R, Lichardus B, Guder W eds: Kidney metabolism and function. 1985.
ISBN 0-89838-749-3.

DiDio LJA, Motta PM eds: Basic, clinical, and surgical nephrology. 1985.
ISBN 0-89838-698-5.

Basic, Clinical, and Surgical Nephrology

edited by

L.J.A. DIDIO
Department of Anatomy
Medical College of Ohio
Toledo, Ohio, USA

P.M. MOTTA
Department of Anatomy
Faculty of Medicine
University of Rome
Rome, Italy

1985 **MARTINUS NIJHOFF PUBLISHING**
a member of the KLUWER ACADEMIC PUBLISHERS GROUP
BOSTON / DORDRECHT / LANCASTER

Distributors

for the United States and Canada: Kluwer Academic Publishers, 190 Old Derby Street, Hingham, MA 02043, USA
for the UK and Ireland: Kluwer Academic Publishers, MTP Press Limited, Falcon House, Queen Square, Lancaster LA1 1RN, UK
for all other countries: Kluwer Academic Publishers Group, Distribution Center, P.O. Box 322, 3300 AH Dordrecht, The Netherlands

Book information

ISBN-13:978-1-4612-9616-4

Library of Congress Cataloging in Publication Data

Main entry under title:

Basic, clinical, and surgical nephrology.

(Developments in nephrology)
Includes bibliographies and index.
1. Kidneys--Diseases. 2. Nephrology. I. DiDio, Liberato J. A., 1920- . II. Motta, Pietro M. III. Series. [DNLM: 1. Kidney--anatomy & histology. 2. Kidney Diseases. Wl DE998EB / WJ 300 B311]
RC903.B38 1985 616.6'1 84-25483
ISBN-13:978-1-4612-9616-4 e-ISBN-13:978-1-4613-2575-8
DOI:10.1007/978-1-4613-2575-8

Copyright

To our late beloved Professor Enzo Nesci, former chairman of the Department of Normal Human Anatomy, University of Palermo, whose premature death left an unfillable gap in our field of study and in our friendship.

To the late Harry Goldblatt in commemoration of the fiftieth anniversary of the experimental production of renal hypertension (1934–1984).

Foreword

This unique volume may very well foreshadow the treatment of renal disease in the twenty-first century. The editors have obviously compiled and reviewed the current clinical problems in which the kidney plays a major role. They then selected as topics for chapters those in which recent scientific investigations have added significant new data. The investigators themselves or their peers have been persuaded to produce a summary of current concepts of renal structure and function for each topic. The result is a volume which will be as invaluable as a clinical guide on the laboratory bench as it will be a reference for the clinician seeking guidance to rational therapy at the bedside.

The strength of the volume lies in the incorporation of those data on renal cellular structure and function which hold the key to the etiology of the majority of renal diseases we now call 'end-stage'. Fully, two-thirds of the volume is devoted to current concepts of renal function and related subcellular structure of various renal tissues. The illustrations, correlations, and explanations are superbly presented in much detail and with an obvious effort to fill out the current knowledge of each subject. We may anticipate this book will remain a valuable reference for many years to come.

In the past quarter century, we have dramatically prolonged life in patients with end-stage renal disease by substitution or support of renal function. Before the next century, we may begin the process of definition, arrest or reversal of renal attrition, are ultimately prevention of many or all of these diseases. If so, much of the currently available fundamental data and the basic patterns of approach to the problem may already be assembled in 'Basic, Clinical, and Surgical Nephrology'.

May 7, 1985

Prof. Dr. William H. Boyce
Department of Surgery (Urology)
The Bowman Gray School of Medicine
of Wake Forest University
Winston-Salem, North Carolina, USA

Preface

In view of the numerous and diverse scientific and medical developments related to the kidney that have occurred within the last few decades, the editors have been prompted to present in condensed and comprehensive form a monograph centering on certain basic, clinical, and surgical aspects of this organ. The focus of each chapter represents what has been considered meaningful by the contributors selected to write this book as well as what is considered of interest to clinicians and scientists.

The book covers the major areas of nephrology, the concept of which is here understood in its broadest sense. The text includes basic knowledge and its application to both clinical and surgical aspects of the kidney. The selection of the topics represents the areas in which, in the view of the editors, new scientific, clinical, and therapeutic trends are developing.

The aim of this volume is to offer both a balanced combination of general and specialized knowledge on the structural, functional, pathological, clinical, and surgical aspects of the kidney for the use of nephrologists, physicians, residents, and medical students.

Anatomical aspects of the kidney have been limited to the recent recognition, description, and surgical application of segmentation as a background for partial nephrectomy. Special findings in the left renal vein were detailed as well as some of its embryological aspects. Renal embryogenesis, and light and electron microscopy of the kidney, including its vasculature, preceded scientific data on tubular transport. Another chapter has been devoted to immunological aspects owing to their importance in renal transplantation. Glomerular and vascular diseases of the kidney have been followed by electron microscopic aspects of renal biopsies. Dialysis, radiological, clinical, and surgical aspects of nephrology complete the contents of this monograph, which also represents an attempt to make such knowledge readily accessible to the generally interested reader.

The emphasis on cell biology of the kidney has been intentional because it is felt that even general practitioners today should be aware of the intricacies of cell biology to understand and utilize their recently developed technology, such as in transplants. On the other hand, basic scientists have to be completely familiar with clinical problems for their investigations, from the planning of each research project to the interpretation of findings. This book should serve as a source also for this kind of information to assist both investigators and practitioners dealing with the kidney.

The authors rely on the reader's indulgence with regard to omissions or errors, hoping to be notified of any such occurrences for deletion or correction in future editions.

The editors wish to express their gratitude to the authors who so kindly contributed to this book. We wish to acknowledge as well the effort and dedication of Mr. J. Smith and his colleagues of the Martinus Nijhoff Publishing staff in the preparation of this book.

September 13, 1984

Liberato J.A. DiDio
Pietro M. Motta

Table of contents

List of contributors

Accinni, Lidia, Clinica Medica II, University of Rome, 00161 Rome, Italy

Allen, Delmas, J., Department of Anatomy, Medical College of Ohio, C.S. 10008, Toledo, OH 43699, U.S.A.

Brand, Paul, Department of Physiology, Medical College of Ohio, C.S. 10008, Toledo, OH 43699, U.S.A.

Casanova, Silvia, Department of Clinical Electron Microscopy, University of Bologna, Policlinico S. Orsola, 40138 Bologna, Italy

Christoforidis, A. John, Department of Radiology, Ohio State University, Columbus, OH 43210, U.S.A.

De Martino, Cesare, Regina Elena Institute for Cancer Research, Viale Regina Elena 291, 00161 Rome, Italy

DiDio, Liberato J.A., Department of Anatomy, Medical College of Ohio, C.S. 10008, Toledo, OH 43699, U.S.A.

Fujita, Tsuneo, Department of Anatomy, Niigata University School of Medicine, Asahi-Machi, Niigata 951, Japan

Gohara, Amira F., Department of Pathology, Medical College of Ohio, C.S. 10008, Toledo, OH 43699, U.S.A.

Goldblatt, Peter J., Department of Pathology, Medical College of Ohio, C.S. 10008, Toledo, OH 43699, U.S.A.

Gross, Michael L., Department of Medicine, Medical College of Ohio, C.S. 10008, Toledo, OH 43699, U.S.A.

Higgins, James T., Department of Medicine, Medical College of Ohio, C.S., 10008, Toledo, OH 43699, U.S.A.

Kaneshige, Tetsuji, Kidney Research Laboratory, Okayama Chuo Hospital, Okayama 700, Japan

Kikuta, Akio, Department of Anatomy, Okayama University Medical School, Okayama 700, Japan

Kropp, Kenneth A., Department of Surgery, Medical College of Ohio, C.S. 10008, Toledo, OH 43699, U.S.A.

Laschi, Renzo, Department of Clinical Electron Microscopy, University of Bologna, Policlinico S. Orsola, 40138 Bologna, Italy

Miyoshi, Masayuki, Department of Anatomy, Fukuoka University School of Medicine, 7–45–1, Nanakuma, Jonan-Ku, Fukuoka 814–01, Japan

Motta, Pietro M., Department of Anatomy, Faculty of Medicine, University of Rome, Viale Regina Elena 289, I–00161 Rome, Italy

Murakami, Takuro, Department of Anatomy, Okayama University Medical School, and Kidney Research Laboratory, Okayama Chuo Hospital, Okayama 700, Japan

Nally Jr., Joseph V., Department of Medicine, Medical College of Ohio, C.S., 10008, Toledo, OH 43699, U.S.A.

Ohtsuka, Aiji, Department of Anatomy, Okayama University Medical School, Okayama 700, Japan

Paquelet, Jean, Department of Radiology, The Ohio State University College of Medicine, Columbus, OH 43210, U.S.A.

Senitzer, David, Department of Microbiology, Medical College of Ohio, C.S. 10008, Toledo, OH 43699, U.S.A.

Sorkin, Michael I, Department of Medicine, Renal-Electrolyte Division, University of Pittsburgh, Pittsburgh, PA 15261, U.S.A.

CHAPTER 1

Segments of the kidney: the anatomical basis for nephrosegmentectomy

LIBERATO J.A. DIDIO

Introduction

The principles of construction of the human body, common to mammals and vertebrates, include general bilateral symmetry (or zygomorphism), metamerism, pachymerism (or tubulation), and stratification [1]. In addition to these, it is recognized that the body is made up of (a) cells or biological units; (b) supracellular functional units, such as nephrons and osteons; (c) tissues; (d) organs; and (e) systems or apparatuses.

Within organs, both hollow and solid or parenchymatous, segmentation, another principle of construction, is recognized: special units, called segments or zones, have been identified, classified, and designated, as for example, in the lungs [2], spleen [3–9], liver [10], stomach [11], heart [12] an also in the kidneys [13–17] and others. Because of the multiple meanings of the word *segment* and owing to the attempts made to replace it with the term *zone*, an etymological analysis follows.

Segment originates from the Latin *segmentum* (in turn, from *sec-, secare,* to cut, plus *ment,* a suffix indicating the product or the action of the verb). It is understood as a division, a section, a portion of a larger structure, each of the parts into which a whole is divided or divisible, or a fragment or a piece divided, cut, or broken off; the term may have a variety of meanings in different fields. For example, in geometry, to which anatomists often refer for terminological and morphological purposes, a segment may be (a) a plane figure limited by a straight line and a portion of the circumference of a circle, (b) the part of a line between two points, (c) a solid figure contained by a portion of the surface of a sphere and an intersecting plane not passing through the center, (d) a part cut off from a figure by a line or plane, and (e) the part contained between a chord and an arc of a circle. In embryology, the word *segment* means each of the longitudinally arranged portions of the developing body, such as a somite, metamere, or a cell formed by segmentation, i.e., the process in Metazoa through which the fertilized egg or ovum is split into numerous cells. In zoology or comparative anatomy, the term may be used as each of the repeating portions of several invertebrates such as Annelids. In anatomy, a *segment* may signify a section of a member between two successive joints, each complete series of bones forming a vertebra, or each division of the spinal cord and nerves. More recently, for practical purposes, an organic segment (segment of an organ) came to be defined anatomically as an independent portion of an organ or a viscus, or any other structure that can be naturally, artificially, arbitrarily or, by imagination limited or separated from the remaining (similar or equivalent) portions. In short, a segment is a territory or part of an organ having an independent function, supply (anatomical or functional terminal arteries), and drainage. The terminal or end-arteries supply independent cuneiform territories or parenchyma, that are called segments. Should the artery be occluded, for example by an embolus or by any other pathological process, the corresponding area of parenchyma, completely isolated because of a lack of collateral circulation, undergoes necrosis and is diagnosed as a segmental infarction. Independence from the other portions is usually based on (a) function (ducts, canals, e.g., bronchial or ventilation territory, biliary drainage), and on (b) vascular distribution (such as lack of arterial or venous anastomosis with adjacent segments) and can be extended to lymphatics and nerves. This concept was further developed and broadened to include tridimensional portions that may be separated by avascular or by paucivascular limits, where vascular anastomosis may be found but do not impede or impair their temporary identification and their permanent surgical removal. From the anatomical and surgical standpoint, 'anatomicosurgical' segments are areas in which an organ can be naturally or artificially divided and separately removed from the

L.J.A. DiDio and P.M. Motta (eds), Basic, Clinical, and Surgical Nephrology. ISBN 0-89838-689-5.

remainder. Each anatomicosurgical segment sometimes has, as occurs in some parenchymatous organs, a hidden morphologic individuality; it functions as a unit and possesses its own vascular (arterial, venous, lymphatic) supply and drainage as well as nervous supply, disposed as a pedicle. In some cases the segment is identified in vivo by clamping its artery, thus stopping the blood supply; the resulting ischemia or anemia restricted to a certain area causes a discoloration on the surface corresponding to the segment the superficial limits of which can, thus, be seen at least temporarily. The duration of this phenomenon lasts until the eventual microscopic vascular anastomoses, by collateral circulation, may blur the intersegmental borders, as it occurs typically in the liver. The longer the persistence of the intersegmental limit the better for the surgical segmentectomy.

The most typical organic, visceral, or splanchnic segments have complete morphologic independence; for instance, the pulmonary segments, when separated by occasional fissures within the same lobe, possess a segmental pedicle each, made up of segmental artery, vein and bronchus (lymphatics and nerves). Even when fissures do not exist, however, segments are identified in solid organs, where their limits are imaginary, invisible on the surface but recognizable nonetheless from their predetermined anatomical features, which allow surgical treatment or removal. Ultimately, organic segments are units that function as the whole; in other words, the total organ is an aggregate or combination of smaller organs called *segments,* each a miniature of the entire viscus. Dévos [18] objected to the term segment used as an independent unit or portion of an organ. His name-zones-and concept were accepted by Lambertini and Catalano [19] as referring to the pulmonary subdivision. According to Dévos

'les zones sont des territoires parenchymateux autonomes, possédant un pédicule bronche-vasculaire propre, qui, accolés les unes aux autres, se trouvent cependent séparées par des cloisons conjonctivo-élastiques interzonaires homologues des scissures. Elles ont la même signification que les lobes. D'ailleurs, en l'absence de scissures, les lobes deviennent des zones et reciproquement une zone isolée par une scissure devient un lobe.'

The term 'zone', from Lambertini and Catalano's viewpoint, though meaning an 'extension of surface' does not exclude a 'tridimensional image' and could be kept as Dévos suggested. They emphasize that 'segment' in anatomy and in embryology commonly refers to a particular symmetry (metameric or segmentary), whereas the (pulmonary) 'zones' are unrelated to this symmetry as they occur in parenchymatous territories and depend upon the division and ramification of the bronchial and vascular trees (broncho-angioarchitecture). In spite of their preference for the word 'zone' instead of 'segment,' the International Anatomical Nomenclature Committee [20] considered segment a general term for a part of an organ or other structure set off by natural or arbitrarily established boundaries, and decided for the term segment, consistently retaining it in Nomina Anatomica for the lungs and other organs, including the kidneys. This introductory discussion on the terminology already shows that the anatomicosurgical concept of *segment* can be generalized, but must take into consideration morphological, functional and, consequently, pathological and surgical feaures related to organic differences. On the other hand, once these differences are described and understood, they serve to assist the surgeon, who is guided by them in designing and performing the necessary and appropriate intervention in each case.

2. Segments of the kidney

The first authors to recognize, classify, and designate the arterial segments of the kidney and to provide the background for surgical application in man were Sohier *et al.* [21] and Graves [22, 25], to whom should be added Cayotte and Brulé [23], who restricted their study to the so-called renal superior pole.

For priority purposes, the data of Sohier *et al.* [21] should have precedence as they were presented to the annual meeting of the 'Association des Anatomistes' held in Genoa, from April 12 through April 14, 1954, though published in the 'Bulletin de l'Association des Anatomistes' in December 1955. As Graves's findings [13] were published in September 1954, that may account for giving him the priority and may explain why his description is the most quoted and best known. In the words of Sohier *et al.* [21], however, it was Gérard [26] who showed

en poussant sous l'écran radiographique des injections, successivement dans chacune des branches de l'artère rénale, que le rein humain est divisé en plusieurs territoires vasculaires absolument indépendants, en nombre exactement égal à celui des divisions de l'artère rénale, répartie en avant et en arrière d'un plan frontal passant un peu en arrière du contour du rein, généralement en quatre territoires:

1° trois antérieurs superposés, supérieur, moyen et inférieur;
2° un postérieur beaucoup moins développé (rétropyélique) empiétant un peu sur les territoires antérieurs au niveau des deux pôles du rein.

Ultimately, as emphasized by Riches [25] in the prologue to Graves's [22] beautiful and informative monograph, ... 'the removal of the whole kidney

should not be necessary if only a fraction of it is diseased', adding that John Hunter [23] had noted since 1794 that there were no anastomoses between the branches of the arteries supplying the different areas of the organ, a precious observation that most textbooks of anatomy have failed to mention.

According to Sohier *et al.* [21], the distribution of the renal artery follows the known pattern, dividing into prepyelic and retropyelic territories, the former corresponding to two-thirds and the latter to one-third of the parenchyma. In each of these portions, they were able to identify three well demarcated arterial territories: superior or superior polar, middle or mesorenal, and inferior or inferior polar. Based on a previous paper, Sohier *et al.* [27] stated that each branch of the renal artery penetrates in the renal sinus at the level of the main incisures (notches), sometimes of the secondary incisures. According to these authors, the incisures constitute the hila of the arterial segments. After labeling each segment with letters and numbers, Sohier *et al.* used the following nomenclature: anterosuperior polar segment (SA-1); anterior mesorenal segment (SA-2); antero-inferior polar segment (SA-3); postero-superior polar segment (SP-1); posterior mesorenal segment (SP-2); postero-inferior polar segment (SP-3).

These authors also found out that the superior pole (SA-1 and SP-1) is supplied by two superior polar arteries, whereas the inferior pole (SA-3 and SP-3) receives only one inferior polar artery. As SA-3 and SP-3 form a unit, as SA-1 and SP-1 are independent, as SA-2 is linked to SA-1, and SP-2 is linked to SP-1, Sohier *et al.* [21] recognized in the kidney three individualized arterial lobes: (1) anterosuperior (SA-1 + SA-2), (2) posterosuperior (SP-1 + SP-2) and (3) inferior (SA-3 + SP-3). The authors emphasized the surgical interest in this description, especially the individuality of the inferior lobe for partial nephrectomy purposes. In the case of this lobe the authors first recommended that hemostasis be performed at the level of the renal pedicle, followed by sectioning, particularly in cases of tuberculosis and in cases which involve the inferior pole because of the latter high vulnerability.

Having in mind the question of partial nephrectomies posed to the 'Congrès d'Urologie', in 1951, Cayotte and Brulé [24] studied the blood supply of the renal superior pole, the site of frequent tuberculotic lesions, aiming at performing their least mutilating or most conservative surgical treatment. They pointed out the difficulty in determining morphologically the limit of the superior pole unless fissures, normally present in fetuses and in several animals, persist in the adult; in such a case, the most cranial of the lobes or lobules corresponds to the superior pole of the kidney. Seeking to determine the superior pole more precisely, the authors modified Bellocq's definition [28], according to which it 'is the portion of renal parenchyma situated above a plane tangent to the supra-hilar tubercle'. Cayotte and Brulé believed that the inferior boundary of the superior pole is represented by an oblique plane medially and inferiorly passing at the level of the inferior portion of the supra-hilar tubercle, and forming with the horizontal plane tangent to this tubercle a dihedral angle of approximately 30°, open superiorly and laterally. Within this definition, the superior pole comprises the superior polar renal pyramid and its surrounding cortical substance, thus representing a miniature kidney, an anatomico-physiological entity; its blood supply is provided by two to four superior polar arteries, the origin and distribution of which prompted Cayotte and Brulé to consider several types. They mentioned the possibility of one (rarely two) accessory polar artery (54% of the cases) penetrating the parenchyma directly instead of running through the renal sinus, and originating from the aorta or from the trunk of the renal artery. These authors were unable to observe, at least macroscopically, any anastomosis between the arteries of a segment and those of the adjacent segments, and they suggested that, from the surgical standpoint, when there is an accessory polar artery it should be ligated prior to a superior polar nephrectomy. They warned, however, that such ligation is usually insufficient because the hemostasis of the polar arteries proper can be performed only in the substance of the renal parenchyma, comprising a minimum of two to a maximum of five arteries.

Concern about persistent bleeding in the postoperative period of two cases of nephrolithiasis, which led to nephrectomy, with a consequent loss of otherwise normal kidneys, and familiarity with the segmental anatomy of the lung led Graves [22] to study the vascular pattern within the renal parenchyma. Casts were obtained by Graves [22] after injection in the renal artery of a plastic substance followed by corrosion in an acid bath from 'more than forty' specimens of normal human kidneys. The author was able to discern that each kidney was divisible into the following five segments:

1. Apical segment, 'a cap of tissue' in the medial and mainly anterior portion of the superior pole.
2. Upper (anterior) segment, in the anterior plane of the kidney, including the superior pole and the upper part of the central area of the organ.
3. Middle (anterior) segment, also in the anterior

plane, corresponding to the inferior central part of the kidney.
4. Lower segment, the inferior pole, in both the anterior and posterior planes of the kidney.
5. Posterior segment, in the posterior plane, between the posterior portion (a) of the apical and (b) of the lower segment.

The nomenclature proposed by Graves reflected the influence of the terminology of the pulmonary segments, which were his starting point and under whose names he attempted to designate the segments of the kidney. The most recent edition of Nomina Anatomica [20] lists among termini generales the anatomically precise words *superior* and *inferior*, without including their more popular synonyms: upper and lower, respectively. Confirming previous editions and in accordance with the morphology of the kidney, each being bean-like and having two 'poles', and not a pyramid as a whole, the International Anatomical Nomenclature Committee [20] designated, in each organ, superior and inferior extremities as well as anterior and posterior surfaces. The similarity between the pulmonary and renal segments was taken further by Banowsky [29] who, after following Graves in naming the superior segment, 'apical' called the inferior segment 'basilar'. As the kidney, in distinction to the pyramid lung, has no apex and no base but two extremities or 'poles' [17], the internationally adopted terminology [20], should be superior, anterosuperior, antero-inferior, inferior, and posterior (Fig. 1). Besides being easier to remember, as general terms of the Nomina Anatomica are used, the term avoids the idea of pyramid, whose morphologic expression (including apex and base) should be reserved for the eight (5 to 11) renal pyramids, a variable number of which, in turn, are contained in each segment. Although Banowsky [29] reduced the total number to four segments by considering only one anterior as a result of the fusion of the anterosuperior and antero-inferior, my observations [14–15] confirmed Graves's [13] description of five renal arterial segments. While the posterior and anterior segments lie in the corresponding regions of the kidney, the superior and the inferior segments occupy areas contained in both the anterior and posterior regions, although the largest portion of the superior segment is found in the anterior renal region.

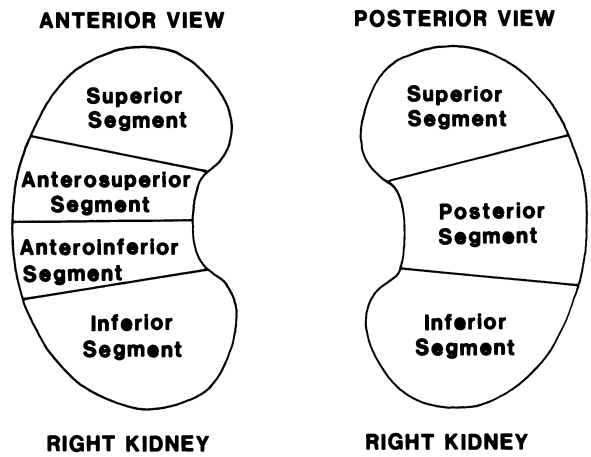

Fig. 1. Diagrams of the anterior and posterior views of the right kidney to indicate the official terminology, published in Nomina Anatomica as adopted by the International Anatomical Nomenclature Committee [20].

3. Renal arteries and segmentation

Each renal artery, after giving off the inferior suprarenal artery (to the homonymous gland) and one or more rami ureterici (to supply the renal pelvis and the proximal or superior portion of the ureter), divided into an anterior and a posterior branch, which Graves [13] called *division*. The anterior branch provided four segmental arteries (superior, anterosuperior, antero-inferior, and inferior) and the posterior branch continued as the posterior segmental artery to supply the homonymous segment [13–15] approximately 85% of the cases [14, 15]. Among variations, in a few cases, the superior segmental artery, for instance, arose from the posterior segmental artery or from the posterior branch of the renal artery, depending on the distance of the origin from the renal hilum.

As done in other organs, the *segmenta renalia* can be numbered (with Roman numerals) and labeled by their initials, from the superior to the anterior, then to the inferior, and ending with the posterior, as follows:

I SS – segmentum superius;
II SAS – segmentum anterius superius;
III SAI – segmentum anterius inferius;
IV SI – segmentum inferius;
V SP – segmentum posterius;

The arteries of the *segmenta renalia* are termed by the names of the corresponding segment:

Arteria renalis
  Ramus anterior (I SS, II SAS, III SAI, IV SI):
    A. segmenti superioris (I SS);
    A. segmenti anterioris superioris (II SAS);
    A. segmenti anterioris inferioris (III SAI);
    A. segmenti inferioris (IV SI).
  Ramus posterior
    A. segmenti posterioris (V SP).

The a. of the superior segment originates from the anterior branch of the renal a. far from the renal parenchyma, thus facilitating its ligation. This segmental a., however, may be given off by the a. of the anterosuperior segment, by the trunk of the renal a. anywhere up to the point of its bifurcation, by the posterior branch of the renal a., and even from the aorta. In the latter case the ligation of the superior segment a. is easiest as long as its extrahilar origin and point of entry in the renal parenchyma are well identified (aberrant or accessory a., which is, actually, a segmental a. having a precocious origin, or as Sykes [30] stated 'an accessory artery is a segmental artery that thas a more proximal origin than usual'). Whereas Graves [13] found the superior segmental a. to be the most variable of all the renal segmental aa. Banowsky [29] stated that the inferior segmental a. showed the most variable origin. In other words, the aa. of the segments located at the extremities of the kidney are those that exhibited most variability.

The a. of the anterosuperior segment originates in the renal hilum and soon after penetrating the parenchyma splits into a superior branch (anteriorly to the superior major calyx) and a lateral branch.

The a. of the antero-inferior segment, which may have a common origin with the preceding a., after supplying the corresponding segment, divides into several branches and its terminal branches establish the limit with those of the posterior segmental a.

The a. of the inferior segment runs anteriorly to the renal pelvis or proximal portion of the ureter, depending on the type of pelvis (ampullary or ramified) and, after a short couse in the parenchyma, divides into an anterior and a posterior branch to supply the major inferior calyx and the inferior extremity of the kidney. The inferior segmental a. may originate with the preceding two segmental aa. or may be given off by the renal a. proximally to the a. of the anterosuperior segment.

The a. of the posterior segment runs at the level of the superior border of the renal pelvis, then posteriorly to the major superior calyx, justifying the former name *retropyelic a.*.

My observations indicated that both Graves [13] and Banowsky [29] are right in stating that each segmental artery is an end-artery with no collateral circulation, thus displaying an arterial arrangement (corresponding to typical segments) in which the anatomical background favors the conservative surgical procedure of partial nephrectomy or nephrosegmentectomy (Fig. 2).

Three posterior segments in addition to four segments supplied by the anterior branch of the renal artery were described by Faller and Ungvary [31].

Fig. 2. Segmental arteries of a left kidney seen from an anterior and medial view. The arteries were drawn longer than normal and the segments artificially separated.

Lacerda *et al.* [32] found five segments in only 15.1% of 33 corrosion specimens obtained from stillborn, whereas Lacerda *et al.* [33] noticed them in 26.7% of 60 casts obtained from adults. Four segments were most frequently observed by Ferreira *et al.* [34] and by Lacerda *et al.* [33] in adults. On the other hand Poisel and Spängler [35] believed that 'the renal arteries develop from a periaortal or perirenal network formed in the embryonal stage and that, for reasons as yet unexplained, they do not develop beyond the intermediate stage, a strict division of the kidneys into 'arterial segments' is rejected as arbitrary and not giving a true picture of the actual conditions'.

Different definitions and terminology of segmental arteries were used by Cordier *et al.* [36]: defining as a segmental artery any artery that can be clamped inside the renal hilum, these authors divided the kidney into three segments, whereas Boijsen [37] described four terminal arteries and Chacon [16] found 13–16 types of renal segments. The surface projections of the arterial segments were studied by Verma *et al.* [38] and by Longia *et al.* [39].

4. Renal segmentation and nephrectomy

The first attempts to perform planned partial nephrectomy made by Czerny [40], in 1887, were marred by hemorrhage, sepsis, and fistulae [41]. Thanks to the surgical application of the anatomical knowledge of the intraparenchymatous renal vasculature, the technique was utilized again four decades ago in patients suffering from nephrolithiasis

and tuberculosis. At present, nephrosegmentectomy is the choice approach for cases of localized renal disease, especially when a non-mutilating conservative procedure is needed to preserve maximum normal parenchyma and function of the kidney. As Graham [41] aptly stated, partial nephrectomy is 'a worthwhile compromise between no surgery and total nephrectomy.'

The surgical approach and technique may differ in accordance with the renal segment involved: for localized disease in the superior or inferior segment the guillotine or the wedge-type techniques can be recommended [41]. These types, however, should not be used for the anterosuperior, antero-inferior, or posterior segmentectomy because their anatomical background causes special difficulties for such surgical techniques, with a possibility of leading to an undesired total nephrectomy. According to Graham [41], the enucleation technique, limited to tumors, may be used in any renal segment with minimal loss of function.

As most if not all the organs of the human body do not function continuously at full capacity and because of the vicarious function of bilateral organs and perhaps, one may extrapolate, owing to the compensatory function of remaining portions of unilateral, median, or residual organs, that the surgical removal of one or more segments maintains most of the renal function. This does not eliminate, however, the possibility that the residual segments or the remaining kidney may not survive.

The surgical approach for a nephrosegmentectomy aims at exposure of the segment to be removed and isolation of its vessels, which can be accomplished with the XI rib flank or supracostal incision [42], the latter in particular for the left superior segment. The anterior approach provides easy access to the vessels but is not recommended for nephrectomy of either the right or left superior segment. As a rule, nephrosegmentectomy is performed from the renal hilum following the vessels toward the periphery of the renal parenchyma.

Once the corresponding renal pedicle is isolated both the artery and the vein are dissected and, when convenient and possible, the artery should be clamped first to reduce the chance of embolism. In fact, occluding first the renal vein, consequently handling the kidney and altering the reno-hemodynamics may enhance the chance of emboli as pointed out by Robson [43] in dealing with radical nephrectomy, when this procedure is also applied.

In left-sided nephrosegmentectomy it may be necessary to ligate and section the left suprarenal vein, the inferior phrenic, and the gonadal (testicular or ovarian) vein, tributaries of the left renal vein; although rare, the right renal vein also may present affluents. It should be remembered that one or more lumbar veins drain into the left renal vein, their orifices being situated in the posterior contour of the latter. Negligence in dealing properly with all these veins will certainly cause bleeding (a common postoperative complication) that may jeopardize the success of the surgical intervention.

Once a segmental artery is clamped, the corresponding territory becomes pale and soft for the duration of the temporary occlusion unless its blood supply is shared by another branch or artery. Meticulous dissection of the segmental arteries and their branches is emphasized by Semb [44]. The renal sinus is exposed by making an incision in the anterior aspect of the parenchyma.

Avoiding as much as possible surgical trauma to the kidney and its vessels, closure of the collecting system should follow. Arcuate vessels should be ligated on the medullary side and interlobar vessels should be tied, according to Parry and Finelli [45], by passing the needle into and then out of the infundibulum of the collecting system. The capsule is closed and manual pressure is applied for 5 minutes, following Poutasse's technique [46].

The guillotine and the wedge resection techniques, limited to the superior and inferior segments, have advantages and disadvantages. To minimize the disadvantages several modifications have been proposed, involving one or more steps of both techniques. The enucleation technique, intended mainly for renal tumors, has the advantage of not being limited to the superior and inferior segments, but has among the disadvantages that of postoperative residual malignancy [41]. On the other hand, this technique may not strictly follow anatomical segmental boundaries.

Follow-up of patients treated with partial nephrectomy [44] correlated with data obtained from investigations performed in dogs [47], indicating a certain degree of vicarious hypertrophy.

An avascular line of Brödel [48] was described along the lateral border of each kidney and considered as the natural route for surgical incisions. As the anterosuperior and the antero-inferior segments invade the posterior 'half' of the kidney, their limits extending beyond the middle frontal plane of the organ, Brödel's 'white line' is not avascular [30], being at its best relatively avascular [29], paucivascular or, in the particular case of the arteries, pauciarterial. An incision along the line of the convex border of the kidney will naturally cut the blood supply of a portion of renal parenchyma. In 10% of

the cases Cordier *et al.* [36] found the 'avascular line' extending to the inferior 'pole', as the posterior artery supplied the posterior part of the inferior extremity of the kidney. The study of the renal segmentation indicated that the real avascular line, separating the posterior from both anterior segments, is found then on the posterior from both anterior segments, is found then on the posterior aspect of the kidney, in other words, the anerior renal territory, suplied by the segmental arteries originating from the anterior branch of the renal artery, is larger than the posterior territory, the plane of separation being posteriorly concave.

5. Venous intrarenal arrangement

It can be noticed, thus, that no particular attention was paid to the veins and their intrarenal arrangement as 'they did not follow the arterial segmental pattern.' With modern advancements in surgical procedures, it has been possible to broaden the purely anatomical concept of renal segment, dictated only by independent territories supplied by end-arteries (without collateral circulation from adjacent or neighboring areas) to an 'anatomicosurgical segment' in which, once intersegmental anastomoses are known, these can be ligated and divided, without being an impediment to nephrosegmentectomy. In fact, in modern surgery the presence of anastomoses, once properly evaluated, should not be a deterrent for the removal of a portion of an organ. Ligation of a vein does not impair drainage because the presence of anastomoses allows other veins to take over the function. On the other hand, if a major, even if only approximate, venous 'segmental pattern' can be recognized, it is better than ignoring it on the basis that anastomoses are present. Ultimately the presence of anastomoses should not be the only factor in determining the surgical approach to a conservative therapeutic procedure. Considering then that the concept of end-vessel and complete vascular independence of territories of an organ was too restrictive I decided to investigate the problem from a different, broader perspective. Toward this end, the concept of 'insufficient' collateral circulation, when anastomoses were present but were not efficient, led to the well-known idea of functional or not functional collateral circulation. The recognition of an anatomical or physiological terminal artery was a departure from the original principle, showing a flexibility that allowed a possible broadening from the practical standpoint. Since the veins must be ligated for the removal of a segment, it is essential to know the major areas of venous drainage, and the most important anastomoses between them, rather than simply ignore what I have called anatomicosurgical 'venous segments.'

While studying the renal angio-architecture and several aspects of the anatomy of the renal veins, I was delighted with Graves's publication [13], whose results were confirmed almost in their entirety by my results [14, 15], particularly those related to the arterial segments, observed with similar techniques. Having investigated both the intra and extrarenal venous distribution, the literature nonetheless indicated several conflicting points that deserved further study. For example, in accord with Lowsley and Kirwin [49], the renal veins correspond to the major subdivisions of the arteries; that is, comprising interlobular, arcuate, interlobar, and straight veins, but differing because there is free anastomosis among the veins. On the other hand, Paitre, Giraud, and Dupret [50] stated that, contrary to what other authors believed, particularly Hyrtl [51], the renal venous circulation does not follow the arterial circulation, as they anastomose abundantly and form true suprapyramidal arches. Paitre *et al.* [50] divided the venous topography into four main zones: sinusal, suprapyramidal, subcapsular, and perirenal, to which they added the sometimes abnormal accessory system of the polar veins; the latter veins leave the parenchyma above or below the hilum, ending in the renal vein or directly in the inferior vena cava. In the sinusal zone, the authors found a 'brush type' of venous distribution and in the 'venous fan' they distinguish superior group (normal superior polar veins), inferior polar group, and middle group. They emphasized the importance of the division of these two or three large prepyelic trunks, occurring anteriorly to the major calyces. In the pyramidal zone, the interpyramidal veins are anastomosed and there is juxtaposition of successive arches. In the subcapsular zone, there are descending veins which, with those of the region of Bellini's tubules, drain into the suprapyramidal arcades. The rich venous anastomosis, in contrast to the arterial 'terminality,' is emphasized by Paitre *et al.* [50], who also described the perirenal zone, corresponding to the veins draining the excretory passages, the adjacent regions, and the neighboring organs. More recently, Warwick and Williams [52], referring to the excellent monographs of Trueta *et al.* [53] and Fourman and Moffat [54], stated that 'with the primary patterns of branching, and their substantial areas of distribution, may be considered the concept of *vascular segmentation* of the kidney'. From the primary

branches of the principal renal artery arise lobar, interlobar, arcuate and interlobular arteries, afferent and efferent glomerular arterioles, cortical intertubular capillary plexuses, and the venous radicles draining the corresponding areas, the vasa recta, and associated capillary plexuses. They called segmental arteries the primary branches of the divisions that supply the vascular segments, and defined accessory renal arteries (30% of the cases) as vessels arising form the aorta, running parallel to the trunk of the renal artery to reach the renal hilum. These accessory arteries may arise from the celiac or superior mesenteric arteries or from the common iliac artery. As there is no anastomosis between a supernumerary and a renal artery, there is no reason for the supernumerary artery to be called accessory [55]. Sykes [30] believed that the term 'accessory renal artery' implied from the surgical standpoint that it could be sectioned with impunity and discussed the terminology that has been used. The term means an 'additional' vessel as 'accessory to the main artery in its extrarenal course' but it is the only source of blood supply to the superior or the inferior segment. 'The term 'accessory' suggests that such a vessel is a supplementary artery, whereas it is in fact complementary'. Aberrant (Graves) is erroneous when applied to the usual (25% or more of the cases) additional vessels, as these are variations rather than abnormalities. Supernumerary may give the impression of a supplementary artery. Sykes [30] concludes, then, that the expression 'accessory renal artery' may be retained if it is understood that a superior accessory artery is a separate superior segmental artery and that an inferior accessory artery is a separate inferior segmental artery.

Besides Graves's description, the authors [52] pointed out that more complex schemes, for example, including three posterior segments [31], or the great variability of the segments [56] have been reported. 'Despite these somewhat divergent views,' Warwick and Williams [52] stated, 'it is nevertheless important to emphasize that the vascular segments are supplied by arteries which have virtually no anastomoses with their neighbours and are thus end arteries. In contrast, the larger *intrarenal veins* have no segmental organization, and anastomose freely'. Graham (1941) underlines this description by stating that the intrarenal venous system does not follow a segmental pattern but instead intercommunicates [57] through a vast plexus of venules. Thus it is the arterial and not the venous system that is surgically important in partial nephrectomy.

When dealing with the interlobular arteries, Hammersen and Staubsesand [58] indicated that a portion of these arteries become perforating arteries, passing through the surface of the kidney to anastomose with the capsular plexus of vessels, which receives capsular branches from the inferior suprarenal, renal and gonadal arteries; their role in collateral circulation (*circulus exorenalis)* was emphasized by Eliska [59].

In the kidney are found glomerular and peritubular capillaries, and from the peritubular plexus arise radicles that join interlobular veins (each accompanying an artery). Many of these veins, beneath the renal fibrous capsule, result from the union of stellate veins, and end as arcuate veins (also following homonymous arteries). Arcuate veins form interlobular veins which, thanks to multiple anastomoses, constitute three roots of the renal vein.

My own observations on the renal segments, confirmed by Grande [60], were based on examination of 28 casts of injection-corrosion specimens [14, 15] in which different colored vinyl acetate was injected in each segmental vessel and in the ureter, followed by corrosion in 10% hydrochloric acid solution. To this series another, comprising 30 kidneys (15 pairs), was recently added, aiming at the identification of renal subsegments [61] utilizing the same technique, following a trend that if carried further may lead someday to microsurgical procedures.

Having confirmed Graves's arterial intrarenal branching into five segments, in each case the veins were studied to find out whether or not they followed the corresponding arteries, and when they followed the arterial segmental pattern if they did it uni or bilaterally. As expected, most of the veins were not satellites of the arteries (in 11 individuals, that is, 22 kidneys), whereas in two individuals they had the same segmental distribution as the arteries (4 kidneys) and in one individual arteries and veins had a similar segmental arrangement only in the left kidney. Without considering the side, a different arterial and venous segmental distribution (23 out of 28 kidneys, that is, 82.1% $\pm$7.2) prevailed over the incidence of a similar segmental pattern (five kidneys, that is, 17.9% $\pm$7.2). As mentioned, it took the adoption of a broader interpretation of the concept of segment, or better, of an anatomicosurgical segment to justify a 'venous segment' (Fig. 3). In other words, it was necessary to disregard the intersegmental venous anastomoses and consider only the territory drained by each major venous trunk to identify a 'venous segment'. Although arteries are of the utmost importance in nephrosegmentectomy, the other structures, particularly the veins, should be known as well, and every effort should be made to establish their pattern, to locate their anastomoses,

Fig. 3. Obs. 309 (male, 40 years old, Caucasian). Diagram of the intraparenchymatous distribution of the veins of the left kidney, in which the vessels were elongated and the segmental areas artificially separated. This represents one of a few cases in which the veins follow the segmental arteries. The major anastomoses between neighboring 'venous drainage' segments are indicated by arrows.

to recognize the existence of one or two venous planes, and to identify the number of their segmental or major trunks, the confluence of which make up the renal vein.

It was already pointed out [52] that there are arterial anastomoses through 'perforating arteries' with the 'capsular plexus of vessels' (and they are not a deterrent to segmentectomy) and that in approximately 18% of the cases [14, 15] the veins follow the same segmental pattern as the arteries (rendering segmentectomy easier). In addition, knowledge of the venous arrangement is also of primary importance if the vein has to be clamped first to avoid embolism, among other justifiable reasons.

Based on these reasons for broadening the concept of segment, based on numerical results, and in spite of the fact that (a) there are multiple venous anastomoses; and (b) there is no clear demarcation or autonomy like those of arterial segmentation, 'anatomicosurgical venous segments' are described and defined simply as 'territories drained by a major or large vein', the trunk of which is found in the renal hilum and is a major root of the corresponding renal vein. In support of these views, it must be emphasized that in the venous intersegmental boundaries of some cases there are portions that show only a few, small anastomoses and that, once the large anastomoses that may be ligated and divided are disregarded, the resulting cleavage planes are long and evident.

In the majority of the cases the 'segmental' veins are not divided into anterior and posterior trunks as are the segmental arteries (Fig. 4). In fact, the anterior and posterior intrarenal small veins join the major veins, which occupy the median plane of the kidney. In most cases, that is, approximately 82% [14, 15], three venous segments were recognized, numbered (with Arabic numerals) and named:

1 SSV – segmentum superius venosum;
2 SMV – segmentum medium venosum;
3 SIV – segmentum inferius venosum.

The veins of these segments were named after the names of the latter:

Vena segmenti superioris venosi (1 SSV);
Vena segmenti medii venosi (2 SMV);
Vena segmenti inferioris venosi (3 SIV).

In the few cases (*circa* 18%) in which venous segments coincided with the arterial ones, the names are the same of the arterial segments with the addition of the adjective venous.

The venous anastomoses in the kidney were classified into intersegmental and intrasegmental, expressions that are self-explanatory; the intersegmental require ligation during the performance of a segmentectomy and the intrasegmental, when more concentrated or dense, facilitate recognition of the segments.

When there was a single drainage plane, anterior and posterior venous radicles or rootlets ultimately converged with the veins of each segment (superior, middle, and inferior) and constituted the 'roots' of the trunk of the renal vein. When there were two drainage plans, and the veins accompanied the arteries, an anterior and a posterior root were recognized. These roots joined each other, then, in the renal sinus to form the trunk of the renal vein.

Intrarenal venous anastomoses between major roots of normal renal veins and between normal and anomalous veins allow the ligation of anomalous veins without embarrassing the circulation of the kidney [62]. Ligation of a radicle or root of the renal vein will not result in kidney damage since collateral venous circulation will provide adequate drainage [29].

6. Concluding remarks

The correspondence between renal lobation and lobulation (evident in newborns and children and occasionally also in adults) and the segments [63–65], the number of renal pyramids and of calyces in each segment [64–66], the recognition of subsegments [61], and the lymphatic and nerve distribution in each segment are as important as the arterial and

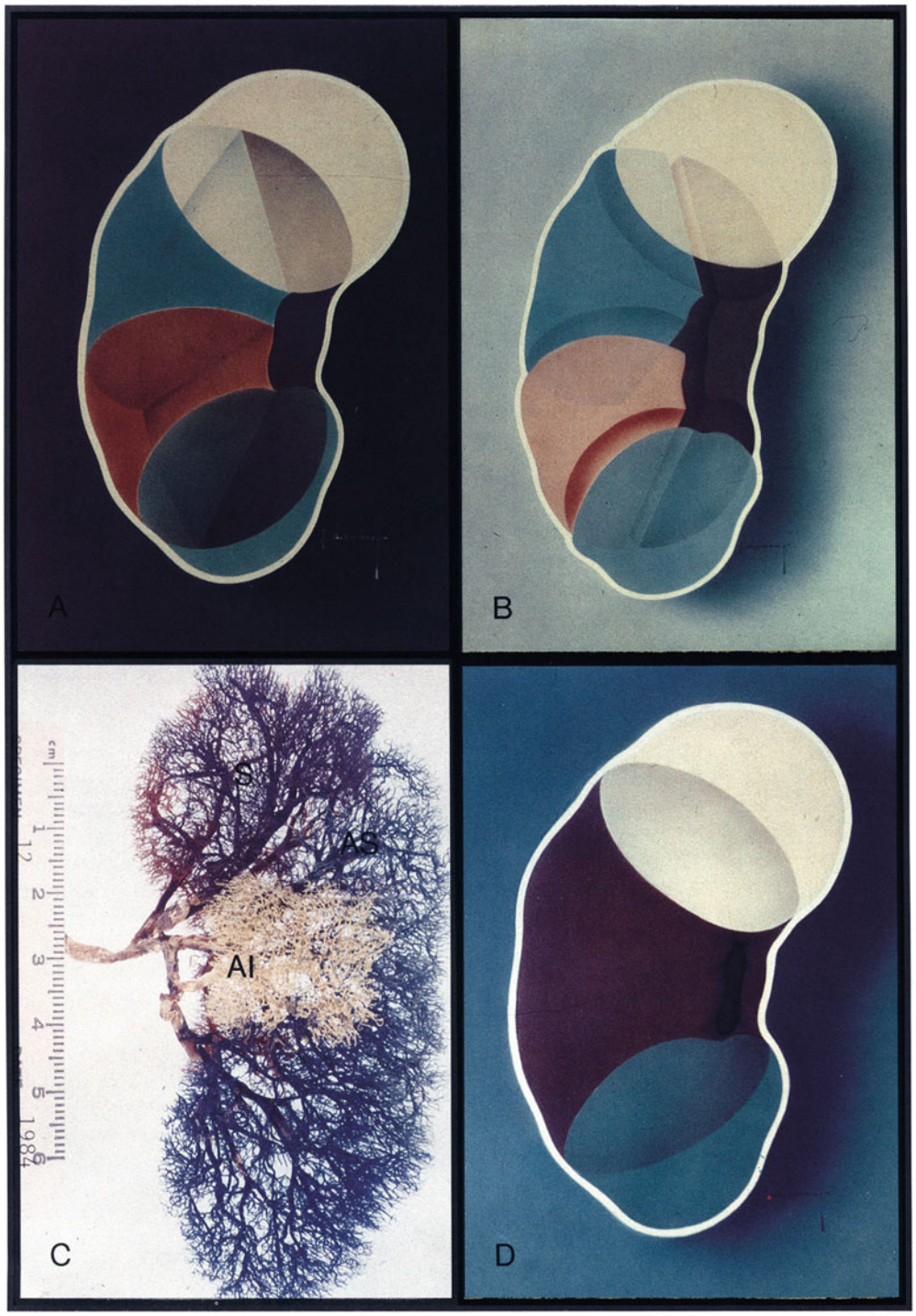
A
B
S
AS
AI
C
D

←
Fig. 4. Ideal diagrams (A, B, D) and an actual multicolored (C) cast (obs. 12, T.B.J., female, 69 years old, Caucasian) of the kidney (prepared with Dr. D. Tose's technical assistance) to illustrate arterial (A, B, C) and venous (D) renal segments. Front views. S, superior; AS, anterosuperior; Al antero-inferior; and I, inferior segment. The artery of the posterior segment is injected with red pigment and is invisible in this figure.

the venous intrarenal arrangement. A great deal of study is, then, still necessary, particularly when considering Wozniak's *et al.* [67] closing statements: 'as the renal artery divides into various number of secondary branches and as there is no constant number even among the primary branches of the renal artery it is difficult or even impossible to distinguish the regular number of arterial segments in the kidney'.

Indications for partial nephrectomy or, more specifically, segmentectomy are based on the presence of localized renal wound injury, lesion, or disease and take into account the natural advantage of preserving as much as possible the normal renal parenchyma and the degree of compensatory function of the residual segments and of the contralateral kidney, with the aim at maintaining the postoperative maximum available amount of the organ.

Simple or multiple nephrosegmentectomy may be suitable in benign renal cysts, congenital atrophy in duplicated system, infections, ischemia (vascular disease), localized hydronephrosis, localized polycystic renal disease, nephrolithiasis, segmental medullary sponge kidney, trauma, tumors, and ureteropelvic junction obstruction [41]. If there is any doubt that a total nephrectomy may result in renal insufficiency, segmentectomy of the kidney should be preferred. In addition, when the use of immunosuppressive drug for renal transplantation, for example, in the treatment of cancer, brings high risk, segmentectomy is naturally indicated.

In Kaufman's experience [68] fewer than 5% of patients fall in the category of those whose segmental renal disease makes partial nephrectomy feasible: the cure following partial nephrectomy has been less than total nephrectomy or vascular repair. The author prefers, once refined surgical techniques and magnification are available, to repair branch or segmental artery stenoses rather than to remove poorly defined ischemic segments.

References

1. DiDio LJA: Synopsis of Anatomy. Saint Louis, CV Mosby Co, 1970.
2. Boyden EA: Segmental Anatomy of the Lungs. New York, McGraw Hill, 1955.
3. Neder AM: Anatomical study of the splenic venous segments and on their drainage in man [in Portuguese]. An Fac Med Univ Minas Gerais Belo Horizonte 18: 265–310, 1958.
4. Zappalá A: Anatomical study of the terminal division of the arteria lienalis. Arterial segments of the spleen [in Portuguese]. PhD dissertation, University of Minas Gerais, Belo Horizonte, Brazil, 1958.
5. Zappalá A: Contribution to the anatomy of the splenic vessels and segments. Anatomical data in man and experimental in dogs for partial splenectomy [in Portuguese]. Chairmanship thesis, University of Recife, Brazil, 1959.
6. Zappalá A: The anatomical basis for segmental resection of the spleen [in Portuguese]. An Fac Med Univ Recife 23: 7–36, 1963.
7. Campos-Christo MB: Splénectomies partielles réglées: à propos de 3 cas operés. Presse Méd 68: 485–486, 1960.
8. Campos-Christo MB: Anatomical and experimental bases for partial splenectomies [in Portuguese]. Rev Bras Cir 46: 80–90, 1963.
9. Pina JAE: Arterial territories of the spleen. Lisboa, Univ Nova de Lisboa, 1979.
10. DiDio LJA: Segments of the Liver: The Anatomical Basis for Partial Hepatectomy. In: Motta PM, DiDio LJA (eds) Basic and Clinical Hepatology. The Hague, Martinus Nijhoff, 1982, pp 1–19.
11. Guerra AJ: Contribution to the study of the vascular territories of the human stomach in adults [in Portuguese]. In: Proceedings 11th Brazilian Congress of Anatomy, Niteroi, Rio de Janeiro, Brazil, 1976, pp 184–186.
12. DiDio LJA, Rodrigues H: Cardiac segments in the human heart. Anat Clin 5: 115–124, 1983.
13. Graves FT: The anatomy of the intrarenal arteries and its application to segmental resection of the kidney. Br J Surg 42: 132–139, 1954.
14. DiDio LJA: Macro and microscopic data on the vena renalis sinistra in man. The venous renal segments [in Portuguese]. Chairmanship thesis, University of São Paulo, Brazil, 1955.
15. DiDio LJA: Applied anatomy of the renal veins. The importance of the mesenterico-aortic forceps. The vascular renal segments [in Portuguese]. An Fac Med Univ Minas Gerais Belo Horizonte 16: 51–202, 1956.
16. Chacon JP: Segmentação Arterial do Rim. Thesis, São Paulo Esc Paul Medicina, 1958.
17. DiDio LJA: Anatomicosurgical vascular segments of the human kidney. Anat Rec 139: 299, 1961.
18. Dévos L: Les zones pulmonaires. La lobation et la zonation chez l'homme et les mammifères. Thèse, Lille in Lambertini and Catalano [18], 1938.
19. Lambertini G, Catalano D: Le zone polmonari. Anatomia e morfogenesi. Napoli, Libr Scientifica-Editrice, 1950.
20. International Anatomical Nomenclature Committee: Nomina Anatomica. Baltimore, Williams & Wilkens, 1983 (5th ed).
21. Sohier HLM, Renon C, Illes JO, Gouazé A: Lobes et segments artériels du rein. Compt Rend Assoc Anat Frenc 87: 921–934, 1955.
22. Graves FT: The Arterial Anatomy of the Kidney. The Basis of Surgical Technique. Baltimore, Williams & Wilkins, 1971.
23. Hunter J: Inflammation and Gun Shot Wounds. London, G. Nicol in Graves [21], 1794.
24. Cayotte J, Brulé A: La vascularisation du pole supérieur du rein. XLIe Réunion (Gênes, 11–14 Avril 1954). Compt Rend Assoc Anat Franc 87: 1019–1027, 1955.
25. Riches E: The Prologue to Graves' The Arterial Anatomy of the Kidney [21], 1971.
26. Gérard: in Sohier *et al.* [20], 1903.
27. Sohier HLM, Renon C, Illes J, Gouazé A: Le hile du rein, ses lèvres et ses incisures. L'artèr rénale au niveau du hile. Compt Rend Assoc Anat Franc 87: 916–920, 1955.
28. Bellocq: in Cayotte and Brulé [23].
29. Banowsky LHW: Surgical Anatomy. In: Stewart BH (ed) Operative Urology. Baltimore, Williams & Wilkens, 1975.
30. Sykes D: The arterial supply of the human kidney with special reference to accessory renal arteries. Brit J Surg 50: 368–374, 1963.
31. Faller J, Ungvary G: Die arterielle Segmentation der Niere. Zentralblatt f Chir 87 (23): 972–984, 1962.
32. Lacerda CAM, Sampaio FJB, Oliveira FGCS, Dallalana EM: Segmentação arterial do rim em natimortos de termo. Rev brasil cir 71 (1): 33–35, 1981.
33. Lacerda CAM, Sampaio FJB, Passos MARF, Dallalana EM, Kano K: Segmentação arterial do rim em adultos. J. Brasil Urol 8(1): 15–17, 1982.

34. Ferreira AS, Pereira JP, Andrea M: Segmentation arterielle du rein. Arq Anat Antropol 35: 137–145, 1971.
35. Poisel S, Spängler HP: The ramifications of the renal artery in relationship to the arterial blood supply of the renal parenchyma. Problem of the so-called renal segment. Acta Anat 76(4): 516–529, 1970.
36. Cordier G, Nguyen-Huu, Bui-Mong-Hung: Segmentation artérielle du rein. Presse Méd 72: 2433–2438, 1964.
37. Boijsen E: Angiographic studies of the anatomy of single and multiple renal arteries. Acta Radiol (Suppl) 183: 1–135, 1959.
38. Verma M, Chaturnedi RP, Pathak RK: Anatomy of the renal vascular segments. J Anat Soc India 10: 12–14, 1961.
39. Longia S, Kumar V, Saxena SK, Gupta CD: Surface projection of arterial segments in the human kidney. Acta anat 113: 145–150, 1982.
40. Czerny: in Graham [41], 1887.
41. Graham SD: Partial nephrectomy. In: Glenn JF (ed) Urologic Surgery. Philadelphia, JB Lippincott, 1983 (3rd ed).
42. Warwick RTT: The supracostal approach to the renal area. Brit J Urol 37: 671–672, 1965.
43. Robson CJ: Radical nephrectomy. In: Glenn JF (ed) Urologic Surgery. Philadelphia, JB Lippincott, 1983 (3rd ed).
44. Semb C: Conservative renal surgery. J R Coll Surg Edinb 10: 9–30, 1964.
45. Parry WL, Finelli JF: Some considerations in the technique of partial nephrectomy. J Urol 82: 562–565, 1959.
46. Poutasse EF: Partial nephrectomy: new techniques, approach, operative indications, and review of 51 cases. J Urol 88: 153–159, 1962.
47. Hoeg K: The early forms of renal tuberculosis and the function of the resected kidney. Acta Chirurg Scand (Suppl) 302: 1–150, 1962.
48. Brödel M: The intrinsic blood-vessels of the kidney and their significance in nephrotomy. Johns Hopkins Hosp Bull 12: 10–13, 1901.
49. Lowsley OS, Kirwin TJ: Clinical Urology. Baltimore, Williams & Wilkins, 1940.
50. Paitre F, Giraud D, Dupret S: Practica anatomoquirurgica Ilustrada. Abdomen. Los Organos Retroperitoneales. Barcelona: Salvat Edit, Fasc III, 1941.
51. Hyrtl: in Paitre *et al.* [50].
52. Warwick R, Williams PL: Gray's Anatomy. Philadelphia, WB Saunders, 1973 (35th British ed).
53. Trueta J, Barclay AE, Daniel PM, Franklin KJ, Prichard MML: Studies of renal circulation. Oxford, Blackwell, 1947.
54. Fourman J, Moffat DB: The blood vessels of the kidney. Oxford, Blackwell, 1971.
55. Hollinshead WH: Renovascular anatomy. Postgrad Med 40: 241–246, 1966.
56. Fine H, Keen EN: The arteries of the human kidney. J Anat 100(4): 881–894, 1966.
57. Brown RKL: The renal circulation. Arch Surg 8: 831–852, 1924.
58. Hammersen F, Staubesand J: Arteries and capillaries of the human renal pelvis with special reference to the so-called spiral arteries. I. Angio-architectural studies on the kidneys. Zeit. Anat Entw 122: 314–347, 1961.
59. Eliska O: The perforating arteries and their role in the collateral circulation of the kidneys. Acta Anat 70: 180–201, 1968.
60. Grande NR Zonas de drenagem venosa em rins de Portugueses africanos. Arq Anat Antropol 34: 165–174, 1968.
61. DiDio LJA, Tose D: Renal subsegments (in preparation), 1984.
62. Smith GT: The renal vascular pattern in man. J Urol 89(3): 275–288, 1963.
63. Lofgren F: Das topographische System der Malpighischen Pyramiden der Menschenniere. Bokhandeln, Lund, A B Gleerupska University, 1949.
64. Sykes D: The morphology of renal lobulations and calices and their relationship to partial nephrectomy. Brit J Surg 51: 294–304, 1964.
65. Sykes D: The correlation between renal vascularization and lobulation of the kidney. Brit J Urol 36: 549–555, 1964.
66. Chevrel JP, Berberian JP, Delmas V, Hureau J: Essai de systematisation pyelo-calicielle. Application à la nephrectomie partielle. Bull Assoc Anat 65(190): 253–263, 1981.
67. Wozniak W, Kiersz A, Wawrzyniak S: The question of the renal arterial segments. Anat Anz 132: 332–340, 1972.
68. Kaufman JJ: Renovascular disorders. In: Glenn JF (ed) Urologic Surgery. Philadelphia, JB Lippincott, 1983 (3rd ed).

CHAPTER 2

Anatomical and embryological aspects of the renal venous drainage

LIBERATO J.A. DIDIO and PIETRO M. MOTTA

1. Introduction

The intraparenchymatous veins of the kidney include the venae interlobares, arcuatae, interlobulares, and the venulae rectae and stellatae. The confluence of these vessels usually forms three major 'segmental' veins, which represent the 'roots' of the right and left renal veins [1]. The arcuate veins describe an arch around the base of the renal pyramids, show several anastomoses, and receive cortical and medullary tributaries. The interlobular veins have rootlets in the periphery of the renal cortex and constitute veins that run parallel to the surface of the kidney. When 3–5 of these rootlets converge, stellate venulae are formed and, from the center of convergence, originate an interlobular vein; the latter is joined by other small veins and drains into an arcuate vein. The straight venules (venulae rectae) originate from the renal medulla, follow the direction of the corresponding arterial vessels in the pyramids, join each other in groups, and terminate in the arcuate veins. A venous network in the adipose tissue surrounding the kidney is a tributary of the venous perirenal arch, which runs parallel to the lateral margin of the organ. This network is also joined by cortical veins and, in turn, gives branches to the stellate venules (and interlobular veins), to the renal and adjacent veins, such as the colic, suprarenal, inferior phrenic, ureteral, gonadal, and lumbar; through these it is connected to the subcutaneous veins of the lumbar region.

2. Embryological data

Early in development (after the 3rd week of intrauterine life), major venous trunks are formed, among them the bilateral superior and inferior cardinal veins, which on each side drain blood from the anterior and posterior portion of the body, respectively, and fuse to form the duct of Cuvier. Later, the inferior vena cava develops from the cardiac end of the right vitelline vein, adjacent to the aorta, next to the medial border of the right mesonephros, from which it receives blood. A left narrow longitudinal vessel, corresponding to the inferior vena cava, also runs next to the left mesonephros, and several transverse anastomoses appear between the two until atrophy of the left longitudinal vessel occurs. On the right side, the inferior vena cava continues to grow and establishes connections with both inferior cardinal veins.

The definitive renal vein originates from a transverse anastomosis that connects the subcardinal veins and the inferior cardinal veins.

By the 7th week, on each side, the longitudinal supracardinal vein appears and joins superiorly and inferiorly with the inferior cardinal vein. Another connection occurs with the subcardinal vein, allowing the blood of the left region of the body to be drained by the superior portion of the right subcardinal vein, that is, the inferior vena cava.

The inferior vena cava is single in its first, primitive portion, and double in the remaining portion, the limit between the two portions corresponding to the renal veins. From the subcardinal veins develop the left renal, the suprarenal, the gonadal veins and a portion of the inferior vena cava.

3. Anatomical data

Fourteen percent of the kidneys show multiple renal veins, especially on the right side, and vascular impressions on the renal pelvis caused by renal veins occur more frequently on the right than on the left side [2].

The renal veins, anteriorly located in relation to the corresponding arteries, are tributaries of the inferior vena cava. The length of each vein is the reverse of that of the companion artery, as the left renal vein is usually more than twice as long as the

L.J.A. DiDio and P.M. Motta (eds), Basic, Clinical, and Surgical Nephrology. ISBN 0-89838-689-5.

right because of the paramedian position of the inferior vena cava (on the right of the median plane of the body) and of the aorta (on the left).

The normal arrangement of the renal vessels occurs in 47.6% of the cases: the left artery is dorsal to the vein and the right renal artery is dorsal to the inferior vena cava and the homonymous vein [3]. In a little lower percentage of cases (42%), the artery runs anteriorly to the corresponding vein, but variations of these relationships are common [4, 5].

The left renal vein measures 8 cm (average), varying from 6 to 11 cm, whereas the right is 3 cm long (average), between a minimum of 2 cm and a maximum of 4 cm (all figures are approximate). Unlike the right renal vein, which may consist of two or three veins and is seldom joined by the right testicular or ovarian vein, the left renal vein is single and among its tributaries frequently receives the left suprarenal, inferior phrenic, lumbar, and gonadal (testicular or ovarian) veins, as well as veins from the perirenal fat and the proximal portion of the ureter. These veins are classified into visceral (suprarenal, gonadal) and parietal (phrenic, lumbar, perirenal). They join the left renal vein (a) superiorly (suprarenal, phrenic veins), (b) inferiorly (gonadal vein), and (c) posteriorly (lumbar vein or veins). Both right and left renal veins anastomose with the ascending lumbar veins; the left also anastomoses with the vena hemiazygos.

The left renal vein, which is included in the angle formed by the superior mesenteric artery and the aorta, bears a close resemblance to the terminal portion of the left common iliac vein, which is compressed between the right common iliac artery, the median sacral artery, and the lumbar region of the vertebral column [6]. This particular topographic relationship was studied from several standpoints because some alterations of the venous wall when subjected to arterial pulsating compression were common to those observed in the left common iliac vein, and had interesting clinical implications.

The projection of the renal vein on the vertebral column has been variably indicated in the literature: (1) the *opening* of the vein in the inferior vena cava at the level of the I LV [7, 8]; (2) the *trunk* of the vein would be at the level of the II LV [9, 10, 11] or of the I LV [12, 13] or of the disc between I and II LV [14, 15]. This variability was noticed by Fagarasanu [16], who observed that the left renal vein crossed the aorta 22 times (out of 48) at the level of the disc of the I LV, 17 at the level of the II LV, 8 between the XII TV and the I LV, and 1 at the level of the II LV. In 80 dissections and 10 cases radiologically studied, this variation was confirmed anywhere between the I LV and the disc above the III LV [1]. Focusing only on the portion of the left renal vein contained in the aorticomesenteric forceps, its projection varied (total of 90 cases) within a rather wide range:
body I LV: 17 cases (18.9% ±4.1)
body of the I LV and disc I LV: 1 case (1.1% ±1.1)
disc I LV–II LV: 35 cases (38.9% ±5.1)
disc I LV–II LV and superior half of II LV: 2 cases (2.2% ±1.5)
body II LV: 33 cases (36.7% ±5.1)
disc II LV–III LV: 2 cases (2.2% ±1.5)

The most frequent percentages corresponded to the projection of the left renal vein at the level of the disc (Fig. 1) above the II LV (38.9%) and at the level of the body of the II LV (36.7%).

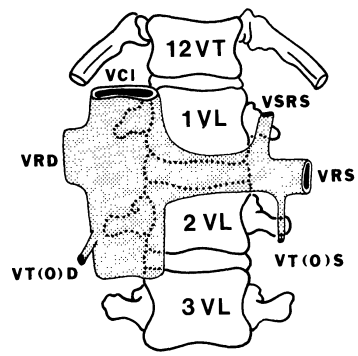

Fig. 1. Projection of the left renal vein on the disc between the first and the second lumbar vertebra. VCI – inferior vena cava; VRS and VRD – left and right renal vein; VT(O)D and VT(O)S, right and left testicular (ovarian) vein; VSRS – left suprarenal vein; VT and VL, thoracic and lumbar vertebra.

The *length* of the left renal vein is differently indicated in the literature:

Dantas [17]:	4.9 cm
Grégoire [18]:	6–7 cm
Barcelos and Byington [19]:	6–8 cm
Banowsky [20]:	6–11 cm
Paitre *et al.* [15] and Maisonnet and Coudane [14]:	8 cm
Brash [21] and Last [11]:	7.5 cm
Purcell *et al.* [22]:	8.3 cm
Testut and Jacob [23]:	8–9 cm

In 132 Brazilian individuals whose ages were 20 years or older, it was found that the minimum length (measured from the junction of its roots to its ending in the inferior vena cava) was 2.1 cm, the maximum 7.3 cm, and the average 4.7 cm. Besides the general factors of variation (age, sex, biotype, race) the technique for measuring the vessel must have an influence in the discrepancies observed [1].

The *external diameter* of the renal vein recorded in

the literature also shows variability:

Testut and Latarjet [24]:	6–10 mm
Charpy [9]:	7–10 mm
Salvi [7]:	8–10 mm
Falcone [25]:	9–10 mm
Purcell *et al.* [22]:	9.2 mm
Barcelos and Byington [19]:	10–18 mm

The external diameter was measured by Almeida [26] in what he called the 'surgical point', meaning the level where it would be sectioned to perform a venous splenorenal shunt, in fixed vessels with and without chronic stasis: the average in the fixed cases was 1.53 cm; in the non-fixed it was 1.45 cm. In cases of chronic stasis it was 1.45 cm and in those without chronic stasis it was 1.53 cm; the global average was 1.49 cm. The external diameter in the initial and terminal portions of the vein were measured by Dantas [17], who obtained 9.4 mm and 11.9 mm, respectively. In 104 adults, measurements [1] resulted in a 16.6 mm average for the external diameter of the juxta-hilar portion of the left renal vein and in 19.8 mm for the terminal portion; whereas the latter in the right renal vein was smaller (14.2 mm) thus in agreement with Fagarasanu [16]. The external diameter of the inter-arterial portion of the left renal vein was 15 mm (average), an indication of a narrowing at the level of the aorticomesenteric forceps, in comparison with the larger diameters found at the level of the initial and terminal portions of the vessel.

The *morphology* of the terminal portion of the left renal vein, related to the external diameters and observable in renophleboradiograms, studied in 160 adult cadavers [1], appeared in five types (Fig. 2):

I.	Hourglass (horizontal)	58.1% ±3.9
II.	Right based cone	23.8% ±3.4
III.	Left based cone	8.8% ±2.2
IV.	Cylinder	6.9% ±2.2
V.	Bulb	2.5% ±1.2

The hourglass morphology, characterized by an intermediate narrowing, appeared as the most frequent, whereas the opposite bulbar type, showing an intermediate wider portion, rarely occurred. It is highly desirable to repeat these observations in children and adults, if possible radiologically, to find out whether or not the morphology of this portion of the vein changes with age and with postmortem conditions.

The *level* of the opening of the left renal vein into the inferior vena cava is described as higher than that of the right by Charpy [9], Salvi [7], Chiarugi and Levi [10], and Warwick and Williams [27]. According to Kolster [28], the right renal vein terminates in a level inferior to that of the left in 55 cases, at the same level in 35, and at a superior level in 13. Similar

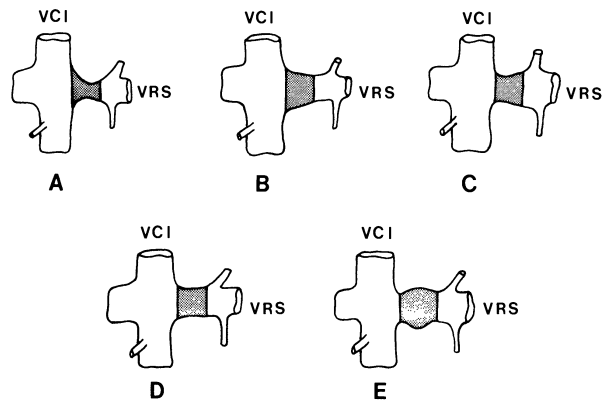

Fig. 2. Diagrams of the types of terminal portion of the left renal vein (VRS); A, hourglass; B, right-based cone; C, left-based cone; D, cylinder; E, bulb. VCI – inferior vena cava.

results were mentioned by Fagarasanu [16], who stated that the left renal vein opens in the inferior vena cava above the level of the right vein but frequently at the same level or at a lower level. This diversity was confirmed in 149 observations in cadavers of adult individuals, but the conclusions were different [1]. In fact, both veins ended in the inferior vena cava in 49.7% ±4.1, the opening of the right was higher in 32.9% ±3.9 and that of the left was higher only in 17.4% ±3.1. Similar results were obtained in different racial groups and in either sex.

The *external left inferior renocaval angle* [1] was measured, as the name indicates, between the inferior contour of the left renal vein and the medial contour of the inferior vena cava, at the level of the termination of the left renal vein. The measurements in 150 adult individuals (20 years of age and older) showed that this angle varied from 50° to 130°, the average being 84°6 confirming descriptions and data provided by Charpy [9], Kristenson [13], Papin [29], Chiarugi and Levi [10], and Paitre *et al.* [15]. The most frequent opening of the left renal vein into the inferior vena cava occurred under an acute angle (43.3% ±4) or perpendicularly (42.7% ±4) and rarely under an obtuse angle (14% ±2.8). The bibliographic search revealed Papin's [29] statement on the variability of the angle, Salvi's [7] description, according to which the left renal vein makes almost a right angle, and Charpy's [9] and Paitre's *et al.* [15] indications of an acute angle. The left renal vein was horizontal (or had a slight cranial direction) in L'Aulnoit [30] and Kristenson's [13] cases, confirmed by Gérard [31], Chiarugi and Levi [10], Fazzari [12], Falcone [25], Almeida [26], and Last [11]. Variations in the angle with age were pointed out by L'Aulnoit [30], Charpy [9] and by Gérard

[31], as the renal veins were found to be obliquely ascending in children and horizontal or forming a less acute angle in adults. An angle, open superiorly, with the vertex at the level of the superior mesenteric artery, was described in the left renal vein by Grégoire [18].

Numerical data were presented by Fagarasanu [16], who described (1) type I – oblique ascending left renal vein – corresponding to an angle between 45° and 70° (42 cases); (2) type II having a right angle (13 cases); and (3) type III – oblique descending left renal vein – (5 cases).

The *aorticomesenteric angle* corresponds to the divergence between the axis of the superior mesenteric artery and that of the aorta. This angle may be called 'axial' as distinguished from the 'inferior' or 'internal' angle, limited by the anterior contour of the aorta and the infero-posterior contour of the superior mesenteric artery, which contains the left renal vein, the tip of the pancreatic uncinate process, and the duodenum (Fig. 3). As the sides or lines of both angles are parallel their measurements give equivalent results.

In accordance with Kristenson [13], the high mobility of the mesentery makes the vascular angle variable during life, for example, depending on the degree of fullness of the abdominal viscera and the position of the body. Considering that after embalming the vessels are fixed in an intermediary position, Kristenson [13] measured the aorticomesenteric angle in several ages:

I group (10 cases): birth to $1^1/_2$ years 72.5°
II group (8 cases): 2–5 years 46°

In the first group, there was obviously no influence of the erect posture and the reduction of the angle is maintained in the subsequent groups with a slight trend to increase beyond 20 years of age.

The *distance between the superior contour of the left renal vein and the vertex of the vascular angle* was also measured by Kristenson [13], who found that it varied from 1 to 25 mm. The distance increased with age: under the age of 50 years the average distances varied between 3.7 and 7 mm; above this age the average distances varied between 8 and 9 mm. In addition, he found that beyond the fiftieth year the left renal is nearer the aorta, practically next to its anterior contour, than in the cases under the age of 50. Fagarasanu [16] also focused on this distance when he alluded to the fact that the left renal vein runs 'under the superior mesenteric artery' from whose origin it is separated by a few mm (between 2 and 5).

Measuring the inferior aorticomesenteric angle only in individuals with ages of 20 years or older, when development is practically completed [1], the results ranged from 10° and 60°, averaging 30°9. The incidence of cases with angles less than 30° (62% ±4.1) is higher than that with angles greater than 30° (38% ±4.1).

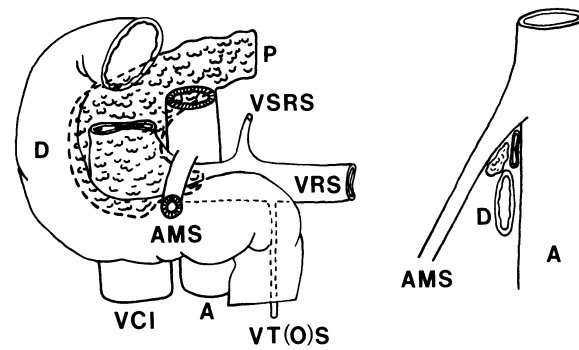

Fig. 3. Diagrams of the aorticomesenteric angle and neighboring structures. On the left the angle is seen to contain the duodenum (D), the tip of the uncinate process of the pancreas and the left renal vein, in cross section. AMS, superior mesenteric artery; A, aorta. On the right, an anterior view of the organs related to the angle: VRS, left renal vein; VSRS, left suprarenal vein; VT(O)S, left testicular (ovarian) vein; P, pancreas; D, duodenum; VCI, inferior vena cava; A, aorta.

For the arteries to exert an influence on the left renal vein the aorticomesenteric angle must be acute and the vein must be close to the vertex of the angle. In fact, even when the angle is acute, a long distance separating the contour of the vein from the vertex of the angle will allow the vessel to escape from the arterial pulsating compression. The same happens when the vein is close to the vertex but the angle is wide.

In a series of 142 observations of individuals aged 20 years or older, the left renal vein was found to be juxtaposed to the vertex of the angle in 18.3 ±3.2 of the cases [1]. Cases in which the distance was shorter than 5 mm occurred (71.1% ±3.8) more frequently than those in which the distance was longer (28.9% ±3.8), the average distance between vein and vertex being 4 mm. The findings correlated with the changes that may take place in the wall of the left renal vein.

4. Normal and pathological structures

The study of the renal veins demonstrated that only in 42% ±3.3 of 224 cases there were no modifications in the wall and no presence of congenital or acquired structures subdividing, reducing, or obliterating the venous lumen [1].

A pathological alteration of the left renal vein was

detected by Kristenson [13] in the portion of the vein located anteriorly to the aorta, and inferiorly to the origin of the superior mesenteric artery; it consisted of an adhesion between the anterior and posterior walls of the vein in its superior contour. The absence of the adhesion in 19 individuals from birth to 6 years of age proved that the alteration was not congenital (the youngest case having an adhesion was an 8-year-old girl). The incidence of such an alteration becomes frequent after 10 years of age, having appeared in 24 out of 115 cases. The author believed in the thrombotic nature of the alteration, after describing cases in which the process was in different developmental stages. Some of these data were confirmed by Caldana [32], among them the presence of one or more adhesions (in 9 out of 28 cases) in the portion of the left renal vein that crosses the aorta.

It was noticed [1] that in the renal veins different kinds of structures both normal and pathological or congenital and acquired, can occur: parietal thickening, adhesion, endovenous septa, and valves.

4.1. Venous parietal thickening.

Parietal thickening (Fig. 4) is an acquired, pathological alteration that appeared in 29 out of 224 cases (12.9% ±2.2), as early as at age 18 years to 57, more frequently (28 cases) in the inter-arterial portion of the left renal vein than outside of this portion (1 case). The thickening appeared more frequently when the projection of the vein occurred at the level of the intervertebral disc (9 out of 14 cases) than when it occurred in front of a vertebral body. A correlation was found between the presence of the parietal thickening and the hourglass type of the terminal portion of the left renal vein (19 out of 28 cases). The average aorticomesenteric angle in cases presenting a parietal thickening was 32° and in those cases without such a thickening it was 30°6. The average distance between the superior contour of the thickened left renal vein and the vertex of the aorticomesenteric angle resulted to be 3.5 mm, and in cases without the thickening it was 4.2 mm.

Taking these findings into account, there are reasons to justify the appearance of a thickening of the wall of the inter-arterial portion of the left renal vein, resulting from the topographical relationship, accentuated by the erect posture of man. Rather than a single factor, multiple factors such as a small aorticomesenteric angle, a juxtaposition of the vein to the vertex, or a projection of the vein in front of a more prominent intervertebral disc, a higher than usual lordosis location, may predispose the development of a thicker wall in the superior contour of the left renal vein.

4.2. Adhesion.

Adhesions of the venous walls, known by different names and corresponding to the fusion of opposite inner or endothelial aspects (Fig. 4), occurred in the left renal vein, especially in its inter-arterial (aorticomesenteric) portion, perhaps as a step following the appearance of parietal thickenings. The thrombotic origin of the adhesions was put forth by Kristenson [13], based on the anatomical conditions of this special vascular portion which may cause a stasis of the blood stream and a lesion of the venous wall. The vein is compressed by the reduction (a) of the vascular or arterial angle and (b) of the distance between the superior margin of the vein and the vertex of the angle. Other factors that may temporarily decrease the angle are a pronounced high lumbar lordosis, a full small intestine hanging in the pelvis or a full stomach pushing down the intestines and mesentery. The compression may cause an endothelial lesion, more likely in the superior contour of the vein, and since the blood stream is only temporarily slowed down there is no blood coagulation, only an accumulation of platelets. The adherence of the inner surfaces of the venous walls may then occur followed by thrombus organization, a thickening of the tunica intima, and the adhesion. Thickening of the tunica media may occur as a reaction to the irritation caused by an organized thrombus and against repeated pressures on the 'inter-arterial' vein, sometimes caused by lymph nodes.

Adhesions of the left renal vein, decreasing its lumen in the inter-arterial portion, were observed in 38 cases out of 224, that is, 17% ±2.5, the earliest at 19 years of age and the oldest at 80 years [1]. Flat adhesions or close fusion of opposite inner aspects of the vein appeared to be more frequent (36 cases out of 38) than adhesions at distance, similar to trabeculae, or columnar adhesions (2 cases). The flat adhesions did not leave a superior canal (35 cases), whereas the columnar adhesions always divided the lumen of the vein for the extension of the junction of the inner surface of the walls.

The measurement of the width of the superior mesenteric artery, anterior arm of the aorticomesenteric forceps, gives an idea of the portion of the left renal vein under pulsating compression to which adhesions may be correlated. In 144 cases [1] the range of the width was 4 mm and 16 mm, the average being 8 mm. There were more cases of adhesions in the left renal vein posterior to the superior mesenteric artery (28 out of 38 cases, that is, 73,7% ±7.1) than outside the inter-arterial portion (10 cases or 26.3% ±7.1). On the other hand, an equal number

of cases with adhesions occurred when the inter-arterial portion of the left renal vein was projected on an intervertebral disc (9) and on a vertebral body (9).

Adhesions appeared more frequently in the hourglass type of the terminal portion of the left renal vein (58.8% ±8.4) than in other types: right based cone (23.5% ±7.3), left based cone (8.8% ±4.9), cylinder (5.9% ±4), and bulb (2.9% ±2.9).

Among the cases that had adhesions, the aorticomesenteric angle averaged 28°2, ranging from 10° to 45°, whereas in the cases without adhesions the average angle was 32°7.

The distance between the superior contour of the left renal vein presenting an adhesion and the vertex of the aorticomesenteric angle varied from 0 to 10 mm and averaged 3.9 mm.

The incidence of adhesions reducing the lumen in the left renal vein, at the level of the aorticomesenteric angle, was found to be 20.9% of 115 cases by Kristenson [13], 32.1% of 32 cases by Caldana [32], and 17% of 224 cases [1].

On the influence that the vertebral column might exert favoring the constriction of the left renal vein, Rieser and Rieser [33] reported that Jehle [34] showed in patients suffering from orthostatic albuminuria the presence of lordosis in the erect posture. They added that lordosis correction might prevent albuminuria and that, in accordance with Sonne's [35] observations in 11 individuals, catheterization showed the right kidney secreting normally whereas the left was albuminuric. Pressure caused by viscera or by the aorta projected forward owing to lordosis will cause the left renal vein to be compressed by the arterial forceps. The authors cautioned that not all lordotic or visceroptotic patients are albuminuric unless the aorticomesenteric angle is sufficiently acute and the left renal vein is in a favorable position to suffer the compression that will cause blood stasis.

Both the prevailing hourglass type as well as those types that showed a narrowing of the terminal portion of the left renal, the smaller aorticomesenteric angle (45° difference), and the relatively large number of cases in which the vein was close to the vertex of the angle correlated with the incidence of venous parietal thickening and adhesions at the level of the inter-arterial portion.

The presence of the duodenum in the aorticomesenteric angle as a possible factor in increasing the compression of the left renal vein was implied by Kristenson [13] and Fagarasanu [16] as well as by Grant [36], who emphasized that both the left renal vein and the duodenum are pinched between the root of the mesentery and the aorta as in a nutcracker, slowing down the flow in the vessel and its tributaries as well as in the viscus. In addition to the duodenum the apex of the uncinate process of the pancreas in the aorticomesenteric angle should be included; however, the visceral variable topography, for instance, when the duodenum and/or the pancreas are located inferiorly to the level of the vein, may help to maintain the degree of the angle or even widen it, and thus protect the vessel against the arterial pulsating compression.

4.3. Endovenous septa.

An endovenous septum is an internal, longitudinal structure that partially divides the vascular lumen (Figs. 4, 5). These septa were pointed out long ago by L'Aulnoit [30], by Hyrtl [37], by Haller [38] as quoted by Franklin [39], Adachi [40], and Ferrari [41] and are comparable to those of the common iliac veins [1]. They are congenital structures, residues of transversal anastomoses in the primitive arrangement of veins that were only partially fused to originate the definitive venous trunks, such as the left renal vein.

Endovenous septa are, then, normal structures, made up of a double wall and arranged in a mirror image, to limit the resulting two channels in to which the lumen is partially divided. They were rarely found [1], that is, in four out of 224 cases (1.8% ±0.9). As they appeared only in adult Caucasians (three males and one female) the incidence of venous septa in this group (117 cases) is 3.4% ±1.7. Of these four cases having endovenous septa one was bilateral and three were observed in the left renal vein: one case had the septum located partially inside and partially outside the inter-arterial portion of the vein, two cases had septa only outside this portion, and the fourth (bilateral) case had a septum in the right renal vein and another outside the inter-arterial portion of the left vein. When present, they may represent an obstacle, for example, to catheterization of the vein or to the performance of venous splenorenal shunt.

4.4. Valves.

Some authors have denied the presence of valves in the renal veins: Verneuil [42], L'Aulnoit [30], Lejars [43], Charpy [9], Papin [29] and Testut and Latarjet [24]. In Franklin's [39] monograph, however, a number of authors who had described valves in the renal veins are mentioned. A study of 11 cases by Rivington [44] revealed that three cases presented valves in

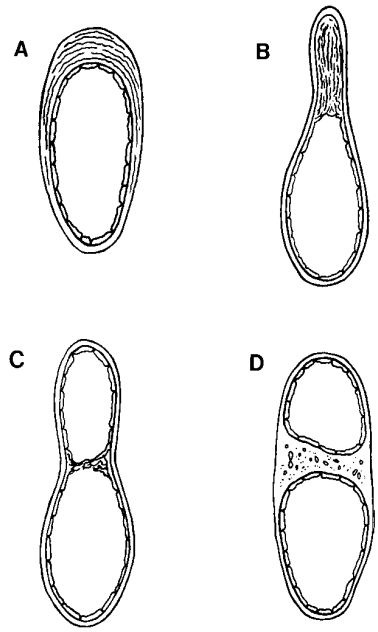

Fig. 4. Diagrams of transversal sections of the left renal vein showing in: A, parietal thickening; B, flat adhesion; C, columnar adhesion; and D, endovenous septum.

the right renal vein and five in the left. Other authors found valves in these veins: Jacquemet [45] in one case out of 68; McDonnell [46]; Kolster [28] in 33 out of 103 cases; Fagarasanu [16], who observed ostial valves in the right and parietal valves in the left; Dziallas [47] in two out of 25 cases; Pick and Anson [48]; Senior [49]; Bruni [50]; Chiarugi and Levi [10]. Out of 224 cases, 82 had valves in the renal veins [1], more frequently in the right (56.1% ±5.5) than in the left (19.5% ±4.4) or in both (24.4% ±4.7). The presence of a single valve (96.3% ±2.1) prevailed over the presence of two (3.7% ±2.1) and parietal valves (65.9% ±5.2) were more frequent than ostial valves (22% ±4.9), or both simultaneously (12.2% ±3.6). Ostial valves are much more frequent in the right renal vein (20.7% ±4.5) than in the left (1.2% ±1.2), but the parietal valves showed no statistically significant difference between those of the right renal vein (30.5% ±5.1) and those of the left (22.3% ±4.7).

Cases having bicuspid (53.7% ±5.5) or unicuspid valves (39% ±5.4) are more frequent than those presenting both types (6.1% ±2.6), the presence of tricuspid valves being very rare (1.2% ±1.2).

Valves possessing cusps which once distended were able to obliterate the lumen or the orifice of the vein were called sufficient or competent; those that were unable to occlude the vessel were termed insufficient or incompetent. The incompetent valves appeared more frequently (90.2% ±3.3) than the competent ones (73% ±2.9), the simultaneous presence of both types in the veins being rare (2.4% ±1.7). In the left renal vein the valves are much less frequent inside its inter-arterial portion (2.4% ±1.7) than outside it (41.4% ±5.4). Valves in the renal veins are, then, common but mostly incompetent and may interfere during catheterization of the vessels.

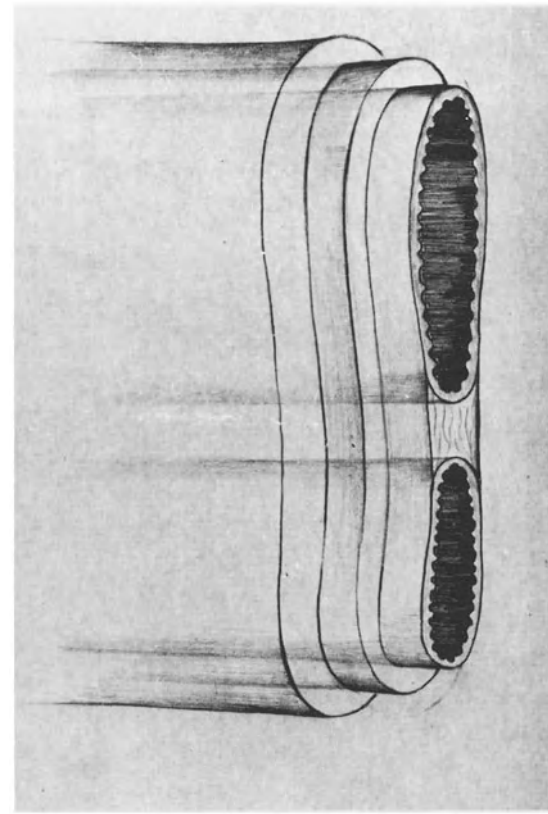

Fig. 5. Ideal drawing of an endovenous septum, dividing internally the lumen of a vein, and corresponding to the juxtaposition of two normal veins.

4.5. Renocaval spur.

Where two vessels join or divide a vascular spur occurs (Fig. 6). At the junction of one vein opening into another, particularly when the tributary has an oblique entrance, the juxtaposition of the venous walls in the acute angle formed by them makes up a crescentic edge or fold, called endovenous spur. Each has a semilunar morphology and a curved free border. Accordingly, as the renal veins drain into the inferior vena cava their junctions show in the inferior contour a renocaval spur, where for some distance,

fusion of the walls takes place, forming a greater or lesser deep common septum. In the left renal vein the spur appeared in 162 out of 163 cadavers, that is, in 99.4% ±0.6 [1]. Its direction (Fig. 6) was found to be more frequently oblique (77.8% ±3.3) than vertical (19.1% ±3.1) or horizontal (2.4% ±1.2), the obliquity always following the same direction as the blood stream.

In the right renal vein the spur occurred in 84 out of 107 cases, that is, in 78.5% ±4, and its direction was more frequently oblique (74.4% ±4.8) than vertical (22% ±4.6) or horizontal (3.7% ±2.1).

Comparing the spur in the renal veins in each case, it was noticed that it is bilaterally present (78.8% ±4) more frequently than it is unilaterally present (21.2% ±4), and that oblique spurs prevailed among the bilateral ones (48.1% ±4.9). Observations in 21 fetuses showed that the spur was always present more frequently bilaterally (90.5% ±6.4) than unilaterally (9.5% ±6.4), whereas L'Aulnoit [30] denied its presence in fetuses.

In phleboradiograms of the renal veins of 12 cadavers, it was possible to demonstrate reduction in the lumen of the terminal portion of the left renal vein, caused by parietal adhesion or thickening.

5. Microscopic anatomy

Microscopic examination of the above-mentioned structures showed that the parietal thickening was caused by increased subintimal and interfascicular connective tissue and by the tunica media. Both flat and columnar adhesions also exhibited thickened venous walls, a disruption of the normal arrangement of the vascular layers, and fusion of the walls facing each other; in the area of fusion there was no endothelium, but there was a large amount of loose connective tissue, numerous fibrils, fibrocytes and capillaries. The endothelium reconstituted its continuity in the limit of the adhesion looking toward the venous lumen. Columnar adhesions are unions or connections at a distance from the venous walls, having the same structure as the flat adhesion but dividing part of the lumen into channels. Both aspects of the columnar adhesion are lined by endothelium but the lamina elastica interna does not penetrate its thickness.

The endovenous septa are longitudinal membranes that divide the vascular lumen; they are made up of a double venous wall, as if two adjacent veins were juxtaposed, each limiting the respective channel. The structure of each endovenous septum shows

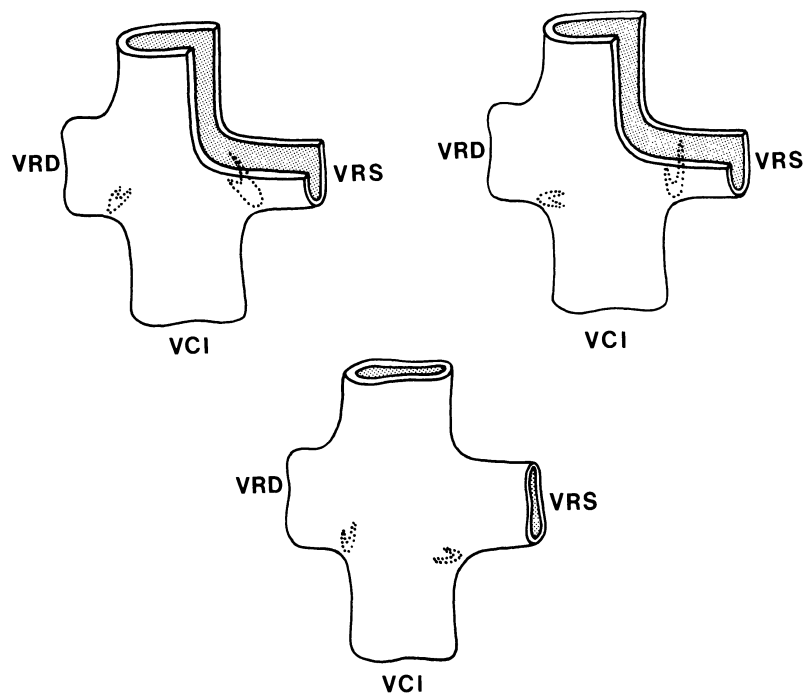

Fig. 6. Diagrams of renocaval junctions to show the direction of the right and left renocaval spurs (seen by transparency): both oblique (the most frequent, that is, 48.1% ±4.9); the right horizontal and the left vertical; and, in the bottom diagram, the right vertical and the left horizontal. VRS, VRD, and VCI, left renal vein, right renal vein, and inferior vena cava, respectively (from [1]).

six vascular layers arranged in a mirror image and occasionally separated between the adventitial layers by connective tissue, and vascular and neural elements. In each endovenous septum of the renal veins the layers are found in the following order: tunica intima (facing the superior canal), tunica media, tunica adventitia, interadventitial elements, tunica adventitia, tunica media, and tunica intima (of the inferior canal).

Histological observations on the renal veins were made by Hochrein and Singer [51], who noticed highly developed muscular fascicles, by Speciale [52], and by Eberth [53], who found an internal circular and an external longitudinal muscular layer. On the other hand, Buschi [54] described the presence of almost only longitudinal bundles, whose hypertrophy he related to the reduction of valves with age. Different findings were reported by Dentici [55] as he observed the tunicae intima, media, and adventitia, and a very complex muscular component: under the intima abundant circular muscular fibers, accompanied by fine connective fibers, formed an almost independent layer lined by longitudinal fibers. The adventitia contained many collagen and elastic fibers and the lamina elastica interna was very thick. According to Banowsky [20], the right renal vein has a more poorly developed muscular layer. Facing such conflicting data, observations of one of us [1], more closely fit Dentici's description [55].

6. Concluding remarks

In spite of Kristenson's [13,56] interpretation of the thrombotic nature of venous adhesions, especially that of the media and adventitia having a different genesis, it seems that Ferrari [41, 57] and Caldana [32] were correct when relating the adhesion to an arterial pulsating stimulus. Macroscopic and especially microscopic data led to the classification of the structures appearing in the renal venous district into:

A. Congenital:
   - I. Valves
   - II. Intervenous spurs
   - III. Endovenous septa

B. Acquired:
   - I. Parietal venous thickening
   - II. Adhesions
     1. Flat adhesions
     2. Columnar adhesions

The congenital formations exhibited a normal structure whereas the acquired formations were of a pathological nature.

Valves occurred more frequently than generally stated, intervenous spurs represented membranes resulting from greater or lesser juxtaposition of confluent vessels (at an acute angle), and endovenous septa are residues, persistent in the adult, of the primitive multiple parallel arrangement of veins which fuse to constitute the definitive trunk.

As a reaction to the constant stimulus provided by arterial pulsating compression (as in the aorticomesenteric angle, also related to erect posture), the acquired venous structures begin with parietal thickening, eventually leading to the flat and/or columnar adhesions, the result of the fusion of opposite venous walls leading to a reduction in the lumen that can be radiologically detected. Extreme cases substantiate these statements and the importance of the presence of these structures. In fact, in an adult, male, Caucasian individual the left renal vein was completely obliterated, his survival probably assured by venous collateral circulation. Unfortunately his clinical history was not available for correlation of the post mortem findings with his symptoms. Such an eventuality would require a phleborenoradiogram previous to the performance of venous splenorenal shunt to avoid unsuccessful surgical treatment, in case of need. Finally, in all four cases in which the left renal vein was found posterior to the aorta and compressed by this artery directly against the vertebral column (thus under a much stronger compression), there was parietal adhesion between the anterior and posterior walls of the vein, corresponding to the aortic impression on the left renal vein.

When L'Aulnoit [30] alluded to the history of the valves he stated that Estienne [58] in 1545 used the vague term 'epiphyses' but cast doubt on whether he actually observed them, adding: 'what he calls epiphyses of the supra-hepatic veins can only be related to the spurs that crown their orifices of entrance in the inferior vena cava, identical to those presented by arteries at their bifurcations'. L'Aulnoit [30] described the spur of the inferior semicircumference of the opening at the end of the renal veins, indicating that its direction is upward oblique in the inferior vena cava. In 11 cases observed by Rivington [44], the spur, or as he called it, the 'inferior semilunar fold', was found in the orifices of the renal veins in the inferior vena cava.

A certain degree of confusion or some relationship was found in the literature as Charpy [9] stated that there was no valve at the end of each renal vein but a spur, owing to oblique direction of the vein, which extended as a 'valvuloid' semilunar fold, in the lumen. The spur was more developed on the left because the vein ended forming a more acute angle

with the vena cava. Along the same line, Kristenson [13] mentioned the spur when stating that the edge of the inferior portion of the circumference at the end of the left renal vein is more or less prominent, often forming a 4–5 mm high crest 'having the aspect of a rudimentary valve.'

Cavorenoradiograms taken in cadavers allowed correlation of each venous partial filling with radiopaque substance, reduced or deformed lumen with parietal thickenings, flat or columnar adhesions, valves, endovenous septa, and spurs. Both in renal vein catheterization, for example to test samples of 'pure' renal or, depending on anatomical variations, relatively pure blood from the right kidney or 'mixed' blood from the left, owing to the suprarenal and gonadal tributaries (among others) and for the performance of surgery, such as venous splenorenal shunt, these structures may have to be considered to assure the success of the intervention.

The concept of direct sampling of renal venous blood in hypertensive patients was established in the mid-1960s by Judson and Helmer [59]: in their patients with renovascular hypertension, renin levels in blood from the ischemic kidney where at least twice as high as renin levels in blood from the contralateral kidney. The concept of lateralization of renin secretion was introduced. Many similar investigations substantiated the finding.

Other applications somewhat related to the basic knowledge of what preceded, includes primary thrombosis of renal veins that occurs often in early infancy, during which the blood flow of the kidney is relatively slow and can further be reduced by dehydration and loss of salt. Renal vein thrombosis can be secondary to primary renal disease, which is responsible for slowing down the renal blood flow. Surgical treatment includes localizing the thrombus, exposure of the inferior vena cava and renal veins, a longitudinal phlebotomy, and clot aspiration. In cases of unilateral thrombosis and contralateral normal kidney, a nephrectomy is indicated [60].

References

1. DiDio LJA: Applied anatomy of the renal veins. The importance of the mesenterico-aortic forceps. The vascular renal segments [in Portuguese]. An Fac Med Univ Minas Gerais Belo Horizonte 16: 51–202, 1956.
2. Smith APF: Vascular impressions on the renal pelvis. Radiol Clin Biol 40: 213–214, 1971.
3. Anson BJ, Daseler EH: Common variations in renal anatomy, affecting blood supply, form, and topography. Surg Gynecol Obst 112: 439–449, 1961.
4. Anson BJ, Cauldwell, Pick JW, Beaton LE: The blood supply of the kidney, suprarenal gland, and associated structures. Surg Gynecol Obst 84: 313–320, 1947.
5. Anson BJ, Kurth LE: Common variations in the renal blood supply. Surg Gynecol Obst 100: 157–162, 1955.
6. DiDio LJA: Estudo anatomico de particularidades normais e patologicas da superficie interna da veia iliaca comum esquerda: Adesões, Septos e Valvulas. Doctoral Thesis, University of São Paulo. Arq Cir Clin Exp 12 (6): 507–616, 1949.
7. Salvi G: Angiologia. In: Balli R *et al.* (eds) Trattato di Anatomia Umana. Milano, C Editr F Vallardi, vol III, 1932.
8. Grégoire R, Oberlin: Précis d'Anatomie. Splanchnologie. Paris, Libr JB Baillière et Fils, 1929.
9. Charpy A: Veines, in Poirier P, Charpy A-Traité d'Anatomie Humaine. Paris, Masson, t II, fasc III, 1903 (2ème éd).
10. Chiarugi G, Levi G: Istituzioni di Anatomia dell'Uomo. Milano, Soc Editr Libraria, 1948 (7.ª ed).
11. Last RJ: Anatomy. Regional Applied. London, J & A Churchill, 1954.
12. Fazzari I: Compendio di Anatomia Topografica. Milano, Soc Editr Libraria, 1940.
13. Kristenson A: Beitrag zur Kenntnis der Pathogenese der orthostatischen Albuminurie und der Varikozele. Upsala Lakareforen. Forhandl. N. F., 31 (3–6): 641–702, 1926.
14. Maisonnet I, Coudane R: Anatomie Clinique et Opératoire. Paris, Doin, 1950.
15. Paitre F, Giraud D, Dupret S: Práctica anátomo-quirúrgica ilustrada. Abdomen. Los organos retroperitoneales. Barcelona, Salvat edit, fasc III, 1941 (1.ª ed).
16. Fagarasanu I: Recherches anatomiques sur la veine rénale gauche et ses collaterales. Leurs rapports avec la pathogenie du varicocèle essentiel et des varices du ligament large. Ann Anat pathol Anat Norm Med Chir 15 (1): 9–52, 1938.
17. Dantas RT: Estudo anatomo-cirurgico do sistema porta, veia renal esquerda e veia cava inferior. (Contribuição ao tratamento cirurgico da hipertensão portal pelas anastomoses venosas). Doctoral Thesis, University of Bahia, 1954.
18. Grégoire R: Anatomie médico-chirurgicale de l'abdomen. La région lombaire et le petit bassin. Paris, JB Baillière et Fils, 1926.
19. Barcelos JMP, Byington CAB: O tronco da veia renal esquerda. Comun à VIII Sem Brasil Debates Cientif São Paulo (personal communication), 1954.
20. Banowsky LHW: Surgical anatomy. In: Stewart BH (ed) Operative Urology. Baltimore, Williams & Wilkins, 1975.
21. Brash JC: Cunningham's Textbook of Anatomy. London, Oxford University Press, 1951 (9th ed).
22. Purcell HK, Connor JJ, Alexander WF, Scully NM: Observations on the major radicles of the extrahepatic portal system. AMA Arch Surg 62: 670–677, 1951.
23. Testut L, Jacob O: Traité d'Anatomie Topographique avec applications médico-chirurgicales. Paris, Doin, 1931 (5ème éd).
24. Testut L, Latarjet A: Traite d'Anatomie Humaine. Paris, Doin, 1929 (8ème éd).
25. Falcone C: Trattato di Anatomia Umana. Milano, C Editr F Vallardi, 1950 (3.ª ed).
26. Almeida AD: O tratamento cirurgico da hipertensão do sistema porta por anastomose venosa direta. São Paulo, Empr Graf Rev Tribunais.
27. Warwick R, Williams PL: Gray's Anatomy. Philadelphia, Saunders, 1975 (35th British ed).
28. Kolster: Studien ueber die Nierengefaesse. Zeit Morphol Anthrop 4: 179–197, 1901; quoted from Pick and Anson.
29. Papin E: Chirurgie du rein. Paris, Doin, 1928.
30. L'Aulnoit AH: Recherches anatomiques et physiologiques sur les valvules des veines. These. Paris, Rignoux, 1854.
31. Gérard G: Manuel d'Anatomie Humaine. Paris, Masson, 1921 (2ème éd).
32. Caldana E: Alterazioni venose nella iliaca comune e nella renale di sinistra, da stimolo pulsatorio arterioso. Biol Lat 4(4): 613–624, 1951.
33. Rieser W, Rieser SL: The etiology of orthostatic albuminuria. Amer Med Assoc 78(9): 644–647, 1922.
34. Jehle: Münch Mediz Woch 55: 12, 1908; in Rieser and Rieser.
35. Sonne: Hospitalstid 61: 800–817, 1918; June 12 in Rieser and Rieser.
36. Grant JCB: A method of Anatomy. Baltimore, Williams and Wilkins, 1952 (5th ed).
37. Hyrtl G: nd Manuale di dissezione pratica (trad ital di G Bassi). Milano, C Edit F Vallardi.
38. Haller: quoted from Franklin.

39. Franklin KJ: Valves in veins: an historical survey. Proc Roy Soc Med 21: 1–33, 1928.
40. Adachi B: Anatomie der Japaner. II Das Venensystem der Japaner. Kyoto, Druk Kenkyusha Tokyo, 1940 (Zweite Lieferung).
41. Ferrari E: Un' interessante alterazione della vena iliaca comune di sinistra al suo sbocco nella vena cava inferiore. Suoi rapporti con la trombosi. Arch Ital Anat Istol Patol 12: 239–293, 1940.
42. Verneuil: Système veineux: thèse de concours, p. 81; in L'Aulnoit, 1953.
43. Lejars F: Les voies de sureté de la veine rénale. Bull Soc Anat Paris A 63, S 5, 2 (17): 504–511, 1888; Les veines de la capsule adipeuse du rein. Arch de physiol, in Charpy, 1891.
44. Rivington W: Valves in the renal veins. J Anat Physiol 7: 163–164, 1873.
45. Jacquemet: Arch Med, in Charpy, 1879.
46. McDonnell R: Recherches sur les valvules des veines rénales et hépatiques et sur la circulation hépatico-rénale. J Physiol Homme 2: 300–308, 1859, in Charpy.
47. Dziallas P: Über die Klappenverhältnisse der Venae spermaticae des Menschen. Anat Anz 97 (4–5): 57–63, 1949.
48. Pick JW, Anson BJ: The renal vascular pedicle. An anatomical study on 430 body-halves. J Urol 44: 411–434, 1940.
49. Senior HD: Blood vascular system, in Morris' Human Anatomy. London: J & A Churchill, p II, 1915 (5th ed).
50. Bruni AC: Compendio di Anatomia Descrittiva Umana. Milano: C Edit F Vallardi, 1948 (3.ª ed).
51. Hochrein M, Singer B: Untersuchungen am venosen Teil des Kreislaufes. II Mitt Untersuchungen über den Bau der Venenwand. Arch exper path Pharmakol 125: 301–325, 1927; in Anat Bericht 18:245, 1930; in Franklin KJ: A Monograph on Veins. Springfield, CC Thomas, 1937.
52. Speciale F: Variazioni strutturali delle vene dell'uomo in rapporto all'età ed ai tipi costituzionali. Ric Morfol 8: 263–281, 1928.
53. Eberth quoted from Speciale.
54. Buschi G: Modificazioni strutturali delle vene nella vecchiaia. Atti Soc Lomb Sc Med Biol 1 (3): 506–523, 1912.
55. Dentici L: La struttura della vena renale. Estratto Boll Soc Natur Econ Palermo 17: 5 pp, 1935.
56. Kristenson A: Zur Kenntnis der localisierten Thrombenbildungen in der Vena iliaca communis sinistra. Acta Med Scandinavica 73 (suppl 33): 1–82, 1930.
57. Ferrari E: Su alcune interessanti malformazioni della vena iliaca comune di sinistra nell'uomo. Briglie congenite tese attraverso il lume. Cuore e Circolazione 24: 455–468, 1940.
58. Estienne CH: De Dissectione partione corporis humani, lib 2, cap 9, et lin 3 Paris: in-folio, p 182, leg 44, p 357, leg 11, in L'Aulnoit, 1545.
59. Judson WE, Helmer OM: Diagnostic and prognostic values of renin activity in renal venous plasma in renovascular hypertension. Hypertension 13: 79–89, 1965.
60. Kaufman JJ: Renovascular Disorders. In: Glenn JF (ed) Urologic Surgery. Philadelphia, JB Lippincott, 1983 (3rd ed).

CHAPTER 3

Embryogenesis of the kidney

CESARE DE MARTINO and LIDIA ACCINNI

1. Introduction

In the last century two apparently conflicting hypotheses were proposed in order to explain the phylogenetic development of the kidneys of the vertebrates. The first one claimed that during evolution the Chordates developed three separate and distinct kidneys, namely the pronephros, the mesonephros and the metanephros, and that the ontogeny recapitulates the phylogenetic history. The second hypothesis maintained that these three kidneys must be regarded as regional specializations of a single primitive, hypothetical, ancestral kidney extended from cervical to caudal somites, i.e. the archinephros. On the basis of more recent phylogenetic observations, which showed that intermediate kidneys such as the opistonephros and the holonephros are present as definitive excretory organs in some vertebrates, the theory of the essential unity of the nephrogenic material has now gained universal acceptance [1, 2],

All embryonic kidneys develop from the nephrogenic cord which arises from the intermediate plate mesoderm. However, although in embryonic and larval periods the pronephros, mesonephros and metanephros are morphologically separated during their development, transitional forms of definitive or adult kidneys are present during the phylogenesis. In fact, while the metanephros is the adult kidney in reptiles, birds and mammals, in amphibians and fishes the definitive kidney develops either from a nephrogenic blastema which is primarily but not entirely of mesonephric origin and incorporates also metanephric material (opistonephros), or, more rarely, from a blastema which derives from the pronephros and the mesonephros (holonephros) [2].

The mammalian kidney develops at the anterior end of the body, extending from here in a posterior direction. The 'first' and the 'middle' kidneys, pronephros and mesonephros respectively, are embryonic kidneys, whereas the 'last', or metanephros, is the definitive adult kidney.

2. Pronephros

In mammals as well as in human embryo the pronephric nonfunctional rudiments extend from somites VI–XIV. These rudiments connect to form a strand separated from the coelomatic cavity by the somatic mesoderm. Successively, these solid rudiments hollow out and form funnels which open into the coelom (nephrostomes). The anterior rudiments degenerate while the most posterior reach full development. The external pole of each nephrostome grows caudally till it fuses with the bud of succeeding nephrostome, giving rise to a tube which extends posteriorly and reaches the cloaca by the end of the 4th week of embryo development (4.3 mm embryo). This nephric duct is variously referred to as pronephric duct (cranial portion), mesonephric duct (middle portion), and Wolffian duct (caudal portion).

Differently from mammals, the pronephric kidney is functional in all species of vertebrates producing free larval forms (teleosts, ganoids, lung fishes and amphibians). Until near the end of the larval period, most anurans retain a functional paired pronephric kidney which degenerates and disappears at the end of metamorphosis [3]. In this species of vertebrates, the pronephros is essentially a water-excreting organ which is mainly involved in the production of an extremely dilute urine containing ammonia, whereas the mesonephros, which succeeds the pronephros during the premetamorphic period, essentially excretes urea [4]. In young premetamorphic amphibians for a short time the pronephros is the sole excretory and osmoregulatory organ. Extirpation of both pronephroi or blockage of both nephric ducts leads to failure in osmoregulation and hence death of the larva [3]. Among the vertebrates, the pronephros is present as adult kidney in Myxinoids which possess both a paired pronephros and a paired mesonephros, separated by degenerating nephron rudiments [5].

L.J.A. DiDio and P.M. Motta (eds), Basic, Clinical, and Surgical Nephrology. ISBN 0-89838-689-5.

Among the mammals, a multinephron pronephros is reported in the lowest animals (Echidna, Opossum) and in the human embryo, while in the cat, rabbit, guinea pig and sheep the pronephros remains a small undifferentiated mass [6, 7]. However, the morphologic features of functional pronephros reported so far regard exclusively the organ of the amphibian larvae [3, 8]. In Xenopous laevis, the initial portion of the pronephric nephrons is formed by very long, ciliated tubules (nephrostomial tubules), which open into the coelom by separate distinct nephrostomes. The nephrostomial tubule continues in a proximal tubule and thence into a distal tubule which opens into the nephric duct [9] (Figs. 1, 2). Some authors [3, 8] describe an intermediate ciliated tubule interposed between the proximal and distal tubules in the larvae of other amphibian species.

3. Human mesonephros

In fishes and amphibians the mesonephros, either as opistonephros or as holonephros, represents the definitive or adult kidney, whereas in reptiles, birds and mammals is only a transitory kidney.

In mammals, there is a strict correlation between size of mesonephros and of allantoid and type of placenta [10]. The mesonephros and the allantoid are usually very large in those animals with a single appositional type of placenta. In fact, in mammals with an epitheliochorial placenta, i.e. pig, the mesonephros is extremely developed and the allantoid contains a considerable amount of fluid, while the size of the mesonephros and allantoid decreases gradually in those animals with an endotheliochorial placenta and reaches the lowest degree of development in rodents, such as mouse and rat, which possess a highly permeable placenta of hemochorial variety.

In the nephrogenic cord, the mesonephros begins to develop from clumps of cells lying along the Wolf-

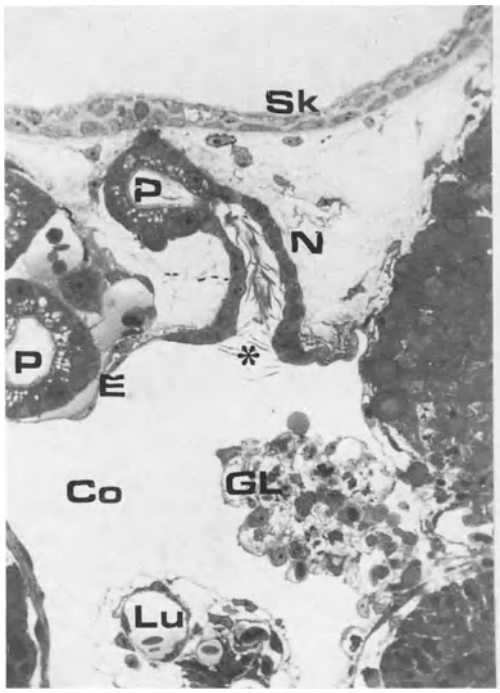

1

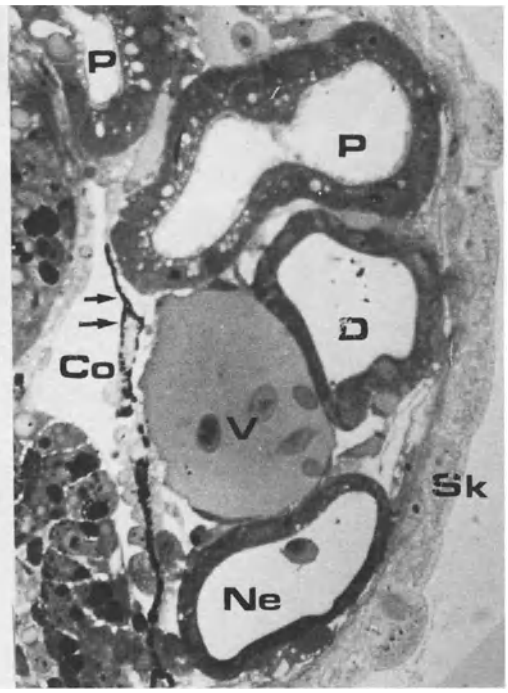

2

Fig.1. A survey picture of the pronephros of a larva of Xenopous laevis. The nephrostomial tubule (N) is composed of cuboidal ciliated cells which are continuous with the flattened coelomatic epithelial cells (E) on one side and with the columnar proximal tubular cells (P) on the other side. The latter cells show an apical brush border and many apical vacuoles. The asterisk indicates the nephrostomial funnel. Gl: glomus floating in the coelomatic cavity, Lu: lung, Sk: skin ×300.

Fig. 2. Pronephros of a larva of Xenopous laevis at higher magnification. In the picture the proximal (P) and distal (D) tubules and the nephric duct (Ne) are visible. Co: coelomatic cavity, Sk: skin, V: vein. The arrows point to the subcoelomatic cell layer containing numerous melanin granules. ×500.

fian duct. Few nephrons develop anteriorly to the 14th somite, thus perhaps overlapping the caudal end of the pronephros. However, in the human embryo the first fully developed mesonephric nephron differentiates at the 18th somite. About 30 to 40 nephrons develop in total, two or three per single somite, reaching at full development the 29th somite. Both development and regression take place in cranial-caudal direction. At the 12th week of embryo development, the cranial nephrons are degenerated, the middle start degenerating and the caudal are fully differentiated. At the end of the 4th month, the mesonephros is completely degenerated except a small middle region which is connected with the reproductive system and will be modified into the epididymis in the male or as nonfunctional vestiges such as the epöophoron in the female.

The human mesonephros, though poorly developed in comparison with the mesonephroi of rabbit, sheep and cat, has such morphological features which suggest that also in man it may be considered as a functional embryonic kidney. This, like the pronephros in amphibians, could assume a main importance before the development of a functional placenta as the sole excretory and osmoregulatory organ indispensable during the embryonic period of intrauterine life. In the foetal period, the mesonephric functions are replaced mainly by the placenta which is also able to replace the metanephros since bilateral renal agenesis is compatible with the survival of the foetus until birth.

The morphogenesis of the mesonephric nephrons is practically similar to that of the nephrons of the metanephric kidney (see section 4). Even though the size of the mesonephros, the number of fully developed nephrons and the diameter of the glomeruli differ among mammalian species, basically the architecture of the nephron is similar in all mammals [11]. The mesonephric nephron is made up of the glomerulus, proximal tubule, distal tubule and collecting tubule which joins the Wolffian duct by means of an intermediary segment, the connecting tubule (Figs. 3–8). There is no Henle's loop interposed between proximal and distal tubules [12–16]. The following description concerns primarily the mesonephros of human embryos from 7 to 10 weeks of intrauterine life, which have been thoroughly investigated by us [12, 15, 16]. The morphological features of the mesonephric nephrons vary according to embryo age and area of development, namely cranial and caudal regions. In the latter region, two types of glomeruli are present (Fig. 3). The first one is located close to the Wolffian duct and is characterized by large glomeruli with wide urinary spaces and capillary lumens, largely convoluted proximal tubules and moderately convoluted distal tubules. The nephrons in the cranial region are similarly organized. The second type of caudal nephrons is situated close to the coelomatic epithelium and possesses smaller glomeruli with narrow urinary spaces and capillary lumens and short unconvoluted proximal and distal tubules. In both types of nephrons, the afferent and efferent glomerular vessels frequently enter and egress from separate and often opposite poles (Fig. 4). The afferent arterioles derive from the mesonephric arteries (Fig. 7), which are lateral branches of the aorta, enter into the glomerulus in a zone which is opposite to the urinary pole and leave the glomerulus as capillaries at considerable distance from the penetration site (Fig. 4). The efferent vessels spread over the surface of the tubules forming a capillary network (Fig. 5) with anastomizing branches of the posterior cardinal vein. These capillaries, reunited into veins (Fig. 8), empty into the subcardinal vein thus establishing the renal-portal circulation. As the mesonephros involution begins, the renal-portal circulation regresses and a new definitive circulation appears with the development of the metanephros. On the basis of morphological features, a functional overlapping appears to exist between fully differentiated mesonephric nephrons and early metanephric nephrons around the 10th week of intrauterine life.

3.1. Glomerulus

The wall of the glomerular capillaries is formed by two cellular layers, namely the endothelium and the visceral epithelium or podocytes (Fig. 9), separated by a basement membrane of irregular width (Fig. 10). The endothelial cells, some of which appear in mitosis, possess scarce fenestrations (Fig. 9). The numerous pinocytotic vesicles present in their cytoplasm suggest the existance of an active transport mechanism of macromolecules across the endothelium rather than a passive filtration which could not be operating at the low levels of blood pressure present in the embryo [12]. The podocytes rest on the glomerular basement membrane either as foot-processes (Fig. 9) or as continuous cytoplasmic sheets containing large bundles of thin filaments (Fig. 10). Numerous microvilli are present on the plasmamembrane facing the urinary space (Fig. 9). The basement membrane is made up of three layers, namely an outer layer or subepithelial zone or lamina rara externa, a thin middle layer or basement membrane proper or lamina densa or basal lamina, and an inner layer or subendothelial zone which in

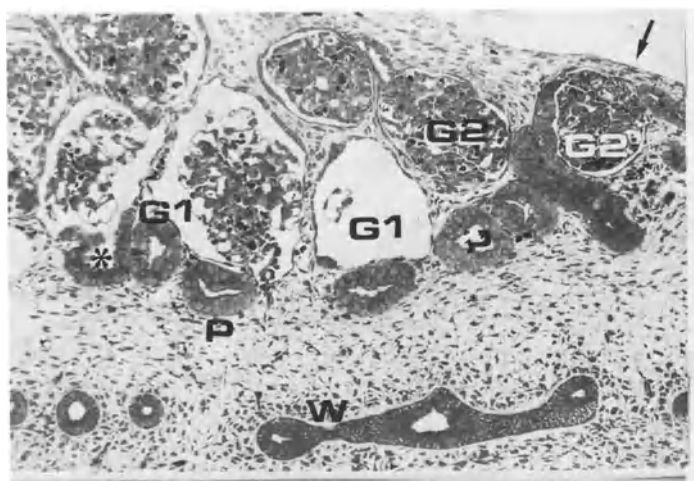

3

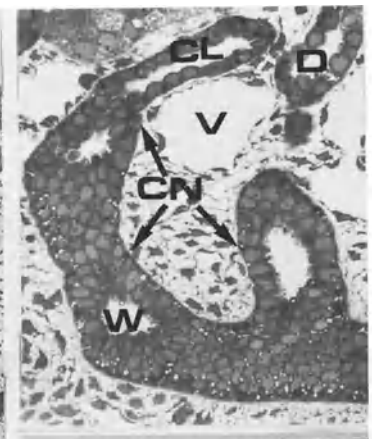

6

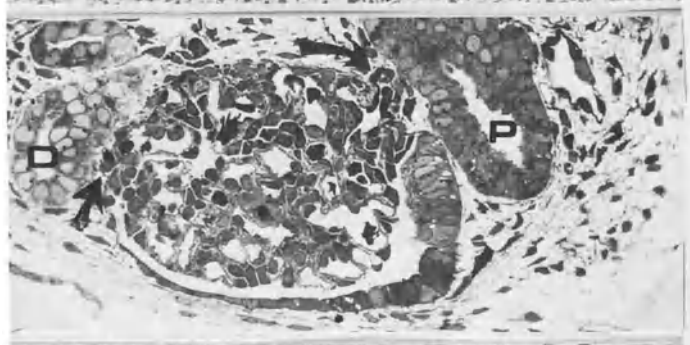

4

7

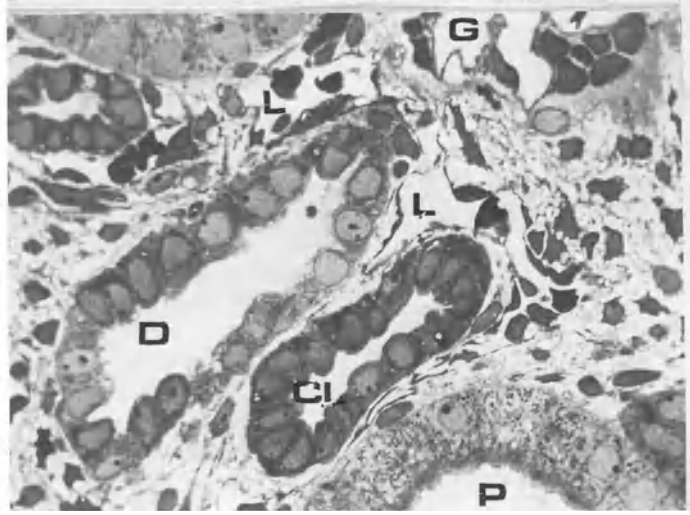

5

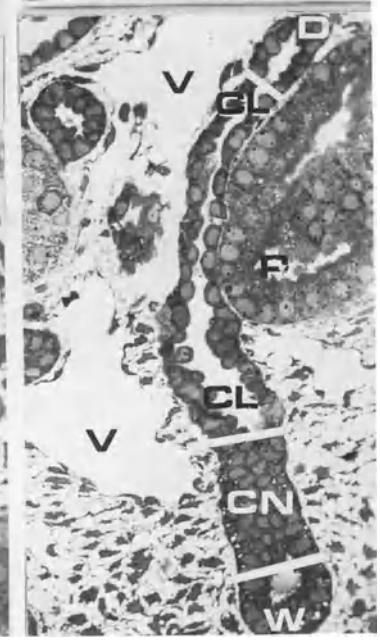

8

Figs. 3–8. Caudal portion of mesonephros of a 10 week old human embryo.
Fig. 3. A survey picture showing two types of mesonephric glomeruli. The first (G1), located close to the Wolffian duct (W), are large and have wide capillary lumens and urinary spaces. The second (G2), located below the coelomatic epithelium (arrow), are smaller and have narrow capillary lumens and urinary spaces. The asterisk indicates the urinary pole of a G1 glomerulus. P: proximal tubules. ×150.
Fig. 4. The picture shows a glomerulus with two opposite vascular poles. The efferent arteriole (curved arrow) is in close relationship with the proximal tubule (P), while the afferent arteriole (straight arrow) is in contact with the first portion of the distal tubule (D) which shows crowded cells. The shape of the capsular cells gradually changes from columnar to flattened. ×400.
Figs. 5 & 6. Proximal (P), distal (D), collecting (CL), connecting (CN) and Wolffian (W) tubules are visible. G: glomerulus, L: lumen of a peritubular capillary, V: vein. Fig. 5, ×1,200; fig. 6, ×500.
Fig. 7. The afferent glomerular vessel (curved arrow) originates from the mesonephric artery which shows a well developed tunica media (straight arrow). G: glomeruli. ×800.
Fig. 8. The picture illustrates a large mesonephric vein (V) closely related with collecting (CL) and connecting (CN) tubules. P: proximal tubule, W: Wolffian duct. ×800.

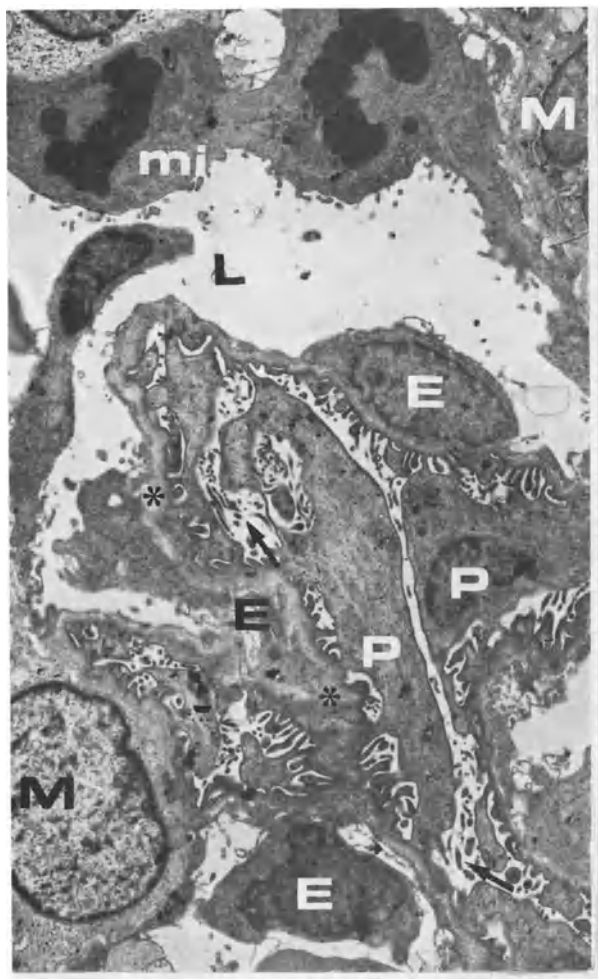

9

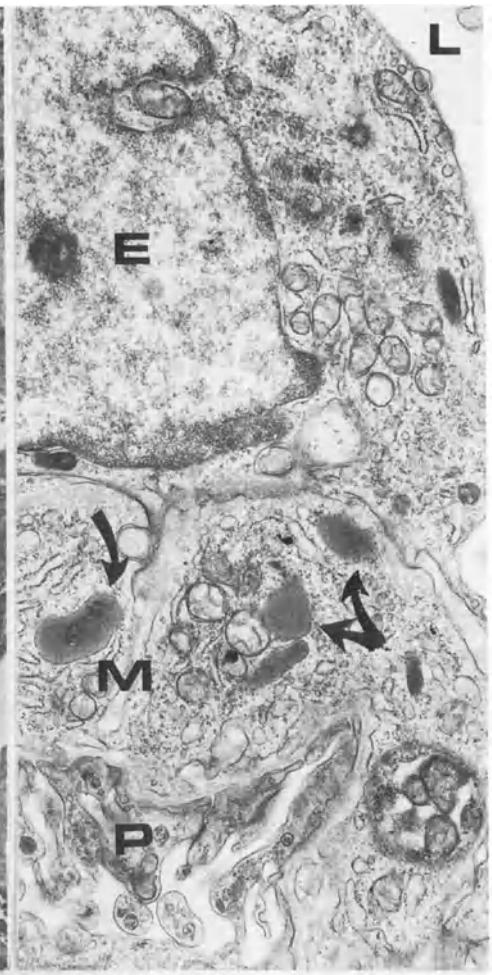

11

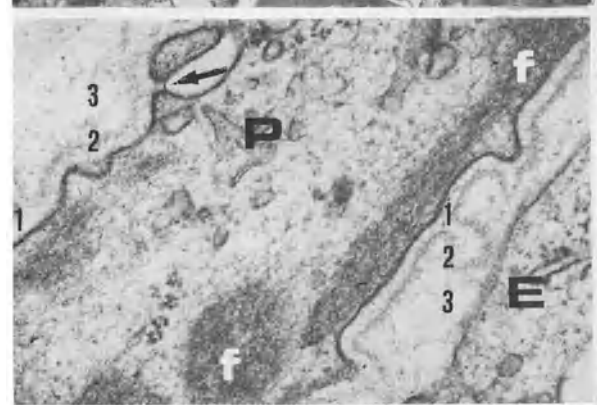

10

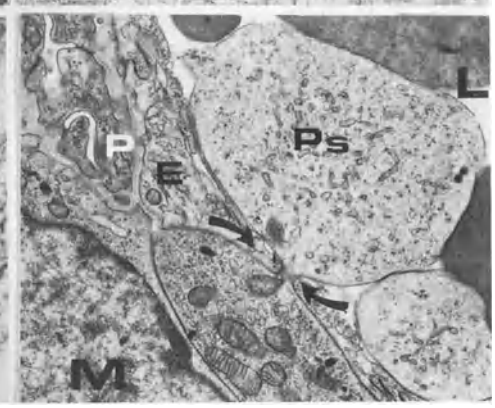

12

Fig. 9. Part of a well developed mesonephric glomerulus. The glomerular capillaries show unfenestrated endothelial laminae (E) and podocytes (P) with well differentiated foot-processes. The arrows point to microvilli on the surface of podocytes. L: capillary lumen, M: mesangial cell; mi: mitotic endothelial cell. ×8,000.

Fig. 10. Part of a glomerular capillary wall of a mesonephric glomerulus at high magnification. The three layers of the glomerular basement membrane are marked as 1) subepithelial zone, 2) lamina densa, 3) subendothelial zone. Bundles of thin filaments (f) are visible in the cytoplasm of a podocyte (P). The arrow points to a slit-membrane between contiguous podocytes. E: endothelium. ×30,000.

Fig. 11. Part of the capillary wall of a mesonephric glomerulus. The mesangial cell (M) shows a well developed ergastoplasm and several dense granules (arrows). E: endothelium, L: capillary lumen, P: footprocesses of podocytes. ×15,000.

Fig. 12. Part of a mesonephric glomerulus. The arrows point to an endothelial gap through which a pseudopodium (Ps) of a mesangial cell (M) reaches the capillary lumen (L). P: podocyte. ×12,000.

some places becomes considerably enlarged (Fig. 10). The mesangial cells are localized in enlarged areas of the subendothelial zone (Fig. 11). They are characterized by a well developed ergastoplasm and Golgi apparatus and by luminar pseudopodia (Figs. 11, 12). Dense granules and crystalloid-shaped bodies [17], similar to those present in the juxtaglomerular granulated cells of the adult kidney [18], are often visible in their cytoplasms (Fig. 11). The epithelium of the Bowman's capsule resembles that of the proximal tubule near the urinary pole, whereas it is flat in the opposite side, cells with transitional features being present between the two regions (Fig. 4).

3.2. Juxtaglomerular-like apparatus

The presence of cells with renin specific protogranules and granules [18] (Figs. 13–20) in the mesangium and in the media of some afferent glomerular arterioles strongly suggests that also in human mesonephros there is a renin production and secretion [16, 19, 20]. Thus, it can be assumed that an autoregolatory mechanism of glomerular filtration rate mediated by the renin-angiotensin I – angiotensin II vasoconstrictor system may be operative and act directly on the contractility of the vascular and mesangial smooth muscle cells. However, a typical juxtaglomerular apparatus with all its components is not observed [11–14]. In fact, in the mesonephric glomerulus the lacis cells lack and the distal tubule is in close association only with the afferent arteriole, being the efferent vascular pole far from the afferent one. Furthermore, although the crowded cells of the first portion of the distal tubule closely resemble the cells of the macula densa, the other ultrastructural characteristics of the macula densa are not observed [21].

3.3. Proximal tubule

The proximal tubule can be divided into two portions. The first one, continuous with the Bowman's capsule, is composed of columnar cells with a well developed brush border and endocytic apparatus, namely apical tubular invaginations, apical dense tubules, apical vacuoles and cytosomes, numerous mitochondria mostly located in the basal cytoplasm and scarce infoldings of the basal plasma membrane (Fig. 21). The second portion, which joins the distal tubule, possesses scarce brush border and endocytic apparatus. The presence of the latter two structures, which are known to be involved in the absorption, digestion and transport of proteinaceous material, strongly suggests that the proximal tubule of the mesonephric nephron actively reabsorbs proteins filtered by the glomerulus [12, 13]. In fact, in fishes with aglomerular kidneys the endocytic apparatus is not present [22] and in human developing metanephros it gradually develops with glomerular maturation [23].

3.4. Distal tubule

The distal tubule is scarcely convoluted and can be divided into two segments. The first segment is continuous with the proximal tubule and runs close to the afferent glomerular arteriole (Fig. 4). In this area, as previously mentioned, the cells are tightly packed simulating a macula densa-like appearance (Fig. 4). In both segments the cells are columnar and contain numerous mitochondria in their basal cytoplasm and around the nucleus while their apical cytoplasm, which is pratically devoid of organelles, largely protrudes into the tubular lumen (Fig. 22).

3.5. Collecting tubule

The collecting tubule is composed of cuboidal cells with large ovoidal nuclei (Figs. 5, 23). Few scattered mitochondria and large amounts of glycogen are present in their cytoplasm. The apical plasma membrane appears smooth and the basal infoldings are scarce or absent (Fig. 23).

3.6. Connecting tubule and Wolffian duct

Both segments are made up of columnar cells which in some areas appear as a pseudostratified epithelium (Figs. 6, 8, 24). The mitochondria, Golgi apparatus and endoplasmic reticulum are usually located above the nucleus which appears indented. Glycogen and apical vacuoles are present in the cytoplasm. Large intercellular spaces containing short microvilli run from the apical cellular junctions to the basal regions (Fig. 24).

3.7. Regression

The glomerular changes which characterize the regression process involve all components of the capillary loops, resulting in a progressive reduction and obliteration of the vascular bed (Fig. 25). At the beginning, the mesangial cells become hypertrophic and, pushing against the endothelium, induce a marked reduction of the capillary lumens. Successively, the mesangial cells decrease in number and assume a fibroblast-like appearance [24]. The

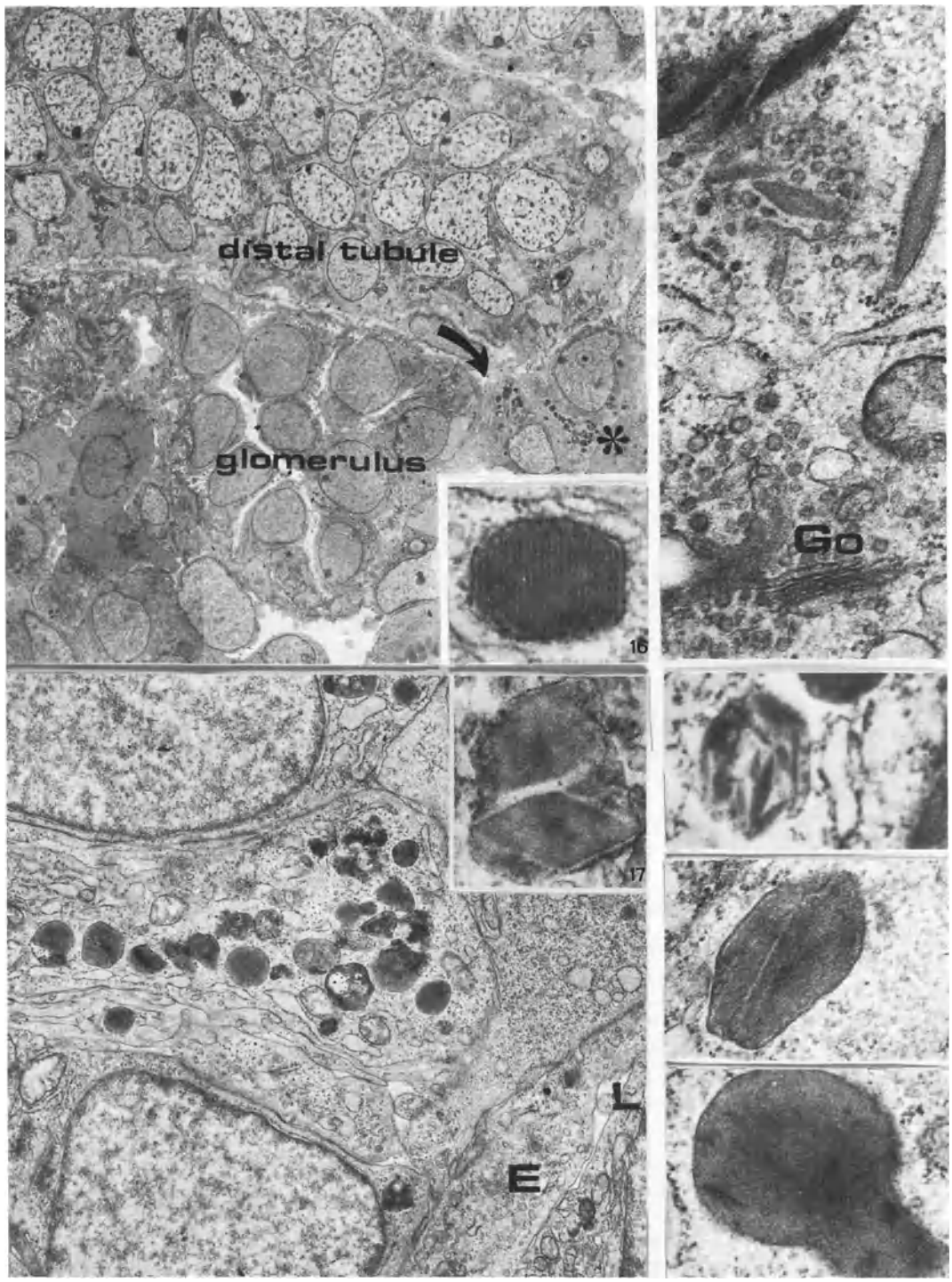

Fig. 13. A survey picture showing the relationship between a mesonephric glomerulus and its afferent arteriole (asterisk) and distal tubule. The arrow indicates the boundary between Bowman's capsule and arteriole. ×3,000.
Fig. 14. The area marked by the asterisk in fig. 13 is shown at higher magnification. Numerous pleomorphic cytoplasmic dense granules are visible in the media of the afferent glomerular arteriole. E: arteriolar endothelium, L: arteriolar lumen. ×18,000.
Figs. 15–20. The pictures illustrate different shapes of dense granules in arteriolar granulated cells. *Fig. 15.* Rod-shaped crystalline protogranules, some of which associated with small vesicles, are located near the Golgi apparatus (Go). *Fig. 16.* Polyhedral crystalline protogranule. *Fig. 17.* Rhomboid-shaped protogranules. *Fig. 18.* Conglomerate of protogranules. *Fig. 19.* Conglomerate of protogranules showing lines of fusion. *Fig. 20.* Amorphous mature granule. ×30,000.

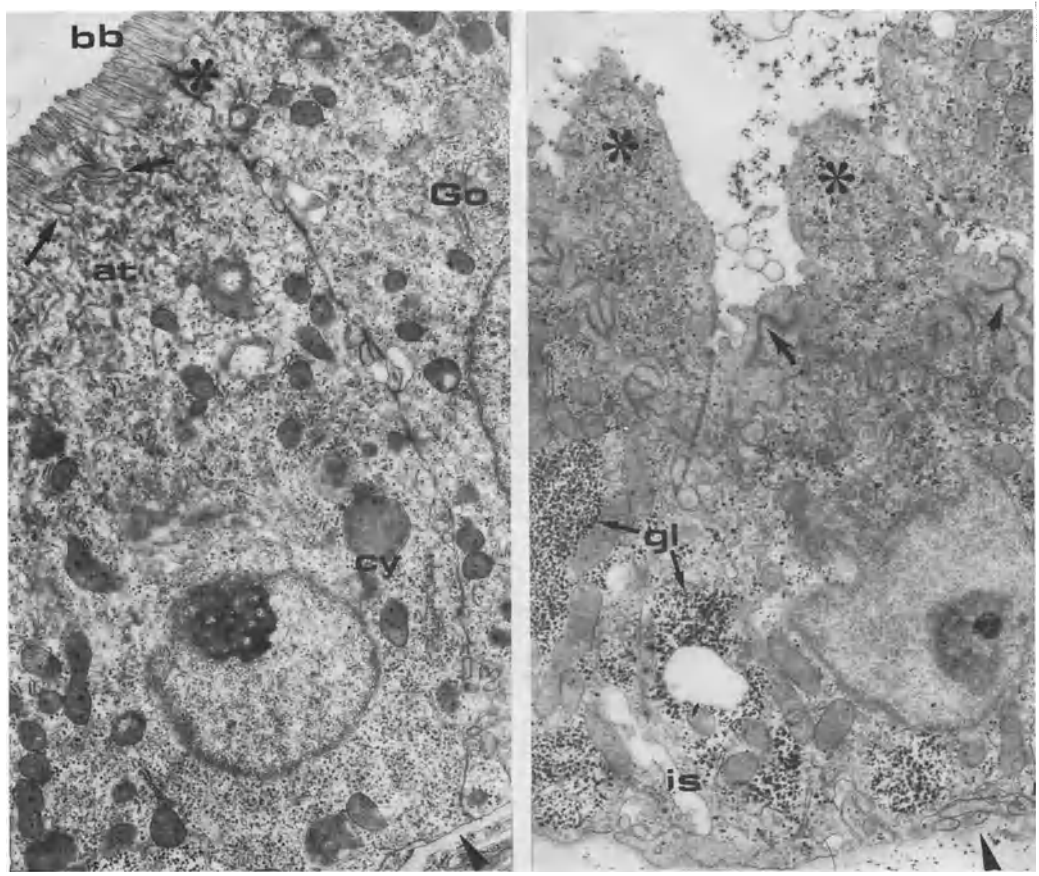

21 22

Fig. 21. Part of a proximal tubule of a mesonephric nephron. The cells show closely packed microvilli forming a brush border (bb), apical tubular invaginations (arrows), apical dense tubule (at), apical vacuoles, numerous cytosomes (cy) and no basal plasma-membrane invaginations and interdigitations. The arrow head points to the tubular basement membrane and the asterisk indicates a terminal bar. G: Golgi apparatus. ×12,000.

Fig. 22. Part of a distal tubule of a mesonephric nephron. The apical cytoplasms (asterisks), devoid of organelles, protrude into the tubular lumen above the level of the junctional complexes (arrows). Short microvilli are visible at the base of the cytoplasmic protrusions. Basal plasmamembrane invaginations and interdigitations (arrowhead) are occasionally visible. gl: glycogen, is: a narrow basal intercellular space. ×12,000.

subendothelial zone progressively swells and considerable amounts of amorphous material and collagen fibers appear in it. The basement membrane proper collapses producing several convolutions. The endothelium thickens and the podocytes lose the foot-processes and develop numerous microvilli toward the urinary space (Fig. 25). In the most advanced stages of regression, the glomeruli are transformed in avascular masses, containing degenerated endothelial and mesangial cells, surrounded by podocytes. The tubular changes are essentially characterized by cell degeneration and necrosis and by the presence of luminar casts [24]. It is worth mentioning that the changes observed during the physiological process of mesonephric regression occur also in the adult kidney as consequence of a wide variety of pathological insults [24].

4. Human metanephros

The metanephros originates from two different systems, namely the metanephric duct, or ureteric bud, and the metanephrogenic blastema which derives from the caudal portion of the intermediate mesoderm. Both systems are of mesodermal origin. The ureter, pelvis, calyces and collecting tubules develop from the first system whereas the distal tubules, Henle's loops, proximal tubules and glomeruli derive from the second one.

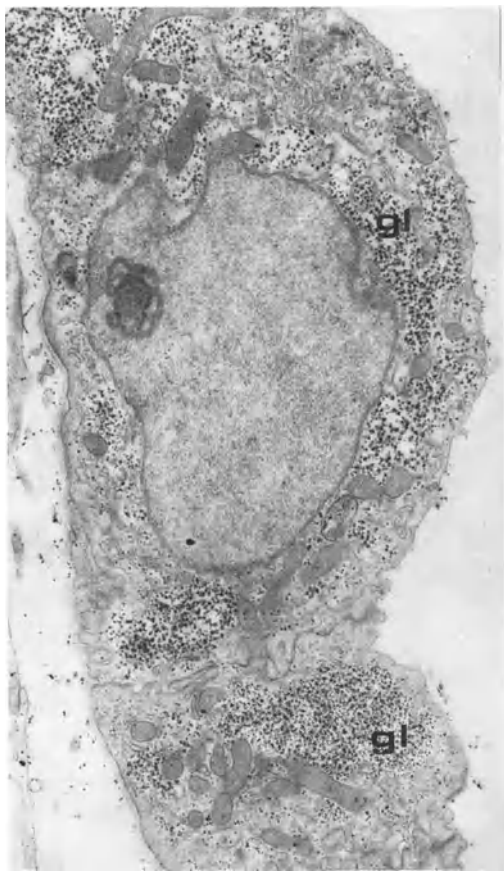

23

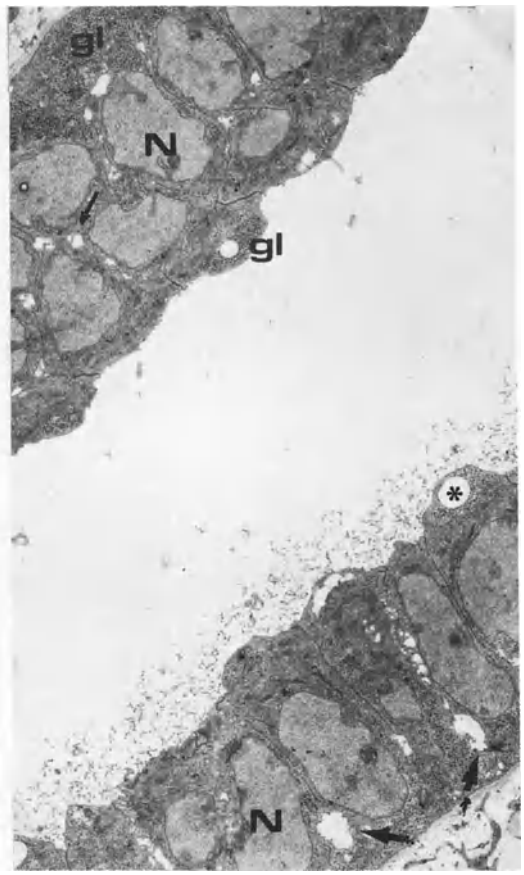

24

Fig. 23. Part of a mesonephric collecting tubule. gl: glycogen deposits ×12,000.
Fig. 24. A survey picture of Wolffian duct. The pseudostratified appearance of the epithelial cells is evident in the upper part of the picture. The majority of the nuclei show indentations. The arrows point to intercellular spaces. The asterisk marks an apical cytoplasm vacuole. gl: glycogen. ×2,500.

The metanephric duct is a paired structure which buds from the dorsal aspect of the caudal portion of the Wolffian duct at the level of 3th–4th lumbar segments (somite XXVI) in the 4th week of embryo development. The ureteric bud extends dorsocranially, pushes into the caudal condensed tissue of the nephrogenic blastema, swells at its extremity giving rise to the primitive pelvis from which the primary and, successively, the secondary calyces develop. From the tip of each secondary calix the collecting tubules generate by dichotomous branching. The terminal branches of the collecting tubules enlarge forming the ampullar extremities or ampullae. The cells of the metanephrogenic blastema condense around the ampullae and form the metanephric caps which successively differentiate into the various segments of the nephrons. The following description concerns the human metanephros from the 10th week (embryo period) (Fig. 26) to the 16th week (foetal period) (Fig. 27) of intrauterine life.

4.1. Stages of development

Although the differentiation of the metanephric nephrons is a continuously evolving process, for descriptive purposes it is divided into six main stages [25].

Stage 1 or stage of metanephric cap. The cells of the metanephric blastema condense in several concentring layers around the tip of the expanded ampullar extremity of each collecting tubule, forming the metanephric cap (Fig. 28). The surrounding stroma is pervaded by numerous capillaries containing red blood cells.

Stage 2 or stage of metanephric vesicle. A nest of cells separates from the metanephric cap on either side of

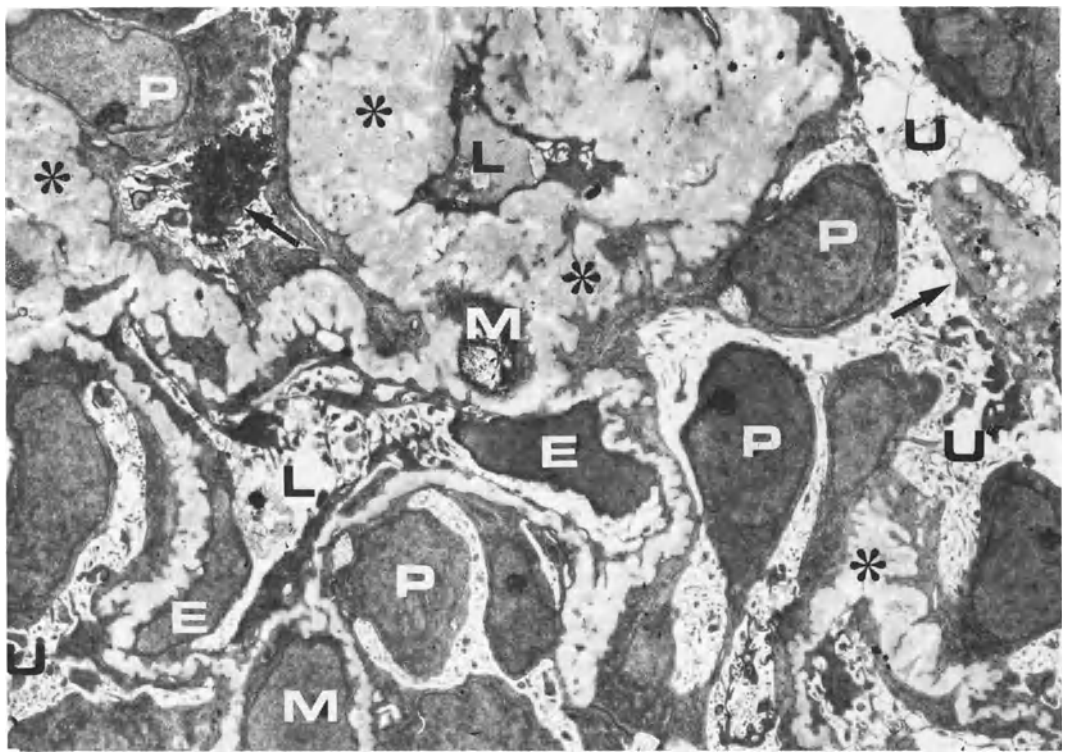

Fig. 25. Part of a mesonephric glomerulus in advanced regression. The podocytes (P) do not show foot-processes and develop numerous microvilli on the surface facing the urinary space (U). The endothelial cytoplasms (E) form numerous projections into the capillary lumens (L). Note the paucity of mesangial cells (M) and the shrinkage of the capillary lumens due to large amounts of amorphous material (asterisks) deposited into the subendothelial zone of the glomerular basement membrane. The arrows point to necrotic cells in the urinary space. ×4,500. (From: C. De Martino *et al.*, Exp. Mol. Pathol. 26: 169–183, 1977).

the ampulla and remains localized in the angle comprised between the expanding tip of the ampulla and the primitive collecting tubule (Fig. 29). Successively, each solid cellular nest develops a central lumen surrounded by a columnar pseudostratified epithelium. This structure is referred to as metanephric vesicle (Fig. 30), with an inner surface facing the collecting tubule and an outer surface opposite to it. Soon after the vesicle developed, communication is established between the lumen of the vesicle and that of the ampulla, which begins to flatten forming the future arched collecting tubule (Fig. 30). Simultaneously, the ampulla divides and a successive order of collecting tubules and related ampullae appears, which induce the formation of new metanephric vesicles. From the 4th month to the end of the 8th month of intrauterine life, the terminal ampullae of the collecting tubules lose the ability to divide by dichotomous branching but remain capable of developing new nephrons, which are first arranged in arcades and successively as separate nephrons [26].

Stage 3 or stage of S-shaped body. The metanephric vesicle becomes elongated and at the lower third of the outer surface an indentation appears (Fig. 30) which deepens forming a sickle-shaped cleft (Fig. 31). The portion of the vesicle below the cleft gradually becomes arranged into two cellular layers. The upper layer, which facies the cleft, is composed of cuboidal pseudostratified cells while the cells of the lower layer flatten. A thin space, which is the renmant of the original lumen of the vesicle, separates the two layers becoming the primitive urinary space. A second indentation simultaneously appears in the upper third of the inner surface of the vesicle (Fig. 31). The progressive deepening of both indentations and the elongation of the portion of the vesicle above the cleft on the outer surface, transform the vesicle into an S-shaped structure composed of three limbs, namely the upper, middle and lower limbs, from which the various segments of the nephron differentiate (Fig. 31). In fact, the distal tubule originates from the upper limb, the macula densa and the proximal tubule from the middle limb. The glomerulus

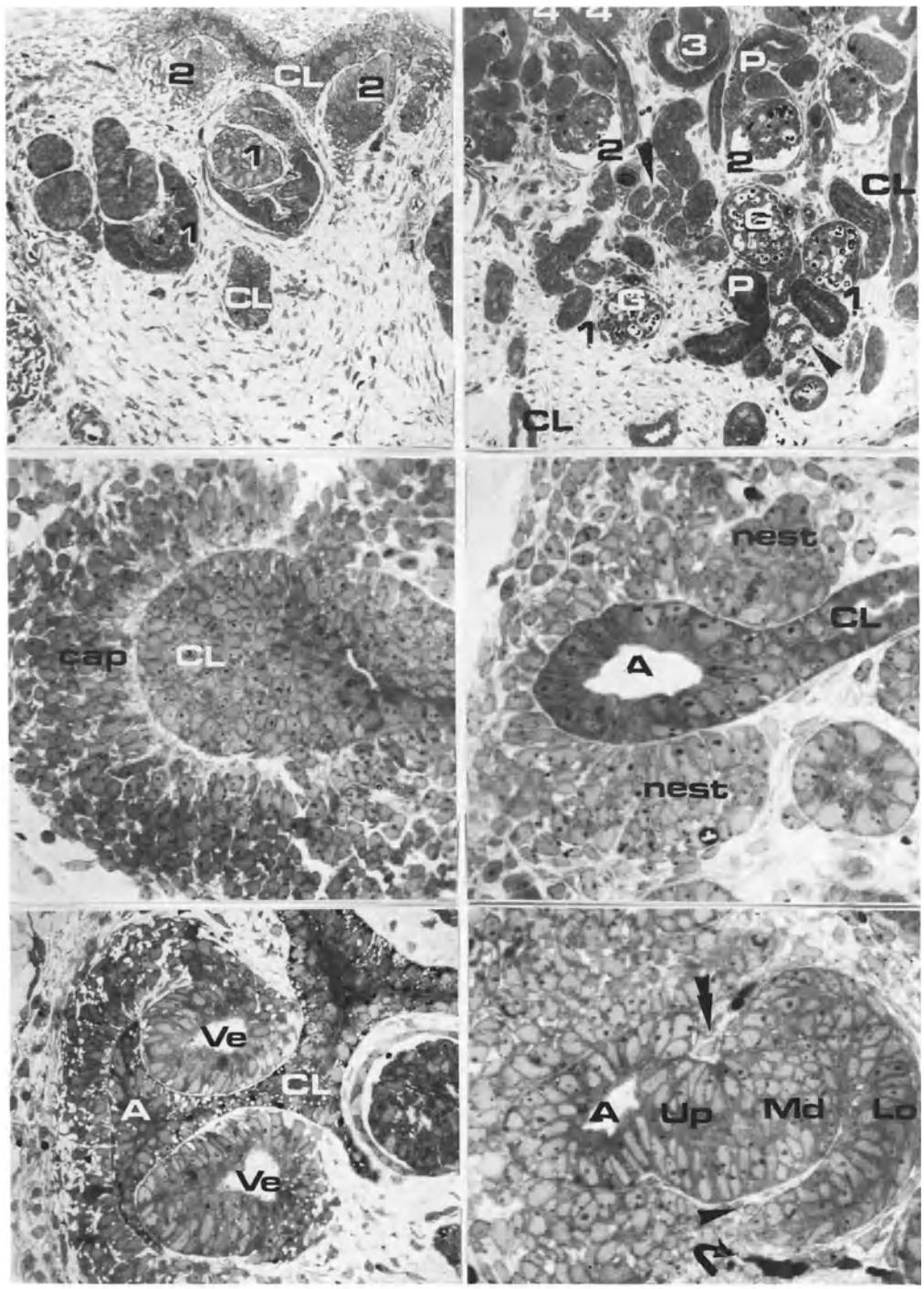

26 27 28 29 30 31

Figs. 26 & 27. Developing metanephros of a 10 week old (Fig. 26) and 16 week old (Fig. 27) human embryo. In Fig. 26, only two generations of metanephric nephrons at the stage of metanephric vesicle [2] and at the stage of double spiral [1] are visible, whereas Fig. 27 shows four generations, the deepest with the most mature glomeruli. CL: collecting tubules, G: glomeruli, P: proximal tubules. The arrows point to distal tubules. Fig. 26, ×120; Fig. 27, ×200.

Figs. 28–31. The pictures show the metanephric cap (Fig. 28, ×300), nest (Fig. 29, ×350), vesicles (Fig. 30, ×300) and S-shaped body with the upper (Up), middle (Md) and lower (Lo) limbs (Fig. 31, ×350). Two indendations are visible at the outer (arrowhead) and inner (double arrowhead) surface of the S-shaped body. A: ampullae, CL: collecting tubules, Ve: vesicles. The curved arrow in Fig. 31 points to a capillary near the mouth of the outer indentation. (Figs. 28, 29, 31, from: L. Zamboni and C. De Martino, Arch. Pathol. 86: 279–291, 1968).

develops from the lower limb which forms the capsular epithelium with its lower layer and the visceral epithelium or podocytes with its upper layer. A capillary is constantly present at the mouth of the glomerular cleft (Fig. 31).

Stage 4 or stage of intracleftal position of the glomerular vessel. The cells of the tip of the lower limb, increasing considerably in number by continuous mitoses, induce further elongation of the cleft by outward growth in the surrounding mesenchyme. Similarly, a further deepening of the inner indentation and a continuous cell multiplication induce the middle and upper limbs to differentiate into the first convolution of the proximal and distal tubules and the S-shape of the metanephric body becomes so

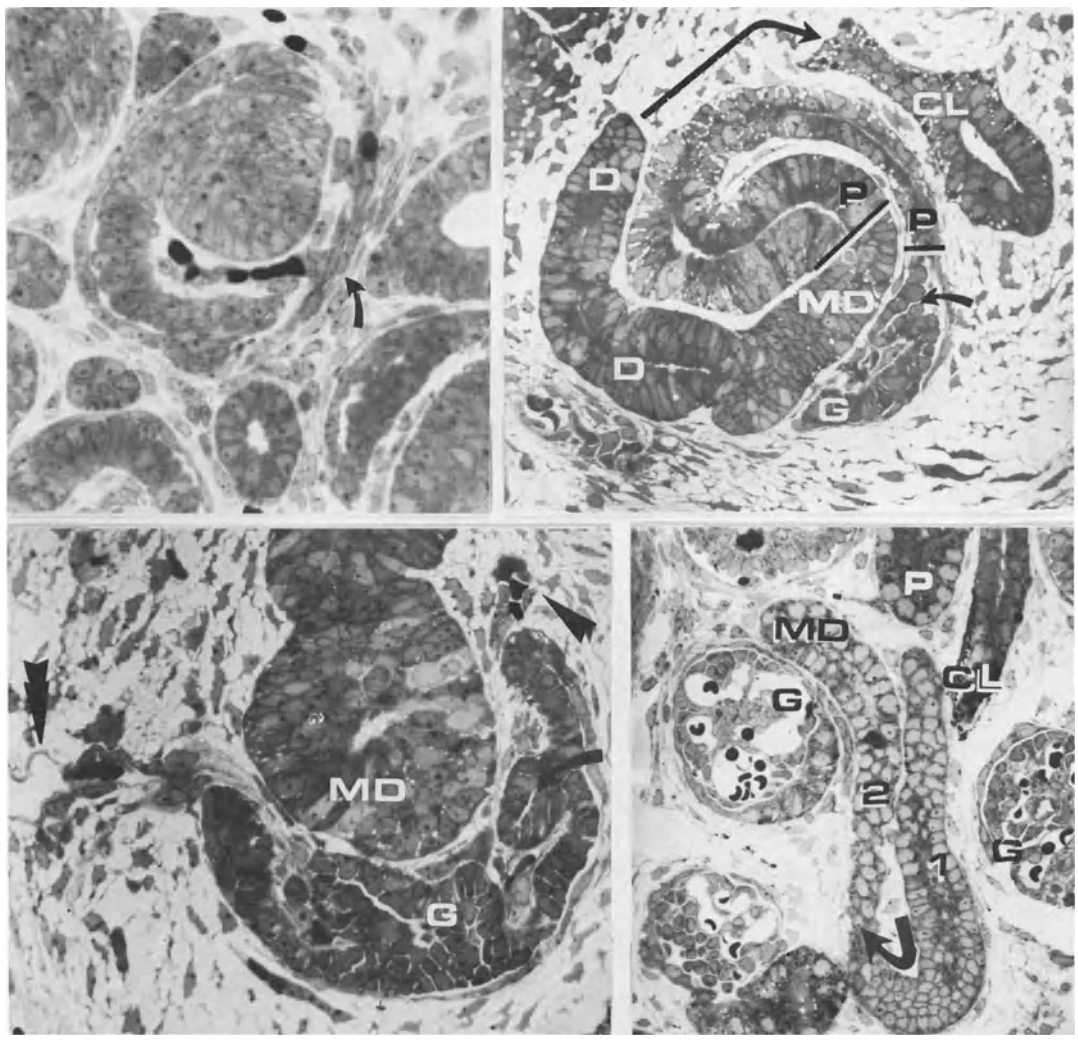

32 33

34 35

Fig. 32. A S-shaped body in more advanced stage of development. The continuity of the interstitial vessel with the intracleftal capillary is evident (arrow). ×300. (From: L. Zamboni and C. De Martino, Arch. Pathol. 86: 279–291, 1968).

Figs. 33 & 34. 'Double spirals' sectioned in two different planes, roughly perpendicular eachother. In the sectioning plane of Fig. 33, all segments of a developing nephron are clearly recognizable, whereas Fig. 34 shows the afferent (arrowhead) and efferent (double arrowhead) vascular poles located on opposite sides. In both pictures, the visceral epithelium begins the glomerular constriction (curved arrow) at the boundary with the proximal tubular cells (P). CL: collecting tubule, D: distal tubule, G: glomerulus, MD: macula densa. Fig. 33, ×300; Fig. 34, ×500.

Fig. 35. Juxtamedullary nephrons of a 16 week old human fetus. At this age, the descending (1) and ascending (2) limbs of Henle's loop are already differentiated. The curved arrow follows the hairpin turn of the loop. CL: collecting tubule, G: glomeruli, MD: macula densa, P: proximal tubule. ×300.

more evident and distorted. The macula densa remains in relation with the cleft assuming close anatomical association with the vascular components of the developing glomerulus (Fig. 32). The origin of the glomerular capillaries is controversial. In fact, some investigators claim that the glomerular capillaries derive from ingrowth of blood vessels present in the surrounding mesenchyme into the cleft of the immature glomerulus [17, 27–29], while others hold that they develop in situ by an anlage of cells which originate from intracleftal bordering cells and that the communication with the extraglomerular vessels is established after these cells are differentiated in endothelial and mesangial cells [30, 31]. Another theory postulates that the glomerular capillaries are formed by mesenchymal cells growing from the adjacent stroma into the cleft of the immature glomerulus [32]. Our personal observations strongly support the first hypothesis [17]. In fact, the capillary, previously localized outside the vesicle, for outward growth of the lower limb becomes embedded within the cleft between the upper layer of the lower limb and the lower surface of the middle limb, running perpendicularly to the long axis of the vesicle (Fig. 32).

Stage 5 or stage of the double spiral. The architecture of the S-shaped body changes into a double spiral in which the glomerulus, proximal and distal tubules can be easily recognized (Fig. 33). This stage is also characterized by growth and development of the glomerular capillary loops (Fig. 34) and increase of convolutions of the proximal and distal tubules (Fig. 33). For repeated splittings, multiple glomerular capillaries derive from the original vessel. The growth of these capillaries within the limited space of the cleft induces tortuosity of the glomerular loops and distortion of the originally regular layer of visceral epithelium (Figs. 33, 34). The afferent and efferent vessels are devoid of the tunica media and appear localized in opposite sites (Fig. 34). The visceral cells at the junction with the proximal tubule begin to proliferate toward the cleft, becoming part of the Bowman's capsule (Figs. 33, 34). This process induces, in the following stages, a gradually increasing separation of the vascular pole from the tubular or urinary pole and together with the proliferation of the tip of the primitive portion of the Bowman's capsule bends and pushes the afferent and efferent vascular poles close to each other, forming a single vascular pole. The phenomenon of glomerular constriction over the vascular pole induces also the rejection of the macula densa out from the glomerular cleft and its anatomical association with both afferent and efferent arterioles, which assume the definitive position gradually developing the vascular portion of the juxtaglomerular apparatus.

Stage 6. This stage collects many continuous evolving processes of metanephric nephron differentiation which end with the development of the Henle's loop (Fig. 35). However, the latter, at the 4th month of intrauterine life, is made up only of the thick descending (or pars recta of the proximal tubule) and thick ascending (or pars recta of the distal tubule) segments, and is present only in the juxtamedullary nephrons (Fig. 35). At this stage, the nephrons show fully differentiated glomeruli with a single vascular pole associated with the macula densa, and more convoluted proximal and distal tubules (Fig. 27). Straight collecting tubules are visible in the papilla, embedded in a loose mesenchyme (Fig. 27).

4.2. Metanephric cap and vesicle

The cells of the cap and nest (stages 1 and 2) are largely irregular and show an ovoidal nucleus, numerous free ribosomes and polysomes and poorly differentiated smooth and rough endoplasmic reticulum and Golgi apparatus. Intercellular spaces, moderately dilated, are sometimes visible. The wall of the collecting tubule and ampulla is formed by high columnar cells which are connected by terminal bars and show elongated nuclei and rare apical microvilli. These cells are separated from the nest by a thin basement membrane (Fig. 36).

As a central lumen appears in the nest, the process of fusion between the newly formed metanephric vesicle and its related collecting tubule initiates [17]. A thin basement membrane, continuous with that of the collecting tubule, evenlops the metanephric vesicle. The cells of the vesicle, many of which in mitosis, possess apical junctional complexes and considerable amounts of ergastoplasm. Large deposits of glycogen appear in the cytoplasm of the cells of the ampulla and collecting tubule (Fig. 37).

4.3. Glomerulus

The main morphological changes in the differentiation of the glomerulus occur during the stages of the S-shaped body and double spiral and are related to the development and growth of glomerular capillaries. At the beginning, a thin capillary, which derives from an interstitial vessel adjacent to the metanephric vesicle (Fig. 31), invaginates into the sickle-shaped cleft (Figs. 32, 38). At the mouth of the cleft, this primitive vessel shows an afferent and efferent

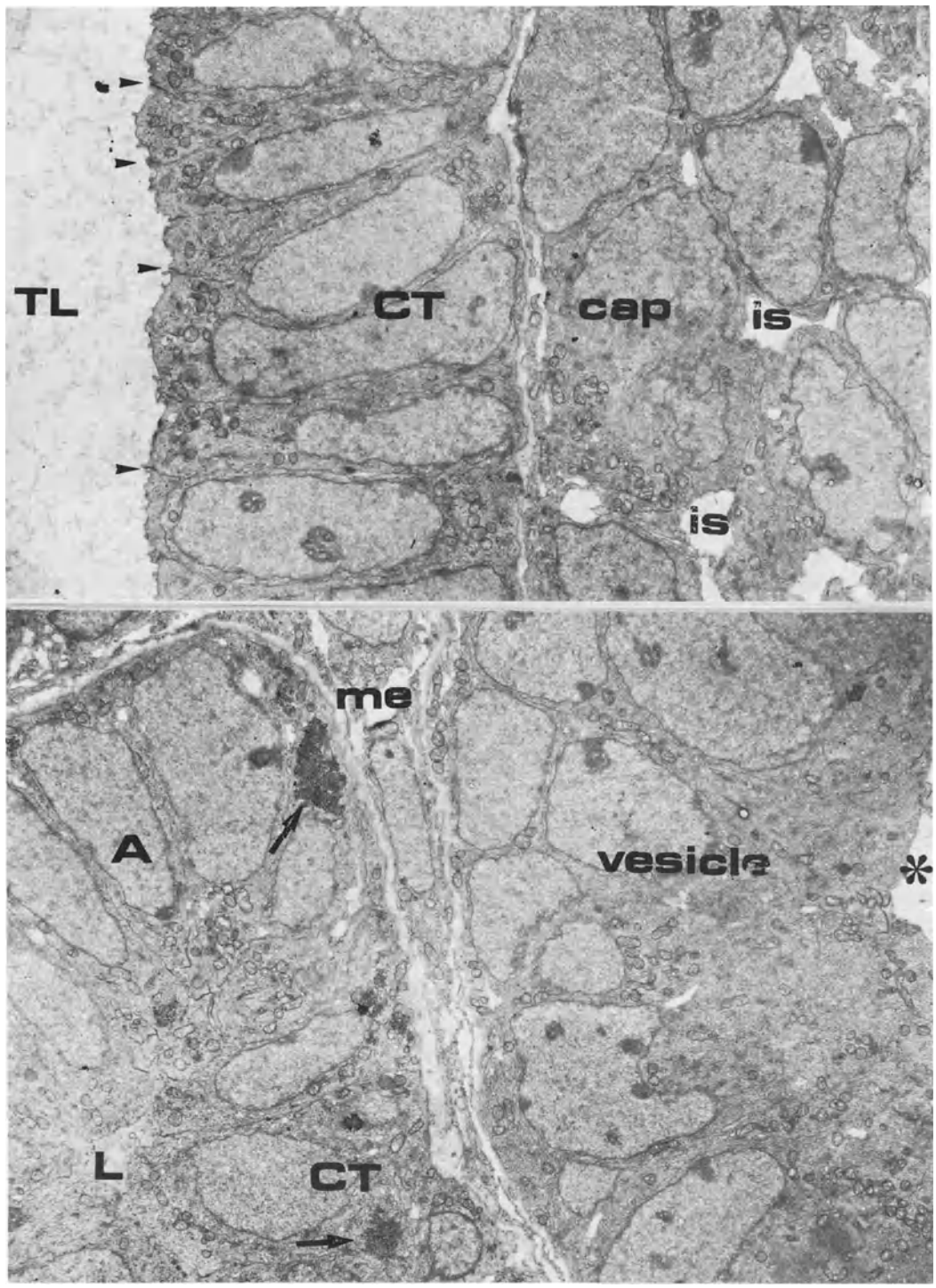

36

37

Fig. 36. The cells of the metanephric cap are closely associated with the high columnar cells of collecting tubule (CT). Intercellular spaces (is) are visible in the cap. The arrowheads point to junctional complexes of collecting tubule. TL: tubular lumen. ×5,000.
Fig. 37. Parts of metanephric vesicle and ampulla (A). CT: collecting tubule, L: lumen of the ampulla, me: mesenchymal cells. The asterisk indicates the lumen of the vesicle. The arrowheads point to glycogen deposits in the collecting tubule. ×5,000.

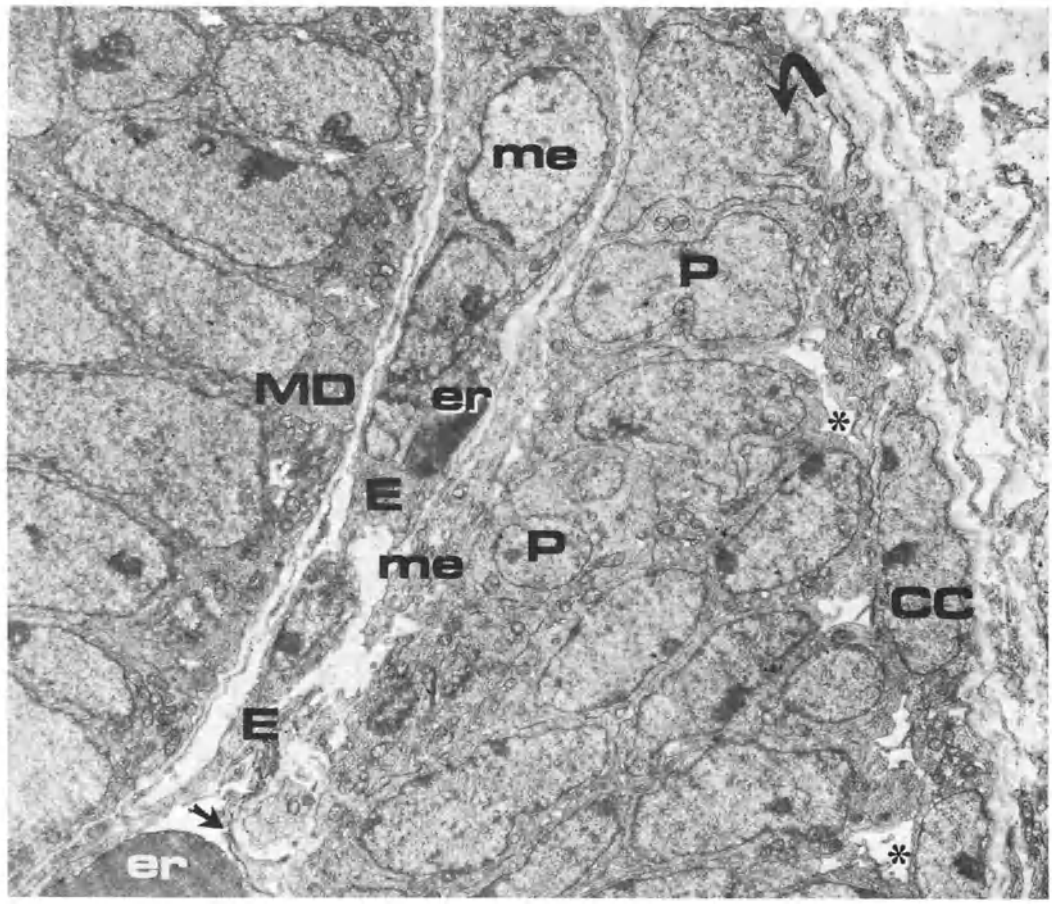

Fig. 38. Part of a S-shaped body. A glomerular capillary is visible within the cleft. Note the multilayered primitive prodocytes (P) separated from the capsular cells (CC) by a narrow urinary space (asterisk). Two mesenchymal cells (me) are close to the endothelium (E) of the intracleftal glomerular capillary. er: erythrocytes, MD: immature macula densa. The boundary between podocytes and capsular cells is marked by curved arrow. Straight arrow points to an endothelial cell junction. ×5,000.

pole (Fig. 39). Its wall is formed only by endothelial cells which on the side of invagination produce numerous villosities toward the narrow vascular lumen. At the afferent pole, the endothelial cells are accompanied by several mesenchymal cells which will become the primitive smooth muscle cells of the afferent glomerular arteriole outside the cleft and the primitive glomerular mesangial cells inside the cleft (Fig. 39). Successively, these cells increase in number in the area comprised between the primitive macula densa and the growing intracleftal capillary which pushes against and invaginates into the visceral epithelium, inducing distortion of the regular pseudostratified layer of the primitive podocytes (Figs. 33, 34, 40). The glomerular capillaries arise from the intracleftal vessel by multiple splitting. A basement membrane network, interdigitating with elongated basal cytoplasmic projections of the podocytes, precedes the invagination of the newly formed glomerular capillaries (Fig. 41).

As the primitive capillary starts invaginating into the cleft, the capsular, visceral, mesangial and endothelial cells undergo the process of cell differentiation, gradually assuming the definitive morphological features of the adult kidney. The capsular cells as well as the podocytes derive from the lower limb of the S-shaped body (Fig. 31) and are separated from eachother by a narrow urinary space (Fig. 38) which progressively enlarges (Figs. 32, 33). The capsular cells are flattened (Fig. 38) except those near the urinary pole which gradually assume the features of proximal tubular cells.

The differentiation of the podocytes is characterized by marked morphological changes [33]. At the beginning, they appear irregularly arranged as a pseudostratified epithelium with the apical portion

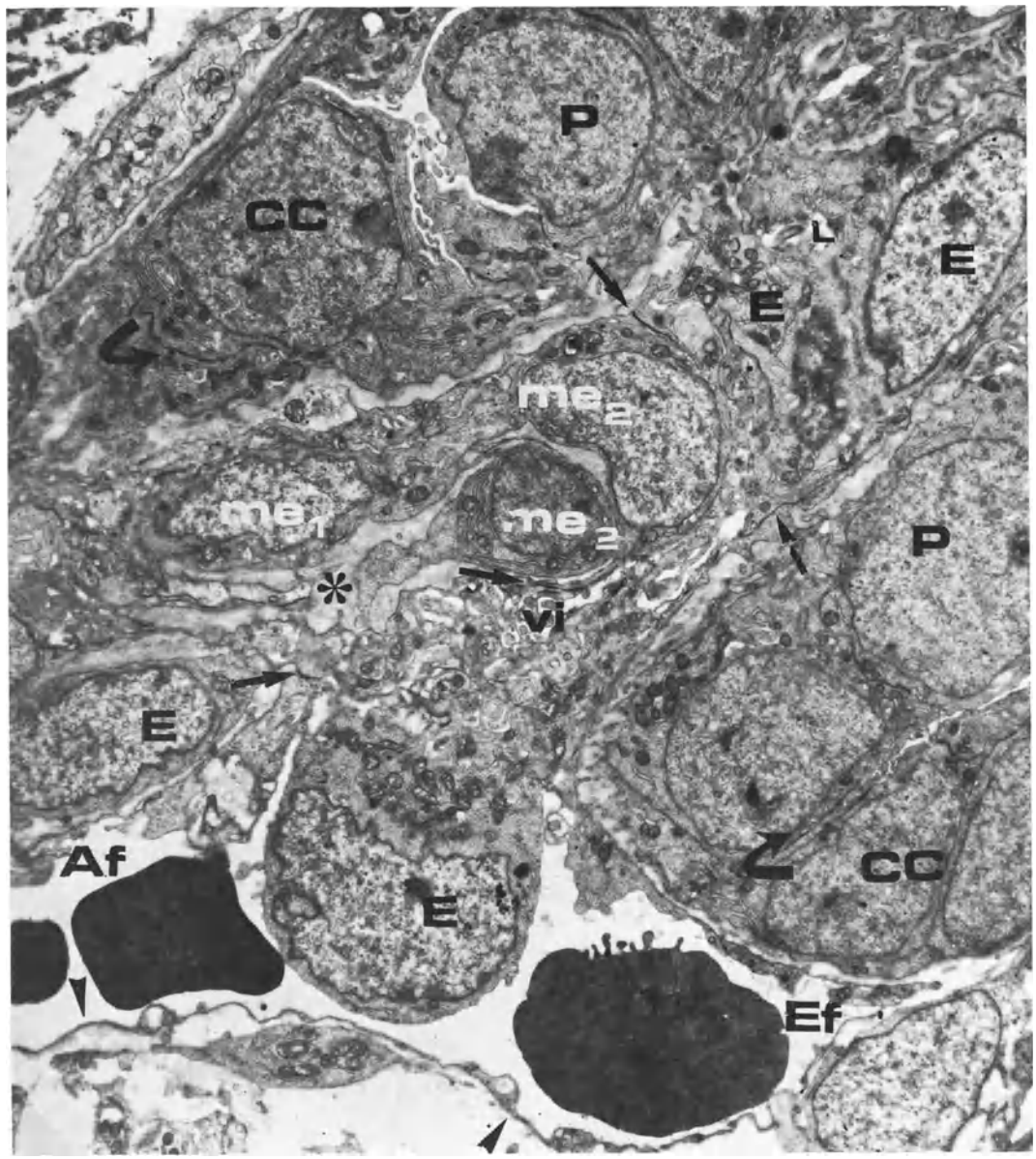

Fig. 39. S-shaped body seen in a plane of sectioning different from that shown in Fig. 38. At the mouth of the cleft, the interstitial vessel shows an afferent (Af) and efferent (Ef) vascular pole. A mesenchymal cell (me_1) which represents a primitive smooth muscle cell of the afferent glomerular arteriole, is visible in the afferent pole on the side facing the glomerulus. Other mesenchymal cells (me_2), or primitive mesangial cells, are present along the invaginating vessel. A thin endothelial lamina forms the wall of the interstitial vessel (arrowheads). The endothelial cells (E) of the portion of the vessel invaginating into the glomerular cleft produce numerous villosities (vi) toward the vascular lumen (L). Straight arrows point to endothelial junctional complexes, curved arrows mark the boundary between capsular cells (CC) and podocytes (P), and the asterisk indicates the extracellular matrix between mesenchymal cells. ×10,000.

facing the narrow urinary space and with the basal part, which rests on a thin basement membrane, facing the sickle-shaped cleft (Fig. 38). As the ingrowth of the glomerular capillaries begins, the podocytes become columnar monostratified. Long intercellular junctional complexes connect them from the apical to the basal portion (Fig. 41). Septate desmosomes (Fig. 42) and intercalated intercellular spaces (Fig. 41) are visible along the junctional complexes. The intercellular spaces localized at the basal region of the cells are dilated, contain a flocculous material and often communicate with the network of

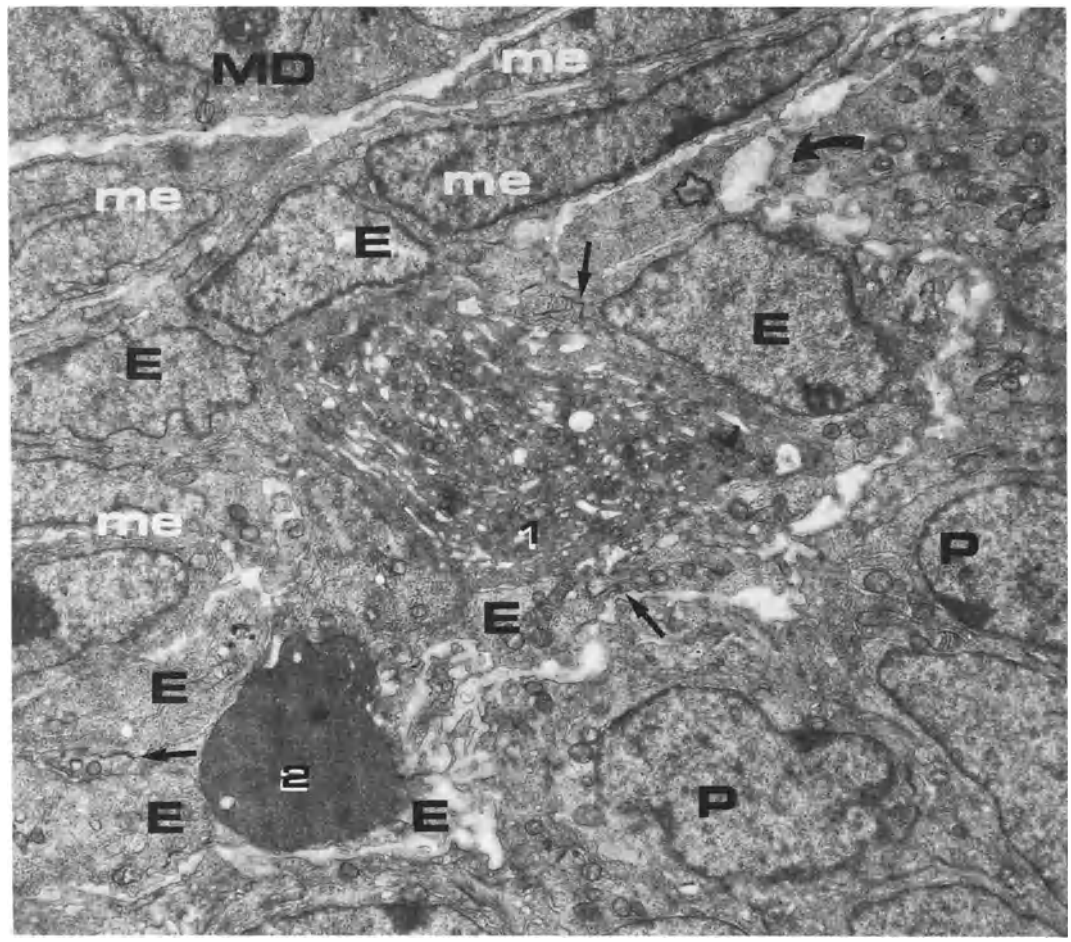

Fig. 40. S-shaped body in advanced stage of development. The invaginating intracleftal capillary, containing a megakaryocyte (1) and a red blood cell (2), begins to protrude into the visceral cell layer (P), from which it is separated by a thin basement membrane. E: endothelial cells, MD: macula densa, me: mesenchymal cells. Straight arrows point to endothelial junctional complexes. ×7,000.

the newly formed basement membrane through narrow gaps (Fig. 41), suggesting a possible role of the podocytes in the synthesis of the glomerular basement membrane [33]. With the further development of the glomerular capillary loops, a variety of morphological changes occur in the podocytes. The junctional complexes lose the terminal bars and the apical septate desmosomes disappear so that the intercellular spaces, which were delimited by them, freely communicate with the urinary space (Fig. 43). The basal septate desmosomes lose all lamellae except the lowest one which probably becomes the slit-membrane between contiguous foot-processes [33]. Slowly, the cells flatten upon the glomerular capillaries, developing long cytoplasmic sheets in which bundles of thin filaments parallel to the glomerular basement membrane are present (Fig. 43). From these primary cytoplasmic processes further processes originate which will form the system of interdigitating foot-processes between contiguous podocytes (Figs. 44–46).

The endothelial cells of the primitive, glomerular capillaries are characterized by unfenestrated cytoplasmic laminae, containing numerous micropinocytotic vesicles. Occasional fenestrae appear only at later stages (Fig. 45). The main cell bodies bulge into the capillary lumens (Fig. 43). The growth and multiplication of the glomerular capillaries are linked to two main processes, namely the proliferation of the endothelial cells by mitotic activity and the multiple splitting of the capillary lumen. The latter is brought about by thin endothelial cytoplasmic projections which reach and join the endothelial cells of the opposite capillary wall (Fig. 44). Afterwards, the mesangial cells move into and fill the space which these cytoplasmic projections delimitate (Figs. 44,

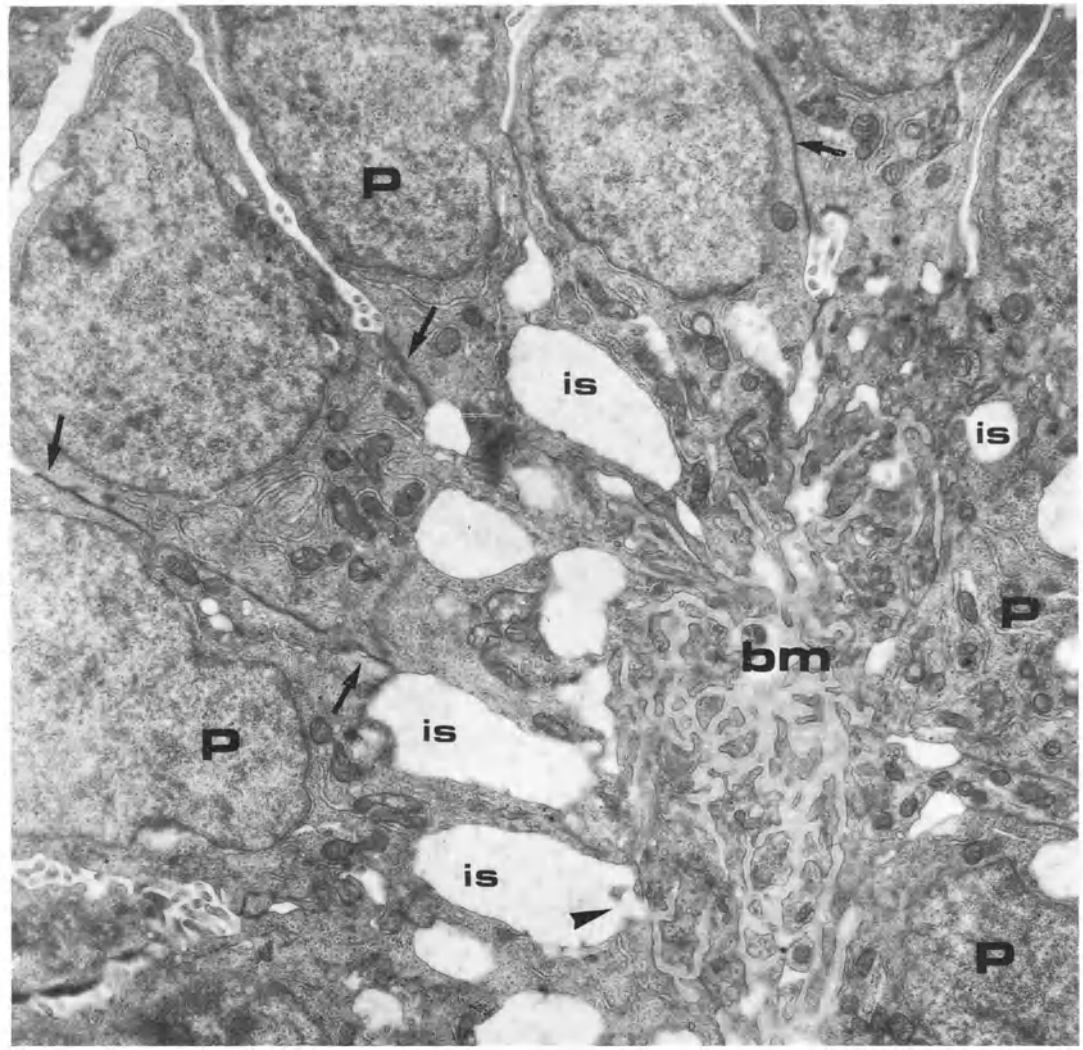

Fig. 41. Part of the glomerulus of a double spiral body. A basement membrane network (bm) interdigitating with basal cytoplasmic projections of podocytes (P) is visible. The podocytes are columnar and show long junctional complexes (arrows) intercalated by large intercellular spaces (is), some of which contain a flocculous material and communicate with the basement membrane network (harrowhead). ×12.000.

45). A thin basement membrane with its three layers, namely the subepithelial zone or lamina rara externa, lamina densa, and subendothelial zone or lamina rara interna, separates the endothelial cells from the podocytes (Figs. 45, 46).

The mesangial cells, which derive from the mesenchymal cells accompanying the primitive glomerular capillary (Figs. 38, 39), are initially poorly differentiated (Fig. 43), reaching complete maturation at the 6th stage. At this stage, they are highly irregular with numerous cytoplasmic projections and abundant ergastoplasm (Fig. 46), and large bundles of actin filaments [34] are visible in their cortical cytoplasms. The mesangial matrix is the latest glomerular component to develop, being initially scarce and loosely arranged (Figs. 45, 46).

4.4. Juxtaglomerular apparatus

At the 16th week of intrauterine life, the juxtaglomerular apparatus of the metanephric nephrons is composed of the macula densa, the afferent and efferent glomerular arterioles, forming a single vascular pole, and a few lacis cells (Fig. 47). The macula densa is characterized by crowded cells which develop basal cytoplasmic projections toward the

42

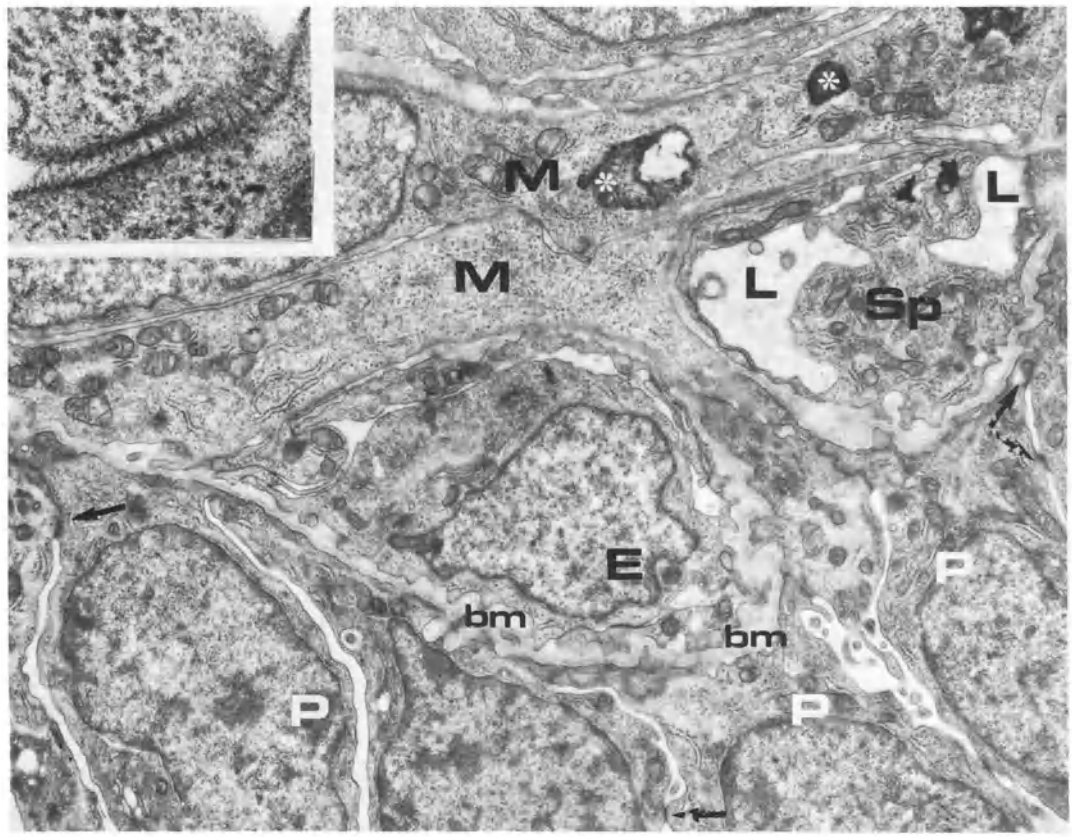

43

Fig. 42. A septate desmosome between podocytes. ×50,000.
Fig. 43. Part of an immature metanephric glomerulus. The podocytes (P) are very close eachother and their junctional complexes are mainly localized in the basal and middle portions (arrows). They rest on the glomerular basement membrane and do not show foot-processes. The hypertrophic unfenestrated endothelial cells (E) bulge into the capillary lumens (L). Numerous cytosomes (asterisks) are visible in the mesangial cell (M). Sp: endothelial splitting. ×12,000. (From: C. De Martino *et al.*, Z. Zellforsch. 140: 101–124, 1973).

glomerular arterioles, preferentially the efferent, from which they are separated by scarce lacis cells (Figs. 47, 48). The cells of the macula densa (Fig. 48) are ultrastructurally similar to the cells of the other segments of the distal tubule since the specialized morphological features, which characterize the macula densa of the adult kidney [21], are not yet differentiated. The afferent arteriole possesses a tunica media formed by smooth muscle and granulated cells. The latter contain abundant ergastoplasm and dense granules similar to the aspecific and specific granules of the juxtaglomerular cells of the adult kidney [18] (Figs. 49–51).

4.5. Proximal tubule

The proximal tubule develops from the inner surface of the middle limb of the S-shaped body (Fig. 31). In early stages of differentiation, the monostratified columnar cells show scarce, short apical microvilli, lipid bodies in the basal portions and glycogen particles scattered throughout the cytoplasms (Fig. 52A). Next, the microvilli increase in number and length and several tubular invaginations, dense tubules and coated vesicles develop in the apical cytoplasms (Figs. 52B, 53). Successively, large clusters of glycogen particles appear in the basal cytoplasms and apical tubular invaginations, dense tubules and vesicles increase in number while the other components of the endocytic apparatus, namely apical vacuoles and cytosomes, appear (Fig. 52C). Ultimately, the brush border and the endocytic apparatus reach full differentiation, numerous cytosegresomes, containing lamellar and myelin-like structures, develop in the basal cytoplasms whereas the glycogen decreases considerably (Figs. 52D, 53, 55). The presence of the apical endocytic apparatus suggests that the proximal tubule is precociously involved in the

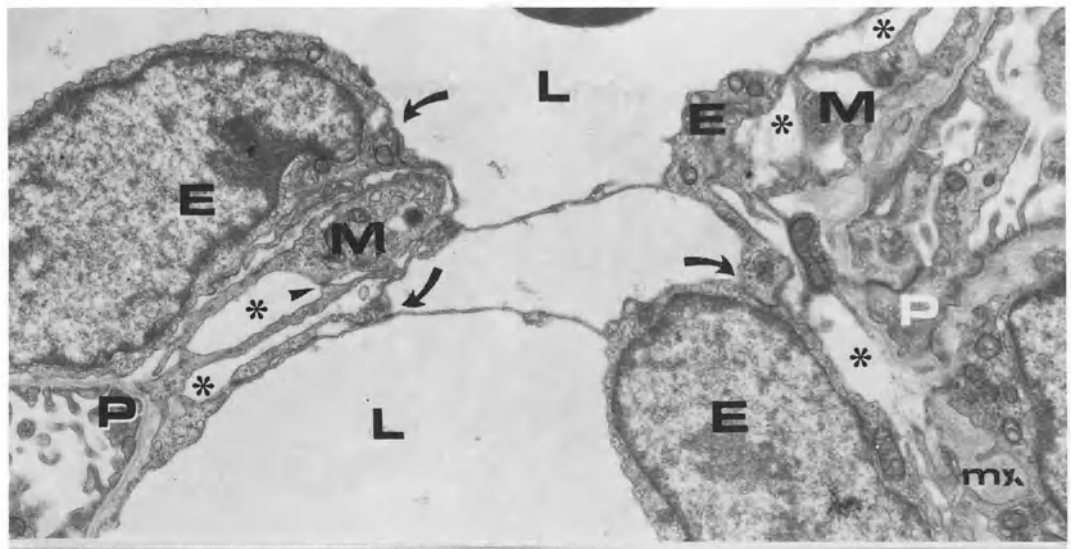

44

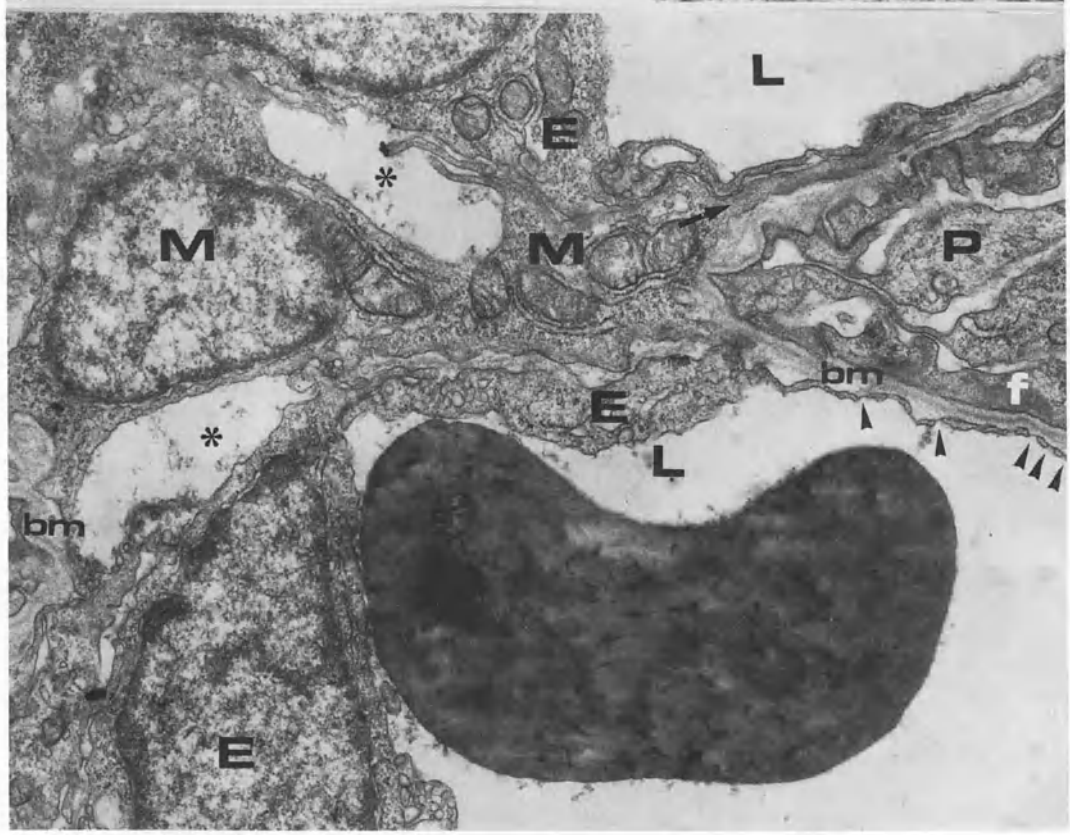

45

Fig. 44. Part of a mature metanephric glomerulus. Two long, thin endothelial (E) cytoplasmic processes bridge the capillary walls, splitting the lumen (L). Mesangial cytoplasmic projections (M) are very close to the space delimitated by the endothelial processes. The mesangial matrix is still lacking (asterisks), being present only in few areas (mx). Arrowhead points to a mesangial gap junction, curved arrows indicate endothelial cell junctions. P: podocytes. ×20,000.

Fig. 45. A complete scission of a glomerular capillary in visible. The mesangial cells (M) also bridge the capillary walls. The mesangial matrix is still lacking (asterisks). The arrow points to a mesangial cytoplasmic projection. bm: glomerular basement membrane, E: endothelium, f: cytoplasmic thin filaments of podocytes (P), L: capillary lumens, arrowheads: endothelial fenestrae. ×20,000.

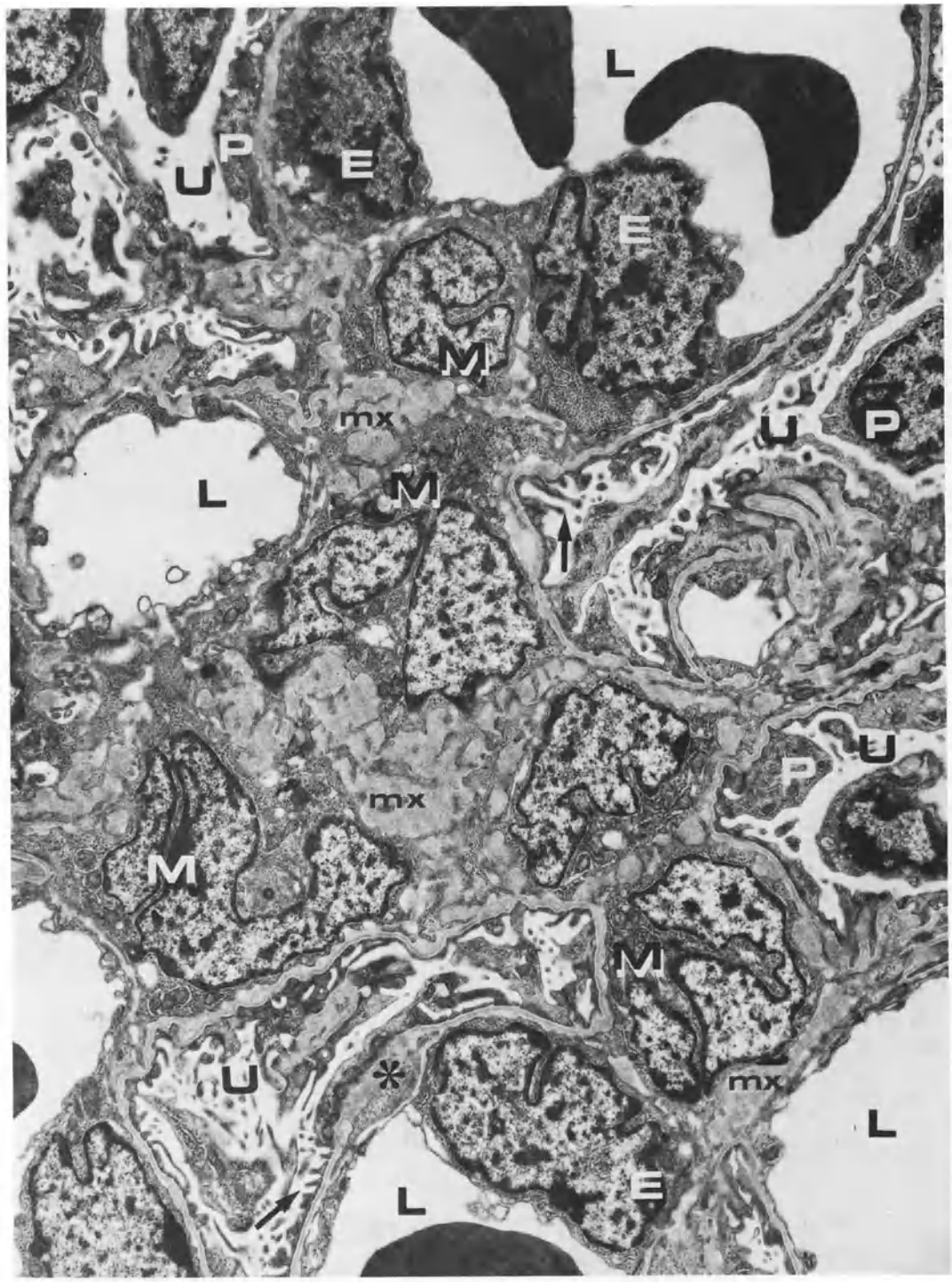

Fig. 46. Part of a fully developed glomerulus. E: endothelium, M: mesangial cells, mx: mesangial matrix, L: capillary lumens, U: urinary space, asterisk: glomerular basement membrane, arrows point to foot-processes. ×6,000.

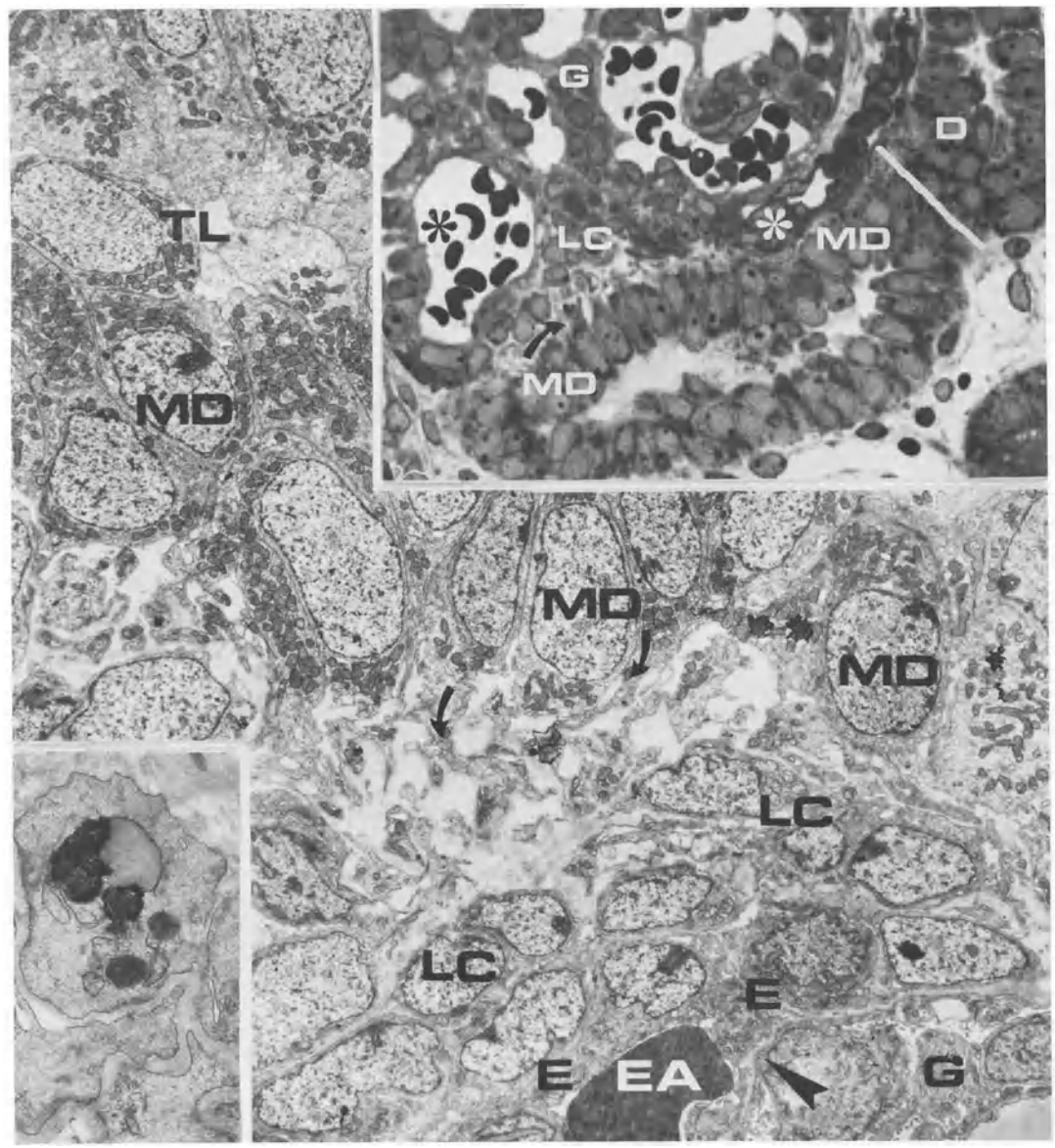

47

48

49

Fig. 47. Juxtaglomerular apparatus of a 16 week old embryo. Note the poorly developed tunica media of the afferent (white asterisk) and efferent (black asterisk) arterioles and the paucity of lacis cells (LC). DT: distal tubule, G: glomerulus, MD: macula densa. Curved arrow points to cytoplasmic projections of the cells of macula densa. ×1,000.
Fig. 48. The morphological relationship between macula densa (MD), lacis cells (LC) and efferent glomerular arteriole (EA) is shown at higher magnification. The cells of macula densa are closely packed, resembling a pseudostratified epithelium. Curved arrows indicate basal cytoplasmic projections of cells of macula densa toward the lacis cells (LC). Arrowhead points to the boundary of the glomerular vascular hilus. G: glomerulus, TL: tubular lumen. ×6,000.
Fig. 49. Aspecific lipofuscin granules in the media of a glomerular arteriole. ×25,000.

reabsorption of proteins contained in the glomerular filtrate. Furthermore, the steps observed during the differentiation of this apparatus indicate that the development of the proximal tubular cells is related to glomerular filtration [24]. In the juxtamedullary nephrons, the pars convoluta and the pars recta (or descending segment of Henle's loop) of the proximal tubules are clearly recognizable (Fig. 35).

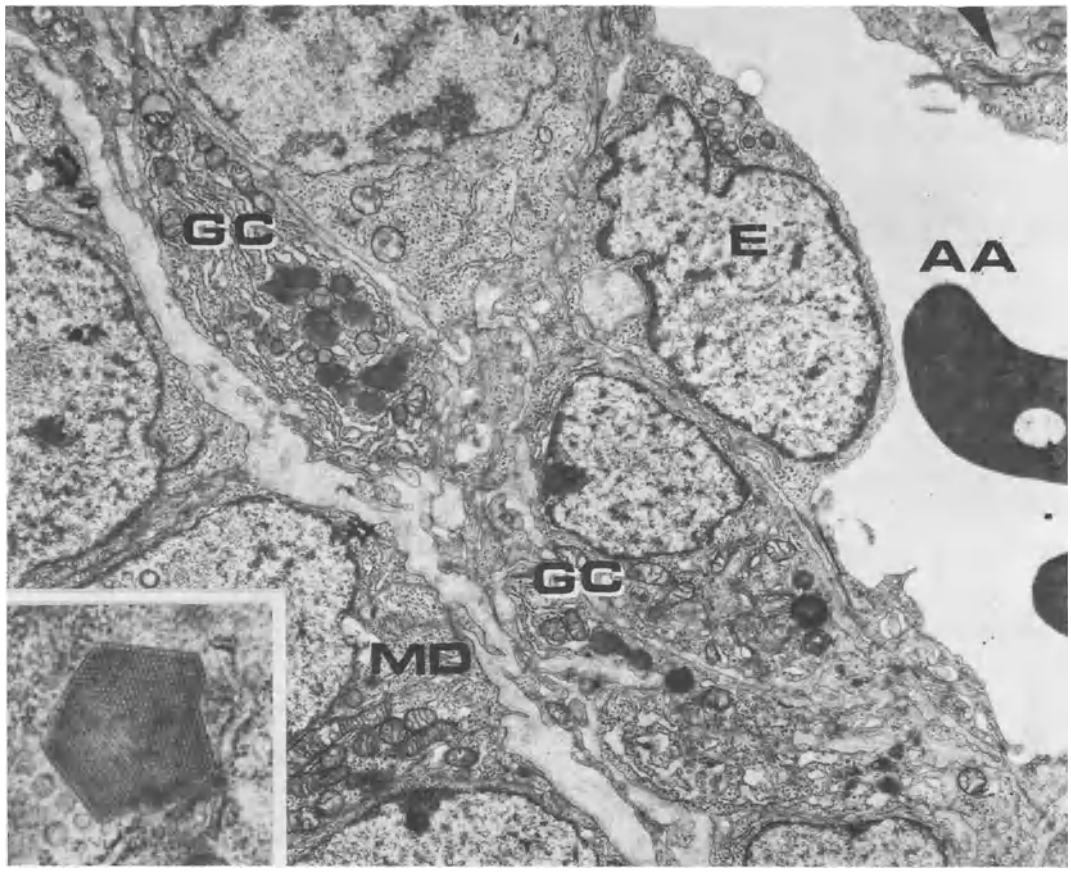

51 50

Figs. 50 & 51. Granulated cells (GC), containing pleomorphic renin-specific granules and large amount of ergastoplasm, are visible in the tunica media of an afferent glomerular arteriole (AA). Some protogranules are rhomboidal with a crystalline pattern (Fig. 51). Arrowhead points to the boundary of the glomerular hilus. E: endothelium, MD: macula densa. Fig. 50, ×6,000; Fig. 51, ×29,000. (Fig. 50, from: C. De Martino *et al.*, Z. Zellforsch. 140: 101–124, 1973).

4.6. Distal tubule

The distal tubule originates from the middle and upper limbs of the S-shaped body (Fig. 31) and differentiates soon after the 4th stage of development, reaching, however, the definitive morphological features much later. In the juxtamedullary nephrons, three portions can be distinguished, namely the ascending limb of Henle's loop (Fig. 35), the macula densa (Fig. 47) and the pars convoluta (Fig. 47). However, no significant morphological features differentiate these segments. In fact, all cells are columnar but less tall than the proximal tubular cells. Furthermore, scarce, short apical microvilli are present for the whole lenght of the tubule. No lateral and basal interdigitations of the plasma membranes are visible. The mitochondria and Golgi apparatus are preferentially localized in the supranuclear cytoplasmic regions (Fig. 56).

4.7. Collecting tubule

The primitive collecting tubules are represented by the ampulla and by the branches of the ureteric bud. During differentiation, the shape of the cells changes from columnar (Figs. 36, 37) to cuboidal (Fig. 57). All collecting tubules are formed by one cell type only, the 'light' cells, since the 'dark' or intercalated cells appear much later. The nuclei of the light cells are located in the apical regions so that they appear to bulge into the tubular lumens. The apical plasma membrane form rare, short microvilli whereas lateral cytoplasmic projections are visible in the basal intercellular spaces. There are no basal plasma membrane invaginations and interdigitations (Fig. 57).

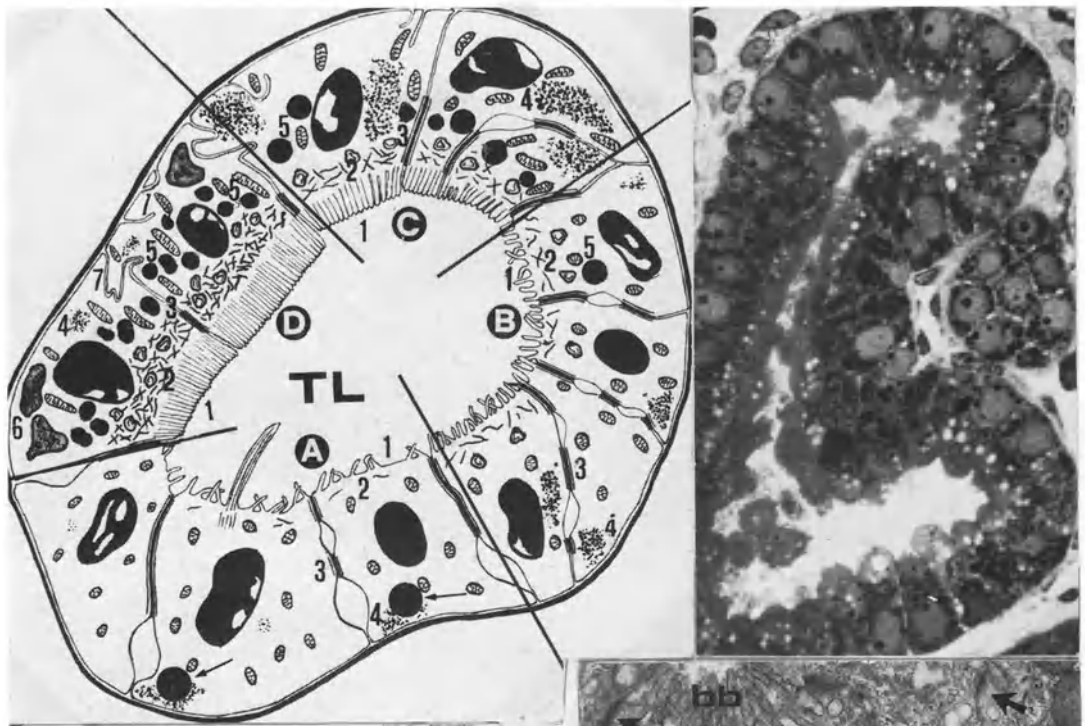

52

53

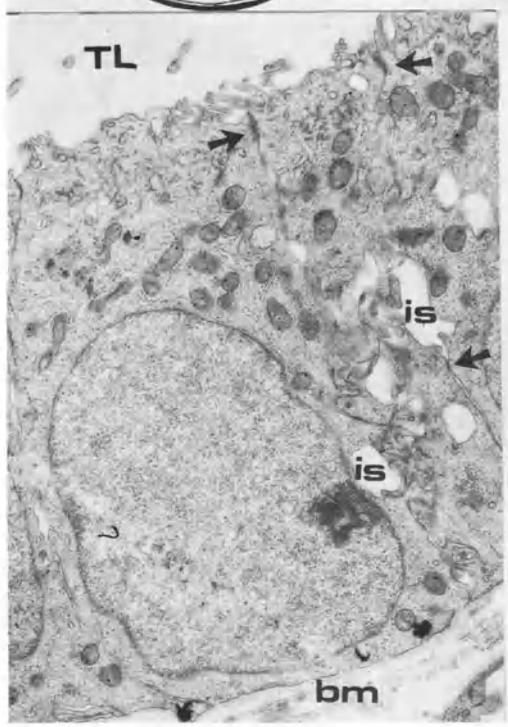

54

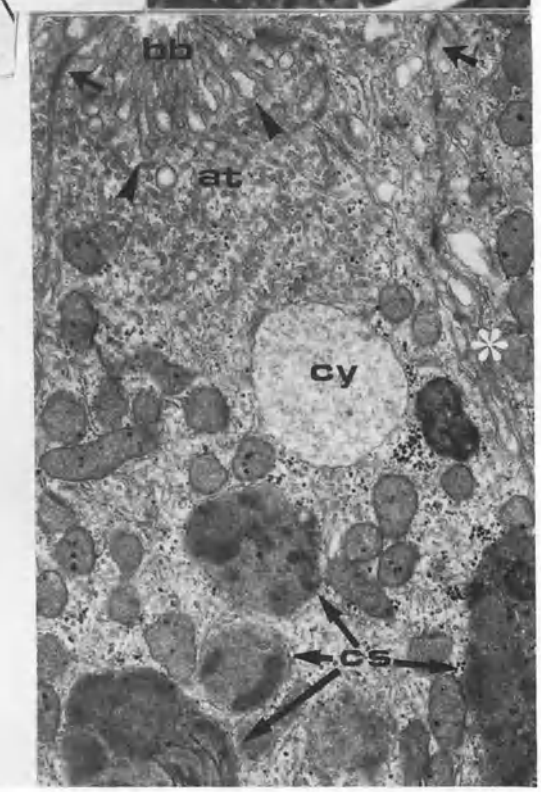

55

Fig. 52. Schematic drawing of the various stages (A, B, C, D) of differentiation of the proximal tubular cells. 1: microvilli of the brush border, 2: endocytic apparatus, 3: intercellular junctions and spaces, 4: glycogen, 5: cytosomes, 6: cytosegresomes, 7: lateral and basal infoldings. Note as the microvilli of the brush border (1), endocytic apparatus (2) and cytosomes (5) progressively increase, while the cytosegresomes (6) develop only at the last stage of cell differentiation. The glycogen (4) also increases but suddenly disappears at te final stage. Lipid bodies (arrows in A) are visible only at early stages. In the last stage, the intercellular junctions [3] remain localized in

the apical cell portion, as junctional complexes, and the intercellular spaces (3) become narrow. Scarce lateral and basal plasmamembrane infoldings (7) appear at the final stage (D).

Fig. 53. Light microscopy of a fully differentiated proximal convoluted tubule. The brush border and apical vacuoles are well recognizable. ×1,000.

Fig. 54. Fine morphology of a proximal tubule at stage B of Fig. 52. bm: basement membrane, is: intercellular spaces, TL: tubular lumen. Arrows point to junctional complexes. ×12,000.

Fig. 55. Fine morphology of a proximal tubule at stage D of Fig. 52. at: apical tubules, bb: brush border, cy: cytosome, cs: cytosegresomes, arrows: junctional complexes, arrowheads: apical tubular invaginations, asterisk: lateral plasmamembrane infoldings. ×25,000.

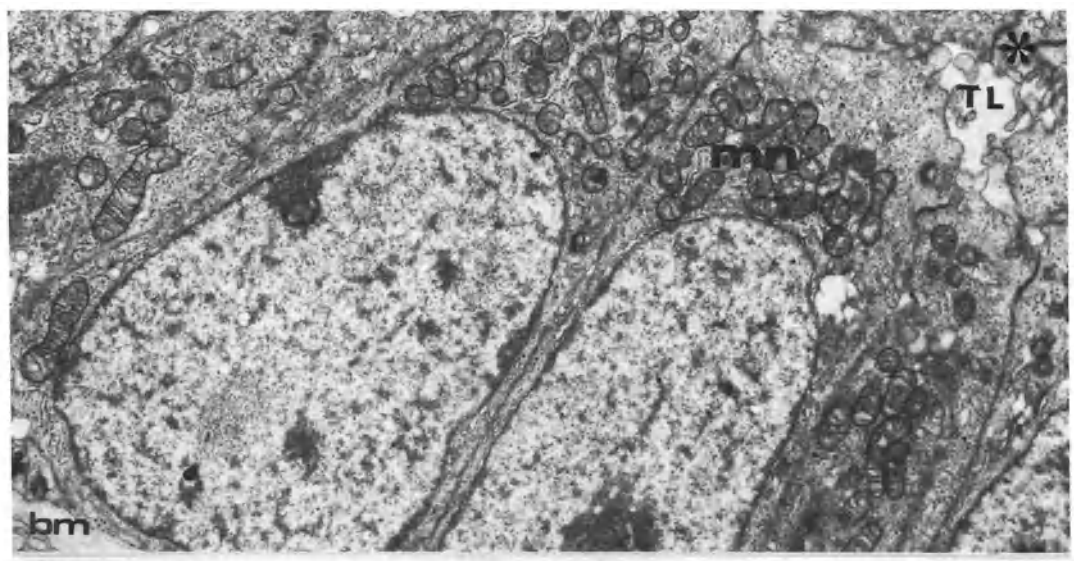

56

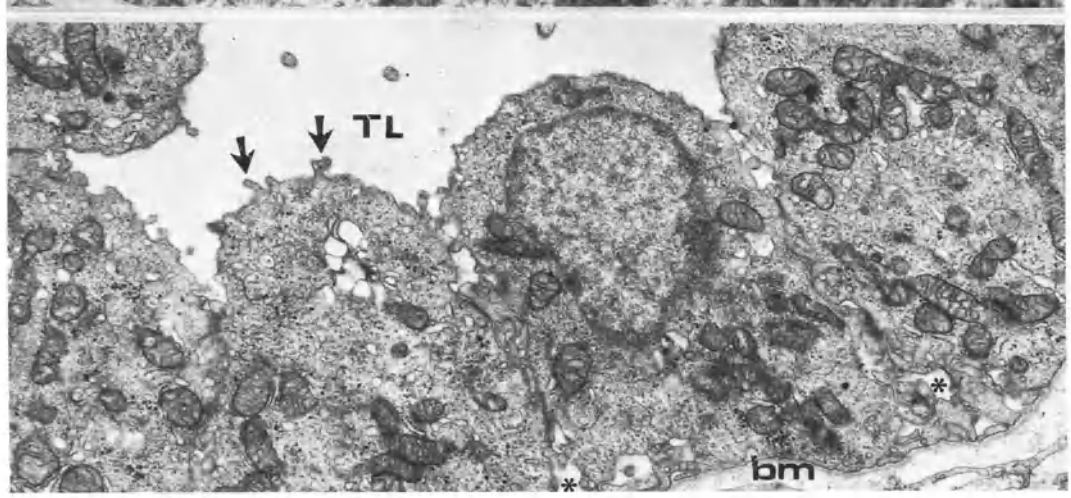

57

Fig. 56. Distal convoluted tubule. The mitochondria are mainly located in supranuclear regions. Rare microvilli of the apical plasmamembranes are visible (asterisk). bm: tubular basement membrane, TL: tubular lumen. ×17,000.

Fig. 57. Collecting tubule. The cells are cuboidal and their apical cytoplasms bulge into the tubular lumen (TL). Rare short microvilli (arrows) are visible along the apical plasmamembranes and narrow intercellular spaces (asterisks) are present in the basal portion of the tubule. bm: tubular basement membrane. ×12,000.

50

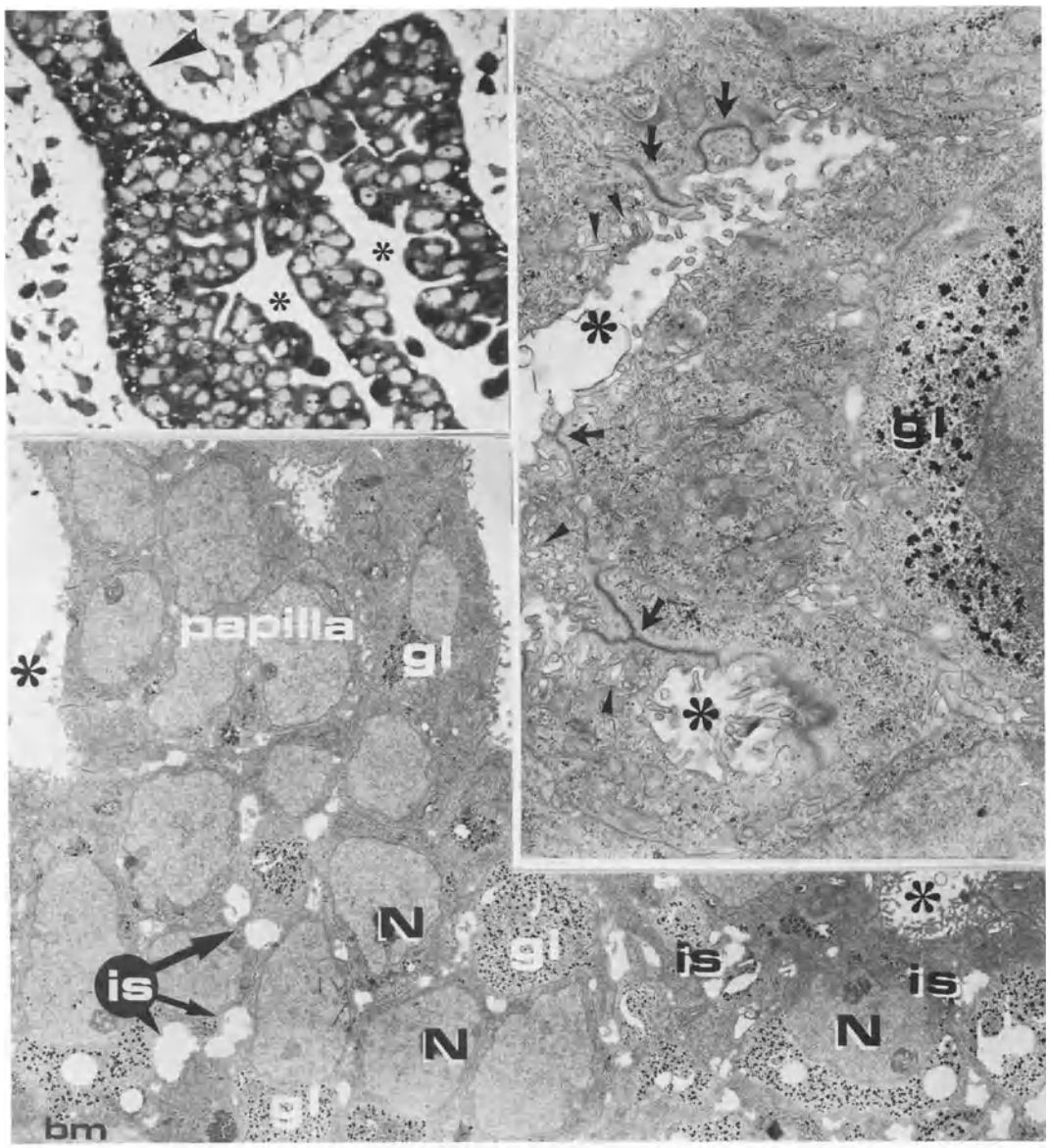

58

60

59

Fig. 58–60. Immature pelvis of 10 week old embryo. The pelvis shows a pluristratified cuboidal epithelium which forms numerous papillae (Figs. 58, 59) toward the lumen (asterisks). Conspicuous glycogen deposits are scattered throughout the cytoplasms (gl, Figs. 59, 60). Numerous intercellular spaces are visible (is, Fig. 59). The apical cells project numerous short microvilli into the lumen (Figs. 59, 60). Several ovoidal vesicles (arrowheads, Fig. 60) are present in the apical cell cytoplasms. N: nuclei, arrowhead in Fig. 58 points to a principal calyx. Fig. 58, ×800; Fig. 59, ×4,000; Fig. 60, ×15,000.

4.8. Pelvis and calyces

At the 10th week of intrauterine life, a prismatic pluristratified epithelium, frequently arranged in numerous papillae, delimits the lumen of the primitive pelvis and calyces (Figs. 58, 59). The cells, many of which in mitosis, are connected by long apical junctional complexes and are provided with short, apical microvilli, apical vacuoles, and large deposits of glycogen (Figs. 59, 60). Intercellular spaces are often visible (Fig. 59).

References

1. Fraser EA: The development of the vertebrate excretory system. Biol Rev (25): 159–187, 1950.

2. Jollie M: Chordate morphology. Reinhold Publishing Corporation, New York, 1962.
3. Fox H: The amphibian pronephros. Quart Rev Biol (38): 1–25, 1963.
4. Cambar R: Valeur et modalités du transit de l'eau chez les jeunes larves d'amphibiens. C R Soc Biol Paris (141): 761–763, 1947.
5. Holmgren N: On the pronephros on the blood in 'Myxine glutinosa'. Acta Zool Stockh (31): 233–348, 1950.
6. Davies, JC: Nephric development in the sheep with reference to the problem of the ruminant pronephros. J Anat, London (85): 6–11, 1951.
7. Torrey TW: The early development of the human nephros. Contrib Embryol Carnage Inst (35): 175–197, 1954.
8. Christensen AK: The structure of the functional pronephros in larvae of Amblystoma opacum as studied by light and electron microscopy. Am J Anat (115): 257–278, 1964.
9. Nardoni C, Tangucci F, Ancinni L, De Martino C: Light and electron microscopic studies of the pronephros of Xenopous laevis. J Submicr Cytol (8): 257–258, 1976.
10. Brenner JL: The interrelations of the mesonephros, kidney and placenta in different classes of animals. Am J Anat (19): 179–210, 1916.
11. Tiedemann K: The mesonephros of cat and sheep. Comparative morphological and histochemical studies. Adv Anat Embryol and Cell Biol, Springer-Verlag, Berlin, vol 52–3, 1976.
12. De Martino C, Zamboni L: A morphologic study of the mesonephros of the human embryo. J Ultrastruct Res (16): 399–427, 1966.
13. Cotrutz Y, Gumpel-Pinot M, Martin C: La morphologie du mésonéphros chez l'homme. Arch Anat (Strasbourg) (54): 191–201, 1971.
14. Koga A: Some observations on the fine structure of the human mesonephros. Arch Histol Jap (34): 185–201, 1972.
15. Zamboni L, Tajana G, De Martino C: Different types of nephrons in the human fetal mesonephros. Ultramicroscopy (5): 402 abs, 1980.
16. De Martino C, Malorni W, Zamboni L: Presence of the juxtaglomerular apparatus in human mesonephros. Ultramicroscopy (5): 402 abs, 1980.
17. Zamboni L, De Martino C: A re-evaluation of the 'mesangial' cells. In: Proc Sixth Int Congr Electr Microsc, R Uyeda (ed), Maruzen, Tokio, 1966, vol 2, p 671–672.
18. Barajas L: The development and ultrastructure of the juxtaglomerular cell granules. J Ultrastruct Res (15): 400–413, 1966.
19. Kaplan A, Friedman M: Studies concerning the site of renin formation in the kidney. The apparent site of renin formation in the tubules of the mesonephros and metanephros of the hog fetus. J Exp Med (76): 307–316, 1942.
20. Sutherland LE, Hartroft PM: Comparative morphology of juxtaglomerular cells in embryos. Can J Zool (46): 257–263, 1968.
21. Rouiller C, Orci L: The structure of the juxtaglomerular complex. In: The Kidney. Morphology, Biochemistry, Physiology, Rouiller C and Muller AF (eds), New York, Academic Press, 1969, vol IV, p 1–80.
22. Ericsson JLE, Trump BF: Electron microscopy of the uriniferous tubules. In: The Kidney. Morphology, Biochemistry, Physiology, Rouiller C and Muller AF (eds), New York, Academic Press, 1969, vol 1, p 351–446.
23. Bellocci M, De Martino C: Development and cytodifferentiation of proximal tubule cells in the metanephros of human embryo. J Sumicr Cytol (4): 105 abs, 1972.
24. De Martino C, Zamboni L, Accinni L: Fine morphology of regressing human mesonephric nephrons. Exp Mol Pathol (26): 169–183, 1977.
25. Zamboni L, De Martino C: Embryogenesis of the human renal glomerulus. Arch Pathol (86): 279–291, 1968.
26. Osathanondh V, Potter EL: Development of human kidneys as shown by microdissection. Formation and interrelationship of collecting tubules and nephrons. Arch Pathol (76): 290–302, 1963.
27. Toldt RC: Untersuchungen über das Wachstul der Nieren des Menschen under der Saugetiere. Akad Wiss Wien (69): 123–150, 1874.
28. Golgi C: Annotazioni intorno all'istologia dei reni dell'uomo e di altri mammiferi e sull'istogenesi dei canalicoli uriniferi. Atti Accad Nazl Lincei Rend Classe Sci Fis Mat Nat (5): 334–361, 1885.
29. Potter FL: Development of the human glomerulus. Arch Pathol (80): 241–255, 1965.
30. Herring R: The development of the Malpighian bodies of the kidney and its relation to pathological changes which occur in them. J Pathol Bacteriol (6): 459–471, 1900.
31. Suzuki Y: An electron microscopy of the renal differentiation. II. Glomerulus. Kejo J Med (8): 129–155, 1959.
32. Jokelainen P: An electron microscope study of the early development of the rat metanephric nephron. Acta Anat (52) suppl 47, 1963.
33. Accinni L, De Martino C: Development and morphological differentiation of podocytes in human embryo metanephros. J Submicr Cytol (4): 101, 1972.
34. De Martino C, Accinni L, Procicchiani G: Ultrastructural study on contractile structures in mammalian nephron. Their development in the metanephros of human embryo. Z Zellforsch (140): 101–124, 1973.

CHAPTER 4

Microscopic structure of the kidney

CESARE DE MARTINO, DELMAS J. ALLEN and LIDIA ACCINNI

1. Introduction

Each of the paired kidneys is a complex, tubular gland comprised of numerous uriniferous tubules. The uriniferous tubule is the basic functional unit of the kidney. Each tubule consists of two distinct morphological entities: (1) the nephron, which produces the filtrate and (2) the collecting tubule which serves to concentrate the filtrate by the further removal of water. The nephron is composed of the glomerulus, the juxtaglomerular complex, the proximal convoluted tubule, the loop of Henle and the distal convoluted tubule. This chapter deals with the light and electron microscopic structure of both the connective tissue capsule and the uriniferous tubule in the parenchyma of the mammalian kidney.

2. The connective tissue capsule

The adult mammalian kidney is closely encapsulated by a comparatively thin, fibrous connective tissue capsule (Figs. 1–4) and embedded within a mass of fatty tissue. In the fetal kidney, internal extensions of the fibrous capsule are distinct, and subdivide the kidney into some 10–12 lobes. During normal development, however, these inward connective tissue extensions become greatly reduced [1]. In the adult kidney, the surface appears comparatively smooth as a result of the reduction or absence of these connective tissue septae (Figs. 5–7) and the ultimate fusion of the lobes.

The cortical stroma (Figs. 6 and 31) consists only of scattered collagen fibrils and occasional fibroblasts [1]. These connective tissue elements increase somewhat in the medulla, but are most prominent in the papilla.

3. The glomerulus

The glomerulus consists of a tuft of specialized capillaries originated from the afferent and drained by the efferent arteriole [2] (Figs. 8–10). These vessels are close together and form the vascular pole (or hilum) of the glomerulus, which is situated in the opposite side of the area where the lumen of the proximal tubule opens into the urinary space (tubular pole). The glomerular capillaries are placed in a space (urinary space) limited by Bowman's capsule (Figs. 11–15). Bowman's capsule is composed of flattened cells which are in direct continuity with the cells of the proximal convoluted tubule. At the hilus of the glomerulus there is the juxtaglomerular apparatus. The wall of the glomerular capillaries is a three layered structure consisting of an inner layer of endothelial cells, of an outer layer of visceral epithelial cells and of an intermediate basement membrane. The axial part of the glomerular capillaries is formed by the mesangium, which is in anatomical continuity with the cells of the media of the glomerular arteriole (Figs. 13–20).

3.1. Endothelium

The endothelium is made up of a single layer of flattened cells [2]. The cell body and the nucleus are usually located in the axial region of the capillary (Figs. 15–17). In the peripheral portion of the capillary, the endothelial cytoplasm is about 400 Å thick and shows round fenestrations of a width of about 600 Å. The fenestrae are closed by a thin diaphragm 40–60 Å thick. A central knob-like structure may be seen in the diaphragm [3]. The perinuclear cytoplasm contains small, round mitochondria, endoplasmic reticulum, a few ribosomes, the Golgi apparatus, pinocytotic vesicles and multivesicular bodies. Adjacent endothelial cells are joined by 'junctional complexes' similar to those of epithelial tissues.

L.J.A. DiDio and P.M. Motta (eds), Basic, Clinical, and Surgical Nephrology. ISBN 0-89838-689-5.

3.2. *Visceral epithelial cells (or podocytes)*

The visceral epithelium is continuous with the epithelium of Bowman's capsule and consists of large cells with an abundant cytoplasm coating the glomerular tuft (Fig. 15). The nuclear region protrudes into the urinary space (Fig. 15). Numerous prolongations of the cytoplasm, the trabeculae, run parallel to the basement membrane to which they are connected by secondary branches, called 'foot-processes' (Figs. 11–13 and 17). The foot-processes are embedded in the subepithelial zone of the basement membrane (lamina rara externa) to a depth of about 400–500 Å (Fig. 18). The foot-processes of a podocyte interdigitate with those of adjacent cells, thus forming a pericapillary lacunar apparatus through which the primitive urine circulates [4, 5]. The functional implications of this complex arrangement are not yet clear but could be related to a possible contractile property of the foot-processes, with a resulting control of the diameter of the filtration slits. Between the foot-processes at or about the level of the basement membrane are epithelial filtration slits or slit pores, which have a width of 200–300 Å [5] (Figs. 16, 17, and 18). Toward the urinary space the epithelial slits widen to 800–1000 Å so that in longitudinal sections the slits appear funnel-like with the apex at the level of the basement membrane. Near the basement membrane, the filtration slits appear closed by a thin membrane or a diaphragm with a central dense spot (filtration slit membrane 40–60 Å thick [6, 7] (Fig. 18). Radiating pedicillar filaments cross the subepithelial zone of the basement membrane bridging the latter with the plasmamembrane of the foot processes (Fig. 18). The plasmamembrane of the podocytes, including that of the foot-processes, possesses a thick cell coat (100–150 Å) or glycocalyx [8] which contains numerous polyanionic sialoglycoproteins. The glycocalyx entends over the filtration slit membrane but is not visible over the portion of the foot-processes embedded in the subepithelial zone of the basement membrane.

The cytoplasm of the podocytes, in addition to the usual cell organelles, contains large number of ergastoplasmic cisternae, lysosomal-like granules, microtubules and filaments. The smooth and rough cisternae of the endoplasmic reticulum are scattered throughout the cytoplasm. The endoplasmic reticulum is probably involved in the synthesis of some components of the basement membrane as suggested by morphologic [9] and immunologic [10] studies. The lysosomal-like granules are components of the apparatus involved in the transport and digestion of reabsorbed proteins [11]. Finally, bundles of filaments are seen in the foot processes. These filaments resemble the myofilaments of smooth muscle cells and probably confer to the podocytes the capacity of contraction, with a consequent important effect on glomerular permeability [12, 13].

3.3. *Basement membrane*

With suitable stains, the basement membrane appears to be formed by three layers (Fig. 18): 1) an outer layer or subepithelial zone' (lamina rara externa); 2) a middle layer, more electron opaque than the other two, called 'lamina densa' or 'basement membrane proper,' and 3) an inner layer or 'subendothelial zone' (lamina rara interna) [2, 5, 6]. The total width of the basement membrane varies with species and age. In man, the average width is 1500 Å in the young to about 3500 Å in the adult.

Chemically, the glomerular basement membrane like other basement membranes is formed by collagenous and non-collagenous glycoproteins and glycosaminoglycans. Type IV and V collagen are the major components of collagenous glycoproteins whereas laminin and fibronectin are the most representative among non-collagenous glycoproteins. Laminin and type IV and V collagen are present in both glomerular basement membrane and mesangial matrix; fibronectin is mainly in the mesangial matrix, with only small amounts of it located in the glomerular basement membrane (see review by Foidart) [14]. Heparan sulphate and hyaluronic acid are the only glycosaminoglycans present in significant quantity in the glomerular basement membrane. By means of their anionic sites, the latter chemical compounds contribute to the electronegative charge barrier of the glomerular basement membrane to neutral or anionic molecules [15].

3.4. *Mesangium*

The mesangium [16] resides within enlarged areas of the subendothelial zone of the glomerular basement membrane (Figs. 15, 19, 20) and is formed by a cellular and an acellular compartment: the mesangial cells and the mesangial matrix. The mesangial cells are characterized by cytoplasmic projections which penetrate into the subendothelial zone of the glomerular basement membrane (Figs. 15 and 19) and by pseudopodia which reach the lumen of the capillary through gaps of the endothelial cytoplasm (Fig. 21) [5] Beside their pinocytotic activity, the luminar pseudopodia are likely to monitor variations in the osmotic and hydrostatic pressure in the glo-

merular capillaries [17]. The mesangial cell cytoplasm containes a large variety of organelles, numerous lysosomes, dense bodies and bundles of filaments which are particularly visible in the pseudopodia. Gap-junctions, similar to those of smooth muscle cells of arterioles, connect the plasmamembranes of adjacent mesangial cells. The mesangial matrix is formed by an amorphous basement membrane-like material and by bundles of thin filaments which penetrate into the subendothelial zone of the basement membrane. The topographic relationship of mesangial cells with other components of the glomerular capillaries and with the cells of the media of the afferent and efferent arterioles are illustrated in Figs. 19, 20 [18]. At the hilus of the glomerulus, the afferent arteriole does not penetrate into the glomerulus (Fig. 20). Thus the endothelium of the arteriole is continuous with the capillary endothelium, and the smooth muscle cells and the intercellular matrix of the arteriole are continuous with the mesangial cells and the mesangial matrix [18]. In the glomerulus the mesangial cells occupy an 'intracapillary' or 'parietal' position comparable to that of smooth muscle cells in the arteriole [18]. The mesangial cells cover only one side of the glomerular capillary wall. This side represents the 'axial region' of the glomerular capillary. The opposite side, which is not covered by the mesangial cells, corresponds to the peripheral (or filtration) zone of the capillary (Fig. 15).

The principal functions of the mesangial cells are [15]: 1) phagocytosis and pinocytosis as indicated by the presence of tracer molecules in cytosomes (Fig. 22) and by the numerous cytoplasmic projections and pseudopodia extending into the lumen and into the subendothelial zone of the basement membrane. Phagocytosis of macromolecules trapped in this part of the capillary wall can contribute to 'cleaning' of the ultrafilter. The phagocytosis and micropinocytosis involve also macromolecules, such as proteins, which are accumulated in the mesangial matrix [19]; 2) local chemical, osmotic and pressure pseudopodia receptors; 3) synthesis and deposition of components of the basement membrane and the mesangial matrix; 4) contractile activity which participates in the control of blood pressure in the glomerular capillaries and regulates the intraglomerular shunts responsible for variations of intraglomerular pressure in single capillary loops; 5) proliferation and 6) transformation into granulated cells similar to the cells of the juxtaglomerular apparatus [20].

The mesangial matrix, which is easily permeated by macromolecules, may have the function of trapping various chemical substances allowing the incorporation and digestion of filtrate residues by the mesangial cells.

In conclusion, it is important to point out that the glomerular capillary is not a permanent structure with a peripheral zone facing the uriniferous space and an axial zone facing the mesangium. These zones are in a continuous modulation whereby a peripheral region may become in part a mesangial region and vice versa [17].

3.5. Bowman's capsule

Bowman's capsule is made up of a basement membrane and a single sheet of epithelial cells or parietal epithelium (Figs. 15 and 23). The basement membrane and the parietal epithelium are continuous with the basement membrane and the epithelium of the proximal convoluted tubule. Furthermore, at the vascular pole the basement membrane of the Bowman's capsule turns in to fuse with the basement membrane of glomerular capillaries and with the subendothelial layer of the afferent and efferent arterioles (Fig. 20).

The epithelial cells are flattened and contain only few ergastoplasmic organelles. In the cytoplasm close to the basement membrane there are bundles of filaments and electron dense bodies similar to the attachment bodies of smooth muscle cells (Fig. 23). These structures suggest that the parietal epithelial cells may have a contractile function.

4. The juxtaglomerular apparatus

The name juxtaglomerular apparatus is given to a functional unit, located at the vascular pole of the glomerulus in a triangular area formed by the afferent arteriole, the efferent arteriole and the distal convoluted tubule [21] (Figs. 24 and 25). The juxtaglomerular apparatus consists of four parts: 1) the granular juxtaglomerular cells of the afferent arteriole, 2) the agranular cells (extraglomerular mesangium or polkissen or lacis cells), 3) the smooth muscle cells of the efferent arteriole, and 4) the 'macula densa' of the distal convoluted tubule.

4.1. Afferent arteriole

The wall of the afferent arteriole is composed of endothelial cells, basement membrane and smooth muscle cells which near the glomerulus are replaced by the granular juxtaglomerular cells [21, 22] (Fig. 26). Smooth muscle cells and juxtaglomerular cells form the media of the vessel. The juxtaglomerular

cells do not progress beyond the hilus while the smooth muscle cells of the arteriole are in anatomical continuity with the mesangial cells (Fig. 20).

The endothelial cells are high and bulge into the lumen (Fig. 26). Filamentous material continuous with (Fig. 20) and similar to (Fig. 26) the mesangial matrix is interposed between the endothelial cells and the cells of the media. The juxtaglomerular cells are larger than the smooth muscle cells and irregular in shape (Fig. 20). They are interconnected by gap-junctions. These junctions are characterized by high permeability and low electric resistance, thus permitting free ionic exchanges and ready transmission of electronic impulses. In man, two main types of granules have been identified in the cytoplasm of juxtaglomerular cells. The first type is not specific and seems to contain mainly lipofuscin; the second type frequently shows crystal-like structures and probably is a secretory granule containing renin [22].

4.2. Extraglomerular mesangium or agranular cells

The cells of the extraglomerular mesangium [22] or lacis cells [23] or polkissen [16] (Figs. 24 and 25) fill the triangular space limited by the two glomerular arterioles and by the macula densa. The cells are embedded in a network of basement membrane-like material and collagen fibrils. The presence of cells with morphologic features intermediate between those of juxtaglomerular cells and lacis cells suggests that both juxtaglomerular cells and lacis cells are derived from the smooth muscle cells of glomerular arterioles.

4.3. Efferent arteriole

The efferent arteriole usually leaves the glomerulus at the vascular pole (Figs. 10 and 24). Sometimes, however, the efferent vessel emerges from the side opposite to that of the afferent arteriole. This is observed in the mesonephric glomeruli of human embryos [24]. The anatomical structure of the efferent arteriole may be muscular or endothelial with a prevalence of the muscular type in the juxtamedullary nephrons.

4.4. Macula densa

The macula densa is formed by the initial portion of the distal convoluted tubule that is in contact with the afferent and efferent glomerular arterioles [21, 22] (Figs. 24 and 25). The cells of the macula densa show short apical microvilli and round mitochondria located in the apical zone. The basal portion of the cell, usually close to the efferent arteriole, has large intercellular spaces and numerous cytoplasmic projections. At this level, the basement membrane of the macula densa and that of the efferent arteriole form a complex network. In the opposite side of the tubule the basement membrane is regular and the cells are similar to those of the distal convoluted tubule (Fig. 25).

5. The urinary tubule

The urinary tubule, which carries the urine from the glomerulus to the papilla, is composed of two structures: the basement membrane and the epithelium.

The epithelium is histologically and functionally different in the various parts of the nephron. Hence, the nephron is divided into proximal tubule, Henle's loop, distal tubule and collecting duct.

5.1. Proximal tubule

The proximal tubule leaves the glomerulus at the urinary pole and initially forms several convolutions ('pars convoluta') before becoming a straight segment ('pars recta') which descends into the medulla and continues in the thin descending limb of Henle's loop. The length of the proximal tubule is about 14 mm. The size of the lumen depends upon the method of fixation. In animals, the lumen is widely patent if fixation is performed by perfusion 'in vivo' (Fig. 27).

5.1.1. Pars convoluta or proximal convoluted tubule. The cells of the pars convoluta are tall and cubical. Their luminar surface is occupied by a brush border, a system of microvilli each 1 μ in length and 700 Å in diameter (Figs. 28–34). There are about 200–250 microvilli per μ^2. A slightly electron opaque, fuzzy material coats their surface. This material is PAS-positive and probably consists of glycoproteins and acid carbohydrate residues. At the base of the microvilli the plasma membrane frequently forms invaginations sometimes connected with apical vesicles and vacuoles (Figs. 34 and 35). In the cytoplasm several types of granules or bodies are visible. According to their morphological and cytochemical characteristics, they can be divided into cytosomes, cytosegregosomes, microbodies and multivesicular bodies [25] (Figs. 34 and 35). These organelles are involved in transport and digestion of proteins, and some of them belong in the category of lysosomes [25]. The Golgi apparatus is localized close to the nucleus. The latter is placed in the middle region of

the cell. One or more nucleoli are also visible. The cytoplasm contains ribosomes, polysomes, microtubules, filaments, glycogen particles and occasional lipid droplets. The filaments are arranged in bundles anchored to thickened zones of the plasma membrane that are similar to the 'attachment zones' of the plasma membrane of smooth muscle cells [12, 26]. The basal part of the cell is characterized by deep infoldings of the plasma membrane which divide the cytoplasm into processes oriented perpendicularly to the basement membrane (Fig. 34). The basal processes of one cell interdigitate with those of neighboring cells thus forming a basal labyrinth of extended surface. The greatest part of the cell, and especially the basal portion, is occupied by mitochondria. The basal mitochondria are elongated and oriented parallel to the basal infoldings of the plasma membrane and contain numerous cristae and a matrix with dense granules (Fig. 34).

Adjacent epithelial cells are joined by junctional complexes [27] (Fig. 35) apparently capable of creating a barrier or 'seal' to diffusion. The junctional complexes result from contact of contiguous apical plasma membranes and are formed by three components: 1) tight junction (or 'zonula occludens'), 2) the intermediary junction (or 'zonula adhaerens'), and 3) the desmosome (or 'macula adhaerens'). The tight junction is placed just below the apical border and results from fusion of the outer leaflets of adjacent cell membranes. A continuous belt-like attachment forms around the cell, thus playing an important role on epithelial permeability. The intermediary junction has an intercellular space of about 240 Å containing a central disc or line. At this point, there is a plaque of dense material in the cytoplasm of both contiguous cells into which bundles of fine fibrils converge. The desmosomes are discontinuous attachments.

5.1.2. Pars recta

The cellular organization of the pars recta appears less complex (Fig. 36). The microvilli are shorter and less tightly arranged. The apical tubules, vesicles and vacuoles are less numerous. The mitochondria are reduced both in size and number, and are randomly distributed. The basal infoldings of the plasma membrane are considerably reduced or even absent. As in the cells of the pars convoluta, bundles of basal filaments and related attachment zones are visible (Fig. 36).

5.2. Henle's loop

The pars recta of the proximal tubule continues in the descending limb of the loops of Henle's which are 14 to 20 μ in diameter and 4 to 10 mm in length [1]. The length of the loops is different according to the position of the glomerulus in the renal cortex. The subcortical nephrons have the shortest loops and the juxtamedullary the longest. The transition from the proximal tubule to the descending limb is rather abrupt, and the epithelium changes from cuboidal to flattened cells (Figs. 27 and 36).

5.2.1. Thin descending limb

5.2.2. Thin ascending limb

According to the morphological features, the thin limb of Henle's loop can be devided into two segments. The first one, or descending thin limb, which runs from the pars recta of the proximal tubule to the hairpin turn of the loop, is characterized by cells with highly complex lateral and basal interdigitations, numerous tight junctions and short apical microvilli (Fig. 39). The second segment, which joins the thick ascending limb or pars recta of the distal tubule and is mainly represented by the thin ascending limb of the loop, possesses only a few tiny apical microvilli and scanty basal interdigitations (Fig. 39). The nephrons with long Henle's loops have both the thin descending and thin ascending limbs, whereas those with short loops have only thin descending limbs but with morphological features of the second segment.

5.3. Distal tubule

The distal tubule is composed of three segments: 1) the 'pars recta' or thick ascending limb of Henle's loop, 2) the 'macula densa' or initial portion of the 'pars convuluta', which is part of the juxtaglomerular apparatus, and 3) the 'pars convoluta' or distal convoluted tubule. The morphology of the macula densa has been described already.

5.3.1. Pars recta or thick ascending limb of Henle's loop

The thick ascending limb of Henle's loop is about 9 mm in length and 33μ in diameter. The transition between the thin limb and the thick limb occurs abruptly (Fig. 40), in the descending (subcortical nephrons) or in the ascending (juxtamedullary nephrons) portions of the Henle's loop. The cellular structure of the thick limb gradually assumes the features of the distal convoluted tubule [2, 6] and is described under the following heading (Figs. 37, 38).

5.3.2. Pars convoluta or distal convoluted tubule

The distal convoluted tubule measures about 5 cm in length and 20–40μ in diameter. The lumen is usually

patent regardless of the method of tissue fixation. The cells are cuboidal and darker than those of the Henle's loop. They have no brush border but only short microvilli (Figs. 41 and 42). Junctional complexes are composed of a tight junction or zonula occludens and an intermediate junction or zonula adherens. The nucleus is large and usually placed in the middle or apical part of the cell (Fig. 41). The Golgi apparatus is well developed and localized laterally to the nucleus. Cytosomes, cytosegregosomes, multivesicular bodies are present in the cytoplasm. Apical microtubules and vacuoles are not visible. A great number of mitochondria are arranged between the infoldings of the basal plasma membrane (Fig. 42).

5.4. Collecting duct

The collecting duct [2, 6] (Figs. 43–46) which follows the distal convoluted tubule has a length of 20–22 mm. Approaching the papilla its diameter increases and reaches 100 μ. The transition between the distal convoluted tubule and the collecting duct is gradual and difficult to pinpoint (Fig. 43). Morphological differences are observed among various segments of the collecting duct placed in the subcortical, juxtamedullary cortical, outer medullary or inner medullary position. As the duct passes from the medullary ray to the inner medulla, the cells become higher and in the ducts of Bellini show a columnar form. Two distinct types of cells are present: the 'light cells' or principal cells, which represent the main cell type in the entire collecting duct, and the 'dark cells' or intercalated cells, which are more numerous in the proximal part of the collecting duct (Figs. 30 and 45). The ligth cells show few cytoplasmic organelles. The nucleus is relatively large. Short microvilli may be seen on the apical surface. The basal infoldings are scarce and do not interdigitate with those of contiguous cells (Fig. 45). The dark cells are characterized by a denser, more osmiophilic ground substance containing more numerous mitochondria, apical microvilli, ribosomes, glycogen and vesicles than the light cells. The basal infoldings are thin and flat (Figs. 29, 30, 44, 45).

6. Peritubular capillaries

The tubules are surrounded by an extensive network of capillaries which are irregularly arranged in the cortex of the kidney. Here the efferent arteriole decreases in diameter after leaving the cortical glomeruli, thus forming the peritubular capillaries. The capillaries are in close apposition to the tubular basement membrane (Figs. 10, 28, 34, 39, 40, 42, 43, 44, 45). The capillary wall is very thin, most having a thickness of about 400 Å. The endothelium shows fenestrations of about 600 Å in diameter. Each fenestra is bridged by a diaphragm 70 Å thick in which a central knob-like structure is frequently visible [3]. The basement membrane is very thin and often is in intimate contact with the tubular basement membrane. The peritubular capillaries eventually transform into venous capillaries which are drained by veins that progressively increase in diameter as they leave the cortex.

The efferent arterioles of the juxtamedullary nephrons descend to the papilla and give rise to the 'vasa recta spuria' which run parallel to the descending and the ascending limbs of Henle's loops. The vasa recta spuria, the Henle's loops and the collecting tubules represent the anatomical complex (Fig. 46) which is involved in the counter current exchange essential for the production of hypertonic urine [28].

References

1. Bulger RE: The urinary system. In: Cell and Tissue Biology, Weise L (ed), New York, Elsevier Biomedical, 1983, p 869–913.
2. Tischer CC: Anatomy of the kidney. In: The kidney, Brenner BM and Rector FC (eds), Philadelphia, WB Saunders Company, 1976, p 3–64.
3. Rhodin J: The diaphragm of capillary endothelial fenestrations. J Ultrastruct Res 6: 171–185, 1962.
4. Arakawa M: A scanning electron microscopy of the glomerulus of normal and nephrotic rats. Lab Invest 23: 489–496, 1970.
5. Yamada E: The fine structure of the renal glomerulus of the mouse. J Biophys Biochem Cytol 1: 551–579, 1955.
6. Rhodin J: Structure of the kidney. In: Diseases of the kidney, Strauss MD and Welt LG (eds), Boston, Little, Brown and Co, 1971.
7. Andrews PM: The kidney glomerular epithelium in response to different physiological states and experimental conditions. In: Three Dimensional Microanatomy of Cells and Tissue Surfaces, Allen DJ, Motta PM and DiDio JJA (eds), New York, Elsevier/North Holland, 1981, p 103–126.
8. Groniowski J, Becrzyskowa W, Walski M: Electron microscope studies on the surface coat of the nephron. J Cell Biol 4: 585–601, 1969.
9. Kurtz SM, Feldman JD: Experimental studies on the formation of the glomerular basement membrane. J Ultrastruct Res 6: 19–27, 1962.
10. Andres GA, Morgan C, Hsu KC, Rifkind RA, Seegal BC: Electron microscopic studies of experimental glomerulonephritis with ferritin-conjugated antibody. J Exp Med 115: 929–936, 1962.
11. Farquhar MG, Wissig SL, Palade GE: Glomerular permeability. I. Ferritin transfer across the normal glomerular capillary wall. J Exp Med 113: 47–65, 1961.
12. De Martino C, Accinni L, Procicchiani G: Ultrastructural study on contractile structures in mammalian nephron. Their development in the metanephros of human embryo. Z Zellforsch 140: 101–124, 1973.
13. Accinni L, Natali PG, Vassallo L, Hsu KC, De Martino C: Immunoelectron microscopic evidence of contractile proteins in the cellular and acellular components of mouse kidney glomeruli. Cell Tiss Res 162: 297–312, 1975.
14. Foidart JM, Mahieu PR, Foidart JB, Boniver J, Lambotte R: Heterogeneity of glomerular basement membrane antigens. In: Immunologia clinica del fegato e del rene e immunoterapia. Recenti progressi. Frada G (ed), Padova, Piccin Editore, 1983, p 347–366.

15. Kanwar YS, Linker A, Farquhar MG: Increased permeability of the glomerular basement membrane to ferritin after removal of glycosaminoglycans (heparan sulfate) by enzyme digestion. J Cell Biol 86: 688–693, 1980.
16. Zimmerman KW: Uber den Bau des glomerulus der Saugetiere. Weitere Mitteilungen. Z Mikr Anat Forsch 32: 176–278, 1933.
17. De Martino C, Natali PG, Zamboni L, Accinni L: Ultrastructural study of mesangial cells and their relationship to smooth muscle cells of glomerular arterioles. In: Contributions to nephrology, Berlyne GM, Giovannetti S (eds), Basel, S. Karger, 1976, vol 2, p 17–24.
18. Zamboni L, De Martino C: A re-evaluation of the mesangial cell of the renal glomerulus. Z Zellforsch u Mikr Anat 86: 364–383, 1968.
19. Farquhar MG, Palade GE: Functional evidence of the existance of a third cell type in the renal glomerulus. Phagocytosis of filtration residues by a distinctive 'third' cell. J Cell Biol 13: 55–87, 1962.
20. Dunihue FW, Boldosser WG: Observation on the similarity of mesangial to juxtaglomerular cells. Lab Invest 12: 1228–1240, 1963.
21. Goormaghtigh N: Les segments neuro-myo-arteriels juxtaglomerulaires du rein. Arch Biol 43: 575–591, 1932.
22. Barajas L: The ultrastructure of the juxtaglomerular apparatus as disclosed by three-dimensional reconstruction from serial sections: the anatomical relationship between the tubular and vascular components. J Ultrastruct Res 33: 116–147, 1970.
23. Oberling C, Hatt PY: Study of the juxtaglomerular apparatus of the rat using the electron microscope. Ann Anat Pathol (Paris) 5: 441–474, 1960.
24. De Martino C, Zamboni L: A morphological study of the mesonephros of the human embryo. J Ultrastruct Res 16: 399–427, 1966.
25. Ericsson JLE, Trump BF: Electron microscopy of the uriniferous tubules. In: The kidney. Morphology, Biochemistry, Physiology, Roullier C. Muller AF (eds), New York, Academic Press, 1969, vol 1, p 351–447.
26. Pease DC: Myoid features of the renal corpuscle and tubule. J Ultrastruct Res 23: 304–320, 1968.
27. Farquhar MG: Palade CE: Junctional complexes in various epithelia. J Cell Biol 17: 375–412, 1963.
28. Berliner RW, Levinsky NG, Davidson DG, Eden M: Dilution and concentration of the urine and the action of antidiuretic hormone. Am J Med 24, 730–744, 1968.

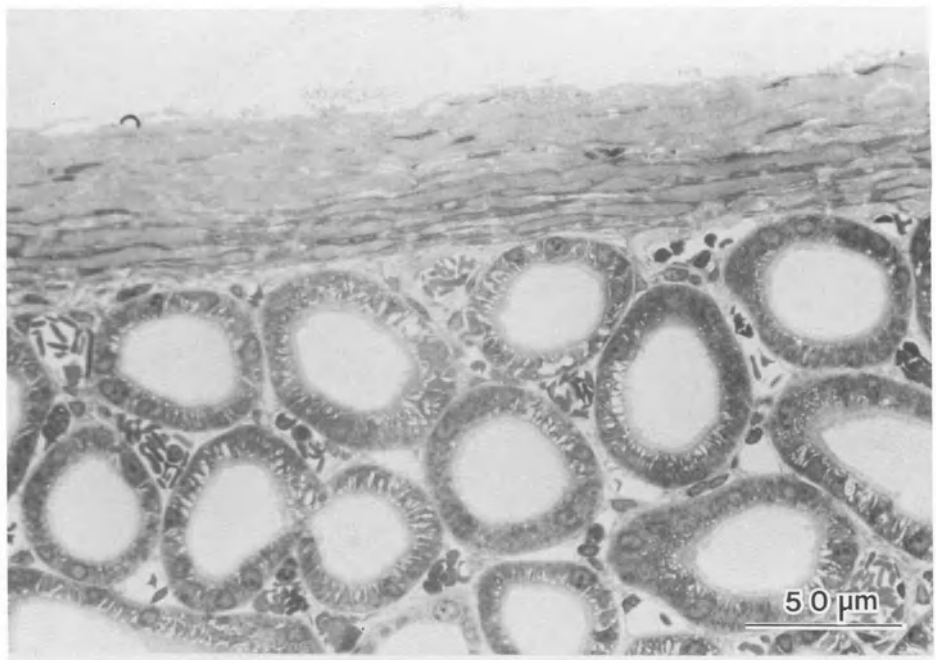

1

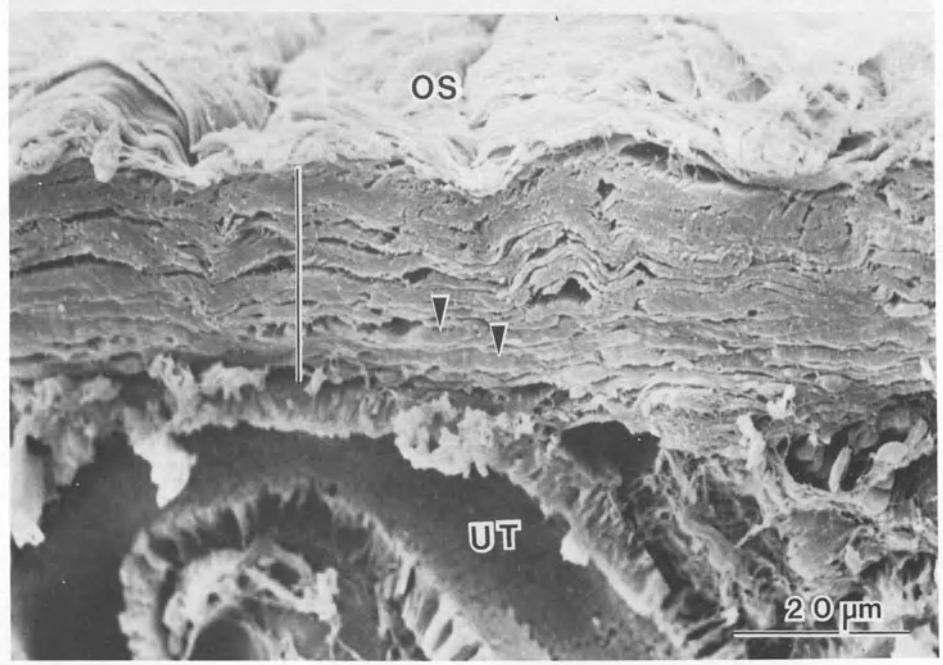

2

Fig. 1. A LM view of a thick-section (toluidine blue stain) of the connective tissue capsule and the underlying outer cortex (through several proximal convoluted segments) of the dog kidney. The cellularity of the capsule and the vascularity of this portion of the kidney parenchyma can be discerned in the otherwise scant cortical stroma.

Fig. 2. SEM of the cut surface of dog kidney capsule and subjacent parenchyma. The cellular and fibrillar components (line) of the capsule proper are observed interposed between the outer surface (OS) and the most superficial portion of the cortex. Cortical stroma and an accompanying blood vessel (lower right) are seen adjacent to a sectioned uriniferous tubule (UT). Cells within the capsule (arrowheads) are difficult to discern in SEM.

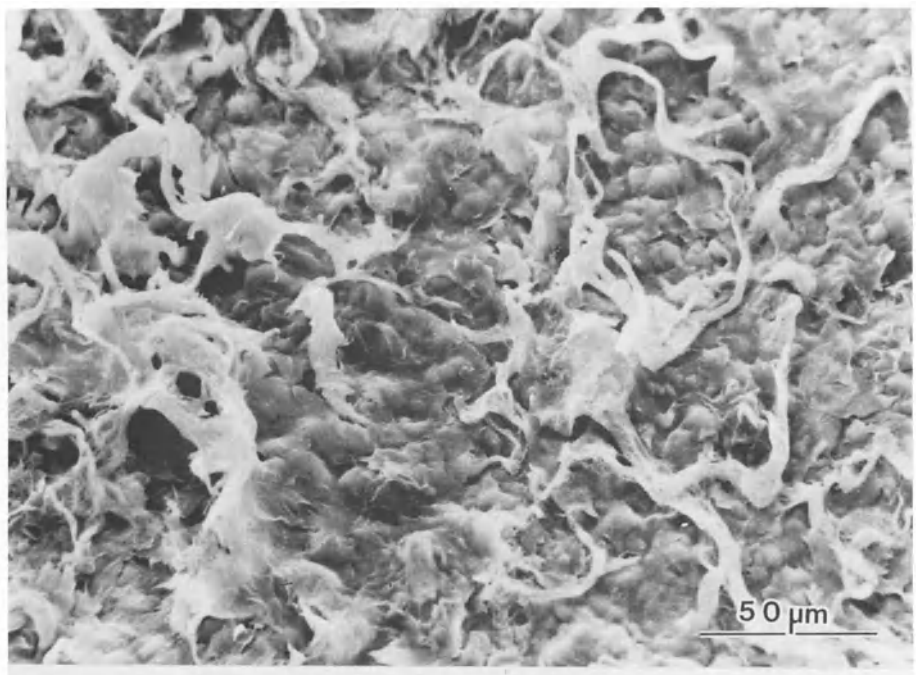

3

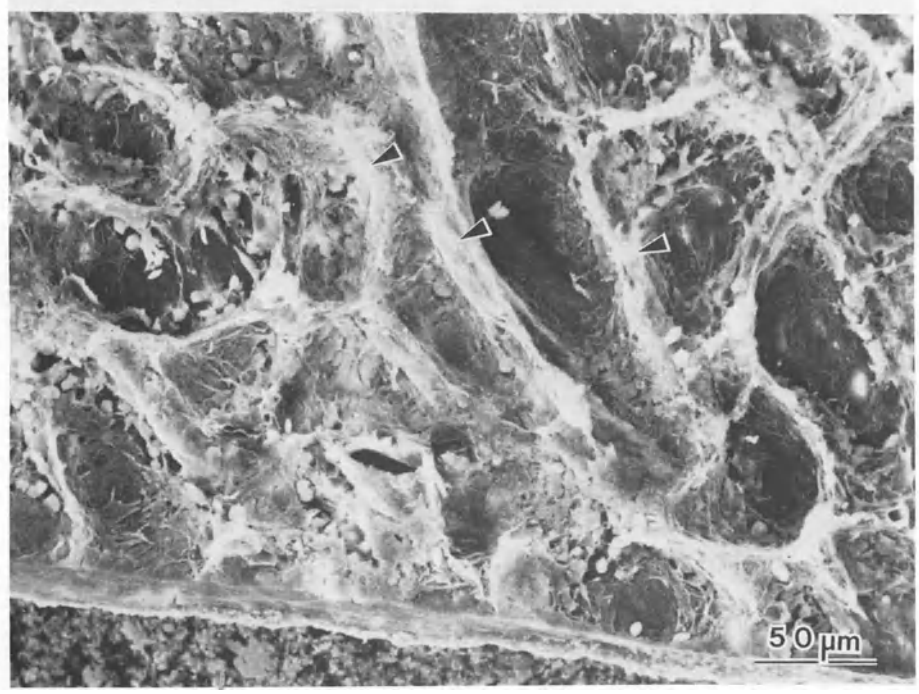

4

Fig. 3. The surface of the renal capsule of the dog as seen in SEM. The outer surface of the dense connective tissue capsule appears less smooth than revealed in LM. Compare the relatively smooth outer surface of the capsule with the inner surface shown in Figure 4.
Fig. 4. The inner (most visceral) surface of the renal capsule of the dog. The depressions in the connective tissue capsule created by the underlying uriniferous tubules and the inward projections (arrowheads) of collagen fibrils contributing to the cortical stroma provide more surface relief to the visceral surface. Blood cells can be seen in the vessels within the connective tissue septae projecting from the capsule proper.

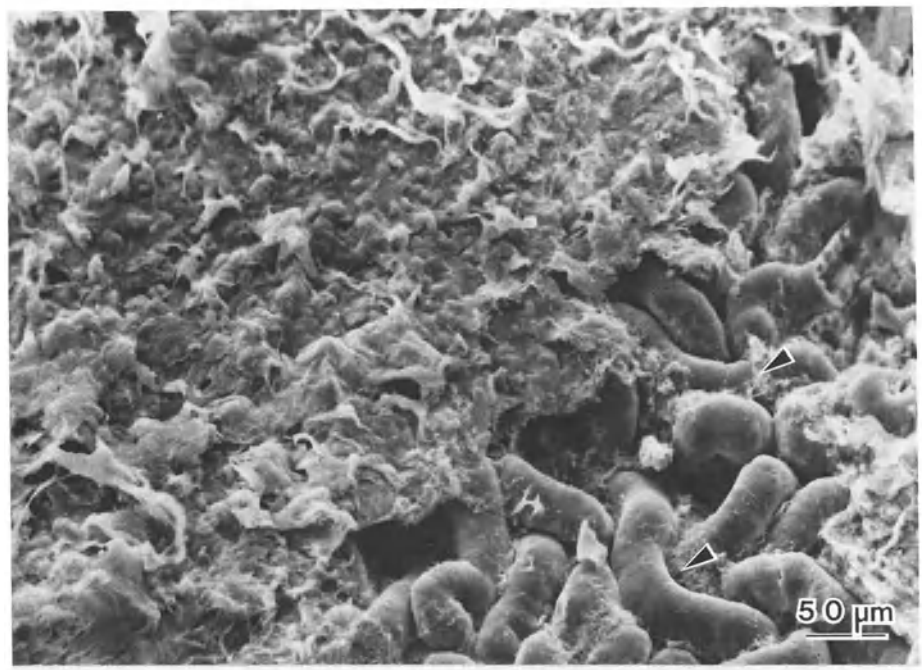

5

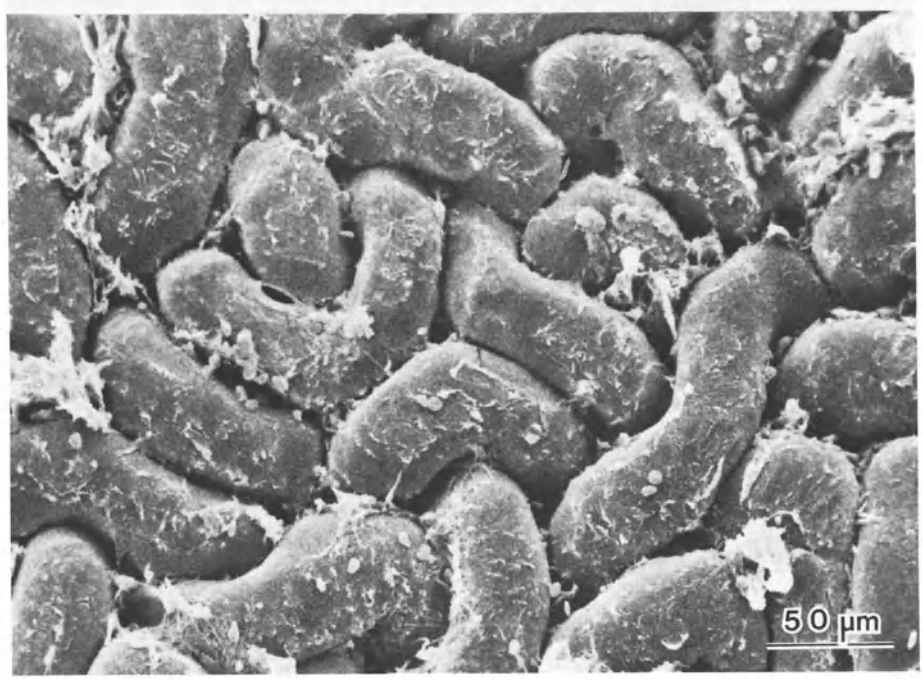

6

Fig. 5. SEM field in an area where the capsule was partially removed to show relationship of capsule (upper left) and underlying uriniferous tubules (lower right). Scant connective tissue septae (arrowheads) can be seen projecting between the tubules.
Fig. 6. SEM of superficial surface of cortex shown in Figure 5 as revealed at a higher magnification. Portions of many uriniferous tubules are seen with intervening scattered cortical stroma. Distinct segments or parts (nephron and collecting tubules) of the uriniferous tubules cannot be identified in this intact surface view.

Fig. 7. TEM of connective tissue capsule of the dog kidney. Collagenous fibers sectioned both longitudinally and transversely and fibroblasts dominate this area of the dense fibrous capsule. Individual collagen fibrils appear as small dots or spheres within the larger cross-sectioned fibers or demonstrate periodicity in longitudinal-sections.

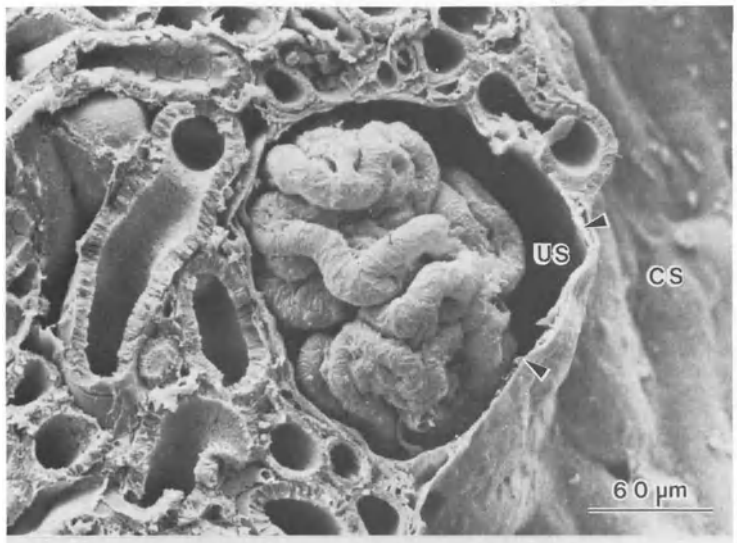

Fig. 8. SEM (low magnification) view of the kidney cortex showing a severed superficial Bowman's capsule and exposed lumina of numerous uriniferous tubules and blood vessels. The cortical surface (CS) of the kidney, the relative thinness of the parietal layer (arrowheads) of Bowman's capsule and the urinary space (US) where ultrafiltrate is initially collected can be distinguished in this cortical field.

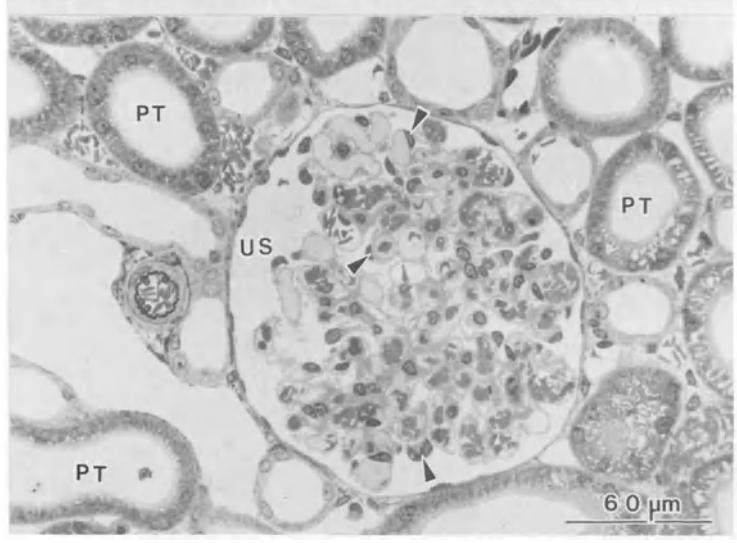

Fig. 9. LM of a section through a renal corpuscle and surrounding cortical structures. The parietal epithelial layer of Bowman's capsule, the urinary space (US), podocytes (arrowheads) of the visceral epithelium, proximal convoluted tubules (PT), peritubular capillaries and an interlobular artery can be distinguished.

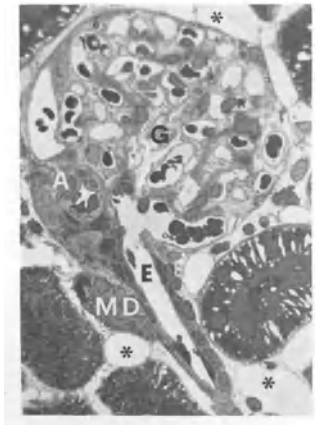

Fig. 10. Rat kidney. Juxtamedullary glomerulus (G). A: afferent arteriole; E: efferent arteriole; MD: macula densa. The asterisks point to peritubular and periglomerular capillaries. ×640.

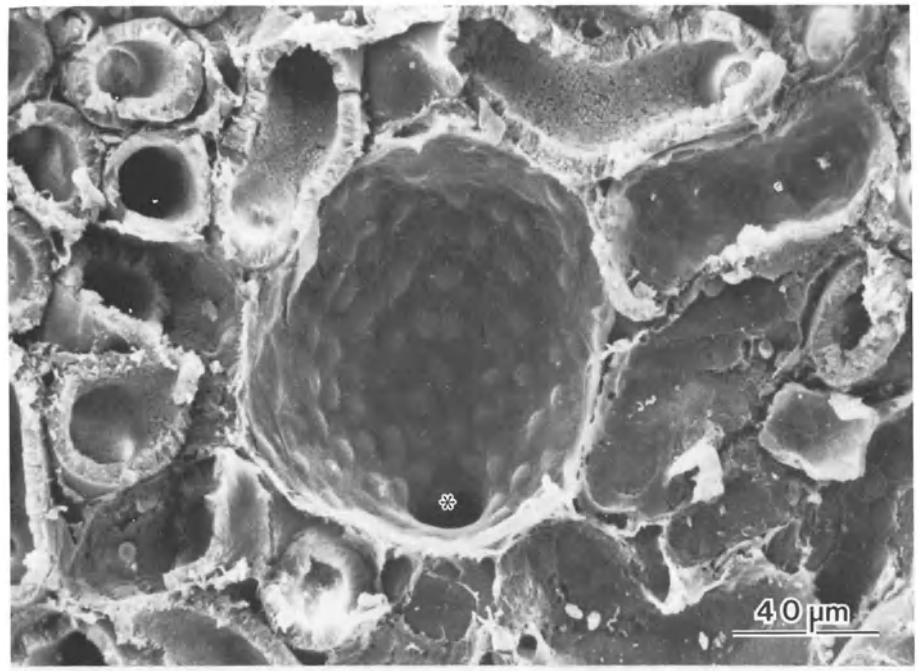

11

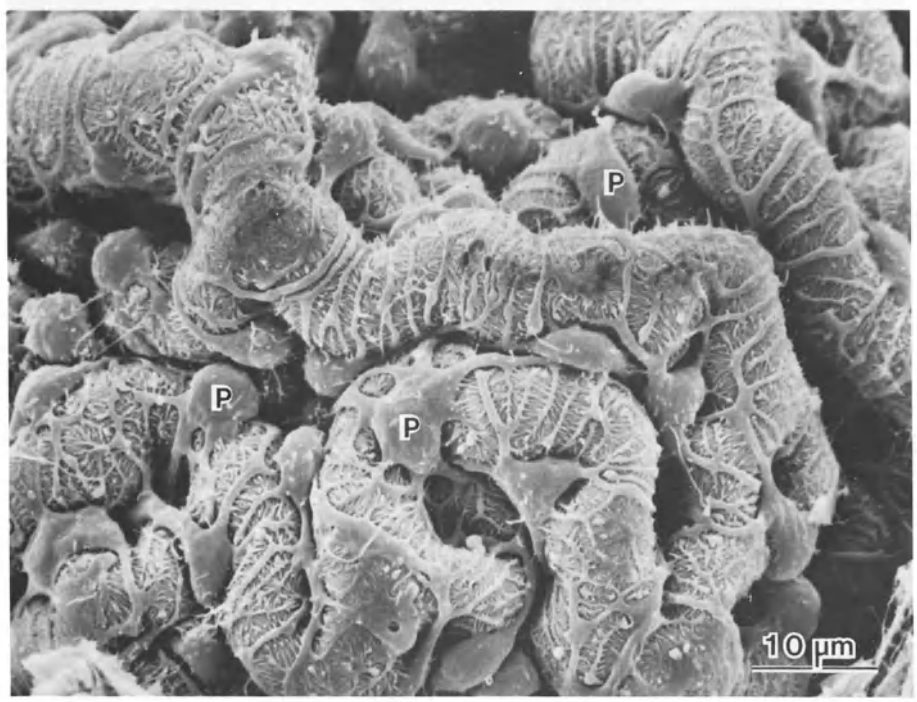

12

Fig. 11. SEM of a portion of the parietal layer of Bowman's capsule after removing the glomerulus. The funnel-shaped urinary pole (*) of the parietal epithelium lies opposite the vascular pole. Note the many rounded protuberances on the parietal surface of the capsule, facing onto the urinary space, created by the underlying nuclei of the otherwise thin squamous epithelial cell layer.
Fig. 12. SEM (low magnification) of the visceral layer of Bowman's capsule showing specialized, polymorphic podocytes (P). The coiled configuration of underlying capillary loops can be recognized with the processes of podocytes interdigitating to enclose and surround the entire glomerular capillary surface.

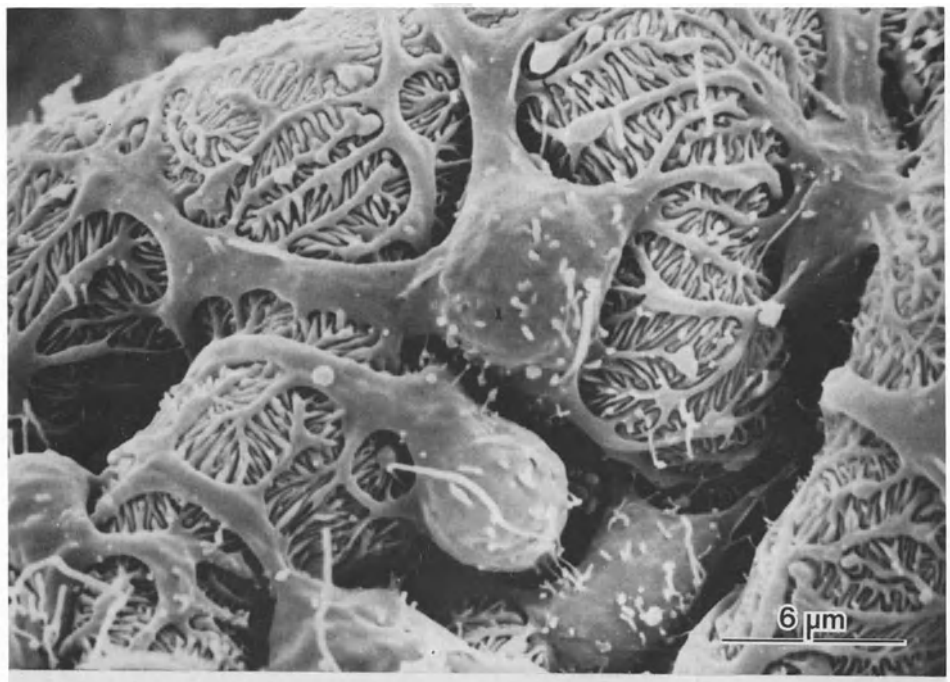

13

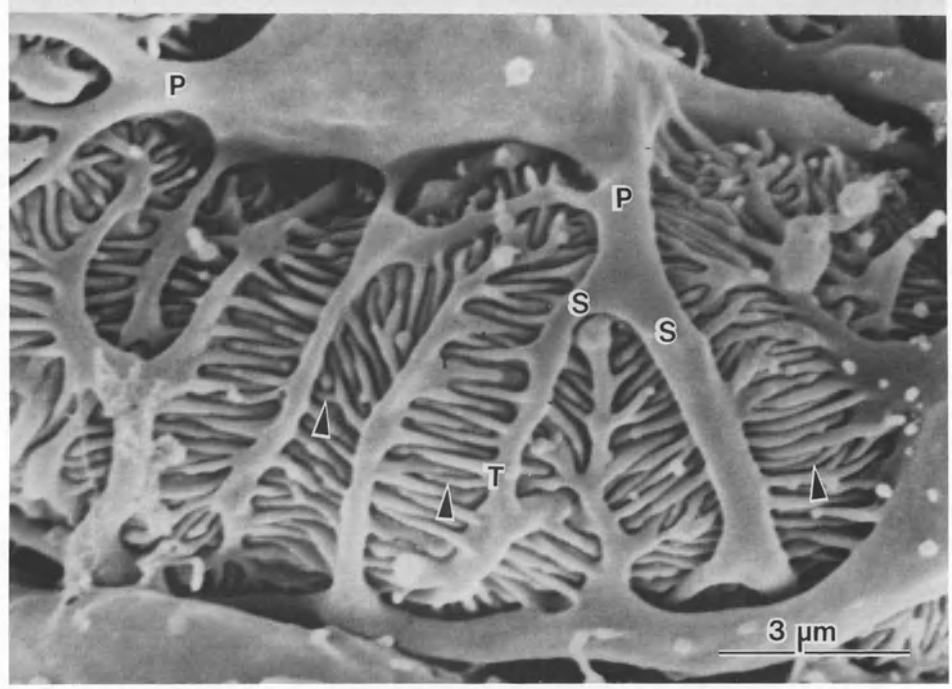

14

Fig. 13. SEM of podocytes, cells which comprise the visceral layer of Bowman's capsule and underlying capillary coils. The cytoplasmic extensions originating from the nucleated cell body of a podocyte vary in size, shape and degree of branching, and account for the polymorphism observed in these specialized cells. Note the variation in number and length of microappendages associated with the free surface of the podocytes.

Fig. 14. Podocyte cytoplasmic bifurcation pattern as demonstrated in SEM. Consecutive branching of the podocyte cytoplasm results in four orders or generations of processes: primary (P), secondary (S), tertiary (T) and quaternary (arrowheads). The fourth or terminal generation of processes is referred to as pedicels, and interdigitate with those from an adjacent podocyte.

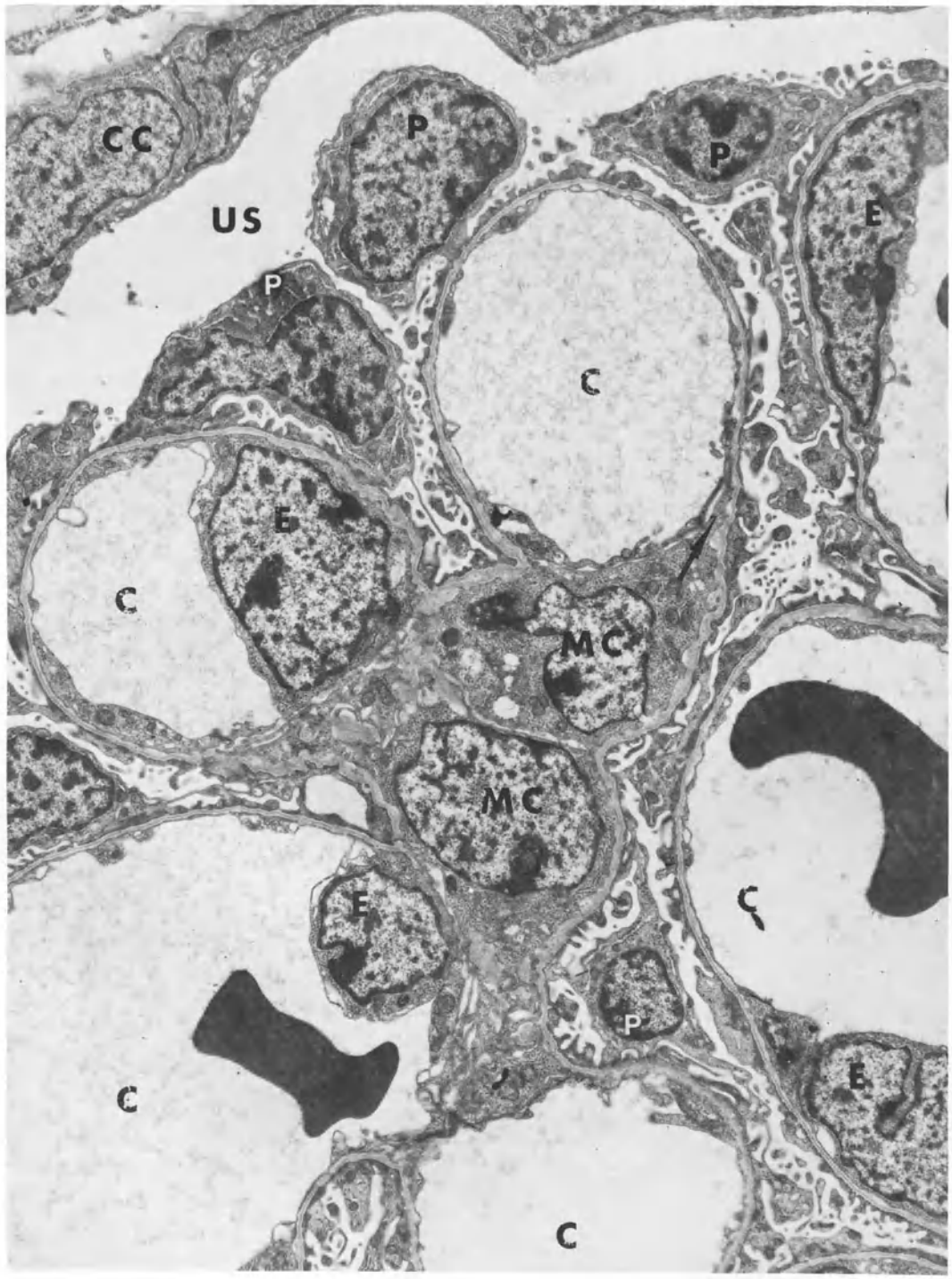

Fig. 15. Peripheral part of human newborn glomerulus. C: capillary lumen; P: visceral epithelial cell or podocyte; E: endothelium; MC: mesangial cells. The arrow indicates a cytoplasmic projection of a mesangial cell. CC: epithelial cell of the Bowman's capsule; US: urinary space. ×4.000.

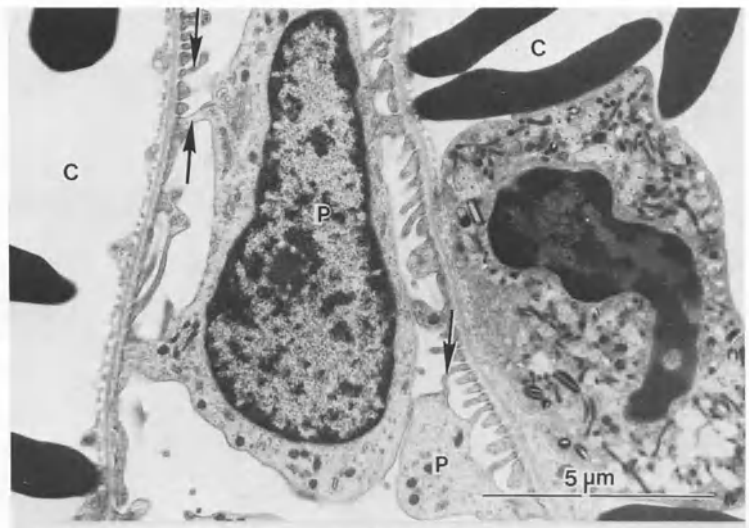

16

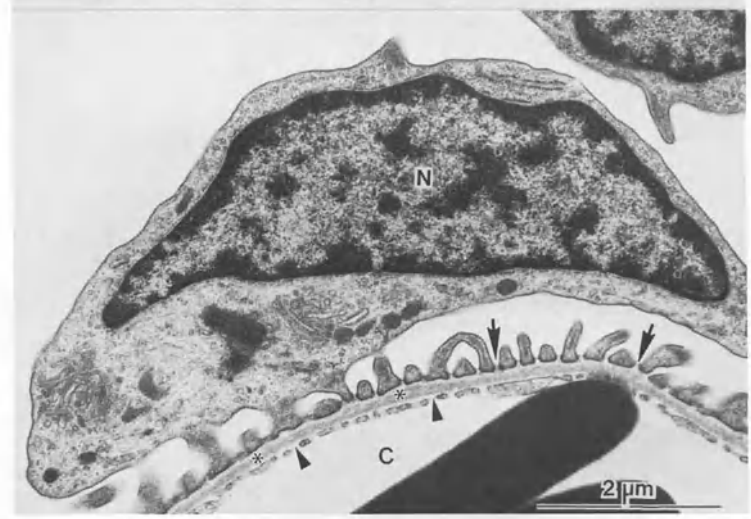

17

Fig. 16. TEM of a renal glomerulus in the dog. Two adjacent capillary loops (C) containing blood cells and portions of glomerular podocytes (P) with their numerous small foot processes referred to as pedicels (arrows) are shown investing the glomerular capillary.
Fig. 17. TEM showing further details of the glomerular capillary (C) and surrounding podocytes. A podocyte cell body with its nucleus (N), well-developed Golgi, rough-surfaced endoplasmic reticulum and many cytoplasmic extensions can be distinguished. The terminal foot processes or pedicels are shown to be contiguous with the basal lamina (*). Note the fenestrations (arrowheads) of the capillary endothelium and the filtration slits (arrows) between juxtaposed pedicels.

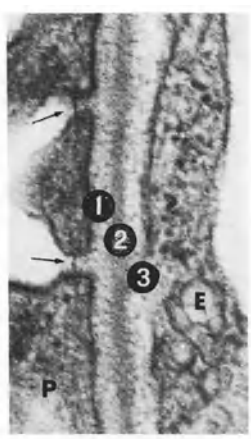

Fig. 18. Human glomerular capillary wall. E: endothelium; P: podocyte; 1) 'subepithelial zone' of the basement membrane; 2) 'lamina densa'; 3) 'subendothelial zone: of the basement membrane. The arrows point to the central knobs of the filtration slit membranes. ×60,000.

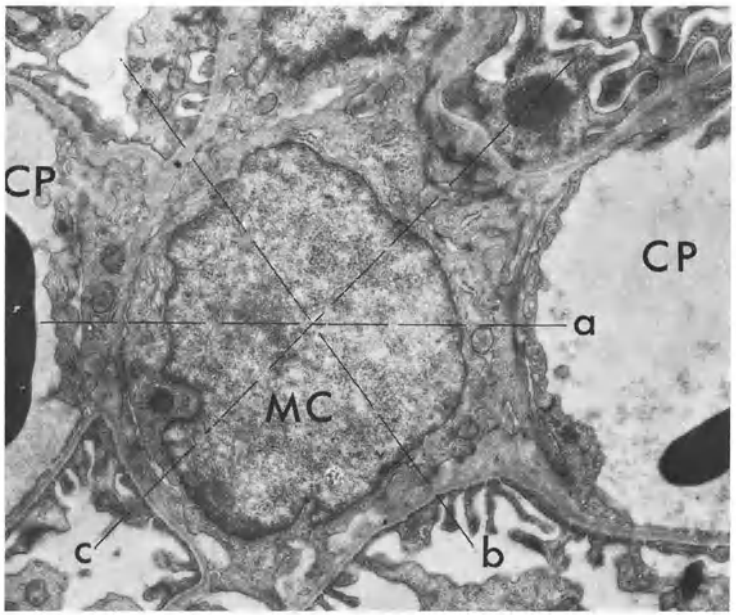

Fig. 19. The electron micrograph shows the topographic relationship between a mesangial cell (MC) and other glomerular structures. The mesangial cell is situated between endothelial cells (plane a) and podocytes (planes b and c). The parietal location of the mesangial cell appears evident considering that the capillary lumina (CP) belong to capillaries shortly after they branch from a common stem (from: Zamboni L. and De Martino C., Z. Zellforsch., 86: 364–383, 1968) ×10,200.

Fig. 20. Rat kidney. The micrograph shows the continuity between the smooth muscle cells (SM) of the afferent arteriole (A) and the glomerular mesangial cells (MC). The arrows indicate the boundaries of the glomerular hilus. Note that the juxtaglomerular granulated cells (GC) do not progress beyond the vascular hilus. P: podocyte; E: endothelium; US: urinary space. (From: Zamboni L. and De Martino C., Z. Zellforsch. 86: 364–383, 1968). ×8,800.

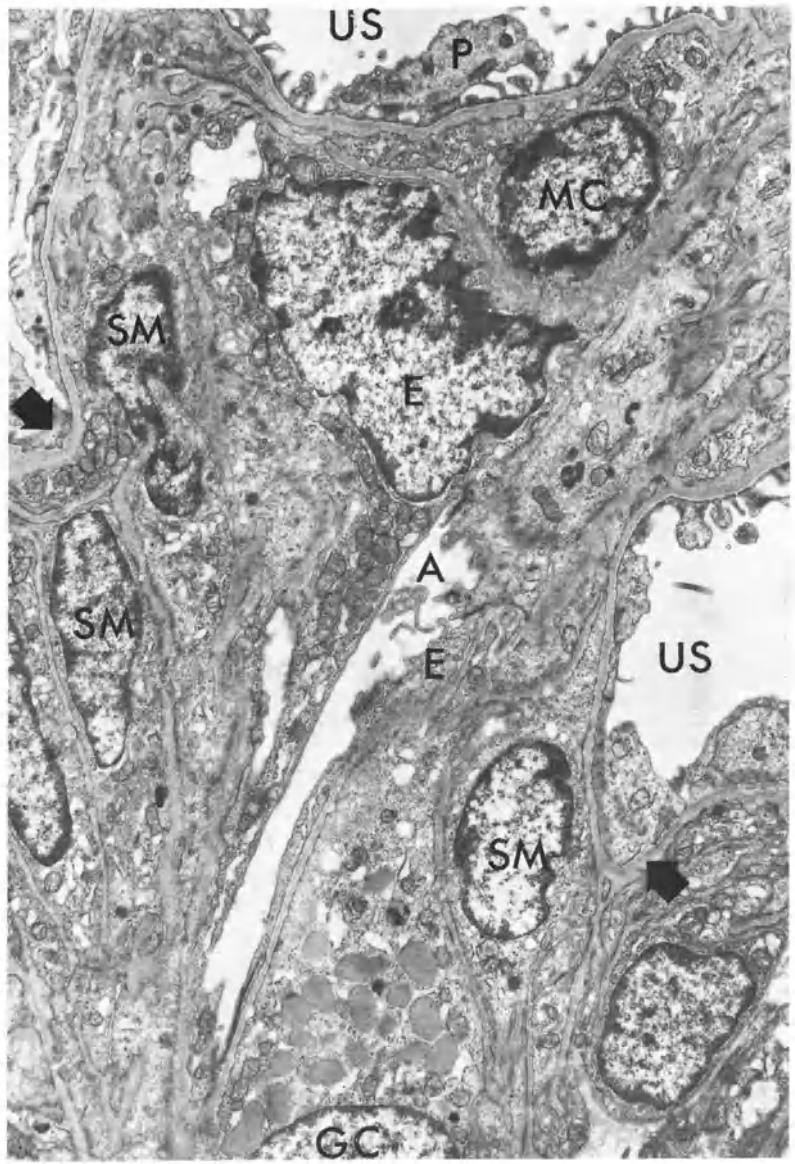

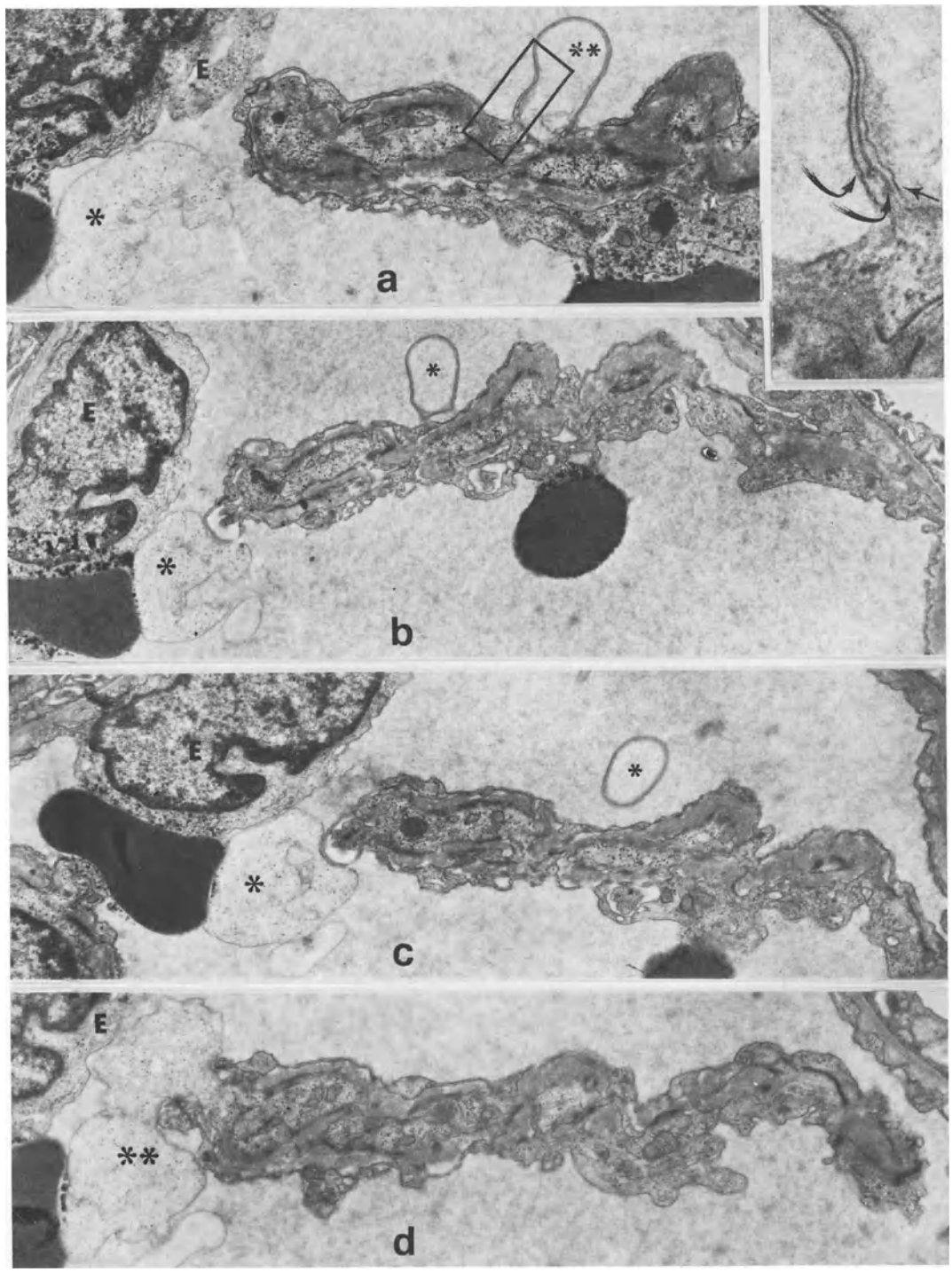

Fig. 21. Serial sections (a, b, c, d) from a human glomerulus showing the penetration of mesangial pseudopodia into the lumen of a capillary. In some sections the connections of the pseudopodia with the mesangium are evident (double asterisk); in others the mesangial pseudopodia are cross-sectioned and appear free in the lumen (single asterisk). The inset in the upper right corner illustrates, at higher magnification, the boxed area of Fig. 21a. The curved arrows point to the outer and inner endothelial plasmamembranes; the straight arrow indicates the plasmamembrane of the mesangial pseudopodium. Fig. 21a, b, c, d, ×6,800; inset, ×25,000.

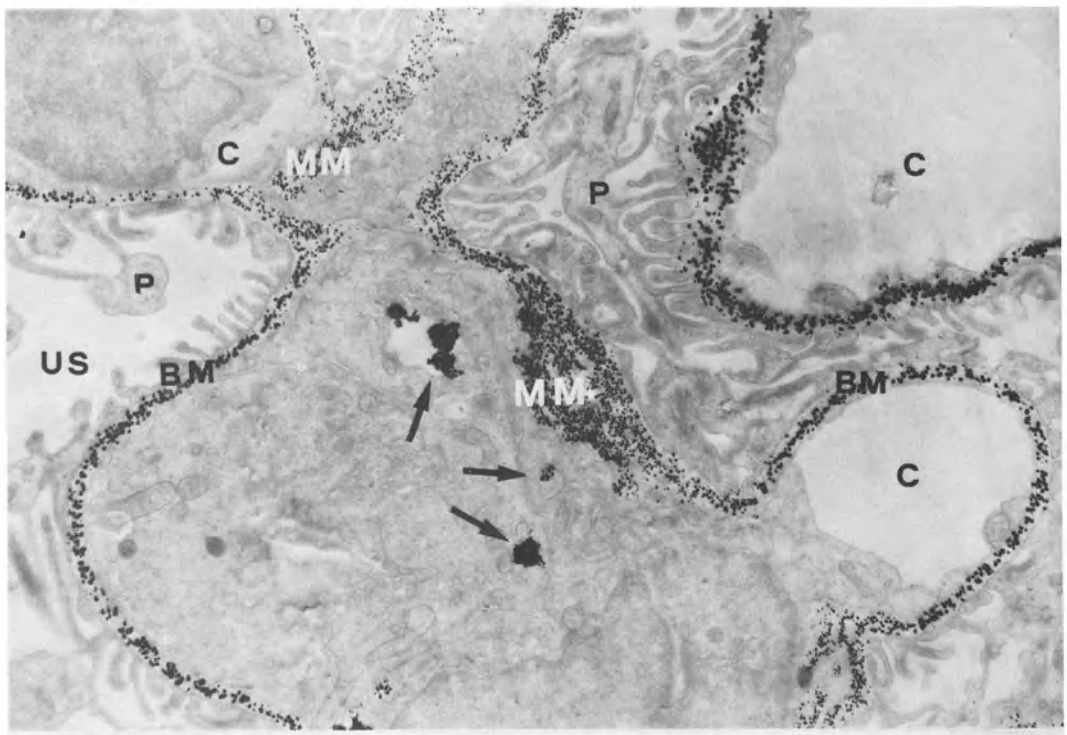

22

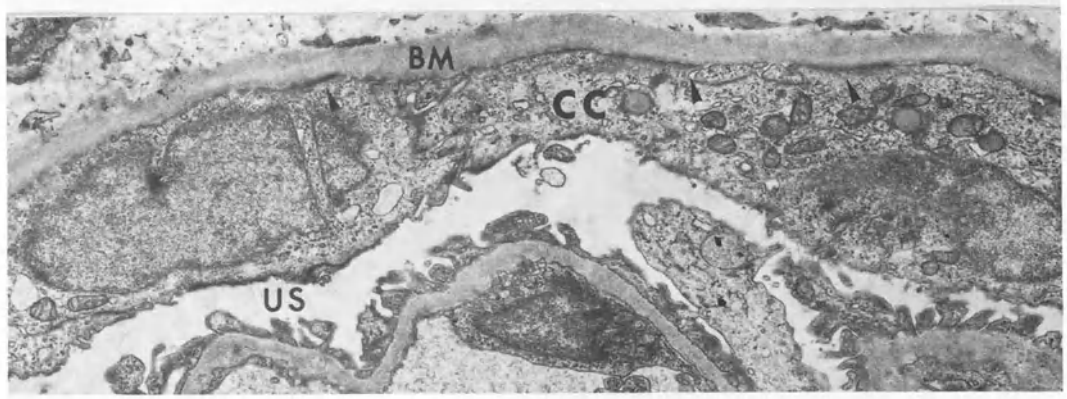

23

Fig. 22. Rat kidney. The animal was given, as drinking water, distilled H_2O containing 0.2% $AgNO_3$ for 3 months. $AgNO_3$ is localized in the glomerular basement membrane (BM), in the mesangial matrix (MM), and in cytosomes (arrows) of the mesangial cells. C: capillary lumen; P: podocytes; US: urinary space. ×9,000.

Fig. 23. Human kidney. The Bowman's capsule is formed by the basement membrane (BM) and a layer of flattened parietal epithelial cells (CC). The arrows indicate myofilaments and their attachment bodies. US: urinary space. ×6,000.

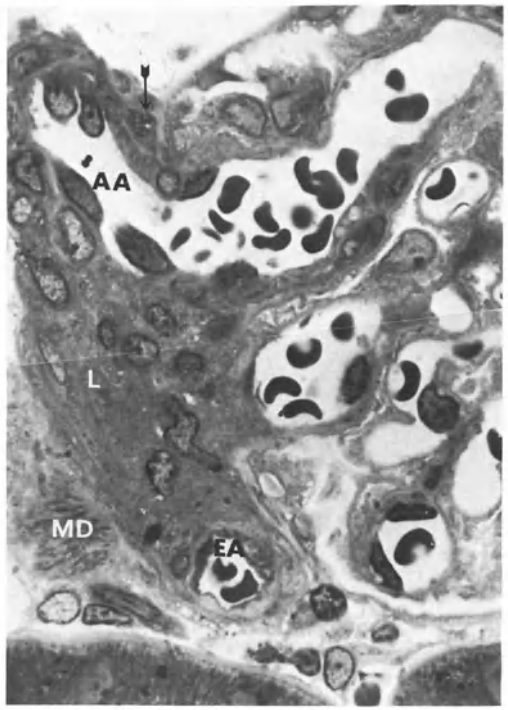

Fig. 24. Juxtaglomerular apparatus of rat kidney. MD: macula densa; L: lacis cells or polkissen; AA: afferent arteriole; EA: efferent arteriole of muscular type. ×800.

Fig. 25. Rat kidney. Morphologic relationships between macula densa (MD), lacis cells (L) and afferent (AA) and efferent (EA) arterioles. The cells of the macula densa are packed together with the appearance of a pseudostratified epithelium. Numerous intercellular spaces are present in the basilar part of the cells (arrows). The tubular basement membrane forms a network with the basement membrane surrounding the lacis cells. On the opposite side, the cells (T) show cuboidal shape and morphological features typical of the distal convoluted tubule. The arrowhead points to the boundary of the glomerular hilus. GL: glomerulus. ×4,880.

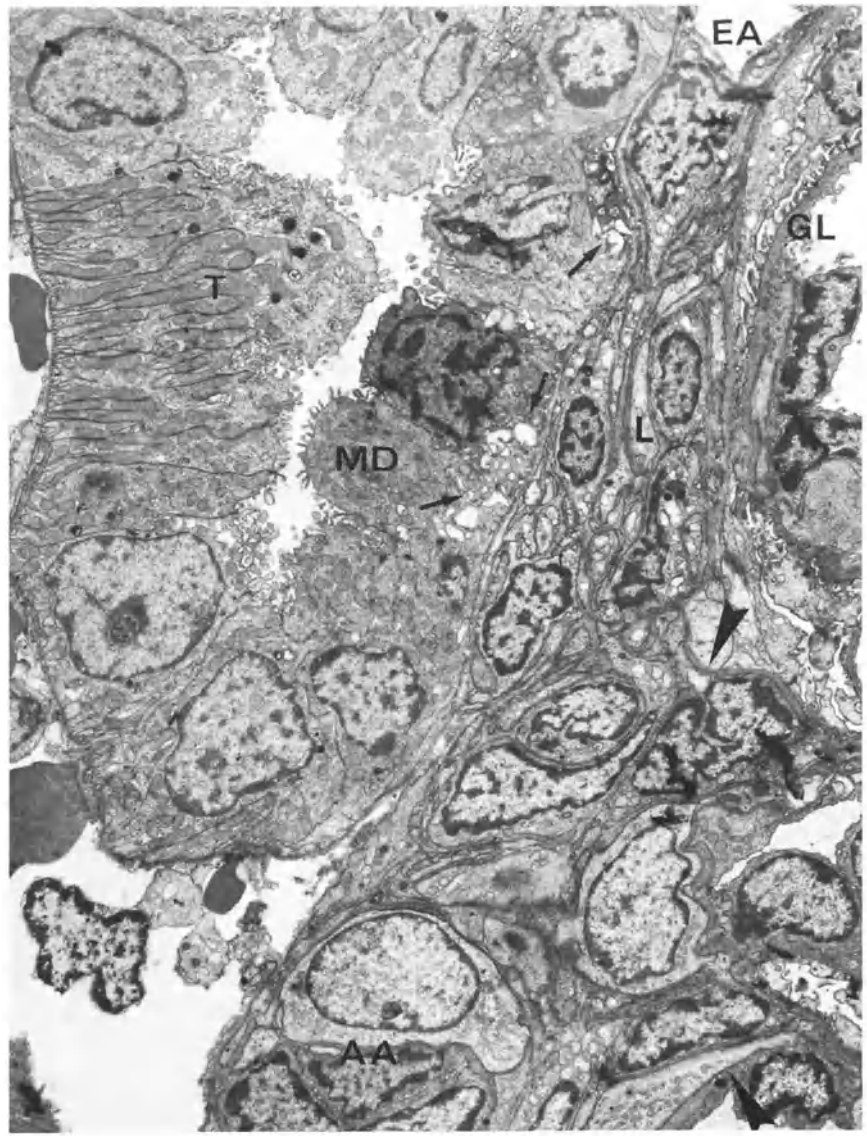

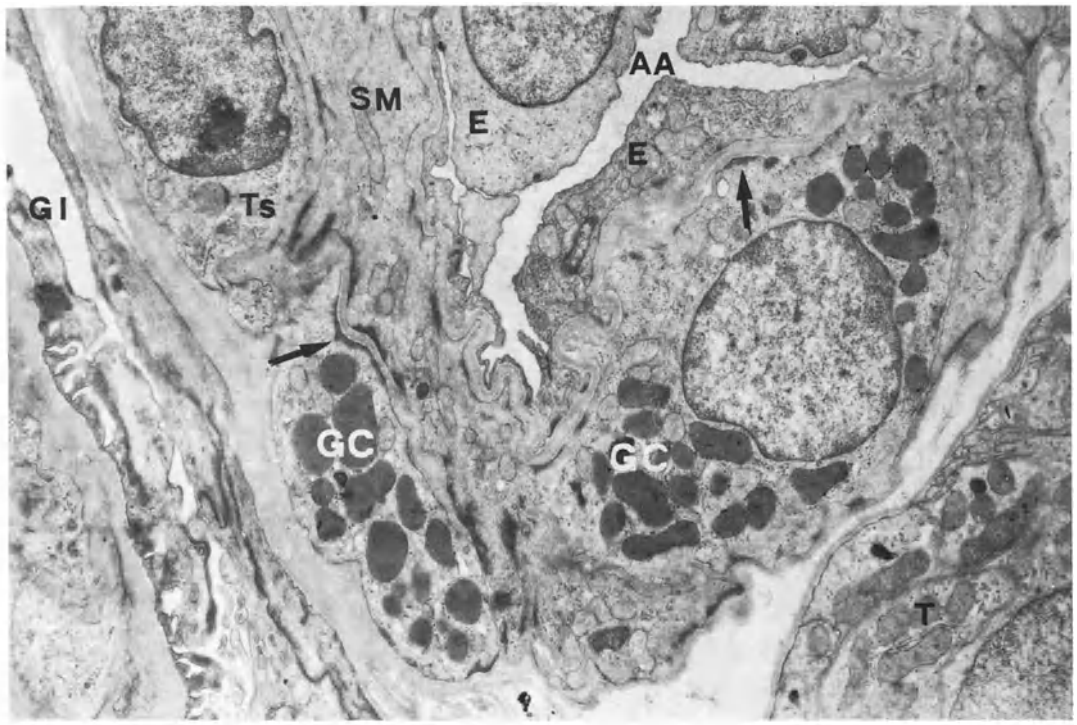

26

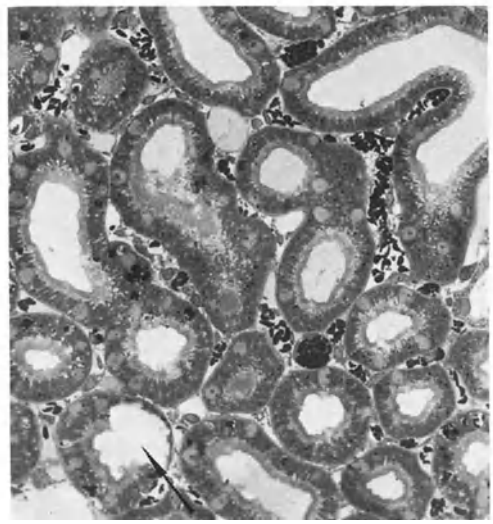

27

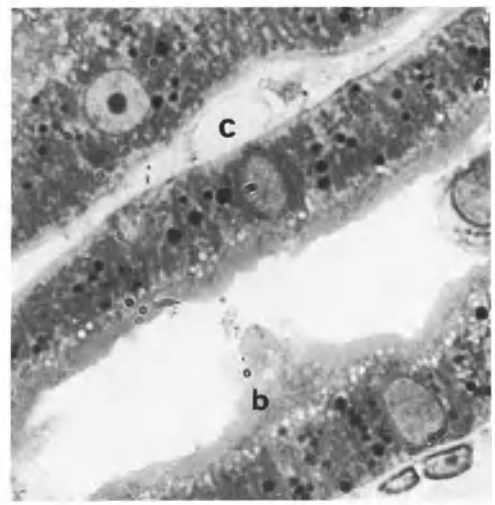

28

Fig. 26. Afferent arteriole (AA) of a rat glomerulus. The media of the vessel is formed by smooth muscle (SM) and granulated (GC) cells. A transitional cell (Ts) is visible. The arrows indicate attachment bodies. E: endothelium; GL: glomerulus; T: tubule. ×7,000.
Fig. 27. Rat kidney cortex. Fixation by 'in vivo' perfusion. Cross-sectioned proximal tubules. The arrow points to the transitional segment between the pars recta of a proximal tubule and the thin descending limb of Henle's loop. Note the widely patent tubular lumina. ×300.
Fig. 28. Rat kidney cortex. Fixation by 'in vivo' perfusion. Longitudinal section of a proximal convoluted tubule. The cell cytoplasms contain dense osmiophilic granules, probably cytosomes. c: peritubular capillary; b: brush border. ×1,000.

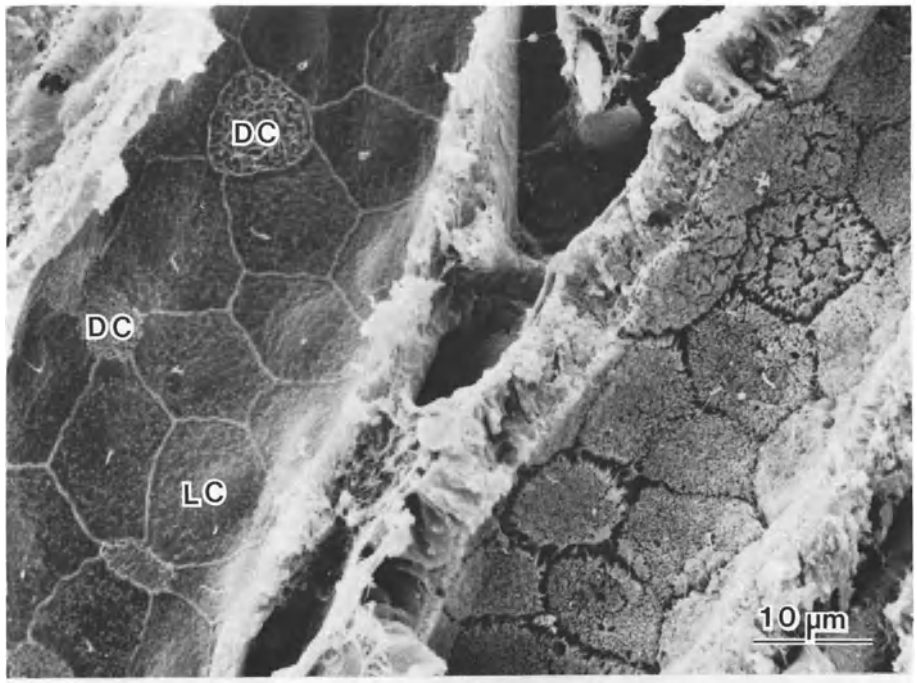

29

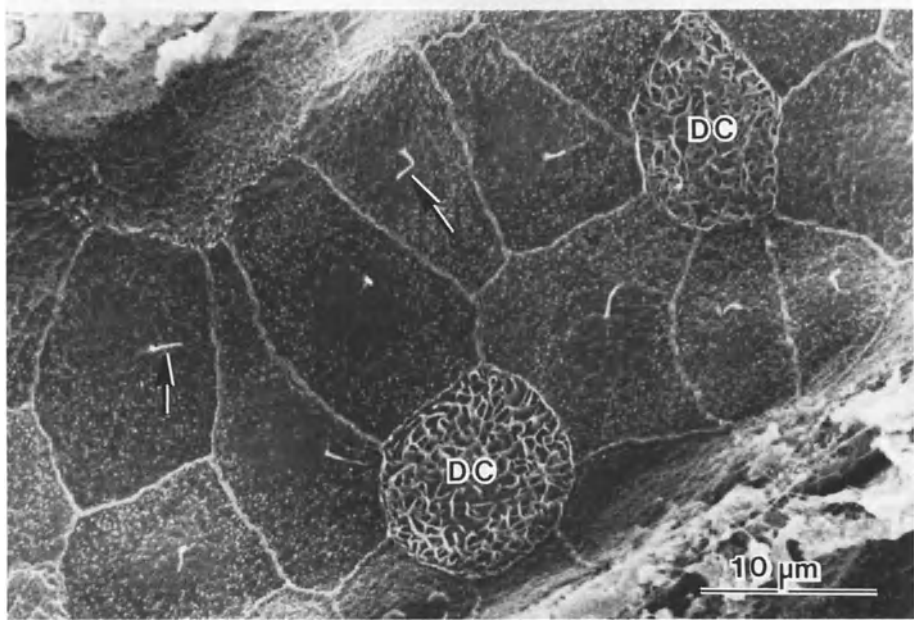

30

Fig. 29. SEM of the luminal surface of a proximal convoluted tubule and a cortical collecting tubule in longitudinal section. The wall of the collecting tubule (left) is comprised of two cell types, the light cell (LC) and the dark cell (DC). The lumen of the distal convoluted tubule (right) is covered by dense apical microvilli projecting from the underlying hexagonal-shaped cells.
Fig. 30. The two cell types found in the wall of a cortical collecting tubule as seen at a higher magnification. The light cells are more numerous and usually possess many short apical microvilli and a single long cilium (arrows), while the dark cells (DC) are identified by their thin apical folds or flaps referred to as microplicae.

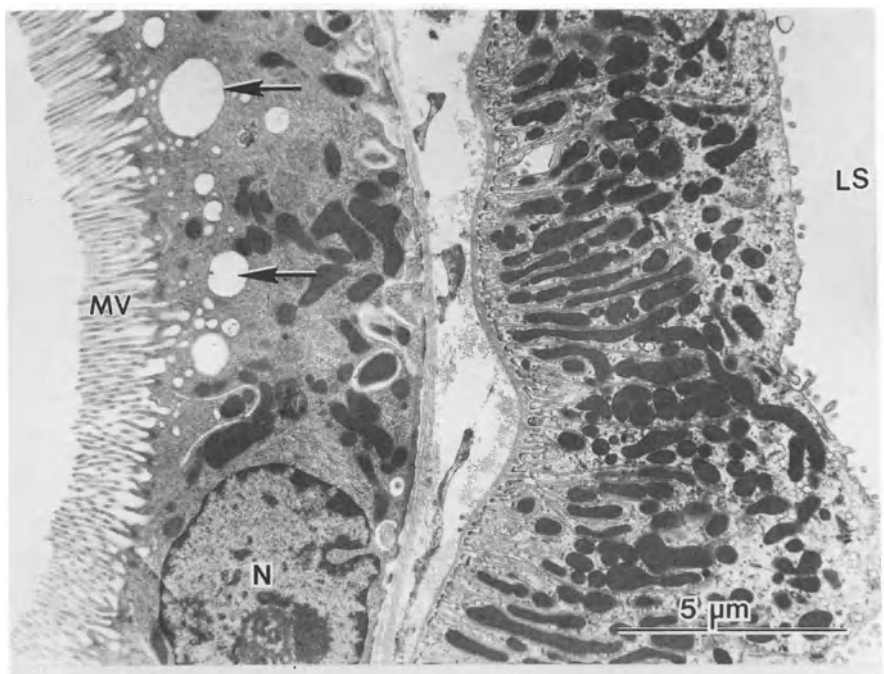

31

32

33

Fig. 31. TEM of a proximal (left) and a distal (right) convoluted tubule cell is characterized at low magnification by a large, oval nucleus (N), apical vacuoles (arrows), numerous mitochondria, and a brush border of microvilli (MV). The distal convoluted tubule cell is identified by short, narrow microvilli on their luminal surface (LS), the absence of a brush border, basal infoldings and long, densely packed mitochondria which are usually oriented perpendicularly to the long axis of the tubule. Note the scattered collagen fibrils in the cortical stroma between these two tubules.

Fig. 32. SEM of a transverse view through a proximal convoluted tubule. A dense, elaborate brush border can be distinguished on the luminal surface (LS) and the complex, interdigitating relationship of the lateral cell processes is discernible in this micrograph.

Fig. 33. The luminal surface of a proximal convoluted tubule as revealed in SEM. Note the density and uniform height of the microvilli which form the brush border in this area, and the underlying apical canaliculi (arrows) where microvilli have been removed.

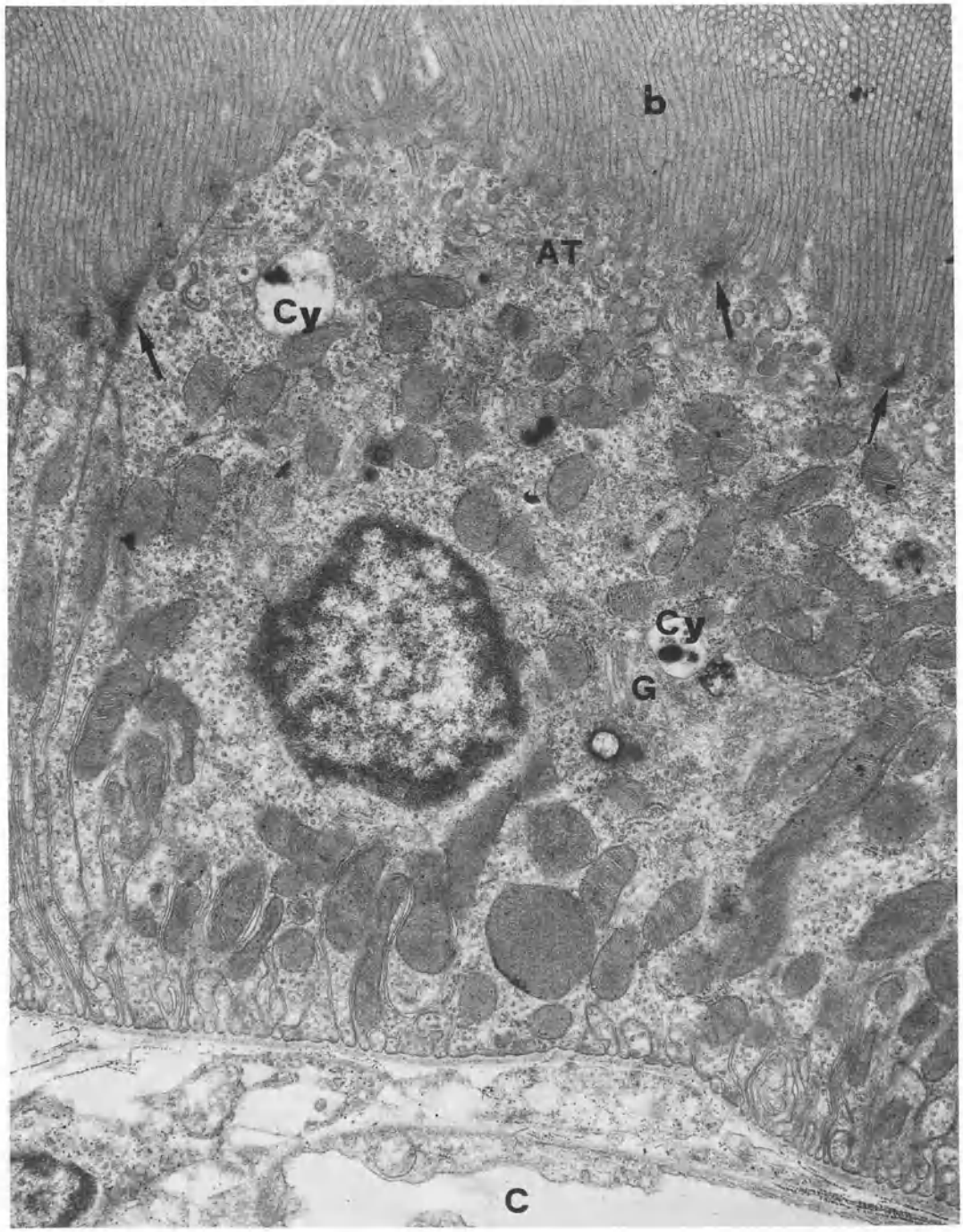

Fig. 34. Rat kidney cortex. Silver methenamine stain without periodic acid oxidation. The micrograph shows part of a proximal convoluted tubule. In the upper part of the picture several junctions (arrows), apical dense tubules (AT), the Golgi apparatus (G) and cytosomes (Cy) are visible. The free surface of the cell is covered by closely packed, long microville constituting the brush border (b). The lower part of the picture shows the infoldings of the basal plasmamembrane and numerous elongated mitochondria. C: peritubular capillary. ×9,000.

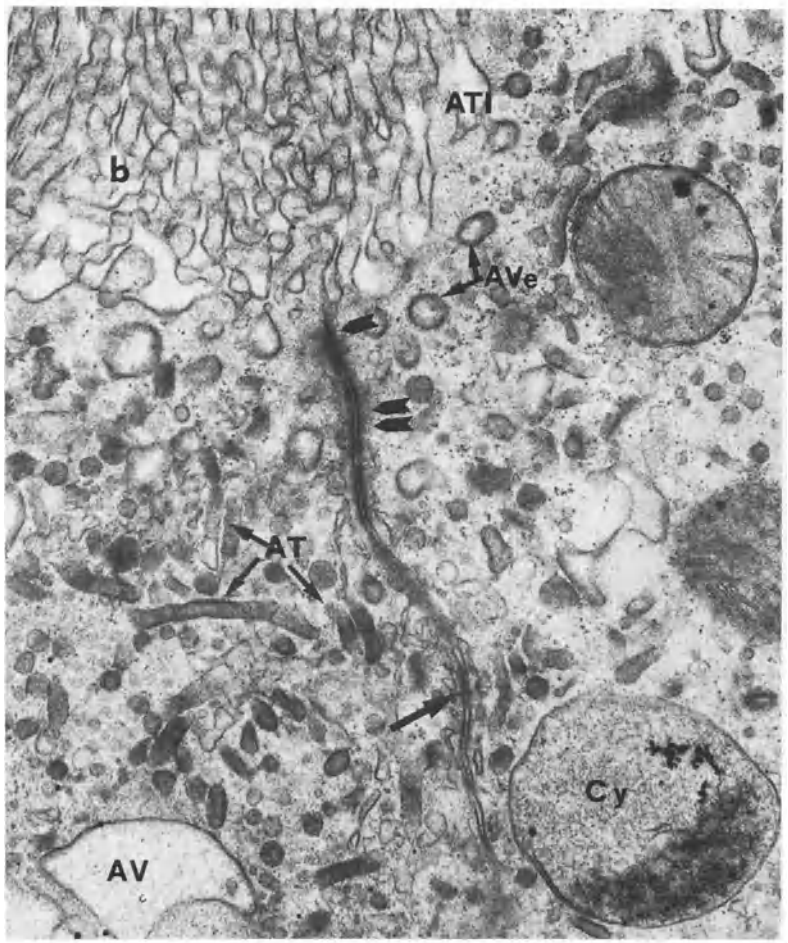

35

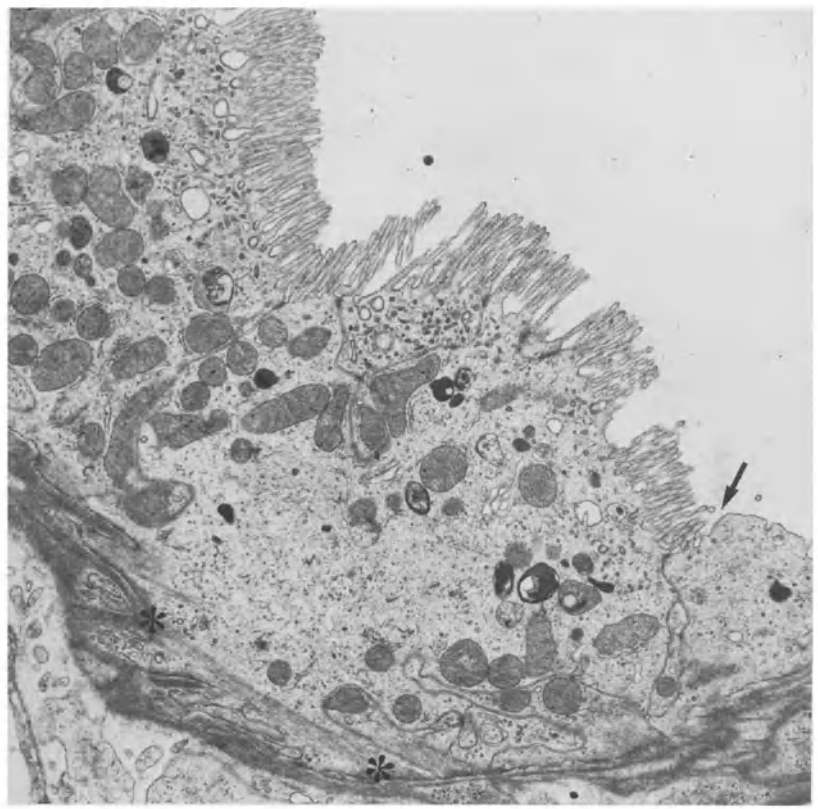

36

Fig. 35. Apical cytoplasm of two adjacent cells of a proximal convoluted tubule. The cell junction consists of a tight junction or zonula occludens (arrowheads), intermediate junction or zonula adherens (double-head arrow), and desmosome (arrow). b: brush border; AV: apical vacuoles; ATI: apical tubular invagination; AVe: apical vesicles; AT: apical dense tubules; CY: cytosome. ×28,800.

Fig. 36. Mouse kidney. Pars recta of a proximal tubule at the transition segment with the thin descending limb of Henle's loop (arrow). The morphological features are less complex than those of the pars convoluta (see text). Note a bundle of basal filaments which joins two attachment bodies (asterisks). ×5,600.

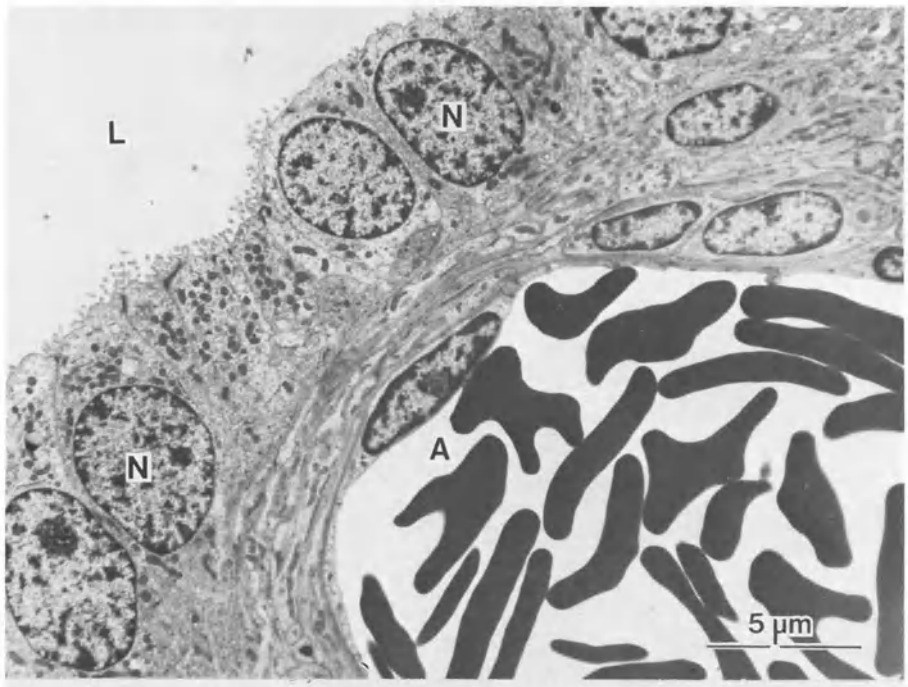

37

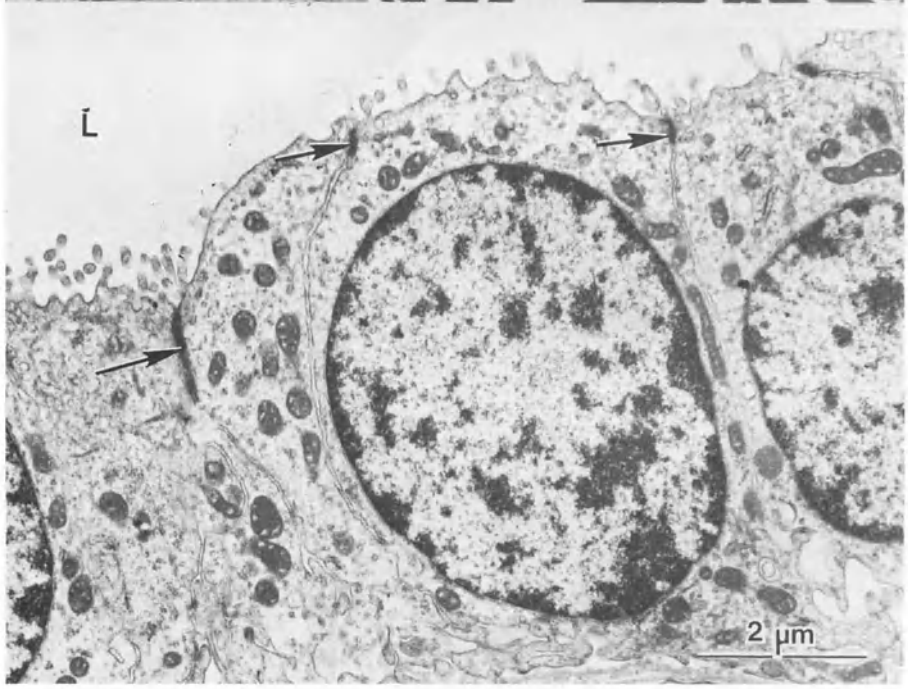

38

Fig. 37. TEM of a transverse section through a distal ascending segment and its associated arteriole (A). The lumen (L) of a tubule returning to its parent renal corpuscle is shown as it passes near one of the arterioles at the vascular pole. The rounded nuclei (N) of tubular epithelial cells and the elongated nuclei of endothelial cells of the arteriole are apparent.

Fig. 38. TEM of distal ascending tubule cells. Portions of several epithelial cells face the lumen (L) of this distal segment in an area near the vascular pole known as the macula densa. Note the very short microvilli projecting into the lumen, the junctional complexes (arrows) and the numerous mitochondria.

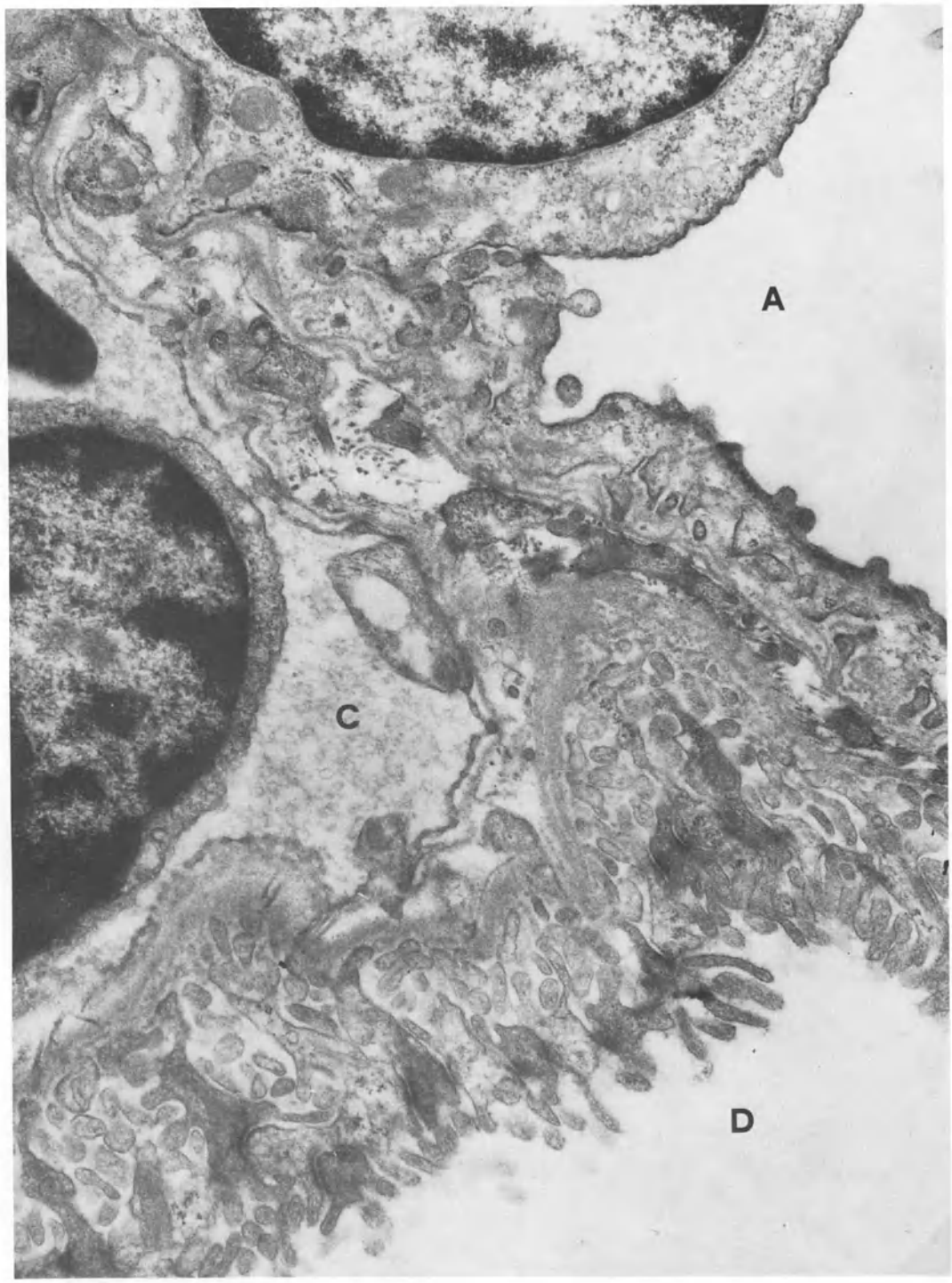

Fig. 39. Mouse renal papilla. Fixation by 'in vivo' perfusion. Descending (D) and ascending (A) thin limbs of Henle's loop. Note the abundance of apical microvilli and basal-lateral interdigitations of the plasmamembranes in the descending thin limb (D) and the paucity of the same structures in the ascending segment (A). C: lumen of vasa recta. ×21.000.

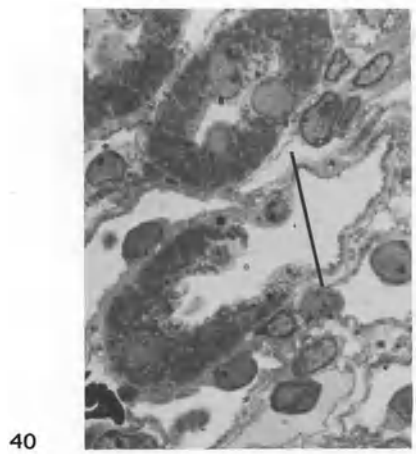

40

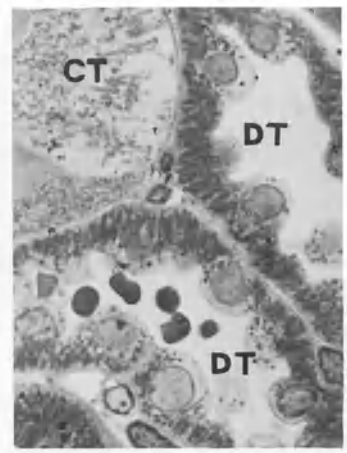

41

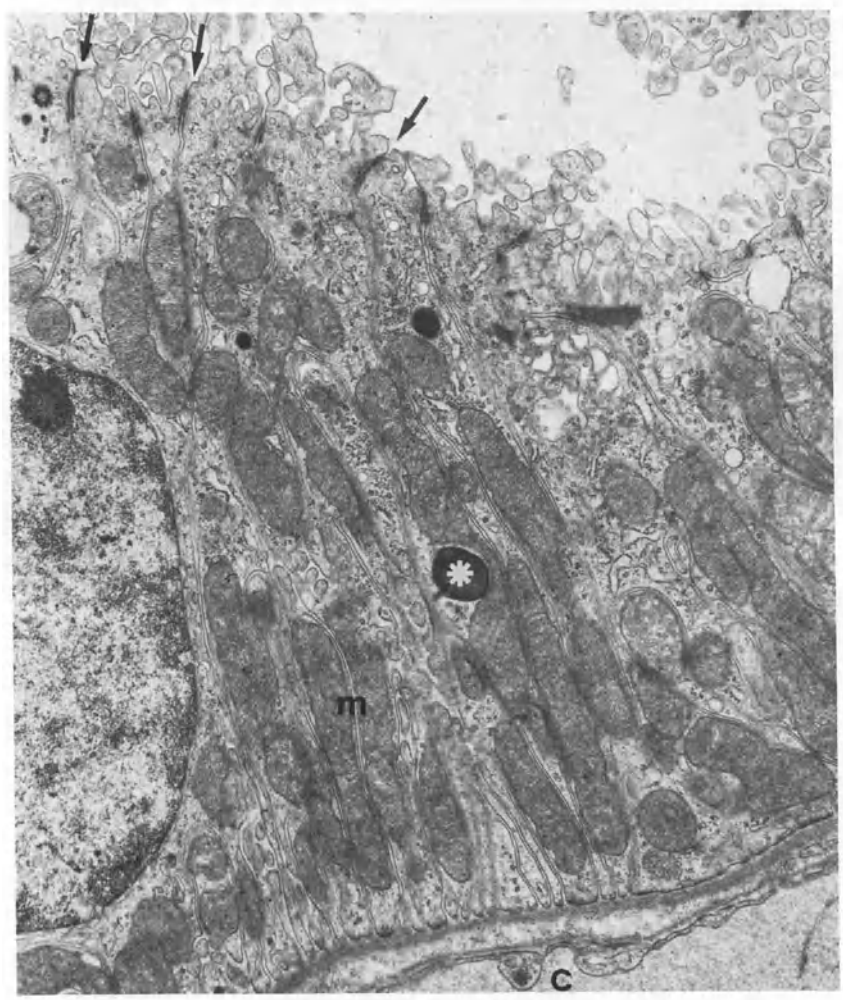

42

Fig. 40. Rat kidney. Transitional part between thin (a) and thick (b) portions of Henle's loop. ×1,000.
Fig. 41. Human kidney. Distal convoluted tubule (DT) and collecting tubule (CT). The nuclei of the cells of the distal tubules bulge into the lumen. ×1,000.
Fig. 42. Human kidney. Distal convoluted tubule. The nucleus (N) is in the mid-part of the cell. Short microvilli are visible in the apical plasmamembrane. The basal cytoplasm contains numerous elongated mitochondria (m) placed between the infoldings of the basal plasmamembrane. The arrows point to apical junctional complexes. Asterisk: cytosome; c: peritubular capillary. ×12,000.

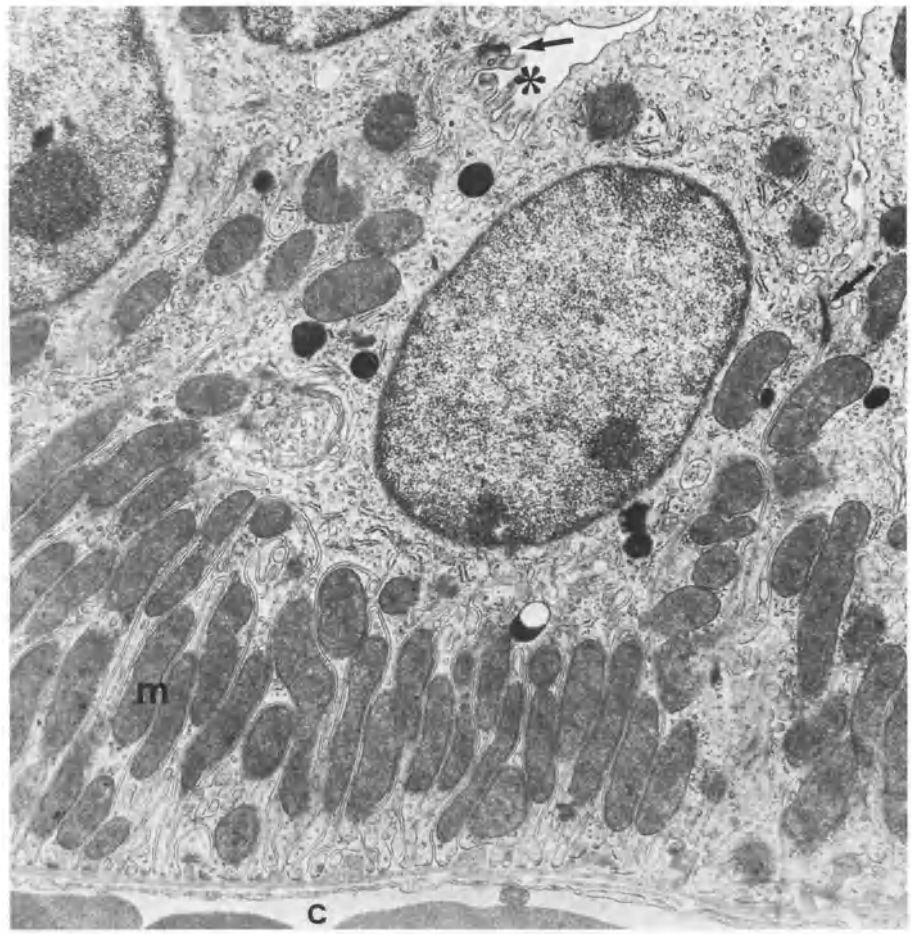

Fig. 43. Mouse kidney. Transitional part between a distal tubule and a collecting tubule. The apical plasmamembrane of the cells possesses occasional microvilli (asterisk). The apical cytoplasm bulges above the level of the junctional complexes (arrows). Numerous vertically arranged mitochondria (m) are present between the infoldings of the basal plasmamembrane. c: peritubular capillary. ×13,500.

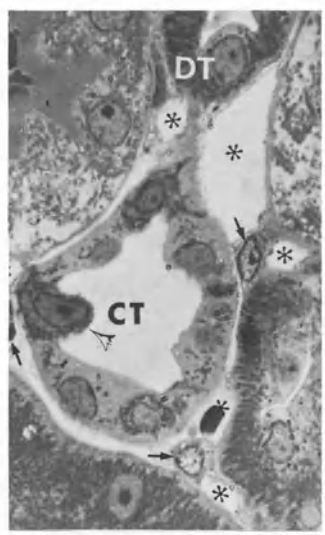

Fig. 44. Human kidney. Collecting tubule (CT) with 'light' or principal' and 'dark' or 'intercalated' (arrows) cells. The asterisks indicate peritubular capillaries. ×1,000.

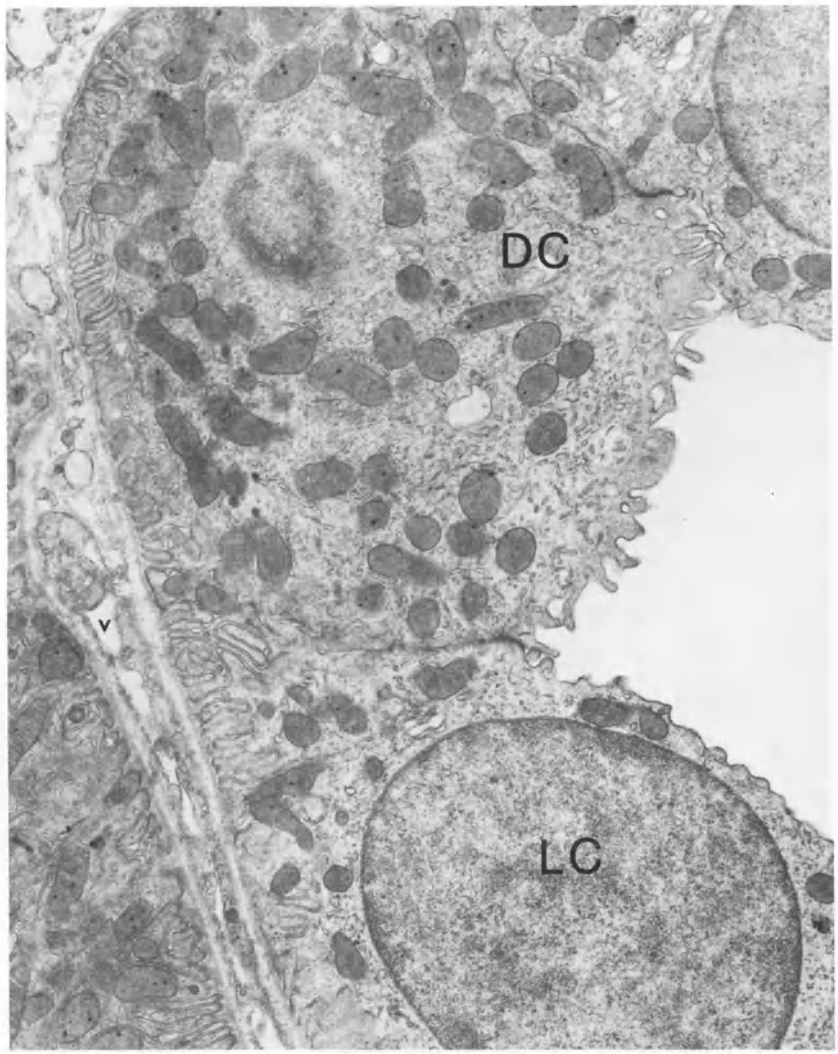

Fig. 45. Collecting tubule in the juxtamedullary cortex. Dark (DC) and light (LC) cells. The dark cell shows more numerous mitochondria, vesicles, and microvilli than the light cell. ×13,000.

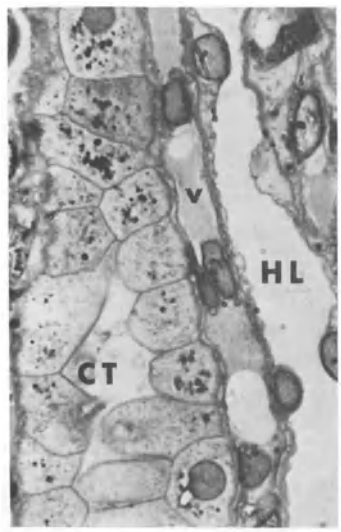

Fig. 46. Human kidney. Longitudinal section of the renal papilla showing the morphologic relationship between Henle's loop HL), vasa recta (v) and collecting tubule (CT). ×1,000.

CHAPTER 5

Renal vasculature as observed by SEM of vascular casts. Basic architecture, development and aging of glomerular capillary beds

TAKURO MURAKAMI, AKIO KIKUTA, AIJI OHTSUKA and TETSUJI KANESHIGE

1. Introduction

Scanning electron microscopy (SEM) of sample casts allows clear three-dimensional and long range viewing of fine blood vascular beds and other vascular systems, previously poorly visualized by conventional light or transmission electron microscopy of sectioned samples [1, 2, 3, 4, 5, 6, 7]. Spatial relations between the vessels and surrounding tissue elements cannot be examined in the cast as it is observed in isolation. Despite this limitation, displaying vascular patterns as independent structures already has proven useful and valuable in the study of microvascular architecture and microcirculation in various organs and tissues, including the kidney [8, 9, 10, 11, 12, 13, 14].

Many injection or casting media are available for preparation of suitable casts for scanning electron microscopy. Low viscosity methacrylate media, including commercially available Mercox and Batson's plastic, usually are used because of ease in handling and good casting of minute vessels [1, 2, 3, 4, 5, 6, 7, 15, 16, 17]. A monomeric methyl and hydroxypropyl methacrylate mixture supplemented with benzoyl peroxide and N,N-dimethylaniline is very fluid, and thus, of great value in casting very fine vessels, and liver bile canaliculi [18].

This chapter reviews renal microvascular architecture, especially glomerular tufts. Scanning electron micrographs of methacrylate casts of human and rat samples are shown as evidence of the power of this method to define fine vascular channels.

1.1. Preparation and scanning electron microscopy of methacrylate casts of renal blood vasculature

Scanning electron microscopy of casts is a three-step process: (1) injection of casting medium, (2) digestion and removal of tissue elements and (3) cast dissection and scanning electron microscopy.

Fresh kidneys, including human autopsy samples, are flushed thoroughly via their arteries with saline or other physiological solutions. Failure to remove blood results in poor penetration of casting media into fine capillaries. Semipolymerized or commercially available low viscosity methacrylate casting media are then injected gently via the same arterial vessels until the efferent veins are filled with the medium. The complete blood vascular beds, including capillaries and veins, are reproduced (for examples see Figs. 2–5). Partial injection via arteries or veins forms partially-injected casts. These partial casts allow preferential observations of arterio-glomerular (see Fig. 8), glomerulo-capillary (see Fig. 6, 7) and veno-capillary connections (see Fig. 9). The partial injection also facilitates isolation of glomeruli, allowing accurate identification of afferent and efferent vessels [8] (examples, Figs. 10, 11).

Injected organs are placed in a warm water bath (60° C) to maintain original form and also to accelerate polymerization. Specimens are subsequently digested in a warm (60° C) hydroxide sodium or potassium solution and washed in running tap water. The corrosion and washing remove tissue elements. The blood vascular casts thus prepared are frozen in water, trimmed into appropriate blocks, air-dried, mounted on metal stubs, and coated with metals such as gold and platinum or exposed to osmium tetroxide vapor [19, 20]. The metal-coated or osmium-impregnated casts are observed by scanning electron microscopy.

Alternating microdissections and microscopy of the casts permit clear visualization of the vessels and thorough examination of their distribution and connections. Microdissection techniques include cutting, fracturing, and sectioning of wet, frozen, ethanol-substituted or dried casts with razor blades, forceps, and needles under the light microscope (see Fig. 15). The ethanol substitution softens the casts, minimizing breakage of vascular connections during microdissection. Dissection in ethanol is of special

L.J.A. DiDio and P.M. Motta (eds), Basic, Clinical, and Surgical Nephrology. ISBN 0-89838-689-5.

value in analysis of conglomerated capillary beds such as those of the renal glomeruli [2, 9]. Osmium vapor treatment provides electron conductivity to the whole block, and is of special value in direct microdissection within the scanning electron microscope.

2. Renal vascular arrangement

The renal artery, arising from the abdominal aorta, reaches the kidney at the hilus. This artery divides into several segmental arteries, which enter the substance of the kidney and give off arcuate arteries at the level of the corticomedullary junction. At this level, parallel to the kidney surface, the arcuate arteries give rise to numerous interlobular arteries. These run radially in the cortex emitting terminal twigs, intralobular arterioles, which flow into renal corpuscle as glomerular afferent arterioles. Repeated divisions and anastomoses of an afferent arteriole in the renal corpuscle forms a capillary tuft, the glomerulus. The glomerular capillary plexus is drained by an efferent arteriole.

The vascular pattern of an isolated rat kidney cast presents clear zonation, which demonstrates three zones: cortical, juxtamedullary or subcortical, and inner medullary zones (Figs. 1–3). Efferent arterioles of glomeruli in the cortical layer branch into fine capillaries, forming a profuse capillary plexus among the proximal and distal convoluted tubules (Figs. 1, 2, 5). Efferent vessels of the juxtamedullary glomeruli descend centripetally into the medulla and give off several straight vessels (*vasa recta*) in the subcortical zone (Figs. 1–3, 7). A few branches of these descending efferent vessels terminate in cortical and subcortical capillary plexuses (Figs. 2, 3, 7).

The arterial vasa recta supply the renal medulla. This system, including its ascending venous counterpart, courses down in vascular bundles in the outer and inner medullary zones. These capillaries form an elongated plexus, which turns back upon itself near the surface of the papilla (Figs. 2, 3).

The medullary capillaries are drained into the ascending vasa recta, which flow either into arcuate veins or directly into proximal segments of interlobular veins (Figs. 1, 9). The subcapsular cortical capillaries drain into the stellate vessels on the cortical surface and converge in the interlobular veins (Figs. 1, 9). Other cortical and subcortical capillaries empty into interlobular veins that flow into arcuate veins (Figs. 1, 9). The arcuate veins discharge into interlobar veins, which finally lead to the renal vein via the segmental veins.

The renal pelvis contains a wide-meshed capillary plexus that is continuous with the ureter's capillary network (Fig. 4). This network extends over the surface of the renal papilla (Fig. 3).

Several short circuit channels bypass the glomeruli: Ludwig's arterioles, which flow directly into the subcapsular capillary plexus in the superficial cortical layer [21], the arteriolae rectae verae (vasa recta vera), which run directly from afferent arterioles into the medulla [22], and direct connections between afferent and efferent glomerular vessels [23, 24, 25, 26]. These aglomerular channels, however, could not be confirmed by our corrosion casting-scanning electron microscope studies in rat [8, 9], monkey [27], and man [2].

3. Glomerular vascular arrangement

The glomerular vascular arrangement has been intensively investigated since Malpighi's first description. The renal glomerulus is the fundamental and most important structure for renal function, namely excretion. However, the glomerular capillary tufts being so small and complicated has led to contradictory models. Bowman [28], Vimtrup [29], and Wilmer [30] presented a 'capillary loop' model in which the glomeruli consists of non-anastomosing capillary loops running from afferent to efferent arterioles. Johnston [31] reconstructed glomeruli based upon a 'capillary plexus' model with glomeruli consisting of anastomosing capillaries. However, his view had been long ignored until Hall [32], Boyer [33], and Lewis [34] confirmed the presence of numerous anastomoses among glomerular capillaries. Hall [32] described, furthermore, completely independent lobulation of glomerular capillary plexuses. A 'blind sacculation' model was proposed by Trabucco and Marquez [35]. Here, the glomerular capillary tuft is formed by evagination of one wall of an arteriole, broken into a digitated arrangement, and ending in blind sacculations. All of these models, however, were based upon light microscopic findings. Because of limitation in resolution and depth of field, the controversy has remained unsettled.

Recently, scanning electron microscopy of casts has confirmed that renal glomeruli consist of capillary plexuses [8]. These plexuses are formed between afferent and efferent arterioles and are organized into fairly independent functional and anatomical units, the glomerular capillary lobules [9].

3.1. Glomerular afferent and efferent arterioles

Glomerular afferent arterioles arise from interlobular arteries. An afferent arteriole enters a renal corpuscle through its vascular pole and forms a capillary tuft within the corpuscle, a glomerulus (Figs. 6–8, 10–15). The efferent rootlets from this glomerular capillary plexus join at the vascular pole and form an efferent arteriole (Figs. 6–8, 10–15). Efferent arterioles leave the glomeruli in opposite directions to afferent arterioles (Figs. 6, 7, 10, 11).

The angle at which afferent arterioles leave the parent trunks, the interlobular arteries, varies. From the proximal part of the interlobular artery, the branch point forms an acute recurrent angle, but the angles gradually open up as the parent vessel is followed peripherally, until the final afferent arterioles are almost in line with the parent trunk [22]. Thus, corrosion casts of an isolated interlobular artery resemble a tree, upon every branch of which hangs a spherical fruit (Figs. 6–8).

Afferent arterioles are usually thicker than efferent arterioles except in the juxtamedullary glomeruli (Figs. 6, 10). These efferent arterioles are thicker than the afferent arterioles and descend into the renal medulla as arteriolae rectae spuriae (vasa recta spuria) [22] (Figs. 7, 11). Constrictions have been observed in juxtaglomerular segments of afferent arterioles [8, 21] (Figs. 6, 11). These constrictions might be due to a sphincter reacting to the infusion pressure but further histological and physiological examinations are required. Similar constrictions or striations are sometimes imprinted in the juxtaglomerular segments of the efferent arterioles [9] (Fig. 11).

Glomeruli with more than two efferent arterioles have been described [8, 21, 22, 36, 37, 38] (Figs. 6, 12, 20). In a series of 1200 rat glomeruli, 0.9% possessed double efferent arterioles, while 4.6% had precocious branching of the efferent arteriole at the glomerular hilum [8]. Casellas and Mimran [25] proposed that one of the double efferent arterioles functions as bypass of the glomerular tuft. However, judging from microdissection analyses of the form and course of these double arterioles, the circulatory pathway seems essentially similar to that of normal efferent arterioles [8] (Fig. 12). The glomerulus with double efferent arterioles could be clearly divided into two parts, each of which was isolatedly supplied by the afferent arteriole and also isolatedly drained into either of the double efferent arterioles [8] (Figs. 6, 12, 20). This anomaly may be called 'twin'.

Earlier we found a rat glomerulus with two afferent arterioles [10]. In this case, the two afferent arterioles arose separately from a terminal twig of an interlobular artery and entered the vascular pole of a subcapsular glomerulus. This anomaly is much rarer than double efferent arterioles (Fig. 6).

3.2. Glomerular capillary plexus

The afferent arteriole divides at the vascular pole of the glomerular tuft into several lobular branches with short but thick trunks (Figs. 8, 11). The lobular branches divide into a few secondary branches of relatively thick caliber. Repeated divisions and anastomoses form a conglomerated capillary plexus (Figs. 6–8, 10–15).

The rat glomerular capillary tuft is always divided into several lobules, usually three to five [9]. Hall [32] described lobulation in the rat glomerular capillary plexus, but this was considered an artifact resulting from uncontrolled injection pressure [33]. Murakami *et al.* [8] stretched and unfolded isolated corrosion casts of rat glomeruli. This clearly delineated the lobulations [9]. Similar lobulation has been described by the corrosion casting-scanning electron microscope method in dog [39, 40, 41], rhesus monkey [27] and man [2] (Figs. 14, 15). Examination of the rat glomerular capillary tufts by reconstruction of ultrathin serial sections also confirmed glomerular lobulation [38].

The secondary branches of the lobular branches ramify into fine capillaries that branch and anastomose to form a genuine plexus (Figs. 10–15). There were neither 'blind-end' vessels nor classically described simple capillary 'loops' [1, 2, 8, 9, 27, 39]. Small, thin protrusions which suggested new capillary formation, were seen (see below).

Each glomerular lobule begins as a single short afferent lobular branch and terminates as a single short efferent rootlet [2, 9, 32] (Figs. 10–15). Usually, the relationship between a glomerular lobule and its afferent and efferent lobular branches is singular. Occasionally, glomerular lobules were found to receive accessory branches from adjacent lobular branches [9] (Fig. 15). Sometimes, lobules drained into distal segments of the adjacent lobule.

Lobule form and size vary in different glomeruli. However, the following characteristics are present. In glomeruli containing more than three lobules, the lateral lobules are most developed (Fig. 14). These lobules originate from branches arising laterally from the sides of the afferent arteriole. The lobules held between the lateral lobules arise from central lobular branches that run opposite to the efferent arteriole. These central lobules are flattened [9, 38]. In the few cases where the glomerular capillary tuft is

comprised of only two lobules, each is fully developed and occupies a hemisphere [9].

Each lobule extends to the urinary pole of the corpuscle where it bends (Figs. 14, 15). The ascending limb returns towards the vascular pole. Thus, the lobules can be divided into three segments, proximal descending limb, the middle turning segment, and distal ascending limb. The proximal and middle segments of lateral lobules are usually well developed, while distal segments are relatively thin. In central lobules the middle segments occasionally are fully developed [9]. Distal segments usually are poorly developed. It is this distal segment where filtration equilibrium is thought to be reached [42, 43].

Distal segments of lobules in the deep cortical layer are thicker than in the superficial cortical layer (Figs. 12, 13). In juxtamedullary glomeruli the distal segments are well developed as judged by thickness and number of vessels; thus part of the glomerular capillary plexus is interposed between the afferent and efferent arterioles, widening the glomerular hilus [9] (Figs. 7, 11).

The lobular efferent rootlets join at the vascular pole medial to the lateral lobular afferent branches to form the efferent arteriole (Figs. 10, 11). Usually efferent rootlets from different lobules form a common trunk that flows into the efferent arterioles. Occasionally, lobules empty into distal segments of adjacent lobules [9].

Each lobule flexes near the vascular pole of the glomerulus leaving a cleft between the afferent and efferent crura. This cleft is probably occupied by the mesangium in intact glomeruli [9].

The branching angle of afferent lobular branches to lateral lobules varies with glomerulus size. In juxtamedullary glomeruli, which are large and contain a portion of glomerular plexus between the afferent and efferent arterioles, the branching angle is much larger than in outer cortical or subcapsular glomeruli [9].

Hall [32] described glomerular lobules as completely independent. Scanning electron microscope observations of microdissected corrosion casts demonstrated that a few vessels usually bridge adjacent lobules in rat [9], dog [39, 40, 41], man [2], and rhesus monkey [27]. These translobular [9], or interlobular [40], vessels are fine capillaries which interconnect proximal or distal ends of the lobules beneath the vascular pole (Figs. 14, 15). Few anastomoses occur between lateral lobules, penetrating the intercalated central lobules. Occasionally lobules are completely independent, with no translobular anastomoses [9]. The lateral or large lobules (see above) sometimes show sublobulations with many trans-sublobular anastomoses [9].

The morphological features of the glomerular lobule, individual afferent and efferent rootlets, and translobular vessels being rudimentary and few, indicate that the lobule is an independent functional and anatomical unit [9]. The 'capillary loop' model, while portraying the glomerulus as composed of fairly independent vascular units – lobules – fails to describe these units not as single vessels but as freely anastomosing capillary plexuses. On the other hand, the 'capillary plexus' model fails to account for the lobular architecture.

It has been suggested that a few large vessels serve as preferential pathways for blood flow from afferent to efferent arterioles [32]. Such direct connections have been reported in rat [24, 25] and man [23]. Most of the recent corrosion casting-scanning electron microscope studies, however, have not found any direct channels or main routes in rat [8, 9], dog [39, 40, 41], man [2], and rhesus monkey [27] (Figs. 12–15). Thus, these channels may be artifacts of either light microscopy or reconstructions.

4. Development and aging of human glomerular capillary tufts

Recently we have examined a series of human kidneys obtained at autopsy from 6-month-old and 10-month-old male fetuses and 45-year-old and 76-year-old men. All specimens were judged normal by histo-pathological examination. Scanning electron microscopy of vascular casts has enabled us to analyze the development and aging of the glomerular capillary tuft and the findings are herein presented.

The human fetal kidneys, especially in the 6-month-old fetus, contained many immature or developing glomeruli interspersed among well developed ones. The simplest, or first stage immature, 'glomerulus' was a single straight vessel, continuous with the interstitial afferent and efferent vessels (Fig. 16). This straight vessel underwent marked dilation and bending, forming a U-shaped capillary loop. The second stage tuft consisted of a few looped capillaries. These looped capillaries emitted small, round or elongated blindly-ending protrusions (Fig. 16). These also were thin self-anastomosing channels (Fig. 17). The third stage tuft consisted of a primitive conglomerated network of anastomosing capillaries (Fig. 17). At this stage, vascular and urinary poles were easily defined. With further development, the networks became larger and contained more capillaries (Figs. 16–18). Even in these later stages, the

freely-ending protrusions and thin anastomoses were noted occasionally, though they were restricted to or near the vascular poles (Fig. 18). The capillary number in mature or well-developed human fetal glomeruli (Figs. 10–15, 18) was comparable to mature adult rat glomeruli (Figs. 5–7).

The glomerular blood vascular tufts of the 45-year-old and 76-year-old men were much larger and contained many more capillaries (Fig. 19) than the well-developed fetal glomeruli (Figs. 10–15, 18). The glomerular capillaries in the 76-year-old man were very tortuous (Fig. 19). Small, freely-ending protrusions and thin anastomosing channels, as noted in developing fetal glomeruli, were occasionally observed in glomeruli of the 45-year-old man, but only rarely in the 76-year-old man. When present, they were restricted, as in the fetus, to or near the vascular pole.

The marked tortuousness of the aged glomeruli increases the total surface area of the glomerular capillary bed. It, thus, may compensate for decreased functioning of aged glomerular capillaries. Such increased tortuousness of the glomerular capillaries is also observed in the aged rat (Fig. 20).

Two main theories for the origin of the glomerular capillary have been proposed, in-growth and in-situ. According to the in-growth theory, the glomerular capillary arises directly from an interstitial vessel [44, 45, 46, 47]. The in-situ theory claims that the glomerular capillary develops in the lower cleft of renal vesicle and subsequently connects with neighboring interstitial vessels [48, 49]. The characteristic loop formation of immature glomeruli in our studies strongly supports the in-growth theory. Similar results have been obtained by our vascular casting-scanning electron microscope investigations of the bullfrog kidney [14].

The glomerular capillaries increased in number from initial development to the aged stage. New capillaries are formed continuously in developing and aging glomeruli. The findings suggested at least one mechanism of capillary formation. Based upon light microscopic studies of Indian ink-injected specimens, the enfaced capillary endothelial surfaces were proposed as protruding into the lumen and producing septa, thus splitting the capillary into several daughter capillaries whose lumens are continuous at the septal margins [44, 45, 46]. Small, freely-ending protrusions were found throughout glomerular development and aging (Figs. 16–19). These protrusions represented luminal discontinuities. Thus, glomerular capillaries multiplied, at least in part, by sprouting daughter capillaries from external surfaces.

The present findings also demonstrated thin anastomosing capillaries. These were considered to be newly formed capillaries that originated in the freely-ending protrusions, and which, in time, developed into thick capillaries [14]. The location of the anastomoses and protrusions suggested that new capillary formation occurs preferentially at the vascular pole. Žlábek [50] observed, under light microscopy of Indian ink-injected sectioned samples, similar thin capillaries in adult rat kidney glomeruli, but regarded them as preferential channels for blood serum.

Previous analyses of microdissected casts have shown that mature kidney glomerular capillary networks are lobulated (see above) [9, 10, 27]. The present findings suggested that these lobulations were demarcated during an early stage of glomerular development. Failure of anastomoses between second-stage looped capillaries possibly results in formation of completely independent lobules.

References

1. Murakami T: Application of the scanning electron microscope to the study of fine distribution of the blood vessels. Arch Histol Jpn 32: 445–454, 1971.
2. Murakami T: Methyl methacrylate injection replica method. In: *Principles and techniques of scanning electron microscopy* 6. Hayat MA (ed) New York, Van Nostrand Reinhold Co, 1978, p 159–169.
3. Nowell JA, Lohse CL: Injection replication of the microvasculature for SEM. In: *Scanning electron microscopy*/ 1974, Johari O, Corvin I (eds), Chicago, IIT Research Institute, 1974, p 267–274.
4. Gannon, BJ: Vascular casting. In: *Principles and techniques of scanning electron microscopy* 6, Hayat MA (ed) New York, Van Nostrand Reinhold Co, 1978, p 170–193.
5. Frasca JM, Carter HW, Schaffer WA: An improved latex injection media for replicating the pulmonary microvasculature. In: *Scanning electron microscopy*/ 1978 II, Becker RP, Johari O (eds), AMF O'Hare, Illinois, SEM Inc, 1978, p 485–489.
6. Hodde, KC, Nowll JA: SEM of micro-corrosion casts. In: *Scanning electron microscopy*/1980/II. Becker RP, Johari O (eds), AMF O'Hare, Illinois, SEM Inc, 1980, p 88–106.
7. Murakami T, Ohtani O, Ohtsuka A, Kikuta A: Injection replication and scanning electron microscopy of blood vessels. In: *Biological research applications of scanning electron microscopy* 3, Hodges GM, Carr KE (eds), London, Academic Press, 1983, p 1–30.
8. Murakami T, Miyoshi M, Fujita F: Glomerular vessels of the rat kidney with special reference to double efferent arterioles. A scanning electron microscope study of corrosion casts. Arch Histol Jpn 33: 179–198, 1971.
9. Murakami T: Vascular arrangement of the rat renal glomerulus. A scanning electron microscope study of corrosion casts. Arch Histol Jpn 34: 87–107, 1972.
10. Murakami T: Double afferent arterioles of the rat renal glomerulus as studied by the injection replica scanning electron microscope method. Arch Histol Jpn 39: 327–332, 1976.
11. Lee ML, Purderson ML, Agata Jr FJ, Dempsy EW: Ultrastructural changes in the renal glomeruli of rats during experimentally induced hypertension and uremia. Am J Anat 135: 191–204, 1972.
12. Morris JL, Campbell G: Renal vascular anatomy of the toad (Bufo marinus). Cell Tiss Res 189: 501–514, 1978.
13. Ohtani O, Naito I: Renal microcirculation of the bullfrog, Rana catesbeiana: a scanning electron microscope study of vascular casts. Arch Histol Jpn 43: 319–330, 1980.

14. Naito I: The development of glomerular capillary tufts of the bullfrog kidney from a straight interstitial vessel to an anastomosed capillary network. A scanning electron microscopic study of vascular casts. Arch Histol Jpn 47: 441–456, 1984.
15. Murakami T: Pliable methacrylate casts of blood vessels: use in a scanning electron microscope study of the microcirculation in rat hypophysis. Arch Histol Jpn 38: 151–168, 1975.
16. Nopanitaya W, Aghajanian JG, Gray LD: An improved plastic mixture for corrosion casting of the gastrointestinal microvascular system. In: *Scanning electron microscopy*/ 1979/ III, Becker RP, Johari O (eds), AMF O'Hare, Illinois, SEM Inc, 1979, p 751–755.
17. Northover JMA, Williams EDF, Terblanche J: The investigation of small vessel anatomy by scanning electron microscopy of resin casts. A description of the technique and examples of its use in the study of the microvasculature of the peritoneum and bile duct wall. J Anat 130: 43–54, 1980.
18. Murakami T, Itoshima T, Hitomi K, Ohtsuka A, Jones AL: A monomeric methyl and hydroxypropyl methacrylate injection medium and demonstration of its use in casting capillaries of rat endocrine organs and liver bile canaliculi for scanning electron microscopy. Arch Histol Jpn 47: 223–237, 1984.
19. Murakami T, Unehira M, Kawakami H, Kubotsu A: Osmium impregnation of methyl methacrylate vascular casts for scanning electron microscopy. Arch Histol Jpn 36: 119–124, 1973.
20. Murakami T, Kubotsu A, Ohtsuka A, Akita S, Yamamoto KJ, Jones AL: Double staining by vaporized osmium tetroxide-hydrazine hydrate of biological specimens for non-coated scanning electron microscopy. In: *Scanning electron microscopy*/ 1982/ I, Becker RP, Johari O (eds), AMF O'Hare, Illinois, SEM Inc, 1982, p 459–464.
21. Shonyo ES, Mann FC: An experimental investigation of renal circulation. Arch Pathol 38: 287–296, 1944.
22. Moffat DB, and Fourman J: The vascular pattern of the rat kidney. J Anat 97: 543–553, 1963.
23. Ljungqvist A: Structure of the arteriole-glomerular units in different zones of the kidney. Nephron 1: 329–337, 1964.
24. Ljungqvist A: Ultrastructural demonstration of a connection between afferent and efferent juxtamedullary glomerular arterioles. Kidney International 8: 239–244, 1975.
25. Casellas D, Mimran A: Aglomerular pathways in intrarenal microvasculature of aged rats. Am J Anat 156: 293–298, 1979.
26. Casellas D, Mimran A: Shunting in renal microvasculature of the rat: A scanning electron microscopic study of corrosion casts. Anat Rec 201: 237–248, 1981.
27. Unehira M: Blood vascular architecture of the rhesus monkey kidney glomerulus. A scanning electron microscope study of corrosion casts. Okayama Igakkai Zasshi 93: 951–961, 1981 (in Japanese).
28. Bowman W: On the structure and use of the Malpighian bodies of the kidney, with observations on the circulation through that gland. Phil Trans Roy Soc London 1: 57–80, 1842.
29. Vimtrup BJ: On the number, shape, structure, and surface area of the glomeruli in the kidneys of man and mammals. Am J Anat 41: 123–151, 1928.
30. Wilmer HA: The arrangement of the capillary tuft of the human glomerulus. Anat Rec 80: 507–518, 1941.
31. Johnston WB: A reconstruction of a glomerulus of the human kidney. Anat Anz 16: 260–266, 1899.
32. Hall BV: Further studies of the normal structure of the renal glomerulus. In: *Proceedings of 6th Ann Conf Nephrotic Syndrome*, New York, Nat Nephrosis Found, 1955, p 1–39.
33. Boyer CC: The vascular pattern of the renal glomerulus as revealed by plastic reconstruction from serial sections. Anat Rec 125: 433–441, 1956.
34. Lewis OJ: The vascular arrangement of the mammalian renal glomerulus as revealed by a study of its development. J Anat 92: 433–440, 1958.
35. Trabucco A, Marquez F: Structure of the glomeruli tuft. J Urol 67: 235–255, 1952.
36. Boenig H: Beiträge zur Kenntnis der Vasa efferentia in der menschlichen Niere. Z Mikrosk Anat Forsch 39: 105–115, 1936.
37. Okano H, Ohta Y, Fujimoto T, Ohtani Y: Cubical anatomy of several ducts and vessels by injection method of acrylic resin. VI. On the vascular system of the kidney in Macacus cynomolgus. Okajimas Fol Anat Jpn 34: 27–41, 1959.
38. Yang GCH, Morrison AB: Three large dissectable rat glomerular models reconstructed from wide-field electron micrographs. Anat Rec 196: 431–440, 1980.
39. Spinelli F, Wirtz H, Brücher C, Pehling G: Non-existence of shunts between afferent and efferent arterioles of juxtamedullary glomeruli in dog and rat kidneys. Nephron 9: 123–128, 1972.
40. Spinelli F: Structure and development of the renal glomerulus as revealed by scanning electron microscopy. In: *International Rev Cytol* 39, Bourne GH, Danielli JF (eds), New York, Academic Press, 1974, p 345–381.
41. Anderson BG, Anderson WD: Renal vasculature of the trout demonstrated by scanning electron microscopy, compared with canine glomerular vessels. Am J Anat, 145: 443–458, 1976.
42. Andreucci VE, Herrera-Acosta J, Rector Jr FC, Seldin DW: Effective glomerular filtration pressure and single nephron filtration rate during hydropenia, elevated ureteral pressure, and acute volume expansion with isotonic saline. J Clin Invest 50: 2230–2234, 1971.
43. Deen WM, Robertson CR, Brenner BM: A model of glomerular ultrafiltration in the rat. Am J Physiol 223: 1178–1183, 1972.
44. Potter EL: Development of the human glomerulus. Arch Pathol 80: 241–255, 1965.
45. Osathanondh V, Potter EL: Development of human kidney as shown by microdissection. Arch Pathol 82: 403–411, 1966.
46. Kazimierczak J: Development of the renal corpuscle and the juxtaglomerular apparatus: A light and electron microscopic study. Acta Pathol Microbiol Scand Secta A supple 218: 1–115, 1971.
47. Kazimierczak J: A study by scanning (SEM) and transmission (TEM) electron microscopy of the glomerular capillaries in developing rat kidney. Cell Tiss Res 212: 241–255, 1980.
48. Suzuki Y: An electron microscopy of the renal differentiation: II glomerulus. Keio J Med 8: 129–142, 1959.
49. Vernier RL, Birch-Andersen A: Studies of the human fetal kidney: I Development of the glomerulus. J Pediatr 60: 754–768, 1962.
50. Žlábek K: Über dünne interkapillare Anastomosen im Nierenglomerulus der Ratte. Acta Anat 85: 175–189, 1973.

Table 1. Abbreviations in Figures.

A.	afferent vessel of the glomerulus
a.	Afferent rootlet of the glomerular capillary lobule
AA.	arcuate artery
AV.	arcuate vein
B.	capillary plexus surrounding the renal corpuscle
b.	interlobular or translobular capillary of the glomerulus (or accessory afferent or efferent rootlet of the glomerular capillary lobule)
C.	cortex
cG.	cortical glomerulus
cv.	cortical vein or venule
D.	collecting duct of urinary tubule
E.	efferent vessel of the glomerulus
e.	efferent rootlet of the glomerular capillary lobule
F.	capillary plexus of the renal pelvis
G.	glomerulus
IA.	interlobular artery
IV.	interlobular vein
J.	juxtamedullary zone or subcortical layer
j.	subcortical branch of the efferent vessel of the juxtamedullary glomerulus
jC.	juxtamedullary or subcortical capillary plexus which supplies the thick ascending and descending limbs of the urinary tubule
jG.	juxtamedullary or subcortical glomerulus
L.	lobule of the glomerular capillaries
M.	medulla
m.	medullary branch of the efferent vessel of the juxtamedullary glomerulus
mC.	medullary capillary plexus
mv.	medullary vein or venule
P.	papilla
pC.	medullary capillary plexus (papilla)
S.	stellate vein
sC.	subcapsular capillary plexus
sG.	subcortical glomerulus
T.	urinary tubule or nephron
U.	ureter
z.	leaked mass of the casting medium or corroded remnant of the tissue elements

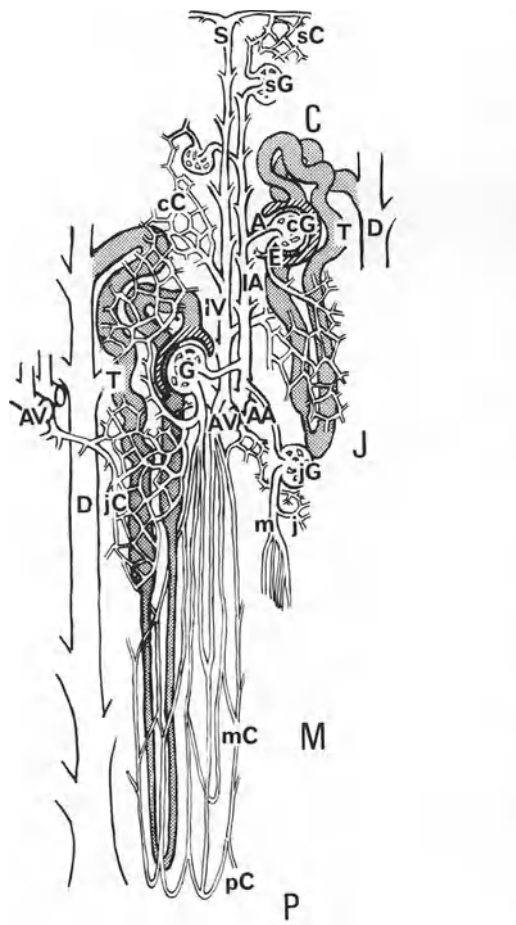

Fig. 1. Diagram of blood supply to the mammalian kidney. See Table 1 for abbreviations.

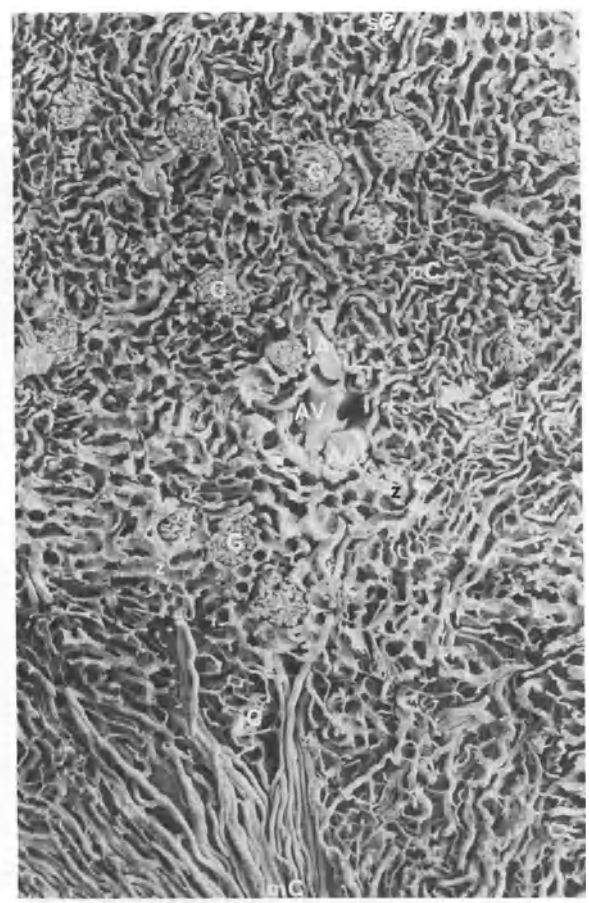

Fig. 2. Scanning electron micrograph (SEM) of methyl methacrylate (MMA)-cast and frozen-cut blood vascular beds of adult rat kidney. Cortico-juxtamedullary layers, ×45. See Table 1.

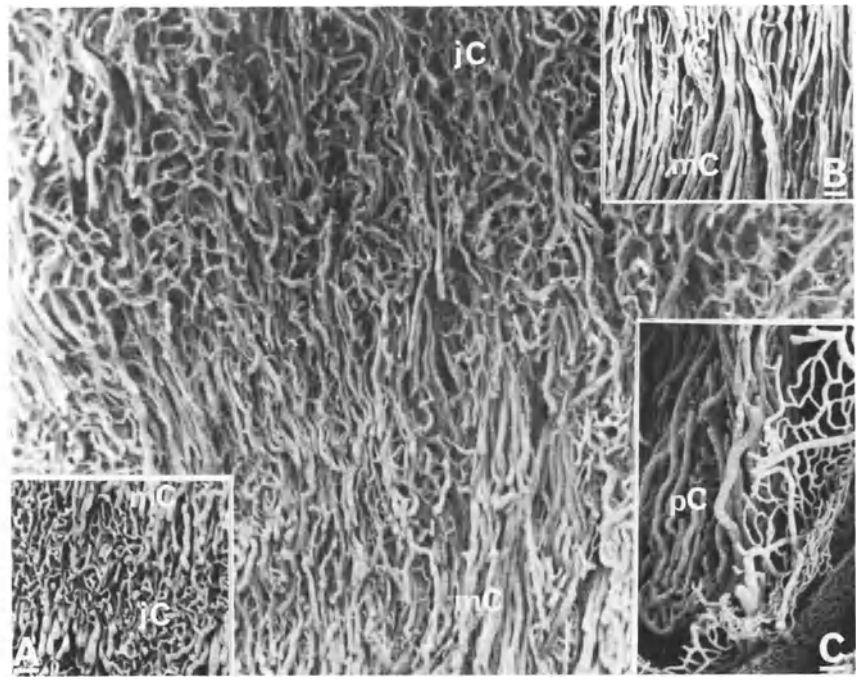

Fig. 3. SEM of MMA-cast and frozen-cut blood vascular beds of adult rat kidney. Subcortico-medullary layers; ×60. Inset A) Transversely cut surface of the subcortical layer, ×60. Inset B) Longitudinally torn surface of the medulla, ×60. Inset C) Longitudinally fractured surface of the papilla, ×60. See Table 1.

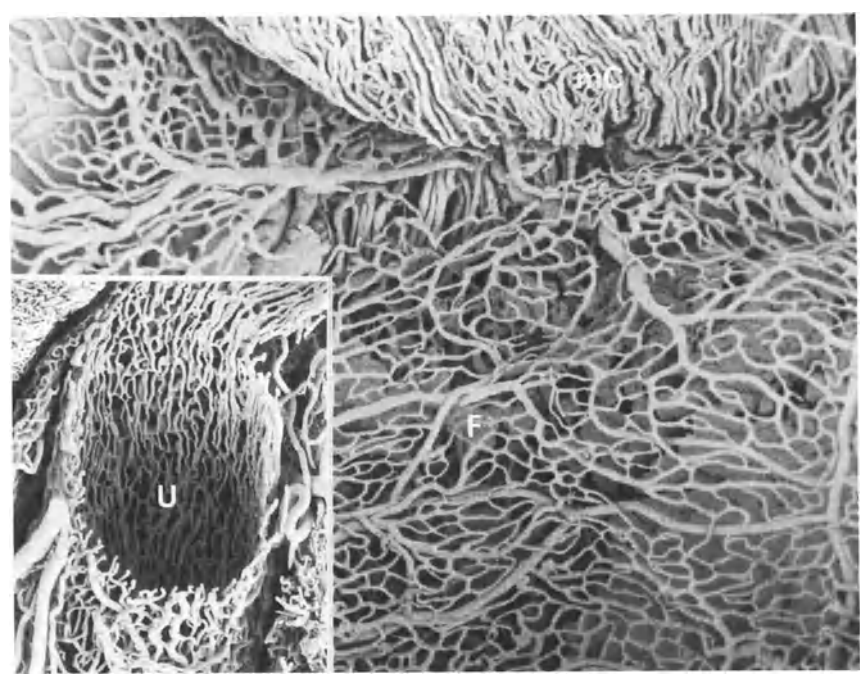

Fig. 4. SEM of MMA-cast and frozen-cut blood vascular beds of adult rat kidney. Renal pelvis, ×80. Inset: Ureter, ×48. See Table 1.

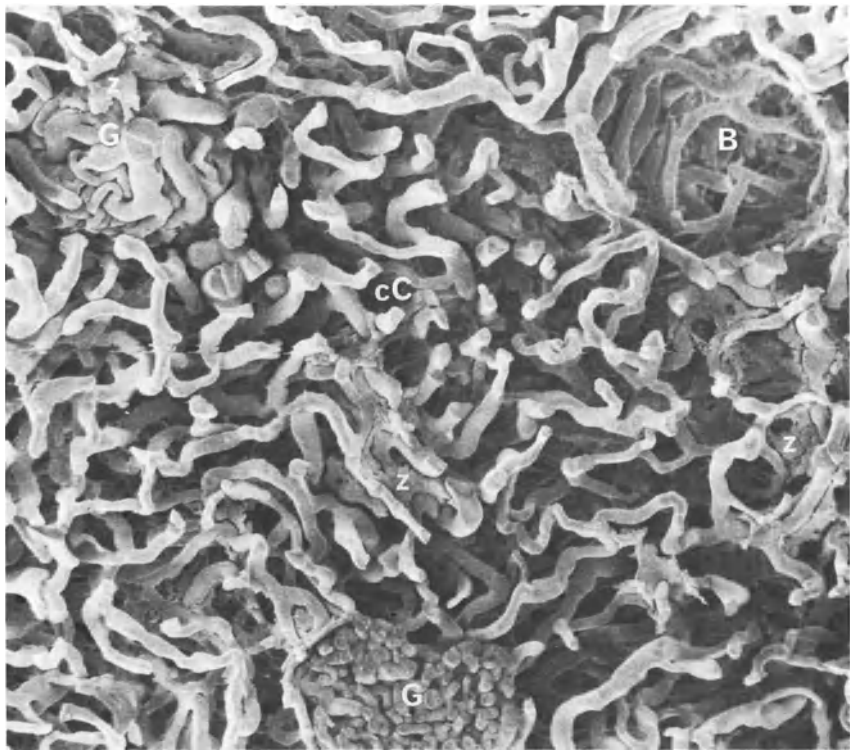

Fig. 5. SEM of frozen-cut surface of MMA-cast cortical vascular beds of adult rat kidney. Cortex, ×180. See Table 1.

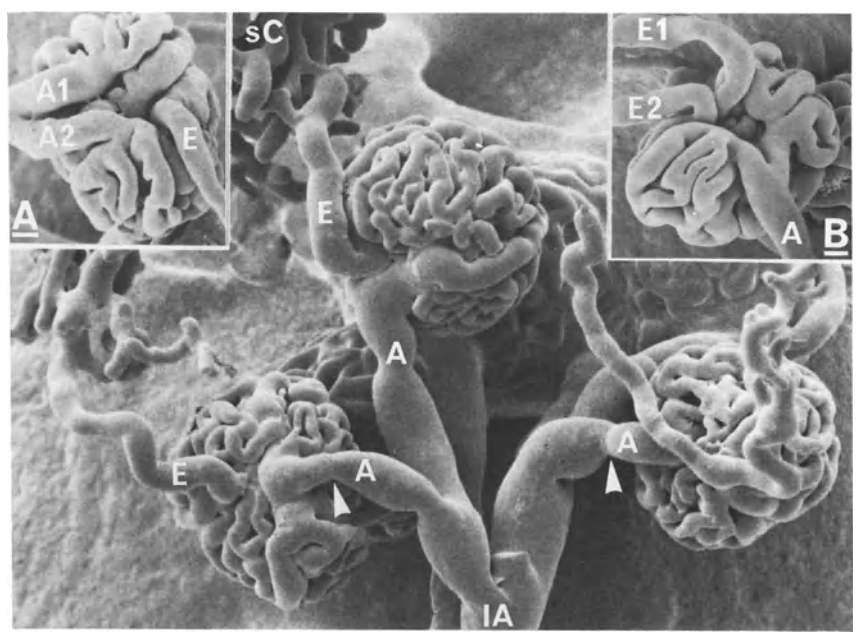

Fig. 6. Partially injected adult rat kidney. Subcapsular layer, ×192. Inset A) Double afferent arterioles, A1 and A2, ×336. Inset B) Double efferent arterioles, E1 and E2, ×280. Arrowheads indicate marked constrictions, possibly representing sphincter resistance of glomerular afferent arteriole against injection pressure of the casting medium. See Table 1.

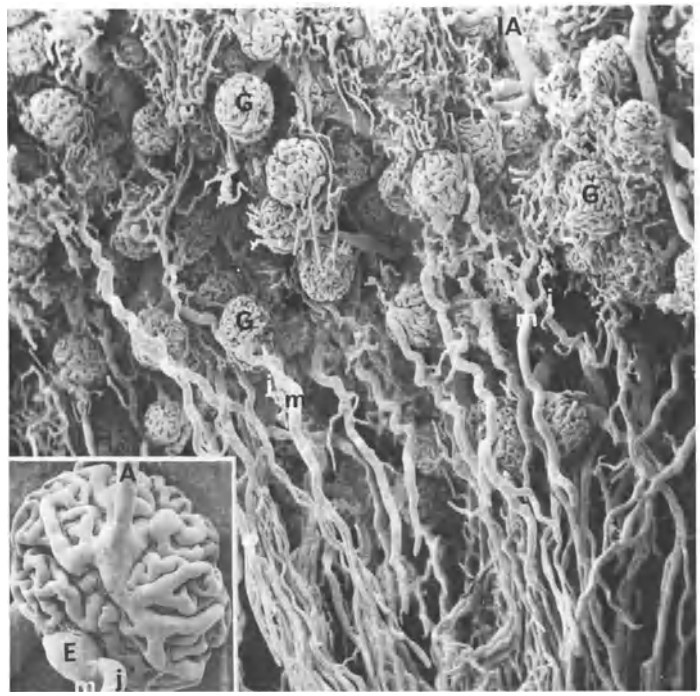

Fig. 7. Partially injected adult rat kidney. Cortico-medullary layers, ×48.75. Inset: a typical glomerulus in the subcortical or juxtamedullary layer, ×130. See Table 1.

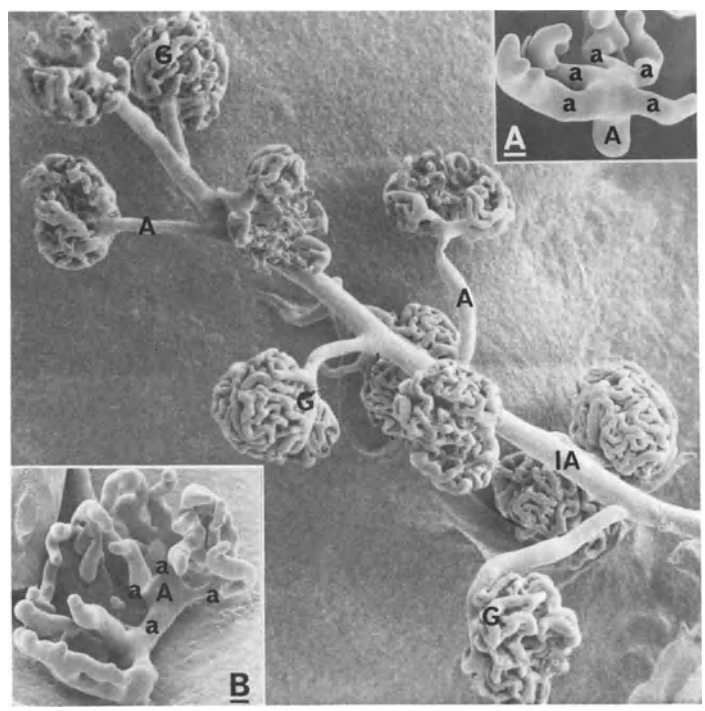

Fig. 8. Partially injected rat kidney showing subcapsular and cortical glomeruli, ×84.5. Note, in the inset A, the afferent vessel (A) branches into five afferent rootlets (a), ×227.5. In the Inset B), the afferent vessel (A) branches into four afferent rootlets (a), ×195. See Table 1.

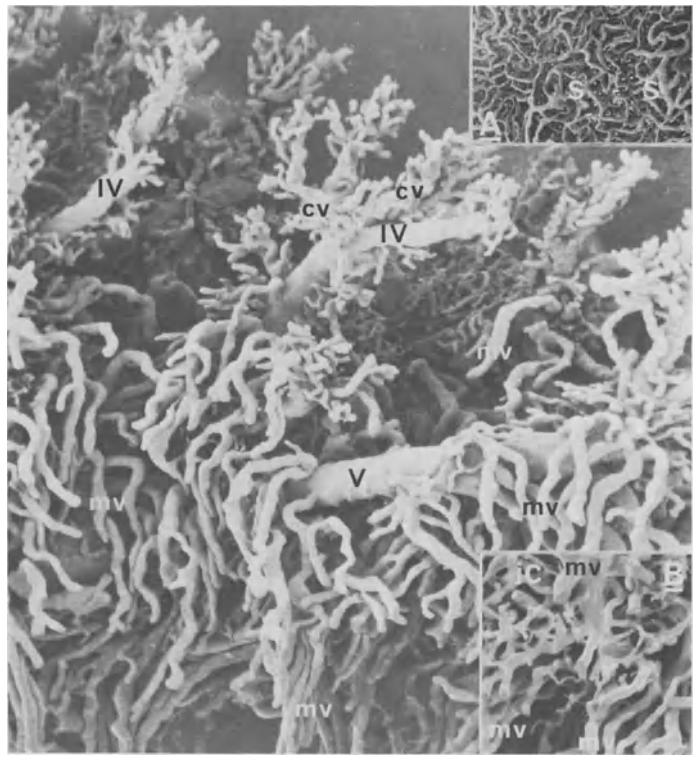

Fig. 9. Venously injected rat kidney, ×65. Inset A) Stellate veins and subcapsular capillaries, ×22.75. Inset B) Subcortical veins and venules, ×65. See Table 1.

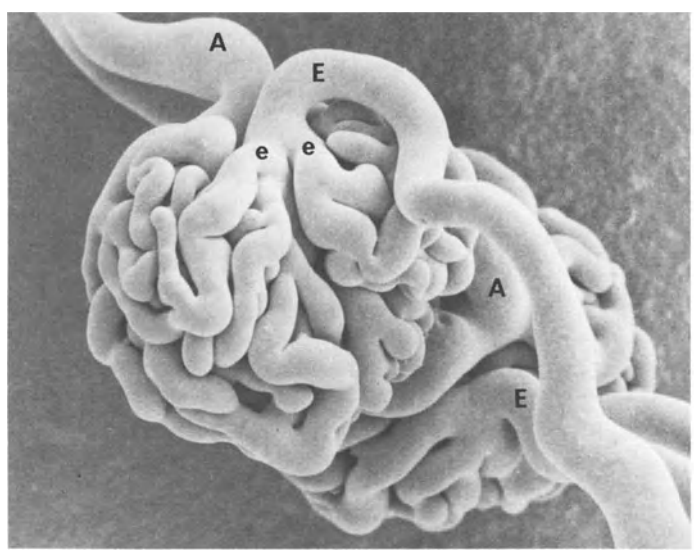

Fig. 10. Thoroughly injected subcapsular glomeruli of a 10-month-old fetal human kidney, obtained from a Japanese fetus who was still-born due to coiling of the umbilical cord, ×325. See Table 1.

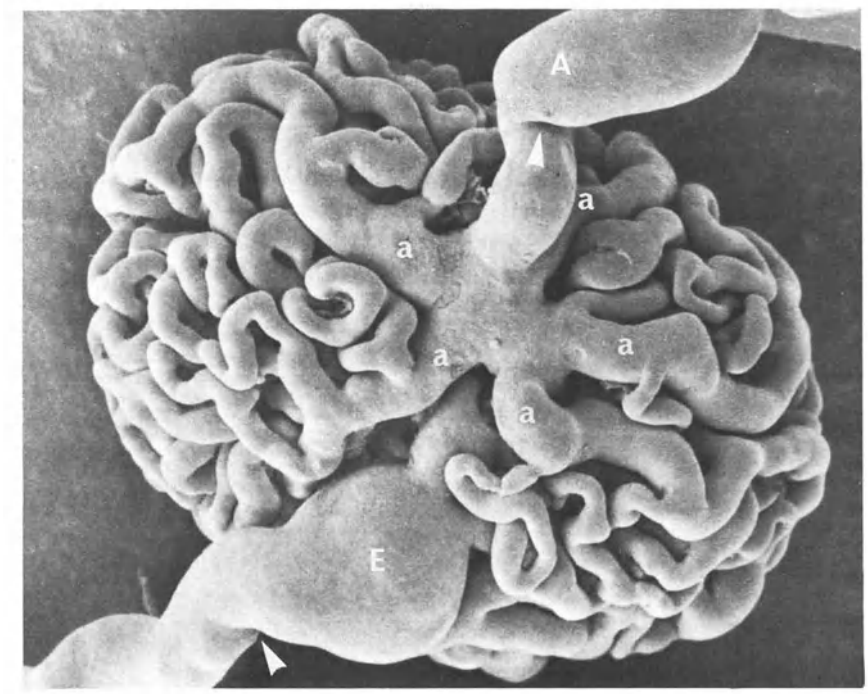

Fig. 11. Typical juxta-medullary glomerulus of 10-month-old human fetal kidney, ×400. Note marked constrictions in the juxtaglomerular segments of the afferent arterioles (arrowheads). See Table 1.

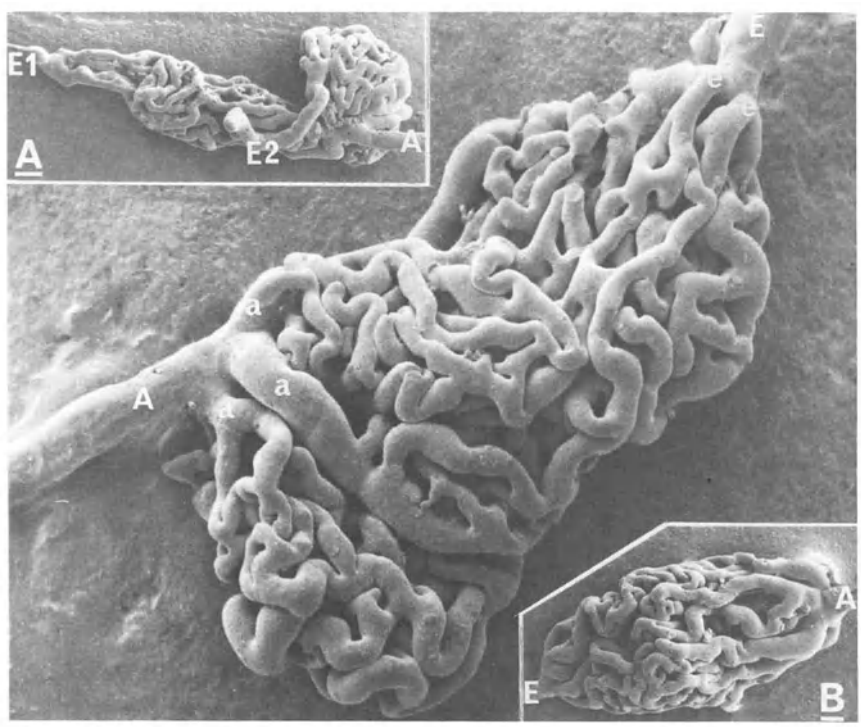

Fig. 12. Extended form of an ethanol-substituted juxta-medullary glomerulus of a 10-month-old human fetus kidney. View from the vascular pole, ×320. Inset A) Extended form of a juxta-medullary glomerulus with double efferent arterioles. View from the vascular pole, ×120. Inset B) Extended form of a cortical glomerulus. View from the vascular pole, ×160. See Table 1.

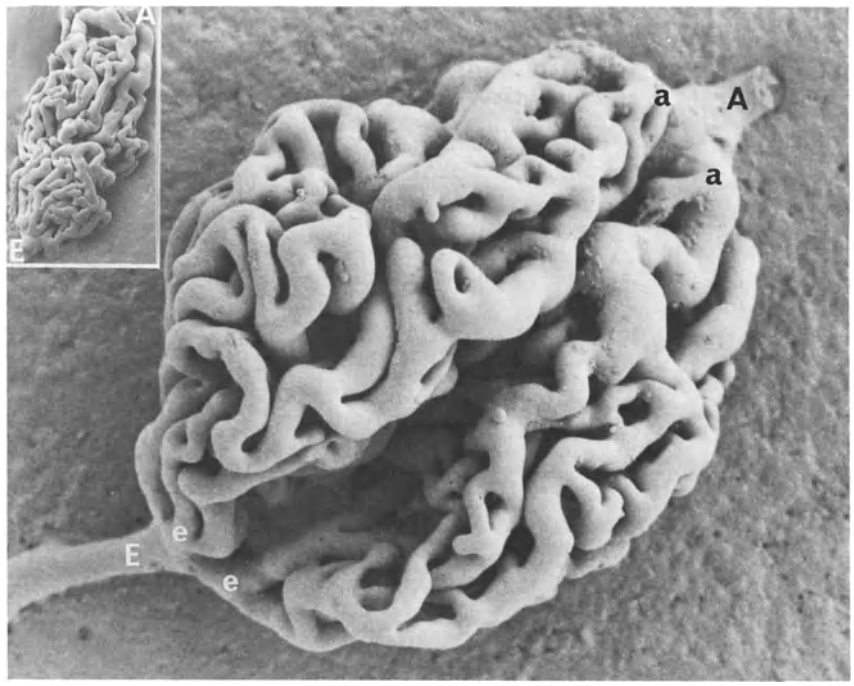

Fig. 13. Extended form of an ethanol-substituted subcapsular glomerulus of the 10-month-old human fetus kidney. View from the urinary pole, ×320. Inset: Extended form of a juxtamedullary glomerulus. View from the urinary pole, ×120. See Table 1.

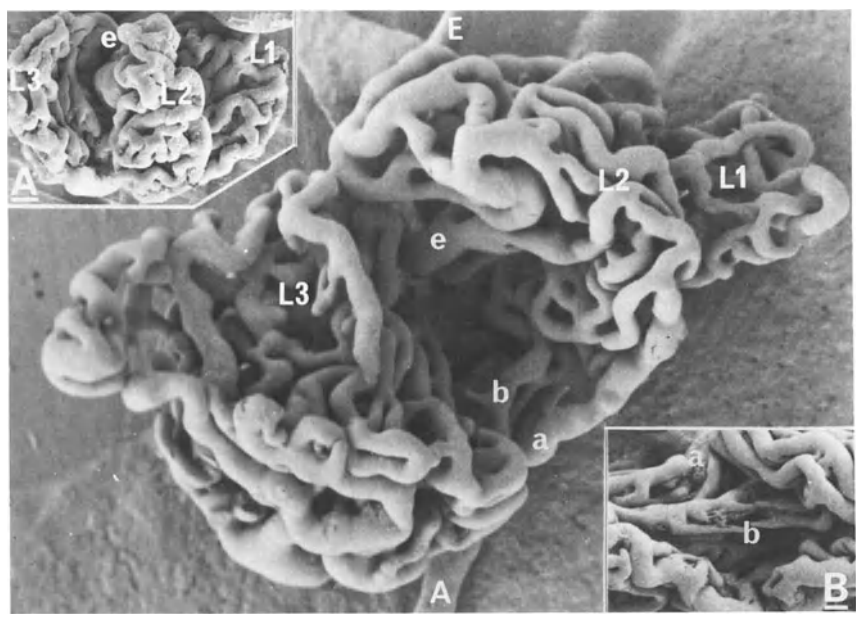

Fig. 14. Extended form of an ethanol-substituted cortical glomerulus of a 10-month-old human fetus kidney. View from the urinary pole, ×400. The glomerular capillary network is subdivided into at least three lobules (L1, L2, and L3). These intercommunicate through a few interbridging capillaries (b). Inset A) A subcapsular glomerulus subdivided into three lobules (L1, L2, L3). View from the vascular pole, ×192. Inset B) Another example of interbridging capillaries of juxta-medullary glomerulus, ×280. See Table 1.

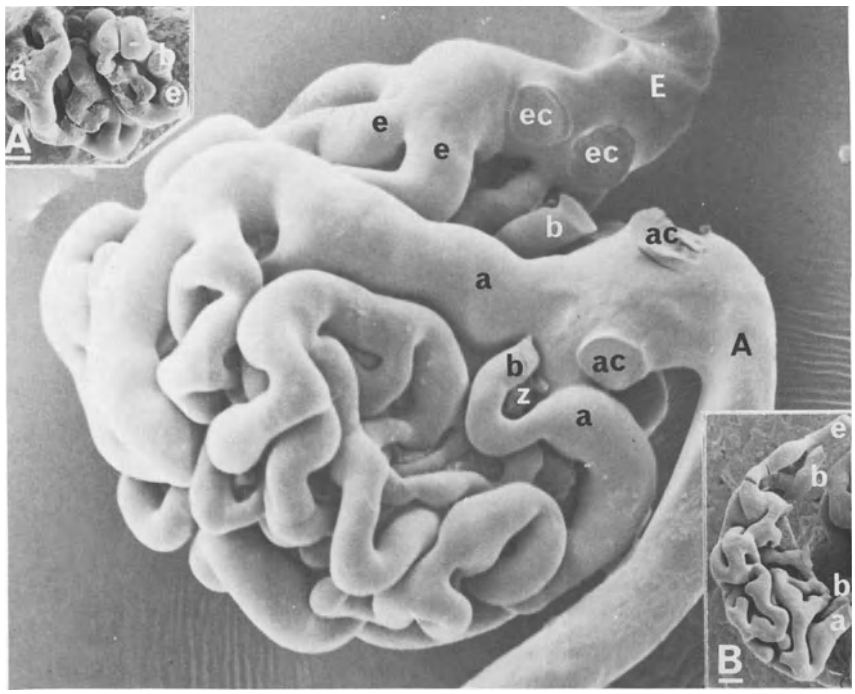

Fig. 15. Microdissected subcapsular glomerulus of a 10-month-old human fetus kidney. Some lobules were removed by microdissection. Afferent (ac) and efferent (ec) rootlets of the removed lobules, ×880. Inset A) and B) Isolated lobules, ×280. See Table 1.

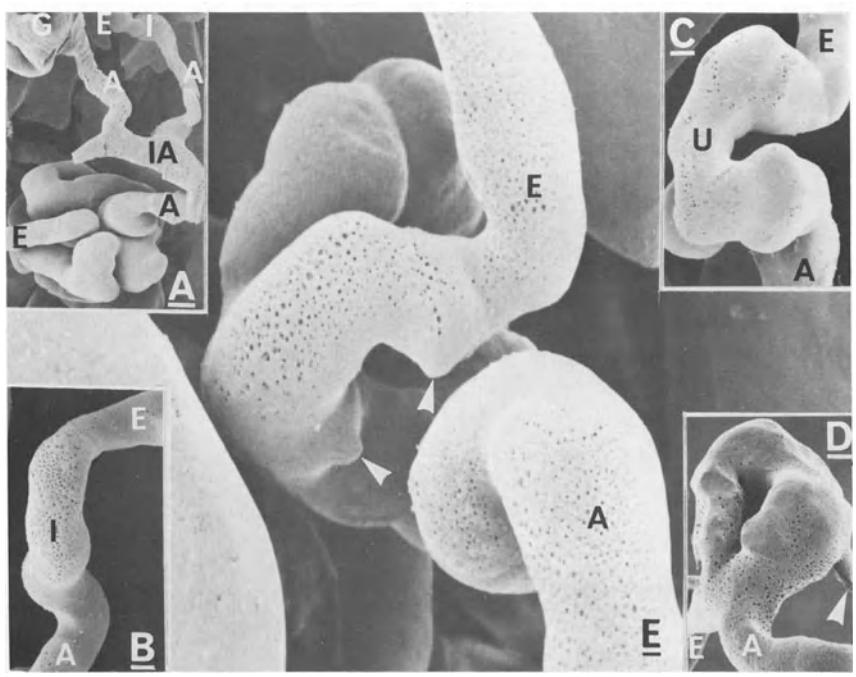

Fig. 16. Developing subcapsular glomeruli of a 6-month human fetal kidney. Abortion was induced because of severe toxemia of pregnancy. A) First stage immature glomerulus with straight appearance (I), ×304. B) Another example of first stage immature glomerulus (I), ×656. C) The intermediate stage immature glomerulus was U-shaped (U), ×896. D) Second stage immature glomerulus, ×800. Arrowhead indicates a small protrusion. E) Another example of second-stage glomerulus, ×1,760. Small protrusions (arrowheads) suggest new capillary formation. See Table 1.

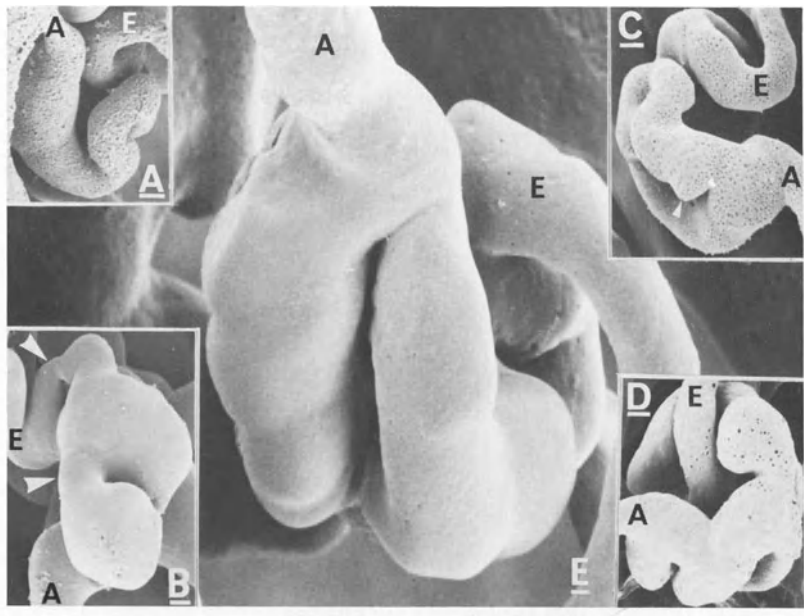

Fig. 17. Immature subcapsular glomeruli with primitive conglomerated capillary networks. These were observed in a 6-month-old human fetal kidney. A) A second stage glomerulus, ×675. B) Note thin anastomosing channels (arrowhead), ×862.5. C) Small protrusions (arrowhead) also were seen, ×577.5. D) A third stage glomerulus, ×600. E) Another example of third stage glomerulus, ×1,650. See Table 1.

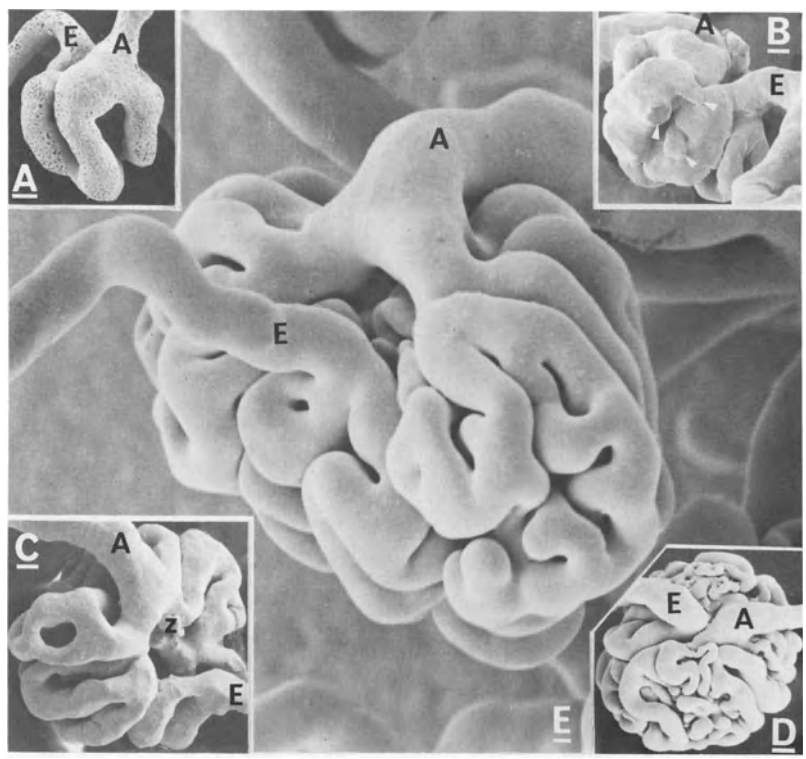

Fig. 18. Subcapsular glomeruli, in middle and final stages of development. The glomeruli were found in a 6-month-old human fetal kidney. A) A middle stage glomerulus, ×450. B). Note small protrusions and thin anastomosing channels (arrowheads), ×525. C) ×525. D) A final stage glomerulus, ×187,5. E) Another example of final stage glomerulus, ×600. See Table 1.

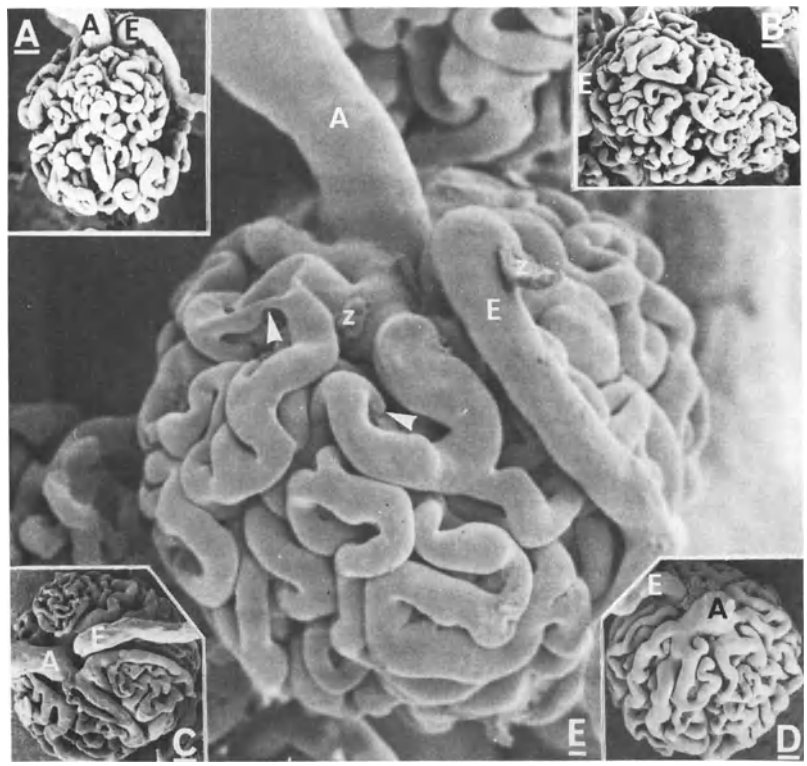

Fig. 19. Subcapsular glomeruli of adult and aged human kidneys. A) and B) Kidney was obtained at necroscopy from a 76-year-old Japanese male, dying with gastric cancer. The senile capillaries are very tortuous, ×142.5. C)–E) Surgically excised kidney from a 45-year-old male Japanese with renal tuberculosis. These glomeruli were isolated from non-affected tissue. Note, in the Figure E), small protrusions or thin anastomosing channels (arrowheads), ×600. C) and D) ×142.5. See Table 1.

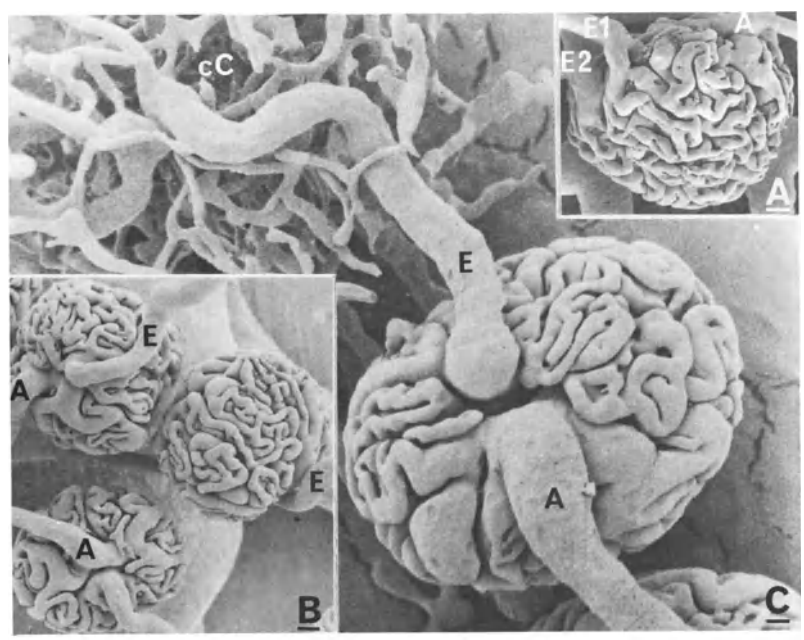

Fig. 20. Kidney glomeruli of a 5-year-old rat. A) subcortical glomerulus with double efferent arterioles (E1 and E2), ×125. B) subcapsular glomeruli, ×135. C) cortical glomerulus, ×256. See Table 1.

CHAPTER 6

Subcellular structure of the renal glomerulus

TSUNEO FUJITA and MASAYUKI MIYOSHI

1. Introduction

It is not exaggerating to say that the essential points in the submicrostructure of the renal glomerulus were elucidated by the earliest transmission electron microscopists like Hall [1], Policard *et al.* [2] and Yamada [3] in the middle of the 1950s. Advances in the study of this field were brought about by the fine structural and histochemical analysis of glomerular filtration, including examination of the transfer of ferritin and other molecular markers across the blood-urine barrier [4, 5]. Application of scanning electron microscopy (SEM) in the 1970s intensively promoted the study by supplementing and extending the visualization of the glomerular structures achieved by conventional transmission electron microscopy (TEM).

The glomerulus is a tuft of anastomosing loops of arterial capillaries. The lumen of the glomerular capillaries is lined by fenestrated endothelial cells, whereas their outer aspect is covered by the endfeet (pedicels) of the processes of podocytes, highly specialized epithelial cells of the urinary tubule. These processes also cover the mesangium which, in its connective tissue elements, contain mesangial cells. A well developed basement membrane is intercalated between the endothelium and podocyte and represents the main element of glomerular filtration. The basement membrane extends also surrounding the mesangial cells (Fig. 1).

The cellular and intercellular elements of the glomerulus introduced above will be dealt with in this chapter with special reference to the correlation of their fine structures and functions.

2. Endothelial cells

2.1. The entire shape of the cell

The glomerular endothelium comprises strongly attenuated cells with slightly flattened nuclei swelling into the capillary lumen. Adjacent cells are closely attached by each other, forming undulated boundary lines.

The early TEM studies had described that the endothelial perikaryon extended simply as a thin cytoplasmic plate with densely and uniformly distributed pores or fenestrae. Hall [1] called this plate the 'lamina fenestrata.' The entire structure of the glomerular endothelium was diagrammatically proposed by Wolff and Merker [6] based on their TEM observations, and this visualization was later confirmed as essentially correct by our SEM study [7]. According to those studies, the nuclear swelling extends thickened cytoplasmic ridges in several directions and they, branching into thinner ridges, reach a crest bordering the cell margin. These radiating and bordering ridges separate the fenestrated lamina into larger and smaller portions of oval, polygonal, or irregular shapes, which we proposed to call 'areolae fenestratae' [7] (Figs. 2, 3).

2.2. Microvilli and fenestrae

Both the cytoplasmic crests and the areolae fenestratae possess microvilli of different length, occasionally reaching 1 μm in length [7] (Figs. 2, 5). The microvilli may be remarkably numerous in certain parts of the endothelial surface; they may occur also on the nuclear swelling. Although TEM pictures of the glomerular endothelium contained oblique or crosswise sections of microvilli, researchers either overlooked or neglected their existence. The functional significance of the endothelial microvilli, which have been observed by SEM also in other blood vessels, is unknown.

The pores or fenestrae of the endothelial cell have been recorded in TEM studies as uniformly round in shape and measuring 500–700 Å, or 'up to 1000 Å' in the rat and mouse [8]. Since Rhodin [9] in his TEM study gave the value of 700 Å for the diameter of the

L.J.A. DiDio and P.M. Motta (eds), Basic, Clinical, and Surgical Nephrology. ISBN 0-89838-689-5.

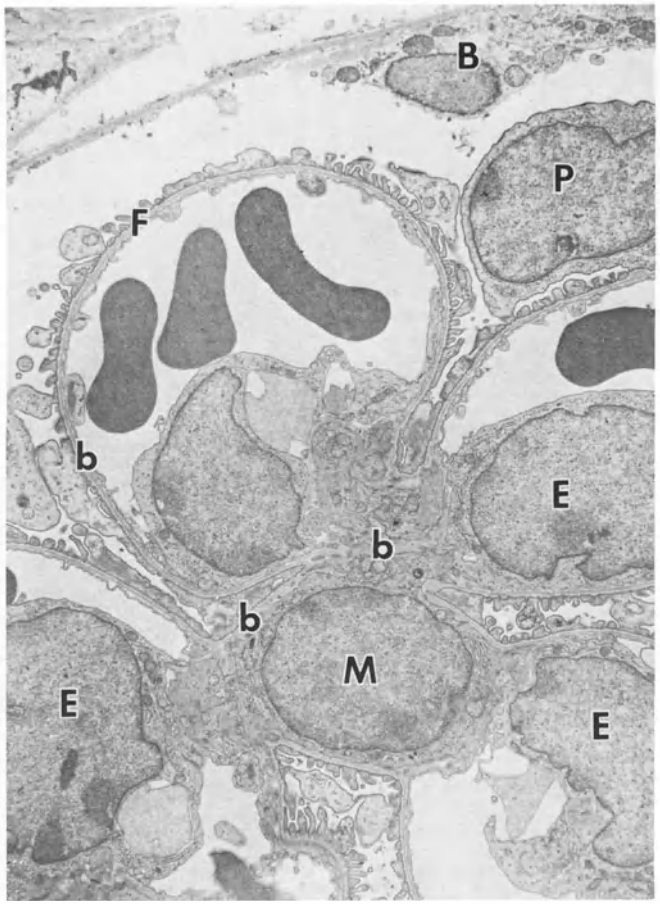

Fig. 1. Low magnification TEM image of a portion of a mouse glomerulus. E: endothelial cells; P: podocytes; M: mesangial cells; F: glomerular filtration membrane; B: epithelial cells of Bowman's capsule; b: basement membrane. (×5,600).

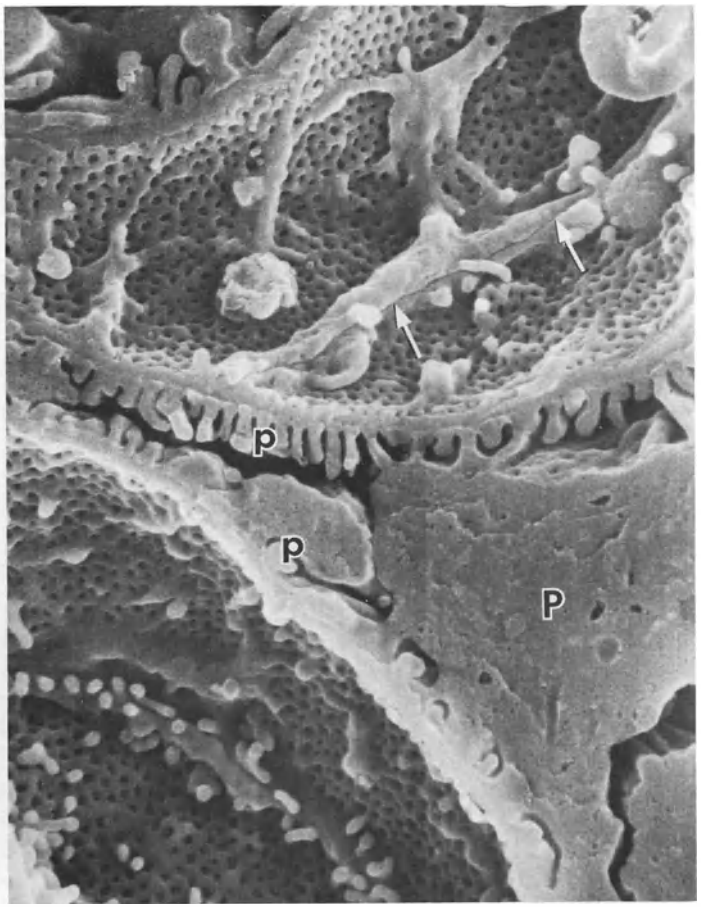

Fig. 2. SEM view of the freeze-fractured aspect of rat glomerular capillaries. Note the clear cytoplasmic ridges of the endothelium and areolae fenestratae separated by them. The marginal crests of adjacent cells are juxtaposed (arrows). Note also the endothelial microvilli, which are especially numerous in the lower capillary. P: podocyte; p: podocyte's endfeet. (×10,500).

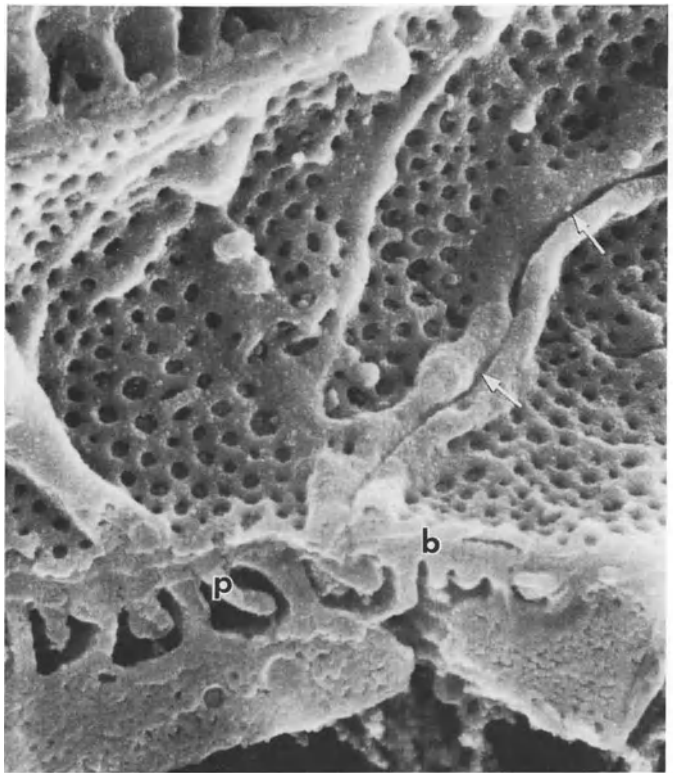

Fig. 3. Closer SEM image of the luminal aspect of a glomerular capillary of a rat. The cytoplasmic crests and areolae fenestratae are clearly distinguished. Marginal ridges of adjacent cells leave a narrow cleft (arrows). Note the uneven size of the endothelial fenestrae. p: Podocyte pedicels; b: basement membrane. (×19,500).

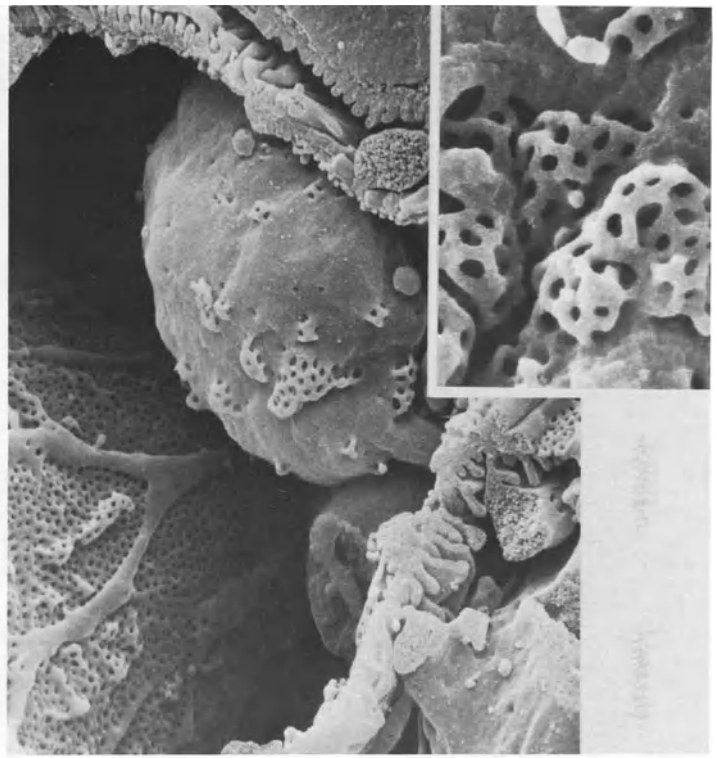

Fig. 4. Fenestrated domes of different sizes found on the perikaryon of rabbit glomerular endothelium. On the upper left side, fenestrated domes are found also on the attenuated part of the endothelium. (×15,000) (Reproduced from T. Yoshinari and T. Fujita, Arch. Histol. Jap. 45: 99–109, 1982). The inset shows a closer view of fenestrated domes from a rat glomerulus. (×22,800).

fenestrations in mouse glomerular endothelium and stated that 'there is a very slight variation in the diameter, mostly explained by a slight compression of the round areas during sectioning,' uniformity in size of the fenestrations tended to be the general belief among the TEM researchers. Recent SEM studies, however, have revealed that the endothelial pores vary much more markedly in size and shape than suggested by TEM researchers. In our observation in the rat [7], the pores measured from 30 to 150 nm in diameter, occasionally even exceeding 200 nm; they varied also in shape: oval, angular, or elongate (Fig. 3).

A thin (60 Å in thickness) diaphram extends across the endothelial fenestra of the mouse, and this membrane is provided with a central knob of about 100 Å in diameter [9, 10]. Numerous papers have dealt with the nature and mechanism of formation, as well as the functional roles of the endothelial diaphragm and knob, arriving at no generally accepted explanation. As reviewed by Latta [8], the diaphragms in the glomerulus are rather infrequently present in other animals and they are usually lacking in the rat. Even if present, they do not seem to form an effective barrier to intravenously injected Thorotrast [8], ferritin [4] and peroxidases or catalases [5].

2.3. 'Pored domes' and related structures

The luminal surface of the glomerular endothelium is often provided with dome-like and irregular shaped swellings formed of a thin cytoplasmic plate (about 80 nm or less in thickness) that is mostly fenestrated in nature (Figs. 4, 5). The profiles of such peculiar structures had been encountered in TEM images of glomerular endothelium but researchers did not like to include them in their publications, except for Wolff and Merker [6] who correctly demonstrated electron micrographs of the structures, which they called 'poröse Vesikeln' (porous vesicles).

Our SEM studies in the rat [7] and guinea pig [11] clearly demonstrated the occurrence and distribution of the pored domes and other irregular elevations on the glomerular endothelium (Figs. 4, 5). They may be remarkably densely populated in some areas of the endothelium. Their dimension varies very widely: from inconspicuous swelling with only a few pores to a large (1 μm or more) construction of complicated shapes. The domes and similar structures are either empty or sponge-like in their interior (Fig. 6). The fenestrae and sponge meshes in the domes are usually identical in size to the ordinary endothelial pores, but occasionally they may be larger or coarser than the latter.

Conspicuously enough, pored domes may occasionally occur on the perikaryon (Fig. 4). Also in this case, the domes cover an empty or spongy space, but its base is not invaginated.

In our SEM study [7] we noticed that microvilli on the glomerular surface occasionally were anastomosed into a small net and we could find different forms suggesting their gradation towards the pored domes (Fig. 5). It may be reasonable to suggest that new pored plates are 'knit' with the material of microvilli and, if so, the pored domes may possibly represent endothelial parts under regeneration. Further studies are naturally needed to confirm this hypothesis.

Whatever their formation mechanism might be, it is stressed that the pored domes, microvilli, and other mentioned structures on the glomerular endothelium are not artifacts caused, for example, by anesthesia or perfusion fixation, but represent normally occurring constituents of the endothelial lining. The idea that fenestrae are present only in the attenuated part of the endothelium for the sake of substance permeation across it must be revised. They may occur on the 'second floor' of the endothelium and even on the perikaryon. What we can say at present is only that the pored endothelium has a tendency or potentiality to form fenestrated plates at every site of its surface, including the perikaryon.

2.4. Nucleus, perikaryon, and organelles

The endothelial nuclei tend to be located toward the center of the glomerular lobule; thus the perikarya often are juxtaposed with the mesangial elements. The nuclei are often deeply indented or folded in profile. Nucleoli are inconspicuous.

The perikaryal cytoplasm contains centrioles, small but distinct Golgi areas, moderate numbers of elongated mitochondria, and a few cisterns of rough endoplasmic reticulum (Figs. 7, 8). Polysomes are numerously scattered. Some cytoplasmic fibrils are seen. Lysosomes are rare [8]. Small vesicles may be numerous and are apparently related to pinocytotic invaginations seen on the luminal and basal aspects of the endothelium. Wolff and Merker [6] presumed that these vesicles might be related to the formation of the fenestrated plates.

Small numbers of mitochondria and other organelles may occur in the cytoplasmic ridges. The marginal cell ridges of adjacent cells come close together and junctional complexes can be occasionally demonstrated there [8].

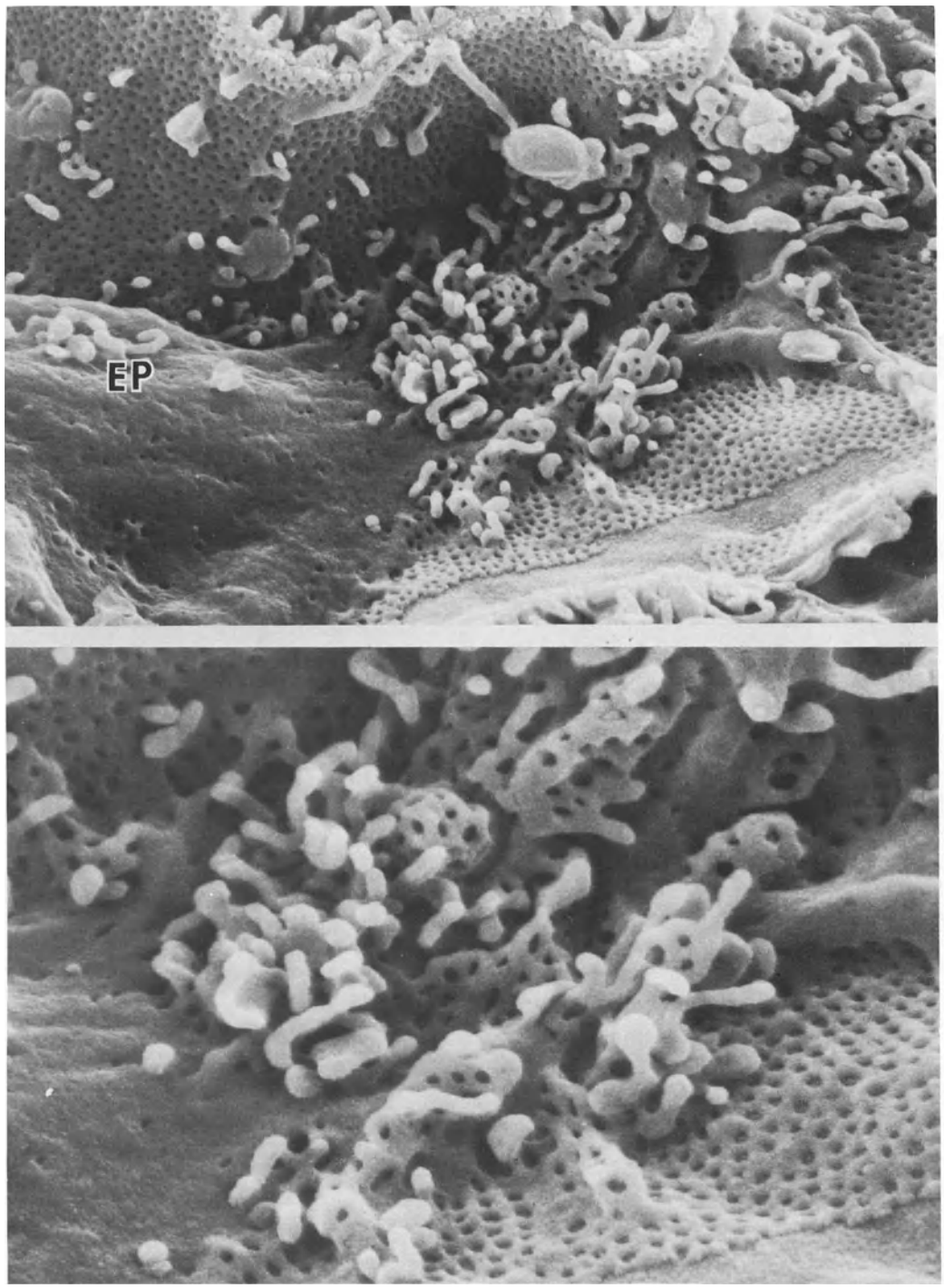

Fig. 5A. The endothelial surface of a guinea pig glomerular capillary showing a group of microvilli and pored projections. EP: endothelial perikaryon. (×12,000). *B*. Closer view of the endothelial microprojections shown in A. Note that there seem to be gradation in forms between microvillous projections and pored domes. (×24,000).

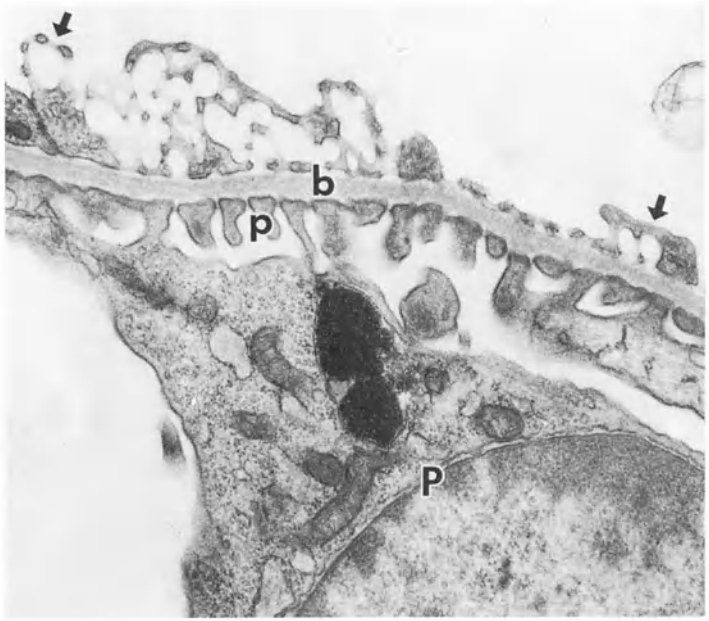

Fig. 6. TEM view of fenestrated domes in a mouse glomerulus. Besides the large complex structure, one may see small domes of simple arch-like structures (arrows). P: podocyte showing dark lysosomes; p: pedicels; b: basement membrane. (×19,500).

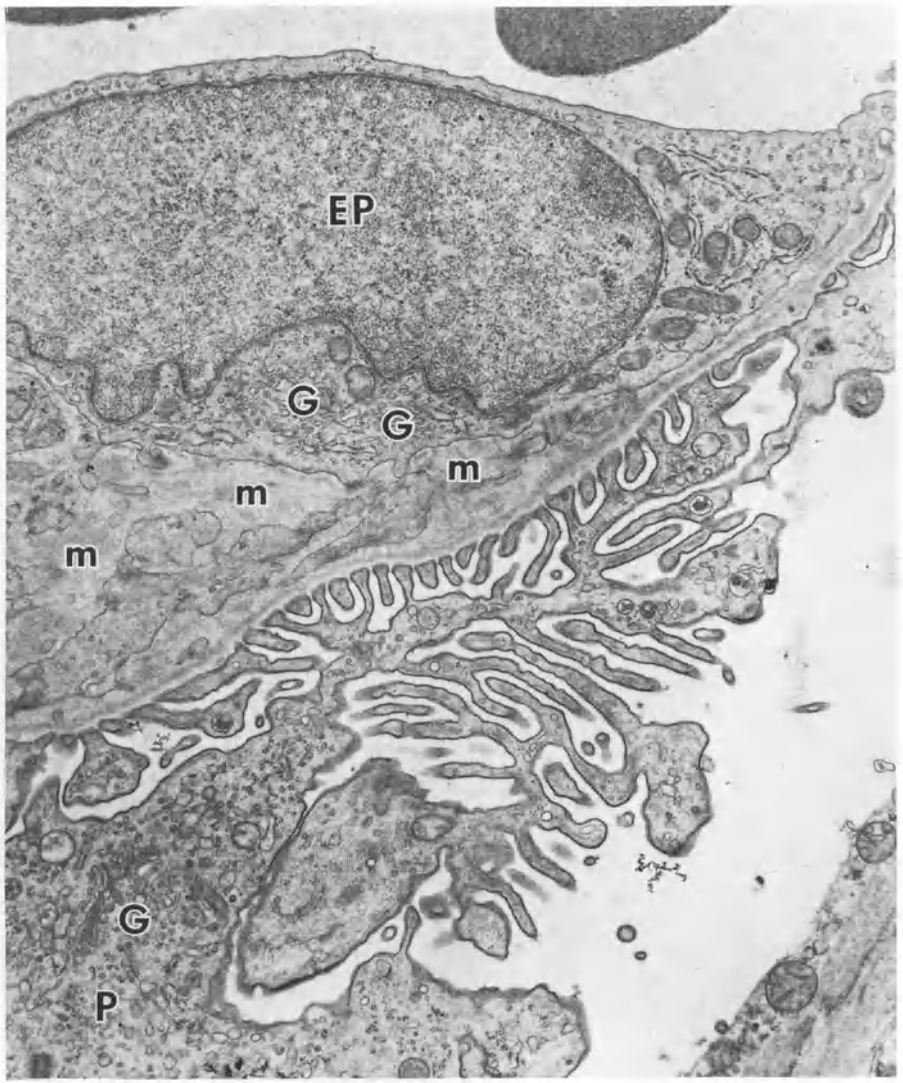

Fig. 7. TEM view of an endothelial perikaryon (EP), mesangial matrix (m) and a portion of a podocyte (P) from a mouse glomerulus. G: Golgi complexes. (×8,250).

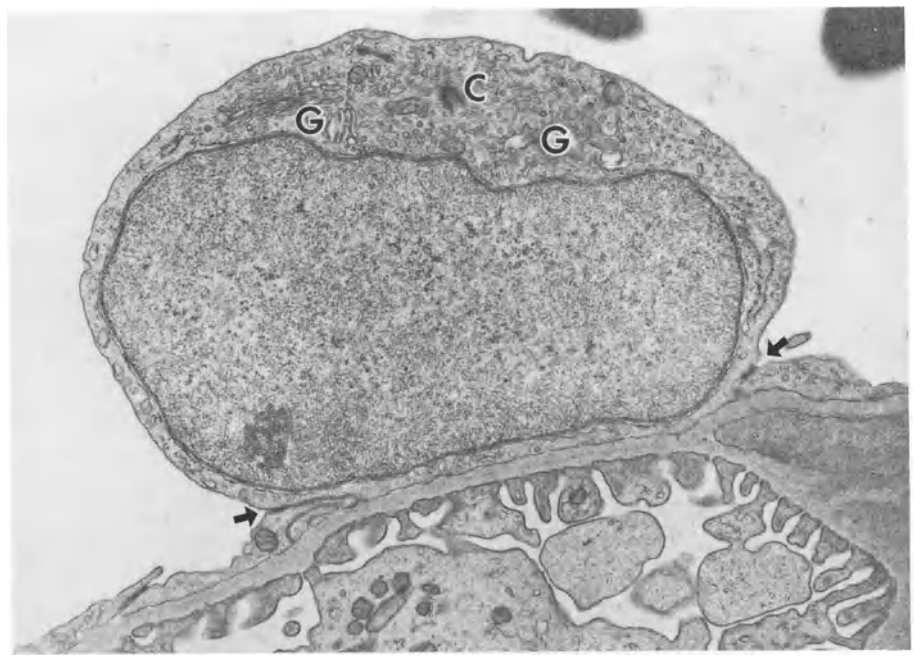

Fig. 8. Endothelial cell with a strongly swollen perikaryon. A centriole (C) and Golgi complex (G) are marked. Endothelial cell boundaries are indicated with arrows. From a mouse glomerulus. (×7,750).

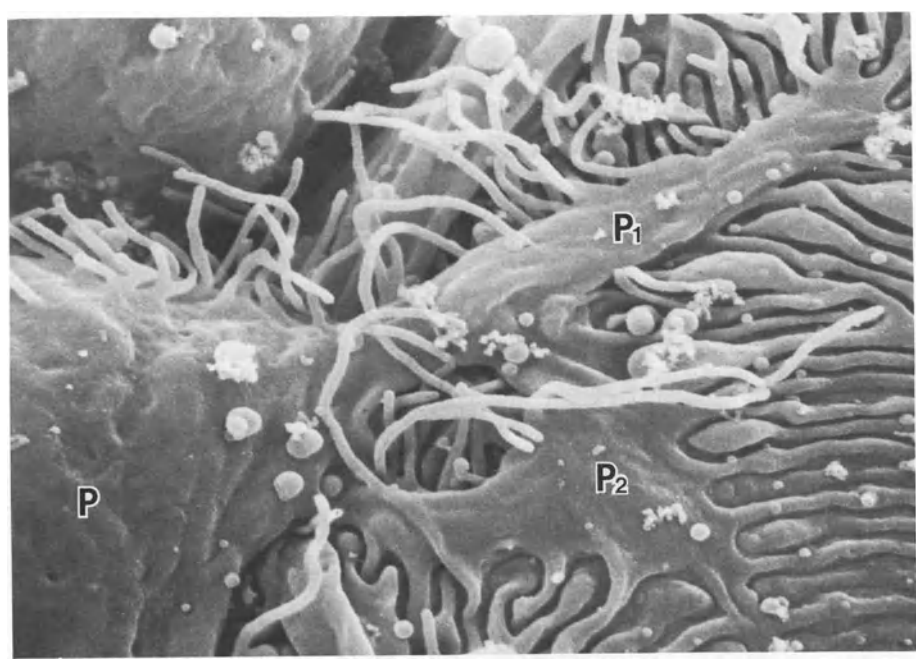

Fig. 9. Podocyte (P), its primary (P_1) and secondary (P_2) processes and endfeet in guinea pig glomerulus. Note the long microvilli on the cell body and processes, which are especially conspicuous in this species. (×10,500).

3. Podocytes or glomerular epithelial cells

3.1. The entire shape of the cell

The three-dimensional shape of the podocyte was only incorrectly visualized by TEM observations, and SEM first made it accurate. The main points are the mode of branching of the cell processes and the interdigitation of their endfeet [12, 13]. SEM further demonstrates microvilli and irregular-shaped microprojections on the cell body (perikaryon) and processes of the podocyte (Fig. 9). Their functions are unknown, but it is known that podocyte microvilli are conspicuously increased in number and length in certain renal disorders including nephrosis, and under cultured conditions [14].

3.2. Pedicels or endfeet

The endfeet of podocytes are engaged in the formation of the glomerular filtration membrane. They are embedded in the outer portion of the basement membrane with their broadened base. The pedicel bases, about 100 nm wide, are juxtaposed, leaving slits 20–50 nm (usually 24 nm) wide [8]. Pedicels derived from the same cell are never juxtaposed with each other [12, 13]. This may imply the alternately different movement of 'massaging fingers' on the capillary wall.

Podocyte cytoplasm contains large amounts of microtubules and filaments that are especially condensed in the endfeet and run longitudinally in each pedicel (Figs. 10, 11). Besides intermediate (10 nm) filaments, microfilaments suspected as actin filaments are densely gathered in bundles, especially in the upper layer of the endfeet (Fig. 10). The occurrence of filamentous structures and the possibility of their contractility have been dealt with by many TEM researchers since the early study of Policard [2]. Recent immunohistochemical and other techniques revealed high concentrations of actin in the podocyte processes and pedicels. Studies with cytochalasins have suggested that contraction of actin may lead to flattening of endfeet and closure of the slits. Relaxation of actin filaments makes the pedicel bases narrow and widen the slits [815].

The surface of the pedicels, except for their basal face embedded in the basement membrane, is coated by an irregular layer of about 12 nm thickness (Fig. 12). The coat is composed of polysaccharides and stained with phosphotungstic acid, ruthenium red, and colloidal thorium and iron. Neuraminidase treatment abolishes the stainability of this layer, suggesting that it contains sialic acid [8].

The lateral surface of the pedicel bases are connected by a particular thin membrane, called the slit membrane [3].

3.3. Podocyte perikaryon and its processes

The nuclei of podocytes are generally oval, sometimes with deep indentations. The nucleolus is not conspicuous.

The cytoplasm of the perykaryon and major processes contains scattered mitochondria, cisterns of rough endoplasmic reticulum, and many polysomes. The Golgi apparatus is usually separated into a few areas in the perikaryal cytoplasm (Fig. 11). Centrioles are occasionally encountered. Smooth surfaced vesicles, coated vesicles, and multivesicular bodies may be numerous [8]. The podocyte cytoplasm is characterized by abundant filaments, which were mentioned in the section 3.2.

4. Glomerular filtration membrane

4.1. Basement membrane

The basement membrane intercalated between the podocytes and endothelial cells belongs to the former cell; the latter possesses no basement membrane in the glomerulus. The basement membrane measures in thickness about 100 nm in children and 200–400 nm in adults. It consists of three layers: an outer less dense layer termed lamina rara externa; a central dense layer, lamina densa; and an inner, less dense layer, lamina rara interna. The lamina rara externa is limited by the slit membrane and embed the lower portion of the pedicels (Figs. 12, 13). The basement membrane consists mainly of type IV collagen and glycosaminoglycans (acid mucopolysaccharides); the former is concentrated in the lamina densa and the latter in the laminae rarae.

4.2. Glomerular filtration

The glomerular filtration mechanism has been and still is a matter of dispute. Examinations of the passage of particulate tracers of different sizes have indicated that the basement membrane stems ferritin particles (about 100 Å in diameter) but does not interrupt the passage of smaller molecules like catalase and human myeloperoxidase. These are, however, interrupted by the slit membrane and/or the pedicel sugar coat mentioned above. Still smaller particles, e.g., horseradish peroxidase, quickly passes through all filtration layers [4, 5, 8].

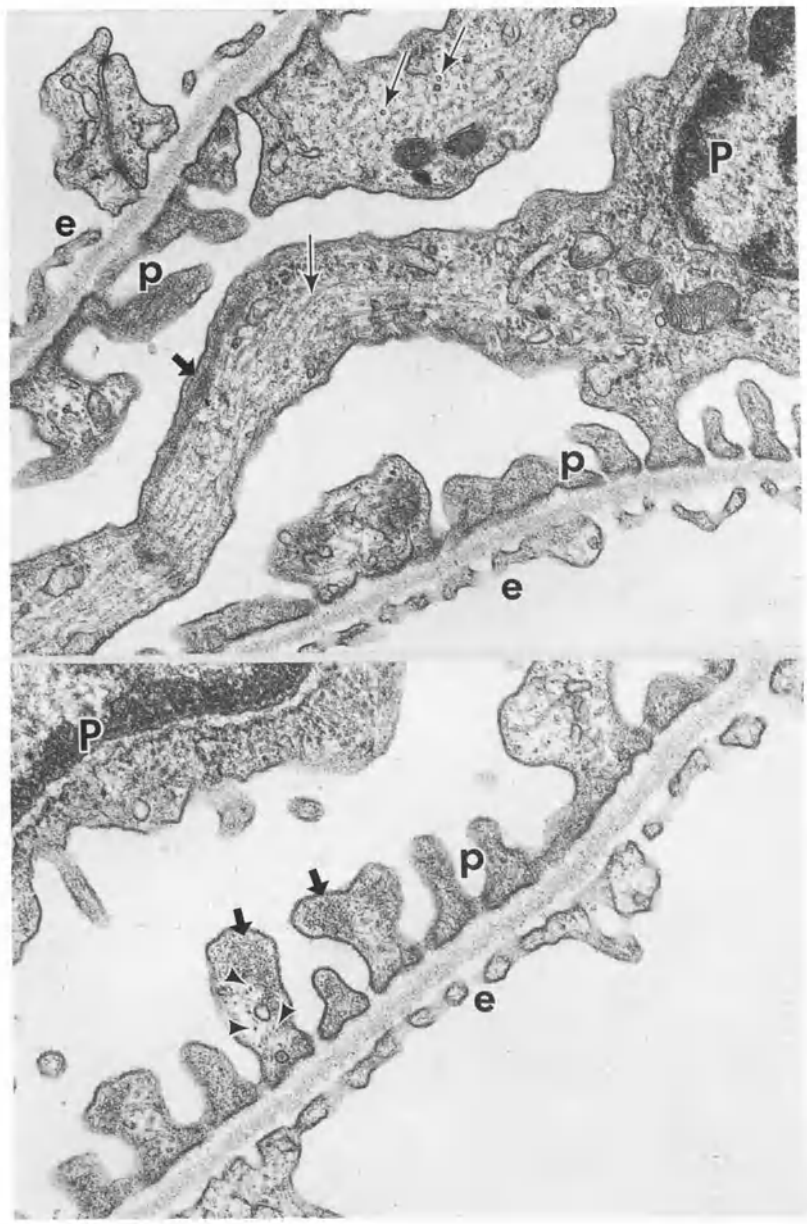

Fig. 10A, B. Supporting and contractile structures in podocyte processes of the mouse. P: podocyte nuclei; e: endothelium. The podocyte processes and endfeet (p) possess longitudinally arranged microtubules (small arrows), intermediate filaments (arrowheads), and bundles of microfilaments (thick arrows). (*A:* ×32,000; *B:* ×44,000). Courtesy of Prof. Harunori Ishikawa, Gunma University Medical School.

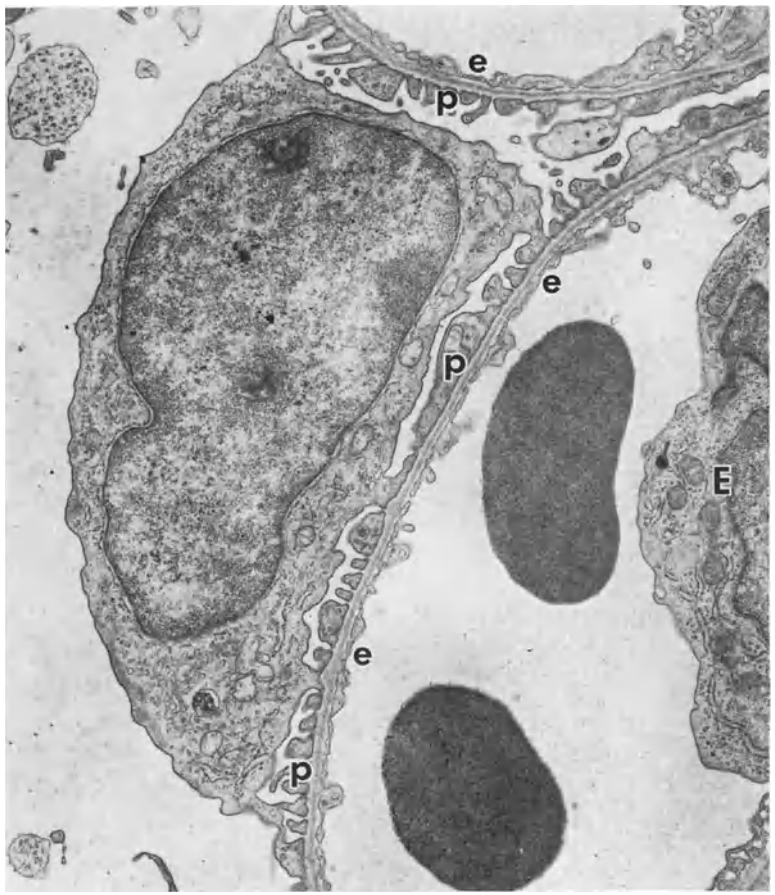

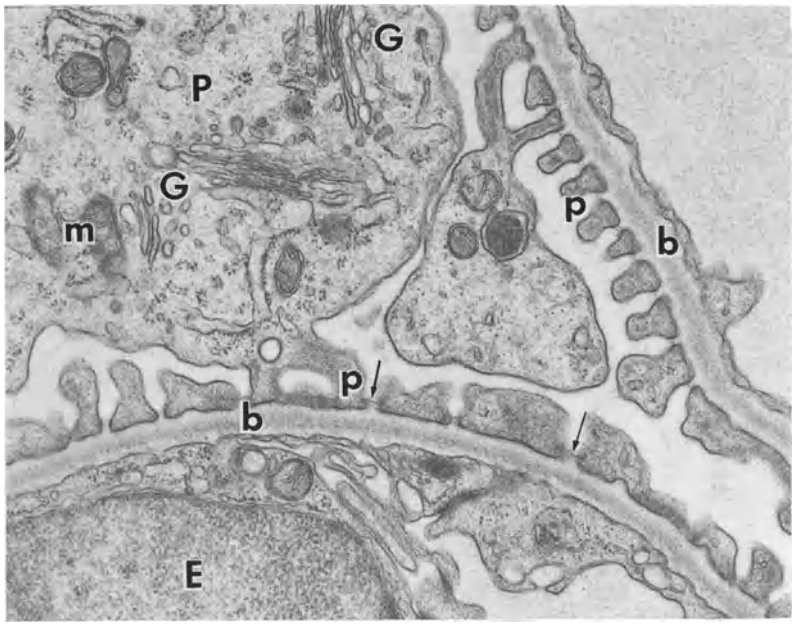

Fig. 12. Podocyte (P), endothelial cell (E) and their processes forming the glomerular filtration membrane in the mouse. G: Golgi complexes; m: mitochondria; p: podocyte endfeet; b: basement membrane; e: attenuate portion of endothelium. Arrows indicate slit membranes. (×21,000).

Fig. 11. Podocyte in a mouse glomerulus. It gives pedicels (p) to the basement membrane (b). E: endothelial cell; e: attenuate portion of the endothelium. (×5,600).

More recently, the polyanionic nature of glycosaminoglycans in the basement membrane has been estimated as an important factor in the selection of substances to be filtrated, since it was demonstrated that ferritin particles, if cationized, could easily permeate into and pass through the basement membrane [16, 17] (Fig. 14).

5. Mesangium

5.1. Mesangial cells

Mesangial cells are characterized by irregular processes radiated from the cell periphery. The nuclei are generally ovoid in shape, often with a clear nucleolus. The electron-lucent cytoplasm contains moderate numbers of elongated mitochondria, cisterns of rough endoplasmic reticulum, and small but distinct Golgi areas [8] (Fig. 15). The phagocytotic activity of the mesangial cells has been reported [cf. 8] to take up large foreign bodies; experimentally-induced India ink or ferritin particles may be incorporated by the cells.

More characteristic of this cell is the occurrence of filaments that are especially numerous in the peripheral cell processes. Immunocytochemical studies using anti-actin antibodies support the view that this cell may be contractile in nature with abundant actin filaments [14, 15]. Andrews [15] stresses that the filaments frequently insert into an electron-dense zone adjacent to the plasma membrane, reminiscent of the dense bodies in smooth muscle cells. The contraction of mesangial cells, which has been confirmed in isolated cells in vitro [cf. 15], has been postulated to serve in the control of the glomerular blood stream, but nothing precise is known about the effects of the contraction.

5.2. Mesangial matrix

The mesangial cells and their processes are embedded in connective tissue matrix consisting of collagen filaments and amorphous substances (Figs. 7, 15). The mesangium is limited by the basement membrane, whose lamina rara interna is incorporated in the mesangial matrix, and only the lamina densa and lamina rara externa can be identified. Podocyte pedicels are studded on the supramesangial basement membrane.

6. Summary and conclusion

Subcellular structures, and possible functions suggested from them, of the cellular and intercellular elements of renal glomerulus were reviewed. In the endothelial cells, hitherto overlooked fenestrated domes on their attenuated cytoplasm and perikaryon were introduced by both TEM and SEM. In the glomerular epithelial cells or podocytes microfilaments of a supporting and/or contractile nature were the main subject. The glomerular basement membrane was dealt with not only as a simple mechanical ultrafilter, but also as a negatively ionized barrier. The mesangial cells were reviewed with special reference to contractile filaments richly contained in them.

The mechanism of glomerular filtration is still largely obscure. Moreover, precise knowledge of normal structure of the glomerulus, which is essential for understanding its pathological changes, is insufficient as yet. TEM, SEM, cytochemistry, and other cell-biological strategies must be combined to promote our knowledge in this field.

References

1. Hall BV: Studies of normal glomerular structure by electron microscopy. In: Proc 5th Ann Conf on the Nephrotic syndrome, New York, National Nephrosis Foundation, 1953, p 1–39.
2. Policard A, Collet A, Giltaire-Ralyte L: Recherches au microscope électronique sur la structure du glomérule rénal des mammifères. Arch Anat microsc Morphol exp 44: 1–19, 1955.
3. Yamada E: The fine structure of the renal glomerulus of the mouse. J biophys biochem Cytol 1: 551–556, 1955.
4. Farquhar MG, Wissig SL, Palade GE: Glomerular permeability. I. Ferritin transfer across the normal glomerular capillary wall. I. Exp Med 113: 47–66, 1961.
5. Karnovsky MJ, Ainworth SK: The structural basis of glomerular filtration. In: Advances in Nephrology, Hamburger J, Crosnier J, Maxwell MH (eds), Chicago, Year Book Medical Publishers Inc, 1972, p 35–60.
6. Wolff J, Merker H-J: Ultrastruktur und Bildung von Poren im Endothel von porösen und geschlossenen kapillaren. Z Zellforsch 73: 174–191, 1966.
7. Fujita T, Tokunaga J, Edanaga M: Scanning electron microscopy of the glomerular filtration membrane in the rat kidney. Cell Tiss Res 166: 299–314, 1976.
8. Latta H: Ultrastructure of the glomerulus and juxtaglomerular apparatus. In: Handbood of Physiology, Section 8, Renal Physiology, Washington, Americal Physiological Society, 1973, p 1–29.
9. Rhodin JA: The diaphragm of capillary endothelial fenestrations. J Ultrastr Res 6: 171–185, 1962.
10. Friedrici HHR: On the diaphragm across fenestrae of capillary endothelium. J Ultrastruct Res 27: 373–375, 1969.
11. Yoshinari T, Fujita T: Scanning electron microscope studies on rabbit renal glomerulus, with special reference to 'podocytic membrane' of Elias and to pored domes on capillary endothelium. Arch Histol Jap 45: 99–109, 1982.
12. Fujita T, Tokunaga J, Miyoshi M: Scanning electron microscopy of the podocytes of renal glomerulus. Arch Histol Jap 32: 99–113, 1970.
13. Arakawa M, Tokunaga J: Further scanning electron microscope studies of the human glomerulus. Lab Invest 31: 436–440, 1974.
14. Andrews PM: Investigations of cytoplasmic contractile and cytoskeletal elements in the kidney glomerulus. Kidney Int 20: 549–562, 1981.

15. Andrews PM, Coffey AK: Cytoplasmic contractile elements in glomerular cells. Fed Proc 42: 3046–3052, 1983.
16. Rennke HG, Cotran RS, Venkatachalam MA: Role of molecular charge in glomerular permeability. Tracer studies with cationized ferritin. J Cell Biol 67: 638–646, 1975.
17. Oite T, Batsford SR, Mihatsch MJ, Takamiya H, Vogt A: Quantitative studies of *in situ* immune complex glomerulonephritis in the rat induced by planted, cationized antigen. J Exp Med 155: 460–474, 1982.

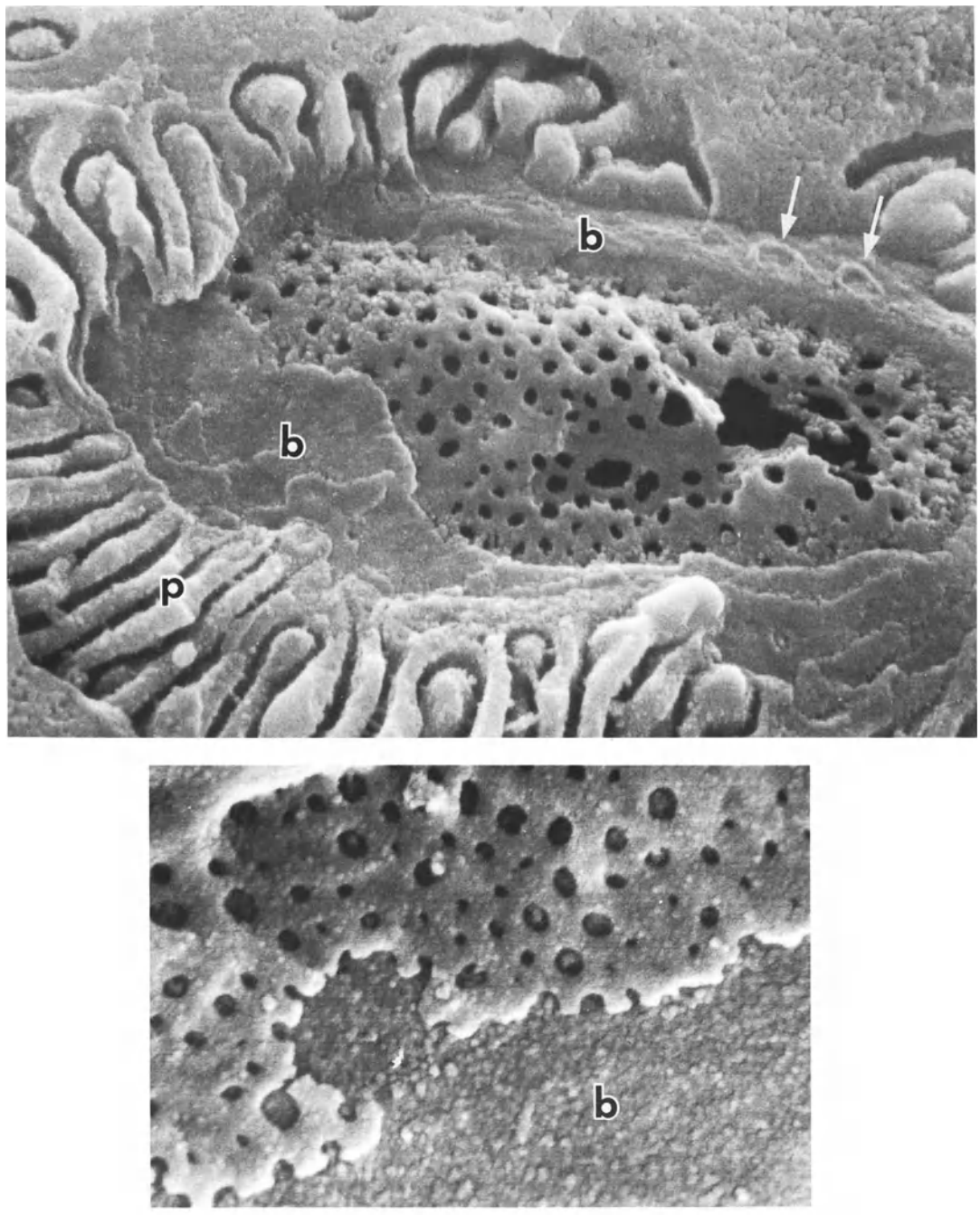

Fig. 13. SEM view of the glomerular basement membrane, seen from the epithelial (urinary) side (*A*) and from the endothelial (hemal) side (*B*). The basement membrane (b) appears laminated in Figure *A*, while granular in Figure *B*. The podocyte pedicels (p) have left their footmarks on the basement membrane (arrows). (*A:* rat, ×25,500; *B:* rabbit, ×34,000).

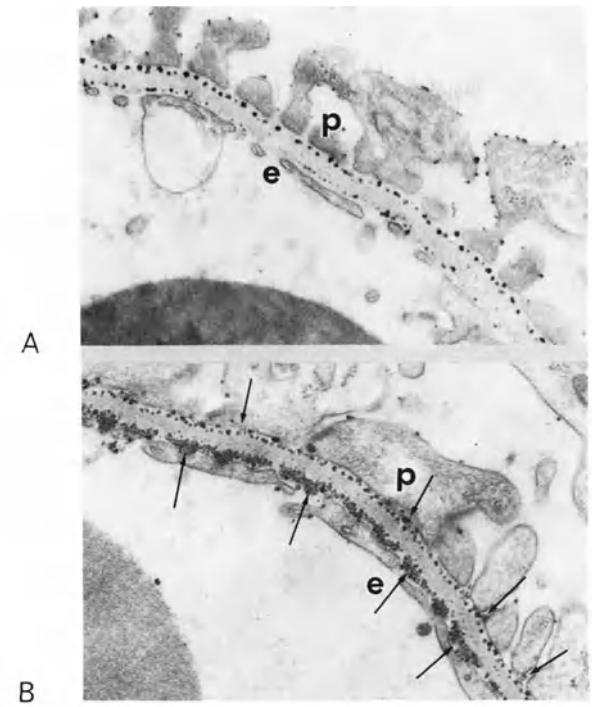

14

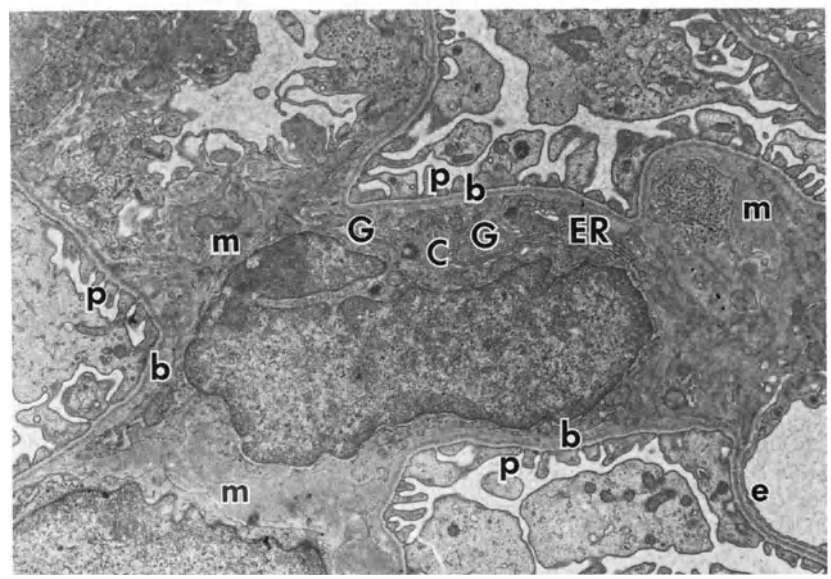

15

Fig. 14A. Glomerular filtration membrane in a rat 15 min after an intravenous injection of polyetheneimine (PEI) (molecular weight 40,000–60,000). Fixation in 10% glutaraldehyde plus 2% phosphotungstic acid. Aggregated PEI particles, which indicate the anionic sites in the tissue, are located in the laminae rarae and partly also on the podocyte pedicels. *B*. In this case the rat kidney was perfused, via the renal artery, with cationized ferritin (isoelectric point: 9.5) 1 hr prior to the injection of PEI. Fifteen min after the PEI injection, the rat was killed and the kidney was fixed as above noted. The ferritin aggregates (arrows), which appear finer than PEI, are mainly located in the lamina rara interna, but small amounts of them have reached the base of the podocyte endfeet. (Cationized ferritin is gathered beneath and between the endfeet within 24 hrs.) e: Endothelium; p: podocyte endfeet. (×22,750). Courtesy of Dr. Takashi Oite, Institute of Nephrology, Niigata University Medial School.

Fig. 15. Mesangial cell surrounded by mesangial matrix (m) from a mouse glomerulus. C: centriole; G: Golgi complexes; ER: rough endoplasmic reticulum; p: podocyte endfeet; b: basement membrane; e: endothelium. (×6,500).

CHAPTER 7

Recent research on some aspects of proximal tubular transport phenomena

PAUL H. BRAND

1. Introduction

Important themes in the study of the metabolism of the kidney have included the relationship between ion transport and energy production, acid-base balance and the control of renal ammonia production, and regional differences in metabolic pathways within the kidney.

The relationship between ion transport and energy production was investigated in the past primarily by determining the effect on renal oxygen consumption of varying net renal sodium reabsorption *in vivo,* usually in the dog. While such studies provided some information on the metabolic cost of sodium transport, quantitative interpretation of these experiments using the intact kidney is difficult [1]. More recently techniques have been developed which permit investigation of the relationship between ion transport and metabolism in different parts of the nephron. The purpose of this chapter is to describe how such recent technical advances are providing a better understanding of the relationship between ion transport and energy production in the mammalian proximal tubule.

Studies of the metabolism of the proximal tubule will be emphasized because recent advances in experimental methodology have allowed the development of a quantitative description of the relationship between active ion transport and oxidative metabolism in this nephron segment. Such recent advances include development of a proximal tubular suspension with improved function [2] and utilization of inhibitors in the isolated, perfused tubule technique.

2. Active cation transport: the 'pacemaker' of respiration

Utilization of these new techniques has provided support for Whittam's hypothesis [3] concerning the regulation of renal tubular oxidative metabolism by changes in the rate of active ion transport (Fig. 1).

Whittman measured the effect of ouabain, or removal of Na^+ from the incubation medium, on oxygen consumption and Na^+ and K^+ transport in slices of brain and kidney cortex. Since inhibition of ion transport by these agents inhibited oxygen consumption, Whittam proposed that 'an ATP-hydrolysing system associated with active transport of cations may act as a pacemaker for about half the respiration of brain and kidney cortex' [3].

A series of elegant experiments analyzing this hypothesis has been published [1, 4, 5, 6]. These studies depended on the development of a collagenase-isolated suspension of rabbit proximal tubules with improved function [2]. Although Burg, *et al.*, [7] had reported the use of a collagenase-isolated rabbit tubule suspension in 1966, the preparation reported by Balaban, *et al.*, [2] has the distinct advantages that the lumina of the tubules are patent, and the tubule segments are predominantly of proximal origin. Patency of the lumen means that transepithelial ion transport may continue to occur, with concomitant metabolism. In contrast, in cortical slices or earlier tubule preparations, the lumina were variably collapsed, thereby inhibiting transcellular ion transport.

Also, predominance of a single nephron segment in Balaban *et al's* suspension means that complications in interpretation of data due to the presence of a mixture of tubule types with different metabolic and transport characteristics, are eliminated.

In this same paper [2] Balaban *et al.* described a chamber for incubation of the tubule suspension which permitted simultaneous measurement of tubule oxygen consumption, NADH fluorescence, and rapid analysis of tubule ATP content. Later, a K^+ selective electrode was added to the chamber for determination of extracellular potassium concentration [6].

Initially, this proximal tubule suspension was used to investigate the role of the ATP/ADP ratio in the

L.J.A. DiDio and P.M. Motta (eds), Basic, Clinical, and Surgical Nephrology. ISBN 0-89838-689-5.

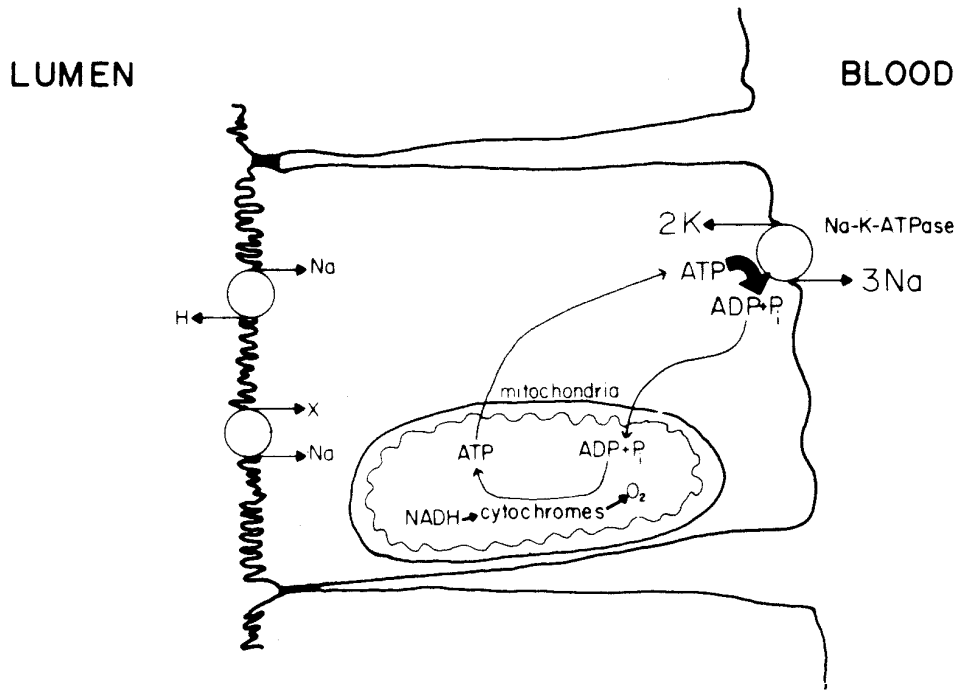

Fig. 1. Whittam's hypothesis as developed by Mandel, that the rate of activity of the Na^+,K^+-ATPase regulates the rate of mitochondrial phosphorylation via cellular ATP and ADP concentrations. The open circles at the luminal membrane represent the Na^+,H^+ antiport and the various co-transport mechanisms (Na^+,X). From Mandel and Balaban, with permission.

coupling of cellular respiration to cellular ion transport [4]. In addition to monitoring oxygen consumption by the tubules, the redox state of the mitochondria was determined by microfluorometry (reduction of NAD to NADH corresponding to an increase in 450 nm fluorescence).

Under control conditions, oxygen consumption, the ATP/ADP ratio and fluorescence (representing the degree of oxidation of NADH) by the tubule suspension were stable until sufficient oxygen in the closed chamber had been consumed so that the PO_2 decreased to 10 mm Hg. At this point, the QO_2 and the ATP/ADP ratio decreased abruptly and fluorescence (reduced NADH) increased dramatically, demonstrating the effects of anoxia on mitochondrial oxidation and oxidative phosphorylation.

Next, to determine the effect of inhibition of the Na^+,K^+-ATPase, ouabain was added (in fresh, oxygenated suspension). Ouabain decreased the oxygen consumption by 54%, increased the NADH fluorescence by 35%, and increased the ATP/ADP ratio by 30%. These changes were interpreted to mean that inhibition of the Na^+,K^+-ATPase by ouabain decreases the rate of ATP hydrolysis, so that the ATP/ADP ratio increases. An increase in this ratio then acts to slow the rate of oxidative phosphorylation, thereby decreasing the oxygen consumption and changing the mitochondria to a resting or reduced state as evidenced by the increased NADH fluorescence.

If the tubules became anoxic before addition of ouabain, then ouabain had no effect on any of the parameters measured.

To observe the effect of stimulating the Na^+,K^+-ATPase, tubules were depleted of K^+ by suspension in a K^+ free Ringers, and then the effect of adding K^+ was observed. Addition of 5 mM KCl to K^+ depleted tubules increased the oxygen consumption by 130%, decreased NADH fluorescence and decreased the ATP/ADP ratio. These changes are all in the opposite direction to those elicited by ouabain and indicate that addition of K^+, by stimulating active ion transport, results in an increase in ATP hydrolysis via the Na^+,K^+-ATPase which depletes cellular ATP. The subsequent decrease in the ATP/ADP ratio then increases the rate of mitochondrial oxidative phosphorylation, NADH is oxidized, (indicative of a more active mitochondrial state) and oxygen consumption and ATP production are increased.

Taken together, these results indicate that the rate of oxidative phosphorylation is under sensitive control via the rate of ATP hydrolysis by the Na^+,K^+-

ATPase. Since, in the renal epithelium, active ion transport is a major consumer of ATP, changes in ion transport rate exert control over mitochondrial respiration via rapid alterations in the ATP/ADP ratio when ion transport rates change.

2.1. Active cation transport: mitochondrial capacity and ion transport

From these experiments a correlation had been established between proximal tubular ion transport (Na^+,K^+-ATPase activity) and mitochondrial oxidative metabolism. In carrying this work further, the proportion of the total ATP generating capability of the renal cell which is used in supporting ion transport, was measured in proximal tubular cells. This was done by determining the maximal mitochondrial oxidative capacity, and the percentage of this capacity utilized to supply ATP for the Na^+,K^+-ATPase. Both the rabbit proximal tubule suspension and a rabbit kidney cortex mitochondrial suspension were used in these experiments [5].

To assess the respiratory capacity of the tubules, oxygen consumption during optimal mitochondrial phosphorylating activity was determined. Optimal mitochondrial phosphorylating activity in the tubules was induced by adding ADP after treating the tubules with digitonin. Digitonin was used to make the cell membrane permeable to exogenous ADP. Addition of exogenous ADP to a digitonin-treated tubule suspension resulted in a four-fold increase in oxygen consumption and ADP/O ratio of 2.1, close to the ratio observed in isolated mitochondria. These results were interpreted to mean that the ADP/O ratio in the intact cell is similar to the ratio in isolated mitochondria.

Next, the turnover of cytochrome A during oxidation was compared in the digitonin-treated tubules to that in mitochondrial suspensions. Cytochrome A content was measured spectrophotometrically in each preparation. The oxygen consumption was also measured during respiration under similar conditions for each preparation. The oxygen consumption rate divided by the cytochrome content gives the turnover, in moles of oxygen per cytochrome A. For proximal tubules the value was 838, and for mitochondria, 844. This similarity in cytochrome turnover indicates that the digitonin treatment had not damaged the mitochondria of the tubular supension.

Since the digitonin-treated tubules have intact respiratory capability, the maximal respiratory capacity in the tubules could be compared to that observed in tubule suspensions under various conditions. For example, spontaneously respiring tubules in the presence of valeric acid, glucose, lactate and alanine had an oxygen consumption rate of ~ 50 nmol/min per mg protein which corresponds to an oxygen, cytochrome turnover of 567 oxygen atoms per minute per cytochrome A. Since the maximal respiratory capacity of digitonin-treated tubules under these conditions corresponds to an 0/cytochrome turnover of 1,010 0/min per cytochrome A, these tubules were utilizing 56% ($567/1010 \times 100$) of their mitochondrial oxidative capacity.

Next, in order to maximize the rate of ion transport and its associated metabolism, the effect of nystatin was examined. Nystatin is thought to increase the permeability of the cell membrane to Na^+, so that cell Na^+ concentration increases and the Na^+,K^+-ATPase is stimulated by internal sodium. Nystatin increased the oxygen consumption and the percentage of mitochondrial capacity utilized. In the presence of nystatin and a short chain fatty acid or ketone body, 100% of the mitochondrial capacity was used. If ouabain was also added, then only 30% of the mitochondrial capacity was used. These data imply that the maximal oxidative capacity of the tubular cell may be enlisted in support of ion transport, and that the non-transport metabolism is about 30% of the total oxidative capacity.

If the only exogenous substrates added were glucose, lactate and alanine, then the oxygen consumption after stimulation by nystatin represented only 70% of the mitochondrial capacity. Endogenous substrates were capable of supporting only 56% of the maximal mitochondrial capacity. Since, as noted above, in the presence of fatty acids, 100% of the mitochondrial capacity is used, the authors suggested that fatty acids or ketone bodies are needed to provide reducing equivalents for optimal mitochondrial oxidative phosphorylation.

In summary, spontaneous rates of respiration in isolated tubules utilize 55% of the cell's mitochondrial respiratory capacity, about half of which is subsumed by the Na^+,K^+-ATPase. Stimulation of the Na^+,K^+-ATPase in the presence of fatty acids results in an increase in ouabain sensitive respiration up to 100%, i.e., complete utilization of the cellular mitochondrial oxidative capacity.

2.2. Active cation transport: stoichiometry

Having described the relationship between ion transport and oxidative capacity in the tubular suspension, Harris *et al* [6] next attempted to determine the stoichiometric relationship between unidirectional active ion transport and oxygen consumption of the proximal tubular cell.

As before, proximal tubular suspensions from rabbit kidney were used. Extracellular K^+ concentration (in the suspending medium) was measured with a K^+ electrode. Tubules were depleted of K^+ by preincubation in K^+ free Ringer's.

Initially, the rate of K^+ uptake and the oxygen consumption were measured after adding K^+ to K^+ depleted tubules. The rate of K^+ uptake was evalued from the change in extracellular K^+ concenration after addition of a bolus of KCl to K^+ depleted tubules. During the 10 second period of measurement, the rate of K^+ uptake was linear with time, indicating that a unidirectional K^+ influx was being monitored. The simultaneously measured oxygen consumption rate was also observed to be linear with time. From these linear initial rates, the ratio of K^+ transported to oxygen consumed can be measured. Since the K^+ transport being measured represented a unidirectional flux via the active pathway, this ratio should directly reflect the coupling of cellular respiration to active ion transport via the Na^+,K^+-ATPase.

A mean ratio of K^+ transported to oxygen consumed was determined in 15 tubule suspensions; the value of the ratio was 10.7. This ratio corresponds exactly to the expected stoichiometry of the Na^+,K^+-ATPase:

Assuming that 2 K^+ are transported per ATP hydrolyzed via the Na^+,K^+-ATPase, and that 3 ATP are generated per oxygen consumed via NADH linked oxidative phosphorylation, the predicted value of the $K^+/0_2$ ratio is 9 to 11, corresponding very closely to the observed value of 10.7. This close correspondence between observed and predicted ratios implies that the stoichiometry of the Na^+,K^+-ATPase *in vivo* is similar to the value *in vitro*. More importantly, there is nearly complete coupling between oxidative phosphorylation and active K^+ uptake (and Na^+ extrusion) in the renal proximal tubular cell.

The $K^+/0_2$ ratio was also determined at different extracellular K^+ concentrations, and was found to be constant over a 3 to 4 fold range of net K^+ uptake. The constancy of the ratio over this range implies that there is tight linkage between ion transport and oxidative metabolism over a wide range of Na^+,K^+-ATPase activities.

How much of the cell's oxidative capacity is required to support maximal ion transport rates? The highest rate of K^+ transport observed in this study corresponded to a Na^+,K^+-ATPase activity of 150 nmol ATP/min per mg protein. This rate is close to the ATP turnover observed under optimal conditions in freeze-thawed rabbit cortical tubules. Similarly, the oxygen consumption observed during the maximal rate of K^+ transport corresponded to the maximal rate of turnover of cytochrome A previously found in proximal tubule suspensions. In other words, the highest rate of active ion transport requires complete utilization of the ATP-synthesizing capacity of the tubular cell.

Further analysis of these data [6] indicates that the rate of ion transport in spontaneously respiring cells is about one-third of the maximal respiratory capacity. Thus the rate of ion transport under physiological conditions equals about one-third of the maximal transport capacity of the tubular cell, and the cell uses about one-half of its oxidative capacity to support this rate.

In summary, these studies [4, 5, 6] have provided strong quantitative evidence in support of Whittam's hypothesis, which provides a mechanistic explanation for the observed dependence of renal cortical oxygen consumption on active ion transport. Tight coupling between generation of ATP by mitochondrial oxidative phosphorylation, and ATP utilization by the Na^+,K^+-ATPase is provided by changes in the ATP/ADP ratio of the cytoplasm. The ATP content of spontaneously respiring proximal tubular cells is small compared to the rate of ATP turnover required to support activity of the Na^+,K^+-ATPase. Consequently, any change in the rate of active ion transport results, within seconds, in a change in cell ATP content and hence in the cytoplasmic ATP/ADP ratio. Changes in this ratio then rapidly adjust the state of mitochondrial oxidative phosphorylation appropriately for the new ATP/ADP ratio.

In addition to demonstrating a tight coupling between ion transport and metabolism, and the central role of the ATP/ADP ratio, these studies imply that maximal rates of active ion transport in the proximal tubule may be supported solely by oxidative metabolism, in keeping with the high oxygen consumption of the kidney.

Conversely, the observation that the ratio of K^+ transported to oxygen consumed is very close to the ratio predicted from *in vitro* observations of the stoichiometry of the Na^+,K^+-ATPase, implies that all of the energy required for proximal tubular Na^+ and K^+ transport is derived from hydrolysis of ATP. This conclusion is at variance with earlier reports indicating that non-ATP sources of energy must be invoked to account for all of proximal tubular active ion transport. However, other recent studies provide independent support for this conclusion (see below).

In addition, since in the proximal tubule, the ac-

tive transport of most other small molecular weight solutes appears to be dependent on active sodium transport, the energy for the transport of these other solutes must also be tightly linked to oxidative phosphorylation. Thus, the active reabsorption of sugars, amino acids, organic acids, phosphate and sulfate and the secretion of H^+ in the proximal tubule, are all energized by co-transport or antiport with Na^+ [8, 9]. Furthermore, to the extent that bicarbonate reabsorption depends on H^+ secretion via the antiport, net proximal bicarbonate reabsorption must also be linked to mitochondrial oxidative phosphorylation via the ATP/ADP ratio. Transport processes whose energetics in the proximal tubule are less well understood, and which perhaps may not be linked to the Na^+,K^+-ATPase, include secretion of organic acids and organic cations, and pinocytosis.

Finally, the observed K^+/O_2 ratio of ~10 in the proximal tubule corresponds, assuming $3\,Na^+$ ejected for each K^+ taken up, to a Na^+/O_2 ratio of 15. A Na^+/O_2 ratio very close to 15 has been recently reported in such diverse preparations as the dog kidney *in vivo* [10, 11], and the toad urinary bladder [12, 13].

These issues will be discussed further below. However, it is first necessary to discuss other experiments which appear to contradict, at least partially, some of the conclusions drawn so far.

3. Inhibitors and proximal tubule ion transport: is there a non-mitochondrial energy source supporting ion transport?

Many attempts have been made to determine the energy sources for proximal tubular fluid reabsorption, by testing the effect of various metabolic inhibitors on fluid reabsorption *in vivo* or *in vitro*. The underlying assumptions in this work are that proximal tubular fluid reabsorption depends on active sodium reabsorption, and that the inhibitors tested may specifically block certain steps in the generation of available metabolic energy. Variable results have been obtained in that some authors have demonstrated complete inhibition of fluid reabsorption by metabolic inhibitors, while others have found differing degrees of partial inhibition. While no attempt will be made here to completely review this literature, two recent thoughtful studies will be discussed.

Gyory and Kinne examined the effect on fluid reabsorption (Jv) of inhibitors of oxidative phosphorylation in rat proximal convoluted tubule, using the split oil droplet technique to measure Jv [14]. The peritubular capillaries were also perfused, so that inhibitors could be applied to the basolateral membrane. In parallel experiments, the Na^+,K^+-ATPase activity was measured in a suspension of rat kidney cortex membranes.

They observed that intratubular application of oligomycin in the presence of bovine serum albumin resulted in a steady state inhibition of Jv of 80%. Antimycin A, again with albumin, also inhibited Jv by 80%. The necessity to provide albumin to achieve inhibition with antimycin A and oligomycin was attributed to binding of the inhibitors to albumin and subsequent uptake of the inhibitor-albumin complex at the luminal membrane by pinocytosis.

On the other hand, cyanide given intratubularly did not inhibit volume absorption. This lack of effect was attributed to very rapid diffusion of CN^- away from the site of action.

Peritubular application of oligomycin or antimycin A produced some inhibition of Jv, but with very large variability and less effect than intratubular application. The authors speculate that the variability may be due to poor ability of the inhibitors to penetrate cells from the basolateral aspect. However, since other studies [15] showed a peritubular effect of antimycin A, another explanation for this variability may be incomplete perfusion of the peritubular capillaries.

Cyanide perfused into the peritubular capillaries resulted in complete inhibition of Jv within 20 seconds. CCCP, an uncoupler of oxidative phosphorylation, had a similar effect to cyanide when given peritubularly.

Oligomycin maximally inhibited ~85% of the Na^+,K^+-ATPase activity in cortical membrane suspensions, whereas antimycin A inhibited Na^+,K^+-ATPase completely. Neither cyanide nor CCCP inhibited Na^+,K^+-ATPase in the membrane suspension.

The complete inhibition of Jv with cyanide and CCCP was taken to indicate that proximal sodium transport depends entirely on oxidative phosphorylation for its energy. However, since oligomycin inhibited Na^+,K^+-ATPase *in vitro* and allowed Jv to continue *in vivo* at 20% of the control rate, the authors concluded that the active sodium transport responsible for 20% of Jv is supported by some unknown oxidative energy source other than ATP, and does not occur via the Na^+,K^+-ATPase. If these data are correct, then there must be some independent non-mitochondrial oxidative energy source which supports a portion of active sodium transport occurring via an undescribed pathway.

To determine if such an independent pathway exists, the degree of inhibition of Jv in the proximal

tubule by inhibitors of oxidative phosphorylation was re-investigated by Gullans *et al* [15] using the isolated, perfused rabbit proximal tubule. To clarify the mechanism of action of the inhibitors, their effects on oxygen consumption, NADH fluorescence and ATP content of a proximal tubular suspension was also measured as were phosphate and glucose reabsorptive transport rates.

Two inhibitors of oxidative phosphorylation, rotenone and antimycin A, were tested and found to produce a dose-dependent inhibition of 85–88% of the oxygen consumption. In fact, antimycin A reduced cellular ATP content by 94%, an effect significantly greater than the 85% inhibition of oxygen consumption.

Rotenone, in addition, increased NADH fluorescence in the tubule suspension, an effect which accords with its role as a site I inhibitor of oxidative phosphorylation. (The effect of antimycin A on fluorescence could not be determined for technical reasons).

Rotenone and antimycin A at concentrations that maximally inhibit mitochondrial respiration completely inhibited proximal tubular volume absorption, phosphate reabsorption and most of glucose reabsorption.

The effects of rotenone and antimycin A on cortical tubular suspensions are similar to their effects in other studies on mitochondrial suspensions. The fact that whith antimycin A, cellular ATP content decreased indicates a mitochondrial site of action rather than inhibition of Na^+,K^+-ATPase. Inhibition of Na^+,K^+-ATPase would produce an increase in cellular ATP content such as is seen with ouabain.

The more complete inhibition of Jv and other transport processes observed in this study was attributed to technical improvements both in the measurement of Jv and in the application of the inhibitors to the proximal tubule. Gullans found [15] that albumin increased the K^+ of these inhibitors, making the drugs less available, and that the inhibitors did act from the peritubular side, in contrast to other results [14].

Gullans *et al* then concluded that, in the proximal convoluted tubule, there is a close correlation between oxygen consumption, cellular ATP content, mitochondrial redox state, and net sodium and water reabsorption. Inhibition of mitochondrial oxidative phosphorylation completely inhibits net sodium reabsorption and therefore, Jv. Inhibition of glucose and phosphate reabsorption would be expected as these transport processes depend on the electrochemical sodium gradient. Residual glucose reabsorption could be energized by glycolysis. No evidence was found for any non-mitochondrial, ATP-independent energy source for proximal tubular sodium transport.

3.1. Inhibitors and proximal tubule ion transport: two pumps?

A hypothesis that bears on the Whittam model as described above is that of Whittembury [16], who postulated the existence of two different modes of Na^+ transport in the proximal tubule on the basis of studies primarily in slices of renal cortex. According to Whittembury's hypothesis, one mode of Na^+ transport involves net Na^+, Cl^- and water extrusion from cells, and is refractory to ouabain but inhibited by ethacrynic acid. Whittembury speculated that this mode may be primarily responsible for net NaCl reabsorption in the proximal tubule. If so, then volume absorption should be insensitive to ouabain. The second mode of sodium extrusion was thought to be a ouabain sensitive exchange for K^+, and to occur without any change in cell volume.

Whittembury's hypothesis of two modes of sodium transport is contradicted by the numerous observations in the isolated, perfused rabbit proximal tubule that administration of ouabain both inhibits net volume reabsorption completely, and causes cell swelling [17].

Linshaw [18] recently re-examined one aspect of Whittembury's hypothesis, that there is a ouabain-insensitive mechanism responsible for regulation of renal proximal tubular cell volume. The effect of several inhibitors on cell volume was measured using isolated, nonperfused rabbit proximal tubules. Proximal straight tubules from rabbit renal mid-cortex were dissected and held with both ends crimped shut between micropipets. Outer tubular diameter (with the lumen collapsed) was measured and tubule volume calculated assuming that the tubule shape can be approximated by a cylinder. Inhibitors were applied in the bath and the tubule outer diameter measured every minute to observe the time course of changes.

Tubules in ouabain, 2,4-dinitrophenol (DNP), cyanide or azide all swelled to a similar degree. Addition of DNP plus ouabain produced no further increase in volume above that seen in ouabain alone. The cell volume in tubules treated with ouabain, DNP and cyanide together was also not different than the cell volume in tubules treated with ouabain alone.

The lack of an additive effect of ouabain and other inhibitors argues against the existence of a distinct, ouabain-insensitive mechanism for regulation of cell

volume, as does the observation that ouabain alone causes cell swelling.

4. Glucose transport and metabolism

The effect of glucose on oxygen consumption by the rabbit proximal tubule is a good example of the tightness of coupling between sodium transport and metabolism in this segment. Gullans *et al.* [19] investigated the question of whether the stimulatory effects of glucose on sodium transport seen in the perfused kidney [20, 21] are due to a direct metabolic effect of glucose, or are secondary to co-transport of glucose and sodium into the cell and subsequent increased availability of sodium for basolateral active extrusion.

Suspensions of rabbit proximal tubules were used. Oxygen consumption was determined polarographically, and NADH fluorometrically.

Results showed that removal of glucose from the suspension decreased oxygen consumption by about 20%, whether or not butyrate was present. Since butyrate is readily oxidized by renal cortex, the limitation on oxygen consumption with removal of glucose is not due to decreased availability of oxidizable substrate.

Substitution of alpha-methyl glucose for glucose had no effect on oxygen consumption, with or without butyrate. Oxygen consumption with nystatin was the same with or without glucose, and in the presence of ouabain, was low and unaffected by glucose. On the other hand, phloridzin decreased oxygen consumption by 10%, but only in the presence of glucose or alpha-methyl glucose. Addition of glucose or alpha-methyl glucose resulted in oxidation of NADH, consistent with an increased activity of the Na^+,K^+-ATPase and an increased rate of oxidative phosphorylation.

In this study it was concluded [19] that the effect of glucose on oxygen consumption occurs via increased sodium entry by co-transport with glucose, which stimulates the Na^+,K^+-ATPase, thereby increasing ATP hydrolysis. Changes in the ATP/ADP ratio then activate the mitochondria, oxygen consumption increases and NADH is oxidized.

This conclusion, that the effect of glucose on oxygen consumption is secondary to glucose, Na^+ co-transport, is consistent with the picture of tight coupling of oxidative metabolism to sodium transport in the proximal tubule described above. However, the conclusion does not satisfactorily explain observations on the effect of glucose on net sodium reabsorption in the intact kidney. For example, Frega *et al.* [20] found that addition of glucose to the perfusate increased net sodium reabsorption by the isolated, perfused rat kidney. This effect could not be mimicked by transported but non-metabolized analogues of glucose, even though the analogues themselves did undergo net reabsorption. Furthermore, both Frega *et al.* [20] and Gregg *et al.* [21] calculated that the observed increase in net sodium reabsorption upon addition of glucose to the perfused kidney was too large to be accounted for by sodium-glucose co-transport.

In the isolated proximal tubule addition of glucose primarily stimulates sodium uptake and thereby oxygen consumption, but in the intact kidney there are additional incompletely understood metabolic effects of glucose on sodium transport and on glomerular filtration rate and perfusate flow rate as well [20, 21]. These effects of glucose in the intact kidney may occur both in the proximal tubule and some more distal segments. While experimentation with an isolated proximal tubule suspension has provided important insights about coupling of transport to metabolism, extrapolation of these results to the intact kidney must be done with caution.

The recent studies with the isolated perfused tubule and proximal tubule suspensions have provided strong evidence for an extended version of Whittam's hypothesis that active cation transport sets the pace of oxidative metabolism in the renal proximal tubule. These data indicate that changes in sodium transport rate in this segment are rapidly translated into changes in oxygen consumption. The absolute changes in transport rate and oxygen consumption that occur correspond closely to the changes that may be predicted on the basis of the stoichiometry of oxidative phosphorylation in mitochondrial suspensions, and of the stoichiometry of the renal Na^+,K^+-ATPase as revealed by the activity of the isolated enzyme. The quantitative description of metabolism-transport coupling in the proximal tubule which has derived from these studies represents a major advance in our understanding of renal physiology.

5. Ion transport and oxygen consumption in vivo

Kiil's group [10, 11] has attempted to examine the question of coupling of active sodium transport to oxygen consumption in different nephron segments by measuring these parameters in the dog kidney *in vivo* under the influence of various inhibitors.

Net renal sodium reabsorption and renal oxygen consumption were measured in dogs receiving a 15% mannitol infusion [10]. To observe the effect of

changes in sodium transport on oxygen consumption, glomerular filtration rate (GFR) was decreased in stepwise fashion by gradual aortic constriction. Observations of sodium transport and oxygen consumption were made at the different levels of GFR obtained. The ouabain was infused into the renal artery and the maneuvers repeated, so that the relationship between net sodium reabsorption and oxygen consumption could be observed before and after ouabain.

Infusion of hypertonic mannitol by itself reduced fractional sodium reabsorption to 0.78, so that a massive natriuresis was established before determination of the Na^+/O_2 ratio. During stepwise reduction of GFR, net sodium reabsorption and oxygen consumption were proportionately reduced, as expected. By combining these results with those obtained after administration of ouabain, the Na^+/O_2 ratio for ouabain-sensitive transport was calculated.

Before discussing the ratio observed, some of the complications in interpretation of these experiments should be mentioned. The animals had been subject to extracellular fluid volume expansion combined with the diuretic effect of mannitol. Net proximal and loop sodium reabsorption were decreased presumably due to increased passive sodium backflux plus the development of a limiting sodium concentration gradient. An increased backflux of sodium should produce an increased recycling of sodium between peritubular capillary and lumen in the proximal tubule. Sodium recycling would be expected to increase oxygen consumption without affecting net sodium reabsorption, and should thereby decrease the Na^+/O_2 ratio.

Other complications in interpretation of this kind of experiment abound. Even in the presence of ouabain, fractional sodium reabsorption was 0.46, indicating a sizeable rate of continued sodium transport. The inhibitory effect of ouabain will be exerted in all portions of the nephron which show Na^+,K^+-ATPase activity, i.e., all segments except the thin limbs of the loop of Henle [22]. Determination of the Na^+,K^+-ATPase activity in cortical and outer medullary homogenates obtained from the kidney at the end of these experiments showed that ouabain inhibited the enzyme by 70%. Therefore, the persistent sodium transport during ouabain infusion probably represents continued activity of the partially inhibited Na^+,K^+-ATPase.

The observed Na^+/O_2 ratio then represents a minimal value obtained from partial inhibition of Na^+, K^+-ATPase activity, averaged for all segments of the nephron, with variable degrees of recycling of sodium perhaps occurring.

Surprisingly, despite the many complications, the observed Na^+/O_2 ratio was 14.5, very close to the ratio predicted for isolated proximal tubule suspensions (see above). It seems unlikely that observation of a stoichiometric ratio so close to the theoretical value could be coincidental. One conclusion that seems likely then, is that the underestimation of the ratio due to purported sodium recycling, as described above, cannot be too great.

Observation of a Na^+/O_2 ratio so close to that obtained in isolated proximal tubules means either that the net sodium reabsorption in these in vivo experiments is dominated by proximal tubular function, or that the Na^+/O_2 ratio is similar in all nephron segments.

In the face of mannitol diuresis and ouabain administration in vivo, it is difficult to estimate the proportion of the net sodium reabsorption which could be due to proximal versus loop or distal nephron function. However, the possibility that similar Na^+/O_2 ratios may obtain in different nephron segments is supported by recent observations of similar values for the Na^+/CO_2 ratio in amphibian urinary bladder, an epithelium often used as a model for distal nephron function (see below).

An attempt to more specifically evaluate the Na^+/O_2 ratio in the proximal tubule of the dog kidney in vivo was made by Mathisen *et al.* [11]. In these experiments, anaesthetized dogs subject to a large volume expansion were given ethacrynic acid. This diuretic was administered to attempt to block NaCl reabsorption in the loop of Henle.

Under these conditions, net renal Na^+ reabsorption and oxygen consumption were measured during either hypercapnia (increased inspired PCO_2) or hypocapnia (hyperventilation). Plasma bicarbonate concentration was maintained at a constant level by bicarbonate infusion. Because ethacrynic acid was also administered, most of the net sodium reabsorption occurring in these experiments was thought to be occurring in the proximal tubule.

Since net renal bicarbonate reabsorption is dependent on arterial PCO_2, in these experiments, the relationship between net Na^+ reabsorption and oxygen consumption could be determined at various rates of bicarbonate reabsorption.

Changing bicarbonate reabsorption during hypercapnia produced nearly proportional changes in net sodium reabsorption and small, disproportionate changes in oxygen consumption. The ratio of the change in net sodium reabsorption to the change in oxygen consumption was ~54. However, if only changes in sodium bicarbonate reabsorption were considered, the $NaHCO_3/O_2$ ratio was 18–20.

Mathisen *et al.* (11) interpreted their data to mean that the $NaHCO_3/O_2$ ratio reflects primarily proximal tubular active $NaHCO_3$ transport dependent on the activity of the Na^+,K^+ATPase. Proximal $NaHCO_3$ reapsorption is dependent primarily on the Na^+,H^+ antiport, and the energy for this antiport ultimately derives from the Na^+,K^+-ATPase. The similarity in value of the $NaHCO_3/O_2$ ratio to the Na^+/O_2 ratios observed in isolated proximal tubules certainly supports this conclusion. Mathisen *et al.* then speculate that the osmotic force generated by active reabsorption of each mole of $NaHCO_3$ is sufficient to cause passive, paracellular reabsorption of two moles of NaCl in the proximal tubule. This hypothesis would account for the observation that the Na^+/O_2 ratio was 50–54, approximately three times greater than the $NaHCO_3/O_2$ ratio. In other words according to Mathisen *et al.*, approximately $^1/_3$ of the reabsorbed sodium is transported actively via the Na^+,K^+-ATPase and two thirds passively.

Although these data are internally consistent, they are difficult to reconcile with other observations. Even assuming that virtually all of the sodium reabsorption occurring in Mathisen *et al.*'s experiments [11] is in the proximal tubule, there are other modes to account for active sodium reabsorption in this segment besides $NaHCO_3$ reabsorption.

Co-transport of sodium with organic solutes will account for a small proportion of the Na^+,K^+-ATPase dependent net sodium reabsorption in the proximal tubule. However, given the relatively low concentration of organic solutes in the glomerular filtrate, further diluted by the large volume expansion in these experiments, the amount of sodium transported in association with these organic solutes may have been too small to detect.

There is direct evidence from isolated perfused tubule studies for the existence of simple, active Na^+ transport independent of H^+ secretion (bicarbonate reabsorption) or organic solutes, in proximal straight [23] and perhaps, in proximal convoluted tubules [24] which should contribute to proximal Na^+ reabsorption *in vivo*. In fact, in a recent review, Berry and Rector [24] estimated that about 80% of the sodium reabsorption in the proximal tubule occurs by active transport by all modes [24]. Many of the studies cited in this review were carried out in isolated rabbit proximal tubules, or using the rat kidney.

The estimate by Mathisen *et al.* [11] that only $^1/_3$ of proximal sodium reabsorption in the dog kidney is active could perhaps be due in part to a species difference. In addition, the unusual conditions of Mathisen *et al.*'s experiments could have resulted in exaggeration of the relative contribution of the Na^+,H^+ antiport to net sodium reabsorption while perhaps minimizing the detectable contribution of other sodium transport processes.

In any case, these in vivo studies both lend some support to the hypothesis that there is a close coupling between active sodium transport and oxidative metabolism in the proximal tubule, and illustrate both the need for, and the difficulty of studying renal sodium transport and metabolism in vivo.

6. Na^+/O_2 ratios in the toad bladder

As mentioned above, Na^+/O_2 ratios near 15 have been found recently in the toad urinary bladder in vitro, during continuous measurement of metabolic CO_2 production with spontaneous [12] or induced [13] changes in active sodium transport. Assuming a respiratory quotient of 1.00, a Na^+/CO_2 ratio has the same significance as a Na^+/O_2 ratio. Demonstration of Na^+/O_2 ratios of 15–18 in the toad bladder [12] suggests a tight coupling between oxidative metabolism and ion transport in this preparation as in the proximal tubule. Additionally, to the extent that the toad bladder represents a model for distal nephron function, the similarity of the Na^+/O_2 and Na^+/CO_2 ratios suggests that the same fundamental stoichiometry between oxidative metabolism and Na^+,K^+-ATPase dependent active transport may obtain in various nephron segments. Of course, given the differences in mechanisms of ion transport and in the net electrochemical gradients opposing transport in different nephron segments, this tentative conclusion awaits extensive experimental verification.

7. Summary

Recent studies have provided a detailed description of the relationship between active ion transport and oxidative metabolism in the renal proximal tubule. Strong evidence has been provided that there is a tight coupling between mitochondrial oxidative ATP generation and ATP utilization by the Na^+,K^+-ATPase responsible for active ion transport. The rate of hydrolysis of ATP by the Na^+,K^+-ATPase sets the cellular ATP/ADP ratio, and this ratio in turn determines the rate of mitochondrial oxygen consumption. Since the ATP content of proximal tubular cells is small compared to the rate of ATP turnover via the Na^+,K^+-ATPase, changes in ion transport very rapidly (within seconds) induce appropriate changes in the oxygen consumption rate.

At least in the proximal tubule, it appears that all of the active sodium transport is energized by oxidative metabolism. This mechanism accounts for the interdependence of oxygen consumption and ion transport in this nephron segment.

Questions that remain to be answered include: is the fundamental stoichiometry of transport and metabolism quantitatively similar in different nephron segments? How do changes in the electrochemical gradient opposing transport affect the stoichiometric ratio? How are organic anion and cation secretion energized? How is H^+ secretion in the distal nephron energized? How can the conclusions described in this chapter, based largely on in vitro studies, be reconciled with sometimes contradictory conclusions from in vivo studies?

References

1. Mandel, LJ and Balaban RS: Stoichiometry and coupling active transport to oxidative metabolism in epithelial tissues. Amer J Physiol 240: F357–371, 1981.
2. Balaban RS, Soltoff SP, Storey JM and Mandel LJ: Improved renal cortical tubule suspension: spectrophotometric study of O_2 delivery. Am J Physiol 238: F50–F59, 1980.
3. Whittam R: Active cation transport as a pace-maker of respiration. Nature 191: 603–604, 1961.
4. Balaban RS, Mandel LJ, Soltoff SP and Storey JM: Coupling of active ion transport and aerobic respiratory rate in isolated renal tubules. Proc Natl Acad Sci 77: 447–451, 1980.
5. Harris SI, Balaban RS, Barrett L and Mandel LJ: Mitochondrial respiratory capacity and Na^+ and K^+-dependent adenosine triphosphatosemediated ion transport in the intact renal cell. J Biol Chem 256: 10319–10328, 1981.
6. Harris SI, Patton L, Barrett L and Mandel LJ: (Na^+,K^+)-ATPase kinetics within the intact renal cell. The role of oxidative metabolism. J Biol Chem 257: 6996–7002, 1982.
7. Burg MB, Grantham J, Abramow M and Orloff J: Preparation and study of fragments of single rabbit nephrons. Am J Physiol 210: 1293–1298, 1966.
8. Aronson PS: Mechanisms of active H^+ secretion in the proximal tubule. Am J Physiol 245: F647–F659, 1983.
9. Ullrich KJ: Renal transport of organic solutes. In: *Membrane Transport in Biology*. Vol. IVA, G. Giebisch (Ed.) Heidelberg, Springer-Verlag, 1979, p. 413–448.
10. Sejersted OM, Mathisen O and Kiil F: Oxygen requirement of renal Na-K-ATPase-dependent sodium reabsorption. Am J Physiol 232: F152–F158, 1977.
11. Mathisen O, Monclair T and Kiil F: Oxygen requirement of bicarbonate-dependent sodium reabsorption in the dog kidney. Am J Physiol 238: F175–F180, 1980.
12. Al-Awqati Q, Beauwens R and Leaf A: Coupling of sodium transport to respiration in the toad bladder. J Membr Biol 22: 91–105, 1975.
13. Beauwens R and Al-Awqati Q: Further studies on coupling between sodium transport and respiration in toad urinary bladder. Am J Physiol 231: 222–227, 1976.
14. Gyory AZ and Kinne R: Energy source for transepithelial sodium transport in rat renal proximal tubules. Pflugers Archiv 327: 234–260, 1971.
15 Gullans SR, Brazy PC, Soltoff SP, Dennis VW and Mandel LJ: Metabolic inhibitors: effects on metabolism and transport in the proximal tubule. Am J Physiol 243: F133–F140, 1982.
16. Whittembury G: Sodium and water transport in kidney proximal tubular cells. J Gen Physiol 51: 303s–314s, 1968.
17. Grantham JJ, Irish III JM and Hall DA: Studies of isolated renal tubules in vitro. Ann Rev Physiol 40: 249–277, 1978.
18. Linshaw MA: Effect of metabolic inhibitors on renal tubule cell volume. Am J Physiol 239: F571–F577, 1980.
19. Gullans SR, Harris SI and Mandel LJ: Glucose-dependent respiration in suspensions of rabbit cortical tubules. J Memr Biol 78: 257–262, 1984.
20. Frega NS, Weinberg JM, Ross BD and Leaf A: Stimulation of sodium transport by glucose in the perfused rat kidney. Am J Physiol 233: F235–F240, 1977.
21. Gregg CM, Cohen JJ, Black AJ, Espeland MA and Feldstein ML: Effects of glucose and insulin on metabolism and function of perfused rat kidney. Am J Physiol 235: F52–F61, 1978.
22. Katz AI: Renal Na-K-ATPase: its role in tubular sodium and potassium transport. Am J Physiol 242: F207–F219, 1982.
23. Schafer JA, Troutman SL, Watkins ML and Andreoli TE: Volume absorption in the pars recta. I 'Simple' active Na^+ Transport. Am J Physiol. 234: F332–F339, 1978.
24. Berry CA and Rector Jr FC: Active and passive sodium transport in the proximal tubule. Min Elect Metab 4: 149–150, 1980.

CHAPTER 8

Immunologic aspects of renal transplantation

DAVID SENITZER

1. Introduction

Renal transplantation has been accepted as therapy for end-stage renal failure. However, over the last ten years renal graft survival has not really improved. Recently, major advances in the immunogenetics of rejection and new modes of therapy suggest that we may be on the threshold of a significant breakthrough in renal transplantation.

It is nearly a quarter of a century ago since the first clinical organ-grafting experiments were done. Morbidity and mortality among renal transplant recipients have declined sharply. Patient mortality within the first year posttransplant, during which most deaths occur, is at present less than 5% in most transplant centers. Graft survival at one year remains approximately 70–90% for living-related donor and 40–60% for cadaveric renal transplants. These levels of patient and graft survival have been achieved due, in large part, to less vigorous immunosuppressive therapy and sacrifice of the kidney to rejection rather than the recipient's life to fatal infections.

Immunologic rejection has been and still is the major stumbling block to the survival of renal transplants. There are two ways by which immunologic rejection can be diminished or controlled. Determining the best biologic match between donor and recipient pretransplantation would preclude encountering problems of rejection posttransplantation. There is some difficulty in finding good matches between unrelated individuals. The major histocompatibility complex (MHC) of humans (the HLA system) has been identified, and matching for the HLA system plays a significant role in allograft survival when donor and recipient are siblings. However, the HLA system is highly polymorphic, making the discovery of unrelated individuals who share one or more HLA haplotypes difficult at best. That HLA-A and HLA-B matching does improve kidney allograft survival has been grudgingly accepted.

Recently, several factors other than HLA-A and HLA-B matching alone have been recognized as significantly influencing kidney allograft survival. We will divide these into pretransplantation and posttransplantation for purposes of discussion. Pretransplant blood transfusion and HLA-DR matching have a beneficial effect on kidney allograft survival. This constitutes the pretransplant approach to enhanced kidney allograft function. The second approach would be to develop the ability to diagnose rejection at an early stage before renal function is impaired and implement more rational protocols of immunosuppression for reversing or preventing the injury caused by the immune response.

That lymphocytes consist of a heterogeneous group of subpopulations has been recognized by the discovery of differential expression of cell surface antigens on lymphoid cells. In addition, a close correlation between the expression of these antigens and the functional capabilities of cells bearing these antigens has been found. Hybridoma technology, together with the analytical and separation capabilities of fluorescence-activated cell sorting has resulted in the classification of lymphocytes into defined subsets. The survival or destruction of a kidney allograft depends upon the interactions between effector lymphocyte subsets and regulatory lymphocyte subsets. Our knowledge of these interactions has enabled a more rational approach toward managing the renal allograft recipient. Two of the more promising approaches to posttransplant management of immunologic rejection are the monitoring of lymphocyte subsets and the use of immunosuppressive agents designed to interfere with the subset interaction necessary to generate an immunologic response.

L.J.A. DiDio and P.M. Motta (eds), Basic, Clinical, and Surgical Nephrology. ISBN 0-89838-689-5.

2. Pretransplantation

2.1. Transfusions

Transfusions for symptomatic relief of anemia in patients with chronic renal failure were fairly common until 1966. In 1966 two cases of hyperacute rejection were attributed to the presence of lymphocytotoxic antibodies in the pretransplantation serum of the recipients [1]. The widespread adoption of restrictive blood transfusion policies for transplant candidates did not produce the desired effect of increasing allograft survival. In fact many studies demonstrated that recipients who received pretransplant transfusions had as much as a 40% higher allograft survival rate than that of recipients who were not transfused [2, 3]. Figure 1 depicts the results from an international collaborative effort to determine the effect of pretransplant blood transfusion on renal allograft survival.

Immunologic responses to red cell transfusions are not yet clearly defined. Antibody responses to HLA antigens does occur since these antigens are found in lymphocytes, granulocytes, and platelets, all of which are contained in whole blood, red blood cells, and even white blood cell poor blood transfusions. The role of these antibodies in precluding transplantation or in affecting allograft survival are critical considerations.

Microlymphocytotoxicity tests employed for the detection of antibodies have yielded somewhat confusing results. There were reports that lymphocytotoxic antibodies were [4, 5] and were not [6, 7, 8] adversely affecting allograft survival. However, all studies did not employ the same methodology. The variables are numerous and have been demonstrated to be important in distinguishing different types of lymphocytotoxic antibodies and their effect on renal allograft survival. Furthermore, the sensitivity of the final donor lymphocyte crossmatch technique can affect the determination of the presence or absence of irrelevent antibodies.

The presence of antibodies may or may not be deleterious. Most will agree that the presence of antibodies reactive with T cells at 37° C are a contraindication to transplantation. Antibodies to B cells that react at 4° C may enhance graft survival [9] while warm (37° C) B cell reactive antibody may be harmful [8, 10]. Table 1 summarizes these results. In addition, it has been demonstrated that the anti-

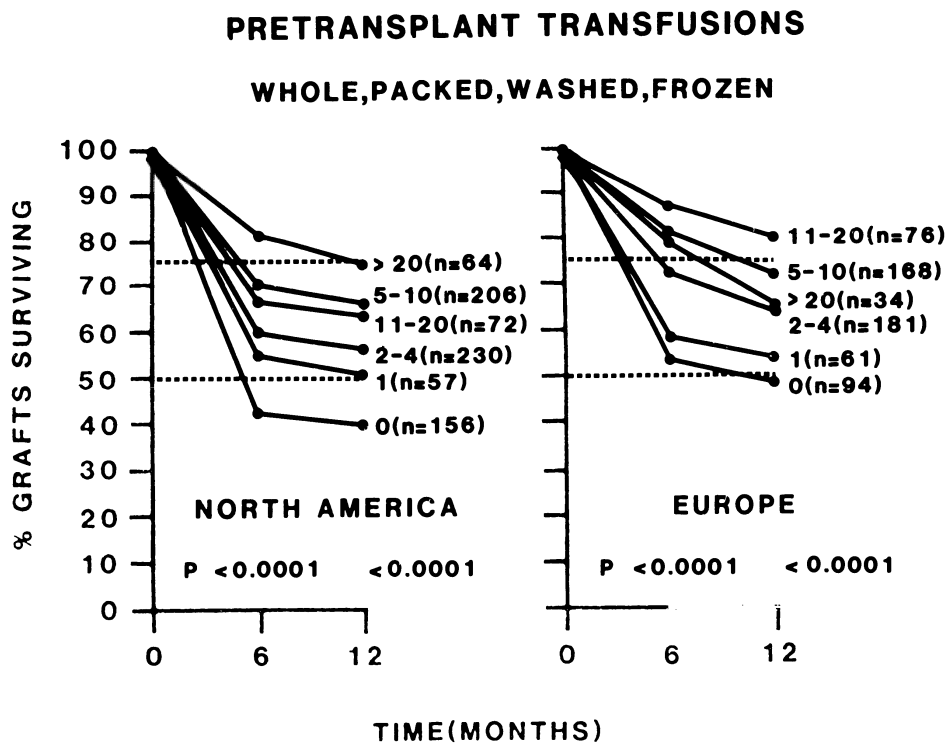

Fig. 1. Correlation of pretransplant transfusions with allograft outcome in transplants submitted by North American or European centers. Opelz and Terasaki, Transpl. 1982 (with permission).

Table 1. Antibodies that may be elecited by blood transfusion and their effect on kidney grafts.

Type of antibody	Temperature of reactivity	Effect on graft
Reactive with T cells	37° C	Destructive
	4° C	Destructive
Reactive with B cells	37° C	Destructive
	4° C	Enhancing?

bodies induced by transfusion appear and disappear within the same patient in an unpredictable manner. Testing sera at different times in an individual patient is likely to produce widely different results. It is interesting to note that lymphocytotoxic antibodies detected after transplantation seem to fluctuate less often than those elicited by transfusion [11].

The rate of exclusion from transplantation due to sensitization resulting from transfusions has been a legitimate concern. Sensitization rates of as high as 50% were expected in multiply transfused patients. Opelz *et al.* [12] found that after 10 transfusions, fewer than 16% of patients had lymphocytotoxic antibodies against more than 90% of a 30 cell panel. It would be reasonable to conclude from these data that the danger of sensitizing large numbers of transplant candidates is minimal. This is especially true when compared with the increases in graft survival that are obtained in multiply transfused recipients.

The concept of using donor-specific transfusions (DST) arose from the difficulty in obtaining good graft survival in patients with a one-haplotype matched living related donor. Such donors may also produce a strong mixed lymphocyte culture (MLC) respone. Seventy percent of patients who underwent DST prior to transplantation received a renal allograft from their blood donors. However, in patients who had already rejected a previous transplant, the sensitization rate was about 70%. Sensitization was defined as having either warm T and/or warm B cell antibody cytotoxic for blood donor lymphocytes [13, 14]. Graft survival was significantly enhanced (about 30% at 12 months posttransplant) in those patients who received the graft from the planned donor [15].

There are several possible mechanisms to explain the results achieved with either random or donor-specific transfusion therapy. Simple selection is an easily recognized explanation. Renal transplantation is never performed when there is a positive crossmatch (donor specific lymphocytotoxic antibody). Blood transfusions, by eliciting such antibodies, select out those who synthesize donor-specific antibody from receiving a renal allograft that they would have rejected. The induction of specific unresponsiveness to the antigens presented in transfusion can also be theorized. Induction of unresponsiveness by activation of suppressor T cells by blood transfusions has been reported [16, 17]. Yet another possible explanation was presented by Dr. Terasaki at the 1983 annual meeting of the Transplantation Society of Michigan. The usual protocol of immunosuppressive therapy is to start with a high dose of immunosuppressive drug at the time of transplantation and gradually decrease the dose of the immunosuppressive drug with time. A transfused recipient who would mount a secondary immune response, but would do so at a time when the dose of immunosuppressive drug is high. Thus, a rejection response would be rendered difficult. In an unsensitized recipient, rejection would occur via a primary immune response; i.e. somewhat later than that expected for a secondary response. The primary response would therefore occur at a time when a lower dose of immunosuppressive is being administered. The immune response would be better able to overcome the lower dose of immunosuppressive drug and cause more graft injury. These relationships are shown in Figure 2. Thus, the explanation of the transfusion effect on graft survival could very likely be the result of the immunosuppressive drug protocol adhered to by most transplant centers. Resolution of the mechanism(s) involved in the enhancing effect of blood transfusions on renal allograft survival must await further research.

2.2. DR matching

Serologic determination of histocompatibility antigens led to the application of leucocyte typing for matching donors and recipients of renal transplants. Two series of MHC antigens in man (HLA) were

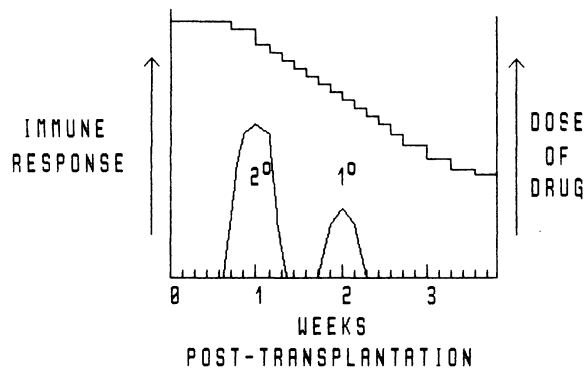

Fig. 2. Correlation of amount of immunosuppressive drug with time of secondary (2°) and primary (1°) immunologic response.

initially shown to be controlled by two loci on chromosome 6 (HLA-A and HLA-B). Extensive studies of matching for HLA in both living related and in cadaver transplantation were performed in an effort to enhance kidney graft survival.

Family genotyping for HLA allows a precise determination of HLA identity of a recipient and potential donor. The success of intrafamilial kidney grafts correlate with the genetic similarity in HLA between donor and recipient. In contrast, cadaveric kidney transplantation began to show little correlation. The consensus reached was that grafts well matched for HLA-A and HLA-B showed about a 10% better graft survival at one year than poorly matched grafts.

Recently, it was recognized that reactivity of lymphocytes from two different individuals *in vitro* (MLC) was not determined by differences in HLA-A and HLA-B between the cell donors, but by differences at a separate locus with the MHC, subsequently named HLA-D. The strong response often seen in MLC between cells identical for HLA-A and HLA-B could now be attributed to disparity of HLA-D. In addition, the MLC resulted in the production of cytotoxic T lymphocytes directed against the cells which stimulated the responding population in the first place. Obviously this seemed to be an *in vitro* model of immunologic rejection. These results quickly led to the use of the MLC for selecting donor and recipient and for predicting the outcome of cadaveric kidney transplantation, but with confusing results.

Homozygous typing cells, in one way MLC, were used to define a number of HLA-D determinants. Antisera were soon developed that were either detecting the same HLA-D determinants or very closely linked antigens, hence their being called HLA-DR (D related) antigens [18]. HLA-D typing for kidney transplantation with homozygous typing cells has not been widespread because results of the test can not be obtained prospectively in cadaveric kidney donor transplants. Serologic recognition of HLA-DR antigens is believed to represent a good approximation of the same HLA-D antigen.

If the MLC is accepted as an *in vitro* model for compatibility it is clear why matching for HLA-DR is conceptually pleasing. HLA-DR matching is directed at the induction phase of the immune response, whereas matching for HLA-A and HLA-B is directed at the effector arm of the immune response to the kidney graft. This is the rationale for the studies undertaken to determine the effects of HLA-DR matching on renal allograft survival.

In single-center analyses of the influence of HLA-DR matching on renal allograft survival the results have been encouraging. An improvement of 15% in graft survival at 12 months was reported by Morris and Ting [19] in transplants with 0 HLA-DR incompatibilities compared to those with 2 HLA-DR incompatibilities. Similar improvements in kidney graft survival have been reported by many transplant centers [20]. HLA-DR matching can significantly improve the survival of cadaveric kidney transplants, even in multiply transfused recipients [21].

International studies, unfortunately, have not confirmed the results from single-center analyses [22]. There was no correlation of kidney graft survival with the number of HLA antigens mismatched or shared between recipient and donor at the HLA-A and HLA-B loci or at the HLA-DR locus in first transplants. In second transplants HLA-DR matching was significantly correlated with kidney graft survival; there was as much as a 30% improvement in 0 HLA-DR mismatched transplants compared with 2 HLA-DR mismatched transplants.

3. Posttransplantation

3.1. Introduction

Humoral as well as cellular immunologic mechanisms have been demonstrated in the pathogenesis of renal allograft rejection [23, 24]. Matching for the MHC antigens HLA-A, HLA-B, and HLA-DR has increased allograft survival somewhat. In addition, the widespread use of deliberate blood transfusions prior to transplantation has contributed to better graft survival. Nevertheless, the central obstacle to successful kidney transplantation remains even today, that of immunologic rejection.

Improved graft survival could be achieved if therapeutic protocols were designed to provide effective immunosuppression with only minimal compromise of the recipient's ability to protect against infections. Such protocols would have to precisely regulate the immune response based on data regarding the current state of responsiveness of the recipient. New technologies coupled with a better understanding of immunologic responses have shown a great deal of promise in realizing this goal.

This section shall deal with the emerging use of monoclonal antibodies to monitor immunologic responsiveness and as immunosuppressive modalities in the treatment of graft rejection. In order to accomplish these goals we will first briefly discuss the interactions among lymphocytes that result in an immunologic response, the monoclonal antibodies

used in identifying lymphocyte subpopulations, and flow cytometry which is used in the high speed quantitation of these cells.

3.2. *Lymphocyte interactions*

The human immune response is a very complex system involving many different cell types interacting in a highly regulated fashion. Initiation of the immunologic response begins with the introduction of antigen, and results in the synthesis of specific antibody molecules and in the generation of 'effector' lymphocytes specific for the stimulating antigen. The central steps in this process are activation of competent lymphocytes, proliferation and differentiation of these cells, and the regulation of these processes. We will deal primarily with the latter.

In the normal immune response the antigen is bound to the surface of adherent cells which are usually macrophages. The macrophages bearing the antigen then present the antigen to the T lymphocytes capable of producing lymphokines, helper T lymphocytes, and proliferating T lymphocytes. The suppressor T lymphocytes seem to be capable of recognizing free (soluble) antigen. Although suppressor T lymphocytes may not require cellular interactions for their priming, their functions are entirely dependent on such interactions.

Suppressor cells function to diminish or even prevent antibody synthesis by B lymphocytes and to limit the generation of effector T lymphocytes. They are able to accomplish these functions by interacting with other T cells, either by direct cell-cell contact or through the production of soluble factors that inhibit the positive functions of helper and regulator T cells. There is now convincing evidence that suppressor cells participate in both positive and negative 'feedback' loops. Thus, even suppressor cells are themselves highly regulated.

3.3. *Monoclonal antibodies*

The production of monoclonal antibodies specific for T cell subpopulations has initiated a new era in the evaluation of T cell subsets in a variety of experimental and clinical settings. In the recent past, the E rosette (sheep red blood cell binding) test and its variants, anti-T cell xenoantisera and the Tμ and Tγ have allowed for the quantitative evaluation of T cells. Correlation of functions with these methods was very poor. Many investigations were based upon the evaluation of data from stimulation of cultured lymphocytes with mitogens, soluble antigens, or alloantigens, as well as the cell-mediated cytotoxicity assay and the study of helper and suppressor cells after conconaval in A or pokeweed mitogen activation. These methods are very cumbersome and difficult to employ on the large scale required for human studies.

The development of monoclonal antibodies specific for functionally distinct subsets of human lymphocytes has allowed for the analysis of the immune response [25]. The E rosette test may soon be abandoned. However, the other cellular assays mentioned above will no doubt remain essential for determination of the relationship between surface antigen and cellular function. Table 2 is a listing of some of the more useful monoclonal antibodies.

Monoclonal antibodies that identify T cells in general include the OKT1, OKT3[26], OKT11A [28],

Table 2. Selected monoclonal antibodies to human leucocyte subpopulations.

Name	Class	T cell			B Cell	Monocyte	NK	Ref
		Helper	Suppressor	Cytotoxic				
OKTI	IgG1	+	+	+	(CLL)	−		26
Leul	IgG2a	+	+	+	(CLL)	−		27
OKT3	IgG2a	+	+	+	−	−	−	26
Leu4		+	+	+	−	−	−	27
OKT11A	IgG2	+	+	+	−	−	±	28
OKT4	IgG2b	+	−	−	−	−	−	26
Leu3a	IgG1	+	−	−	−	−		27
OKT8	IgG2a	−	+	+	−	−	−	29
OKT5	IgG1	−	+	+	−	−	−	30
Leu2a	IgG1	−	+	+	−	−		27
OKM1	IgG2b	−	−	−	−	+	±	31
OKIal	IgG2	−*	−*	−*	+	±		32
HNK1	IgM	−	−	−	−	−	+	33

* not detectable unless activated.

Leu1 [27], and Leu4 [27] antibodies. It is worth mentioning that different monoclonal antibodies recognizing the same cell type may not be reacting with the same cell surface molecule or even the same antigenic determinant on a single molecule. Therefore, one should not assume that subset antibodies are interchangeable. The helper subset is recognized by the OKT4 [26] and Leu3a [27] antibodies. Note that the suppressor and cytotoxic subsets are not separable, both are identified by OKT8 [29], OKT5 [30], and Leu2a [27]. Monocytes are detected by OKM1 [31], which also reacts somewhat with human Natural Killer (NK) cells. The antibody HNK1 has been reported to react with NK cells exclusively [33]. OKIa1 detects an antigen on resting B cells, some monocytes, and on activated T cells, not resting T cells [32].

3.4. *Flow cytometry*

Recently there has been a great deal of interest in the application of flow cytometry to the analysis of immunologic responsiveness in a variety of patients. In this subsection we will discuss what flow cytometry is, and then in the next section how it and the monoclonal antibodies have been applied to human kidney transplantation.

3.4.1. *Basic concepts*

The basic concept of flow cytometry depends upon the ability to move cells single file through a light beam and measure the fluorescence emitted by individual cells. Scattered light from the beam can also be simultaneously measured. Modern flow cytometry uses a laser light source because of it locally high intensity. Fluorescein is the most commonly used dye for attachment to monoclonal antibodies, and therefore an argon ion laser set at a wavelength of 488 nm is an excellent choice. The emitted fluorescent and scattered light is detected by photomultiplier tubes appropriately placed around the detection chamber (Fig. 3).

The laser beam is focused on the cells as they flow single file in a narrow sheath of fluid. Particles (cells) passing through the laser beam scatter the light in all directions. Light scattered in the forward directions, with respect to the laser beam, can be correlated with size of the cells passing through the laser beam.

The emitted fluorescence is detected at 90° to the laser path. Scattered laser light is excluded from detection by a filter which only allows light of wavelengths longer than 488 nm to pass to a photomultiplier tube, i.e. only the scattered fluorescent light is detected by the photomultiplier tube.

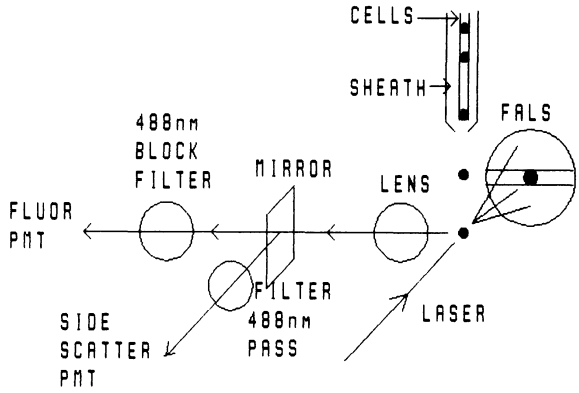

Fig. 3. Schematic diagram of the optical system of a flow cytometer.

A third signal that can be detected is laser light scattered at 90° from the laser. A third photomultiplier tube detects this 90° scattered laser light after filters have removed the emitted fluorescent light. This signal has a good correlation with the surface and interior complexity of the cells being analysed. Cells with an abundance of granules (e.g. neutrophils) will scatter the laser light in the 90° direction much more so than cells of similar size but with few granules.

These three light signals are transformed into electrical pulses, amplified, and converted into a digital signal for computer analysis and storage. The results are stored as a histogram, which displays the number of cells counted with a given amount of fluorescence (Fig. 4). Data can be acquired at the rate of 300,000 cells per minute.

3.4.2. *Gating*

One powerful feature of the modern flow cytometer is its ability to correlate several signals simultaneously. A selected or 'gated' population of cells can be defined based on their light scatter signals. The fluorescence emitted by this gated population can be separately analysed. If one wanted to measure the fluorescence of a lymphocyte population, one would record only the fluorescence signals from the cells with the lower range of light scatter while ignoring those from all other cells. The gates are selected by a two dimensional plot of forward and 90° scatter for each cell, such as the one shown in Figure 5.

Analysis of peripheral blood buffy coat cells gives four discrete clusters of cells separated on the basis of their forward and 90° light scatter (Fig. 5). These clusters have been identified as debris (red cell ghosts, platelets), lymphocytes, monocytes, and

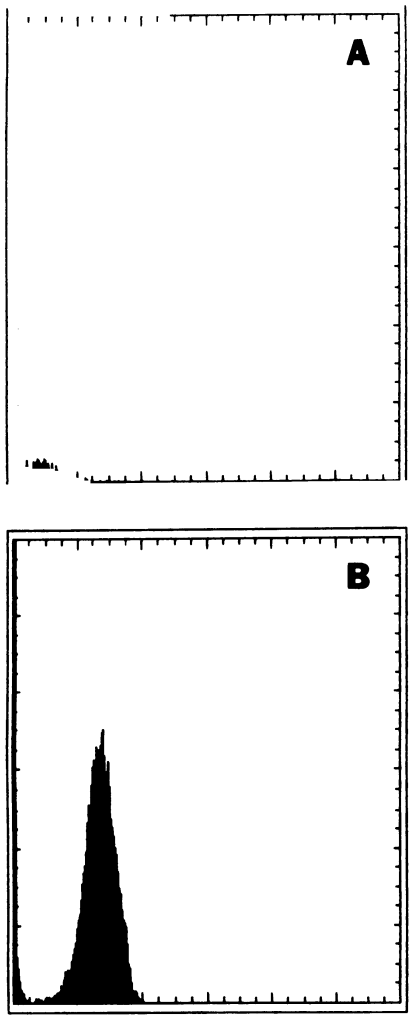

Fig. 4. Fluorescence histogram of lymphocytes stained with an anti-mouse IgG antibody (A) and a monoclonal antibody OKT3 (B). Cell number is plotted on the vertical axis, fluorescence intensity in linear fluorescence units on the horizontal axis.

neutrophils [34]. Thus, the direct analysis of lymphocytes in buffy coat or even whole blood can be accomplished without a Ficoll-hypaque separation step, which would be a saving of time and cells.

3.4.3. Sensitivity

The level of sensitivity reached by flow cytometers is beyond that of fluorescence microscopes. Approximately 3,000 molecules per cell can be detected. This is equivalent to 0.4 femtograms (4×10^{-16} gm) of antibody (at a F/P ratio of 2), a level that is also beyond most radioimmunoassays [35]. This means that a population of positive cells that are 1% of the total population can be reliably detected. In addition, there are the advantages of objectivity and a marked (10–100 fold) increase in the number of cells

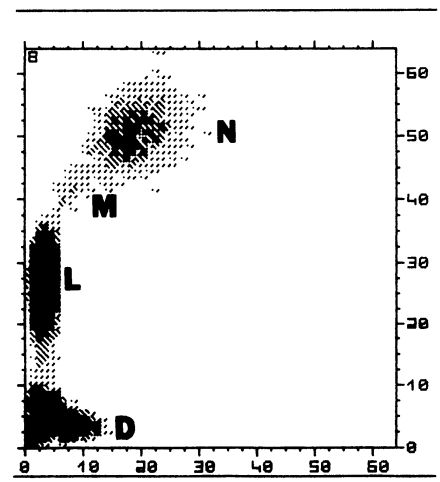

Fig. 5. Two parameter histogram of 90° light scatter (horizontal axis) vs forward angle light scatter (vertical axis) of peripheral blood buffy coat cells. Each dot represents one or more cells. L, lymphocytes; M, monocytes; N, neutrophils; D, red blood cell ghosts, platelets, debris.

counted (rate of analysis at 1–3,000 cells per second) compared with fluorescence microscopy. Results from different groups of patients can be compared with greater statistical accuracy.

3.4.4. Lymphocyte subset analysis

One of the most useful applications of flow cytometry is the analysis of lymphocyte subsets. To obtain this kind of data mononuclear cells may be obtained as a whole blood, buffy coat, or Ficoll-hypaque purified preparation. The cells are incubated at 4° C in the presence of the desired monoclonal antibody, which binds to the specific lymphocyte subset [36]. After an incubation period to allow binding of the monoclonal antibody to the subset of cells to be analysed, the cells are washed to remove exces monoclonal antibody. The cells are then exposed to a second antibody which is a fluorescein conjugated anti-mouse antibody. Let us say we are trying to evaluate the number of helper cells, then the monoclonal antibody of choice would be OKT4 or Leu3a (binds only to helper cells). The second antibody would bind all cells having OKT4 or Leu3a bound, and would render all the helper cells fluorescent as measured in the fluorescence microscope. However, due to the tediousness and subjectivity of microscopic evaluation it is easier and more accurate to analyze the cell preparation by flow cytometry. Analysis of a sample from a patient is shown in Figure 6. This is a three dimensional histogram which depicts the log fluorescence intensity on the X axis and the light scatter intensity on the Y axis. The

cell number is on the Z axis which extends out of the plane of the paper.

The next step is to determine the percentage of helper (OKT4 or Leu3a positive) cells in the total population. In order to accomplish this the operator merely integrates the number of cells in the peak containing the lymphocytes and divides by the total number of cells analyzed (see Fig. 6). This kind of analysis can be run quite easily with a great deal of precision using a flow cytometer.

3.5. T subset monitoring

Interactions between immunologic effector and suppressor mechanisms ultimately determine the outcome of kidney transplantation. There is general agreement that cytotoxic T cells, helper T cells, especially those producing interleukin-2, and macrophages activated by lymphokines are responsible for graft destruction, while suppressor T cells and anti-idiotypic immunization play protective roles. Immunosuppressive therapy is not antigen-specific, and certainly leads to increased risk of infection, and possibly neoplasia. The immunologic events occurring after kidney transpantation remain poorly characterized. In addition, the precise effect of may immunosuppressive agents on these events is still a matter of intense investigation.

In those recipients with good graft survival induced by nonspecific immunosuppression one can only speculate on the mechanism of specific unresponsiveness responsible. In view of the number of such poorly defined factors, the notion of *in vitro* monitoring of the immunologic status of kidney graft recipients, suggests a very complex undertaking. In fact, the investigation of cytotoxic T cells in graft recipients has proved to be disappointing [37]. Only isolated reports have reported success in the search for blocking factors or suppressor T cells [38, 39]. Evaluation of lymphocyte subsets by E rosette tests has not proven to be a reliable parameter of rejection [40]. Finally, despite the enormous gain in basic knowledge about allograft immunity, most transplant centers still rely excessively upon the clinical signs and symptoms of kidney failure to establish the diagnosis of rejection.

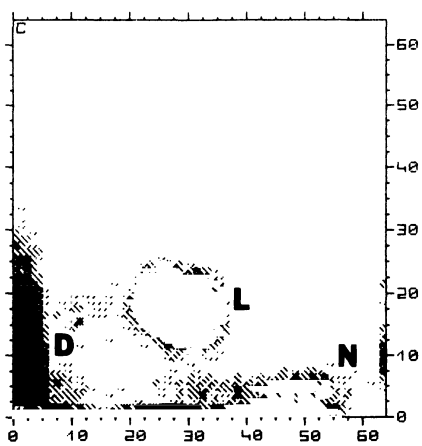

Fig. 6. Two parameter histogram of log integrated green fluorescence (horizontal axis) vs forward angle light scatter (vertical axis). Each dot represents one or more cells. L, lymphocytes staining with OKT3; N, autofluorescing neutrophils; D, red blood cells ghosts, platelets, debris.

3.5.1. Results of monitoring immunologic status

In normal individuals the percentage of OKT4-positive (helper) cells is twice that of the percentage of OKT8-positive (suppressor-cytotoxic T) cells. The sum of these two subsets usually will equal the percentage of OKT3-positive cells.

Cosimi *et al.* [41] sequentially monitored 24 recipients of HLA-nonidentical kidney grafts. They evaluated 16 rejection episodes in these patients. The number of OKT3-positive cells and the ratio of OKT4 to OKT8 were found to correlate with a high probability of allograft rejection. Nine of 11 patients in whom the OKT4/OKT8 ratio was greater than 1.3 experienced acute rejection during the first six weeks posttransplantation. The diagnosis of rejection was reached in only two of the 11 patients with a low OKT4/OKT8 ratio, due to high proportion of OKT8-positive cells. All of these patients received immunosuppressive therapy of azathioprine and prednisone with (15 patients) or without (9 patients) anti-thymocyte globulin (ATG).

It is quite interesting to note there is a clear correlation of the OKT4/OKT8 ratio at the onset of clinical rejection and the irreversibility of injury to the graft [42]. In those patients who experienced the onset of clinical rejection with an OKT4/OKT8 ratio >1.0, 93% were reversible. However, if the OKT4/OKT8 ratio was <1.0 only 22% were reversible. Our experience at MCO confirms and extends the correlation of the OKT4/OKT8 ratio and the reversibility of rejection. As can be seen in Figure 7 the OKT4/OKT8 ratio is responsive to standard pulse therapy for rejection with Solumedrol. We found that the numerical value of the OKT4/OKT8 ratio is not as valuable as reported by others, but that a change in the ratio is significant. It is important to realize that we monitor the T cell subsets on a daily basis beginning with the day of transplant, unlike that of many others who perform T subset analysis

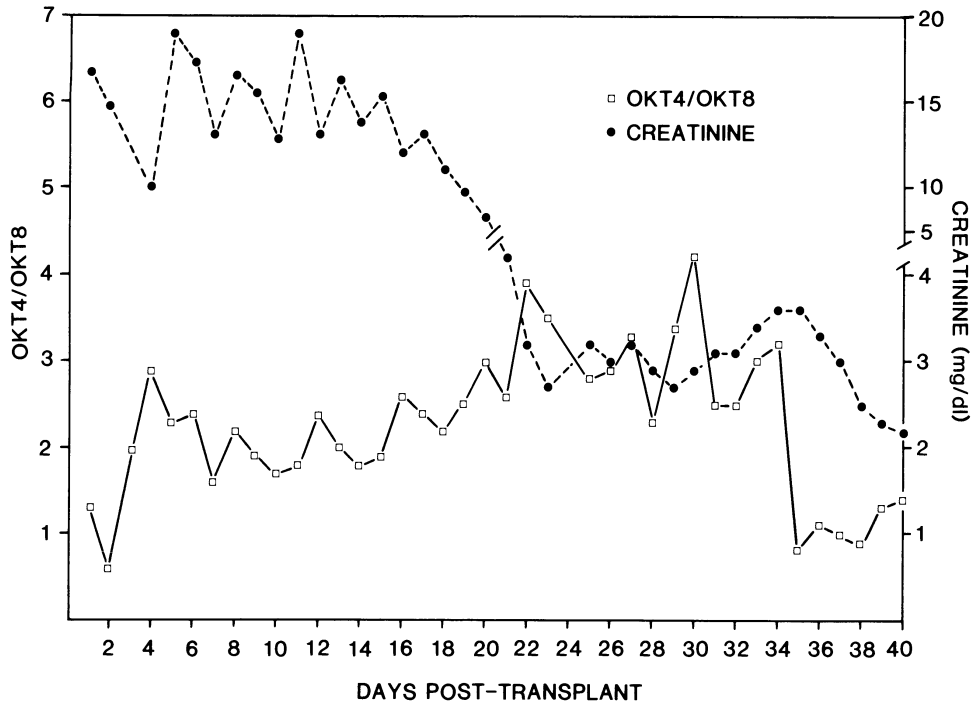

Fig. 7. Clinical course of renal allograft recipient whose T lymphocytes were monitored on a daily basis. OKT4/OKT8 ratio decreased with pulse therapy, but rebounded one or two days later.

every 2 or 3 days or even once per week. On the days Solumedrol was administered the ratio declined sharply, and then it began to recover usually the very next day. The ratio continued to increase until another dose of Solumedrol or ATG therapy was instituted. This pattern of recovery of the OKT4/OKT8 ratio following pulse therapy is indicative of the failure of the pulse therapy.

A point worth mentioning is that the OKT4/OKT8 ratio often begins to rise before clinical signs of rejection appear and before the serum creatinine levels increase. This pattern is more easily seen in Figure 8. It can be seen that the OKT4/OKT8 ratio increases from as much as 1 to 2 days before serum creatinine levels rise. Others have reported similar increases in the ratio by as much as 5 days preceeding diagnosis of rejection [43]. This relationship has not been observed in every instance of rejection, and increases in OKT4/OKT8 ratio may not precede rejection in any given individual patient [44, 45]. Therefore, the interpretation of the T subset ratio must be made with caution.

In patients being treated with low dose corticosteroids and azathioprine the OKT4/OKT8 ratios are sensitive indicators of the success or failure of subsequent treatment for rejection. It has been reported [46] that OKT4/OKT8 ratios >1.6 before the start of rejection therapy correlated with reversible rejection episodes and that OKT4/OKT8 ratios <1.6 correlated with irreversible rejection. In our experience to date, the numerical value of the OKT4/OKT8 ratio is not as important as whether or not there is decrease in the ratio after administration of rejection therapy or a rebound in the ratio once therapy is discontinued.

There are several explanations for the variety of results one finds in the current literature. One of the first is the effect of nonlymphoid cells on the interpretation of the results. The percentages of monoclonal antibody positive cells would be greatly affected by contaminating nonlymphoid cells. This problem can be alleviated by ensuring the purity of the cell preparations and by better standards of gating durng flow cytometric analysis.

A second more serious problem is that of the doubly labelled cell. In peripheral blood from normal volunteers there is no overlap between OKT4 and OKT8 cells. Thus, the use of the OKT4/OKT8 ratio is a valid measure of the balance between the helper/suppressor cytotoxic subsets. In kidney graft recipients on immunosuppressive therapy the presence of doubly labelled cells (OKT4 and OKT8 positive) makes the interpretation of the ratio difficult [47]. The immunologic significance and their

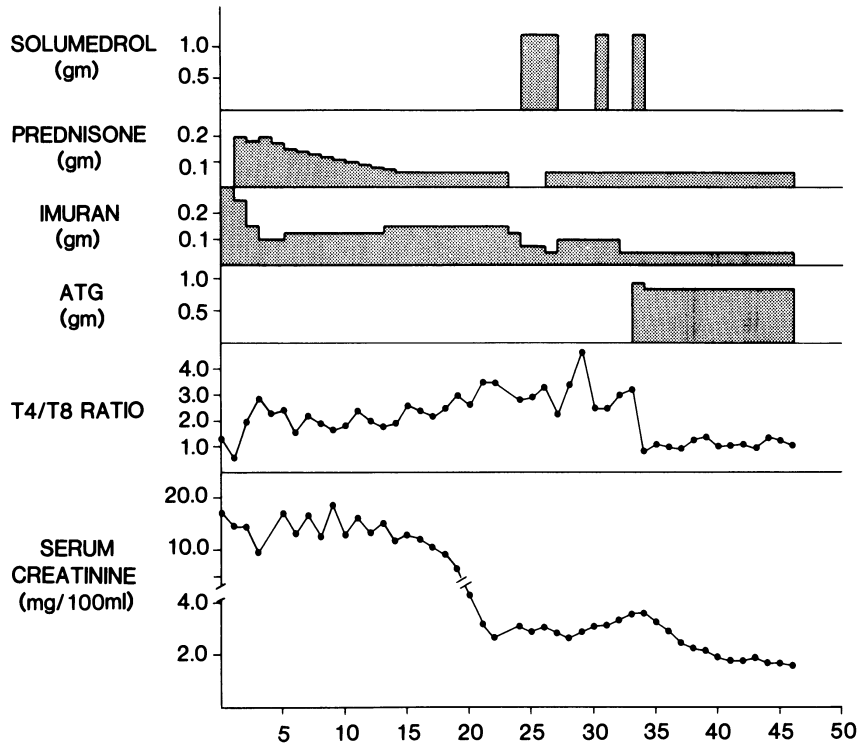

Fig. 8. Correlation of OKT4/OKT8 ratio with serum creatinine levels. Same patient as in Fig. 7. Increases in creatinine level usually was accompanied or preceded by a rise in the OKT4/OKT8 ratios (days 22, 27, 29).

correlation with particular clinical events is speculative. A suggested solution is simply to ignore the results when such doubly labelled cells are encountered.

3.6. Treatment with monoclonal antibody

The rationale behind the use of monoclonal antibody against T cell subsets is derived from the desire to better regulate the immune response of transplant recipients. As we have previously discussed, the regulation of immunologic responsiveness lies at the level of interaction of effector and regulatory subpopulations of lymphocytes. Renal allograft rejection involves both humoral and cellular immunologic mechanisms. It has been shown that the cells infiltrating a graft undergoing rejection are predominantly T cells (41), the majority of which were, in one report, OKT8 positive (48).

Currently used immunosuppressive agents result in nonspecific suppression of the recipient's immune system. The availability of monoclonal antibody specific for human T cell subsets makes it possible to suppress selected subsets rather than the entire population of proliferating cell types. One of the first human studies employed OKT3 antibody rather than antibody specific for a subset of T cells (49). This antibody was chosen to ensure that adequate immunosuppression would be obtained (Fig. 9). It was employed for the treatment of acute rejection. The most encouraging result was the initial reversal in all cases of the established rejection episode without the use of any other therapy than the OKT3 antibody and despite the continued reduction of the dose of steroid. ATG is often used to treat rejection but patients have developed antibody against the horse proteins contained in the ATG. It should be noted the dose of OKT3 antibody (17 to 56 mg total) was much lower than that of ATG (50 to 100 mg/kg/day). The rate of sensitization to the monoclonal antibody protein should be much less compared to the rate for ATG. Use of the monoclonal antibodies for rejection therapy would produce less of a problem of hypersensitivity reactions.

A recent study employed monoclonal OKT12 antibody for treatment of acute rejection [50]. OKT12 antibody reacts with all postthymic T cells. The results suggest that OKT12 is of use in the treatment of cellular rejection, but is not effective when humoral mechanisms have caused significant vascular damage.

Together these studies have demonstrated the

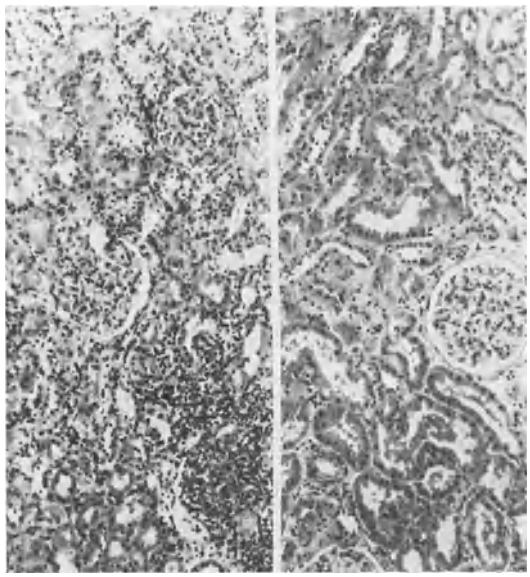

Fig. 9. Histopathological picture of renal allograft biopsies before (left) and after (right) OKT3 monoclonal antibody therapy. Almost complete disapppearance of interstitial mononuclear infiltrate and reversal of endothelial damage was noted after treatment. Cosimi *et al.*, Transpl. 1981 (with permission).

safety of therapy with monoclonal antibodies. Furthermore, they both reported favorable results with such therapy. The treatment of acute renal allograft rejection with more specific monoclonal antibodies can now be anticipated with the hope for ever increasing success.

4. Summary

During the last 10 years, several concepts have had a significant impact on renal allograft transplantation. We have discussed several of these in relation to the timing of transplantation, i.e. pre- and posttransplantation. Pretransplantation, the two concepts have been multiple blood transfusions and HLA-DR matching.

Blood transfusion has a beneficial effect on renal allograft survival in one haplotype matching living related donors, and especially on cadaveric graft survival. There is no general agreement on the influence of different variables such as the exact number of blood transfusions, composition of the transfusate, and the time interval between transfusion and transplantation. In addition the mechanisms underlying this beneficial effect of blood transfusions on renal allograft survival remain open to speculation.

One of the most consistent observations in the published literature is that HLA-DR matching does have a beneficial impact on renal allograft survival in nontransfused recipients, while the correlation is much less clear in transfused patients. HLA-DR typing is a notoriously difficult procedure, note that DR matching with currently available antisera does not always ensure low MLC reactivity. Combined HLA-A, HLA-B, and HLA-DR matching does hold the promise of better long term allograft survival. Better HLA-DR typing reagents are needed if this promise is to be fulfilled.

Recent studies into the mechanisms of graft rejection have highlighted the complexity of this response. Although current immunosuppressive therapies are crude, many studies on the mechanisms of graft rejection have demonstrated the efficacy of various approaches which may assist in the early diagnosis of rejection, in the prognosis of a rejection episode, in the assessment of the reversibility of rejection, and in the development of more specific therapy to prevent and treat rejection. Even now the monitoring of T cell subsets in blood and graft infiltrates is of considerable value. The use of monoclonal antibodies directed against T cell subsets is already in use, and as more specific monoclonals become available ever more specific and subtle immunosuppressive therapies will result. In the long term, the goals are induction of specific immunologic unresponsiveness to the graft, the development of more refined techniques to assess adequacy of immunosuppression and detect the presence of specific unresponsiveness.

References

1. Kissmeyer-Nielsen F, Olsen S, Petersen VP, Fjeldborg O: Hyperacute rejection of kidney allografts, associated with pre-existing humoral antibodies against donor cells. Lancet 2: 662–665, 1966.
2. Persijn GG: Blood transfusion in renal transplantation. Ann Clin Res 13: 215–223, 1981.
3. Opelz G, Terasaki PI: International study of histocompatibility in renal transplantation. Transplantation 33: 87–95, 1982.
4. Patel R, Merrill JP, Briggs WA: Analysis of results of kidney transplantation: comparison in recipients with and without preformed antileucocyte antibodies. N Engl J Med 285: 274–276. 1971.
5. Morris PJ, Dumble LD: Use of lymphoblastoid cell lines in determining responsiveness in cadaveric renal transplantation. Lancet 2: 16–18, 1973.
6. Opelz G, Terasaki PI, Graver B, Cohn M, Chun C: Blood transfusions and renal transplantation. Transplant Proc 11(4): 1889–1891, 1979.
7. Iwaki Y, Terasaki PI, Heintz, Cardman L, Hermes M: Enhancing antibody in human renal transplantation. Transplant Proc 11(4): 1899–1902, 1979.
8. Opelz G, Terasaki PI: Dominant effect of transfusions on kidney graft survival. Transplant 29(2): 153–158, 1980.
9. Ayoub G, Park MS, Terasaki PI, Iwaki Y, Opelz G: B-cell antibodies and crossmatching. Transplant 29(3): 227–229, 1980.
10. Soulillou JP, Bignon JD, Peyrat MA, Guimbretiere J, Guenel J: Systematic transfusion in hemodialized patients awaiting graft. Kinetic

of anti-T and -B lymphocyte immunization and its incidence on graft function. Transplant 30(4): 285–289, 1980.
11. Ayoub GM, Terasaki PI, Iwaki Y, Park MS: Presensitization tests for potential transplant recipients. Dial Transplant 7: 496–504, 1978.
12. Opelz G, Graver B, Mickey MR, Terasaki PI: Lymphocytotoxic antibody responses to transfusion in potential kidney transplant recipients. Transplant 32: 177–183, 1981.
13. Salvatierra O, Iwaki Y, Vincenti F, Amend W, Terasaki PI, Garavoy M, Duca R, Hopper S, Feduska N: Update of the University of California at San Francisco experience with donor-specific blood transfusions. Transplant Proc 14: 363–366, 1982.
14. Schweizer R, Bow L, Generas D, Bartus S: Serologic considerations in donor-specific transfusion therapy for kidney transplantation. Transplant Proc 14: 374–377, 1982.
15. Anderson CB, Gregorio A, Sicard MD, Etheredge EE: Pretreatment of renal allograft recipients with azothioprine and donor-specific blood products. Surgery 92: 315–321, 1982.
16. Van Es AA, Terasaki PI: Blood transfusions and kidney allograft survival. Transplant Proc 13: 1284–1287, 1981.
17. Fischer E, Lenhard V, Seifert P, Kluge A, Johannsen R: Blood transfusion-induced suppression of cellular imunity in man. Hum Immunol 3: 187–194, 1980.
18. Bodmer WF, Batchelor JR, Bodmer JG, Festenstein H, Morris, PJ: Histocompatibility testing 1977. Munksgaard, Copenhagen, 1978.
19. Morris PJ, Ting A: Studies of HLA-DR with relevance to renal transplantation. Immunological Reviews 65: 105–131, 1982.
20. Madsen M, Graugaard B, Fjeldborg O, Petersen VP, Hansen HE, Kissmeyer-Nielsen F: The impact of HLA-DR antigen matching on the survival of cadaveric renal allografts. Transplant 36: 379–383, 1983.
21. Vanrenterghem Y, Vandeputte I, Lerut T, Roels L, Gruwez J, Michielsen P: Importance of HLA-DR matching in polytransfused cadaveric kidney transplant recipients. Transplant 36: 384–387, 1983.
22. Opelz G, Terasaki PI: International study of histocompatibility in renal transplantation. Transplant 33: 87–95, 1982.
23. McPhaul JJ, Stasney P, Freeman RB: Specificities of antibodies eluted from human cadaveric renal allografts. J Clin Invest 67: 1405–1414, 1981.
24. Strom TB, Tilney NL, Carpenter CB, Busch GJ: Identity and cytotoxic capacity of cells infiltrating renal allografts. N Engl J Med 292: 1257–1263, 1975.
25. Reinherz EL, Schlossman SF: The differentiation and function of human T lymphocytes. Cell 19: 821–827, 1980.
26. Kung PC, Goldstein G, Reinherz EL, Schlossman SF: Monoclonal antibodies defining destructive human T-cell surface antigens. Sci 206: 347–349, 1979.
27. Ledbetter JS, Evans RL, Lipinski M, Cunningham-Rundles G, Good RA, Herzenberg LA: Evolutionary conservation of surface molecules that distinguish T-lymphocyte helper/inducer and cytotoxic/suppressor subpopulations in mouse and man. J Exp Med 153: 310–323, 1981.
28. Lanier LL, Engelman EG, Gatenby P, Babcock GF, Warner NL, Herzenberg LA: Correlation of functional properties of human lymphoid cell subsets and surface market phenotypes using multiparameter analysis and flow cytometry. Immunol Rev 74: 143–160, 1983.
29. Reinherz EL, Kung PC, Goldstein G, Levey RH, Schlossman SF: Discrete stages of human intrathymic differentiation: analysis of normal T-lymphocytes and leukemic lymphoblasts of T-cell lineage. Proc Natl Acad Sci 77: 1588–1592, 1980.
30. Reinherz EL, Kung PC, Goldstein G, Schlossman SF: A monoclonal antibody reactive with the human cytotoxic/suppressor T-cell subset previously defined by a heteroantiserum termed TH_2. J Immunol 124: 1301–1307, 1980.
31. Beard J, Reinherz EL, Kung PC, Goldstein G, Schlossman SF: A monoclonal antibody reactive with human peripheral blood monocytes. J Immunol 124: 1943–1948, 1980.
32. Reinherz EL, Kung PC, Pesando JM, Ritz J, Goldstein G, Schlossman SF: Ia determinants on human T-cell subsets defined by monoclonal antibody: activation stimuli required for expression. J Exp Med 150: 1472–1482, 1979.
33. Abo T, Blach CM: A differentiation antigen of human NK and K cells identified by a monoclonal antibody (HNK-1). J Immunol 127: 1024–1029, 1981.
34. Salzman GC, Growell JM, Martin JC, *et al.*: Cell classification by laser light scatterings: Identification and separation of unstained leucocytes. Acta Cytol 19: 374–377, 1975.
35. Herzenberg LA, Herzenberg LA: Analysis and separation using the fluorescence activated cell sorter (FACS). In: Handbood of Experimental Immunology, Weir DM (ed), Oxford, Blackwell Sci Publ, 1978, Ch 22.
36. Reinherz EL, Kung PC, Breard J. Goldstein G, Schlossman SF: T-cell requirements for generation of helper factor in man: Analysis of the subsets involved. J Immunol 124: 1883–1887, 1980.
37. Stiller CR, Sinclair NRSC, McGirr D, Jennikar A, Ullan RA: Diagnosis and prognosis of donor-specific posttransplant immune responses: clinical correlates and in vitro variables. Transplant Proc 10: 525:530, 1978.
38. Quadracci LJ, Hellstrom IE, Striker GE, Marchioro TL, Hellstrom KE: Immune mechanisms in human recipients of renal allografts. Cell Immunol 1: 561–566, 1971.
39. Liburd EM, Parderka V, Kotihavongs T, Dossetor JB: Evidence for suppressor cells and reduced CML induction by the donor in transplant patients. Transplant Proc 10: 557–561, 1978.
40. Tursz T, Fournier C, Kreis H, Crosnier J, Bach JF: T-lymphocytes in kidney allograft recipients. Br Med J 1: 799–801, 1976.
41. Cosimi AB, Colvin RB, Burton RC, *et al.*: Use of monoclonal antibodies to T-cell subsets for immunologic monitoring and treatment in recipients of renal allografts. N Engl J Med 305: 308–314, 1981.
42. Colvin B, Cosimi AB, Burton RC, *et al.*: Circulating T-cell subsets in 72 human renal allograft recipients: The $OKT4^+/OKT8^+$ cell ratio correlates with reversibility of graft injury and glomerulopathy. Transplant Proc 15: 1166–1169, 1983.
43. Ellis TM, Lee HM, Mohanakumar T: Alterations in human regulatory T-lymphocyte subpopulations after renal allografting. J Immunol 127: 2199–2203, 1981.
44. Guttman RD, Poulsen RS: Fluorescence activated cell sorter analysis of lymphocyte subsets after renal transplantation. Transplant Proc 15: 1160–1162, 1983.
45. Keiman RH, Van Buren CT, Payne W, Flechner S, Kahan BD: Monitoring of T-cell subsets and immune events in renal allograft recipients. Transplant Proc 15: 1170–1172, 1983.
46. Van Es A, Tanke HJ, Baldwin WM, Oljans PJ, Ploem JS, Van Es LA: Ratios of T-lymphocyte subpopulations predict survival of cadaveric renal allografts in adult patients on low dose corticosteroid therapy. Clin Exp Immunol 52: 13–20, 1983.
47. Chatenoud L, Chkoff N, Kreis H, Bach JF: Interest in and limitation of monoclonal anti-T cell antibodies for the follow-up of renal transplant patients. Transplant 36: 45–50, 1983.
48. Platt JL, LeBien TW, Michael F: Interstitial mononuclear cell populations in renal graft rejection. Identification by monoclonal antibodies in tissue sections. J Exp Med 155: 17–3, 1982.
49. Cosimi A, Burton RC, Colvin RB, *et al.*: Treatment of acute renal allograft rejection with OKT3 monoclonal antibody Transplant 32: 535–539, 1981.
50. Kirkman RL, Araujo JL, Busch GJ, *et al.*: Treatment of acute renal allograft rejection with monoclonal anti-T12 antibody. Transplant 36: 620–626, 1983.

CHAPTER 9

Current concepts of glomerular diseases

AMIRA F. GOHARA and PETER J. GOLDBLATT

Introduction

The main objective of this chapter is to provide the reader with a review of current concepts of glomerular diseases including the classification of glomerulonephritis with associated clinical picture, differential diagnosis, laboratory findings, course and complications. Since it is very important to know the normal to be able to understand the pathologic processes, we have included in our discussion a brief review of the anatomy, physiology and biochemistry of the glomerulus including its ultrastructure as well as an update of the mechanisms of glomerular injury and how they lead to the morphologic patterns seen in the various types of glomerulonephritis. Each kidney is made up of a cortex which contains the glomeruli and proximal and distal convoluted tubules and a medulla made up of the collecting tubules. Both cortex and medulla have a very rich and intricate blood supply which is very important for the normal function of the glomerulus, the latter being the cornerstone of normal renal function.

1. Structure and function of the glomerulus

1.1. Structure

A few important features of glomerular structure will be presented for emphasis. For a more extensive discussion, see Chapters 6, 7, 13.

Each normal glomerulus contains six to eight lobules, each of which is composed of anastomosing capillaries supported by a mesangial matrix.

The glomerulus is made up of capillaries surrounded by Bowman's capsule. It receives its blood supply from an afferent arteriole that enters the capsule then divides into several branches which coalesce to form the efferent arteriole which exits from the capsule. The glomerular capillaries are supported by a mesangial matrix. Each capillary loop has a basement membrane lined on its inner aspect by endothelial cells and on its outer aspect by epithelial cells. Using electron microscopy the basement membrane appears to have three zones: a central lamina densa bounded by a lamina rara externa and a lamina rara interna. The total thickness of the basement membrane is 3000–3500 Å.

In addition to the basement membrane of the capillaries the glomerulus has three cellular elements:

The mesangial cells, which act as macrophages and possess phagocytic abilities. They also contain contractile elements and appear to play a role in regulating blood flow through the glomerulus.

The endothelial cells which line the internal surface of the basement membrane. On electron microscopy they reveal regularly spaced 500–1000 Angstrom fenestrations.

The epithelial cells, or podocytes, which form the external component of the capillary loop. On EM they appear to branch repeatedly terminating in foot processes which attach to the outer aspect of the glomerular basement membrane. The podocytes are separated by filtration pores bridged by a thin filtration slit membrane. In each glomerulus the capillary tufts are surrounded by Bowman's capsule which is lined by flattened parietal epithelial cells. The highest concentration of glomeruli is in the outer cortex of the kidney. Each kidney contains 1 million glomeruli with a total filtering surface of roughly one half a square meter/kidney.

1.2. Physiology and biochemistry [1]

The main function of the renal glomerulus is filtration of water and solutes. Roughly 25,000 mEq of sodium ion are filtered every 24 hours. Active filtration of potassium also takes place through the glomerulus. The normal glomerulus acts as a barrier against the spillage of large amounts of protein permitting a maximum of 200 mg/24 hours in the urine

L.J.A. DiDio and P.M. Motta (eds), Basic, Clinical, and Surgical Nephrology. ISBN 0-89838-689-5.

of a normal individual. In glomerular diseases, this balance is disturbed and protein as well as RBCs and large quantities of RBC casts appear in the urine. The biochemical integrity of the capillary basement membrane is very important in maintaining the normal function of the glomerulus.

Chemical analysis of the glomerular basement membrane indicates that it is composed of two distinct types of glycopeptides: a nonpolar collagen-like component rich in glycine and hydroxyproline and a polar non-collagenous fraction rich in tyrosine and aspartic acid with a high content of sialic acid.

Further assessment of the glomerular basement membrane using cationic stains indicates that the lamina densa are neutral and have a high concentration of nonpolar collagen-like moiety, while the laminae rarae contain the polar non-collagen component and have a negative charge. The latter plays a major role in filtration in both normal and diseased states. For example, under normal conditions albumin molecules do not go through the basement membrane because of electrostatic repulsion.

Changes in the metabolic constituents of the capillary basement membrane lead to increased permeability to macromolecules and result in proteinuria [2].

In addition to the factors mentioned above hemodynamic flows and pressures play a major role in glomerular filtration. Therefore in trying to explain filtration abnormalities in disease states all factors have to be considered.

2. Mechanisms of glomerular injury

2.1. Mechanisms of glomerular diseases

Although glomerular diseases can be caused by immunologic infectious, metabolic and as yet unknown mechanisms, the majority of the glomerular diseases appear to be immunologically mediated. In this review we will concentrate on the immunologic mechanisms that initiate glomerular injury.

2.2. Antiglomerular basement membrane antibody

Glomerular injury is due to the formation of antibodies to an antigen fixed to the capillary basement membrane. The antigen could either be a constituent of the basement membrane or a foreign antigen fixed to the basement membrane. The interaction between the antigen and the antibody activates the complement cascade which releases chemostatic factors. The latter initiate an acute inflammatory response with release of lysosomal enzymes from the polymorphonuclear leucocytes and results in glomerular damage. The example of this mechanism in humans is Goodpasture's syndrome.

2.3. Immune complex diseases mediated by circulating immune complexes [3]

The patient develops circulating antigen, antibody immune complexes which deposit in the glomerular basement membrane, activate complement, release chemostatic factors and initiate the inflammatory response which leads to tissue damage through the release of lysosomal enzymes and the release of vasoactive amines. In this type of glomerular injury the following factors play an important role.

3. Important factors in immune mediated injury

3.1. The size of the complex

Only complexes formed with a moderate excess of antigen can cause damage. These usually have a molecular weight of approximately 1,000,000. Larger complexes are removed by the reticuloendothelial system. Smaller complexes are removed by filtration.

3.2. The titer of the complexes

The presence of vasoactive amines: In experimental studies the use of histamine antagonists in the presence of immune complexes prevent the deposition of the complexes in the glomerulus. Examples of immune complex glomerulonephritis in man include acute poststreptococcal glomerulonephritis and systemic lupus nephritis.

3.3. Activation of the alternate complement pathway in glomerular diseases

In this setting there is cleavage of C_3 bypassing C_1, 2 and 4. The cleavage of the third component of complement leads to tissue damage through its lytic effect and also through initiation of the inflammatory response. Examples of diseases mediated through this mechanism are IgA nephropathy and Henoch-Schonlein purpura.

3.4. Cellular immunity in glomerulonephritis [4]

The role of cellular immunity in the initiation of glomerular damage is still unclear although some

experimental studies seem to indicate a possible role of lymphokines in glomerular diseases.

3.5. Monocyte involvement in crescent formation [5]

In several studies investigators have assessed the role of the monocyte in crescent formation in antiglomerular basement membrane and immune complex diseases using cytochemical stains for monocytes and electron microscopy. The results indicate that monocytes participate actively in crescent formation in antiglomerular basement membrane disease but appear to be of minor importance in immune complex diseases associated with crescents.

4. Alternative mechanisms of glomerular injury

Although less important than the ones discussed previously, they include:

4.1.

Trapping or binding of antibodies to the capillary basement membrane resulting in alterations of its physical and chemical characteristics which leads to changes in permeability.

4.2. Kinin mediated injury.

The coagulation system appears to play a major role in glomerular diseases.

4.3.

IgE and histamine mediated injuries have been studied in animal models but their role in human diseases is not clear.

5. Special techniques and definitions used in the study of glomerular diseases [5]

Optimal interpretation of renal biopsy requires an adequate sample appropriately prepared for combined examination by light microscopy, immunofluorescence and electron microscopy. The needle core is usually split longitudinally into three segments:

5.1.

For light microscopy the tissue is fixed in 10% buffered formalin solution, then routinely processed and embedded in paraffin, then serial. 2–4 micron sections are cut and the following stains are routinely used, hematoxylin and eosin, periodic acid-Schiff (PAS) to assess the mesangial matrix; trichrome stain to assess the amount of fibrosis, as well as the presence of deposits, which appear as bright red spots; Jones silver stain to assess the capillary basement membrane. Additional stains could be added if needed, e.g. Congo red stain for amyloidosis. The slides are then scanned, the glomeruli counted and assessed for the type as well as the distribution of the lesion. The following terms are commonly used in describing the light microscopic features of glomerular diseases: Focal = means some glomeruli are involved and some are not. Segmental = means only parts of the glomerulus are involved. Diffuse = means the entire glomerulus is involved. Generalized = means all the glomeruli are involved. Crescent = means proliferation of the cells lining the Bowman's capsule.

5.2. Immunofluorescence (IF)

The core is rapidly frozen in liquid nitrogen, then multiple sections are cut and monospecific fluorescein, conjugated antihuman IgG, IgA, IgM, C_3, C_4, properdin, fibrinogen and albumin are used to stain the sections to assess the presence as well as the type and location of immunoglobulin and complement deposits.

5.3. Electron microscopy (EM)

The tissue is minced and fixed in gluteraldehyde, then dehydrated and embedded in Epoxin, then micron sections are prepared as well as thin 600–000 Angstrom's sections. The micron sections are stained with Toluidine blue. The thin sections are stained with uranyl acetate and examined with the transmission electron microscope. The value of scanning electron microscopy in the study of glomerular diseases is still under investigation.

6. Specific diseases of the glomerulus

Glomerular diseases can be classified in a variety of ways based on morphology, clinical presentation, pathogenesis and associated diseases. In this chapter we will use the following classification:

6.1. Primary glomerular diseases

6.1.1. Nephrotic syndromes

The nephrotic syndrome consists of
- proteinuria – due to leaky capillary basement membrane, secondary to changes in the chemistry and electric charge of the basement membrane.
- hypoproteinemia – due to spillage of protein in urine.
- edema – due to decreased oncotic pressure.
- hyperlipidemia – the mechanism of which is unclear. It could be due to increased synthesis of lipoprotein in the liver or excessive loss in the urine of factors that regulate lipoprotein synthesis and disposal. The following diseases are associated with nephrotic syndrome.

6.1.1.1. Lipoid nephrosis. Incidence – 60–80% of cases of primary nephrotic syndrome occur in children. 20–30% of cases of primary nephrotic syndrome present in adults. Male to female ratio – 2.5:1 in children; – 1:1 in adults. Peak age incidence – 1–5 years.

Clinical presentation: Nephrotic syndrome with highly selective proteinuria (albuminuria). 10% of the patients tend to have recurrent episodes of nephrotic syndromes.

Pathogenesis: Not known.

Diagnostic features: Light microscopy – no changes.

Immunofluorescence – negative.

EM – fusion of the foot processes and swelling of the epithelial cells. These changes are nonspecific and disappear.

Course: 90–98% of children respond to steroids.
66–77% of adults respond to steroids.
10% recurrence.
7% mortality

Differential diagnosis: Early membranous nephropathy may be misdiagnosed as lipoid nephrosis by light microscopy but IF and EM reveals deposits in membranous nephritis.

6.1.1.2. Focal glomerulosclerosis. Incidence: second most common cause of nephrotic syndrome in children. Approximately 10% of primary nephrotic syndrome.
3:1 female predominance. Age range 5–45 years.

Clinical presentation: 60–80% nephrotic syndrome, 30–60% of the patients have azotemia, 20–40% of the patients are hypertensive. The proteinuria in focal glomerulosclerosis is nonselective. The disease does not respond to steroids. Focal glomerulosclerosis recurs in renal allograft. Some patients have microscopic hematuria.

Pathogenesis: It was thought that focal glomerulosclerosis represents an advanced stage of lipoid nephrosis but recent investigations indicate that they are two different diseases.

Diagnostic features: Light microscopy – focal mesangial sclerosis starting in the juxtamedullary glomeruli and spreading superficially as the disease progresses [8].

Immunofluorescence: large focal mesangial IgM deposits. Occasional focal mesangial C_3 and C_4 deposits.

Electron microscopy: Wrinkling of the basement membrane. Endothelial cell degeneration. Focal increase of mesangial matrix. Electron dense deposits in sclerotic segments. Lipid droplets in mesangial cells.

Course: The disease usually progresses to renal failure.

Differential diagnosis: If the biopsy does not include the juxtamedullary glomeruli, it could be misinterpreted for lipoid necrosis.

6.1.1.3. Membranous glomerulonephritis. Incidence: Membranous nephropathy represents approximately 1–9% of childhood cases of nephrotic syndrome and about 20% of adult cases of primary nephrosis. Male:Female – 1.5:1. Mean age – 35 years.

Preceding illness: Several preceding illnesses have been reported with membranous nephritis including: poison oak, chronic hepatitis B antigenemia, syphilis, malaria, Guillain-Barre syndrome, systemic lupus, renal vein thrombosis and extra renal tumors namely lymphoma and GI cancer. Gold therapy for rheumatoid arthritis has also been associated with membranous nephritis.

Clinical presentation: Cases present with nephrotic syndrome with 10–50% of the cases associated with hypertension and azotemia at the onset of the disease. The proteinuria is nonselective, serum C_3 level is normal except in membranous nephropathy asssociated with systemic lupus.

Pathogenesis: This disease appears to be a chronic immune complex disease. The antigens include gold, treponemata, tumors, renal tubular antigen in experimental models and hepatitis B surface antigen. In some cases there is no identifiable antigen, and these cases are referred to as idiopathic membranous nephritis [9, 10].

Diagnostic features: Light microscopy: uniform diffuse thickening of the capillary basement membrane. Occasional small subepithelial 'spikes' on silver (Jones) stain.

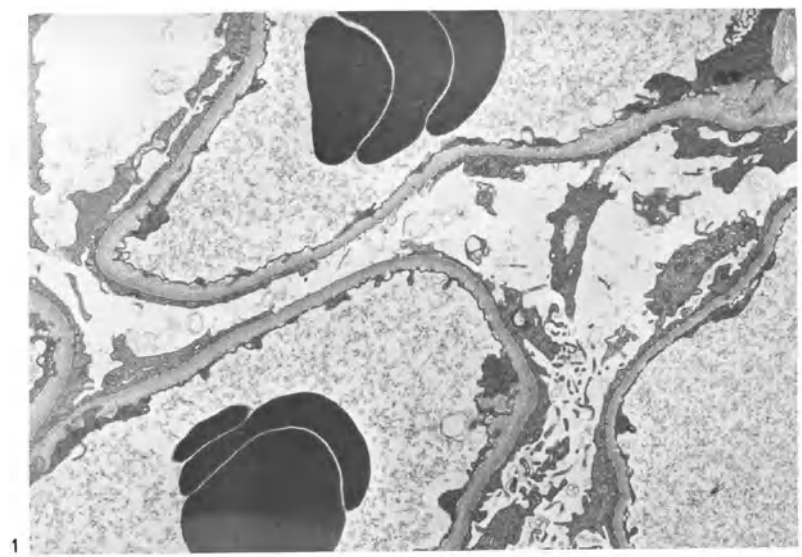

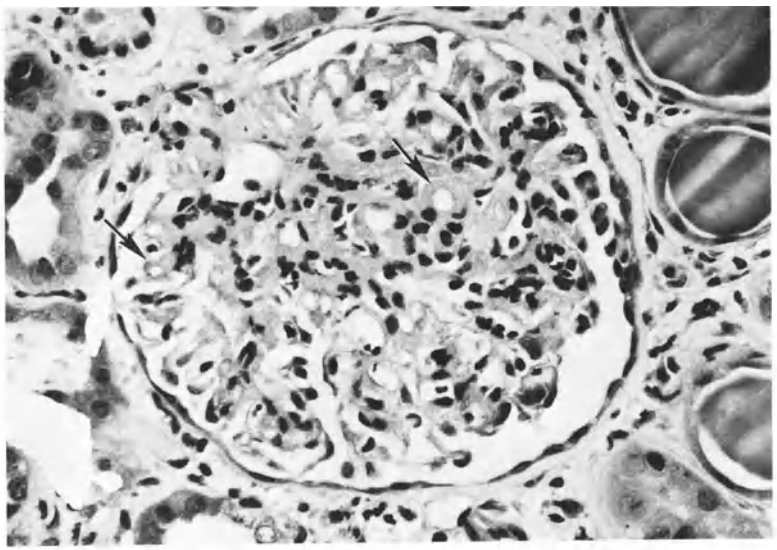

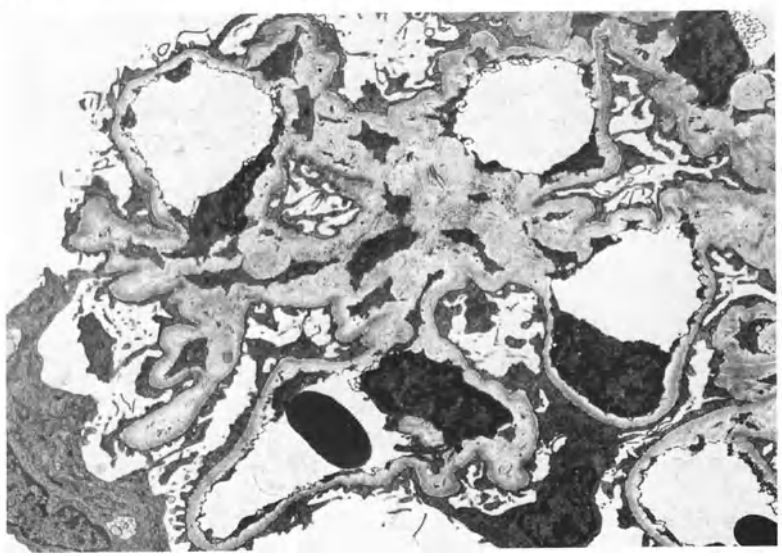

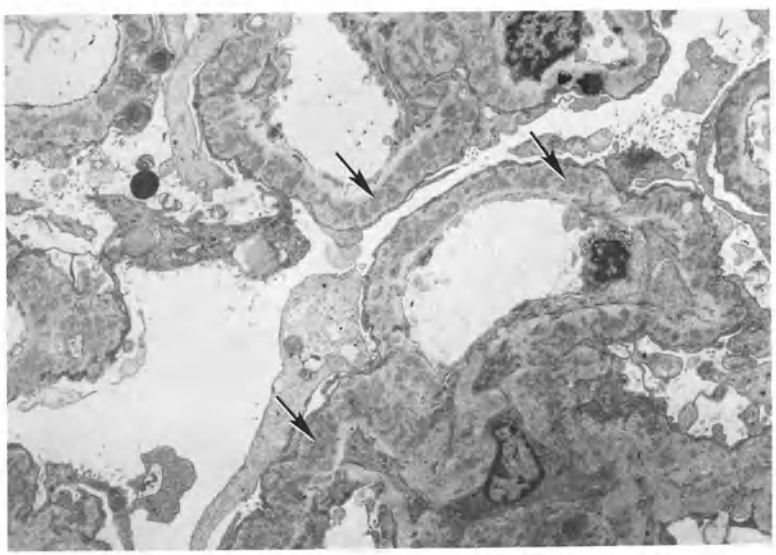

Fig. 1. Electron micrograph showing diffuse fusion of the podocytes in a case of lipoid nephrosis. ×3,250. *Fig. 2.* Electron micrograph showing focal sclerosis of the mesangial matrix from a case of focal glomerulosclerosis. ×2,275. *Fig. 3.* Light microscopy of membranous glomerulonephritis showing thickening of the capillary loops. ×97.50. *Fig. 4.* Electron micrograph showing multiple large intramembranous electron dense deposits in membranous glomerulonephritis. ×2,275.

Immunofluorescence: Diffuse, peripheral granular IgG and complement.

EM: 4 stages: 1 – epimembranous electron dense deposits.
2 – intramembranous deposits with spikes.
3 – intramembranous deposits.
4 – intramembranous clear areas at the site of deposits.

Course: Thirty-eight percent of the patients develop renal failure in <5 years. Twenty-five percent develop chronic renal failure in 15–20 years. Eight to 15% go into complete remission, but there is a 35% recurrence rate. The prognosis in children is better.

6.1.1.4. Membranoproliferative glomerulonephritis. There are three types of membranoproliferative glomerulonephritis. *Type I* is also known as mesangiocapillary glomerulonephritis [11, 12, 13].

Incidence: 5–20% of cases of primary nephrotic syndrome. There is a slight female predominance. Age: 4–65 median age at onset, 13 years.

Clinical presentation: Nephrotic syndrome and hypocomplementemia are present in 80% of the cases; C_4 is normal but C_3 shows fluctuations.

Pathogenesis: The pathogenesis of membranoproliferative glomerulonephritis may involve both classical and alternate pathways. In addition, the sera of many patients with this type of nephritis contain the C_3 nephritic factor which initiates the alternate complement pathway.

Diagnostic features: Light microscopy: The glomeruli reveal mesangial cell proliferation and increase in mesangial matrix with lobular accentuation. Silver stains reveal splitting of the capillary basement membrane.

Immunofluorescence: The glomeruli show C_3 deposits in a peripheral lobular distribution. Some cases also reveal properdin deposits.

Electron microscopy: Reveals a split double contoured basement membrane due to extension of the mesangial cells with the capillary loops giving them a 'train track' appearance.

Course: The disease usually follows a chronic progressive couse and it tends to recur in allografts.

Type II is also called dense deposit disease [14].

Incidence: Less frequent than Type I and no sex predilection.

Clinical presentation: Nephrotic syndrome, hypertension with or without hematuria. Complement studies reveal low C_3, normal C_4 and oftentime shows C_3 nephritic activity.

Pathogenesis seems to be due to activation of the alternate complement pathway.

Diagnostic features: Light microscopy: diffuse mesangial cell proliferation with increased mesangial matrix and thickening of the capillary loops.

Immunofluorescence: Segmental linear C_3 deposits.

Electron microscopy: Segmental ribbon-like electron dense deposits in the lamina densa.

Course: Chronic progressive with recurrence in transplanted kidneys.

Type III. Incidence: 3–8% of cases of primary nephrotic syndrome. Age range 3–15 years. No sex preponderance.

Clinical presentation is the same as Types I and II.

Pathogenesis: unknown.

Diagnostic features include on light microscopy mesangial cell proliferation with thickening of the capillary basement membrane. On immunofluorescence there is a mixture of peripheral and mesangial deposits of IgM and C_3. Electron microscopy reveals subepithelial and subendothelial electron dense deposits as well as disruption of the lamina densa [15].

Differential diagnosis: Membranoproliferative glomerulonephritis Type I, the differentiating features being the hypocomplementemia and double contour basement membrane in the Type I, both of which are absent in the Type III.

Course: Favorable course with possible complete remission.

6.2. Hematuria syndromes

6.2.1. Acute post-infectious glomerulonephritis

Incidence: Approximately 0.2/1000/year in children between 5–14 year of age, usually following an episode of streptococcal pharyngitis due to beta hemolytic streptococcus type 12. The glomerulonephritis usually occurs 10–12 days post-pharyngitis.

Clinical presentation: Sudden onset of periorbital edema, dark urine 10–12 days following a streptococcal pharyngitis or tonsillitis.

Pathogenesis: This disease represents an immune complex process.

Physical examination: There is moderate hypertension. The urinalysis shows RBCs, RBCs casts and mild proteinuria. Additional laboratory finding include:

- elevated ASO titers >500 Todd units
- elevated anti-DNASE B
- decreased CH_{50} and C_3, they return back to normal in 12 weeks
- Moderate azotemia
- 5% of the patients present with nephrotic syndrome.

Diagnostic features: Light microscopy: Diffuse

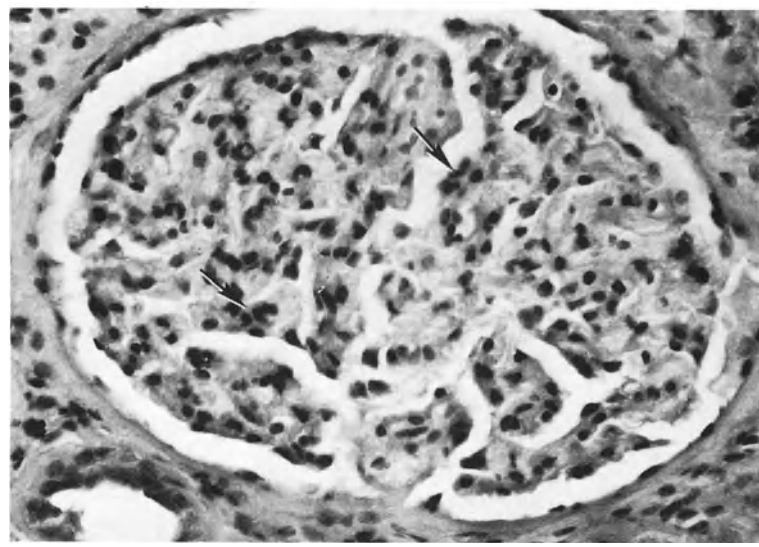

Fig. 5. Light microscopy of membranoproliferative glomerulonephritis showing mesangial cell proliferation of lobular pattern of the mesangial matrix. ×97.50.

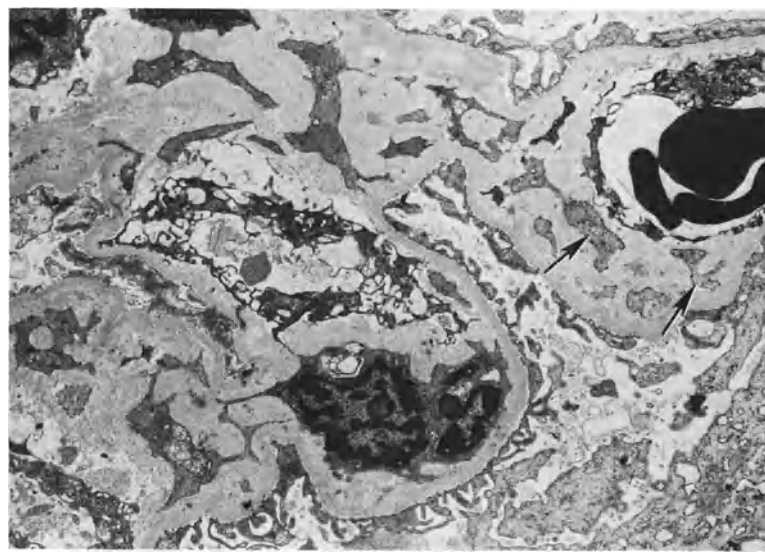

Fig. 6. Electron micrograph showing mesangialization of the capillary basement membrane in a case of membranoproliferative glomerulonephritis, Type I. ×3,250.

proliferation of mesangial cells, swelling of endothelial cells and few scattered polymorphonuclear leucocytes within the mesangial matrix.

In the rapidly progressive type of acute post infectious glomerulonephritis the renal biopsy reveals crescent formation, in addition to all of the above findings.

Immunofluorescence: reveals diffuse, lumpy, bumpy, coarse granular peripheral deposits of IgG, and C_3. Occasionally C_4 and IgM deposits are present.

Electron microscopy: reveals multiple subepithelial electron dense deposits or humps.

If the renal biopsy is obtained late in the course of the disease the deposits are more prominent in the mesangium in contrast to the peripheral deposits in the acute stage.

Course: In children 80–95% cured; in adults 50–70% cured.

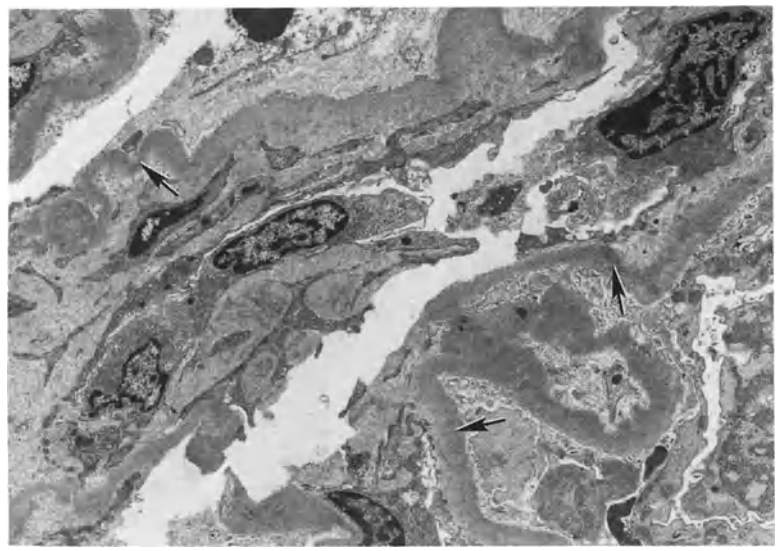

Fig. 7. Electron micrograph showing ribbon-like dense deposits in lamina densa in dense deposit disease. ×3,250.

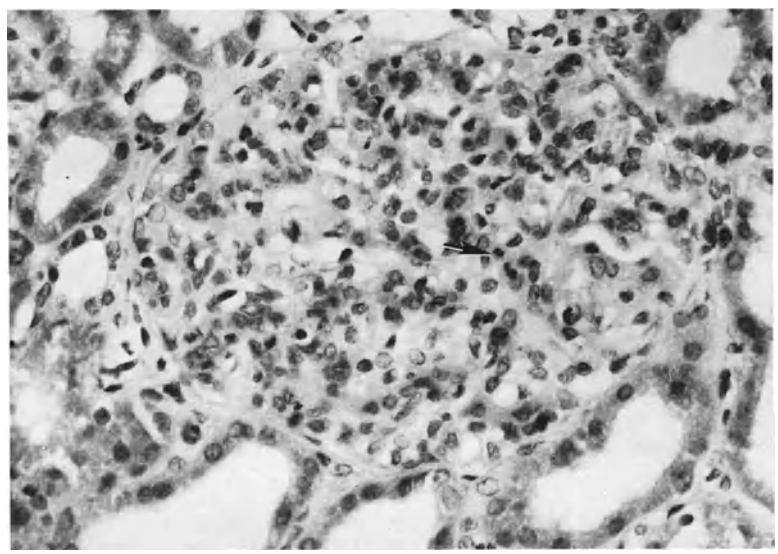

Fig. 8. Light microscopic picture showing diffuse mesangial cell proliferation and scattered polymorphonuclear leucocytes within the glomerulus in a patient with acute proliferative poststreptococcal glomerulonephritis. ×97.50.

Differential diagnosis: Other types of post infectious glomerulonephritis. Example: glomerulonephritis associated with SBE has a very similar morphology to post streptococcal nephritis except on electron microscopy the glomeruli appear to contain subendothelial deposits [16, 17].

6.2.2. IgA Nephropathy (Berger's disease) [18]:
Incidence: This disease represents approximately 15% of all primary chronic glomerulonephritis. The mean age is 35 years. There is a male predominance. Male: female is 2:1.

Clinical presentation: Usually it is preceded by an upper respiratory tract infection. Recurrent gross or microscopic hematuria with or without mild proteinuria may appear.

Pathogenesis: Two major hypothesis have been used to explain IgA nephropathy.

Immune complex disease (with the complexes being rich in IgA).

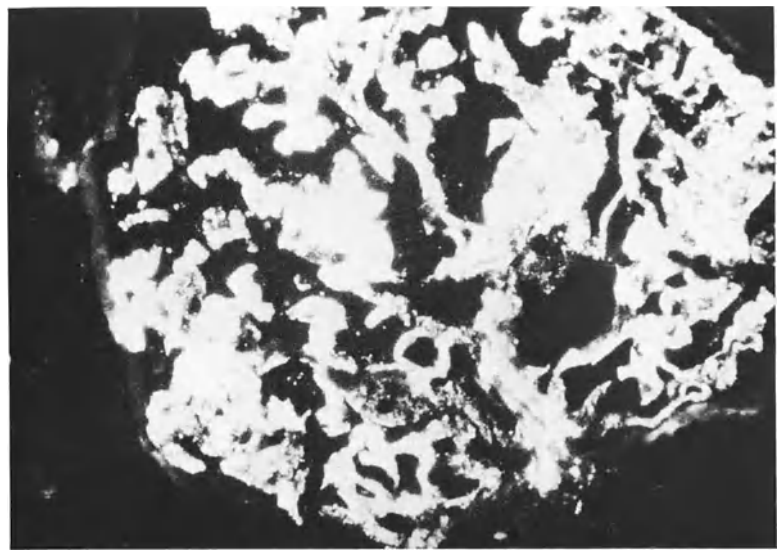

Fig. 9. Immunofluorescence picture of lumpy bumpy deposits of IgG and C_3 in acute poststreptococcal glomerulonephritis. ×97.50.

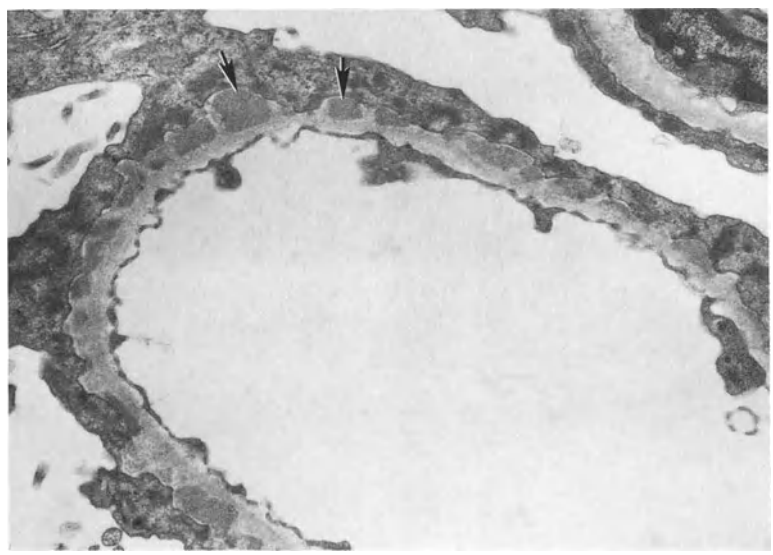

Fig. 10. Electron micrograph showing multiple subepithelial electron dense deposits 'humps' in acute poststreptococcal glomerulonephritis. ×7,500.

Activation of the alternate complement pathway. This is supported by the fact that in IgA nephropathy immunofluorescence reveals mesangial deposits of C_3 but not C_4 or C_{19}.

Diagnostic features: Light microscopy: Variable findings including normal appearing glomeruli, focal mesangial cell proliferation, diffuse mesangial cell proliferation, focal necrosis and occasional crescents.

Immunofluorescence: Diffuse mesangial IgA and C_3 deposits, occasional IgG.

Electron microscopy: Variable findings including multiple mesangial electron dense deposits, thining of the capillary basement membrane and occasional subendothelial deposits.

Course: Benign in children. In adults, 30% of the patients develop hypertension and 20% go into chronic renal failure. The disease tends to recur in renal allografts.

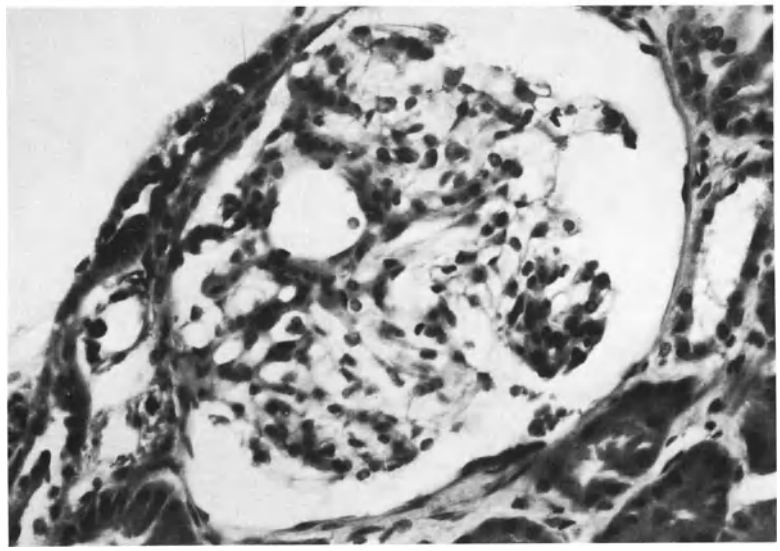

Fig. 11. Light microscopic picture showing segmental mesangial cell proliferation from a patient with IgA nephropathy. ×97.50.

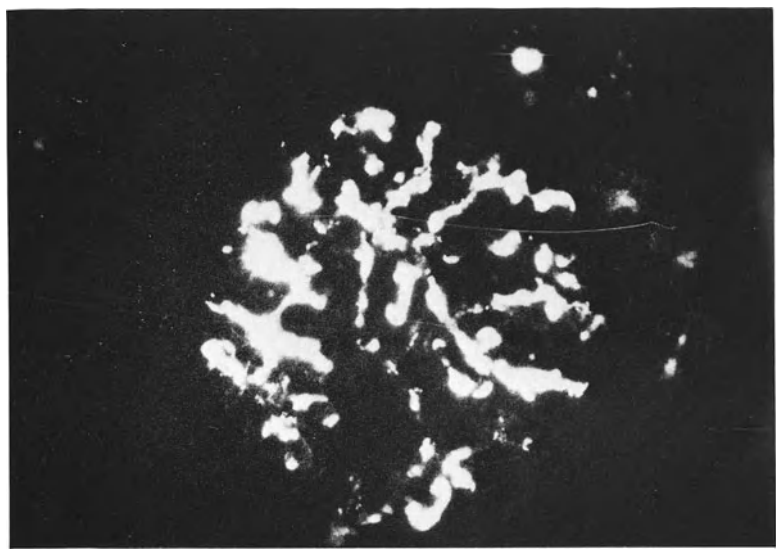

Fig. 12. Diffuse mesangial IgA deposits in Berger's disease. ×97.50.

6.2.3. Benign recurrent hematuria

Incidence: Median age 10 years, range infancy – 65 years.

Clinical presentation: Recurrent episodes of microscopic and gross hematuria.

Pathogenesis unknown. It is a familial disease and its mode of transmission is not clear.

Diagnostic features: The diagnostic morphologic features of this disease include normal appearing glomeruli on light microscopy, negative immunofluorescence and diffuse thinning of the capillary basement membrane on electron microscopy, sometimes as thin as 500 Å.

Course: The course of the disease is usually benign but whether benign recurrent hematuria represents a stage in the spectrum of Alport's syndrome or is a disease entity is still under investigation.

6.2.4. Alport's Syndrome: Hereditary nephritis [19, 20]

Incidence: To date there have been approximately 100 families described with this syndrome.

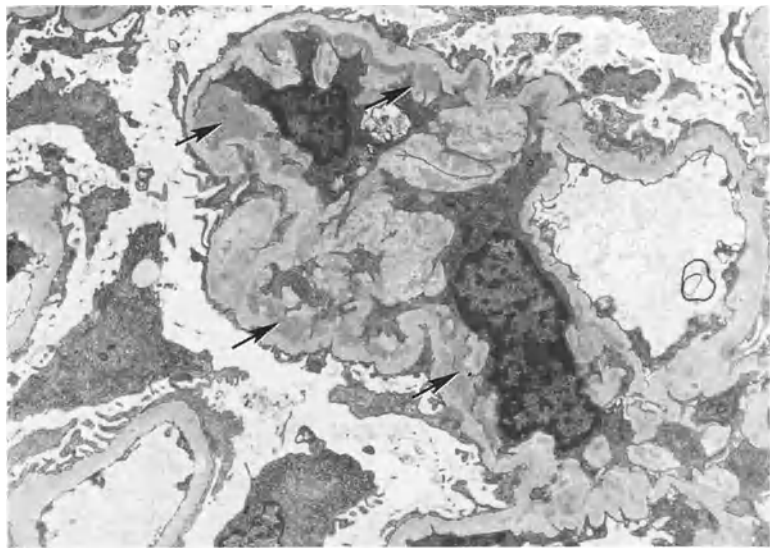

Fig. 13. Electron micrograph showing multiple intramesangial electron dense deposits from a case of IgA nephropathy. ×3,250.

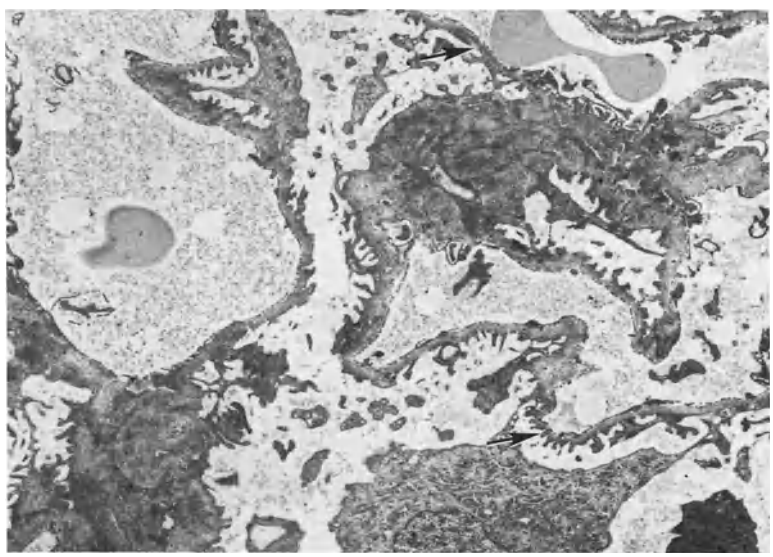

Fig. 14. Electron micrograph showing segmental thinning of the capillary basement membrane in benign recurrent hematuria. ×2,275.

Age: The disease is usually detected in the first decade. Females tend to have a milder form while males usually have a more fulminant course.

Clinical presentation: The early renal manifestations of this syndrome are variable. They include hematuria following upper respiratory tract infection in 25% of the patients, mild proteinuria in 40% of the patients, microscopic hematuria in 80% of the cases. Fifty percent of the patients have deafness, 20% of the patients have ocular abnormalities and there is an increased incidence of toxemia and spontaneous abortions. Male patients usually progress to chronic renal failure.

Pathogenesis: The exact mode of genetic transmission is not clear. Three possible modalities have been suggested:

1. autosomal dominant;
2. preferential segregation;
3. partial X-linked dominant.

Diagnostic features: Light microscopy: variable in females. In males with early disease, the glomeruli are within normal limits. The interstitium shows ag-

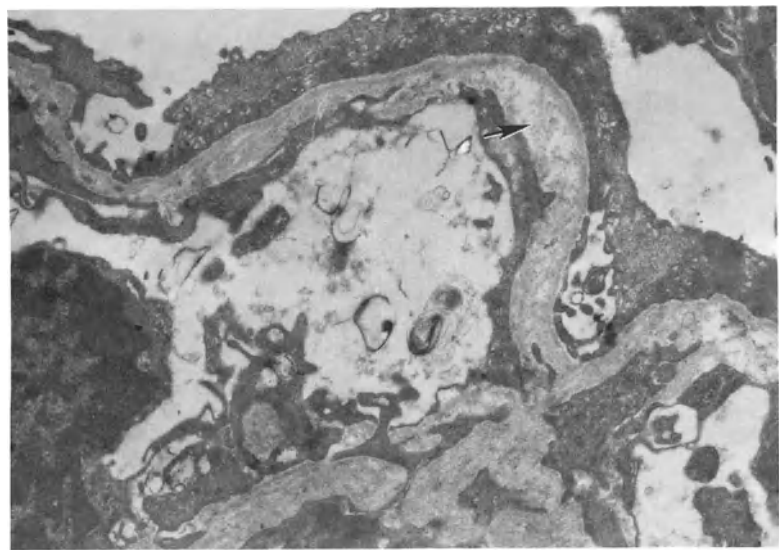

Fig. 15. Electron micrograph showing lamellar splitting of the capillary basement membrane in Alport's syndrome. ×4,875.

gregates of foam cells and focal fibrosis.

As the disease progresses the glomeruli become sclerotic, more interstitial scarring develops as well as tubular atrophy and vascular sclerosis.

Immunofluorescence: Negative.

Electron microscopy: Splitting of the lamina densa giving the capillary basement membrane a lamellated appearance. Segmental thinning of the basement membrane is also noted.

Course: Males develop renal failure by the fourth decade. In some families some females have also progressed to renal failure.

Differential diagnosis: Benign recurrent hematuria which shows thinning of the capillary basement membrane but no splitting.

7. Glomerular diseases associated with systemic diseases

7.1. Nephrotic syndrome

7.1.1. Diabetes

The development of nephropathy in diabetes is related to the duration and severity of the disease. In the majority of the cases the patients are diabetics for 10 to 12 years before they develop the renal disease.

Incidence: 35% in juvenile diabetes and 12% in adult onset diabetes.

Clinical presentation: In nodular glomerulosclerosis the patient presents nephrosis and hypertension. In diffuse glomerulosclerosis the patient has proteinuria, hypertension and azotemia.

Pathogenesis: The underlying change in diabetic nephropathy is capillary microangiopathy.

Diagnostic features: Light microscopy: The glomeruli reveal two different patterns of sclerosis, a diffuse pattern and a nodular pattern also known as Kimmelsteil Wilson syndrome. The tubules show thickening of their basement membrane and vacuolation of their epithelial lining. The interstitium is fibrotic. The afferent and efferent arterioles are hyalinized. Other arterioles are also sclerotic.

Immunofluorescence: Diffuse linear IgG without complement in the capillary and tubular basement membrane.

Electron microscopy: reveals diffuse thickening of the lamina densa and large insulative lesions that appear as granular electron dense deposits in a subendothelial location.

Course: patients with diabetic nephropathy usually have a downhill course.

Differential diagnosis: Nodular glomerulosclerosis and amyloidosis.

7.2. Amyloidosis

Incidence: Renal amyloidosis is more common in secondary amyloidosis and less frequent in primary amyloidosis. It is also seen in association with multiple myeloma in 33% of the cases. There is a slight male preponderance. This is also seen in 14% of patients with Mediterranean fever.

Clinical presentation: Nephrotic syndrome.

Pathogenesis: Although the exact etiology of

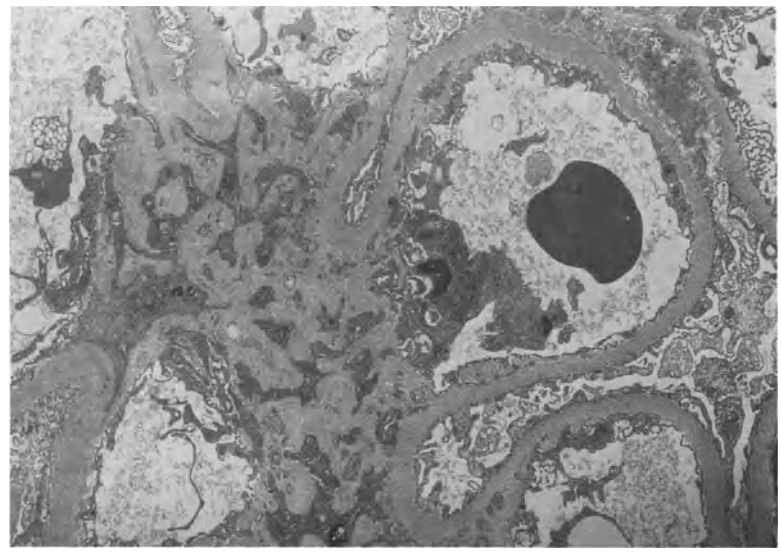

Fig. 16. Electron micrograph showing focal nodular increase of mesangial matrix from a patient with diabetic nephropathy. ×2,275.

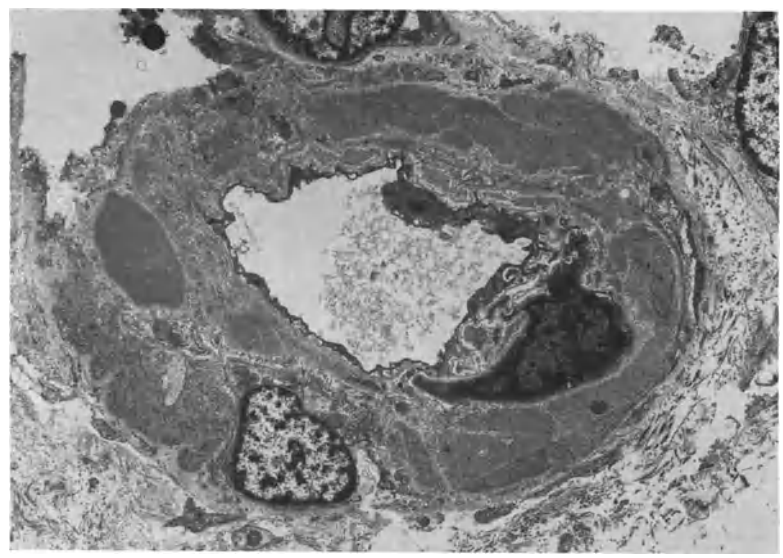

Fig. 17. Arteriole with multiple intramural hyaline deposits and thickening of the wall from a case of diabetic nephropathy. ×2,275.

amyloidosis is unknown, it is important to know that there are at least two chemical types of amyloidosis. LA related to the variable fragment of monoclonal immunoglobulin light chains. This type is seen in myeloma and macroglobulinemia. The second type known as AA is seen in familial forms of amyloidosis and it represents a more immunoglobulin protein.

Diagnostic features: Light microscopy: Nodular mesangial deposits. Also deposits in the arterioles. The congo red reaction is positive and if congo red stained slides are examined under polarized light the amyloid deposits reveal an apple green birefringence [21].

Immunofluorescence: Occasional monoclonal light chain deposits in glomeruli vessels and interstitium.

Electron microscopy: Nonbranching 70–80 Å diameter aggregates of fluid in the mesangium as well as in the capillary basement membranes and vessel walls.

Course: Progressive course to chronic renal failure with persistent heavy proteinuria.

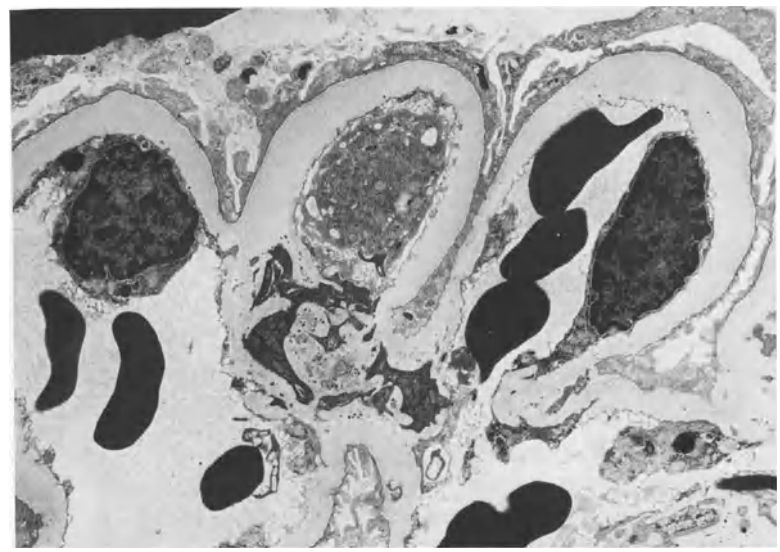

Fig. 18. Electron micrograph showing marked thickening of the capillary basement membrane 'microangiopathy' in diabetes. ×2,275.

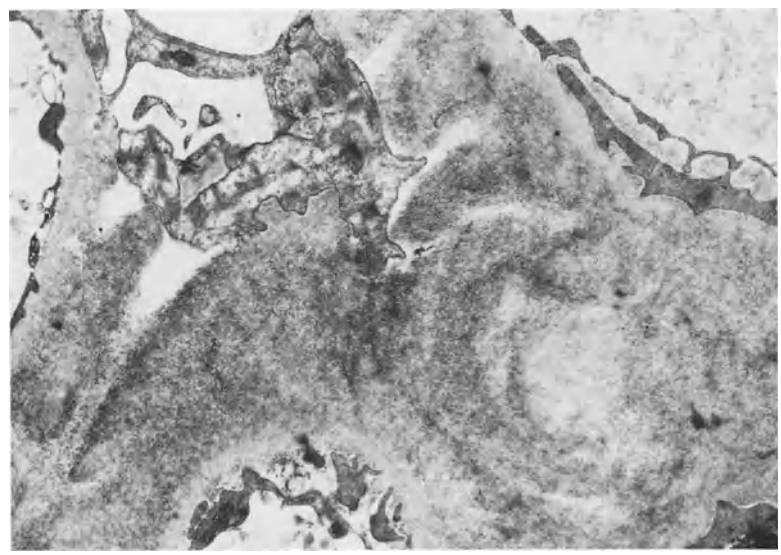

Fig. 19. Electron micrograph showing intramembranous and intramesangial amyloid fibrils from a case of renal amyloidosis. ×4,875.

Differential diagnosis: Diabetic nephropathy and focal glomerulosclerosis.

7.3. Membranous glomerulonephritis in systemic lupus

See membranous nephritis.

8. Hematuria syndromes

8.1. Goodpasture's syndrome [22]

Incidence: Approximately 3% of glomerular diseases. Usually in males: male to female ratio 4:1. The age range is very wide from 15–70 years. The patient usually has a preceding upper respiratory tract infection.

Clinical presentation: In a majority of the patients, pulmonary involvement occurs at the same

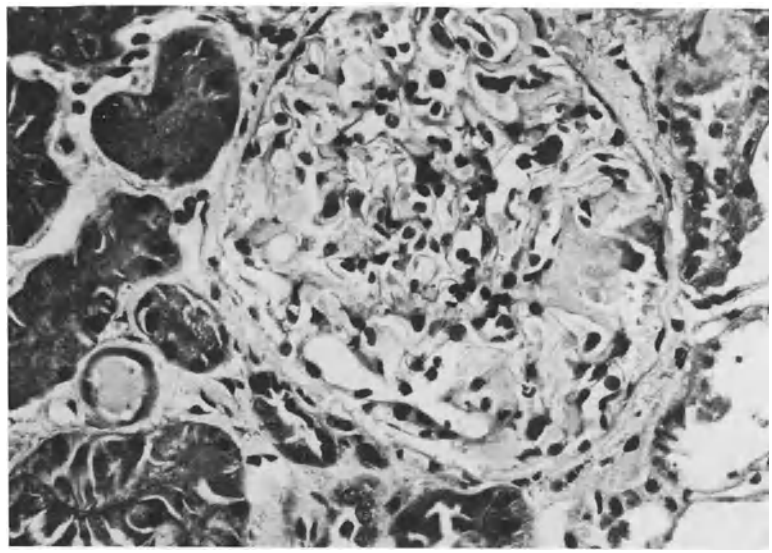

Fig. 20. Light microscopic picture from a case of Goodpasture's syndrome showing massive glomerular necrosis and mesangial cell proliferation. ×97.50.

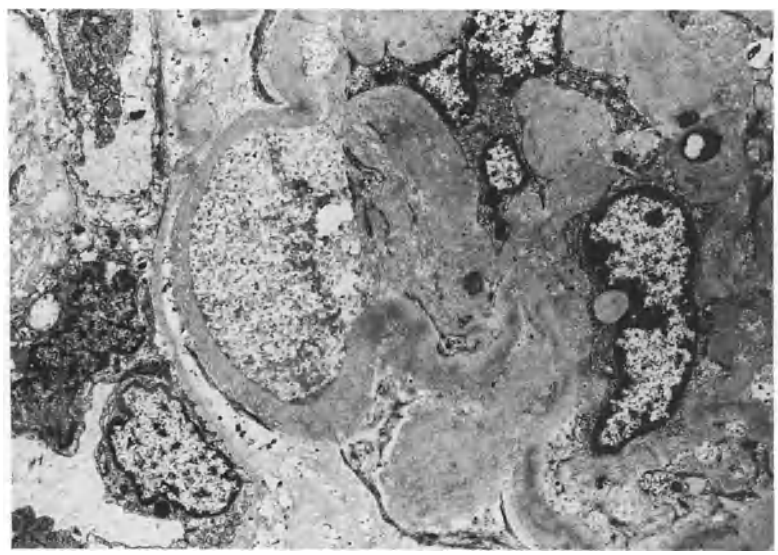

Fig. 21. Electron micrograph from a patient with Goodpasture's syndrome showing massive necrosis. ×3,250.

time or precedes the renal disease, sometimes as early as one year prior to the onset of the renal manifestations. In a small percent of patients, approximately 15%, renal involvement occurs first. The patient usually presents with hemoptysis, cough, dyspnea and hematuria. Serologic tests for lupus and streptococcal disease are negative. Serum complement studies are all normal.

Pathogenesis: Antiglomerular basement membrane antibodies.

Diagnostic features: Light microscopy: The glomeruli reveal a mixture of mesangial cell proliferation, necrosis and fibrin thrombi within the capillaries and large crescents.

Immunofluorescence: Diffuse linear IgG deposits, less frequently C_3 deposits, fibrin deposits in the crescents. Linear IgG deposits along the alveolar septa.

EM: Crescents – collapse of the capillary basement membrane and swelling of the endothelial cells, fibrin deposits in the crescents as well as fibrin and platelet thrombi within the capillaries.

Course: Rapidly progressive course, most of the patients develop fatal pulmonary hemorrhage.

Differential diagnosis: Rapidly progressive post streptococcal glomerulonephritis.
- Wegener's granulomatosis.
- Angitis.

The diagnostic feature in Goodpasture's syndrome being the linear deposits seen with immunofluorescence.

8.2. Wegener's granulomatosis

Incidence: Very rare, only 0.1% of renal biopsies. Slight male preponderance.

Clinical presentation: Characterized by a triad of sinusitis, pneumonitis and nephritis. The pathogenesis of the disease is not clear. Immune complexes, hypersensitivity as well as cellular immunodeficiency have been implicated.

The majority of the patients have hematuria with or without mild proteinuria.

Pathogenesis: Possible hypersensitivity, angitis.

Diagnostic features: Light microscopy: In the kidneys include focal proliferation of mesangial cells with necrosis and crescent formation. This is usually associated with a necrotizing vasculitis with occasional intramural giant cells. The interstitium usually contains scattered granulomas.

Immunofluorescence: Fibrin deposits in the crescents.

Electron Microscopy: Variable.

Course: Very poor, rapidly fatal course.

8.3. Henoch-Schonlein purpura

Also known as anaphylactoid purpura with glomerulonephritis [23].

Incidence: Mostly children.

Clinical presentation. The syndrome usually follows an upper respiratory tract infection and is characterized clinically by renal, gastrointestinal and cutaneous manifestations. The renal manifestations vary from microscopic hematuria to acute nephritic syndrome.

Pathogenesis: The pathogenesis of the disease is a diffuse vasculitis, most probably secondary to a transient immune complex reaction.

Diagnostic features: Features on light microscopy, immunofluorescence and electron microscopy and very similar to IgA nephropathy.

Skin biopsy in patients with Henoch-Schonlein purpura have IgA deposits at the dermal epidermal junction.

Course: The disease tends to recur in 20–40% of the patients. The course depends on the severity of renal involvement with approximately 25% developing renal failure.

8.4. Periarteritis nodosa

Incidence: 0.5% of routine renal biopsies.

Clinical presentation: Systemic disease characterized by involvement of the renal, GI, musculoskeletal, CNS, pulmonary and cardiovascular systems as well as the skin.

The onset is usually in the fourth to sixth decade with a marked male preponderance, 15:1.

Pathogenesis: The pathogenesis of the disease is thought to be a chronic immune complex disease. 30% of the cases have been associated with persistent hepatitis B antigenemia.

Diagnostic features: Light microscopy: Multiple stages of the disease are usually present in the same biopsy. Acute necrotizing lesions alternating with old scarred vessels. The lesion of the blood vessels is characteristically segmental with involvement of large and medium sized arteries in the classic type. In the microscopic form of PAN the glomeruli and small vessels reveal focal areas of fibrinoid necrosis in the acute stage. The vessels involved reveal fibrinoid necrosis and intramural and perivascular inflammatory cells. Long standing lesions reveal scarring.

Immunofluorescence: Reveals intramural and focal mesangial fibrin deposits.

Electron microscopy: Reveals endothelial cell swellings, crescents and fibrin deposits.

The clinical picture is very variable and depends on the location, number and size of the involved vessels.

Renal manifestations include hematuria and mild proteinuria.

Course: Generally a progressive disease with death resulting from renal failure or hypertension and its complications.

8.5. Systemic lupus nephritis [26]

Incidence: This is an immune complex disease with 50–80% of the patients developing renal disease. The disease has a predilection to middle age females.

Clinical presentation: Renal manifestations are variable depending on the underlying renal lesion. They include mild hematuria and proteinuria, nephritic syndrome, nephrotic syndrome and renal failure.

Serologic findings include ANA high titers, high Anti-DNA titers, and low CH_{50} and C_3 in the active disease.

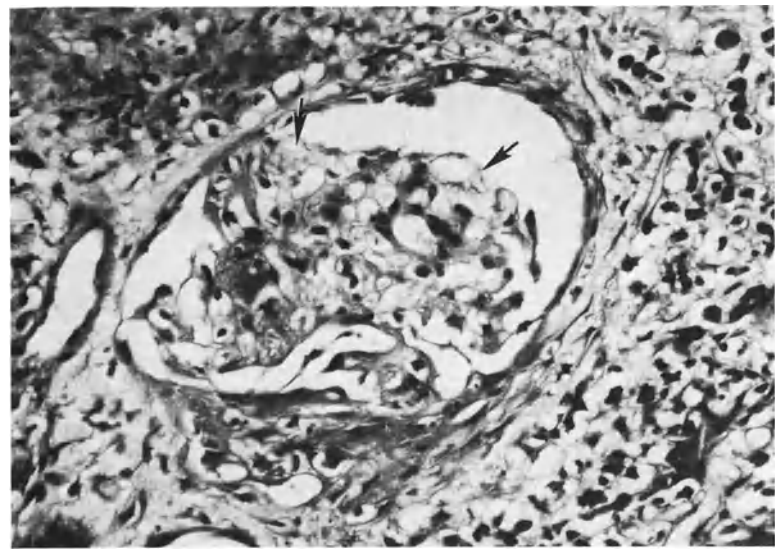

Fig. 22. Light microscopy picture showing glomerulus with focal necrosis from a case of periarteritis nodosa. ×97.50.

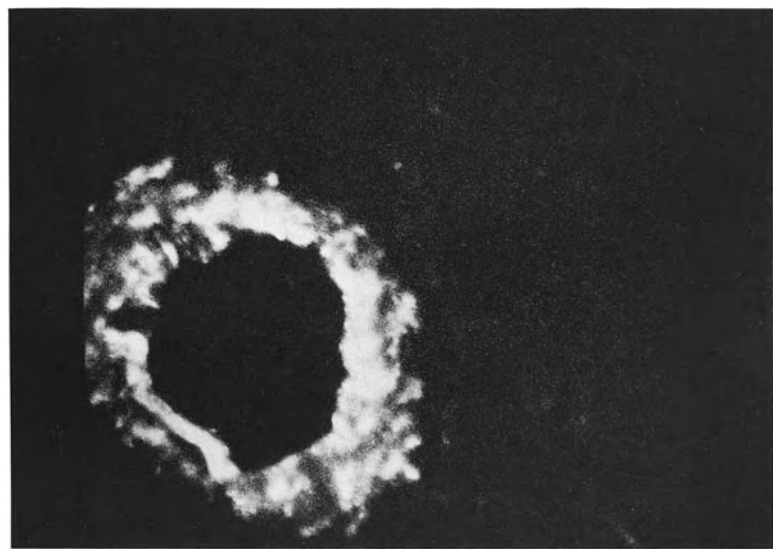

Fig. 23. Immunofluorescence picture showing intramural fibrin deposits in the arterioles in a case of periarteritis nodosa. ×97.50.

Pathogenesis: Immune complex disease.

Diagnostic features: Light microscopy variable. Focal mesangial proliferation. Patients with this lesion will present clinically with mild hematuria and proteinuria.

Diffuse mesangial proliferation characterized clinically by gross hematuria, moderate proteinuria and azotemia.

Membranous nephropathy characterized clinically by nephrotic syndrome.

Necrosis with crescent formation and hematoxylin bodies. In addition to the glomerular lesions, patients with SLE have tubular necrosis, vasculitis and interstitial inflammation.

Immunofluorescence: The extent and intensity of the glomerular deposits of immunoglobulin and complement components usually correlates with the histologic features. The diffuse proliferative lesions are usually associated with diffuse mesangial IgG, IgA and complement. Immunoglobulin deposits are also seen in the tubular basement membrane and in the vessel walls. Fibrin deposits are seen in the necrotizing variety.

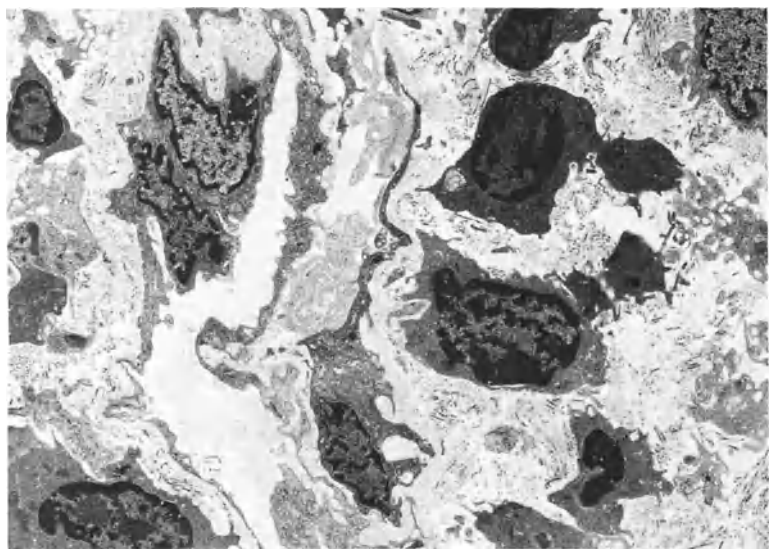

Fig. 24. Electron micrograph showing a blood vessel with swollen endothelial cells and intramural lymphocytic infiltrates from a case of periarteritis nodosa. ×2,275.

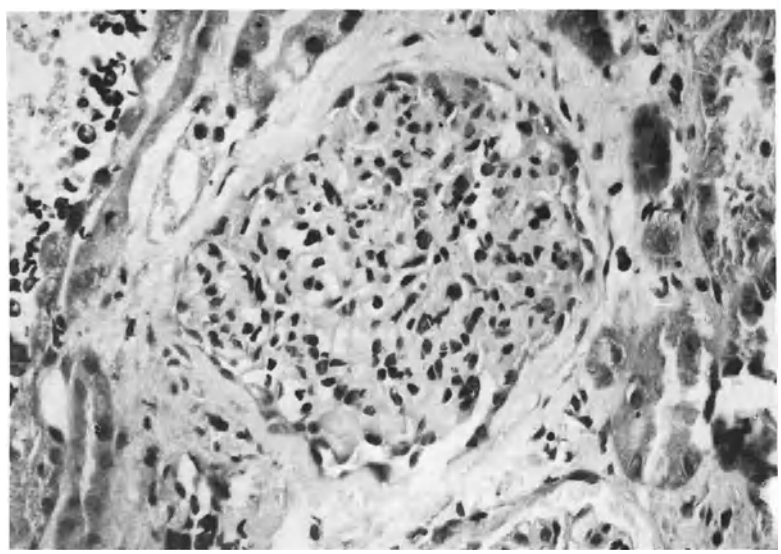

Fig. 25. Light microscopic picture showing diffuse mesangial cell proliferation from a patient with systemic lupus nephritis (diffuse proliferative type). ×97.50.

Electron microscopy: Multiple mesangial, intramembranous and subendothelial electron deposits with occasional paracrystalline (fingerprint pattern). In addition, viral-like particles have been described in the endothelial cells. Electron dense deposits have also been seen in the tubules, Bowman's capsule and blood vessels.

Course: Depends on the histologic feature and the degree of renal involvement.

9. Oliguric and hypertensive syndromes

9.1. Progressive systemic sclerosis (Scleroderma)

Incidence: Also known as scleroderma is a systemic disease with between 45% of patients developing renal disease. There is a female predominance.

Clinical presentation: Patients usually have the systemic manifestations of the disease before they develop the renal manifestations. The latter include

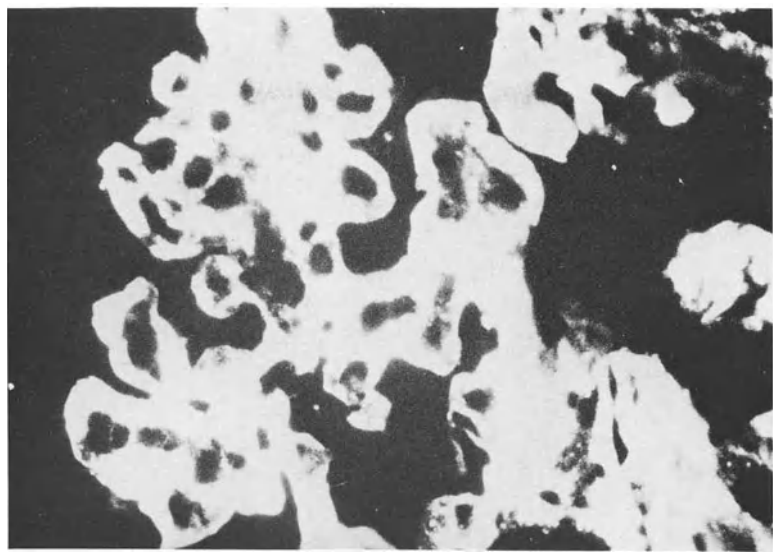

Fig. 26. Immunofluorescence micrograph showing diffuse mesangial and peripheral fluorescence with IgG in a patient with active lupus nephritis. ×97.50.

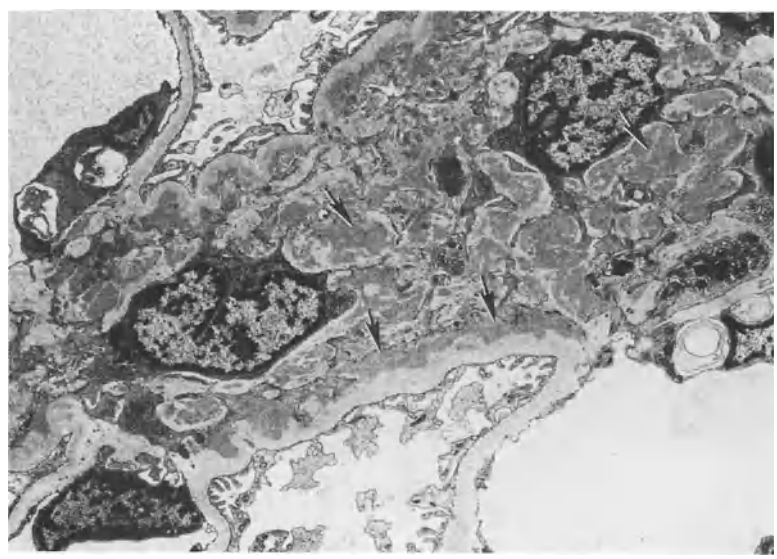

Fig. 27. Electron micrograph from a patient with active lupus nephritis showing multiple large subendothelial and intramesangial electon dense deposits. ×3,250.

proteinuria, hypertension and renal failure.

Pathogenesis: The pathogenesis of the disease is not clear but appears to be secondary to a disorder in collagen, metabolism and although there are no specific serologic tests for progressive systemic sclerosis, patients with this disease have positive anti-ANA low titers especially nucleolar pattern. Some patients also have low RA titers.

Diagnostic features: Light microscopy: The arterioles reveal marked thickening of their walls with intimal hyperplasia and focal fibrinoid necrosis. Secondary sclerosis of the glomeruli, tubular atrophy and interstitial scarring are present.

Immunofluorescence: variable

Electron microscopy: No specific findings.

Course: rapidly progressive renal failure.

9.2. Hemolytic uremic syndrome

Incidence: Postpartum. Children <1 year after viral

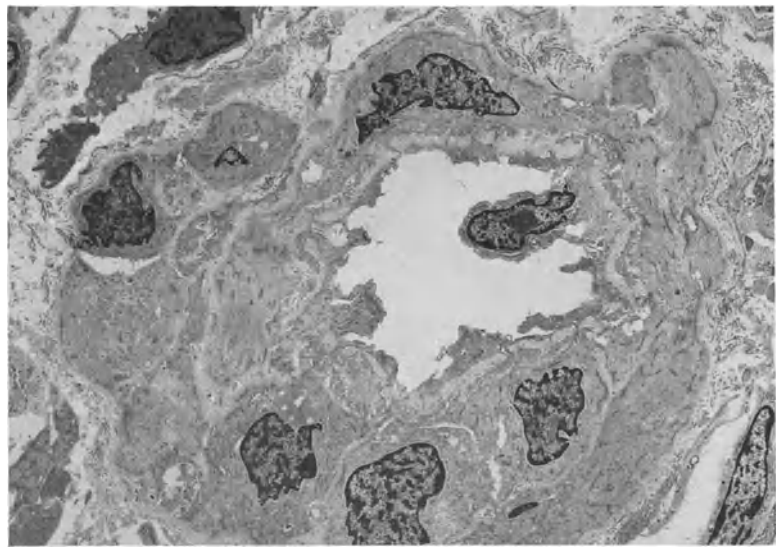

Fig. 28. Arteriole showing marked intimal hyperplasia and focal endothelial cell swelling from a case of scleroderma. ×2,275.

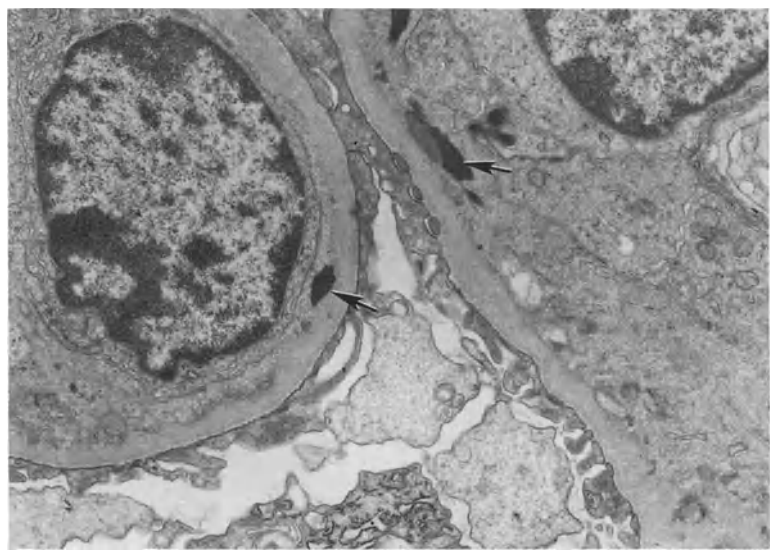

Fig. 29. Electron micrograph from a patient with hemolytic uremic syndrome showing subendothelial and mesangial fibrin deposits. ×6,500.

diseases, particularly viral gastroenteritis.

Clinical presentation: Oliguria, renal failure, hemolytic anemia, thrombocytopenia, bleeding tendencies.

Pathogenesis: Intravascular coagulation. This is supported by the fact that coagulation studies reveal decreased platelets and increased fibrin split products.

Diagnostic features: Light Microscopy: Cortical necrosis, glomerular necrosis with intracapillary fibrin thrombin, fibrinoid necrosis of the arterioles and intraluminal fibrin and platelet thrombin.

Immunofluorescence: Fibrin deposits in the mesangium and in the arteriolar walls.

Electron microscopy: Disrupted basement membrane and subendothelial and mesangial fibrin deposits.

Course: 40% of the patients die in the initial stage of the disease. The remainder develop renal failure and hypertension.

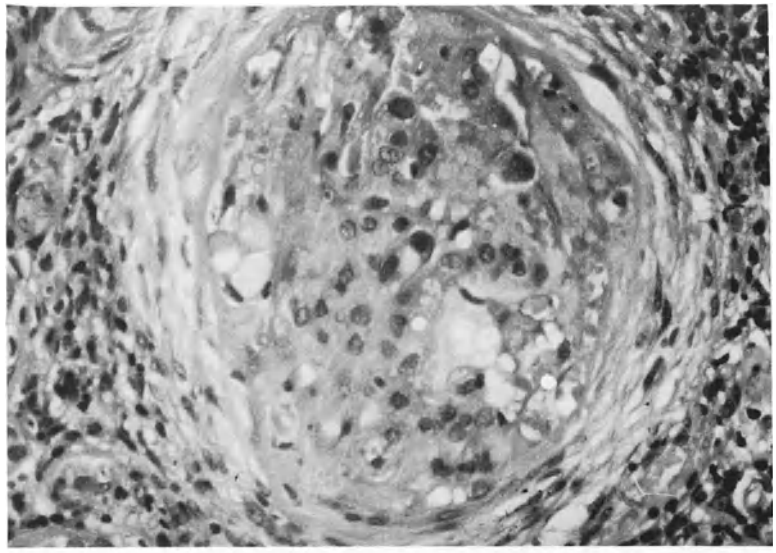

Fig. 30. Light microscopic picture from a case of crescentic glomerulonephritis showing crescents and marked mesangial cell proliferation. ×97.50.

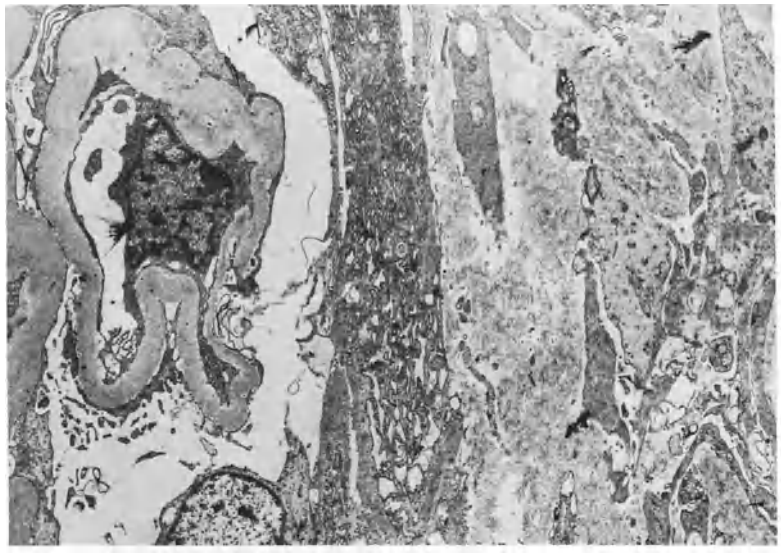

Fig. 31. Electron micrograph showing a crescent from a patient with crescentic glomerulonephritis. ×3,250.

9.3. Crescentic glomerulonephritis

Many glomerular diseases are associated with crescent formation (proliferation of the cells lining Bowman's capsule). These include poststreptococcal glomerulonephritis, IgA nephropathy, malignant hypertension, Alport's syndrome, membranoproliferative glomerulonephritis, Wegener's granulomatosis, Goodpasture's syndrome and even diabetes. The presence of large numbers of crescents is associated clinically with a rapidly progressive course. In some instances the patient presents with a crescentic nephritis with no underlying identifiable glomerular disease. These cases are referred to as idiopathic crescentic glomerulonephritis or primary crescentic glomerulonephritis.

Diagnostic features: Light microscopy reveals multiple crescents with or without necrosis. Immunofluorescence reveals a variable pattern but a constant finding is the presence of fibrin deposits

within the crescents. Electron microscopy reveals variable findings plus the presence of epithelial crescents.

The clinical course of crescentic nephritis is usually very rapidly progressive leading to renal failure.

10. Concluding remarks

From the above review of glomerular diseases it is clear that there are several questions unanswered in relationship to glomerulonephritis, the major and most important one being the pathogenesis of immunologically mediated glomerular diseases and the role of circulating immune complexes versus the formation of in situ deposits, delayed hypersensitivity reaction and the role played by HLA haplotypes and other host factors that predispose to glomerular diseases.

In most patients with glomerulonephritis it is very difficult if not impossible to identify the antigen which initiates the immune complex process leading to glomerular damage.

The second limitation in the study of glomerular diseases is the fact that there are no unique diagnostic morphologic changes characteristic of each disease because there are only few limited histologic and subcellular patterns which the glomerulus exhibits in response to injury, and although in most instances there is a good correlation between the histologic picture of the glomerulus and the clinical course of the disease with the current techniques available for the study of glomerular diseases we cannot identify, specific morphologic changes for each clinical syndrome.

In this chapter we have attempted to summarize the current concepts of glomerular diseases and we hope that advances in immunologic, cytochemical and ultrastructural techniques will help resolve soon some of the answered problems in the study of glomerular diseases.

Acknowledgements

We thank Mrs. Marilyn Cline for her secretarial assistance in preparing this chapter and Mr. William Gunning, M.S. for preparing all the illustrations used in this chapter.

References

1. Kidney Disease Present Status: Churg J, Spargo B and Abell M (eds), Williams and Wilkins, Baltimore, 1979.
2. Myers BD, Okauma TB: Mechanisms of proteinuria in human glomerulonephritis. J Clin Invest 17: 732–746, 1982.
3. Belovezlidov N, Altankova I: Immunologic studies in patients with glomerulonephritis. Clin Nephro 17(3): 141–148, 1983.
4. Schmitt E, Seyforth M, Weiner H, Klinkman H: Cellular immunity in glomerulonephritis. Clin Nephro 17(6): 271–276, 1982.
5. Magil AB, Wadsworth L: Monocyte involvement in glomerular crescents. Lab Invest 47(2): 160–166, 1982.
6. Jenis, Lowenthal: Kidney Biopsy Interpretation, Davis FA, Philadelphia, pp 1–11, 1977.
7. Enery DT, Strife CF: Nephrotic syndrome in childhood: Management and treatment in patients with minimal change, disease, mesangial proliferation or focal glomerulosclerosis. Pediatric Clinics of North America, 89(4): 875–894, 1982.
8. Walker R, Bailey RR, Lynn KL, Burry AF: Focal glomerulosclerosis – another familial renal disease? NZ Med J 95: 686–688, 1982.
9. Furuse A, Hattori S, Terashima T, Karashima S, Matusa I: Circulating immune complex in glomerulonephropathy associated with hepatitis B virus infection. Nephron 31: 212–218, 1982.
10. LePetit JC, Laurent B, Berthoux FC: HLA-DR3 and Idiopathic membranous nephritis (IMN) association. Tissue Antigens 20: 227–228, 1982.
11. Jones E, Magil A: Nonsystemic mesangiopathic glomerulonephritis with 'full house' immunofluorescence: Pathological and clinical observations in 5 patients. Am J Clin Path 78: 29–34, 1982.
12. Strife CF, MacAdams AJ, West CD: Membranoproliferative glomerulonephritis characterized by focal, segmental proliferative lesions. Clin Nephro 18(1): 9–16, 1982.
13. Jermanovich NB, Giammarco R, Ginsberg SJ, Tinsley RW, Jones DB: Small cell anaplastic carcinoma of the lung with mesangial proliferative glomerulonephritis. Arch Intern Med 142: 397–399, 1982.
14. Thorner P, Baumal R: Extraglomerular dense deposits in dense deposit disease. Arch Path Lab Med 106: 628–631, 1982.
15. Helin H, Mustonen J, Pasternack A, Antonen A: IgM-associated glomerulonephritis. Nephron 31: 11–16, 1982.
16. Stark JL: Acute poststreptococcal glomerulonephritis. Nursing 12(5): 114–115, 1982.
17. Dawson KP, Martin DR: Streptococcal involvement in childhood acute glomerulonephritis: A review of 20 cases at admission. NZ Med J 95: 373–6, 1982.
18. Whitmouth JA, et al.: IgA and glomerular disease. Clin Nephro 5: 33–36, 1976.
19. Spear GS: Alport's syndrome. A consideration of pathogenesis. Clin Nephro 1: 336–337, 1973.
20. Spear GS: Alport's syndrome emphasizing electron microscopic studies of the glomerulus. Am J Pathol 69: 213–220, 1972.
21. Heptinstall RH: Pathology of the kidney. Vol 3, Ed 3, Little Brown & Co, Boston, 1983, p 1015–1030.
22. Dash SC, Malhotra KK, Sharma RK, Kumar R, Srivastava RN, Bhuvan UN: Spectrum of rapidly progressive (crescentic) glomerulonephritis in northern India. Nephron 30: 45–50, 1982.
23. Heptinstall RH: Pathology of the Kidney, Vol II, ed 3, Little, Brown and Co, Boston, 1983, p 741–761.
24. Baldwin D: Clinical usefulness of the morphological classification of lupus nephritis. J Kid Dis 2(1), Suppl 1, July 1982.
25. Dawson KP: A comparative study of the clinical patterns of acute glomerulonephritis from a high and a low incidence area of New Zealand. JZ Med J 95: 262–4, 1982.
26. Jordan SC, Lemire JM: Acute glomerulonephritis: Diagnosis and treatment. Pediatrics Clinics of N. America 29(4): 857–873, 1982.
27. Tany J, Kida H. Abe T, Tomosugi N, Saito Y, Asamoto T, Hattori N: B lymphocyte subset patterns and their significance in idiopahtic glomerulonephritis. Clin Exp Immunol 48: 201–204, 1982.
28. Kefalides NA, Alper R, Clark C: Biochemistry and Metabolism of basement membranes. Int Rev Cytol 61: 167, 1979.
29. Jorgensen F: The ultrastructure of the normal human glomerulus. Lab Invest 18: 42, 1968.
30. Morrin PA: Rapidly progressive glomerulonephritis: A clinical and pathologic study. Am J Med 65: 446, 1978.

CHAPTER 10

Renal vascular diseases: Their relationship to hypertension

PETER J. GOLDBLATT and AMIRA F. GOHARA

1. Introduction

1.1. Relationship of hypertension to renal vascular disease

Since the initial observations of Richard Bright (1832) [1] an increasing body of knowledge has established a firm relationship between changes in the renal vasculature and the presence of systemic hypertension. The predominant view, which is essentially that expressed in the late 1800's by Mahommad, [1] is that *persistent hypertension* through a mechanism which is as yet incompletely understood, *causes widespread pathologic changes in the structure of arteries and arterioles.* These include atherosclerosis of the major elastic vessels such as the aorta and its principal branches, and arterial and arteriolar sclerosis, in vessels throughout the body. With particular reference to the kidney, arterial and arteriolar sclerosis with scarring of the parenchyma (nephrosclerosis) of some degree is virtually always present in human cases of essential hypertension [2]. The well known experiments of Harry Goldblatt beginning in the early 1930's [3] established that constriction of the main renal artery, even to a single kidney, resulted in systemic hypertension closely simulating essential hypertension in man. These experiments led him to postulate that the raised blood pressure was the *result* of changes in the renal vasculature, rather than the cause. Stemming from those investigations, a great deal of experimentation has established a humoral mechanism (renin-angiotensin-aldosterone, see Figures 1 and 2), which is acknowledged to play an important role in some types of hypertension.

Despite the demonstration of a pressor mechanism that could be initiated by constriction of the main renal artery, investigations directed towards the establishment of the sequence of vascular changes in the kidney have generally resulted in conflicting hypotheses. The early work of Moritz and Oldt [3] established beyond question the prevalence of intrarenal vascular disease in individuals with essential hypertension. The continuing studies of Castleman and associates [4, 5] in differing stages of hypertension, emphasized the lack of morphologic changes in what they characterized as an early stage of essential hypertension. Even these studies documented the presence of moderate to severe intra-renal vascular disease in the vast majority of hypertensive human beings. A series of investigations in the rat by Byrom, Dodson and Wilson [6, 7] are widely quoted as establishing the 'vicious circle' of hypertension. These investigators and others asserted that constriction of a renal artery and other modes of inducing hypertension, cause widespread vascular disease which then results in the perpetuation of the hypertensive state. Constriction of a main renal artery, it is alleged, 'protects' the renal microvasculature distal to the constriction from the effects of hypertension [7].

While this view has become so dominant that the alternative is rarely discussed, there are many instances, such as the appearance of hypertension *following* the development of intra-renal vasculitis, which show clearly that disturbance of intra-renal hemodynamics can *initiate* systemic hypertension. Then too, restoration of normal circulation to a kidney with compromised extra-renal vessels has frequently been shown to lower the blood pressure of affected individuals. In the subsequent discussion we shall present some of the pathologic and pathophysiologic changes seen in the most important vascular diseases affecting the kidney, with the emphasis on extra-renal and intra-renal arteriosclerosis, and then return briefly to a consideration of the 'chicken vs. egg' controversy as we consider directions for future research. The literature is voluminous and sometimes conflicting so the interested reader is urged to explore further.

L.J.A. DiDio and P.M. Motta (eds), Basic, Clinical, and Surgical Nephrology. ISBN 0-89838-689-5.

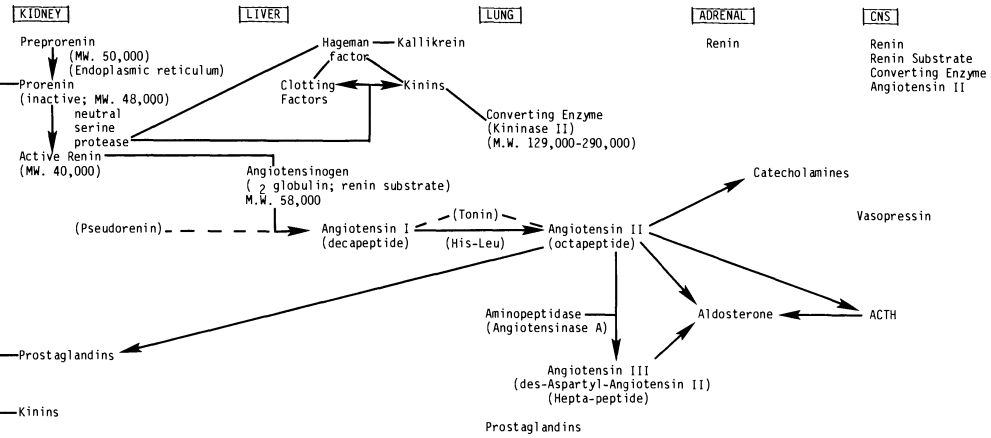

Figure 1.

1.2. Important aspects of intra- and extra-renal vasculature

The renal vasculature has been discussed in other sections of this book (see Chapters 1, 2 and 6) so that only brief comment will be made here for emphasis. The extra-renal arterial supply is somewhat variable, but consists of one or more arteries which are elastic in type at their origin from the aorta, and become musculo-elastic vessels as they enter the kidney and arborize further. The inter-lobular vessels are muscular arteries which give rise to arterioles (afferent) which have specialized granular cells in their muscle walls as they approach the glomeruli they supply. The specialized endocrine function of the granules (renin) will be commented on briefly below. The structure of the glomerulus has been discussed extensively elsewhere (see Chapter 7) but it is worth noting that the efferent 'arteriole' is little more than a capillary with the exception of a smooth muscle mass at its origin from the glomerulus. The latter may possess an important sphincteric action. The capillaries and veins, while important in renal function, will not be discussed. The major point to be remembered, is the variety of arteries and arterioles present in the kidney. These will be affected by specific pathologic changes which may be confined to certain classes of vessels in other parts of the body as well. Some of these affect the kidney with particular frequency or severity.

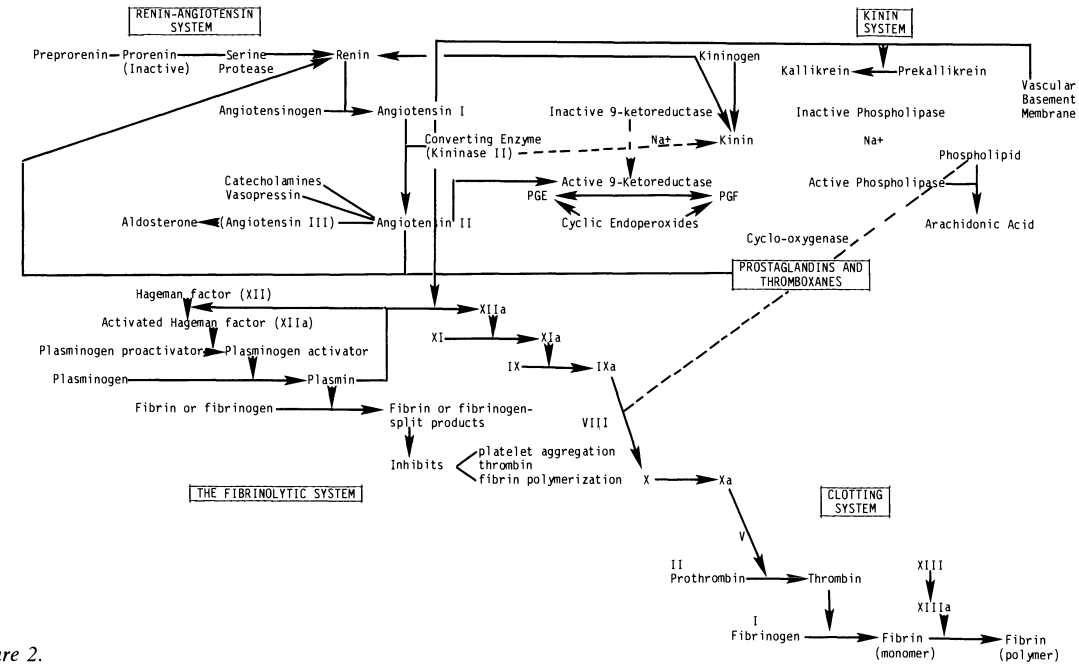

Figure 2.

2. Blood pressure and autoregulation of renal blood flow

The kidney receives over 20% of the cardiac output under physiologic conditions. As a high pressure filtration system with selective secretion and reabsorption mechanisms, it must be able to closely regulate the pressure and flow of blood to and from the glomeruli, as well as the various divisions of the tubular system. Thus, the ability to autoregulate appears to be well developed in the kidney and both anatomic and physiologic mechanisms are present to permit primarily cortical or medullary blood flow. The principal mechanisms are the pressor (cortical) and depressor (medullary) substances which reside within the kidney.

2.1. Renal pressor (vasoconstrictor) systems

The principal vasoconstrictor system of the kidney is the renin-angiotensin system. This multi-enzyme system generates the most powerful pressor substance known, but has even greater importance because of its interrelationships with other systems for control of extra-cellular fluid volume and vascular tone (see Figures 1 and 2). It is now recognized that the system is considerably more complex than the initial postulations [3]. It appears that a precursor molecule, preprorenin, of 50,000 daltons is converted first in the endoplasmic reticulum to inactive prorenin ('big' renin, 48,000 m.w.) which then is converted to active renin, a proteolytic enzyme of 40,000 daltons [8]. The latter conversion is poorly understood, but may involve a neutral serine protease and/or kallikrein and Hageman factor. Active renin splits a leucyl-leucyl bond in its substrate, angiotensinogen, a 58,000 dalton α_2 globulin produced by the liver [9]. This produces angiotensin I, a decapeptide which is then further split by a chloride requiring *converting* enzyme (kininase II) which is in high concentration in lung and blood, to form the active vasoconstrictor octapeptide, angiotensin II. Further degradation by aminopeptidases was initially thought to inactivate the molecule, but it is now felt that the des-aspartyl angiotensin II (Angiotensin III) may be a regulatory factor for aldosterone secretion [9, 10].

While mounting evidence supports the notion that the granules of the juxtaglomerular afferent arteriole are renin, the control of their release, and their site of action is less well established [10–12]. Local activation of Angiotensin II was thought to be precluded, until converting enzyme was demonstrated in renal lymph [13]. Release appears to involve baroreceptor, neural or sodium sensing mechanisms [12]. Surface contact between the macula densa and the arteriole with their common basal lamina has been proposed [14]. Although it seems likely that angiotensin is important in regulation of glomerular filtration, it would obviously work antagonistically if it constricted the afferent arteriole rather than the efferent vessel. This is not a trivial problem, and it creates a problem of interpretation of experiments in which angiotensin is infused, since it would reach the afferent vessel primarily. It may also act on glomerular mesangial cells [15]. Then, too, renin may reside in blood vessel walls, [16], and thus measurement of circulating levels of these substances may be misleading in elucidating their local effects. Finally, the concentrations necessary to produce a response in experimental systems (pharmacologic doses) may exceed those necessary to produce a profound effect under physiologic conditions [19]. Much remains to be learned about this system and in particular its relationship to other vasoactive substances (see below). Among the vasoconstrictors which are important, vasopressin (ADH) must be mentioned, not only for its role in water reabsorption, but because it may also play a significant part in abnormal vascular reactivity in hypertension [19].

2.2. Renal anti-pressor (vasodilator) systems

Soon after the major pressor system of the kidney was elucidated, evidence of an anti-pressor role was produced (renoprival hypothesis) [19]. A number of vasodilator substances have now been demonstrated to exist in the kidney, particularly the medulla, to have significant effects on renal blood flow, or to have interrelationship with the renin angiotensin system. In particular, the prostaglandins are in high concentration in the medulla, and production of prostaglandin E_2 may in part be regulated by the angiotensin converting enzyme [20]. A similar relationship to bradykinin has been postulated [21]. The possibility that bradykinin works together with renin as a 'cofactor' has also been suggested [22]. These interrelationships are shown in Figures 1 and 2.

2.3. Other renal pressor and depressor substances

As mentioned above, in addition to the renin-angiotensin system, vasopressin as a vasoconstrictor, and bradykinin as a vasodilator may play a part in the regulation of renal blood flow. The principal kinins are bradykinin and lysyl-bradykinin which are formed by the enzymatic action of kallikrein on the kininogens which are α_2 globulins. Of the two types

of kallikrein (plasma and glandular) the circulating plasma forms may be inactive (prekallikrein) and require activation by Hageman factor [21]. Bradykinin is inactivated in the lungs by kininase II an enzyme which appears to be identical to angiotensin converting enzyme. Interconversion of lysylbradykinin to bradykinin takes place in the kidney via an aminopeptidase. Bradykinin has been postulated to act as a 'co-factor' in the renin-angiotensin system, to antagonize the action of angiotensin, although this remains to be proved [22].

A number of other factors have been identified in the kidney. These include *nephrotensin* [23], *renopressin [24] and tonin* [25]. Their role in renal hypertension and vascular diseases remains to be elucidated.

2.4. Renal volume regulation in relation to hypertension

There are only two mechanisms by which sustained arterial hypertension can be achieved: *vasoconstriction* and intra-vascular *volume expansion*. The former appears to be responsible for the majority of human hypertension, since the latter has not been conclusively demonstrated. However, it is clear that, since the kidney's major role is to regulate extracellular fluid volume and composition, disturbances in its function could easily result in volume expansion. While this obviously does occur in renal failure, the majority of the fluid leaves the vascular compartment, and thus its contribution to the hypertension that co-exists with most primary renal disease (secondary hypertension) has not been satisfactorily demonstrated. Although the kidney is listed as the major cause of secondary hypertension, the mechanism by which the blood pressure is elevated is still not agreed upon [3, 9, 11, 26].

Since sodium is a major determinant of extracellular fluid volume, and mineral corticoids are involved in its re-absorption, the renal-adrenal axis, through the renin-angiotensin system's ability to regulate aldosterone secretion is clearly involved in determining the sodium concentration of body fluids. Even in primary aldosteronism, however, it has been difficult to demonstrate intra-vascular fluid accumulation as the primary event in the accompanying hypertension. Among those who ascribe a central role to volume regulation as a principal player in the pathogenesis of hypertension, Guyton's [26] analysis of renal function has contributed the clearest evidence of a probable contribution from even minor extra-vascular fluid expansion. Although his argument is complex, and his approach has required computerization, it appears to be leading to new insights into the central role of the kidney in both essential (primary) and secondary hypertension.

3. Diseases of extra-renal vessels

As indicated above, the kidney usually has one main renal artery which is a principal branch of the aorta, although separate polar arteries are also frequent. The draining veins rapidly coalesce as they reach the capsule and emerge to form a single renal vein outside the renal parenchyma (see Chapter 2).

The vessels supplying the kidney are prone to all the diseases which affect similar sized arteries and veins throughout the body, but there are some diseases which are more or less unique to these vessels.

3.1. Atherosclerosis of main renal arteries

Atherosclerosis is a disease of the intima affecting large elastic and musculo-elastic vessels. It should be distinguished from arteriosclerosis which affects the media of muscular arteries and arterioles, although the two are undoubtedly related, in part, pathogenetically. The latter term is unfortunately often used loosely to denote both diseases. The role of lipids in the pathogenesis of atherosclerosis appears to be central, and they are richly deposited in the intimal plaque which is the hallmark of the disease (Plate 1, panels 1–3). They may be the principal mitogenic stimulus for myointimal cell proliferation [27]. Several recent references may be consulted for a more extensive discussion of this important subject [27, 28].

Atherosclerosis is the principal disease of the extra-renal arteries, and is usually found to be most severe at or immediately past the origin of these vessels from the aorta. Turbulence of flow is probably a factor in this distribution, as it is thought to be in other sites. Unquestionably, atherosclerosis is more prevalent in individuals with long standing hypertension. It is also established that significant stenosis of the main renal artery by an atherosclerotic plaque (Plate 1, panels 1–3) can produce hypertension, which can then be reversed by relieving or bypassing the obstruction [11, 29]. What is not clear, is how frequently this is the cause of hypertension, or how often it contributes significantly enough to warrant intervention. The newer techniques of angiography [30] and less invasive approaches to angioplasty [31] may yield an answer in the future. It must be mentioned that thrombi propagating in the aorta (Plate 1, panel 1) or emboli of various types may

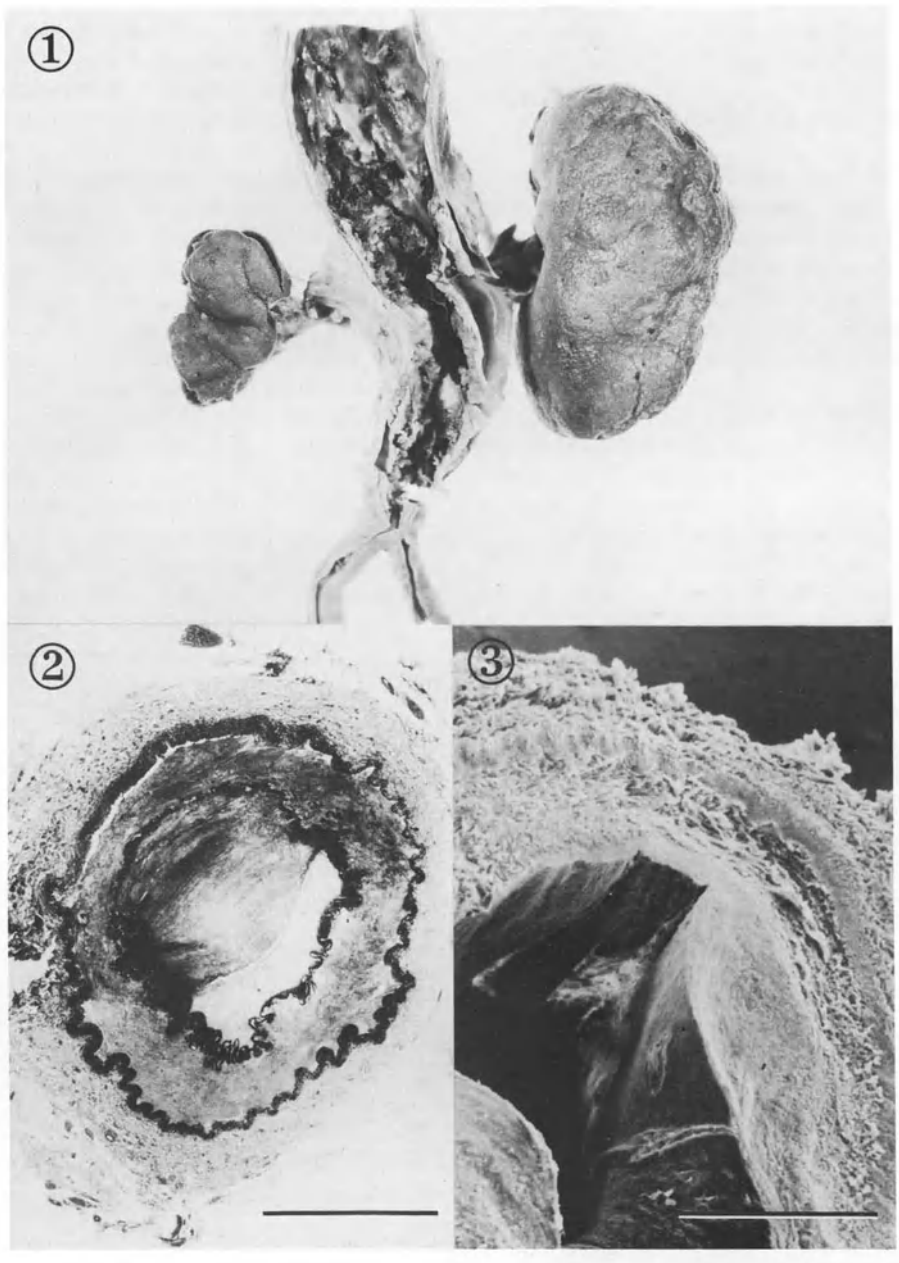

Plate 1. (1) Gross photograph of aorta and kidneys of elderly hypertensive female. The aorta has been opened posteriorly showing marked atherosclerosis with mural thrombosis. The left kidney is atrophic as a result of virtually complete atherosclerotic stenosis of the left main renal artery. (2) Histologic preparation of left main renal artery from case illustrated above stained with Weigert's elastic stain. Note intimal plaque virtually occluding lumen. Internal elastic lamella is darkly stained. (×25; bar equals 1000 μ (3) Adjacent ring of same renal artery processed by critical point drying for scanning electron microscopy. Note irregular narrowing of lumen by atherosclerotic plaque. Internal elastic lamella is faintly visible as irregular wavy area on surface. (1200 μ wide; bar equals 500 μ).

partially occlude the main renal artery and occasionally lead to acute hypertension.

3.2. *Fibromuscular dysplasia (hyperplasia)*

This disorder of the extra renal vasculature is now recognized to have several variants (Figure 3) which can be separated from one another on the basis of natural history and morphology, particularly with reference to the vascular coat which is most severly affected (intima, media or adventitia). Overall, these disorders account for 32% of patients with renovascular hypertension. As shown in the table taken from Gaspar the *intimal form* of the disease is rare and affects children primarily. There is accumulation of loose fibrous tissue in the intima, but lipid is not present, and inflammatory changes are not seen. In the adult there is only fibrosis of the intima, but the elastic lamellae may be affected in children. Limb vessels and interstitial arteries may be affected in both adults and children. A secondary form of intimal fibroplasia is seen in endstage renal disease such as pyelonephritis, and affects the distal branches of the extra-renal arterial system. The latter's relationship to the primary disorder, and to the genesis of hypertension, is unclear.

The most frequent and characteristic form of the disease is medial hyperplasia, which may also take several forms. A rare form, affecting young women predominantly, involves hyperplasia of a short segment of the media with consequent significant reduction in luminal diameter. The most frequent form, usually seen in the distal two thirds of the artery, and also affecting young women most frequently, is produced by fibromuscular ridges alternating with thinned areas of the arterial wall. This gives the characteristic radiologic appearance of a 'string of sausages' or 'string of beads'. This disorder is frequently bilateral. The internal elastic lamina of the vessel is lost in the thinned areas, and this may be important in the pathogenesis of the disease [11, 29]. *Perimedial fibroplasia* is the second most frequent form. It is also seen in young women and may be bilateral.

Peri-arterial fibroplasia is the least common variety of the disorder. Here the adventitia is affected and the fibroplasia sometimes extends to the surrounding fibro-fatty tissue of Gerota's fascia. The disorder may be related to idiopathic retroperitoneal fibrosis [11, 29, 31].

Figure 3. Fibromuscular dysplasia.*

	Incidence	Sex & age	Pathology	Location	X-ray film	Progression	Bilateral	Thrombosis
Intimal Fibroplasia	1–2%	Children	Fibrous material inside internal elastic lamina	Orificial or major branches	Smooth focal	Yes	Yes	Yes
Medial Fibromuscular Dysplasia	98%							
Medial fibroplasia	60–70%	Women 25–50	Stenotic ridges formed by loose collagen replacing muscle with thinning of muscle between ridges producing aneurysms	Distal 2/3 and major branches	'String of beads' (beads larger than normal artery)	Mild	40–60%	Rare
Medial hyperplasia	5–15%	Women 10–30 Men 35–45	Hyperplasia of media and fibrous tissue	Main artery and branches	Smooth linear	Yes	Yes	Rare
Perimedial fibroplasia	15–25%	Women 15–30	Thick fibroplasia of outer half of media	Main artery and branches	Stenosis and 'beads' not larger than main artery	Yes (Note: may have rapid increase in blood pressure)	Yes	Yes
Medial dissection	5–10%	Channel in outer 1/3 of media						
Adventitial fibroplasia	Rare (less than 1%)		Fibroplasia in adventitia and periarterial fibrofatty tissue					

From: Gaspar, MR (MD) in barker WF (MD). Peripheral Arterial Disease, Volume IV, Major Problems in Clinical Surgery, 1981, Saunders, Philadelphia, reprinted with permission of authors.

While each of these disorders is relatively rare, their prevalence in young women is significant in that they represent a curable form of hypertension. A recent report of spontaneous remission of hypertension after several years with documented fibromuscular hyperplasia of both main renal arteries may also have important implications with regard to the thesis that prolonged hypertension in and of itself is the *cause* of vascular disease [33].

4. Intra-renal arterial and arteriolar sclerosis

Hyalinization and hypertrophy of the media of the muscular arteries and arterioles of the kidney is the most important vascular problem in relationship to hypertension. Grossly, the kidneys may be of normal size, or sometimes, their mass may be significantly reduced. In the latter case, there is loss of renal parenchyma with atrophy of the tubules, narrowing of the cortex and interstitial fibrosis which produces punctate scars. The scarring gives the kidney a pebbled or finely granular appearance when the capsule is stripped away. At times, the capsule adheres to these foci of scarring. Additionally, there are protein casts in renal tubules, sometimes resulting in areas of 'thyroidization'. That is, flattened atrophic tubular epithelium surrounding colloid-like pink protein casts which give a resemblance to thyroid follicles. Usually, significant interstitial inflammation is lacking, as is scarring and inflammation of the renal medulla. These features distinguish the scarring of primary renal vascular disease from that seen in pyelonephritis. When scarring of the parenchyma is significant the term arterial (or arteriolar) *nephrosclerosis* is used. This may appear to be a trivial distinction, but since arterial and arteriolar sclerosis can occur in older individuals in the absence of hypertension, and usually without significant *nephrosclerosis,* while the latter is almost always present in individuals with essential hypertension, the distinction may have value. Further, since the changes described above closely resemble those of pyelonephritis, it is important to separate nephrosclerosis from the infectious or inflammmatory diseases. In up to 50% of individuals with chronic pyelonephritis, even when severe, significant hypertension is lacking [11, 15]. Since chronic pyelonephritis may greatly reduce renal mass this lack of association with hypertension may support the notion that renal disease in association with hypertension is more likely to be due to pressor substances than the lack of depressor influences, (renoprival hypertension). We shall first discuss arterial and arteriolosclerosis, and then nephrosclerosis in relation to hypertension.

4.1. Arterial and arteriolosclerosis of the kidney

The changes in muscular arteries which are agreed to contribute light microscopic evidence of arteriosclerosis include adventitial fibrosis, medial thickening which is due both to hypertrophy and some hyperplasia of medial smooth muscle cells, and hyaline changes (increased eosinophilia or acidophilia with glass-like opacity) and fraying or splitting of the internal elastic lamella (Plate 2, panels 4, 5). While intimal fibrosis may also be present, intimal lipid deposition as is blood pressure [39]. Little has, as yet, appeared correlating the severity of intra-renal vascular disease in long standing hypertension with the degree of control.

Hyaline arteriolosclerosis involving the afferent arteriole is characteristic of benign nephrosclerosis in association with essential hypertension (Plate 2, panels 6, 8; Plate 3, panel 12). The vascular pole of the glomerulus may also become encased in a collagenous proliferation which is said to begin within the Bowman's space [11]. Ultimately, ischemic atrophy and sclerosis of the glomerular tuft is also seen [11]. Curiously, the efferent arteriole is virtually never involved in this hyalinizing process. However, in Diabetes Mellitus, (Plate 3, panel 10) hyaline change of a similar degree to that seen in the afferent arteriole is frequently present in the efferent vessel as well. This change is so characteristic as to be useful as a differential diagnostic feature when diabetic renal disease is suspected. Further, diabetic glomerulosclerosis accompanied by severe intra-renal vascular disease may frequently be seen in the *absence* of significant hypertension. This can be used first as evidence that intra-renal vascular disease does not *always* cause hypertension, but secondly it appears to support the notion that vascular disease, even of the severe hyalinizing type, can develop independent of hypertension, and therefore hypertension is certainly not the *only* cause of arteriosclerosis. The possibility that the efferent vascular disease significantly alters either the signal for renin release, or the response to the renin-angiotensin mechanism, aborting further renin secretion, appears to have received little attention in the literature thus far. It is interesting that the nephrotic syndrome (loss of volume control) is frequent in diabetic glomerulosclerosis.

Immunofluorescence studies of the vascular disease in benign nephrosclerosis have indicated that at least some of the hyaline material is derived from components of plasma proteins, presumably leaking

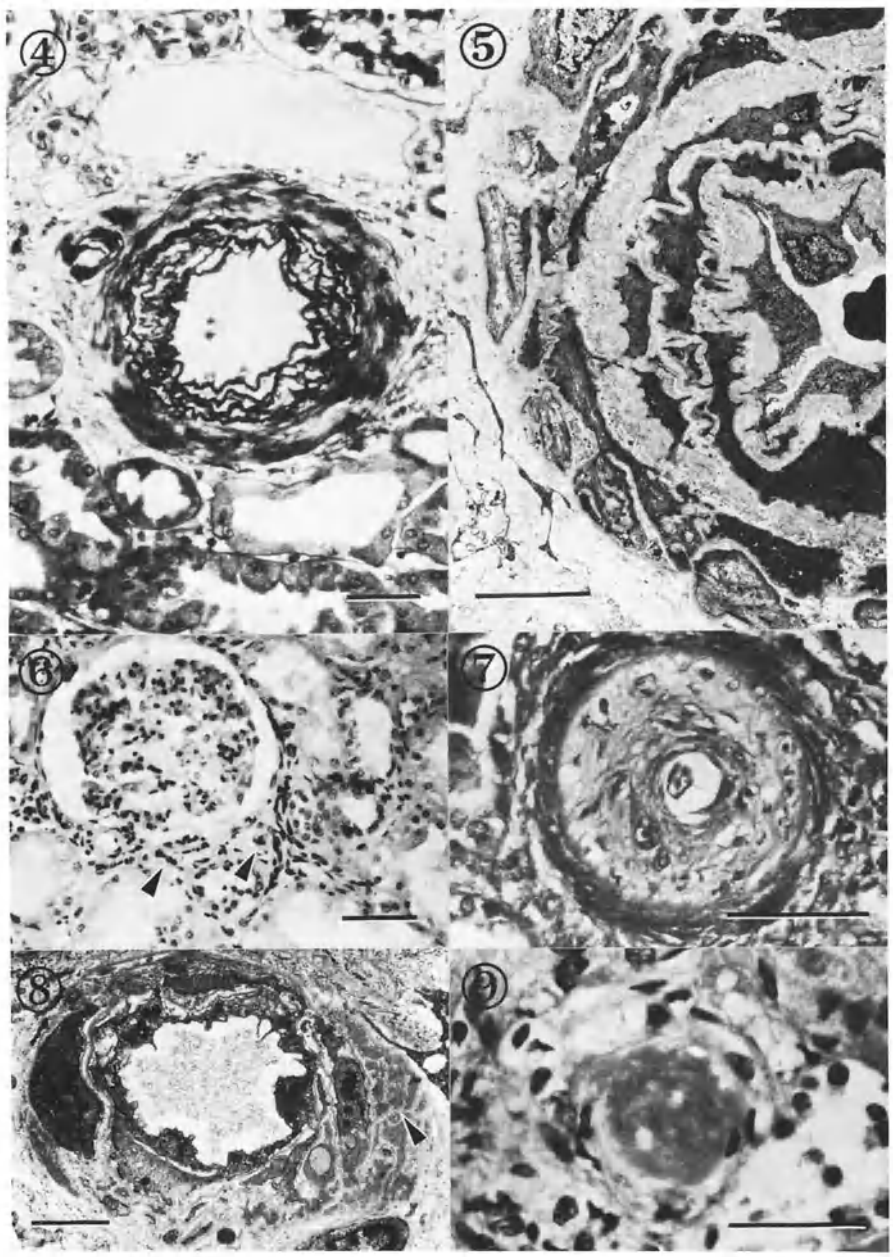

Plate 2. (4) Photomicrograph of interlobar vessel from kidney of patient with history of benign essential hypertension. Note the reduplication of the internal elastic lamella in this elastic stained section (×400; bar equals 25 μ). (5) Electron micrograph of similar sized vessel from kidney of hypertensive individual. Note reduplication of elastic lamellae (less dense, wavy area). There is also proliferation of adventitial cells and an increased amount of basal lamina material surrounding the vessel. (×1,500; bar equals 10 μ). (6) Low magnification photomicrograph showing glomerulus in individual with benign essential hypertension. Arrowhead to left indicates delicate efferent arteriole. Arrowhead to right points to thickened afferent arteriole. The vascular pole of the glomerulus most frequently is affected in nephrosclerosis, sometimes showing fibrosis beneath Bowman's capsule, which is not seen here. (×100, bar equals 100 μ). (7) Photomicrograph of medium sized artery from individual with malignant hypertension. The media is thinned, and there is subintimal fibroplasia with a suggestion of 'onion skin' change. The intima also shows mucoid degeneration. (×800; bar equals 25 μ). (8) Electron micrograph of renal arteriole from patient with benign essential hypertension. Note increased amount of basal lamina-like material (×1,000; bar equals 10 μ). (9) Photomicrograph of small artery in kidney of individual with malignant hypertension. The lumen shows hyaline thrombus, and the wall shows fibrinoid necrosis. Note that there is little or no perivascular inflammation. (×800; bar equals 25 μ).

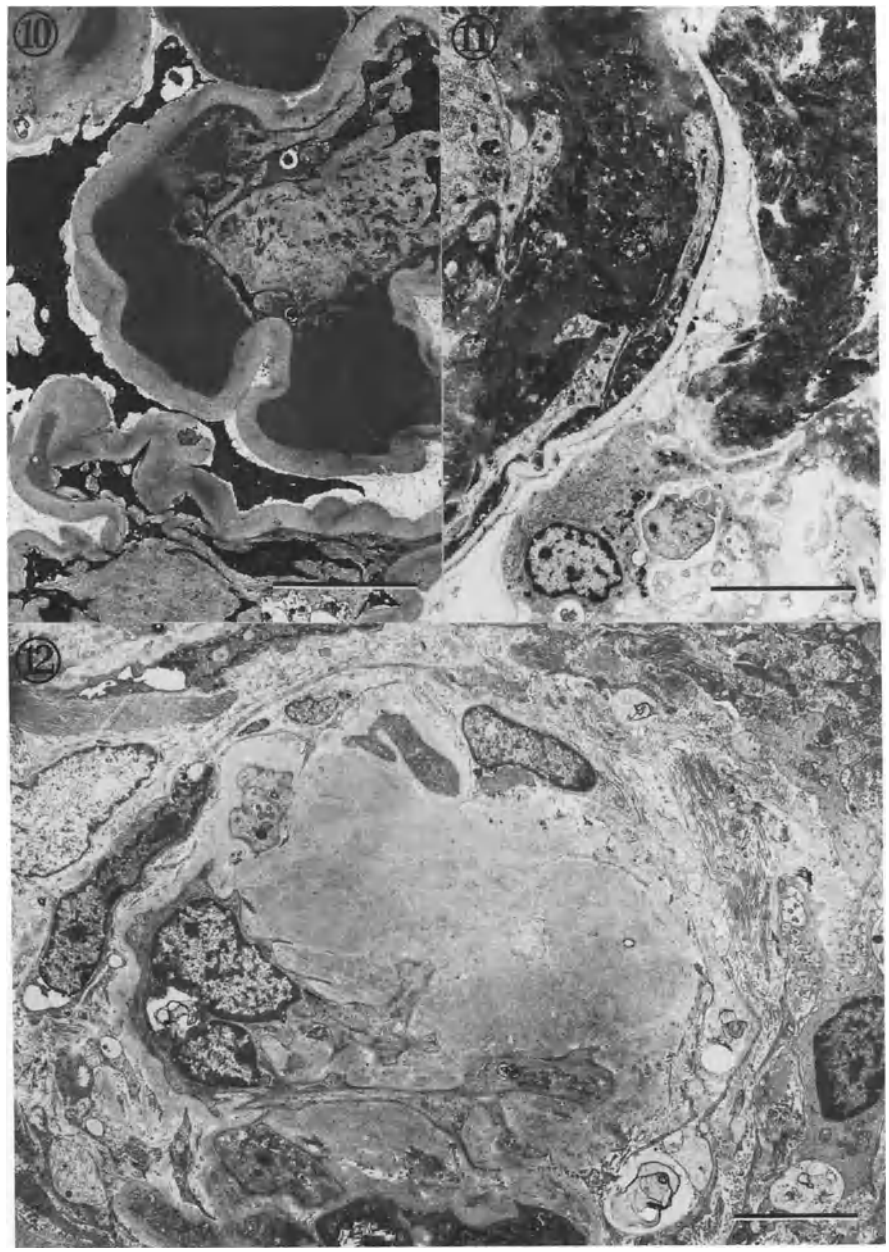

Plate 3. (10) Electron micrograph of glomerular capillary from diabetic individual. Note intense hyaline deposition (insudative lesion). Compare density with hyaline change in Figure 12 below. (×4,000; bar equalss 5 μ). (11) Electron micrograph of glomerular capillary in individual with malignant hypertension. There is fibrin deposition both in the lumen and in Bowman's space. Fibrinoid change (necrosis) is commonly seen in the smaller arteries and arterioles, but also in glomerular capillaries in malignant hypertension. (×4,000; bar equals 5 μ). (12) Electron micrograph of pre-glomerular arteriole from individual with benign nephrosclerosis. There is an increase in fibrous collagen and intense hyaline change with deposition of material with the density of basal lamina. The lumen is virtually obliterated. (×3,500; bar equals 5 μ).

into the vessel wall through an altered endothelium. Although additional studies are needed, IgM, and C_3 have been demonstrated in the wall of arteriosclerotic vessels in one study [40] and fibrinogen, IgG, IgA, and IgE have been seen, in addition, in other investigations [41].

While it is logical to assume that increased vascular tone, like exercise, might lead to muscular hypertrophy, the stimulus to endothelial fibroplasia, elastic reduplication, and the exact nature of the hyaline change remain to be elucidated. Evidence from investigations in experimental animals will be discussed briefly below (6.0).

4.2. Malignant nephrosclerosis

Since the early 1900's when Volhardt and Fahr [3, 11] classified hypertension into primary and secondary types, it has been recognized that some hypertensive patients have an accelerated disease which, if untreated, is relentlessly progressive and results in death in weeks to months, usually from renal failure. Some of these, more frequently black males in the United States, appear *de novo* without an apparent antecedent raised blood pressure. Others have a documented benign essential hypertension which suddenly progresses to show manifestations of severe retinopathy and deteriorating renal function.

In patients whose blood pressure was not documented to be in the hypertensive range prior to the development of malignant hypertension, the kidneys are usually of normal size and have a smooth capsular surface. There are punctate hemorrhages in the cortex, corresponding to areas of fibrinoid necrosis of small arteries and arterioles, but the vascular scars described above (4.0, 4.3) are not seen. They are present only in patients with a clear-cut history of benign essential hypertension in whom the malignant phase has developed. It therefore would seem better to refer to these two pathologic pictures as malignant *vasculopathy,* and *nephrosclerosis* with *malignant vasculopahty,* to distinguish a probably different pathogenesis. None-the-less, the term malignant nephrosclerosis (flea-bitten kidney) is ingrained in the literature.

The vascular lesions which are characteristic of the malignant phase of hypertension are seen in both instances, though there is also significant hyaline arteriosclerosis in kidneys which show nephrosclerosis grossly. The two lesions which accompany the accelerated phase are an endoproliferative process in medium sized and larger vessels termed '*onion skin*' change because of its resemblance to the concentric layers of a sliced onion, sometimes accompanied by mucoid degeneration, and *fibrinoid necrosis* which is seen in smaller arteries and arterioles (Plate 2, panels 7, 9; Plate 3, panel 11). There are other, perhaps more precise descriptive terms for the latter such as *plasmatic arteriolosis* [11], and others, which indicate that the lesion is due to *insudation* of plasma proteins into the wall of the vessel. The exact nature of these two vascular reactions to injury, and their relationship to hypertension, is still a matter of some debate. Neither of these is unique to malignant hypertension, and both can apparently be seen under clinical circumstances where high blood pressure may not have been documented (see below, 6.0). In malignant hypertension there is the distinct impression from the literature that the height of the blood pressure, and the presence of renal failure, may be important in their pathogenesis [3, 11]. The latter has led to a search for a 'toxic' principal which may directly injure the endothelium. Although several candidates have been suggested, conclusive evidence is lacking. Among the agents which have been suggested is renin itself. Raised renin levels appear to be a consistent feature of the malignant phase, whereas in benign essential hypertension the renin concentration is often low or within the normal range [42]. Laragh's group has brought forth evidence that the renin level may correlate with the presence and severity of vascular disease in both the benign and the malignant phase [42].

The mitogenic stimulus for the endoproliferative reaction in medium and larger muscular arteries is unknown. The very similar change seen in scleroderma and a mucinous degeneration of the intima which is sometimes seen late in pregnancy simulate the vascular lesions of malignant hypertension (6.0). As pointed out by Heptinstall [11], these divisions of the renal vascular tree are proximal to the arterioles and would be expected to be subjected to the full force of the hypertension. However, as they become narrowed by the endothelial proliferation the effect would appear to diminish blood pressure and flow more distally. Thus, it becomes difficult to understand how both this lesion and the fibrinoid change in arterioles relate to hypertension. The vascular lesions of the retina, including focal hemorrhaging and exudates which accompany the malignant phase of hypertension have been suggested to be a visible counterpart of the changes occurring in small renal vessels. On the other hand, as pointed out by Pickering (personal communication), they may also be seen following massive gastrointestinal hemorrhaging accompanied by *hypotension.*

The lesions of malignant hypertension in humans have received some detailed ultrastructural and im-

munologic study [11, 37, 41] (Plate 3, panel 11). These are summarized in the general references given [11, 37, 41] and indicate that fibrinogen is present in glomeruli, arteries and arterioles. C_3 is also frequently present, and IgM, IgG and IgA as well as IgE have been demonstrated in scattered reports [11]. Electron microscopic studies have detailed a large number of changes. Wrinkling of the basement membranes of capillaries, visible at the light microscopic level, is also seen in the electron microscope. Reduplication of the basal lamina, electron dense deposits within the basal lamina and beneath endothelial cells, which are often swollen, have been seen. In areas of fibrinoid necrosis, fibrin tactoids are seen (Plate 3, panel 11) and platelets may also be found on occasion [11, 37, 41].

5. Other forms of renal vascular disease

The kidney is susceptible to all of the forms of vasculopathy which affect arteries or arterioles throughout the body. The evidence favors the notion that vasculitis such as that seen in scleroderma, lupus erythematosus and polyarteritis nodosa (periarteritis) are *primary,* and the hypertension which develops in association with these conditions *is seen only when and if* there is significant compromise of the renal circulation. This appears to be unequivocal evidence for the contention that vascular compromise can precede and initiate hypertension of renal origin. Again, the mechanism has not been totally elucidated, but there is evidence that the renin-angiotensin mechanism may be involved [11].

Three forms of vascular disease are worthy of some further comment because of their resemblance to the lesions of the malignant phase of essential hypertension. These are the lesions of *scleroderma,* those sometimes seen following *pregnancy,* and the so-called *hemolytic-uremic syndrome.*

In each case, patients may begin with normal or only slightly elevated blood pressure and end with severe hypertension. They are associated with evidence of intra-vascular coagulation and so-called microangiopathic hemolytic anemia in which there is a negative Coombs' test and fragmentation of red blood cells producing forms such as *helmet* cells and *burr* cells. The vascular lesions in post-partum acute renal failure, scleroderma and hemolytic-uremic syndrome include the gamut of those seen in the malignant phase of hypertension. These include: mucinous endovascular degenerative and onion skin change, in large and medium vessels, and fibrinoid change in arterioles and glomeruli. So similar are the changes that the pathogenesis must involve similar mechanisms. The primacy of intra-vascular coagulation has been suggested, and raised circulating renin levels may play a role [11].

6. Experimental studies of vascular disease and hypertension

Much of the controversy over the relationship between hypertension and the pathogenesis of vascular disease stems from the lack of an experimental animal which develops vascular lesions identical to those seen in human essential hypertension, either in the benign or the malignant phase. While fibrinoid change without accompanying inflammation occurs in the dog, the endoproliferative lesion is not seen [43]. Interestingly, the early observation by H. Goldblatt of fibrinoid changes in vessels throughout the body, but not in the kidney distal to a clamp on the main renal artery [44] has led to the concept of the 'protected kidney'. That is, that hypertension is *necessary* to produce the vascular changes, and that they are more severe on the side that is not protected by renal artery stenosis. Goldblatt himself suggested that the lesions of *malignant hypertension* appeared to require at least normal perfusion pressure [44]. How this relates to the lesions of benign essential hypertension (arterial and arteriolar sclerosis) is not clear and has led to some confusion. Clarity has not been gained from studies of the rat (see below). Neither the dog nor the rat develops a lesion simulating hyaline arteriosclerosis in man. The dog may show medial hypertrophy [43] in small and medium sized vessels, but does not develop significant hyaline change [43]. The lesion seen most frequently in the rat, particularly in salt or steroid induced hypertension is an inflammatory arteritis simulating periarteritis nodosa in man [6, 7, 11, 45]. This lesion does not resemble those of the malignant phase in man, and certainly has little similarity to benign arteriosclerosis. Because some authors have failed to recognize this lack of similarity, much confusion has been generated.

Despite these objections, there have been some significant studies of lesions induced by experimental hypertension. The early studies of Byrom and associates [6, 7] are often cited as establishing the vicious circle of hypertension. Several strains of rats which develop hypertension, such as the Kyoto, SHR and Dahl strains have been developed [11]. The latter is especially important since Rapp [45] has inbred both a salt sensitive animal (S) which develop rapidly progressive hypertension, and a salt resistant

strain (R) which does not get raised blood pressure on a similar level of salt intake. The availability of the control animals will be extremely important in unraveling the factors which are most important in the pathogenesis of the vascular lesions which have only been partially characterized to date.

It appears from numerous studies that more than one mechanism is operative in the pathophysiology of experimental renal hypertension [9, 11]. These are typified by so-called two-kidney Goldblatt hypertension, in wich raised renin levels probably play a major role, and one-kidney Goldblatt hypertension, in which renin levels are low, and other factors are felt to predominate [9, 11]. The literature is voluminous and confusing. There is a need to be somewhat cautious about interpreting failure of pharmacologic agents, such as converting enzyme inhibitors, to abrogate the hypertension as meaning that the renin angiotensin mechanism is not involved. It is naive to assume that pharmacologic agents act monospecifically, act identically under different physiological conditions, and finally, the effect could still involve the renin *system* indirectly through one of its multiple interrelationships. Much work remains to finally establish the relationship of the kidney to the pathogenesis of essential hypertension.

7. Summary and future directions

We have discussed the principal forms of intra and extra-renal vascular disease and their probable relationship to hypertension. It is clear that when there is significant compromise of the lumen of the main renal artery, whether it be from atherosclerosis or fibromuscular dysplasia, that hypertension follows and can be cured by nephrectomy or correction of the stenosis. The pathogenetic relationship between intra-renal arteriosclerosis and hypertension is not as clear. It appears that either can exist without the other, but when severe, they almost invariably coexist. The renin-angiotensin mechanism appears to be related to the development of the vascular lesions in malignant hypertension, but its relationship to renal hypertension, arteriosclerosis and essential hypertension is still not entirely delineated. Future studies need to be carried out to firmly establish the relationship of hypertension to vascular disease. This is very difficult because an animal model is lacking at present. Moreover, many compensatory reactions, so subtle as to be undetectable, may take place in *in vivo* experiments, and mislead investigators. The development of an *in vitro* model may be essential before all variables can be controlled. Finally, the balance between depressor and pressor substances, and the role of volume expansion in the generation of high blood pressure require further elucidation.

References

1. Pickering GW: High Blood Pressure. Churchill, London, 1955.
2. Moritz AR, Oldt MR: Arteriolar sclerosis in hypertensive and nonhypertensive individuals. Am J Path 13: 679–728, 1937.
3. Goldblatt H, Lynch J, Hanzal RF, Summerville WW: Studies on Experiment Hypertension. I. The production of persistent elevation of systolic blood pressure by means of renal ischemia. J Exper Med 59: 347–379, 1934.
4. Casleman B, Smithwick RH: The relationship of vascular disease to the hypertensive state based on a study of renal biopsies from one hundred hypertensive patients. JAMA 121: 1256–1261, 1943.
5. Castleman B, Smithwick RH: The relationship of vascular disease to the hypertensive state. II. The adequacy of the renal biopsy as determined from a study of 500 patients. N Eng J Med 239: 729–732, 1948.
6. Byrom FB, Dodson LF: The causation of acute arterial necrosis in hypertensive disease. J Path Bact 60: 357–368, 1948.
7. Wilson C, Byrom FB: The vicious circle in chronic Brights' disease. Experimental evidence from the hypertensive rat. Quart J Med 10: 65–93, 1941.
8. Poulsen K, Vuust J, Bravo R, Lund T: Preprorenin and prorenin from mouse kidney and submaxillary gland identified by translation of messenger RNA and cell free systems and frog oocytes. In: Sambhi MP (ed.) Heterogeneity of Renin and Renin Substrate. Elsevier, New York, 1981, pp 27–32.
9. Skeggs KJ, Dorer FE, Kahn JR, Lentz KE, Levine M: Experimental renal hypertension: The discovery of the renin angiotensin system. In: Suffer R (ed) Biochemical Regulation of Blood Pressure. Wiley, New York, 1981.
10. Goodfriend TL: Angiotensin receptors and specific functions of angiotensins I, II and III. In: Genest J, Kuchel O, Hamet P, Canton M (eds) Hypertension, Physiopathology and Treatment. McGraw-Hill, New York. 1983 (2nd ed), pp 271–279.
11. Heptinstall RH: Pathology of the Kidney. Little Brown and Co., Boston, 1983 (3rd Ed), pp 147–300.
12. Freeman RH, Davis JD: Factors controlling renin secretion and metabolism. In: Genest J, Kuchel O, Hamet P, Cantin M, (eds) Hypertension, Physiopathology and Treatment. McGraw-Hill, New York, 1983 (2nd ed) pp 225–250.
13. Thurau K, Mason J: Renin-angiotensin, a local determinant for glomerular filtration. In: Sambhi MP (ed) Mechanisms of Hypertension. Excerpta Medica, New York, 1973.
14. Barajas L: Renin secretion. An anatomical basis for tubular control. Science 172: 485–487, 1971.
15. Cantin M: Morphopathology of the renin-angiotensin system. In: Genest J, Kuchel O, Hamet P, Cantin M (eds) Hypertension, Physiopathology and Treatment. McGraw-Hill, New York, 1983 (2nd ed) pp 280–308.
16. Gould AB, Skeggs LT, Kahn JR: The presence of renin activity in blood vessel walls. J Exp Med 119: 389–399, 1964.
17. Goldblatt H, Haas E, Haas R: Studies on Renin. II. Continuous infusion of homologus renin at very low rates in intact or nephrectomized, conscious or anesthetized dogd. Circ Res 31: 74–81, 1972.
18. Baracek KH, Barron KW, Webb RL, Brody MJ: Vasopressin-Central nervous system interactions in the development of DOCA hypertension. Hypertension 4 (Suppl II): 131–137, 1982.
19. Grollman A, Muirhead EE, Vanatta J: Role of the kidney in pathogenesis of hypertension as determined by a study of the effects of bilateral nephrectomy and other experimental procedures on the blood pressure of the dog. Am J Physiol 157: 21–30, 1949.
20. Muirhead EE, Brown GB, Germain GS, Leach BE: The renal medulla as an anti-hypertensive organ. J Lab Clin Med 76: 641–651, 1970.
21. Levinsky NG: The renal kallikrein-kinin system. Circ Res 44: 441–451, 1979.

22. Haas E, Goldblatt H, Lewis L et al.: Interplay of vasodilator and vasoconstrictor substances in the femoral arterial bed: identification of the angiotensin Co-factor. Lab Invest 28: 1–7, 1973.
23. Grollman A, Krishnamurty VSR: Differentiation of nephrotensin from angiotensin I and II. Proc Soc Exp Biol Med 143: 85–88, 1973.
24. Skeggs LT, Kahn JR, Levine M, Dorer RE, Lentz KE: Chronic one-kidney hypertension in rabbits. III. Renopressin, a new hypertensive substance. Circ Res 40: 143–149, 1977.
25. Schiffrin EL, Genest J: Tonin-Angiotensin II System. In: Genest J, Kuchel O, Hamet P, Cantin M (eds) Hypertension, Physiopathology and Treatment. McGraw-Hill, New York, 1983 (2nd ed), pp 309–319.
26. Guyton AC, Coleman TG: Quantitative analysis of the pathophysiology of hypertension. Circ Res 24/25 (Suppl) I1, 1969.
27. Ross R, Glomset JA: The pathogenesis of atherosclerosis. New Eng J Med 295: 369–376; 420–425, 1976.
28. Benditt EP: The origin of atherosclerosis. Sci Ann 236: 74, 1977.
29. Gaspar MR: Renovascular hypertension. In: Barker WF (ed) Peripheral Arterial Disease, Vol IV. Major Problems in Clinical Surgery. Saunders, Philadelphia, 1981, pp 383–411.
30. Osborne RW, Goldstone J, Hillman BJ, Ovitt TW, Malone JM, Nudelman S: Digital video subtraction angiography: screening technique for renovascular hypertension. Surgery 90: 932–939, 1981.
31. Kuhlman U, Vetta W, Furner J et al.: Renovascular hypertension: treatment by percutaneous transmural dilatations. Ann Int Med 92: 1–6, 1980.
32. Breslin DJ, Swinton NW Jr, Libertino JA, Zinman L: Renovascular Hypertension. Williams and Wilkins, Baltimore, 1932, p 225.
33. Siegler RL, Miller FJ, Mineau DE, Moatamed F: Spontaneous reversal of hypertension caused by fibromuscular dysplasia. J Ped 100: 83–85, 1982.
34. Biava CG, Dyrda I, Genest J, Benscome SA: Renal hyaline arteriosclerosis. An electron microscope study. Am J Path 44: 349–363, 1964.
35. McGee WG, Ashworth CT: Fine structure of chronic hypertensive arteriopathy in the human kidney. Amer J Pathol 43: 273–299, 1963.
36. Orizuka H: Electron microscopical studies on the renal arteriole in hypertensives and non-hypertensives. I. Renal arteriole in hypertensives. Kumamoto Med J 27: 1–26, 1974.
37. Weiner J, Giacomelli F: Hypertensive vascular disease. In: Genest J, Kuchel O, Hamet P, Canton M (eds) Hypertension, Physiopathology and Treatment. McGraw-Hill, New York, 1983 (2nd ed), pp 498–524.
38. Veterans Administration Cooperative Study Group on Antihypertensive Agents: Effects of treatment on morbidity in hypertension II. Results in patients with diastolic blood pressure averaging 90 through 114 mmHg. JAMA 213: 11143–1152, 1970.
39. Kannel WB: Importance of hypertension as a major risk factor in cardiovascular disease. In: Genest J, Koiw E, Kuchel O (eds) Hypertension, Physiopathology and Treatment. McGraw-Hill, New York, 1977, pp 888–910.
40. Captopril Collaborative Study Group: Does Captopril cause renal damage in hypertensive patients? Lancet 1: 988–990, 1982.
41. Gerber MA, Paronetto F: New patterns of immunoglobulin deposition in the lesions of malignant nephrosclerosis with special reference to IgE. Am J Path 65: 535–542, 1971.
42. Laragh JH: The renin system in high blood pressure, from disbelief to reality: converting enzyme blockade for analysis and treatment. Prog Cardiovasc Dis 21: 159–166, 1978.
43. Goldblatt H: The renal origin of hypertension. In: Harvey Lecture Series. Charles Thomas Publishing, 1947.
44. Goldblatt H: Studies on experimental hypertension. VII. The production of the malignant phase of hypertension J Exp Med 67: 809–826, 1938.
45. Rapp JP: Age related pathologic changes, hypertension and 18 hydroxydeoxycorticosterone in rats bred for high and low juxtaglomerular granularity. Lab Invest 28: 343–351, 1973.

CHAPTER 11

Renal biopsies: glomerular subcellular features

SILVIA CASANOVA and RENZO LASCHI

1. Introduction

Electron microscopy is nowadays a routine method in the study of renal biopsies. The doubts existing some years ago about the true validity of such a method, which was considered too sophisticated and too expensive, are now definitively overcome by the accurate analysis of the cost/benefit ratio.

The increased skill of pathologists in interpreting the information inherent in electron micrographs leads more and more to the distinction among lesions which earlier seemed to be totally superimposable, and at the same time to a better understanding of the findings of light and fluorescence microscopy. Moreover, the simplification of the preparation procedures allows a considerable shortening of the times of processing of the specimens and thus a particularly quick report to the clinician.

Therefore the analysis of the subcellular and particularly glomerular features assumes a precise inequivocal clinical meaning in the course of renal disease and should possibly be performed regularly on each renal biopsy in parallel with the conventional light and immunofluorescence microscopy.

In this chapter, we describe only those ultrastructural lesions of the various glomerular components which, in our experience, are of a precise pathological significance at the present state. Other lesions with a still imprecise significance and uncertain evaluation were deliberately neglected.

2. Alterations of endothelial cells

The endothelial cells line the inner surface of glomerular capillaries with a thin lamina of fenestrated cytoplasm coated by a layer of negatively charged glycoproteins. The glycocalix can retard the filtration of some circulating cationic proteins such as albumin and repels the circulating cells. Blood group antigens (ABO) and histocompatibility antigens (class 2DR) can be found on the endothelial surface. Moreover, the endothelium performs important coagulation control functions by means of the secretion of procoagulative and fibrinolytic factors. Under pathological conditions the endothelium may detach from the basement membrane and desquamate in the lumen; this phenomenon is often associated with coagulation disorders. The endothelial cells can proliferate in order to repair the interruptions, as demonstrated by the presence of mitosis.

In the course of some proliferative glomerulonephritides, circulating monocytes may infiltrate the glomerulus, contributing to the glomerular hypercellularity. This monocytic infiltration can be demonstrated either by means of histochemical techniques or by electron microscopy. The latter method, however, presents some limits because of the reduced sampling and the lack of definite morphological identification features of the monocytes.

Various alterations of the endothelial cells can be observed at the electron microscope in the course of different nephropathies, but they seldom are specific, especially if they are of modest degree. The honeycomb transformation of the endothelium seems to be detected frequently also in normal glomeruli [1] (Fig. 1). The swelling of the endothelium occurs in response to a wide range of stimuli and only in toxaemia of pregnancy it is particularly evident (endotheliosis). Occasional endothelial foam cells can be observed in toxaemia of pregnancy, and in other nephropathies (Fig. 2).

Tubuloreticular inclusions in the cisternae of the endoplasmic reticulum can be found frequently in the course of systemic lupus erythematosus (Fig. 3]. Initially they were considered as paramyxoviruses, but in fact they are nuclease and RNAse resistant. They seem to contain mucoproteins. Some authors suggest that they represent an unspecific sign of cellular damage. In this connection it is known that lymphoblastoid cells in vitro develop tubuloreticular structures after being exposed to human interferon [2].

L.J.A. DiDio and P.M. Motta (eds), Basic, Clinical, and Surgical Nephrology. ISBN 0-89838-689-5.

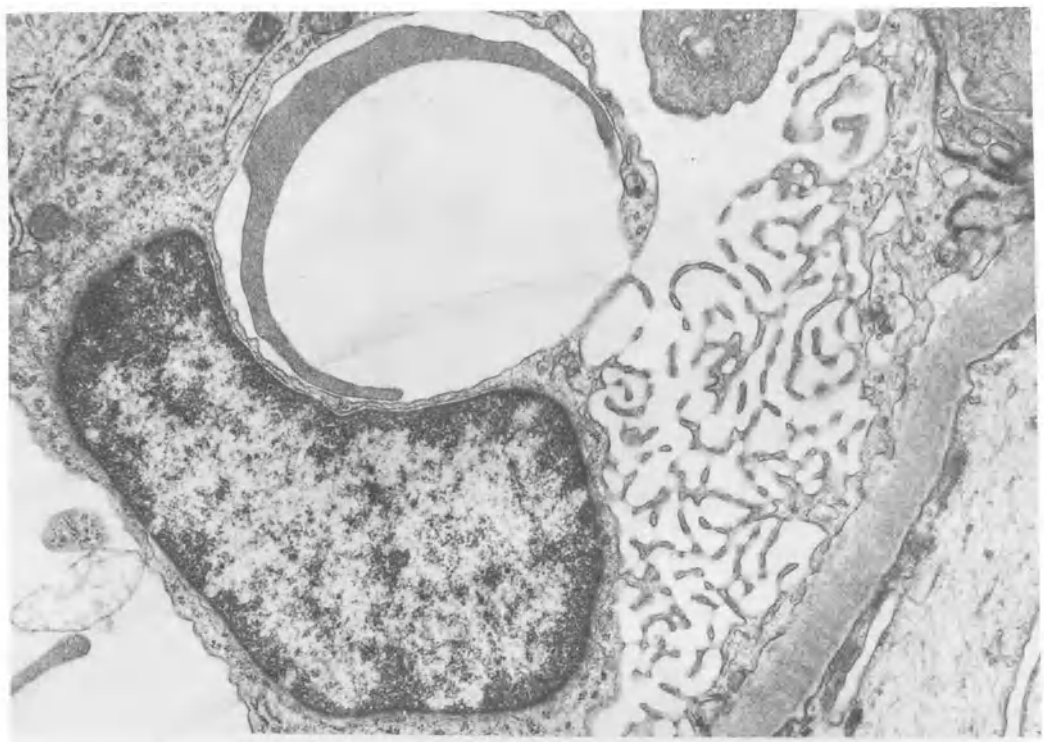

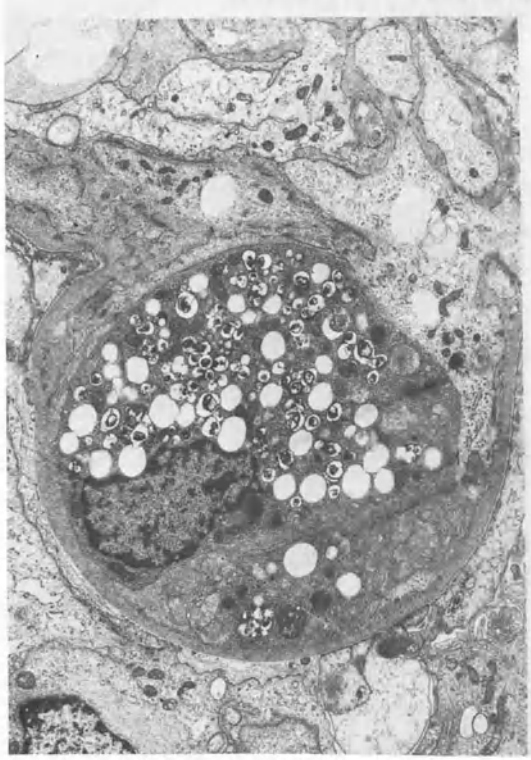

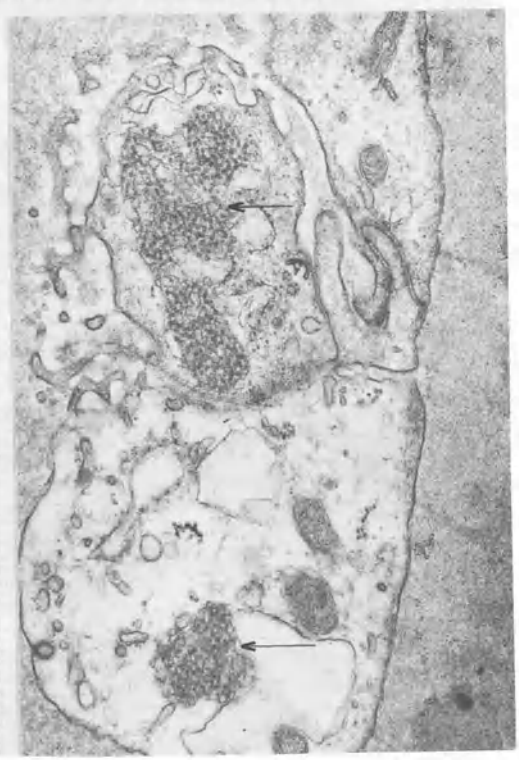

Fig. 1. Focal proliferative glomerulonephritis. Honeycomb transformation of endothelial cell (×18,700).
Fig. 2. Toxaemia of pregnancy. The endothelial cell cytoplasm is laden with clear vacuoles (foam cell) (×5,500).
Fig. 3. Lupus nephritis. Clusters of tubulo-reticular structures into the endothelial cells (arrows) (×23,000).

3. Alterations of the basement membrane

The glomerular basement membrane results from the fusion of the epithelial and endothelial basement membranes. Hence, it has a trilaminar aspect with a lamina densa interposed between two laminae rarae, interna and externa. In humans the basement membrane reaches a thickness of about 350 nm with a significant difference between the sexes: 373 nm in men and 326 nm in women [3]. Until the fourth decade of life, the thickness increases with age and then stabilizes or decreases.

Among the constituents of the glomerular basement membrane some intrinsic components are secreted by the cells resting on it. Other extrinsic components are entrapped in the membrane during the filtration process, even if their presence if likely to have functional significance. Among the intrinsic components type IV collagen is distributed in all layers of the basement membrane, forming its structural frame, to which other components anchor. Laminin and heparan sulfate are predominant in the laminae rarae. The heparan sulfate seems to be the major responsible of the charge selectivity of the glomerular filter. Among the extrinsic components fibronectin is localized on the endothelial side of the basement membrane [4].

3.1. Gaps of the basement membrane

Focal discontinuities or gaps of the basement membrane can be observed in the course of various glomerulonephritides. The interruptions can involve large segments (up to 4 μm) of the basement membrane and be associated with cellular necrosis. Masses of fibrin frequently fill the capillary lumen and spill through the gap in the urinary space, mixed with blood elements. Such interruptions may be observed in rapidly progressive glomerulonephritis, severe postinfective glomerulonephritis, lupus nephritis, etc. (Fig. 4).

Sometimes the gaps in the basement membrane are small without any evidence of cellular necrosis and sealed with epithelial or endothelial cell cytoplasm (Fig. 5). In other cases, a thin irregular layer of lamina densa remains among the closely apposed epithelial and endothelial cells. Electron-dense deposits can also be present.

The gaps of the basement membrane may have a causal role in the formation of epithelial crescents, as they are frequently found in extracapillary proliferation. The presence of fibrin, serum proteins and monocytes in the urinary space are regarded as the triggering stimulus [5].

Several factors appear to play a role in the damage of the glomerular capillary wall: the basement membrane may be digested by cellular collagenases or weakened by the presence of immune complexes as well as by intravascular coagulation or it may be interrupted by mechanical stress. However, none of these factors is inequivocally proved.

3.2. Thickening of the basement membrane without morphological alterations

The increase in thickness of the morphologically inaltered basement membrane represents an important finding in diabetic glomerulosclerosis, both in diffuse and nodular form. It is associated with increased protein permeability of the glomerular filter. The basement membrane appears homogeneous, dense and sometimes lamellated (Fig. 6). The thickness varies in the different loops. The outer contour is smooth with occasional crater-shaped depressions.

Quantitative analyses have shown that the thickening begins early and is followed by an increase of the mesangial matrix in either diffuse or nodular form.

Most authors consider the altered carbohydrate metabolism to be the determinant cause of the basement membrane changes [4], but the physiopathologic mechanism is still obscure. Recent biochemical data on diabetic glomeruli have shown a reduced content of heparan sulfate proteoglycans, which might explain the increased permeability of the basement membrane [6]. Even if the thickening of the glomerular basement membranes is characteristic of diabetic glomerulosclerosis, it can be detected in various other glomerulopathies such as hepatic glomerulosclerosis and glomerular ischemia. In the first case, the thickening may be associated with transparent areas containing osmiophilic particles; in the second case, it is possible to observe wrinkling of the membrane.

3.3. Thickening of the basement membrane with morphological alterations

The basement membrane assumes irregular contours, the lamina densa appears divided into several differently interwoven lamellae, interrupted by lucent areas with electron-dense granulations (Fig. 7). If these alterations are sufficiently diffused, they are suggestive of Alport's syndrome, a chronic familial progressive nephritis often associated with nerve deafness. Nevertheless, not all patients with clinical features of and positive inheritance for the Alport's

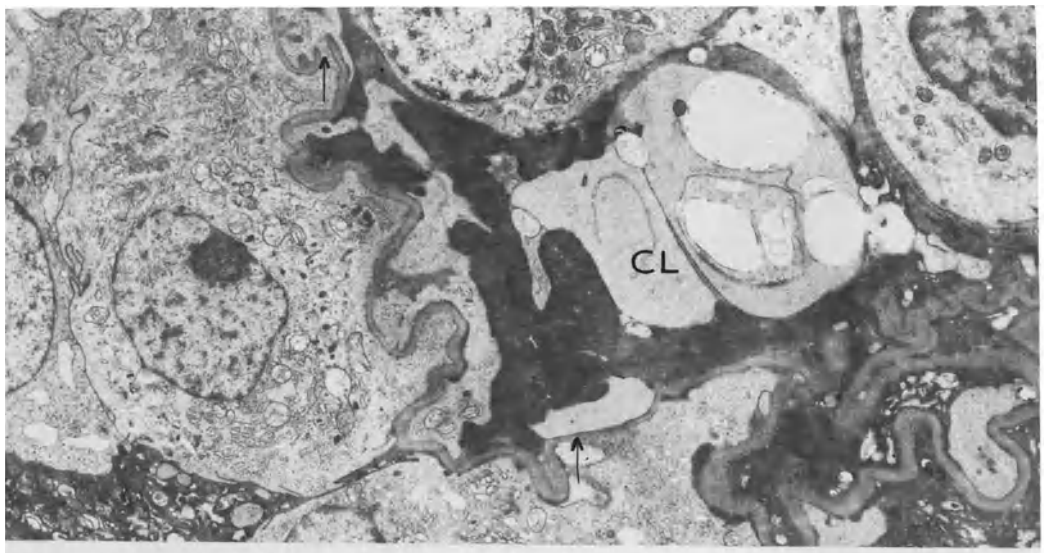

4

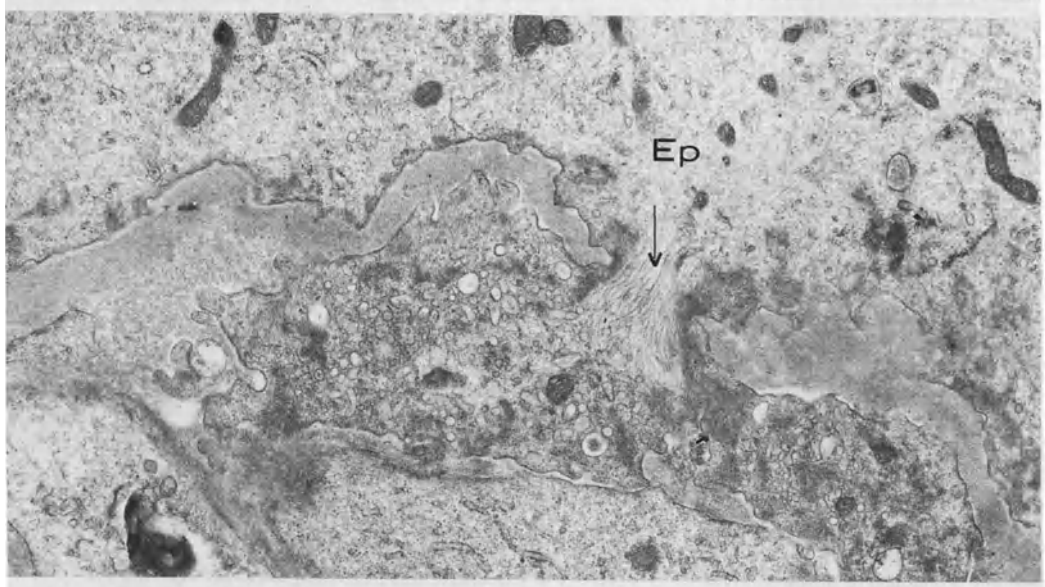

5

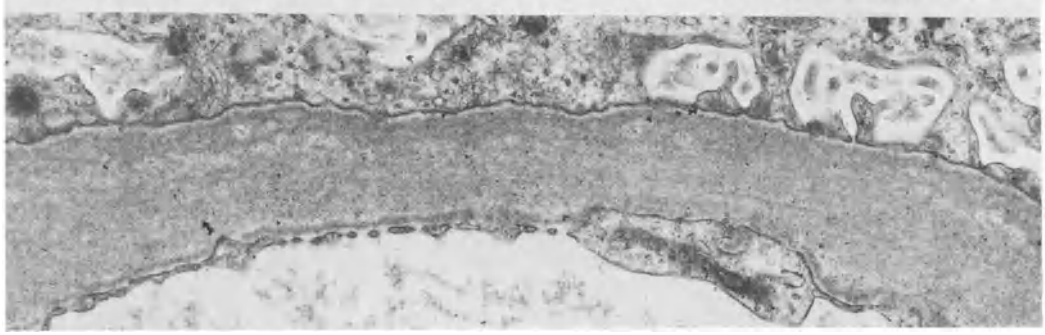

6

Fig. 4. Goodpasture's syndrome. The capillary lumen (CL) is occluded by a fibrin trombus. The basement membrane is thin and focally interrupted (arrows) (×5,400).
Fig. 5. Proliferative glomerulonephritis. Gap of the basement membrane sealed by a process of the epithelial cell (EP) (arrow) (×13,400).
Fig. 6. Diabetic glomerulosclerosis. The basement membrane appears severely thickened (×15,600).

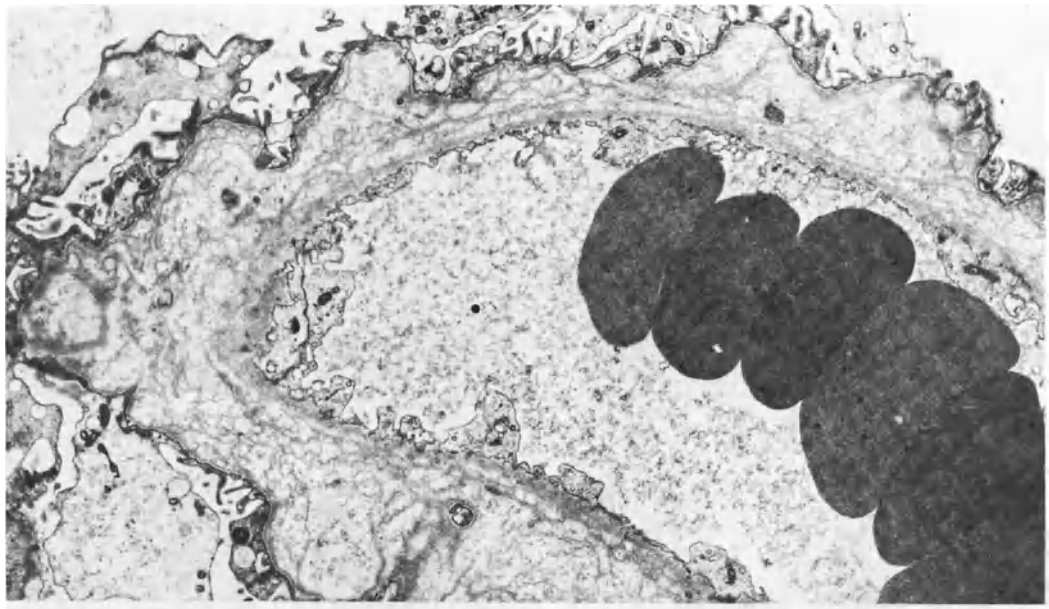

7

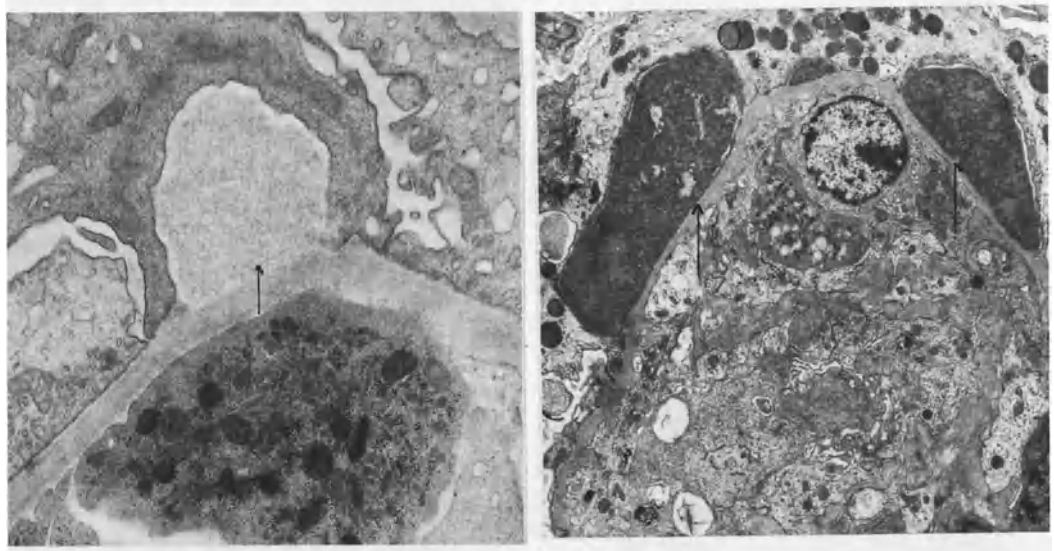

8

10

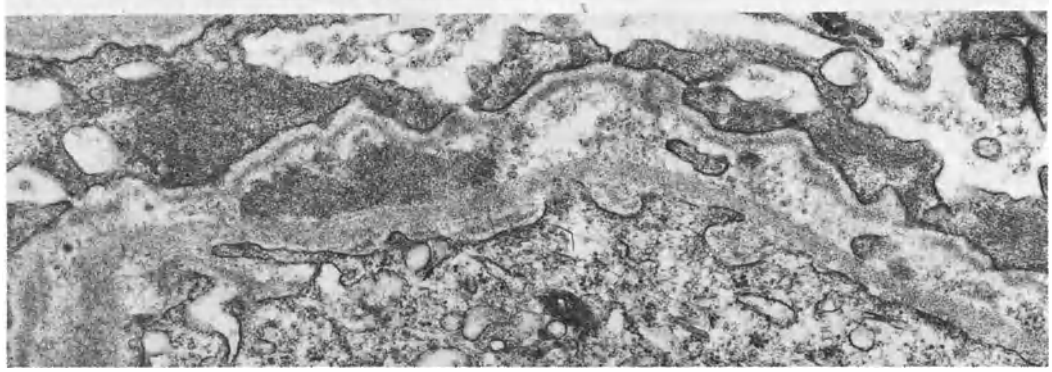

9

Fig. 7. Alport's syndrome. Characteristic appearance of the basement membrane with lamellation and lucencies (×4,400).
Figs. 8, 9, 10. Proliferative glomerulonephritis. Different aspects of humps (arrows) (Fig. 8, ×15,300; Fig. 9, ×38,400; Fig. 10, ×4,250).

syndrome present these alterations [7]. In fact, some patients show normal basement membranes, others only a diffuse thinning and others still present patchy splitting.

On the other hand, focal lamellation of the basement membrane can be observed in patients with different glomerulopathies such as IgA glomerulonephritis and postinfective glomerulonephritis [8]. Therefore these alterations, even if they suggest the Alport's disease, cannot be considered to be the sole and indispensable criterion for diagnosis.

Spear suggested that the Alport's syndrome could be the expression of an inherited defect of the basement membrane assembly [9]. Some authors have described a defective binding of anti-basement membrane antibodies to the glomeruli of patients with Alport's syndrome [10], whereas Habib et coll. [7] report a decreased biochemical content of collagenous polypeptides with a normal distribution of the different constituents of the basement membrane at immunofluorescence. These last authors conclude with the assumption of an altered collagen degradation rate.

In other hereditary disorders with renal involvement, a thickening of the basement membranes is produced: the familial deficiency of lecithin-cholesterol acyltransferasis and the hereditary onychoosteodysplasia or nail patella syndrome. In the first case the basement membrane contains lucent areas and electron-dense membrane-like material on the subepithelial side. The glomerular histological picture suggests a membranous glomerulonephritis with negative immunofluorescence for immunoglobulins and complement [11]. In the second case, the basement membranes appear homogeneously thickened and contain cross-banded collagen fibers [12]. The renal involvement is associated with proteinuria, sometimes in nephrotic range, with histological evidence of segmental glomerular sclerosis and cortical fibrosis. Patients present dystrophic and hypoplastic nails, bone alterations (rotula and ilium) and iris pigmentation.

3.4. Basement membrane thickening by apposition

This type of thickening is due to the presence of material which differs in structure and/or density from the lamina densa. The deposition may occur on either sides or within the lamina densa. It is common use to indicate as deposits amorphous areas of increased electron density. Often their presence is associated with the deposition of immunoglobulins and/or complement, which can be demonstrated by means of immunofluorescence. The areas with increased lucency are generally indicated as lucent areas.

3.4.1. Subepithelial deposits are located between the lamina densa and the plasma membrane of visceral epithelial cells. The deposits may be isolated, dome-shaped and sharply marked off from the lamina densa; the epithelial cytoplasm covering them shows increased density and loss of foot processes. These deposits are called 'humps' and are considered the hallmark of acute postinfective glomerulonephritis. Nevertheless, they can be detected in other glomerulonephritides such as idiopathic membranoproliferative glomerulonephritis, glomerulonephritis in the course of infective endocarditis, Schoenlein-Henoch purpura. In postinfective glomerulonephritis humps appear during the acute stage; after 4–8 weeks they lose density and form empty spaces (Fig. 8), which collapse and are filled by the epithelium. In some cases they may be incorporated into the basement membrane, where they give rise to electronlucent lacunae (Fig. 9) which persist for a long time (up to 4 years) [13]. Closely packed large humps (atypical humps) have been described in cases with slow resolution (Fig. 10) [14].

Round or flat subepithelial deposits occurring in large number distinguish idiopathic and secondary membranous glomerulonephropathy. By immunofluorescence microscopy the deposits contain IgG and complement and in some cases antigens have been detected. Such deposits are therefore considered to contain antigen-antibody complexes either pre-formed in the circulation or formed in situ.

In the course of membranous glomerulonephropathy, the initially subepithelial deposits (I stage) are in part (II stage) and totally (III stage) incorporated into the projections of the lamina densa. They may lose their electron density (IV stage) and, in some cases, disappear completely (V stage) (Figs. 11, 12, 13, 14).

By light microscopy the diagnosis of stage I may be difficult as well as the differential diagnosis between stages III and IV. At the electron microscope only at stage IV or V, if deposits are minimal or absent, diagnosis may be difficult.

After stage II the basement membrane appears generally greatly thickened; only in a few patients thickening is modest.

Membranous nephropathy may occur as one of the morphological variants of lupus nephritis. Sometimes clinical evidence for lupus is lacking and thus some morphologic features warrant suspicion of lupus. These are: mesangial, subendothelial, and

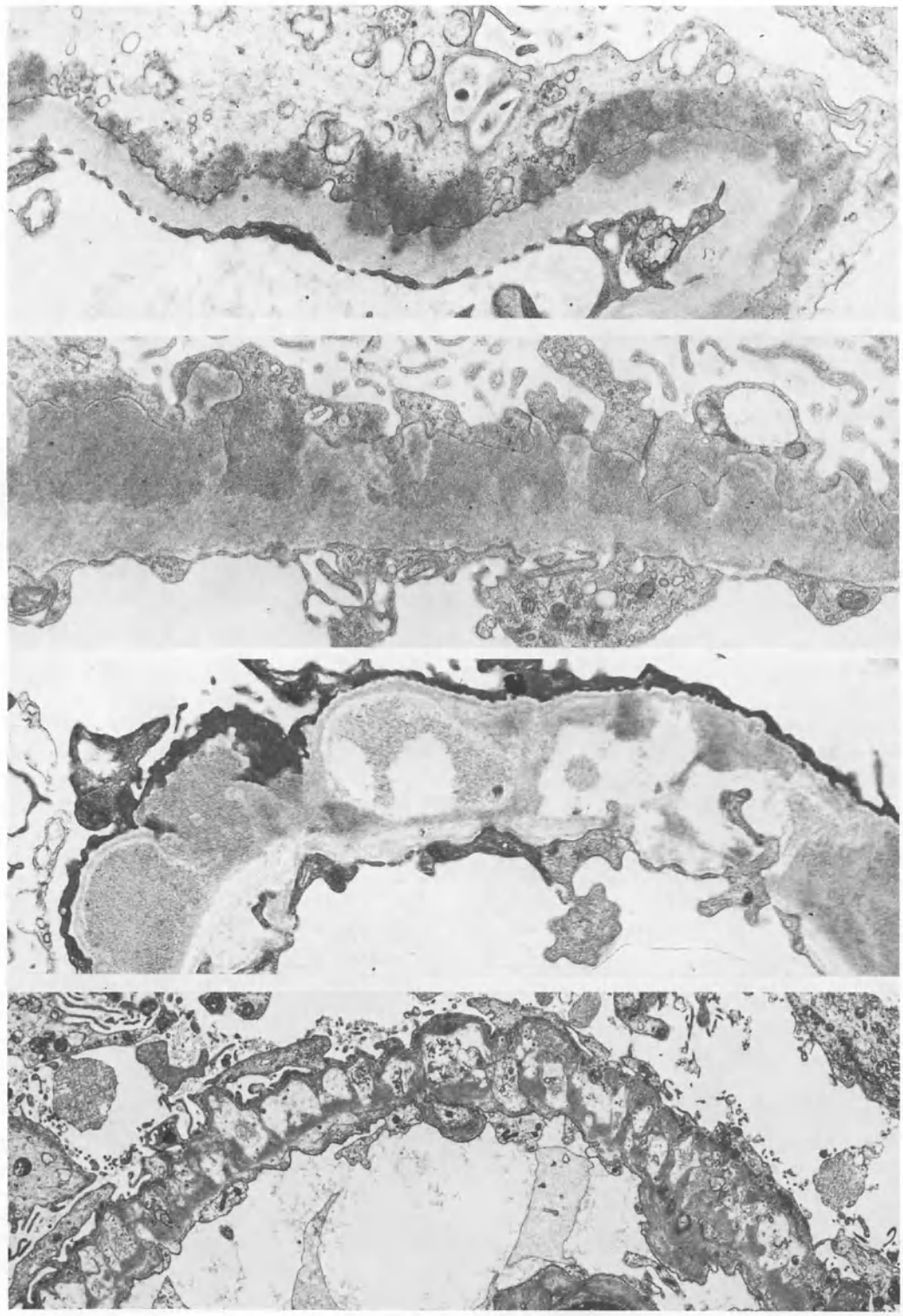

11

12

13

14

Figs. 11, 12, 13, 14. Membranous glomerulonephropathy. The morphology of the basement membrane and deposits within it changes in the different stages of the disease. Fig. 11: stage I (×18,700); Fig. 12: stage II (×18,700); Fig. 13: stage III (×12,000); Fig. 14: stage IV (×4,800).

tubular deposits and tubulo-reticular inclusions in the endothelial cells. If more than one of these features is present, their efficiency in differential diagnosis increases.

3.4.2. Intramembranous deposits. They may be a) discontinuous, b) dense granular, and c) ribbon-like.

a) The electron-dense material lies among more or less regular layers of lamina densa. Some deposits are early located within the lamina densa, others assume this position later because of the formation of new basement membrane material. Primary intramembranous deposits can be found in cases of acute postinfective glomerulonephritis. Generally, they do not induce thickening of the basement membrane. Secondary intramembranous deposits characterize the III stage of membranous glomerulonephropathy and some cases of membranoproliferative glomerulonephritis. In these latter, the basement membrane appears greatly thickened and the lamina densa splitted into lamellae and twisted by the presence of intramembranous, subepithelial and subendothelial deposits (Fig. 15). These forms have been classified by Strife et coll. [15] as a third type of membranoproliferative glomerulonephritis. At present, no clinical or immunopathological feature seems to differentiate type III from type I membranoproliferative glomerulonephritis.

b) The association of lymphoplasmocytic dyscrasia with tissue deposition of granular material containing determinants of monoclonal light or heavy chains has been recognized only recently. The disease is often called light chain deposition disease, although there are cases with heavy chain deposition. The histologic picture of renal biopsy may mimic diabetic nodular glomerulosclerosis, but cases with slight mesangial thickening are described. The mesangial nodules are highly PAS-positive and not argyrophilic. The glomerular sclerosis is often focally distributed. Monoclonal chains can be demonstrated by immunofluorescence. At the electron microscope glomerular basement membranes show the presence of granular electron-dense material (Fig. 16). The deposition involves also glomeruli without any histological alteration. Similar deposits can be observed in the mesangium, in the tubular basement membranes, peritubular capillaries and in the interstitium.

The tissue precipitation mechanism of the monoclonal chains is unknown. Structural changes as well as abnormal glycosilation of the light chains have been demonstrated by Preud'Homme and coll. [16]. The formation of mesangial nodules might be a reaction to the abnormal material or the consequence of mesangiolysis with formation of capillary microaneurysms.

c) The glomerular basement membrane is thickened and the lamina densa replaced by highly electron-dense, homogeneous, ribbon-like material (Fig. 17). The same material can be found in mesangium, Bowman's capsule and tubular basement membranes. Some glomerular basement membranes have a normal aspect. The picture is specific of dense deposits disease. At light microscopy most patients with this disease show the features of membranoproliferative glomerulonephritis. For this reason dense deposits disease has been classified as a subgroup of membranoproliferative glomerulonephritis (type II). Immunofluorescence does not show immunoglobulins within the deposits, whereas anti-C3 antiserum outlines the dense material with a double-track pattern along the basement membrane and a ring-shaped pattern in the mesangium.

Dense deposit disease recurs in transplanted kidneys, suggesting the importance of circulating factors. Deposits appear early at the vascular pole. Deposition of complement takes place later as a secondary phenomenon. The relapse does not lead to loss of the graft.

The nature of the electron-dense material is still unknown. The available data indicate it is glycoproteic and contains less cystine and more sialic acid than the normal basement membranes. According to Kim *et al.* [17], the electron-dense material is not immunogenic and the basement membranes cannot fix anti-basement membrane antibodies eluted by Goodpasture kidneys. The latter datum is contested by Droz *et al.* [18].

3.4.3. Subendothelial deposits. These deposits can reach considerable dimensions, extending along the whole capillary loop. They can therefore easily be recognized at the light microscope. Subendothelial deposits are typical of type I membranoproliferative glomerulonephritis and of lupus proliferative nephritis (Fig. 18), but they can be observed in various nephropathies.

Peculiar deposits with crystalline structure may be found in cryoglobulinemia: deposits with cylindric or annular configuration in mixed cryoglobulinemia (Fig. 19), whereas deposits with fibrillary form in monoclonal cryoglobulinemia [19]. Deposits with organized pattern may be present in lupus glomerulonephritis as well (Fig. 20).

In view of the functional continuity between subendothelial space and mesangium, it has been presumed that subendothelial deposits form as a consequence of mesangial overloading with immunocomplexes.

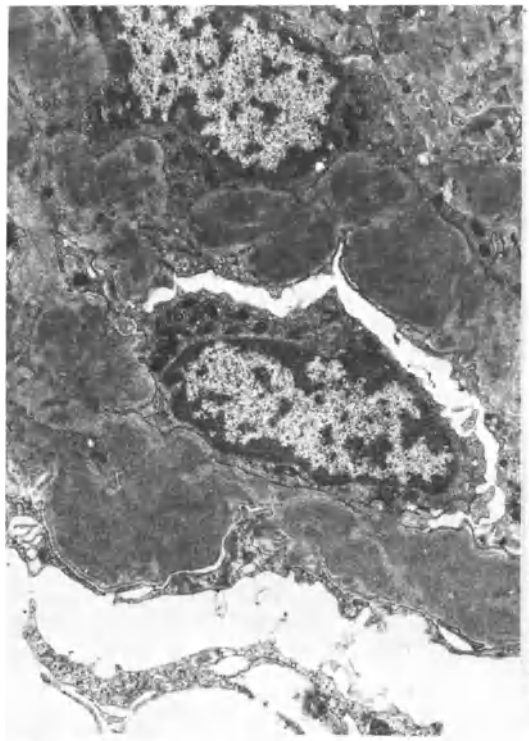

15

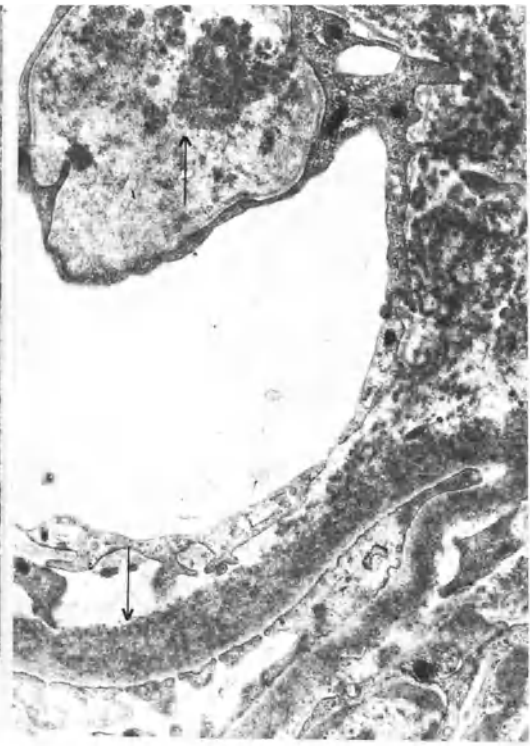

16

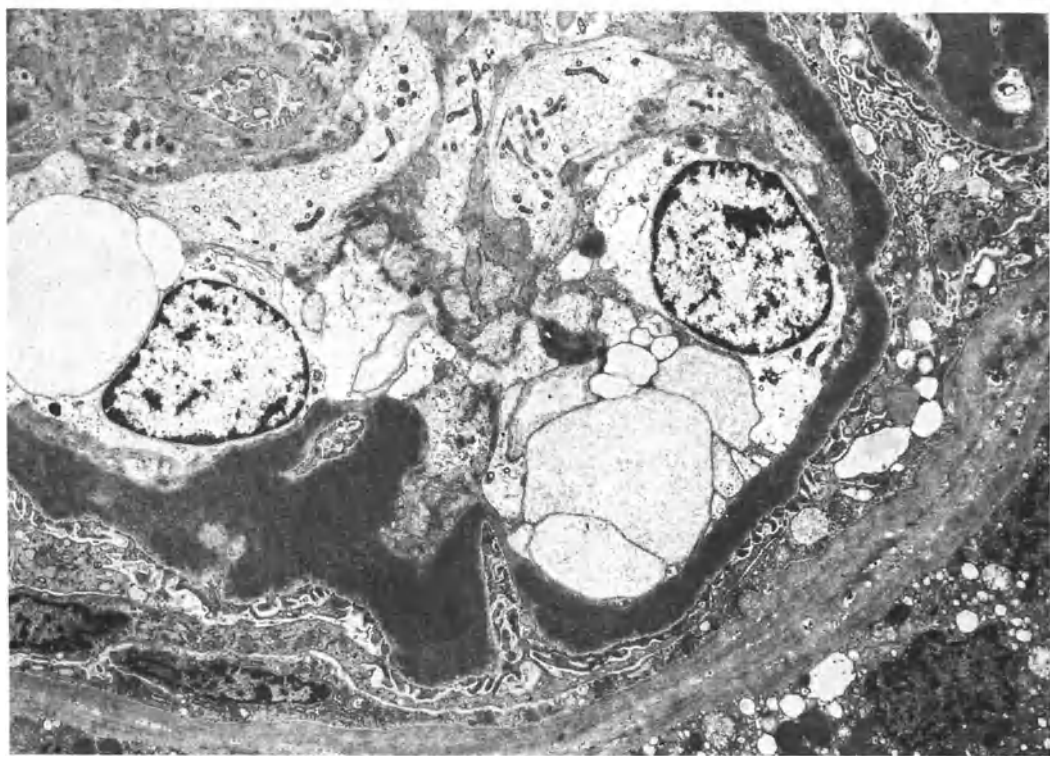

17

Fig. 15. Membrano-proliferative glomerulonephritis. Discontinuous deposits into the basement membrane (×6,000).
Fig. 16. Light chain deposition disease. Dense granular deposits (arrows) in the basement membrane and mesangial matrix (×11,400).
Fig. 17. Dense deposits disease. Ribbon-like dense transformation of the basement membrane (×4,300).

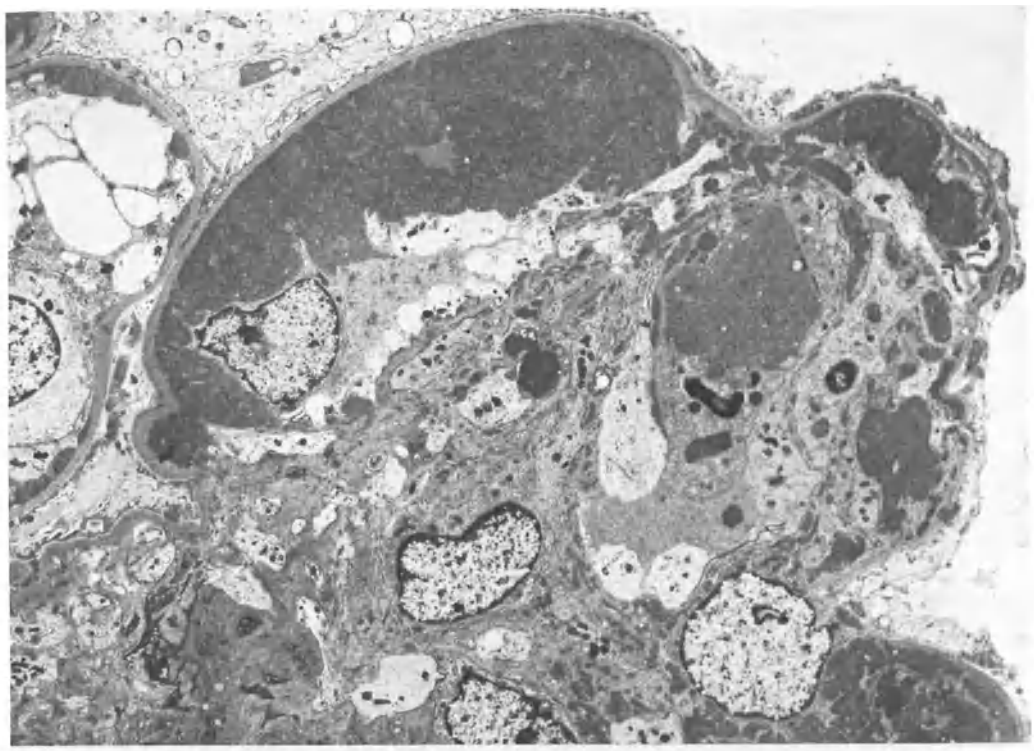

18

19

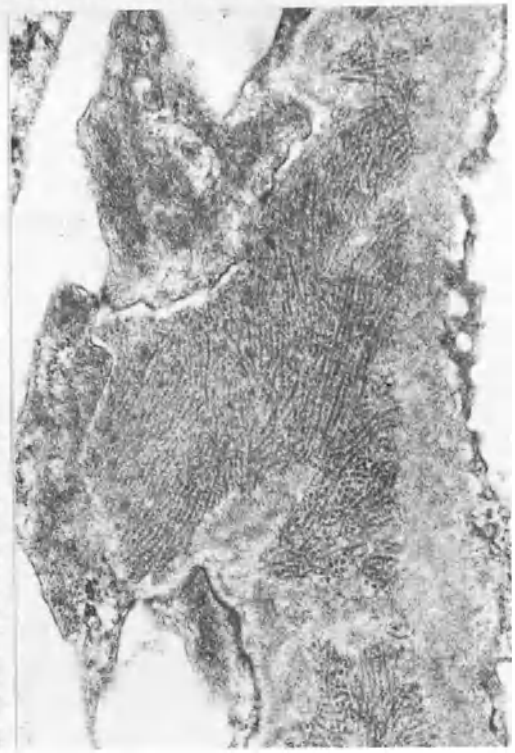

20

Fig. 18. Lupus nephritis. Subendothelial large deposits in the basement membrane (×3,000).
Fig. 19. IgG-IgM cryoglobulinemia. Deposits organized into cylindrical paracrystalline structures (×33,600).
Fig. 20. Lupus membranous glomerulonephritis. Organized deposits in the basement membrane (×32,000).

3.4.4. Deposition of fibrillar material

a) Amyloid. At least three types of amyloidosis are recognized: a systemic hereditary form the isolated fibrils of which seem to contain pre-albumin, a primary acquired or myeloma-associated form with fibrils containing light immunoglobulin chains or frangments of them, and an acquired form secondary to inflammatory processes containing AA protein.

Electron microscopy does not allow to distinguish among the three types of amyloid, which appears in all cases as rigid, unbranched fibrils with a diameter of about 100 Å (Fig. 21). Amyloid glomerular deposits may vary in extension and location. The glomerular involvement may be segmental, diffuse, nodular or mixed. Amyloid fibrils may permeate all glomerular structures and greatly distort the basement membranes.

The deposition pattern and the extent of capillary wall involvement do not significantly correlate with the degree of proteinuria or the renal function. However the presence of massive proteinuria and a fulminating clinical course may be associated with the deposition of amyloid fibrils in spicular form on the subepithelial side of the basement membrane [20]. The absence of spicules and the formation of new basement membrane on the subepithelial side of the capillary wall seem, on the other hand, to be associated with modest proteinuria and the rare cases of recovery.

b) Microfibrils within the size range of amyloid fibrils, but with a regular parallel arrangement can be detected in the subendothelial space of the basement membrane and in mesangium in various nephropathies (Fig. 22) [21] (transplant glomerulopathy, toxaemia of pregnancy, nodular glomerulosclerosis . . .). On cross section the microfibrils show a lucent core surrounded by a dense rim. They contain collagenous glycoproteins.

3.4.5. Widening of the lamina rara interna. This appearance is caused by the deposition of non-fibrillar electron lucent material. This alteration, if limited, can be observed in various nephropathies without being specific. If extensive, is typical of severe ischemic glomerular damage (essential malignant hypertension, renal involvement in the course of scleroderma) or lesions associated with disseminated intravascular coagulation (uremic hemolytic syndrome, thrombotic thrombocytopenic purpura, toxaemia of pregnancy, transplant glomerulonephropathy). Fibrin, immunoglobulin and fibronectin deposits are detectable in the subendothelial space by immunofluorescence. Widening of the lamina rara interna may associate with mesangial interposition or with intracapillary thrombi (Figs. 23 and 24).

3.5. Thickening of the basement membrane by mesangial interposition

It is well known that the lamina rara interna is in anatomical and functional continuity with the mesangium. In low class vertebrates the lamina rara interna normally contains mesangial cells [22]. It is therefore not surprising that in pathological conditions mesangial cells migrate into the subendothelial space, surrounding partially or totally the capillary lumen. On the inner side of the capillary loop a new layer of basement membrane is layed down. At light microscope the involved loops appear therefore with a double contour pattern. The stimuli which induce mesangial cells to migrate are not yet understood. Occasionally, the interposition is associated with electrodense deposits in the subendothelial mesangium. Therefore, it has been assumed that mesangial migration may represent an attempt to degrade material, which otherwise could not be eliminated from the subendothelial space.

Mesangial interposition in the basement membrane occurs with frequency in the course of some glomerulopathies such as membranoproliferative glomerulonephritis, transplant glomerulonephritis, toxaemia of pregnancy (Figs. 23–24). The process may lead to a remarkable narrowing of the capillary lumen.

3.6. Thinning of the basement membrane

The diffuse and significant reduction of the basement membrane thickness to about 1500–1900 Å is considered to be the morphologic hallmark of essential benign haematuria (Fig. 25), although this lesion has been described also in Alport's syndrome [7].

Familial essential benign haematuria shows dominant autosomic transmission and differs from the Alport's disease, as no proteinuria, renal insufficiency or auditive deficiencies can be observed. In doubtful cases, familial essential benign haematuria is to be excluded in the presence of proteinuria and evolution into renal failure in a family member.

4. Alterations of epithelial cells

Under normal conditions the glomerular visceral epithelium represents about 54% of the total glomerular cytoplasm [1]. It consists of podocytes, which are highly specialized cells with a characteris-

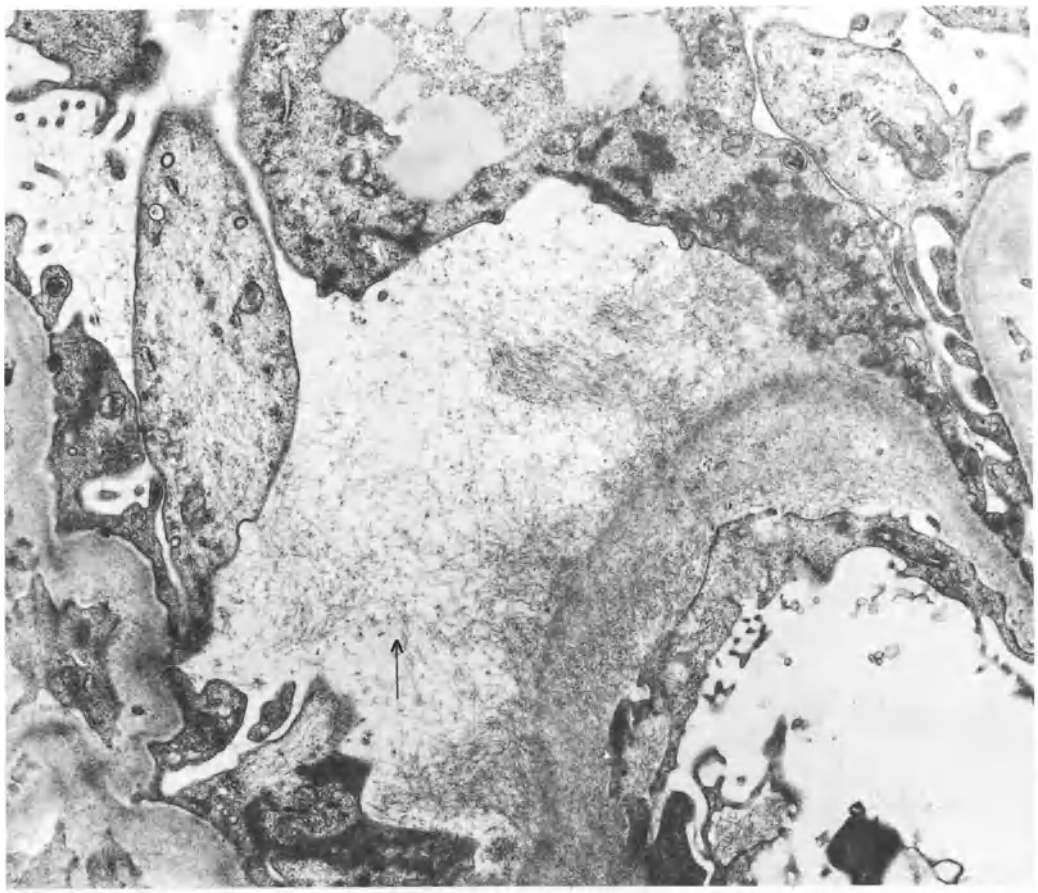

21

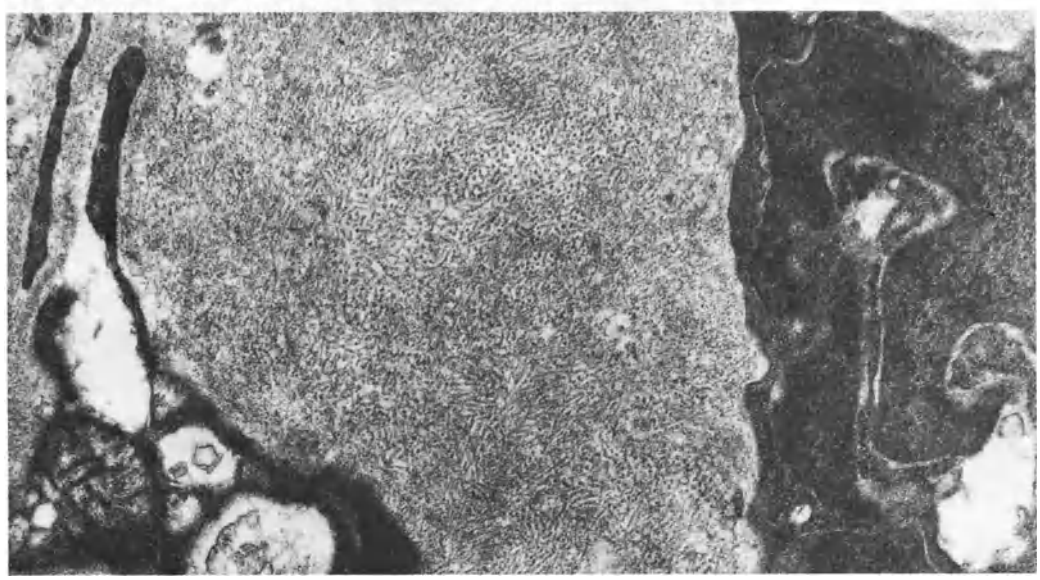

22

Fig. 21. Renal amyloidosis. Amyloid fibrils penetrating beneath the epithelial cells (arrow) (×12,000).
Fig. 22. Membrano-proliferative glomerulonephritis. Microfibrillar structures in the mesangium (×36,800).

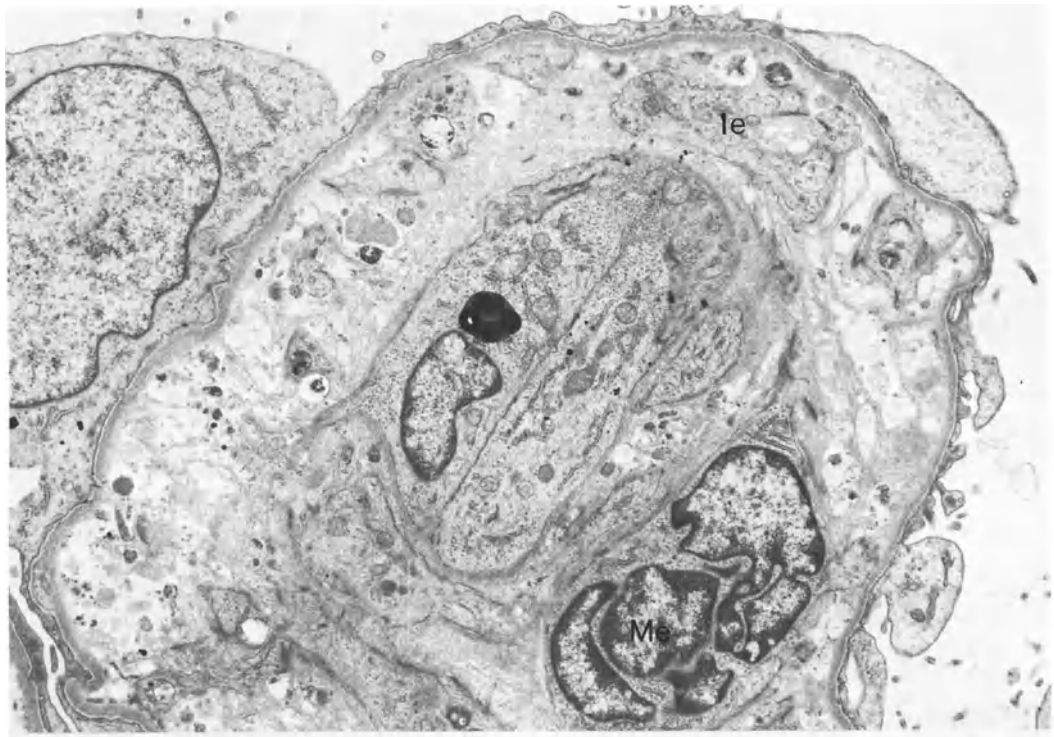

23

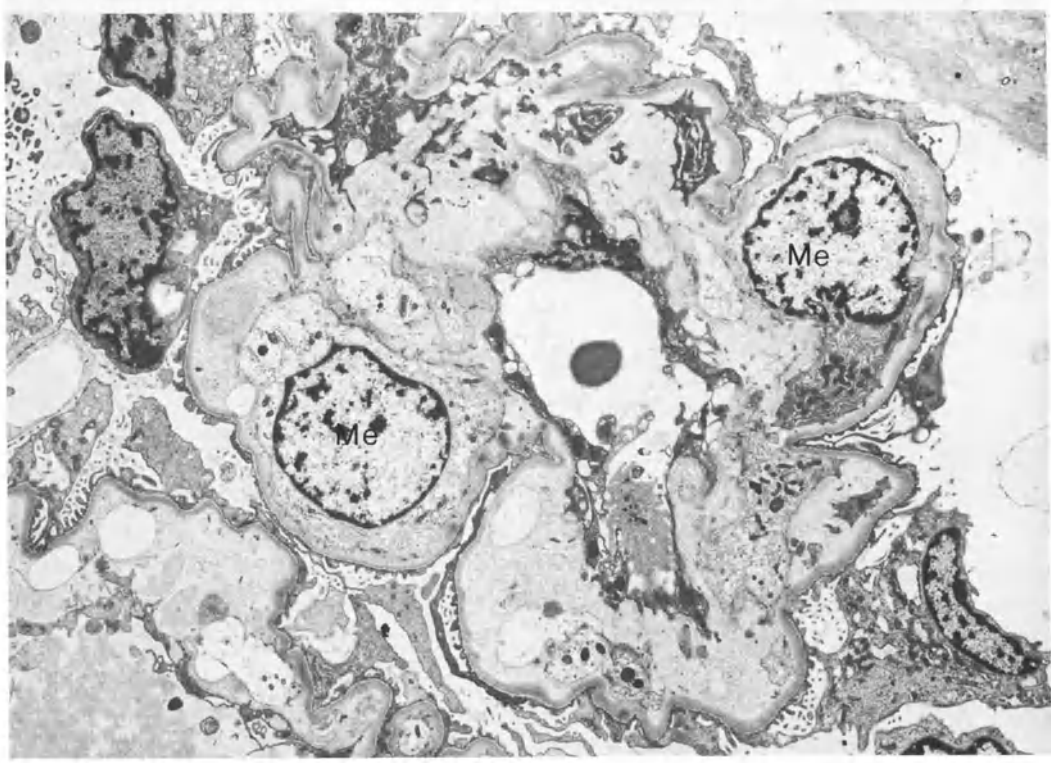

24

Figs. 23, 24. Transplant glomerulopathy (Fig. 23) and uremic haemolytic syndrome (Fig. 24). Prominent thickening of the lamina rara interna of the basement membranes and mesangial interposition (Me) (Fig. 23, ×6,000; Fig. 24, ×4,000).

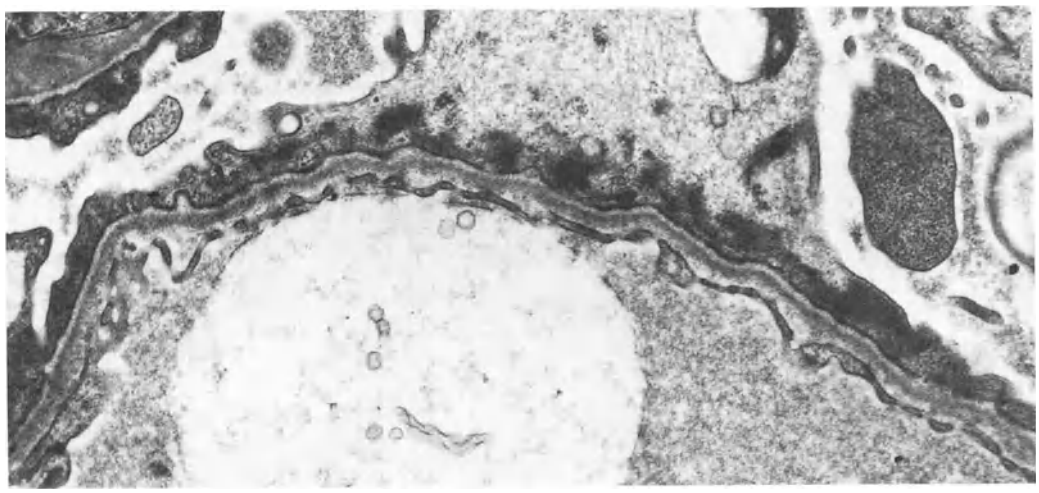

Fig. 25. Familial benign haematuria. Thinning of the basement membrane (×20,000).

tic tridimensional structure. It is likely that the elements of the cytoskeleton, regional differences in the composition of the plasma membrane and an extracellular lining of polyanionic sialoproteins concur to maintain this structure. The functions of synthesis of some constituents of the basement membrane, of supporting the membrane itself and of controlling the hydraulic flow through the glomerular capillary wall are attributed to the visceral epithelium.

The best known podocyte alteration is the disappearance (fusion) of foot processes (Fig. 26). According to Haynes [1], an apparent modest fusion of the foot processes can be detected also in normal conditions; lenghts of fusion of about 12 μm must be a regular finding before the degree of fusion can be considered significant. The disappearance of the foot processes occurs because of retraction of the cytoplasm towards the cell body and is associated with distortions and dislocations of the slit diaphragms (Fig. 26, inset). According to the more generally accepted opinion, this alteration is consequent upon the reduction of the negative charges on the epithelial surfaces, even if the data supporting this hypothesis are still inadequate. The disappearance of the foot processes represents the main ultrastructural lesion in minimal change nephropathy. Moreover, this lesion can be observed in the course of various proteinuric states.

The relation between proteinuria and the fusion of the foot processes is still controversial. Results published by various authors seem to indicate that proteinuria in itself is not responsible for the epithelial alterations [23–24]. As the basement membrane seems to be the main size and charge filter of the glomerular capillary wall, it is also unlikely that epithelial alterations may be primarily responsible of proteinuria. The two phenomena may represent separate answers to an underlying pathologic process.

In the course of various glomerular diseases, the visceral epithelium may present degenerative and necrotic changes followed by its detachment from the basement membrane. Depending upon the extent of the injury,sclerosis may result (Fig. 27).

In Fabry's disease the visceral epithelial as well as endothelial and mesangial cells contain intracytoplasmic vacuoles full of myelin-like material (Fig. 28).

5. Mesangial alterations

The mesangium is the structure supporting the glomerular flocculus. The mesangial matrix is in functional continuity with the internal lamina rara of the basement membrane, whereas it is structurally and chemically distinct from the lamina densa. It contains in fact different types of sulphated glycosaminoglycans [25], fibronectin, type IV procollagen and type V collagen. Moreover, it is more easily soluble than the lamina densa. From a structural point of view, it is less homogeneous and often contains fibrotubular structures.

Recent observations in experimental animals seem to indicate that there are two different populations of mesangial cells: one similar to the smooth muscle cells containing myosin and able of contracting in response to local stimuli, thus controlling the glomerular perfusion and filtration, and a second with phagocytic ability derived from the bone marrow, expressing antigens Ia. In normal conditions

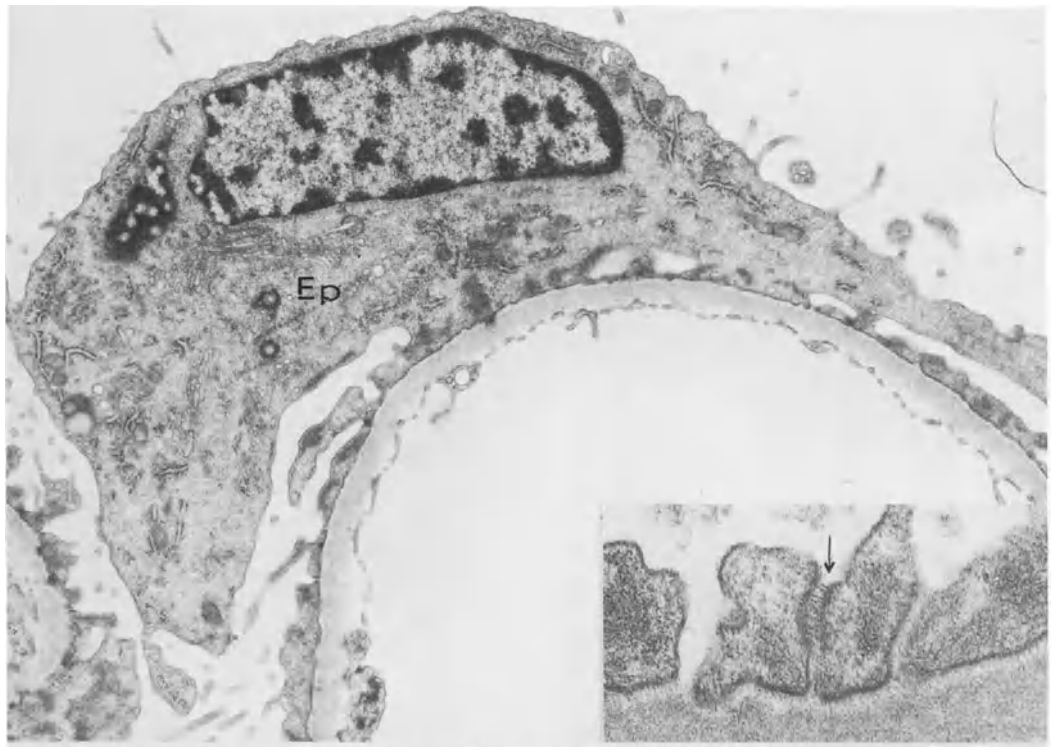

26

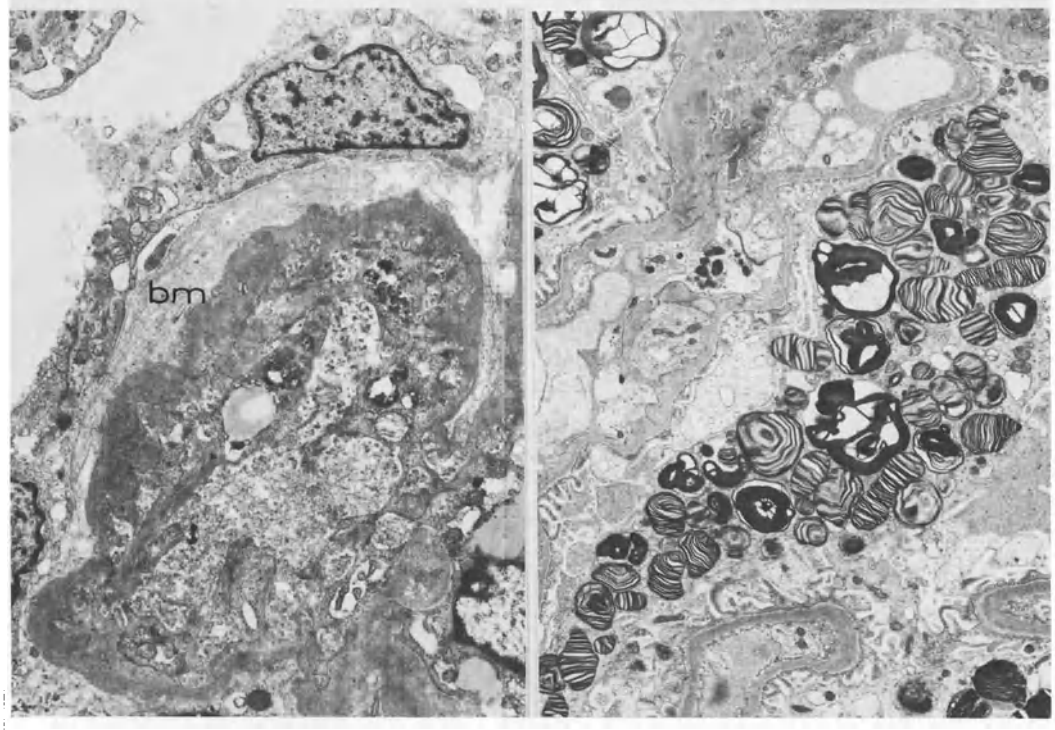

27 28

Fig. 26. Minimal change disease. Fusion of the foot processes of epithelial cell (Ep) (×14,000). Inset: high magnification of foot processes. The remaining slit diaphragms are either lacking or multilayered (arrow) (×6,400).
Fig. 27. Focal glomerulosclerosis. Epithelial cells (Ep) are severely damaged and under them new layers of basement membrane (bm) appear (×6,400).
Fig. 28. Fabry's disease. Typical Zebra bodies into the lysosomes of epithelial cells (×3,900).

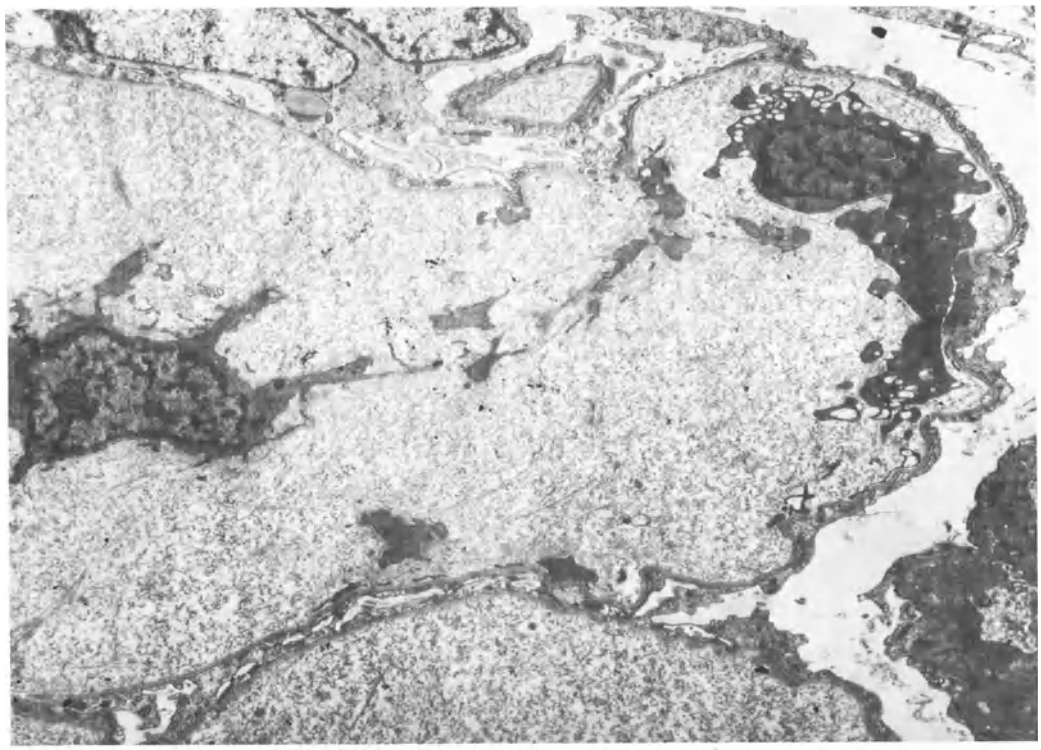

Fig. 29. Proliferative glomerulonephritis. The mesangial matrix appears completely dissolved and mesangial cells are free into proteinaceous material (×4,100).

such a population represents about 2% of the mesangial cells.

Little is known about the factors controlling the access of circulating macromolecules to the mesangium and the elimination of the products filtered and possibly degraded in the mesangium. Moreover, the stimuli which induce the increased synthesis of matrix by mesangial cells must still be examined more thoroughly.

Electron microscopy, which has definitively demonstrated the existence of this third population of glomerular cells, up to this moment seems of limited help in the diagnosis of mesangial changes. Such changes, being more of quantitative than of qualitative nature, can be studied easily by the traditional histology, whereas the evaluation of immune deposits can more properly make use of immunohistochemical techniques.

Apart from the presence of immune deposits, alterations of the mesangial matrix structure are the presence of amyloid fibrils in amyloidosis, fibrotubular structures in nodular glomerulosclerosis (diabetes and others), and collagen fibers in chronic glomerulopathies.

Mesangiolysis may occur, indicating the disintegration of the mesangial matrix with oedema and accumulation of proteinaceous material within the matrix and the subendothelial space, which appears enormously enlarged. The basement membranes lose their anchorage on the mesangial axis and form capillary aneurysms full of blood cells. The mesangial cells degenerate rapidly. Phenomena of mesangiolysis (Fig. 29) can be observed in various inflammatory glomerulopathies and others (acute and chronic glomerulonephritis, radiation nephritis, thrombotic microangiopathies, transplant, diabetes). Such alterations may possibly lead to glomerulosclerosis.

Conclusions

In the years to come, the ultrastructural investigation will certainly lead to new and important informations in the study of renal biopsies. It will in fact be able to make use of new associated techniques, such as refined cytochemistry and immunocytochemistry, freeze-fracturing, x-ray microanalysis and other methods which are being developed. This will allow a more and more precise correlation between morphology and function.

References

1. Haynes VDG: The normal human renal glomerulus. Virchows Arch (Cell Pathol) 35: 133–158, 1981.
2 Grimley PM, Barry DW, Schaff Z: Induction of tubular structures in the endoplasmic reticulum of human lymphoblastoid cells by treatment with 5-bromo-2′deoxyuridine. J Natl Cancer Inst 51: 1751–1755, 1973.
3. Steffes MW, Barbosa J, Basgen J, Sutherland DER, Najarian JS, Mauer SM: Quantitative glomerular morphology of normal human kidney. Lab Invest 49: 82–86, 1983.
4. Martinez-Hernandez A, Amenta PS: The basement membrane in pathology. Lab Invest 48: 656–677, 1983.
5. Thompson NM, Holdsworth SR, Glasgow EF, Atkins RC: The macrophage in the development of experimental glomerulonephritis. Am J Path 94: 223–240, 1979.
6. Parthasarathy N, Spiro RG: Effect of diabetes on the glycosaminoglycan component of the human glomerular basement membrane. Diabetes 31: 738, 1982.
7. Habib R, Gubler MC, Hinglais N, Noël LH, Droz D, Levy M, Mahieu P, Foidart JM, Perrin D, Bois E, Grunfeld JP: Alport's syndrome: experience at Hôspital Necker. Kidney Int 21: S20–S28, 1982.
8. Hill GS, Jenis EM, Goodloe S: The nonspecificity of ultrastructural alteration in hereditary nephritis. Lab Invest 31: 516–532, 1974.
9 Spear GS: Alport's syndrome: A consideration of pathogenesis. Clin Nephrol 1: 336–337, 1973.
10. Olson DL, Anoud SK, Landin BH, Heuser E, Grushkin CM, Lieberman E: Diagnosis of hereditary nephritis by failure of glomeruli to bind anti-glomerular basement membrane antibodies. Pediatrics 96: 697–699, 1980.
11. Magil A, Chase W. Frohlich J: Unusual biopsy findings in a patient with familial lecithin-cholesterol acyltransferase deficiency. Hum Pathol 13: 283–285, 1982.
12. Hoyer JR, Michael AF, Vernier RL: Renal disease in nail-patella syndrome. Clinical and morphological studies. Kidney Int 2: 231–238 1972.
13. Törnroth T: The fate of subepithelial deposits in acute poststreptococcal glomerulonephritis. Lab Invest 35: 461–474, 1976.
14. Hinglais N, Garcia-Torres R, Kleinknecht D: Long-term prognosis in acute glomerulonephritis. The predictive value of early clinical and pathologic features observed in 65 patients. Am J Med 56: 52–60, 1974.
15. Strife CG, McEnery PT, Mac Adams AJ, West CD: Membranoproliferative glomerulonephritis with disruption of the glomerular basement membrane. Clin Nephrol 7: 65–72, 1977.
16. Preud'Homme JL, Mihaesco E, Guglielmi P, Morel-Maroger L, Ganeval D, Danon F, Brouet JC, Miahesco CM, Seligmann M: La maladie des dépôts de chaînes légères ou d'immunoglobulines monoclonales: concepts physiopathogéniques. Nouv Presse Med 11: 3259–3263, 1982.
17. Kim Y, Vernier RL, Fish AJ, Michael AF: Immunofluorescence studies of dense deposits disease. The presence of railroad tracks and mesangial rings. Lab Invest 40: 474–480, 1979.
18. Droz D, Noël LH, Nabarra B, Leibovitch: The dense deposits disease of the renal basement membranes. Renal Physiol 3: 415–417, 1980.
19. Feiner H. Gallo G: Ultrastructure in glomerulonephritis associated with cryoglobulinemia: a report of six cases and review of the literature. Am J Pathol 88: 145–162, 1977.
20. Dikman SH, Churg J, Kahn T: Morphologic and clinical correlates in renal amyloidosis. Hum Pathol 12: 160–169, 1981.
21. Hsu H-C, Churg J: Glomerular microfibrils in renal disease: A comparative electron microscopic study. Kidney Int 16: 497–504, 1979.
22. Pak Poy RKF: Electron microscopy of amphibian renal glomerulus. Austr J Exp Biol Med Sci 35: 583–593, 1957.
23. Zucchelli P, Casanova S., Sasdelli M, Cagnoli L, Pasquali S: Correlation of proteinuria and ultrastructural glomerular changes in toxaemia of pregnancy. In: Functional ultrastructure of the kidney. Maunsbach AB, Olsen TS, Christensen EI (eds) Academic Press New York, 1980, pp 151–161.
24. Seefeldt T, Bohman O, Jørgen HJ, Gundersen G, Maunsbach AB, Posborg Petersen V, Olsen TS: Quantitative relationship between glomerular foot process width and proteinuria in glomerulonephritis. Lab Invest 44: 541–546, 1981.
25. Kanwar JS, Rosenzweig LJ, Jabubowski ML: Distribution of the novo synthesized sulfated glycosaminoglycans in the glomerular basement membrane and mesangial matrix. Lab Invest 49: 216–225, 1983.

CHAPTER 12

Dialysis

MICHAEL I. SORKIN

1. Introduction

Progressive chronic renal failure was uniformly fatal twenty years ago. Now patients need not die of renal failure. Not because we have a cure for the underlying disease but because we have the technology to replace renal function. When renal failure progresses to its end stage, life can be maintained by dialysis or transplantation. Over the past decade many important changes have improved the treatment of these patients with End Stage Renal Disease (ESRD). I have selected only a few of these new dialysis-related techniques for discussion. I have tried to choose topics that either have had a recent important impact on ESRD treatment, should have an important impact, or are interesting enough to be discussed regardless of impact.

Continuous Ambulatory Peritoneal Dialysis (CAPD) is clearly the most important innovation in the dialysis treatment of patients with end stage renal disease. It's simplicity has led to a marked increase in the home dialysis population. This 'steady state' dialysis provides excellent middle molecular clearance, good blood pressure control, increase dietary flexibility and patient mobility. CAPD does suffer from the risk of peritonitis and lower small molecule clearance than hemodialysis.

Hemofiltration (also known as hemodiafiltration) looks like hemodialysis but is not dialysis. It depends on the convective transfer of solute produced by high rates of ultrafiltration across a special membrane to remove metabolic waste products. The advantages of hemofiltration include better middle molecule removal, less side effects than hemodialysis and better blood pressure control.

The recent introduction of continuous arteriovenous ultrafiltration provides an interesting 'continuous' form of hemofiltration, especially adaptable to the acute intensive care setting. This technique depends on the patient's own arterial pressure to drive blood through highly permeable membrane to produce continuous ultrafiltration over relatively long periods of time – on the order of several days for each treatment. Although best for fluid removal, continuous arterio-venous ultrafiltration can be used to treat patients with renal failure if enough ultrafiltration is produced.

2. CAPD

2.1. Development

CAPD was first reported in 1976 but its widespread clinical use began in 1978. At that time Medicare recognized this therapy as a variant of peritoneal dialysis and agreed to reimburse dialysis centers and physicians for its use in the United States. In this short period of time CAPD has enjoyed an incredible growth. More than 20,000 patients will be using this form of treatment worldwide by the time this book goes to press. It is the single most important factor in the growth of home dialysis in the United States and now accounts for most of home dialysis training. At least 50% of patients currently 'at home' on any form of dialysis therapy use CAPD.

CAPD was devised to meet the needs of a single patient who could no longer be treated with hemodialysis because he had no vascular access. By applying existing knowledge of ultrafiltration and solute transfer across peritoneal membranes, calculations indicated that five 'exchanges' per day would keep a functionally anephric patient healthy [1]. Clinical trials, beginning in late 1976 and early 1977, suggested that four exchanges per day were optimal for most patients [2]. By late 1977 the introduction of dialysis solutions in plastic bags made this procedure safer and more convenient [3]. The major advantages of CAPD are its extreme simplicity (which allows more patients to go to home dialysis) and its 'steady state' characteristics which allow continuous solute removal and ultrafiltration (which are com-

L.J.A. DiDio and P.M. Motta (eds), Basic, Clinical, and Surgical Nephrology. ISBN 0-89838-689-5.

patible with easy adjustment to individual diets). The major risks are peritonitis and infection around the peritoneal access device. Only now do we have enough data to begin to draw some preliminary conclusions as to the efficacy and effectiveness of CAPD so that we can place it in its proper relationship with other modes of therapy, especially hemodialysis.

2.2. CAPD technique

Until the introduction of CAPD in 1976, all efforts to improve peritoneal dialysis systems centered around attempts to improve dialysis efficiency by increasing dialysis solution flow rates. Under conditions of virtually continuous peritoneal lavage some investigators were able to achieve peritoneal urea clearances in the range of 40 ml/min. The combination of efficiency, coupled with economic factors, led to the relatively standard use of exchanges consisting to two liters every half hour or a dialysis flow rate of 67 ml/min. This system is only possible using automated or semi-automated devices since the nursing time required for manual exchanges would be prohibitively expensive. Most Intermittent Peritoneal Dialysis (IPD) patients are maintained on 36 to 40 hours of dialysis per week – usually divided into two 20-hour segments twice weekly or 12-hour treatments thrice weekly. Automated systems made it possible for patients to perform their own dialysis treatment overnight at home without a helper. With the fully automated systems the complication rate is low and peritonitis is a relatively minor problem. The introduction of the chronic peritoneal dialysis catheter by Tenckhoff in 1968 made peritoneal access simple and relatively trouble free [4].

In 1976, Popovich and Moncrief reported a novel approach to improving peritoneal dialysis [1]. It took advantage of the relative inefficiency of the peritoneal dialysis system. They proposed that the patient be dialyzed continuously (24 hours/day, seven days/week) using 'long dwell exchanges'. The patient would perform his own exchanges by infusing two liters of dialysis solution, allowing it to dwell between four to eight hours, then allowing it to drain – all by gravity using no automated equipment. The patient could perform these exchanges virtually anywhere given reasonably clean controlled surroundings and appropriate sterile technique. These long dwell exchanges resulted in low dialysis solution flow rates – between six and eight ml/min. The original calculations indicated that the very long dialysis times – 168 hours/week – would more than make up for the low dialysis solution flow rate inefficiency. Sometimes called equilibrium dialysis or steady state dialysis, the system depends on the fact that small molecules (including urea 60 daltons and creatinine 113 daltons) are nearly completely equilibrated between four to six hours but that larger molecules such as B_{12} (1355 daltons) or inulin (5500 daltons) reach equilibrium much more slowly. Clearances calculated on a weekly basis rather than on a minute basis indicated that the removal of small molecules is better than the usual intermittent peritoneal dialysis clearances but not quite as good as hemodialysis clearances. Removal of middle molecules (500 to 5,000 daltons) is considerably better than both IPD and hemodialysis. Only hemofiltration rivals CAPD for middle molecule removal (see Table 1). Although the original description of CAPD required five exchanges per day, clinical practice now suggests that average patients can be maintained on only four exchanges a day depending on residual renal function and diet. Timing of exchanges is not critical and patients are able to regulate the dialysis program around daily activities. Since dialysis is occurring at all times (except when the patient is draining solution from his peritoneal cavity or infusing new solution into his peritoneal cavity) blood chemistries are maintained at a steady state concentration rather than exhibiting the sawtooth pattern seen with the intermittent forms of dialysis. Fluid and sodium removal are continuous and, therefore, blood pressure regulation tends to be better than with intermittent dialysis. Dietary planning is much simpler since the patient has the flexibility provided by the ability to alter his dialysis solution four times a day rather than having to wait a day or two until his next dialysis treatment to remove extra sodium or water.

No machines are involved and the operation of the system is virtually as simple as changing a plastic intravenous solution bag. The patient does have to wear the empty bag along with the solution administration set (called a transfer set or simply 'tubing') at all times. Usually the patient becomes quite adept at concealing this relatively small mass so that it is not noticeable to the uninitiated.

This CAPD system gives the patient more mobility than any other dialysis system. The time required

Table 1. Solute clearance (liters/week).

	Urea	Creatinine	B_{12}	Inulin
Hemodialysis	135	90	90	5
CAPD	70	60	50	30
Hemofiltration	70	70	70	65

(Figures are approximate for comparison purposes.)

to 'do an exchange' (drain, change bags, fill) is about 30 minutes, but the patient is only actually occupied for the 10 minutes it takes to change the bag of spent dialysate for a fresh bag. Care of the catheter exit site is usually performed in the shower with a daily soap and water or povidone-iodine scrub. A well healed exit site requires no dressing. Most CAPD system suppliers will ship supplies directly to alternate addresses so the patient does not have to carry bags on vacation or for business trips.

2.3. CCPD

Continuous Cycler-assisted Peritoneal Dialysis (CCPD) is a variant of CAPD [5]. Instead of four exchanges performed by the patient during the waking hours, the CCPD technique uses a semi-automated system to perform the exchanges while the patient sleeps. The nighttime hours are divided into three or four long dwell two-liter exchanges – each between two and three hours. Dialysis solution in standard, commercially available plastic bags is placed on the cycler. Multi-pronged tubing connects the bags through a manifold to a single patient inflow line. The patient inflow line is connected to the patient's peritoneal dialysis catheter in the evening before bedtime. The cycler automatically warms the solution, delivers it to the patient by gravity, times the dwell and outflow and monitors the system for failures or unsafe situations. When the patient arises in the morning, he drains the last two liters from his peritoneal cavity, infuses two additional liters and disconnects from the cycler tubing. He is free from dialysis-related activity for the day but is still being dialyzed by the the two liters of dialysis solution which remains in his peritoneal cavity from the time he disconnected to the time he reconnects to the cycler tubing in the evening. CCPD is usually performed seven days a week and thus qualifies as a continuous form of dialysis.

The advantage of CCPD is that the patient is not required to take time out during the day to 'do exchanges'. The disadvantage is that he is dependent on a machine and the machine is not very portable.

CCPD is slightly less effective than CAPD at removing water and unwanted solutes but still superior to intermittent peritoneal dialysis. The inefficiency of the daytime 14-hour long dwell exchange is partly offset by the more efficient two to three nighttime exchanges.

The risks in CCPD are the same as for CAPD. The major problem is peritonitis. Recent figures from the National CAPD Registry indicate that peritonitis rates for CCPD are about the same as for CAPD [12]. The number of CCPD patients followed by the National CAPD Registry are small (about 350) compared with CAPD (over 8,000) so the CCPD statistics must be interpreted with caution.

The cost of CCPD is higher than for CAPD because the tubing sets are more complicated and thus more costly, plus the cycler cost must be added to the total. Technological changes already in the development phase promise to simplify the system and reduce the cost so that it is comparable to CAPD.

A very intriguing possibility is to train a patient for both CCPD and CAPD. This would allow a normal working day free of CAPD procedure but the option to travel, leaving the cycler at home, and using CAPD. Most nephrologists have been reluctant to offer this option because the success of each technique depends in part on the constant practice that comes from exclusive use of one technique. With standard connectors compatible with both systems and simpler cycler systems, this CAPD–CCPD combination may become more popular.

2.4. Advances in understanding peritoneal physiology

Investigation into the physiology of long dwell exchanges has expanded our understanding of peritoneal physiology greatly. Basic clinical studies of the kinetics of long dwell exchanges have complimented the classic studies of short dwell exchanges. Instead of looking at the efficiency of the system or ways to increase clearance of solute, we must now look at the inefficiency of the system and the total solute removed. The end result of both systems is the same – the removal of enough metabolic waste products and water to maintain the patient in reasonable health.

Of the three components involved in any dialysis system – blood flow, peritoneal membrane, and dialysate flow – blood flow is the least limiting factor in the peritoneal dialysis system. Blood flow may be significantly reduced without significant change in solute clearance. An unexpected finding of early CAPD investigations was the fact that the addition of commercially available solutions actually optimizes peritoneal blood flow by increasing the number of capillaries perfused [6]. From laboratory investigation this appears to be the result of a combination of osmolality and the buffer used in the peritoneal dialysis solution [7].

If we consider the peritoneal membrane as beginning with the capillary endothelium and ending at the mesothelial cell layer, the membrane thickness is considerable. Measurements indicate that the aver-

age peritoneal membrane thickness is about 100 microns. This distance plus the characteristics of the membrane provide a significant resistance to the movement of both large and small molecules but is most noticeable in molecules of relatively small size – like urea and creatinine. Because most molecules do not move through cell bodies rapidly, the surface area available for moleculer movement through the capillary wall most likely occurs between cell bodies – through the intercellular space. This space accounts for an area available for filtration which is probably about 0.2% of the total capillary surface area of the peritoneal membrane. The width of intercellular spaces is great enough so that it does not impose any selection for molecular size. Access to the basement membrane is not increased by endothelial cell fenestrae as in the glomerular capillary.

Certain 'vasoactive' substances can increase solute transfer from capillary lumen to dialysis solution. Since we believe that blood flow is virtually optimal using commercial peritoneal dialysis solutions, a phenomenon other than increased blood flow must be sought to explain the observation of increased solute clearance using these substances. Experiments using the intravital microscope indicate that changes in permeability of the venular end of the capillary arcade may be important in controlling solute transfer – especially large molecular transfer. Topical application of histamine has been shown to selectively increase the intercellular gaps of the venules while causing no change in the intercellular gaps in the capillaries or arteriolar end of the capillary arcade [8]. Topical application of sodium nitroprusside selectively increases the diameter of the venule [6]. These test substances (intraperitoneal sodium nitroprusside and histamine) appear to act by effects on the venule rather than by changing blood flow, even though they are primarily known for their generalized vasodilatory effects.

Thusfar, these findings provide a tool for laboratory investigation but have not been useful clinically for several reasons. First, the agents tend to increase large molecule clearance to a greater extent than small molecule clearance. This is not necessary for CAPD patients since they appear to achieve more than adequate large molecule clearance. Second, in the long dwell exchange systems, small molecule equilibration is nearly complete before draining the fluid from the peritoneal cavity. Enhanced permeability of the peritoneal membrane for these molecules does not result in significantly greater solute removal.

Movement of solute and water across the peritoneal membrane appears to be governed only by passive forces. There is no evidence that active transport plays an important role. The mesothelial surface of the peritoneal membrane may be an important limiting factor in this dialysis system. Although little is known about the normal function of the peritoneal mesothelium, agents which affect the mesothelial cells have been shown to increase the permeability of the peritoneal membrane. Thus, the application of protamine, mechanical damage caused by drying and the damage caused by bacterial infection all cause a spectrum of damage ranging from a small increase in intercellular gaps to total mesothelial denudation [9, 10]. These changes are clearly associated with increased peritoneal permeability. Thus far, it has been impossible to totally separate the effects these agents may have on vascular permeability from their effects on mesothelial permeability but correlation of histologic changes of damaged mesothelium with permeability changes in the peritoneal membrane is striking.

Large molecular clearance is most likely increased by agents that increase intercellular spaces since they do not easily pass across cell membranes. Small molecule movement may be affected by agents that change to microtubular structure of the mesothelial cells or by calcium channel blockers as well as changes in the distance between cells since some small molecules do cross cell membranes.

In the peritoneal dialysis system, increased efficiency can be obtained by increasing dialysis solution flow rates. The greater the flow the greater the average concentration gradient. Thus, the system gains an advantage from increasing diffusive movement of solute. Even under very high solution flow rates the clearance of small molecules does not achieve the clearance rate expected from our knowledge that the average peritoneal blood flow through the capillary is about 70 to 100 ml/min. This limitation in clearances is probably imposed by the peritoneal membrane thickness and characteristics. Calculation of clearances under optimal conditions with the largest gradient possible have been used to characterize peritoneal membrane permeability. This factor is known as the mass transfer area co-efficient (MTAC) [11]. This is somewhat analogous to the ultrafiltration co-efficient used in renal physiology. It is determined by the product of the peritoneal surface area and peritoneal permeability. Stated another way, it is the maximum clearance of a given solute under optimal conditions. Although it is useful in the laboratory, it is relatively difficult to measure and has not been commonly used in the clinical setting.

In long dwell systems like CAPD, dialysis solution

flow rates are so low that for most small solutes they are only a fraction of the maximum achievable clearances and, therefore, dialysis solution flow rate is a factor limiting the clearance of small molecules. Since almost complete small molecule equilibration occurs before the solution is drained, the clearance cannot be greater than the dialysate flow regardless of theoretical maximum rate. Total dialysis solution flow rate for a week of CAPD is still only about half the dialysis solution flow rate for the standard weekly IPD treatment of 40 hours (70 liters and 160 liters respectively). Fortunately, the prolonged time and greater equilibration more than makes up for the deficit in flow rate. Overall clearances of all molecules are better in the CAPD system than in the IPD system [11].

2.5. National CAPD registry

The progress of CAPD in the United States is being monitored by the National CAPD Registry sponsored by the National Institutes of Health. The development of CAPD, expecially in the United States, has been unusually well controlled. Clinical trials at the University of Missouri which expanded the initial experiences of the CAPD system designers in Austin, Texas occurred under the auspices of the NIH. The current Registry grew from data collected during the early CAPD pilot studies beginning in 1977. Some measure of control over the development of the technique – limiting it to centers of known expertise – was maintained by the Health Care Finance Administration agreement to reimburse only centers selected by the NIH. The rapid growth of CAPD occurred after the Health Care Finance Administration modified its reimbursement regulations in September 1978 to include CAPD as a reimbursable variant of peritoneal dialysis. Although the National Registry was intended to be much more comprehensive than its final form allowed, this project does collect demographic information, infection experience (including tunnel and exit infections as well as peritonitis), mortality figures, reasons for leaving CAPD, and hospitalization figures. The Registry has officially been in existence since January 1, 1981 and currently has more than 8,000 patients registered for about 260 participating centers. Participation is entirely voluntary.

CAPD is an effective form of dialysis therapy. Because there is no reporting system for hemodialysis data in the United States at the present time, it is difficult to make comparisons between CAPD and hemodialysis. According to the recent National CAPD Registry, the mortality rate for all CAPD patients followed at one year is 15% and for 18 months 21% [12]. When ideal patients are segregated out – those without diabetes and between the ages of 20 and 50 – the mortality rate is only 7% at one year and 9% at 18 months. CAPD-related problems account for only about 1/3 of the hospitalization days although CAPD patients tend to spend an unusually large number of days in the hospital – averaging 26 days per patient/year. Hospitalization rates are higher for older patients and diabetics and tend to be lower for otherwise healthy young patients. It is interesting to note that the hospitalization rate is higher in patients with diabetic nephropathy but CAPD-related hospitalizations are no greater than in non-diabetic groups. The greater incidence of cardiovascular disease in diabetic patients accounts for the difference. Evidence indicates that diabetics have no greater likelihood of peritonitis or catheter-related infections.

2.6. Peritonitis

Peritonitis remains the single most important peritoneal dialysis complication. It accounts for the greatest number of patients transferring from CAPD. Peritonitis has been relatively stable at about 1.7. episodes of peritonitis per patient year since the national CAPD Registry began reporting. More sophisticated statistical tools are now applicable since we have been following a large enough population from the time they began CAPD. Life table analysis of Registry data is now being used to predict the probability of a certain event occurring. For instance, the probability of a CAPD patient developing peritonitis after six months on CAPD is 40%. At the end of one year 68% of the patients will have had one episode of peritonitis. Put in a slightly different way the likelihood of remaining free of peritonitis at one year is 32%. This is not to say that patients cannot remain free of peritonitis. About 50% of patients will not have peritonitis during any given year. 25% of the patients account for 75% of the infections!

It is important to note that most episodes of peritonitis do not present with the same intensity we expect from the non-peritoneal dialysis patient experience. Rather, the training program teaches the patient to try to make the diagnosis before symptoms strike by observing each bag of dialysate for turbidity. Many times the 'cloudy bag' is the only indication of peritonitis. Some patients experience a mild flu-like syndrome accompanied by abdominal pain. The diagnosis is made by the observation of signs and symptoms compatible with peritonitis and/

or the development of a cloudy dialysate – this, in fact, usually precedes the development of symptoms. The patient is instructed to call his CAPD center as soon as cloudy dialysate is observed.

If the patient is treated within a reasonable amount of time – usually several hours from the time turbid dialysate is detected – the majority of patients will not require hospitalization and will experience relatively little in the way of discomfort. Patients are generally trained to administer their own antibiotics in the peritoneal dialysis solution and are followed closely by telephone at home. If the dialysis solution does not clear or if symptoms persist or worsen in the first 12 to 24 hours the patient is then admitted to the hospital. Of course, if the patient is unusually symptomatic or the physician is concerned for any reason on initial examination, the patient is admitted to the hospital.

Cloudy fluid usually coincides with a peritoneal dialysate leukocyte count of greater than 100 white blood cells per microliter with more than 50% neutrophils. Bacteria can be seen on a centrifuged dialysate sample about 50% of the time. Cultures grow an organism more than 80% of the time. Gram positive cocci are cultured from 70% of the episodes. Of that 70%, two-thirds are Staph Epidermidis and one-third Staphlococcus Aureus. Standard cephalosporins, either intraperitoneally or in combination with an intravenous leading dose, are quite effective in controlling these infections. Recently the convenience of the long half life of vancomycin, plus its superior coverage of Staph Epidermidis, has made it the first line drug in many centers. Like the cephalosporins, vancomycin may be administered in the appropriate doses intraperitoneally or intravenously. With either route of administration appropriate concentrations are achieved at the infection site as well as in the blood [13, 14]. The preferred treatment for peritonitis is to continue the long dwell exchanges rather than making attempts to do continuous peritoneal lavage. Initial treatment does require two or three short dwell exchanges to reduce symptoms and reduce the likelihood that the catheter will be obstructed by the fibrin or proteinaceous exudate caused by the peritonitis. It appears that the long dwell exchanges are superior in controlling peritonitis because the leukocyte function is more normal during more of the dialysis cycle. The dialysis solution when first instilled has a pH of 5.5 and osmolality greater than 400. Within a relatively short time, however, the pH becomes physiologic and the osmolality falls to levels that are more compatible with leukocyte phagocytosis. Abdominal discomfort is usually gone within one to two doses of antibiotics and peritoneal leukocyte counts usually return to normal within three to five days. Patients very rarely experience bacteremia as a result of these episodes [2].

Since peritonitis can be caused by organisms entering the peritoneal cavity across the bowel rather than through the peritoneal catheter, great care must be taken to insure the diagnosis of peritoneal dialysis-induced peritonitis is correct. The finding of gram negative organisims, organisms other than gram positive cocci, or multiple organisms arouses the suspicion that this is not a 'run of the mill' peritonitis. Since the mortality from a perforated bowel and peritonitis is quite high under the best of circumstances and is even higher in patients with renal failure, aggressive treatment must be pursued if a perforated viscus is suspected.

Most centers have some fixed protocol to help determine whether the patient should remain on CAPD or would be better treated by changing modalities. One example, commonly in use, would be the occurrence of more than three episodes of peritonitis in six months. Should a patient exceed these criteria, many centers would transfer the patient to hemodialysis because we believe the risk of unusual organisms (including fungi and yeast) increases as the number of episodes of peritonitis and the number of courses of antibiotics increases.

2.7. Nutrition

An important consideration in maintaining the health of patients in general, and especially CAPD patients, is carefull attention to nutrition, Patients on peritoneal dialysis do lose 6 to 8 grams of protein in the dialysate daily. This protein loss is increased during peritonitis. A dramatic fall in total protein and serum albumin concentrations may occur during an episode of peritonitis. One reason for changing from CAPD or excluding a patient from a CAPD program is protein malnutrition. Patients with low plasma proteins or those who fail to improve their nutritional status and are unable to achieve positive nitrogen balance are best treated by other techniques. To that end, maintenance diets for CAPD patients usually include 1.2 grams of protein per kilogram per 24 hours – considerably more protein than most physicians prescribe for patients in renal failure [15].

An advantage of the CAPD system is the absorption of calories in the form of glucose across the peritoneal cavity from dialysis solution to blood. This may account for the considerable increase in calorie intake which is an important part of the de-

velopment of positive nitrogen balance. This increased energy absorption results in improved growth rates reported in children on CAPD compared with children on IPD or hemodialysis. Unfortunately, glucose absorption has the side effect of causing marked weight gain in many CAPD patients [2].

3. Hemofiltration

3.1. Theoretical aspects

The hemofiltration system depends on the convective movement of solutes driven by ultrafiltration to remove accumulated water and metabolic waste products in patients with end stage renal disease [16]. Diffusion is not involved, therefore, solute removal is controlled only by the membrane characteristics and solute concentration in the plasma. This is in contradistinction to dialysis which depends on membrane characteristics, concentration, and molecular size because diffusion is more important than convection for solute removal. The theoretical advantage of hemofiltration is better removal of middle moleculer weight solutes than achieved by hemodialysis. In return, hemofiltration results in clearances of small molecules somewhat less than achieved by hemodialysis. Large molecules are not removed to any appreciable extent in either the hemodialysis or hemofiltration system. No dialysis solution is used for hemofiltration. The process depends on a high rate of ultrafiltration across a special membrane to achieve clearances capable of sustaining relatively normal life.

The success of the system depends on a membrane that is capable of high water flux driven by transmembrane pressures that are clinically achievable. A second important part of the system is the production of sterile replacement solution so that the patient maintains a normal blood volume during the procedure. The rate of ultrafiltration and replacement of fluid is balanced carefully so that the net fluid loss during the treatment approximates the amount of weight the patient gained between treatments.

The safest and most cost effective techniques use inline filtration to make the replacement fluid free of micro-organisms and pyrogens [17]. This inline filter has characteristics similar to the membrane used for the hemofilter. Usually fluid replacement in the range of 20 to 40 liters is required during each treatment. The composition of the replacement is very similar to standard dialysis solutions.

The formation of ultrafiltrate depends on the net transmembrane pressure – as in any ultrafiltration system. This means that high rates of filtration result in increasing protein concentration on the plasma side of the membrane and, therefore, increasing oncotic pressure which retards ultrafiltration. When filtration equilibrium occurs – when oncotic pressure retarding ultrafiltration equals hydraulic pressure favoring ultrafiltration – filtration stops. This system is exactly analogous to the dynamics of ultrafiltration occurring in the glomerulus of a normal kidney. Of course, no tubular functions are performed by the hemofilter and, therefore, solute reabsorption does not occur. Substances moving with the ultrafiltrate are discarded.

Fluid balance can be achieved by adding the replacement solution to blood as it leaves the hemofilter (called post-dilution hemofiltration) or it may be added as the blood enters the hemofilter (called pre-dilution hemofiltration). Post-dilution has the advantage that solute concentration of the ultrafiltrate is the same as in plasma water. The disadvantage is that rapid increase in protein concentration limits the ultrafiltration rate. On the other hand, pre-dilution results in a greater ultrafiltration rate but lowers the solute concentration in the blood being hemofiltered. These two methods would seem to have similar results but careful clearance studies indicate that optimal results are obtained by using pre-dilution hemofiltration with maximum blood flow and maximum transmembrane pressure [18]. However, the optimal treatment must be tempered by practical considerations. High blood flow may not be possible. The pre-dilution technique requires considerably more fluid replacement than post-dilution. Therefore, the cost of preparing the infusion solutions is an important factor. Generally, the solutions prepared using online filtration result in relatively little cost differences and pre-dilution hemofiltration may be the preferred method [18].

3.3. Technical aspects

The hemofiltration system requires two components. The first is essentially the same as the hemodialysis system. Blood must be pumped from the patient through the hemofilter and back to the patient. Appropriate monitoring units must be included to prevent air embolism and provide for heparin infusion along with appropriate pressure monitors.

Although the system does not require a dialysis solution delivery system, it does require a system to make the replacement solution and regulate the rate

of infusion of this solution so that the patient does not die of volume overload or volume depletion. This is usually accomplished by using two pumps. One pump regulates the rate of replacement solution infusion and a second pump creates a negative pressure on the hemofilter to drive the ultrafiltration. The hemofiltration machine measures the ultrafiltrate, computes the net ultrafiltration pressure, adjusts the speed of the ultrafiltration pump to maintain a pre-set ultrafiltration pressure and regulates the rate of replacement solution infusion so that a pre-set net volume is removed from the patient. The length of the treatment generally is determined by the total amount of ultrafiltrate to be removed. Under the best circumstances this volume loss should be accomplished smoothly throughout the duration of the treatment. The high flux membranes and large amounts of replacement solutions required make this a delicate sounding procedure. Currently available equipment, however, has performed amazingly well.

3.3. Current role of hemofiltration

At the time this book goes to press, hemofiltration is still considered an experimental treatment in the United States with only a few centers performing this procedure on a regular basis. It has found somewhat wider acceptance in Europe.

The two major advantages of hemofiltration over hemodialysis are: 1) lower incidence of intradialytic symptoms, and 2) better control of diastolic blood pressure. Reports consistently indicate that patients on hemofiltration experience fewer episodes of hypotension and muscle cramps. Comparison of hemodialysis and hemofiltration consistently shows lower post dialysis diastolic blood pressures in the hemofiltration group [19, 20]. Inspite of the huge amount of fluid required for replacement, problems with septicemia and infection appear to be no greater than those experienced with hemodialysis patients. Mortality and morbidity rates are similar among hemofiltration patients, hemodialysis patients and CAPD patients [19, 20]. The commonest cause of death still remains cardiovascular disease.

4. Continuous arteriovenous hemofiltration

This amazingly simple system utilizes a hemofiltration membrane (more permeable than the standard hemodialysis membrane) to remove an ultrafiltrate of plasma driven usually by the patient's own blood pressure. It requires the cannulation of an artery, heparinization of blood which is passed through this special 'filter', and the return of blood to the patient through a large vein. It does not involve dialysis since no dialysis solution is involved.

Fluid and solute are removed purely by the procedure of ultrafiltration. Since the fluid removed is an ultrafiltrate of plasma, it contains most of the constituents of plasma in the same concentration as plasma water with the exception of very low concentrations of a very large moleculer weight substances or substances that are highly protein bound. The membrane used is more permeable to middle molecules (between 500 and 5,000 daltons) than standard cellulosic membranes and, therefore, yields better clearances of these molecules. Since ultrafiltration is driven by net filtration pressure, even relatively small blood flows (in the range of 30 to 90 ml/min) can result in reasonable rates of ultrafiltration and, therefore, successful treatment. Continuous hemofiltration was initially proposed for the removal of fluid in unstable patients who are 'poor' candidates for hemodialysis or peritoneal dialysis. If large enough volumes of ultrafiltrate are formed like standard hemofiltration (see Section 3), enough metabolic waste products may be removed to control azotemia, hyperkalemia and acidosis in those patients with renal failure. The secret, like CAPD, (see Section 2) lies in the length of the treatment.

Access to the vascular system may be obtained in any of the ways commonly used for hemodialysis. The presence of a functioning arteriovenous fistula or vascular graft placed for hemodialysis provides an easy entry to remove 'arterial' blood under relatively high pressure. A Scribner-type shunt may also be placed to obtain access to arterial blood. If one of these high pressure access points is not available, an artery must be cannulated since subclavian vein or femoral cannulation will not supply adequate pressure to drive ultrafiltration unless a pump is inserted in the circuit.

Blood must be returned to the patient through a low resistance, low pressure vessel since the higher the ultrafiltration pressure the greater the rate of ultrafiltration. This means that the return site for a patient with a existing hemodialysis arteriovenous fistula or vascular graft must be in a vein at a site distant to the hemodialysis access so that it is of lower pressure. The Scribner arteriovenous shunt that uses a cannula inserted in both an artery and a vein, usually in the foot, is an ideal access for this system. If a large caliber artery is cannulated virtually any peripheral vein that is accessible can be used for venous return.

This system has been used with a blood pump to

augment blood flow and pressure thus providing a greater efficiency in ultrafiltration. The tendency at the present time is to take advantage of the simplicity afforded by the system without a blood pump. This allows the system to be used in settings where the personnel are not trained in the use of hemodialysis techniques.

The filter is very much like the hollow fiber dialyzer in standard use in hemodialysis units today. Heparin must be infused to prevent clotting in the hemofilter. A loading dose of heparin is given to the patient through the 'arterial' side of the hemofilter, then a continuous infusion of heparin is adjusted to maintain clotting times in the desired range. As with standard hemodialysis, the coagulation can be closely monitored and adjusted to provide little increased risk of bleeding during the procedure.

The volume of ultrafiltrate formed is monitored and replacement solutions are adjusted to provide the desired volume loss over the period of hemofiltration. Since no dialysis solutions are involved, the ultrafiltrate is simply collected from the outflow part of the hemofilter and measured at convenient intervals. Expected ultrafiltration rates in the current system are about 600 ml/hour but this can be increased by providing more or less pressure with the ultrafiltrate side of the system. Since ultrafiltration depends on net filtration pressure (the algebraic sum of hydraulic pressure within the blood path and the oncotic pressure of the plasma proteins) a fall in the patient's own blood pressure will decrease the ultrafiltration rate thus decreasing the likelihood of hypotensive complications during this procedure [21]. On the other hand ultrafiltration can be augmented by adding a vacuum to the ultrafiltrate side of the hemofilter. Ultrafiltration can be reduced by impeding the flow of the ultrafiltrate by simply applying a screw clamp to the outlet and allowing hydrostatic pressure to build up on the ultrafiltrate side of the hemofilter. If the system is to be used to replace or partially replace the dialysis procedure, relatively large rates of ultrafiltration and thus large volumes of ultrafiltrate are required to remove appropriate amounts of solute. This requires that relatively large amounts of replacement solutions be used. This can be done quite easily in the setting where careful monitoring is possible – as in the intensive care unit where most of these acutely ill patients are placed under these conditions anyway. Duration of treatment has been reported as low as four hours and as long as 300 hours with good results [22].

Although this is a relatively simple system, it should be used only by those who are familiar with the techniques and problems of dialysis or plasmapheresis-type systems.

5. Summary

Where do these new treatment modalities fit in the management of patients with end stage renal disease? Hemodialysis is the most commonly used treatment. This is appropriate since we have the most background information on hemodialysis and we have the most experience in its use. Many small technical changes have improved it significantly over the past twenty years. Many options now exist so that the hemodialysis procedure can be tailored to individual patient requirements. The use of 'high sodium' dialysis solutions and the use of bicarbonate-based dialysis solutions have reduced symptoms and made management of acutely ill patients easier. Hemodialysis is still the least expensive of the treatment options available.

CAPD is a technique designed for home dialysis. It is a technique designed to be used by the patient himself. It requires a motivation to request and carry out home dialysis and the meticulous life style and attention to detail required to perform the procedure without contamination. It requires a patient who is able to assume the basic day to day management of his dialysis program and to make appropriate choices of dialysis solution requirements based on his training program and repeated assessment of his own situation. CAPD provides excellent 'steady state' dialysis with wide latitude in diet and improved blood pressure control. Middle molecule clearances are superior to hemodialysis. For diabetic patients it can be used as the vehicle for the administration of insulin – a distinct advantage in providing normalization of blood glucose. On the other hand it is a procedure that must be performed daily, in fact four times a day, every day. Small molecule clearances are not as good as hemodialysis. It is not a dialysis form suited to the acute care of patients. Because of its simplicity, patients have selected CAPD as the primary mode of home dialysis therapy – especially in the United States. The growth in the home hemodialysis population has come almost exclusively from CAPD training programs and relatively little increase has been due to hemodialysis home training programs in the past several years. Therefore, hemodialysis will remain the mainstay of dialysis therapy but CAPD can be expected to capture a larger number of home dialysis patients – in fact even expanding the home dialysis population. Technological advances should reduce peritonitis rates so that this is no longer a significant problem.

Hemofiltration remains more expensive and more complicated than hemodialysis at the present time. It has the distinct advantages over hemodialysis of bet-

ter blood pressure control, fewer symptoms during the procedure and better middle molecule clearance. At the present time, the advantages of this procedure are not perceived to be great enough to warrant the increased investment in time and money to change a significant number of patients to hemofiltration. Because there is relatively little demand for hemofiltration, there are relatively few manufactures supplying equipment. Improvements in the hemofiltration procedure have been relatively slow but steady over the past decade. I believe hemofiltration will continue to have a few followers in the United States and perhaps more in Europe but will not compete seriously with hemodialysis or CAPD in the near future.

Continuous arteriovenous hemofiltration is a variant of hemofiltration designed primarily for fluid removal. With proper use it may substitute for dialysis in patients with acute renal failure. The advantages of the system are simplicity, 'steady state' dialysis when used continuously over several days, and relative freedom from adverse side effects usually seen in hemodialysis. Since it does depend on ultrafiltration and not dialysis, its use to replace dialysis in the acute care setting will still depend on the supervision by a nephrologist and nephrology staff. It provides another option for acute removal of fluid in the intensive care setting. It does depend on the cannulation of an artery or a high flow, high pressure vascular device if the simplicity of the system is to be maintained. Although preliminary results have been good using this technique, cannulation an artery long term, i.e., days, is not without hazard. Bleeding and infection coupled with potential for distal embolization of thrombi still is a real hazard. Therefore, I expect limited but increasing use of this technique as an adjunct to existing treatment forms in specific specialized settings.

References

1. Popovich RP, Moncrief JW, Decherd JF, Bomar JB, Pyle WK: The definition of a novel portable/wearable equilibrium peritoneal dialysis technique (abstract). Trans Am Soc Artif Intern Organs 5: 64A, 1976.
2. Nolph KD, Sorkin M, Rubin J et al: Continuous ambulatory peritoneal dialysis: Three-year experience at one center. Ann Intern Med 92: 246–256, 1980.
3. Oreopoulos DG, Robson M, Izatt S, Clayton S, deVeber GA: A simple and safe technique for continuous ambulatory peritoneal dialysis (CAPD). Trans Am Soc Artif Organs 24: 484, 1978.
4. Tenckhoff H, Schecter H: A bacterialogically safe access device. Trans Am Soc Artif Intern Organs 14: 181–187, 1968.
5. Diaz-Buxo JA, Walker PJ, Farmer CD, Chandler JT, Holt KL: Continuous cyclic peritoneal dialysis (Abstract). Kidney Int 19: 145, 1980.
6. Miller FN, Wiegman DL, Joshua IG, Nolph KD, Rubin J: Effects of vasodilators and peritoneal dialysis solutions on the microcirculation of the rat cecum. Proc Soc Exp Biol Med 161: 605–608, 1979.
7. Miller FN, Nolph KD, Harris PD, Rubin J, Wiegman DL, Joshua IG, Twardowski ZI, Ghods AJ: Microvascular and clinical effects of altered peritoneal dialysis solutions. Kid Int 15: 630–639, 1979.
8. Wayland H: Transmural and interstitial molecular transport. Proceedings of the Internation Symposium on CAPD, paris 1979, Excerpta Medica, Amsterdam, 1980, pp 18–27.
9. Alavi N, Lianos E, Andres G, Bentzel CJ: Effect of protamine on the permeability and structure of rat peritoneum. Kid Int 21: 44–53, 1982.
10. Verger C, Luger A, Moore HL, Nolph KD: Acute changes in peritoneal morphology and transport properties with infectious peritonitis and mechanical injury. Kid Int 23: 823–831, 1983.
11. Popovich PR, Pyle WK, Moncrief JW, Bomar JB: Peritoneal dialysis. Am Inst Chem Eng Symp Ser 75: 31:45, 1979.
12. Steinberg SM, Cutler SJ, Novak JW, Nolph KD: Characteristics of Participants and Selected Outcome Measures for the Period January 1, 1981 through June 30, 1983. National CAPD Registry of the National Institutes of Health, 1984.
13. Bunke CM, Aronoff GR, Brier ME, Sloan RS, Luft FC: Vancomycin kinetics during continuous ambulatory peritoneal dialysis. Clin Pharmacol Ther 34: 631–637, 1983.
14. Rubin J: Comments on Dialysis Solution Composition, Antibiotic Transport, Poisoning, and Novel Uses of Peritoneal Dialysis. In: Nolph KD (ed) Peritoneal Dialysis. The Hague, Boston, London: Martinus Nijhoff, 1981, pp 249–251.
15. Blumenkrantz MJ, Kopple JD, Moran JK, Coburn JW: Metabolic balance studies and dietary protein requirements in patients undergoing continuous ambulatory peritoneal dialysis. Kidney Int 21: 849–861, 1982.
16. Henderson LW, Besarab A, Michaels A, Bluemle Jr LW: Blood purification by ultrafiltration and fluid replacement (dialfiltration). Trans Am Soc Artif Intern Organs 13: 216–221, 1967.
17. Henderson LW, Beans E: Succussful production of sterile pyrogenfree electrolyte solution by ultrafiltration. Kid Int 14: 522–525, 1978.
18. Van Stone J: Dialysis and the treatment of renal insufficiency. New York, Grune & Stratton, 1983, p 221.
19. Quelhorst EA, Schuenemann B, Hildebrand U: Morbidity and mortality in long-term hemofiltration. ASAIO J 6: 185–191, 1983.
20. Baldamus CA: Clinical value and technical feasibility of long-term hemofiltration. ASAIO J 6: 192–196, 1983.
21. Lauer A, Saccaggi A, Ronco C, Belledonne M, Glabman S, Bosch JP: Continuous arteriovenous hemofiltration in the critically ill patient. Ann Intern Med 99: 455–460, 1983.
22. Kaplan AA, Longnecker RE, Folkert VW: Continuous arteriovenous hemofiltration. Ann Intern Med 100: 358–367, 1984.

CHAPTER 13

Radiological modalities in the examination of the kidney

JEAN PAQUELET and A. JOHN CHRISTOFORIDIS

1. Introduction

Radiology of the kidneys is of great importance to every practicing physician and particularly to the radiologist, urologist and nephrologist. This is reflected by the fact that a significant number of hospital admissions is related to kidney diseases. Excretory urography, a time honored examination, is still routinely used in the study of the urinary tract (Fig. 1). In 1980 4.2 million intravenous urograms were performed in the United States [1]. In addition, a larger number of examinations for kidney disorder was conducted by ultrasound, nuclear studies or plain abdominal radiographs. Multivolume editions and many monographs are devoted exclusively to the radiology and the various imaging modalities for kidney diseases. More than 100 articles related to this subject are published monthly in the radiological literature alone.

It is understandable that when the editors of this volume asked us to contribute a short on the radiology of the kidney we were confronted with an unrealistic task. Considering that this monograph is addressed not only to clinicians but also to other life scientists it was considered appropriate to devote this short chapter primarily to an outline of the newer radiological modalities developed in the last 10 to 15 years. These newer modalities, some of which are undergoing further evolution, have broadened the participation of the radiologist in the study of renal diseases. It is possible now to obtain new information unattainable a few years ago. This is contributing to an earlier and more accurate diagnosis. While some of these modalities added to the cost of the diagnostic workup, it should be quickly emphasized that these examinations decrease the days of hospitalization by an earlier and more accurate diagnosis. The fact that most of these examinations can be performed on an outpatient basis is another positive step in the direction of health cost containment. This becomes more evident when one considers the fact that the single most important factor in the health expenditure is the length of hospital stay. At this point we should also mention the fact that radiological procedures, in the last few years, are contributing more actively not only in the diagnostic work-up of the patient, but also, through a variety of percutaneous techniques, are utilized as therapeutic procedures in a variety of pathologic conditions. These interventional radiological procedures can successfully substitute for conventional surgical treatment methods which necessitate as a rule, longer hospitalization. Some of these procedures will be mentioned under the title of 'Interventional Techniques'.

Mass lesions of the kidney have been always one of the most important topics of kidney pathology. The exact diagnosis of mass lesions, so important because of the difference in the treatment and in the prognosis, has been phenomenally improved with the newer modalities. Some of these new diagnostic procedures are competing for early diagnosis and mainly for accuracy. Accuracy rates of ninety to ninety five percent are common in large series of patients, undergoing these diagnostic examinations.

Renal trauma, sometimes difficult to diagnose, or to assess accurately the extent of the injury, with the time honored conventional methods, has been simplified by expediting an early diagnosis and markedly improving its accuracy. Trauma in general, as well known, is a leading cause of disability to millions and the cause of death to approximately 105,000 per year in this country alone with approximately half of these being due to automobile accidents. Trauma is the leading cause of death below the age of forty. This is not going to decrease significantly in the foreseeable future particularly in a society where shortening of working hours will allow more free time, used frequently for traveling and for an increasing participation in sports, some of which have a built in percentage of expected trauma.

Interventional techniques, as mentioned, ex-

L.J.A. DiDio and P.M. Motta (eds), Basic, Clinical, and Surgical Nephrology. ISBN 0-89838-689-5.

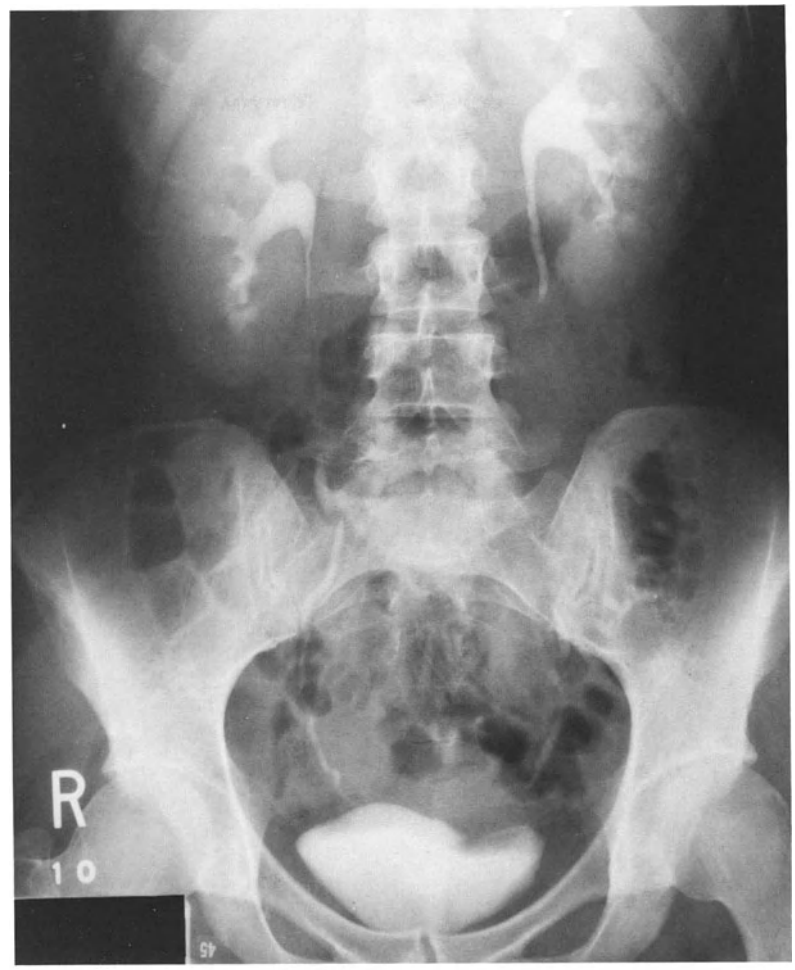

Fig. 1. Medullary sponge kidney. The excretory urogram demonstrates fine linear collections in the medullary pyramids representing contrast in the dilated collecting tubules.

panded the spectrum of the radiologist's contribution to the patient's care. Biopsy of the kidneys, percutaneous nephrostomy, abscess drainage, angioplasty and stone extraction are some of the most important areas where the radiologist is daily an active participant not only in the diagnosis but also in the treatment of renal diseases.

The imaging of inflammatory lesions, where conventional urographic techniques are still used routinely and effectively (Fig. 1), have been enhanced by the introduction of the the new imaging modalities.

Digital subtraction angiography has simplified, to some extent, the evaluation of renal hypertension. This 'less invasive' procedure in comparison with the well established renal angiography can be performed on an outpatient basis and therefore it can be utilized, to some extent as a screening test.

Radionuclide imaging in renal diseases has been in routine used in general hospitals for the last 20 years. It still has its place particularly with the refinements of instrumentation and the introduction of new radionuclides.

The introduction of magnetic resonance not only as a superb imaging tool but particularly as a potential spectrographic imaging technique presents a new dimension in diagnosis and holds a great hope for the early detection and the evaluation of the treatment of renal as well as other diseases.

An outline of the above mentioned radiological modalities will follow this introduction.

2. Mass lesions of the kidney

Mass lesions in the kidneys are readily demonstrated

with both ultrasonography and computed tomography. Masses which appear cystic at excretory urography are best further evaluated by sonography. If their cystic nature is confirmed, no further work up is necessary. Sonographically, renal cysts are seen to have a sharp, smooth distal wall, acoustic enhancement distal to the lesion, and lack of internal echoes (Fig. 2). Renal cysts are commonly encountered incidentally when computed tomography of the abdomen is performed for other indications. Benign cysts are characterized by attenuation values near water, imperceptibly thin wall in that part of the cyst protruding from the renal margin, sharp margination from the renal cortex, and lack of enhancement after contrast administration.

While simple renal cysts present no problem in diagnosis, complicated cysts still require cyst puncture and cytologic evaluation of the fluid which is withdrawn. Hemorrhagic cysts appear as very dense well defined masses at computed tomography examination. Infected cysts also have computed tomography attenuation numbers above that of water. Sonographically, hemorrhagic or infected cysts often have internal echoes and may lack the acoustic enhancement which is characteristic of simple cysts. Eventually, the wall of the complicated cyst may calcify and demonstration of this peripheral calcification by computed tomography suggests a previously complicated cyst. However, since the computed tomography and sonographic appearance are not pathognomonic, cyst puncture or surgery is required to differentiate the infected or hemorrhagic cyst from necrotic or hemorrhagic tumor and to differentiate the calcified cyst from the renal cell carcinoma which occasionally demonstrates rim-like calcification.

Masses which appear solid at excretory urography are best further evaluated by computed tomography. On computed tomography renal cell carcinoma appears as a renal mass with a lobulated contour, often heterogeneous in appearance, with attenuation values near that of renal parenchyma and having an indistinct interface with the normal renal parenchyma (Fig. 3). Secondary signs include invasion of perinephric space, regional lymphadenopathy and invasion of the renal vein or the inferior vena cava. Venous involvement is most accurately evaluated by injecting a bolus of contrast material and obtaining rapid sequential scans at the level of the renal vein.

Computed tomography has proven to be highly accurate in staging of primary renal cell carcinoma. The commonly employed staging criteria are as follows:

Stage I – indicates lesions confined within the renal capsule.

Stage II – denotes lesions which have extended through the capsule into the perinephric fat but not beyond Gerota's fascia.

Stage III – indicates involvement of renal veins or lymph nodes.

Stage IV – denotes either invasion of adjacent visceral structures such as liver or spleen or distant metastases.

Ultrasound also can demonstrate renal cell carcinoma but is considered to be less valuable in tumor staging [2]. It accurately predicts inferior vena caval and renal vein involvement, but is less sensitive than computed tomography for detection of adjacent organ and lymph node involvement.

Traditionally, renal arteriography and venography have been used in preoperative staging of renal cell carcinoma. However, computed tomography is more accurate and sensitive than angiography in detecting perinephric extension, more sensitive in assessing lymph node involvement, and equally accurate in detecting main renal vein and vena caval involvement [3]. Because of this, computed tomography has reduced the need for preoperative angiography [4]. Arteriography remains helpful in selected cases when computed tomography is equivocal and when the surgeon desires vascular mapping for pertinent information. When transcatheter tumor infarction is planned, angiography is necessary to visualize accurately the arterial anatomy including variations. Venography frequently provides additional useful information when large right sided masses compress or distort the renal vein or the inferior vena cava. In these cases computed tomography is frequently equivocal as to whether the inferior vena cava and renal vein are merely distorted by adjacent tumor, or actually contain tumor thrombus within the vessel.

Tumors other than primary carcinoma are detectable with current body imaging techniques. Renal angiomyolipoma for example, can be diagnosed on computed tomography by the detection of fat in the renal tumor [5] (Fig. 4). Increased echogenicity in a renal mass at sonography suggests this diagnosis, but is nonspecific.

Renal oncocytoma, an unusual solid renal mass that has an excellent prognosis and is said to be adequately treated by local excision, has a distinctive appearance on computed tomography exam (Fig. 5). The oncocytoma has a distinct margin, a smooth contour and enhances homogeneously after injection of intravenous contrast [6]. On the other hand, renal cell carcinoma is frequently polylobulated, enhances inhomogeneously and has an irregular interface with normal renal parenchyma. While the

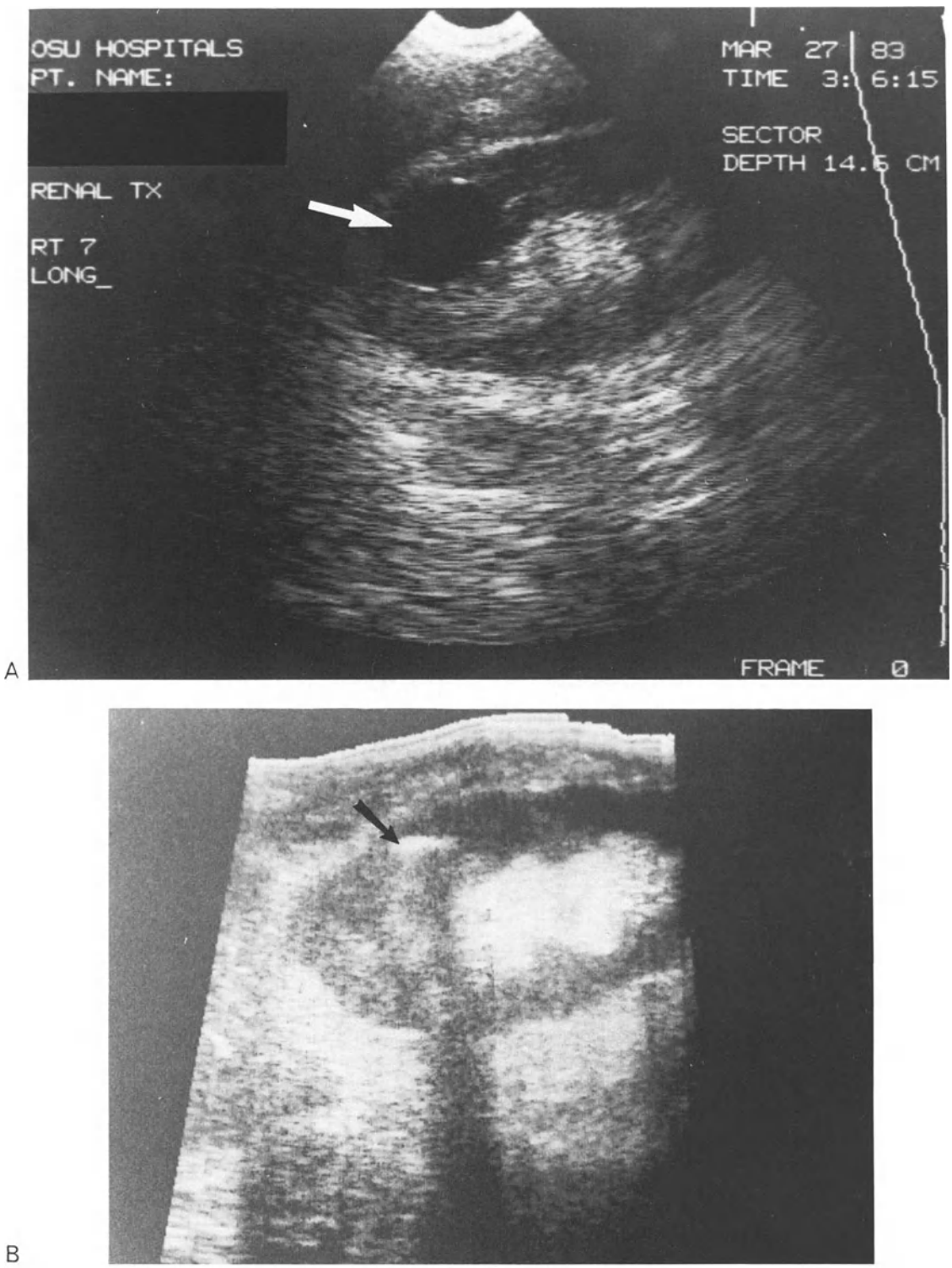

Fig. 2. Renal cyst aspiration under sonographic guidance. (A) Typical renal cyst (arrow) with no internal echoes, well defined thin walls and acoustic enhancement. (B) After cyst puncture, the cyst is no longer seen. The echogenic area (arrow) with acoustic shadowing represents minimal air in the collapsed cyst cavity.

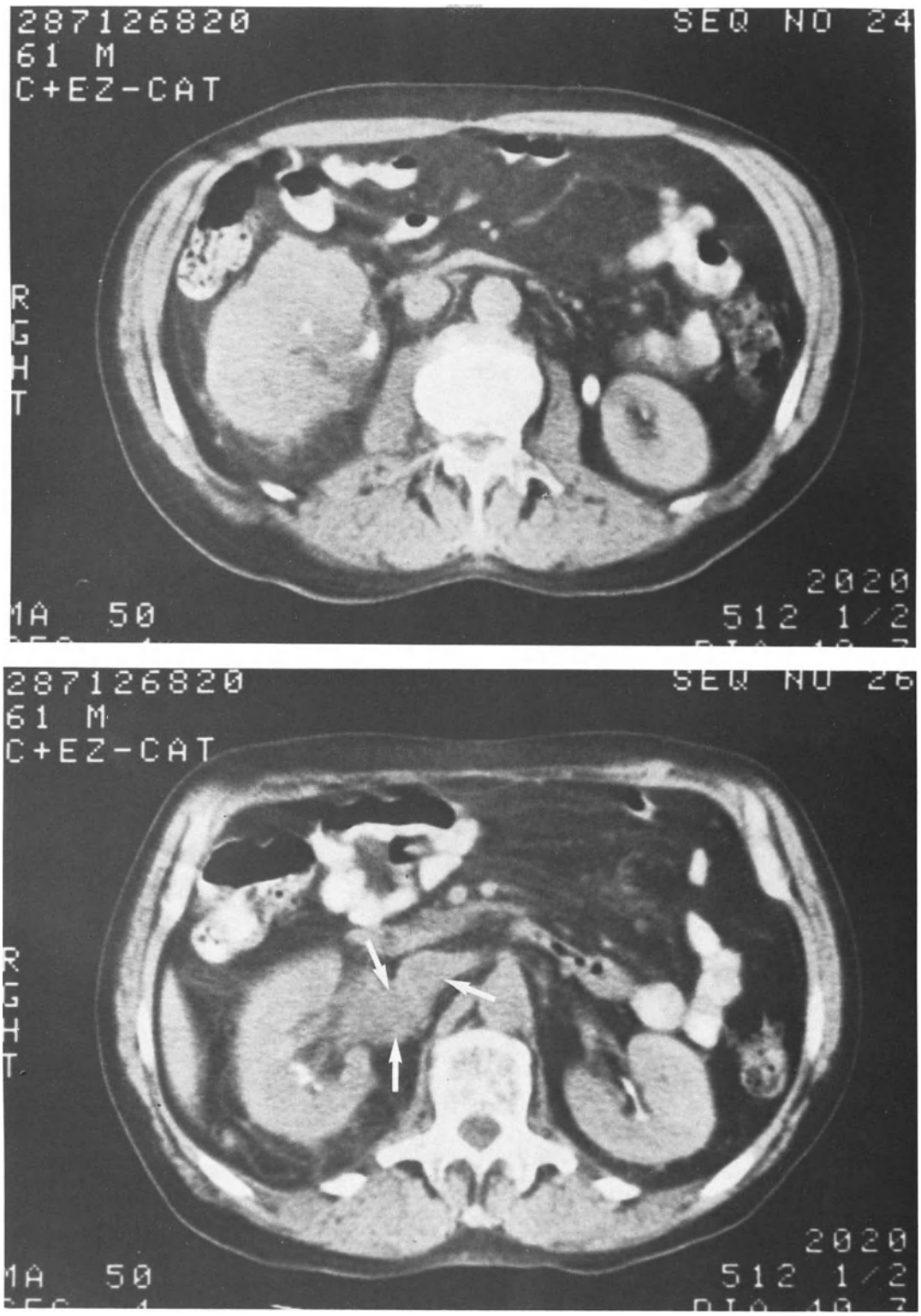

Fig. 3. Carcinoma of the kidney. (A) A large polylobulated nearly isodense tumor mass is present in the right kidney. (B) At a slightly higher level, tumor thrombus is seen in the renal vein and inferior vena cava (arrows).

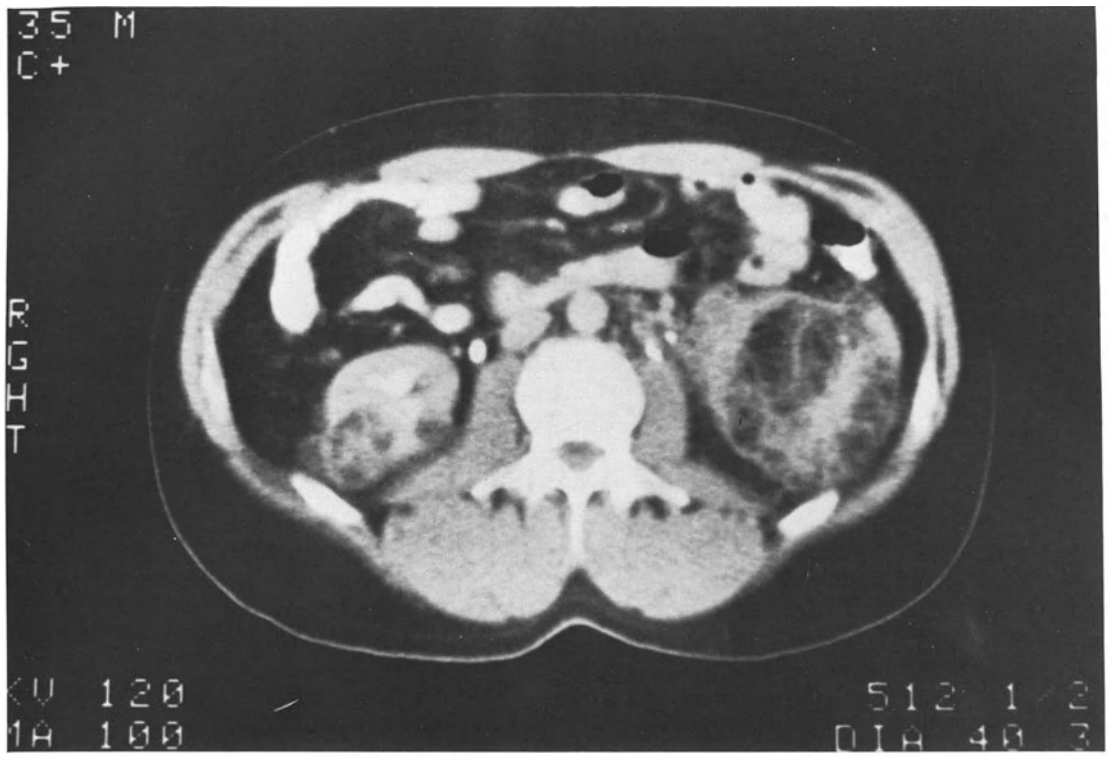

4

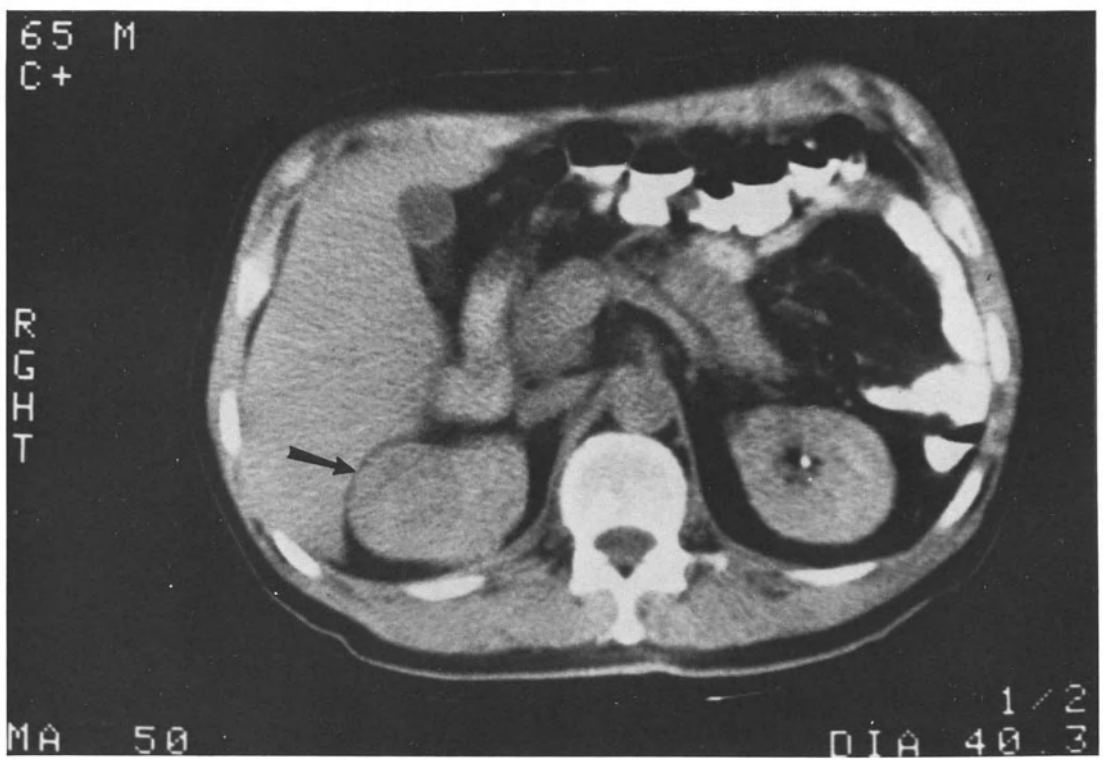

5

Fig. 4. Renal angiomyolipomas in a patient with tuberous sclerosis. There are bilateral renal masses with very low density areas of fat.
Fig. 5. Right renal oncocytoma. CT demonstrates a well defined, homogeneous, nonlobulated right renal mass. (arrow) The tumor has a lower absorption coefficient than the surrounding renal parenchyma. Histologic diagnosis was oncocytoma.

computed tomography appearance of oncocytoma is not pathognomonic, the presumptive diagnosis of oncocytoma would allow the surgeon to biopsy the mass rather than proceed with radical nephrectomy, the procedure of choice in renal cell carcinoma. If frozen section confirms the diagnosis of oncocytoma, the tumor may be treated by excisional biopsy. Lymphomatous and metastatic lesions to the kidney are more frequently recognized with computed tomography and sonography, either of which can provide guidance for percutaneous biopsy (Figs. 6, 7).

3. Radiologic evaluation of renal trauma

Computed tomography of the kidney has dramatically altered the radiographic evaluation of the traumatized urinary tract. Traditionally, excretory urography has been the screening procedure of choice, followed by arteriography in those patients with abnormal urograms. Excretory urography remains the screening procedure of choice in patients with blunt abdominal trauma who are stable and have minimal or no signs of renal injury. If the urogram is normal, no further work up is necessary. If it is abnormal, computed tomography is then performed for more accurate delineation of the extent of injury, as the urographic abnormality is frequently nonspecific. In patients with labile vital signs, hematuria or other strong clinical indicator of renal injury, computed tomography should be performed as the initial step in the investigation of the upper urinary tract, in order to expedite a probably necessary surgical procedure.

Computed tomography offers excellent anatomic detail. Contusions, lacerations, subcapsular and perinephric hematomas are accurately diagnosed. Renal contusion, the least serious renal parenchymal injury, is characterized at computed tomography, by an area of prolonged nephrographic stain, probably due to interstitial extravasation of contrast. Intrarenal hematomas are seen as poorly marginated rounded areas of decreased attenuation, compared to the contrast enhanced kidney [7] (Fig. 8). Intrarenal hematomas or lacerations are frequently accompanied by an area or subcapsular hematoma. If there is extension of the laceration into the collecting system, computed tomography is very sensitive for detection of extravasated contrast material into the perinephric space. Areas of infarction due to traumatic occlusion of renal arterial branches are also fairly commonly detected. The infarcted areas have a sharply marginated border and are wedge shaped. They usually are not accompanied by an associated subcapsular hematoma.

Subcapsular hematomas appear as lens shaped collections in the immediate extrarenal area with intact perirenal fat. The fluid collection is low in density compared to the contrast enhanced kidney. Perinephric hematomas surround the kidney in a crescentic fashion. Below the kidney, these hematomas have a rounded appearance on axial sections, as they conform to the shape of Gerota's fascia which extends to the pelvis [8].

Computed tomography seems to be the ideal way to examine the traumatized kidney. It is non-invasive, requires minimal time and patient cooperation. It has the important additional advantage, in the traumatized patient, of evaluating adjacent liver and spleen frequently suspected for associate injury. The method is also useful for monitoring patients during conservative treatment or postoperatively for complications such as abscess or urinoma.

Angiography remains useful in penetrating trauma for the detection of arterio-venous fistulae or traumatic aneurysms. Angiography is also the procedure of choice in patients with blunt trauma in whom nonvisualization of the kidney at excretory urography suggest arterial or venous thrombosis.

4. Imaging of inflammatory lesions of the kidney

Acute pyelonephritis in adult patients will usually resolve with appropriate antibiotic treatment and usually does not warrant imaging procedures in the acute phase. However, radiologic investigation is indicated in patients unresponsive to medical therapy and in those with underlying medical disease, making severe infection likely. Excretory urography and angiography have been in the past the usual methods of evaluation. Excretory urograms are frequently normal or have nonspecific findings. Because of this, and because of the incomplete evaluation of the perirenal and pararenal spaces with angiography, sonography and computed tomography have largely replaced these methods.

Acute bacterial nephritis indicates a solid inflammatory renal mass without drainable pus. At sonography, this disease appears as unifocal or multifocal renal mass(es) which are solid, usually less echogenic than normal kidney, with poorly defined margins [9]. Computed tomography also demonstrates a poorly defined mass lesion of similar or slightly lower density than normal kidney. After contrast administration, the area shows patchy enhancement, but remains less dense than the surrounding parenchyma.

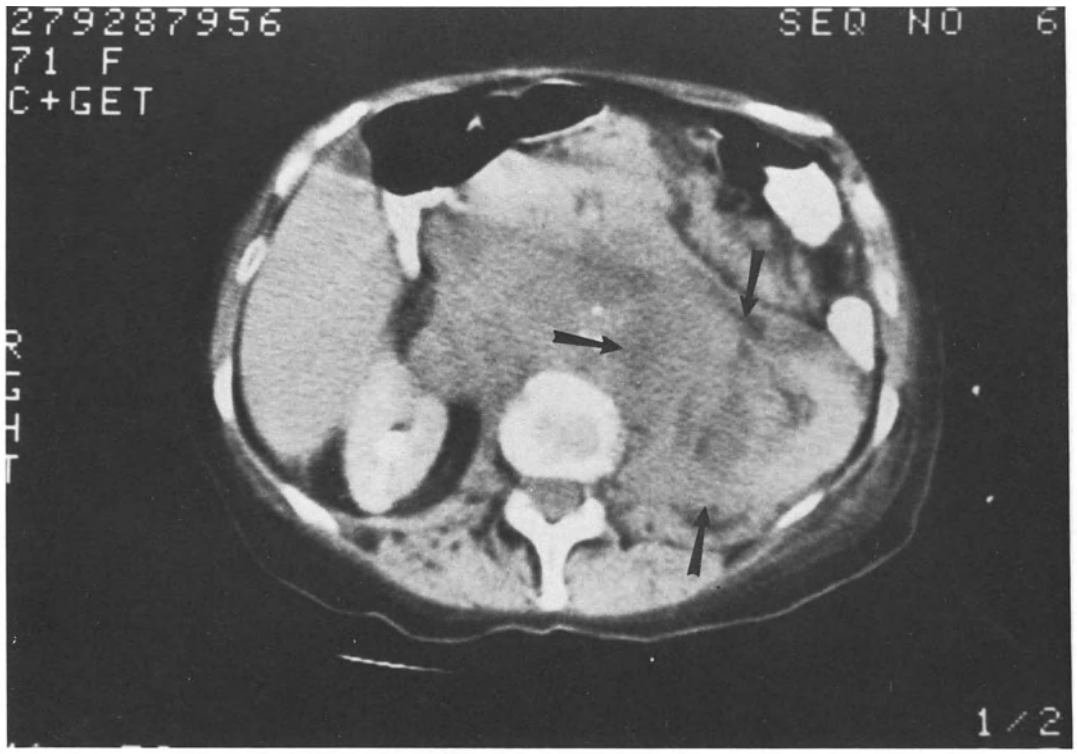

6

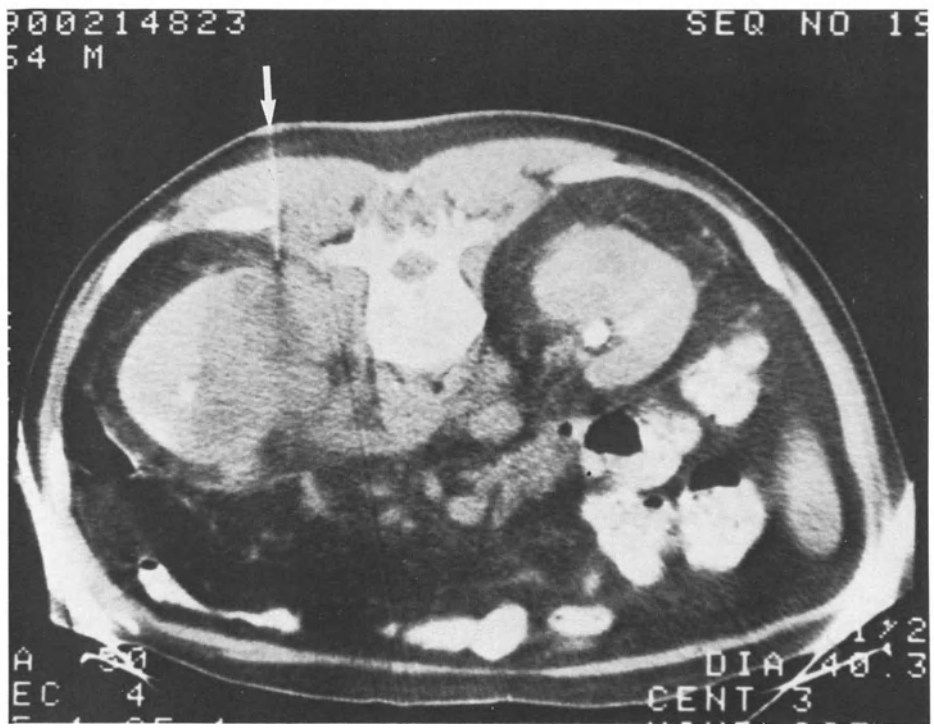

7

Fig. 6. Histiocytic lymphoma of the kidney. A large retroperitoneal mass extends into the perinephric space and invades the left kidney (arrows). Mesenteric adenopathy is also present.

Fig. 7. Bilateral metastatic renal masses in a patient with bronchogenic carcionoma. Bilateral renal masses are seen. Arrow indicate the biopsy needle with its tip at the margin of the left renal mass. Histologic diagnosis was metastatic squamous cell carcinoma.

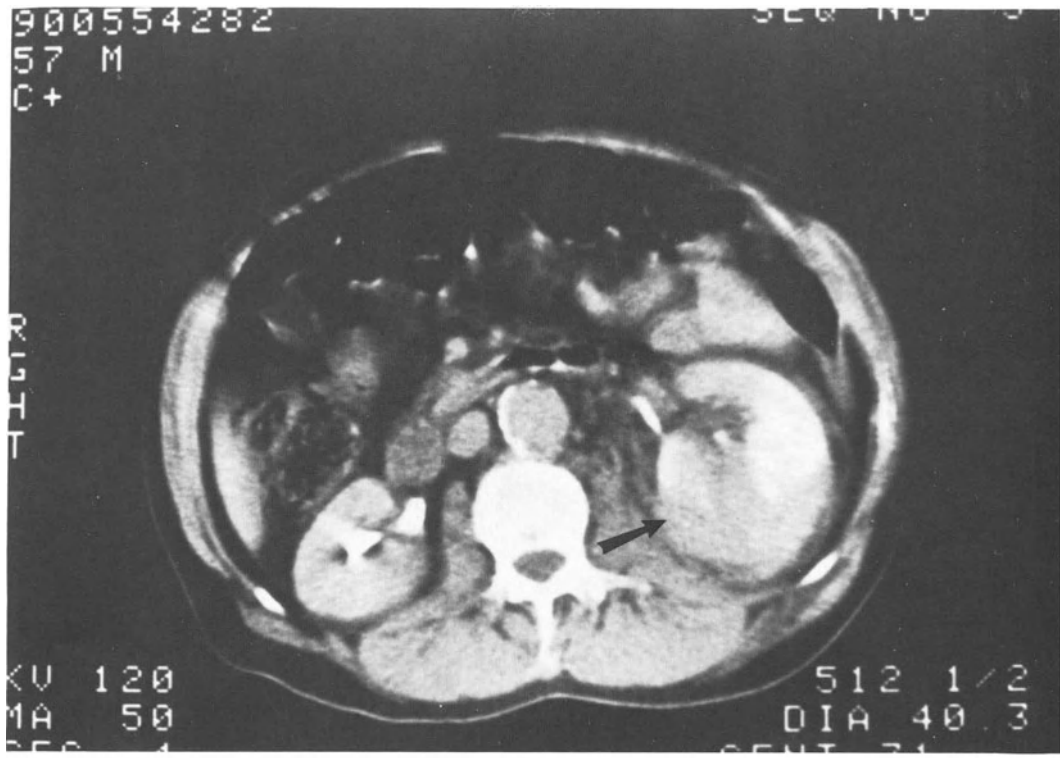

8

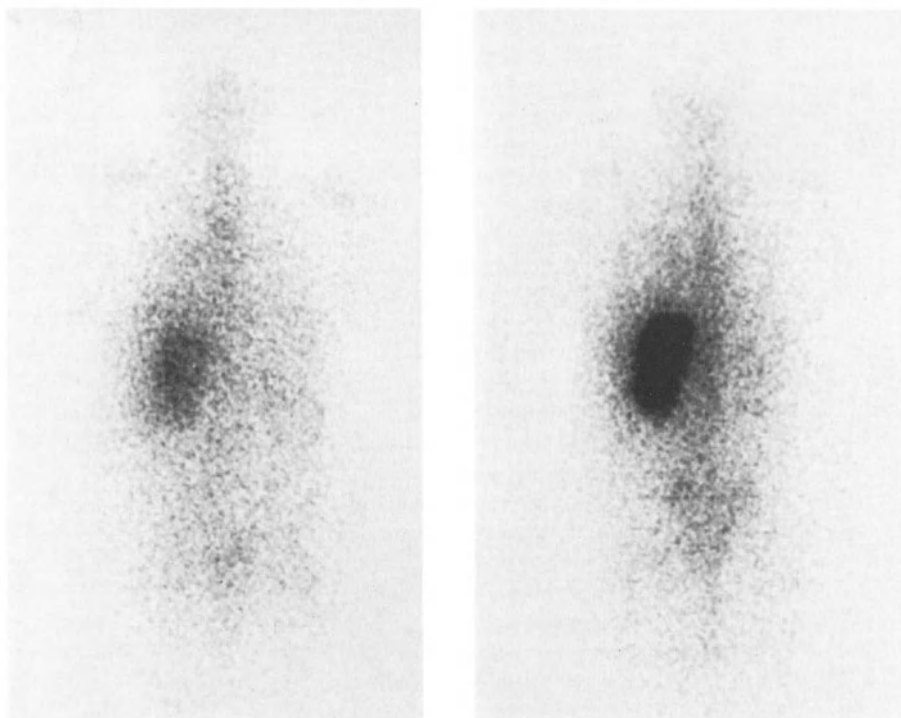

9

Fig. 8. Left renal trauma. The arrow indicates a wedge-shaped renal parenchymal hematoma and posterior perinephric hematoma.
Fig. 9. Gallium^{67} citrate scan in pyelonephritis. Total body (anterior and posterior) images reveal intense activity in the right kidney in patients who subsequently had laboratory evidence of pyelonephritis.

Acute focal bacterial nephritis may progress to frank abscess. At sonography, an abscess appears as a nearly anechoic mass with good through transmission, irregular walls and a variable amount of debris causing internal echoes. If the abscess contains air, this appears very echogenic. The computed tomography image of abscess shows irregular margination of a low density lesion with a thick wall. The central liquified area does not enhance after contrast administration and may contain air. Associated thickening of the adjacent renal fascia may also be present.

Radionuclide investigation of the kidney can also be very helpful in inflammatory disease. In patients with pyuria radionuclides which accumulate in inflammatory lesions can indicate whether there is pyelonephritis or if the infection is merely limited to the lower urinary tract. These radionuclides can also be useful in patients presenting with fever of unknown origin, in demonstrating that renal infection is the cause. Gallium 67 citrate, which localizes in polymorphonuclear leukocytes, after being cleared from the blood where it is bound to transferrin, has been used extensively in some centers (Fig. 9). Of the administered dose of gallium, 20–30% is excreted by the kidneys in the first 24 hours, but scanning at 48 hours should show no significant activity in the kidneys, unless there is inflammatory disease [10].

More recently indium 111 labeled white cells have gained popularity. Indium 111 white cell scans seem to be at least equal in diagnostic accuracy to gallium scans. Indium is not normally excreted by the kidney, does not require the bowel preparation that gallium does and quite specifically localizes in inflammatory collections. Gallium, on the other hand accumulates in a variety of tumors, in addition to inflammatory lesions, but this rarely presents a problem clinically. Indium 111 has the additional advantage of providing diagnostic information earlier since the patient can be scanned 12 hours after administration of the radionuclide. The major drawback of Indium 111 white cell scanning is that its preparation is cumbersome and requires an in hospital radiopharmacy, which usually is available only in large hospitals.

Neither radionuclide can differentiate perinephric abscess from pyelonephritis but scanning with a renal cortical agent, such as Technetium 99m glucoheptonate would differentiate the two since it shows a distinctive striated 'flare' pattern in pyelonephritis [10].

Xanthogranulomatous pyelonephritis, an unusual inflammatory process of the kidney occurring in patients with long standing obstruction due to calculus disease, has a characteristic computed tomography appearance that allows differentiation from renal cell carcinoma and accurate preoperative diagnosis [11] (Fig. 10). The diagnosis is suggested by the presence of a renal mass, calculus disease and history of infection. Computed tomography demonstrates the enlarged kidney with dense renal parenchyma peripherally with central low density areas representing dilated pus-filled calyces and xanthomatous tissue. Thickening of Gerota's fascia, perinephric abscess and psoas abscess may be present. Calculi in the renal pelvis are also demonstrated.

Perinephric abscess is usually a complication of severe renal infection. These abscesses can be diagnosed by both computed tomography and ultrasound by the demonstration of a perirenal fluid or gas collection with distortion of the renal contour [12] (Fig. 11). Computed tomography will also demonstrate thickening of perirenal fascia and either method can be used as a guide for percutaneous drainage of the collection.

5. Interventional techniques in uroradiology

In the past decade, the role of the radiologist has expanded greatly. While diagnostic procedures remain important, newly developed and applied percutaneous techniques have expanded the radiologist's role to include patient therapy and management. This is particularly the case in the urinary tract where, percutaneous nephrostomy, stent placement, stone extraction, biopsy, abscess drainage and angioplasty have come to be performed routinely.

Ultrasonically guided renal cyst puncture, once a frequently employed technique in the work up of renal cysts, is now reserved for atypical appearing cystic masses. Cysts can be punctured through a special biopsy transducer with a central channel for the needle, or the cyst can be punctured after ultrasound localization with a regular transducer used to monitor needle tip location. Cytologic study of the fluid withdrawn is helpful in differentiating cystic or necrotic neoplasm from simple cyst.

Computed tomography guided biopsy of solid renal masses is employed in the diagnosis of renal cell carcinoma in patients with widespread metastatic disease at time of presentation, in whom surgery would not be curative. In a patient with known primary malignancy elsewhere, such as lung or breast, a metastatic lesion of the kidney must be differentiated from primary renal malignancy. Percutaneous biopsy under local anesthetic with computed tomography guidance, provides the informa-

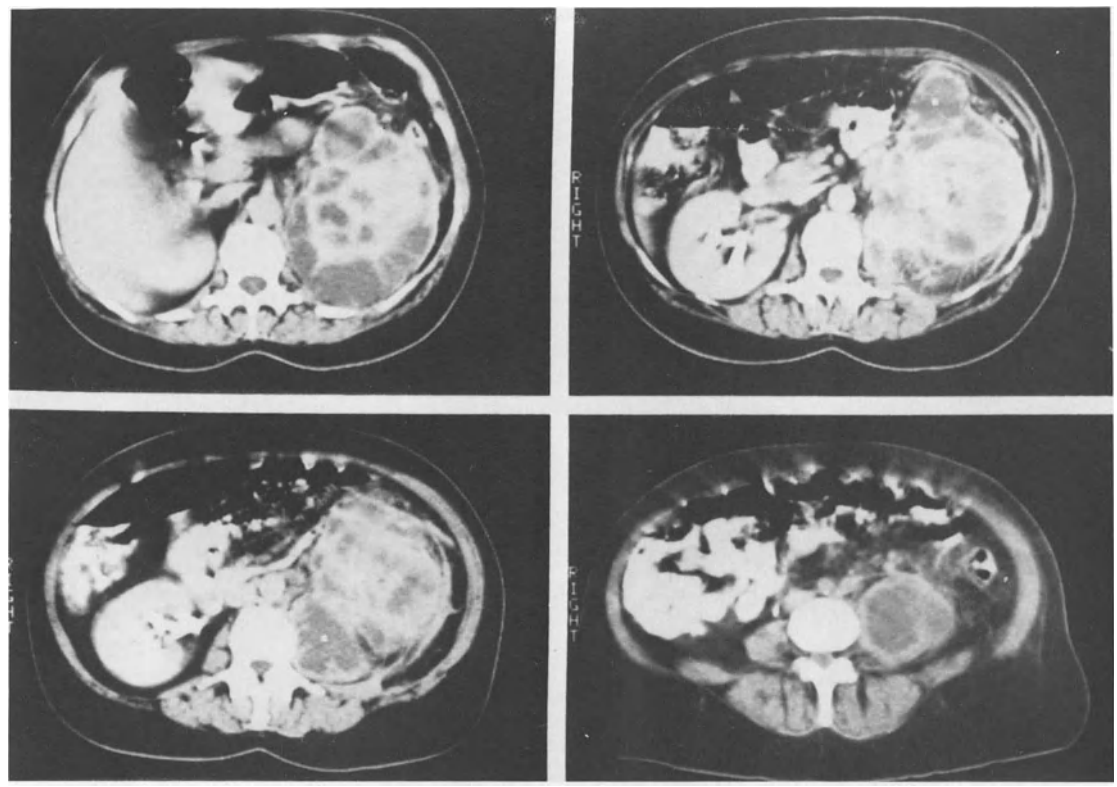

Fig. 10. Xanthogranulomatous pyelonephritis-Serial CT images demonstrate central dilated calyces filled with pus and xanthomatous material and perinephric abscess extending around and below the kidney.

tion quickly, at reasonable cost, and with minimal morbidity and shorter or no hospitalization as the procedure can be done on an outpatient basis.

The perinephric space can also be needled under computed tomography or ultrasonic guidance for diagnosis or perinephric collections. In the case of perinephric abscess, a drainage catheter can be placed percutaneously for treatment. After needle placement in the perinephric collection and withdrawal of fluid to determine if it is purulent, a guide wire is placed through the needle. One of the many commercially available drainage catheters is then advanced over the guidewire and into the abscess cavity. The cavity is then aspirated as completely as possible, and the aspirate cultured for planning of the appropriate antibiotic therapy. The cavity size is then followed serially by computed tomography sonography or sinography performed through the catheter. The drain may be removed when the patent's temperature has returned to normal for 2–3 days, the white blood count has improved, the amount of catheter drainage has markedly decreased, the cavity has collapsed and the patient's general clinical condition has ameliorated [13]. Complications are unusual. They may include hemorrhage and also pneumothorax and empyema if the pleural space is inadvertantly entered.

Definitive treatment of intrarenal abscess has recently been described using percutaneous drainage in a small series of patients [14]. The technique is similar to that used elsewhere in the abdomen and provides an attractive alternative to surgery for treatment of this condition.

Percutaneous nephrostomy is a frequently performed procedure in most larger radiology departments. Both fluoroscopy and sonography have been used for renal localization and needle guidance. Zegel et al. [15] favor ultrasonic guidance since intravenous contrast administration is unnecessary, and in their hands, allowed introduction of a larger caliber needle and was quicker than fluoroscopic guidance.

The most common indication for percutaneous nephrostomy is ureteral obstruction due to pelvic or retroperitoneal malignancy. Ureteral obstruction complicated by infection is a situation in which this procedure is frequently requested. The procedure is outlined below briefly:

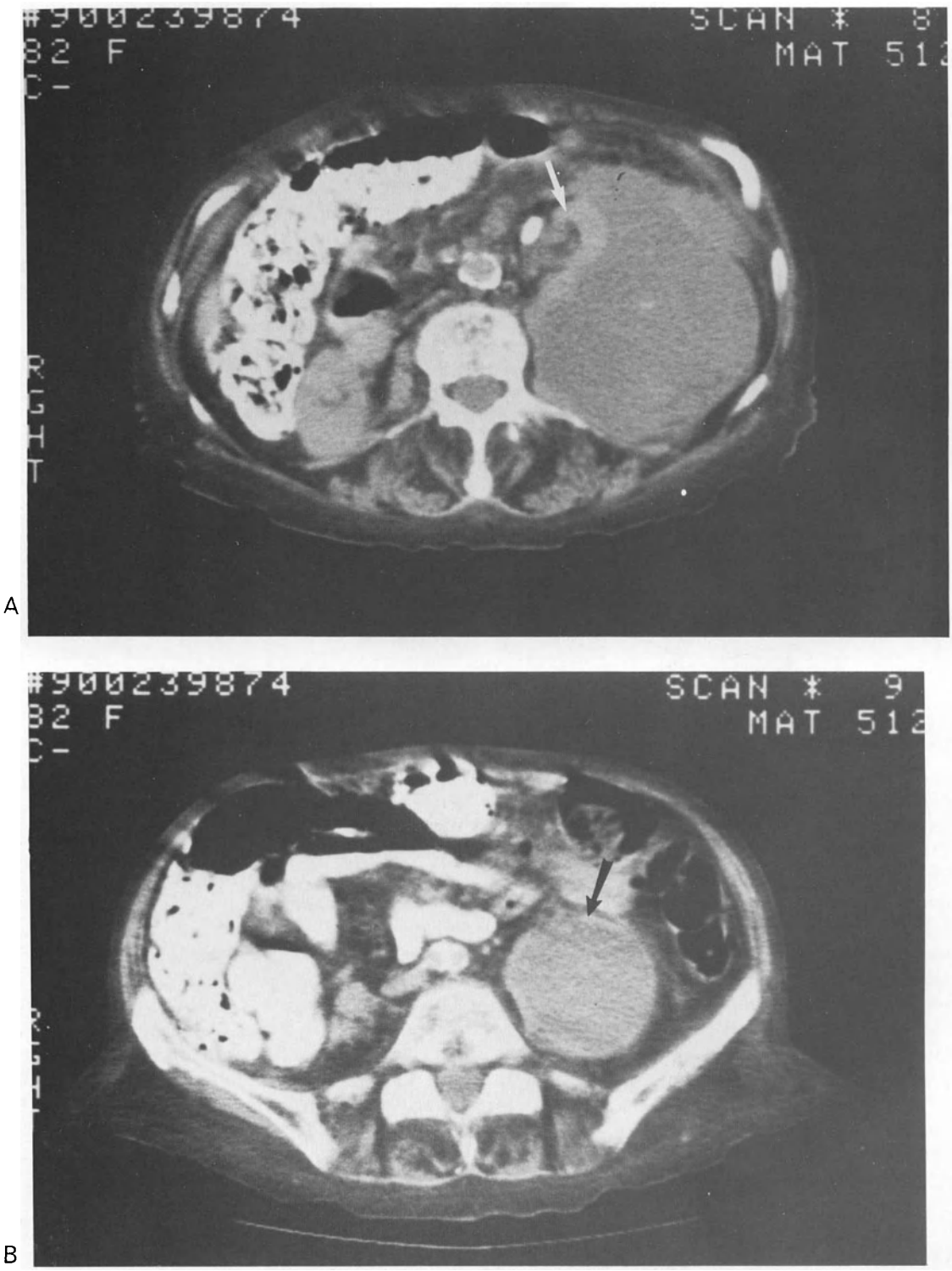

Fig. 11. Perinephric abscess. (A) CT examination shows the abscess as a large low density collection surrounding a small kidney (arrow) of slightly higher density. There is a high density calculus in renal pelvis. (B) A lower section demonstrates pus filling Gerota's fascia below the level of the kidneys.

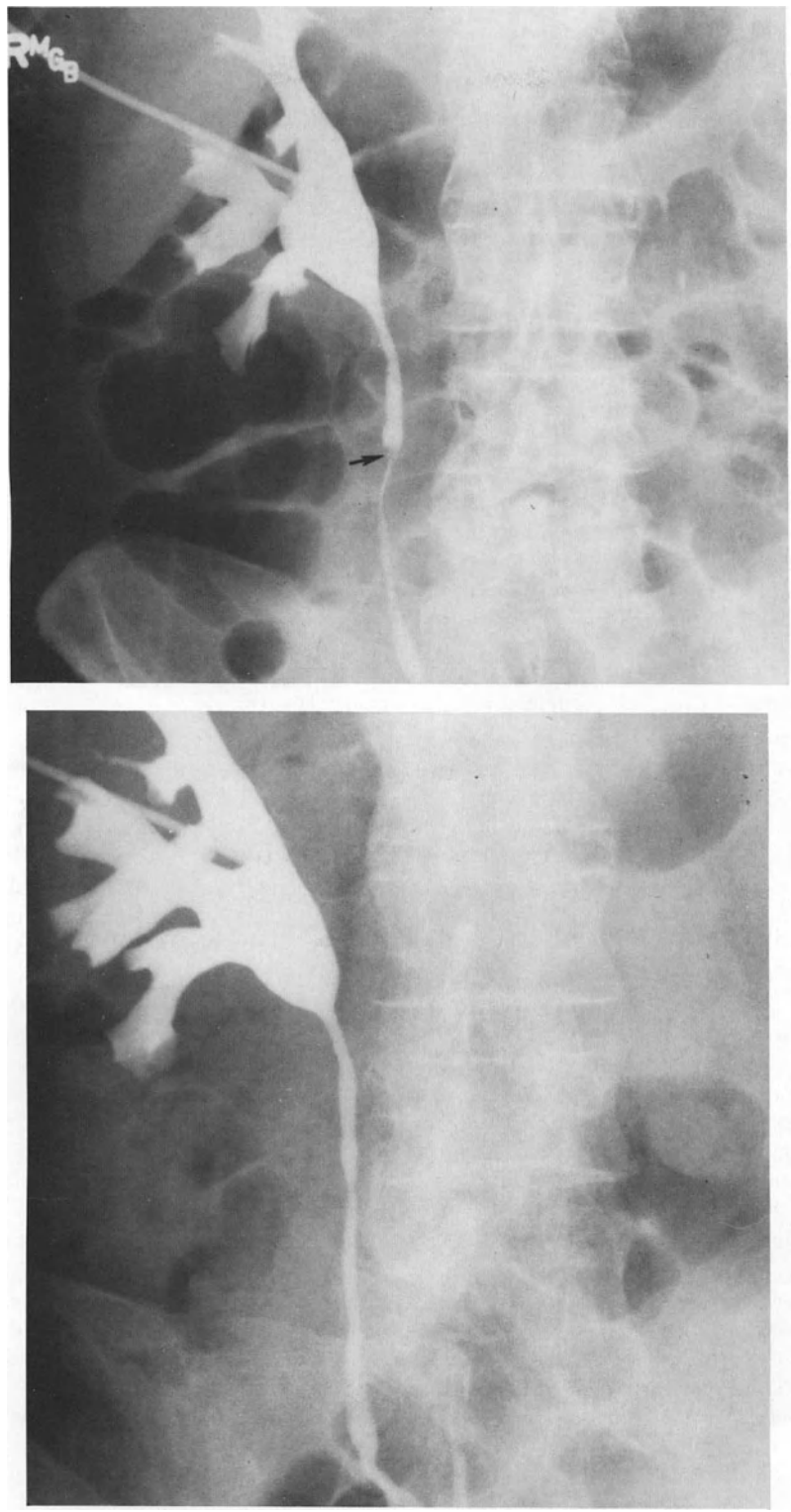

Fig. 12. Percutaneous ureteral calculus extraction. (A) Antegrade pyelogram through a percutaneous nephrostomy tube demonstrates a ureteral calculus (arrow) with mild dilatation of the upper ureter. (B) Antegrade pyelogram after calculus extraction shows no ureteral calculus and resolution of upper ureteral dilatation.

a) After administration of broad spectrum antibiotics to the patient, the renal collecting system is opacified either by administration of intravenous contrast or by antegrade pyelography, using ultrasonic guidance for needle puncture of the collecting system.
b) After a second puncture for placement of a larger needle into the desired calyx, a guidewire is placed through the needle into the renal pelvis.
c) The needle is removed and a drainage catheter is advanced over the guidewire and into the renal pelvis or ureter.

Temporary external drainage of the urinary tract can be accomplished in this way, and in some cases, it is possible to establish antegrade drainage into the bladder using a double-pigtail endoprosthesis with the proximal holes in the renal pelvis and the distal ones in the bladder. Ureteral catheters can be placed percutaneously as stents in patients with ureteral fistulas, and strictures [16]. In addition to providing drainage, these stents maintain luminal caliber and allow healing.

Nephrostomy tracts can be dilated to allow percutaneous extraction of urinary calculi (Fig. 12). A variety of techniques are used for stone removal. Calculi can be grasped using stone forceps or wire baskets similar to those used in the biliary system. Large calculi can be fragmented using a mechanical or ultrasonic lithotriptor and the fragments extracted or flushed into the bladder using intermittent flushing and suction. Castenada-Zuniga [17] reported a success rate of 87% with no mortality. Complications include hemorrhage, infection, ureterocutaneous fistula, perforation of renal pelvis requiring surgical repair, pneumothorax, and paralytic ileus.

In recent years, percutaneous transluminal angioplasty has been gaining widespread acceptance as nonsurgical treatment of renovascular hypertension caused by renal artery stenosis (Fig. 13). All types of fibromuscular dysplasia and short segmental atherosclerotic lesions respond well to the procedure. After a lesion is deemed amenable to dilatation based on its angiographic appearance, a percutaneously inserted guidewire is manipulated across the stenosis. An appropriately sized balloon catheter is then inserted and the renal artery is dilated. Angiography is immediately performed to monitor the results. The mechanism of dilatation is controlled injury to the vessel wall with stretching or splitting of a portion of the media. Tegtmeyer et al. [18] reported an initial success rate of 95% with redilatation necessary in 11.8% of patients due to recurrent stenosis. The procedure has several advantages when compared to surgery including avoidance of general anesthesia, minimal morbidity with short hospital stay, and relatively low cost. Angioplasty does not preclude surgical graft if necessary at a later date.

6. Digital subtraction angiography of the kidney

Digital subtraction angiography (DSA) is a relatively recent innovation in the field of angiography that has found application in the evaluation of the renal vasculature. In appropriately selected patients, excellent images of the main renal artery and its proximal branches can be obtained and information provided concerning their patency, caliber and number (Fig. 14). Very simply, the technique employs injection of a bolus of intravenous contrast during fluoroscopy. The fluoroscopic images are converted into digital format and stored. Images are made before the arrival of the iodinated contrast material and then subtracted from those made after its arrival. Thus, a final image showing only contrast is obtained. Electronic enhancement of the image improves the conspicuity of the vessels and the image is then viewed on a television display screen.

The most common indication for DSA of the kidneys is the investigation of possible renovascular hypertension. Other indications include evaluation of the renal transplant donor, study of arterial patency of renal allograft and evaluation of vascular bypass, endarterectomy and embolization. The overall accuracy of DSA in large series is approximately 90% [19]. The advantages of DSA over conventional arterography include less discomfort, less expense, short examination time and the ability to perform the procedure on an outpatient basis. Limitations include the necessity for considerable patient cooperation, poorer spatial resolution compared to conventional angiography, and difficulty in obtaining technically adequate studies on patients with poor cardiac output or obesity. Many of these problems can be circumvented by careful patient selection. The role of DSA in the evaluation of the renal vasculature is well established and is expanding.

7. Radiographic evaluation of renal allografts

The role of ultrasound in the detection and diagnosis of peritransplant fluid collections is well established. The most common fluid collection causing hydronephrosis of the transplanted kidney is a lymphocele (Fig. 15). Lymphoceles tend to be lobulated and

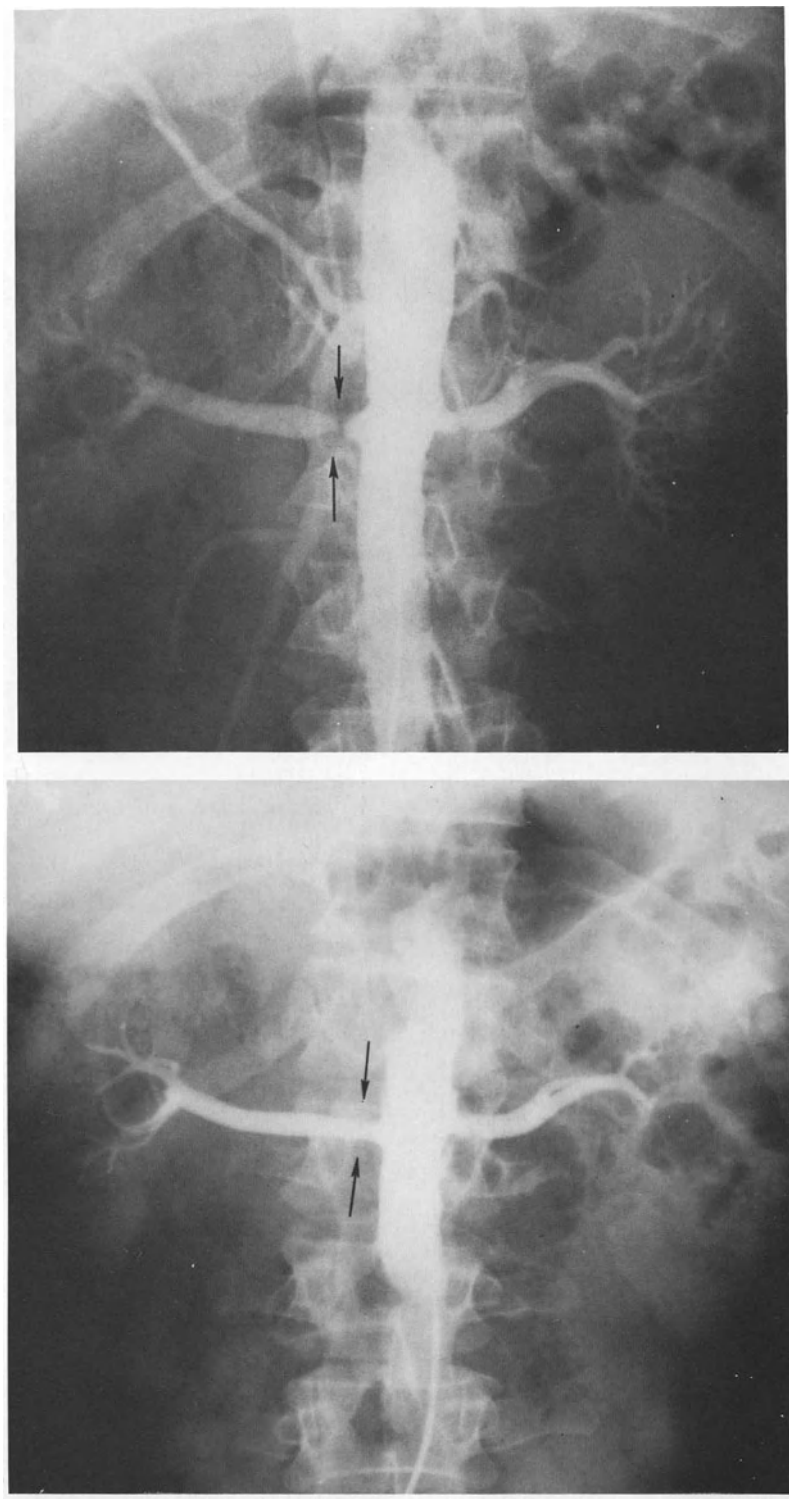

Fig. 13. Percutaneous right renal angioplasty. (A) Aortogram prior to angioplasty demonstrates severe atherosclerotic segmental stenosis in the proximal right renal artery in a patient with systemic hypertension and elevated renin level in blood sampled from the right renal vein. (B) After balloon dilatation a normal caliber of the right renal artery was restored.

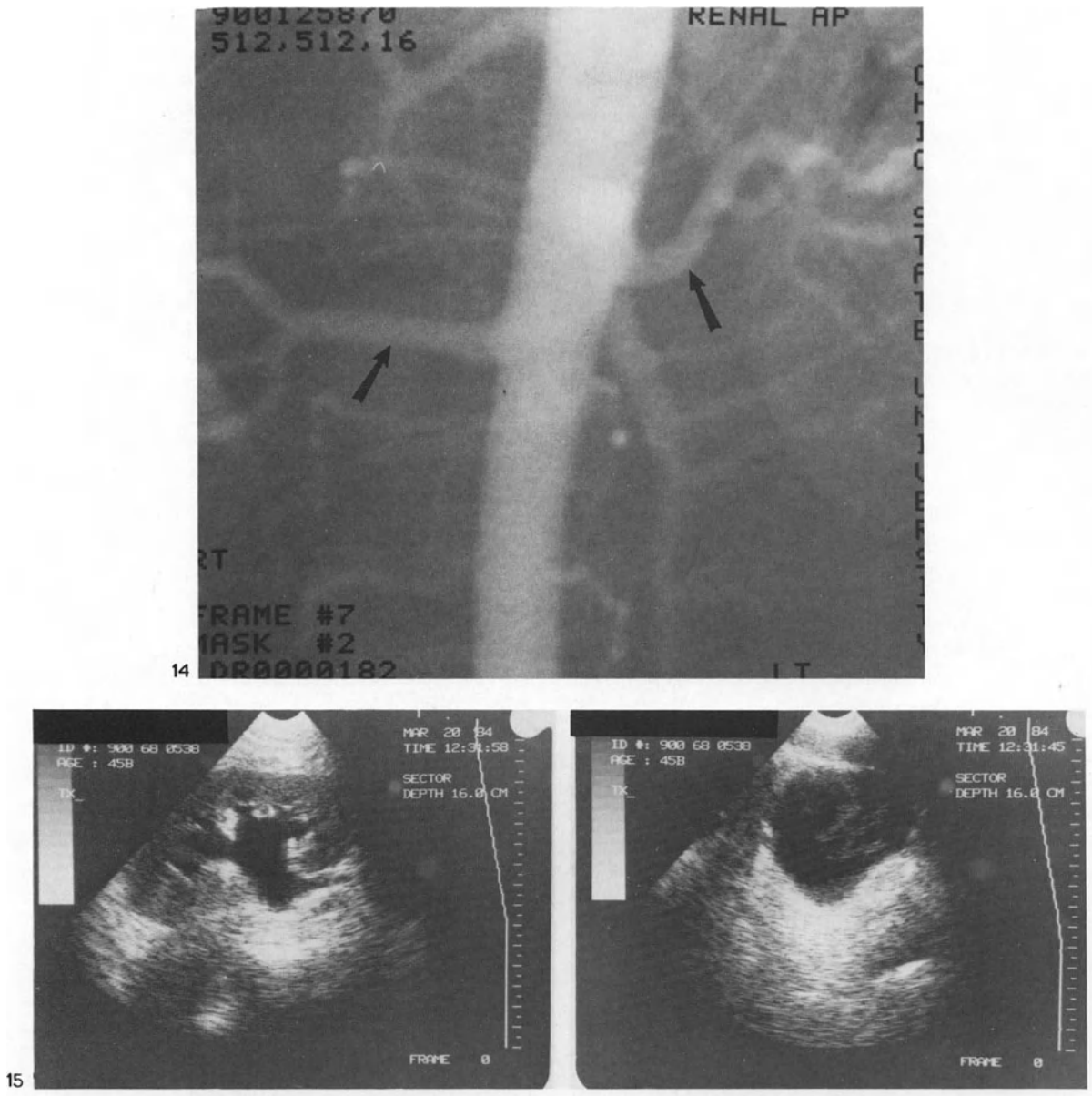

Fig. 14. Digital subtraction angiogram of normal renal arteries. The arteries are marked with arrows.
Fig. 15. (A) Longitudinal sonogram demonstrating hydronephrosis of the transplanted kidney. (B) Just below the kidney, a typical septated lymphocele is present.

contain septations [20]. Urinomas, abscesses and hematomas have no characteristic ultrasound appearance. The temporal relationship of the development of the collection with the time of transplant may be helpful, since urinomas tend to occur earlier after transplantation than do other types of collections. Small asymptomatic crescentic collections are frequently seen after renal transplantation and frequently resolve spontaneously with time. Collections which persist, grow, cause hydronephrosis or are associated with clinical signs of sepsis usually require treatment. Ultrasonically guided aspiration of these collections can diagnose the type of collection preoperatively and thus assist in patient management.

Radionuclide scintigraphy of the renal transplant has a central role in the evaluation of patients who have undergone this procedure. Technetium 99m

complexes are used to gauge perfusion and a parenchymal agent, Iodine ^{131} orthoiodohippurate in our institution, are used to monitor uptake and drainage patterns in transplanted kidneys (Fig. 16). Obstructive uropathy and urinary extravasation are readily detected by these means [21]. Parenchymal failure of the allograft is most frequently caused by acute tubular necrosis and transplant rejection. These can be best differentiated from each other with these methods on the basis of serial studies since acute tubular necrosis usually occurs in the first few days after transplantation and gradually resolves over one to three weeks, while acute rejection usually does not occur until the end of the first week after the surgical procedure.

Technetium 99m sulfur colloid, radioiodinated fibrinogen and gallium67 citrate have all been investigated as indicators of transplant rejection since they usually do not accumulate in normal kidneys, nor in those with acute tubular necrosis. Indium 111m labeled autologous leukocytes and Indium 111 labeled platelets are also under investigation [22]. None of these radionuclide are uniformly accurate in diagnosing acute rejection and their use requires close correlation with other imaging modalities and clinical parameters.

In the past few years, parenchymal sonographic patterns in renal transplants have shown considerable utility in the differential diagnosis of parenchymal failure (Fig. 17). In acute tubular necrosis, sonographically, the allograft appears normal. The renal allograft also appears normal in arterial occlusion and stenosis except for lack of normal post-transplantation hypertrophy. On the other hand, a spectrum of sonographic abnormalities is seen in acute renal allograft rejection, including increased renal volume, decreased renal sinus echogenicity, enlarged medullary pyramids, increased or decreased cortical echogenicity compared to baseline studies and development of perirenal fluid collections [23]. Thus, serial sonographic studies, when correlated with serial radionuclide evaluation and clinical and laboratory data can frequently obviate more invasive studies in the diagnosis of renal transplant failure or other complication.

8. Magnetic resonance imaging of the kidney

Magnetic resonance imaging (MRI) is the newest and most promising imaging method for evaluating the kidney. It is based on the pioneering work of Block and Pursell related to chemical nuclear magnetic resonance (NMR) for which they received the Nobel prize in 1952. The method is attractive because it is noninvasive uses no ionizing radiation and has no known adverse biological effects. Spatial resolution of MRI images is comparable or better than that of computed tomography. Unlike computed tomography, MRI has the ability to produce axial, sagittal and coronal sections without reformatting.

Normal renal anatomy is well demonstrated with MRI. The cortex, medulla, vascular structures and collecting system are discernable [24]. Solid and cystic lesions of the kidney are adequately differentiated. In the staging of carcinoma of the kidney, MRI supplies information similar to that of computed tomography and in some cases gives additional information concerning tumor invasion of the renal vein [25].

It appears that MRI will have a major impact in the evaluation of medical renal disease. Tissue characterization based on the magnetic resonance properties is expected to become an important adjunct to renal biopsy, although further research correlating histology and magnetic resonance properties is needed. MRI will probably also have an important role in the evaluation of patients on long-term hemodialysis. These patients have an increased incidence of renal neoplasia and acquired cystic disease. The superior resolution of MRI compared to ultrasound gives MRI a distinct advantage in the evaluation of these kidneys.

The exact role of MRI in renal imaging is not yet adequately assessed. Its cost effectiveness compared to computed tomography and ultrasound in various disease states is yet to be determined. The equipment is expensive and scanning time is longer compared to computed tomography. Despite these problems, MRI is expected to play a role in the imaging of renal masses and medical renal disease in general. The development of spectroscopic imaging, where extensive research is conducted at the present time, will bring us to a new era of tissue characterization and histologic study in vivo.

9. Concluding remarks

In this short chapter we have attempted to provide an overview of the most recent advances in renal imaging and to outline the percutaneous techniques in the urinary tract which have been developed in the past few years. Space considerations prevent discussion of the basic and time honored method of excretory urography which remains the most frequently used radiographic study for evaluation of the urinary tract.

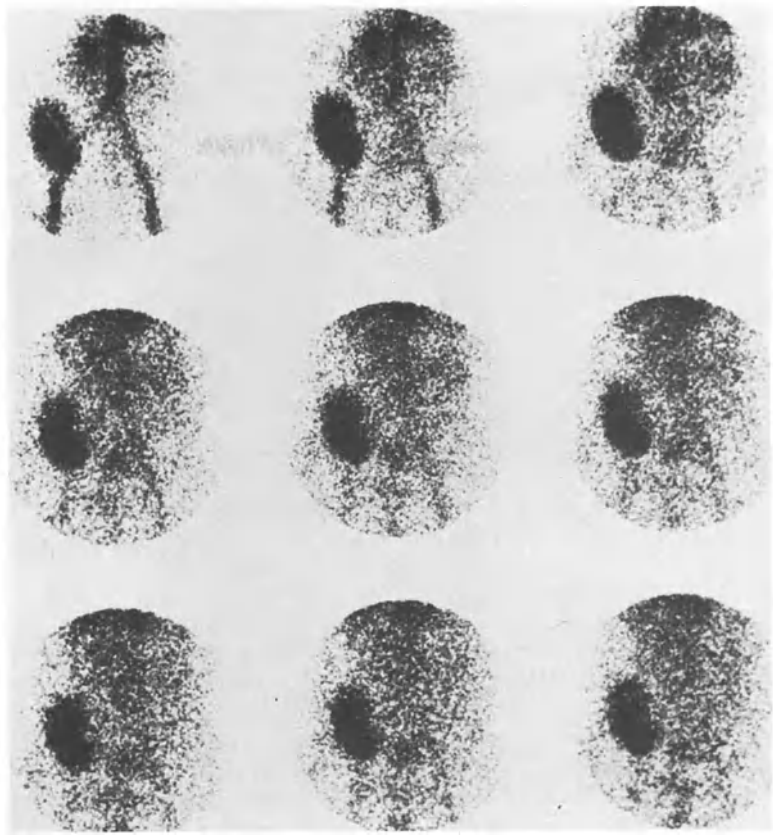

A

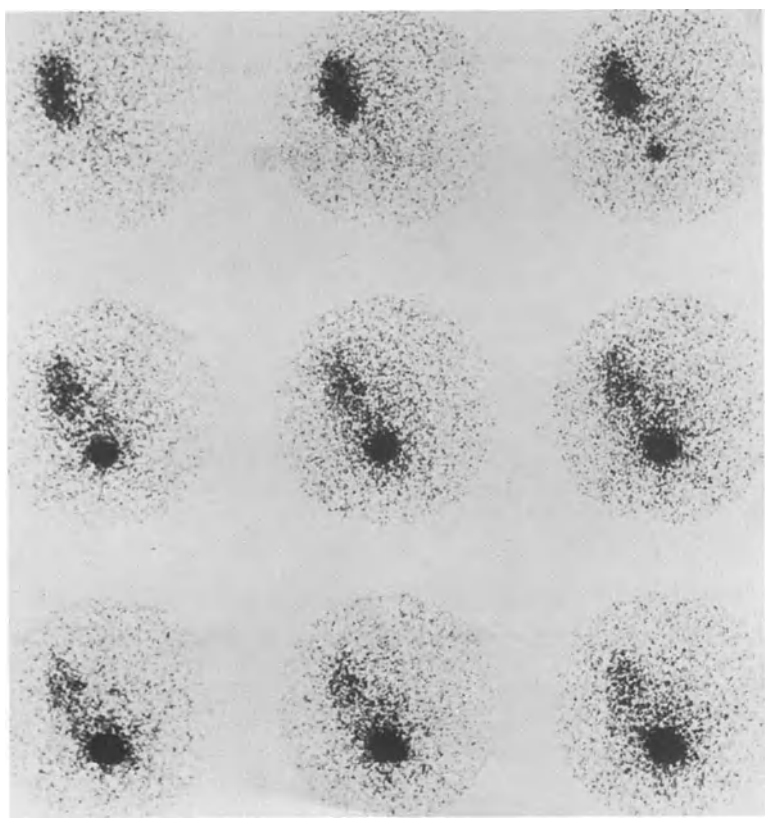

B

Fig. 16. Normal radionuclide evaluation of right renal allograft. (A) Technetium 99m DTPA flow study. These serial images represent three seconds per frame. The first image demonstrates perfusion of the transplanted kidney at the same time as the radionuclide passes through the aorta and iliac arteries. Considerable activity remains in the kidney on later images since Technetium 99m DTPA is excreted by glomerular filtration. (B) Iodine ^{131}Hippuran study of the same kidney with images representing one minute per frame shows good uptake by the kidney then gradual decrease in renal activity as the compound is excreted into the bladder, where there is progressively greater activity.

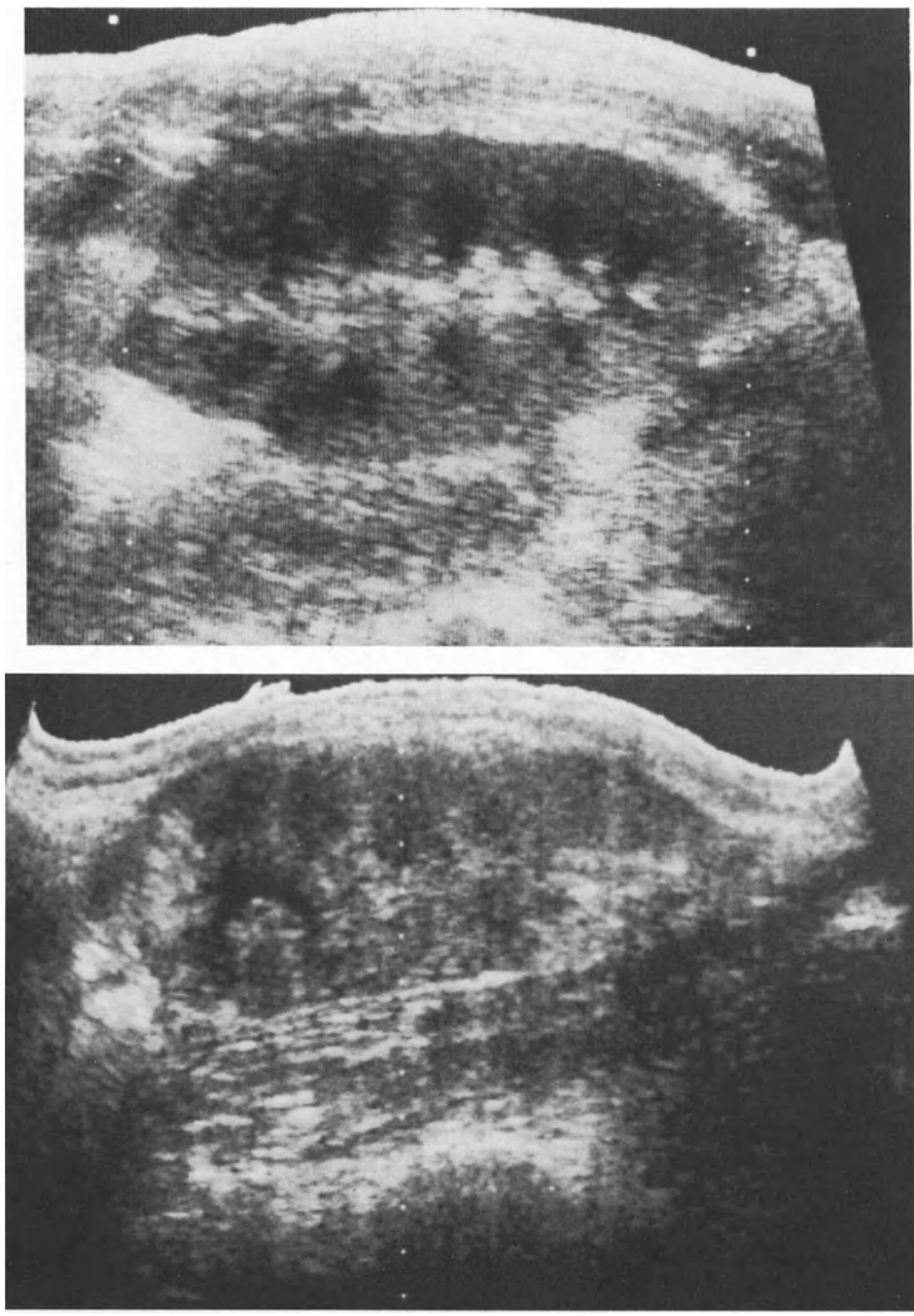

Fig. 17. Sonography of renal allograft rejection. (A) One week after renal transplant, the kidney has normal cortical echogenicity, normal intense central eco complex and well defined normal triangular renal pyramids. (B) Four weeks later, during an episode of clinical rejection, sonographic evidence of rejection is present. There is increased cortical echogenicity, disruption of central echo complex and poor definition of the pyramids.

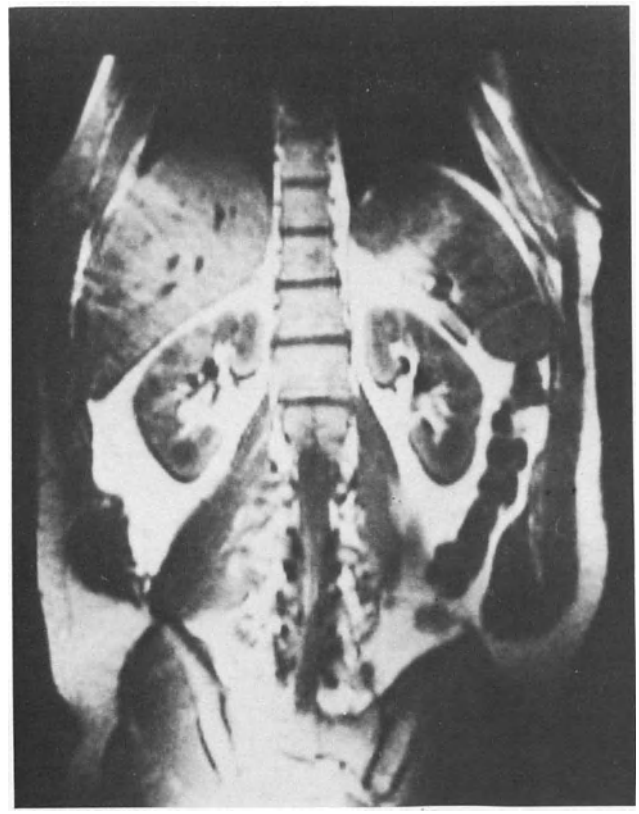

Fig. 18. Coronal magnetic resonance image. High intensity signal from perirenal fat and fat in the renal hila. Renal cortex and medulla are resolved. Courtesy of General Electric.

It is apparent that close cooperation between the physicians responsible for primary patient care and the radiologist is required for selection of the most expeditious series of procedures for diagnosis in patients with renal disease. While these more sophisticated procedures are expensive, the savings in hospital days and patient morbidity and the improved accuracy in diagnosis, contributing to better quality care, more than justifies their utilization.

References

1. Johnson JL, Abernathy DL: Diagnostic imaging procedure volume. Radiology: March, 851–853, 1983.
2. Leving E, Maklad NF, Rosenthal SJ, Lee KR, Weigel J: Comparison of computed tomography and ultrasound in abdominal staging of renal cancer. Urology 16: 317–322, 1980.
3. Maura MA, Wadsworth ED, Stanley RJ, McLennan BL: Renal cell carcinoma: Angiography in the CT era. Am J Roentgenol 139: 1135–1138, 1982.
4. Weyman PJ, McLennan BL, Stanley RJ, Levitt RG, Sagel SS: Comparison of computed tomography and angiography of the evaluation of renal cell carcinoma. Radiology 137: 417–424, 1980.
5. Bosniak MA: Angiomyolipoma of the kidney: A preoperative diagnosis is possible in virtually every case. Urological Radiology 3: 135–142, 1981.
6. Levine E, Huntra KM: Computed tomography of renal oncocytoma. Am J Roentgenol 141: 741–746, 1983.
7. Sandler CM, Roombs BD: Computed tomography of blunt renal injuries. Radiology 141: 461–466, 1981.
8. Federle MP, Kaiser JA, McAninch JW, Jeffrey RB, Mall JC: The role of computed tomography in renal trauma. Radiology 141: 455–460, 1981.
9. Lee JKT, McClennan BL, Melson GL, Stanley RJ: Acute focal bacterial nephritis: Emphasis on gray scale sonography and computed tomography. Am J Roentgenol 135: 87–92, 1980.
10 Handmaker H: Nuclear imaging in acute pyelonephritis. Semin Nucl Med 12: 246–253, 1982.
11. Subramanyam BR, Megibow AJ, Nagesh B: Diffuse xanthogranulomatous pyelonephritis: Analysis by computed tomography and sonography. Urol Radiol 4: 5–9, 1982.
12. Hoddick W, Brooke RB, Goldberg HI, Federle MP, Laing FC: Ct and sonography of severe renal and perirenal infections. Am J Roentgenol 140: 517–520, 1983.
13. Sones PJ: Percutaneous drainage of abdominal abscesses. Am J Roentgenol 142: 35–39, 1984.
14. Cronan JJ, Amis ES, Dorfman GS: Percutaneous drainage of renal abscesses. Am J Roentgenol 142: 351–354, 1984.
15. Zegel HG, Pollack HM, Banner MP, Goldberg BB, Arger PH, Mulhern C, Kurtz A, Dubbins P, Coleman B, Koolpe H: Percutaneous nephrostomy: Comparison of sonographic and fluoroscopic guidance. Am J Roentgenol 137: 925–927, 1981.
16. Mitty HA, Train JS, Dan SJ: Antegrade ureteral stenting in the management of fistulas, strictures and calculi. Radiology 149: 433–438, 1983.
17. Castenada-Zuniga WR, Clayman R, Smith A, Rusnale B, Herrera M, Amplatz K: Nephrostolithotomy: Percutaneous techniques for urinary

calculus removal. Am J Roentgenol 139: 721–726, 1982.
18. Tegtmeyer CJ, Kofler TJ, Ayers CA: Renal angioplasty: Current status. Am J Roentgenol 142: 17–21, 1984.
19. Hillman BI, Ovitt TW, Capp MP, Fisher HD, Frost MM, Nudelman S: Renal digital subtraction angiography: 100 cases. Radiology 145: 643–646, 1982.
20. Silver TM, Campbell D, Wicks JD, Lorber MI, Surace P, Turcotte J: Peritransplant fluid collections. Radiology 138: 145–151, 1981.
21. Kirchner PT, Rosenthal L: Renal transplant evaluation. Semin Nucl Med 12: 370–378, 1982.
22. George EA: Radionuclide diagnosis of allograft rejection. Semin Nucl Med 12: 379–386, 1982.
23. Hricak H, Cruz C, Eyler WR, Madrazo BL, Romanski R, Sandler MA: Acute post-transplantation renal failure: Differential diagnosis by ultrasound. Radiology 139: 441–449, 1981.
24. Hricak H, Crooks L, Sheldon P, Kaufman L: Nuclear magnetic resonance imaging of the kidney. Radiology 146: 425–432, 1983.
25. Hricak H, Williams RD, Moon KL, Moss AA, Alpers C, Crooks LE, Kaufman L: Nuclear magnetic resonance imaging of the kidney: Renal masses. Radiology 177: 765–772, 1983.

CHAPTER 14

Clinical aspects of renal insufficiency induced by drugs and hepatic disease

JOSEPH V. NALLY JR., MICHAEL L. GROSS and JAMES T. HIGGINS JR.

1. Introduction

Progress of any sort commonly carries an element of risk, and clinical medicine is no exception. As the pharmacological armamentarium available to the practitioner expands, so does the risk of adverse reaction in the drug-treated patient. Interest in drug-induced renal disease has several aspects. Not only is there concern for diagnosis, treatment, and prevention of the undesired clinical events, but there is recognition that the elucidation of mechanisms by which drugs injure the kidney, or cause it to malfunction, may shed light on normal and abnormal renal function and on the kidney's reaction to injury.

Modern pharmaceutics is sometime said to have begun with the development of the sulfonamides. If this is true, then the modern era of drug-induced renal disease has the same birthdate for renal injury was one of the first major complications of sulfonamide therapy. Drug-related kidney problems include acute renal failure, chronic renal failure, nephrotic syndrome, fluid-electrolyte disorders, and acid-base disturbances. Since upward of 30–40% of all cases of acute renal failure are caused by drug nephrotoxicity [1], we cannot hope to review all of the nephrologic reactions to drugs, or even the major pathophysiological mechanisms. Thus we have chosen to consider the problems encountered with two of the most used classes of drugs used clinically, the aminoglycoside antibiotics and the nonsteroidal anti-inflammatory drugs, and two of the most commonly recognized types of renal injury, direct injury to renal tubular cells and interstitial nephritis. First we will discuss the direct injury to the renal cells, acute tubular necrosis, produced by the aminoglycoside antibiotics. Next is considered renal interstitial disease caused by several different classes of drugs including some antibiotics and nonsteroidal anti-inflammatory drugs. Finally, we will discuss three clinical states of renal insufficiency or renal failure in which the renal tissues are normal and uninjured, but renal circulation is deranged. The first two of these are caused by drugs which interfere with the intrarenal function of the renin-angiotensin system and the prostaglandin-prostacyclin- thromboxane system. The third of these states of renal dysfunction is the hepatorenal syndrome, in which renal failure follows liver failure, and whose pathogenesis may involve vasoactive hormones or toxins.

2. Drug-induced acute tubular necrosis and acute renal failure

Acute renal failure is defined as a rapid decline in renal function characterized by a rise in the blood urea nitrogen (BUN) and serum creatinine, usually associated with oliguria (less than 400 ml/24-hr), although an increasing incidence of non-oliguric drug-induced renal failure is being recognized.

The prototypic class of drugs causing acute tubular necrosis is the aminoglycosides. Aminoglycosides were first noted to be potentially nephrotoxic in the early 1970's, although before this time were thought to be relatively safe in humans. Despite the development of newer third generation cephalosporins, aminoglycoside use continues and is the most frequent cause of antibiotic-associated acute renal failure. Aminoglycoside nephrotoxicity is estimated to be between 10 and 20% when defined by a rise in serum creatinine of at least 0.4 mg/dl, even when serum concentrations are monitored closely [2].

Although there is a general relationship between cumulative aminoglycoside dose and nephrotoxicity (total dose usually greater than 1.0 gram(s), maintenance of both peak and trough serum antibiotic concentrations at desired levels does not prevent nephrotoxicity. Experimentally in rats, when gentamicin was given once daily (40 mg/kg) compared to the same total dose given three times per day, the rats given gentamycin once daily had a much higher peak serum level but a lower incidence of nephrotoxicity [3].

L.J.A. DiDio and P.M. Motta (eds), Basic, Clinical, and Surgical Nephrology. ISBN 0-89838-689-5.

Older patients and those with pre-existing renal insufficiency seem to be at greatest risk for toxicity. Other predisposing factors include dehydration, hypotension, acidosis, and previous exposure to aminoglycosides. Concomitant administration of a cephalosporin may enhance aminoglycoside toxicity, although this is controversial [4].

Clinically, aminoglycoside nephrotoxicity is nonoliguric, typically occuring after one week of therapy. In rats an increase in urine volume precedes the fall in GFR and is related to a drug-induced concentrating defect with ADH resistance [5].

The exact mechanism related to the nephrotoxicity of aminoglycosides is still debated. In animals proximal tubular necrosis is common but may have a patchy distribution. Tubular regeneration may coexist with necrosis [6]. Electron microscopic changes in proximal tubular cells, including the formation of myeloid bodies, may be seen after a single dose of aminoglycoside, and do not necessarily correlate with toxicity [7]. There is no doubt that aminoglycosides are bound to the luminal brush border and that by pinocytosis become sequestered in the lysosomes of the proximal tubule. The importance of this tissue accumulation is still uncertain. In experimental animals the relative nephrotoxicity of various aminoglycosides does not precisely correlate with their cortical accumulation [8]. Gilbert reported cycling every 10–14 days of renal cortical concentrations of gentamycin with continued dosing for 42 days [9]. He also demonstrated recovery from renal failure with continued dosing in these rats, although improvement in recovery may be more rapid when the drug is discontinued [10]. Although a minimum cortical concentration of the aminoglycoside is necessary it does not suffice as the total explanation for toxicity. Once inside the lysosome there may be effects related to mitochondrial energetics which may be responsible for the toxicity. More recently, Baylis has reported a decline in glomerular ultrafiltration coefficient as a contributing factor [11].

All members of the aminoglycoside family appear to be potentially nephrotoxic. It is of great clinical importance to compare the various aminoglycosides currently in use as to their nephrotoxicity. Numerous studies, both animal and human, have compared gentamycin to tobramycin. In animal studies it appears clear that gentamycin is more nephrotoxic than tobramycin. In dogs renal cortical accumulation of gentamycin is higher than that of tobramycin and gentamycin toxicity is greater [12], but the significance of cortical concentration has been questioned [8]. Numerous human studies have also suggested less nephrotoxicity for tobramycin versus gentamycin [2, 13], although a recent study by Fong [14] showed no significant difference.

Netilmycin is the newest member of the aminoglycoside family to be released. Preliminary animal studies look extremely encouraging [15], although a significant number of human studies to date have not been reported. In the one human study available, nephrotoxicity was extremely low for both tobramycin (4%) and netilmycin (1%) when combined with ticarcillin so that statistical significance was not achieved [16]. Some clinicians would prefer tobramycin over gentamycin if the microbe sensitivity permits, and await the results of more clinical trials concerning netilmycin.

The prognosis for aminoglycoside-induced ARF is usually good with resolution within 1–2 weeks. Patients at highest risk to develop more permanent renal failure are those with pre-existing renal insufficiency.

3. Drug-induced interstitial nephritis

Many drugs may impair renal function by producing an acute interstitial nephritis which may be immunologically mediated [17]. Recognition of this syndrome is of great clinical significance since this is a potentially reversible form of renal failure. Two major types of acute interstitial nephritis will be discussed; one will be the classic drug-induced allergic interstitial nephritis and the other, the newly described interstitial nephropathy secondary to nonsteroidal anti-inflammatory drugs (NSAID), which may not be prostaglandin-dependent. Elsewhere in this chapter the effects of nonsteroidal anti-inflammatory agents on prostaglandin synthesis and renal circulation will be discussed.

Acute interstitial nephritis was first recognized with the use of methacillin. Since 1961 over 100 cases have been reported. Clinically, the patients were treated with normal doses of methicillin and problems occurred after many days into therapy. It is not uncommon for patients to defervess when initially treated with methicillin but then become febrile again when the acute interstitial nephritis begins. Presenting symptoms include fever, skin rash, macroscopic hematuria, eosinophilia and eosinophiluria. Clinical features of acute interstitial nephritis caused by drugs other than methicillin confirms that not all features are present in each case. Pyrexia occurs in approximately 80%, skin rash in 50%, and arthralgias in 20%. Renal function usually deteriorates quickly with oliguria. Eosinophilia and elevated serum IgE level may be seen. Pyuria is com-

mon and the demonstration of eosinophils in the urinary sediment is diagnostic [18]. It must be emphasized that the lack of eosinophilia, increased IgE or eosinophiluria does not exclude the diagnosis since 50% of patients with biopsy-proven acute interstitial nephritis may exhibit none of these features.

The principal difficulty in diagnosing acute interstitial nephritis is differentiation of this entity from other forms of acute renal failure, such as acute tubular necrosis or other drug-induced nephropathies. Classical urinary diagnostic indices have not been helpful, but recently gallium scanning has been demonstrated to be positive in all cases of biopsy-proven interstitial nephritis and absent in all patients with acute tubular necrosis [17].

The pathogenesis of acute interstitial nephritis is not clear. Immunologic mechanisms are suggested by the presence of eosinophils and elevated IgE levels. Antitubular basement membrane antibodies have also been described, as well as complement deposition along the tubular basement membrane. In the vast majority of cases immunoglobulins are absent in the renal biopsy and anti-tubular basement membrane antibodies cannot be identified. Complications of the disease include selective distal tubular dysfunction, and episodes of papillary necrosis. Renal function improves when the offending drug is withdrawn, and the use of steroids for this condition is controversial. In a recent study administration of 60 mg of prednisone daily hastened recovery of renal function and reduced the extent of residual renal damage [18]. The most commonly implicated drugs include most antibiotics, diuretics, and nonsteroidal anti-inflammatory agents.

The prognosis of drug-induced interstitial nephritis is excellent once the offending agent has been discontinued. If unrecognized or the offending drug is continued, permanent renal failure may result.

Three distinct clinical syndromes have been described in patients receiving nonsteroidal anti-inflammatory drugs who developed interstitial renal disease [19]. These include: 1) nephrotic syndrome with acute renal failure, the most common, 2) nephrotic syndrome alone, and 3) renal failure alone. Although the clinical findings in some patients with NSAID interstitial nephritis resembled the classic drug-induced interstitial nephritis, many differences exist. These differences include: 1) the duration of exposure for the NSAID-treated group was much greater than for the patients with allergic interstitial nephritis (5 months versus 15 days), 2) a hypersensitivity response (fever, rash, eosinophilia) occurs in only 20% of the nonsteroidal group compared to 85% in patients with allergic interstitial nephritis; 3) nephrotic range proteinuria occurs in 85% of patients with the nonsteroidal nephropathy in comparison to only 5% for drug induced allergic interstitial nephritis; 4) nonsteroidal interstitial nephritis is seen in older patients in comparison to allergic interstitial nephritis which is seen in all age groups.

Acute interstitial nephritis secondary to drugs is probably a more common cause of acute renal failure than had previously been thought. Its recognition depends upon increased awareness and a high level of suspicion. The prognosis for recovery from the acute renal failure is good if the offending agent can be removed, but failure to recognize this syndrome may lead to progressive and permanent renal failure.

4. Renal insufficiency caused by renal vascular response to drugs

4.1. Normal renal vascular autoregulation

The intrarenal circulation is unique, containing two capillary beds in series, the glomerular and the peritubular capillaries, each supplied by arterioles (Fig. 1). The afferent arterioles supply the glomerular capillaries, which in turn are drained by the efferent arterioles to feed the peritubular capillary bed. The rate of plasma filtration at the glomerular capillary bed depends upon the hydraulic conductivity of the capillary walls, the surface area of the capillary bed, and the driving force for filtration. The net driving force for filtration is the sum of the hydrostatic and oncotic forces on each side of the capillary wall. The hydrostatic pressure within the glomerular capillaries depends upon the level of systemic arterial pressure transmitted through the afferent arterioles, and the resistance to outflow from the capillaries through the efferent arteriole. The rate of blood flow through the glomeruli is largely controlled by the resistance of the afferent arterioles, and over a wide range of systemic arterial pressures the blood flow through the kidney is held remarkably constant by this autoregulatory process [20]. The rate of filtration, on the other hand, appears highly dependent upon the resistance of the efferent arterioles. Thus the glomerular filtration rate can be maintained relatively constant despite variations in systemic arterial blood pressure and renal blood flow rate.

The smooth muscle tone, or arterial resistance, in the afferent arterioles is partially under control of the adrenergic nervous system, and there is also a large element of response to stretch by as yet unex-

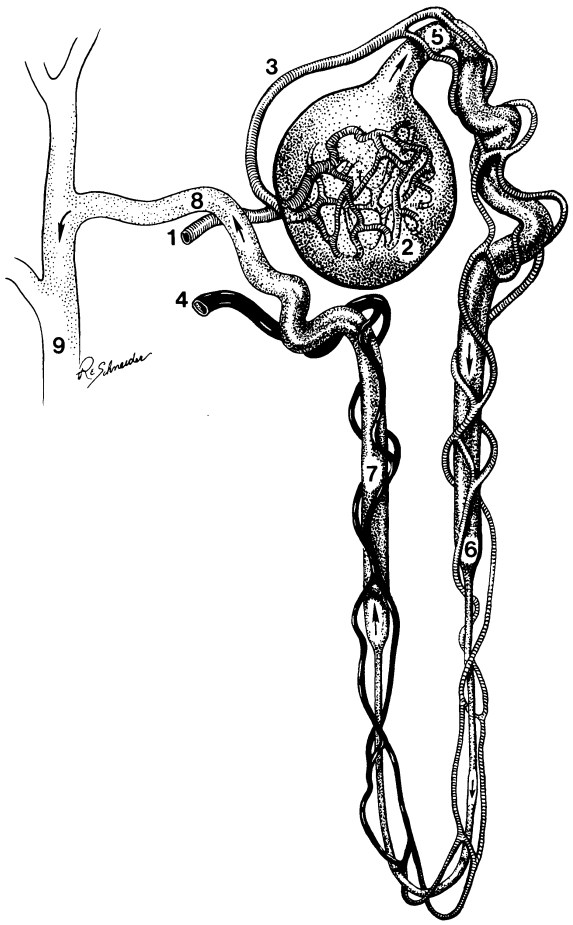

Fig. 1. Schematic representation of an outer cortical nephron segment. The afferent arteriole (1) carries blood into the glomerular capillary tuft (2). The glomerular capillaries are drained by the efferent arteriole (3) which branches into a capillary bed surrounding the renal tubule and carries blood to a vein (4). Fluid filtered from the glomerular capillaries (2) enters Bowman's capsule, proximal convoluted tubule (5), the descending (6), and ascending (7) limbs of Henle's loop, the distal convoluted tubule (8), and the collecting duct (9), Note the proximity of the distal convoluted tubule (8) and the afferent arteriole (1), where specialized epithelial cells in the macula densa of the tubule make contact with renin-secreting juxtaglomerular cells of the arteriole.

plained mechanisms to cause autoregulation of blood flow. Control of efferent arteriole resistance appears to result from several intrarenal hormonal systems acting in concert. The major vasoconstrictor effect is thought to be due to angiotensin II; the vasoconstrictor effect of angiotensin II is counteracted by vasodilator effects of products of the cyclo-oxygenase system, prostaglandins and prostacyclin, and possibly by products of the kallikrein-kinin system.

Space permits only a cursory discussion of this complicated control system. The amount of angiotensin II produced depends on the secretion rate of renin from the juxtaglomerular cells in the walls of the afferent arterioles. The secretion rate of renin is determined by the arterial blood pressure, by β-adrenergic stimulation via renal nerves, and by a poorly understood signal from the macula densa cells of the distal convoluted tubule. There appears to be sufficient renin substrate in plasma, and converting enzyme in vessel walls, to generate angiotensin II in blood as it passes through the glomeruli.

$$\text{Renin substrate} \xrightarrow[\text{enzyme}]{\text{renin}} \text{angiotensin I} \xrightarrow[\text{enzyme}]{\text{converting}} \text{angiotensin II}$$

Prostaglandins, prostacyclin and thromboxanes (collectively referred to as prostanoids) are products of the action of cyclo-oxygenase on arachidonic acid, which is released from cell membrane phospholipids by phospholipases.

Phospholipids
↓ Phospholipase
Arachidonic acid
↓ Cyclo-oxygenase
Precursor prostaglandins
↙ ↓ ↘
Prostacyclin Prostaglandins Thromboxanes

The action of phospholipase appears to be the pivotal step, and is stimulated by angiotensin II as well as by vasopressin, catecholamines, and a number of other stimuli including ischemia and calcium [21]. Prostacyclins and prostaglandins of the E-series have vasodilator properties, whereas the thromboxanes are vasoconstrictors. Although the factors determining the ratio of the products of arachidonic acid oxygenation are unknown, in the renal cortex the production of the vasodilator PGE_2 predominates, and production of prostacyclin exceeds that of thromboxane [22]. Thus, the net hemodynamic effect of increased prostanoid synthesis in the kidney is vasodilatation and increased blood flow.

As mentioned above, angiotensin II is a potent stimulus to prostanoid synthesis. Conversely, the vasodilator prostanoids are potent stimuli of renin secretion. Thus there is an interaction between these intrarenal vasodilator and vasoconstrictor systems to control renal blood flow, and an even more direct and important control of glomerular filtration rate by their effects on the efferent arteriole [21]. Hall *et al.* demonstrated the role of angiotensin II in autoregulation of GFR in dogs [23]. During reduction of renal perfusion pressure, renal blood flow and GFR

autoregulation were well maintained, but when an antagonist of angiotensin II was infused during low perfusion pressure, renal blood flow rose and GFR fell. These results were even more striking in sodium-depleted animals, suggesting that in high renin states the action of angiotensin II on the efferent arteriole is necessary for maintenance of glomerular filtration.

The role of prostaglandins in normal renal function is somewhat more difficult to assess. Infusion of arachidonic acid, prostaglandins or prostacyclin into the renal circulation of dogs and rabbits produces vasodilation and increased renal blood flow. There is little or no change in GFR, thus filtration fraction is reduced. In the rat different results are seen, which emphasize the interrelations of the prostanoids and renin-angiotensin system. In this species, infusion of arachidonic acid increases renal vascular resistance and reduces renal blood flow. Since this effect can be overcome by infusion of the angiotensin II inhibitor saralasin, the vasoconstrictor response to arachodonic acid is thought to be due to stimulation of renin secretion by the products of arachidonic acid metabolism. The response of the rat renal circulation to infusion of prostaglandins and prostacyclin are not so clearcut, and probably represent the complex interplay of vasoconstrictor and vasodilator effects [Reviewed in (21)].

4.2. Renal response to inhibitors of prostaglandin synthesis

Synthesis of the prostanoids is inhibited by a large number of agents including aspirin, indomethacin and newer pharmaceutical compounds such as ibuprofen, sulindac, meclofenamate and others. These drugs are known collectively as nonsteroidal anti-inflammatory drugs (NSAID). The NSAID's are useful in a wide variety of inflammatory and rheumatologic disorders, and together constitute the most widely prescribed class of drugs [24]. Thus, because of their wide use, the potential for harm is great if these drugs have serious side effects.

Administration of NSAID's to conscious, unstressed animals or human subjects does not result in any significant reduction in renal blood flow or glomerular filtration rate. Earlier studies carried out in anesthetized dogs, sometime subjected to surgical trauma, had shown renal vasocontriction in response to inhibitors of prostaglandin synthesis and it is now felt that under such circumstances renal blood flow is preserved by prostaglandin synthesized in response to the vasocontrictor mechanisms produced by trauma and stress. Similar dependence on prostaglandin synthesis to preserve blood flow and glomerular filtration during sodium depletion can be demonstrated using the NSAID's. Other conditions in which prostaglandins are important for maintenance of renal function include reduced renal perfusion due to volume contraction (salt depletion, dehydration, hemorrhagic hypotension) or reduced cardiac output [21], and hepatic disease (discussed below in relation to the hepatorenal syndrome). However, in the normal, unstressed, volume replete, conscious subject the prostanoids are probably not active in control of renal function, and their suppression by drugs does not result in renal dysfunction.

In contrast to the situation in the normal kidney, the diseased kidney may be more dependent on the products of the cyclo-oxygenase system for preservation of function. The observation that two patients with systemic lupus erythematosus developed striking decreases in renal function while taking large doses of aspirin prompted Kimberly and Plotz to carry out a prospective study of 23 patients with this disease [25]. They observed that 13 patients developed significant elevations in serum creatinine and blood urea nitrogen levels while on aspirin; patients with active nephritis or who were hypocomplementemic were more likely to suffer this complication. The reduction in renal function was reversed when the aspirin was discontinued. Later studies of seven women with systemic lupus erythematosus showed that their urinary prostaglandin E excretion was above normal [26]. During aspirin treatment, the urinary PGE excretion fell by 45%, the clearance of creatinine, inulin and para-aminohippurate fell by 18%, 14% and 29% respectively, and it was observed that the degree of reduction in urinary prostaglandin excretion and glomerular filtration rate were highly correlated. These observations, as well as studies in uremic rabbits [27], suggested that increased renal prostaglandin production helps to maintain renal function in states of renal insufficiency. In rabbits made uremic by subtotal nephrectomy, urinary PGE excretion was greatly elevated; during administration of either indomethacin or meclofenamate, urinary prostaglandin excretion fell by 71% and glomerular filtration rate was halved. In normal control rabbits, the NSAID's reduced urinary PGE excretion without an effect on glomerular filtration rate.

In a study of 20 female patients with various types of glomerular disease, and preservation of creatinine clearance to 40 ml/min or above (about 50% of normal or greater), urinary PGE_2 excretion rate was equal to that of normal subjects, and 6-keto-$PGF_{1\alpha}$

excretion (a measure of prostacyclin production rate) was significantly reduced [28]. When 10 of the women with renal disease were given ibuprofen, urinary excretion rates of 6-keto-$PGF_{1\alpha}$ and PGE_2 fell by 80%, creatinine clearance fell 28%, (range 19–44%) and para-aminohippurate clearance was reduced by 35%. The fall in GFR was inversely related to the baseline excretion rate of 6-keto-$PGF_{1\alpha}$, but unrelated to PGE_2 values. These investigators suggested that prostacyclin is the most important of the cyclo-oxygenase products for preservation of function in the diseased kidney. Another important observation in this study was the failure of sulindac to reduce renal function in 10 other patients with glomerular disease, despite evidence of inhibition of nonrenal cyclooxygenase activity. This finding suggests organ-specificity of cyclo-oxygenase inhibition by the NSAID's and indicates that sulindac may be safe for use when an anti-inflammatory drug is needed in the patient with impairment of renal function.

Another potentially serious complication of the use of NSAID's is hyperkalemia [24]. As is the case of the acute renal insufficiency described above, the patients at greatest risk of developing hyperkalemia are those with preexisting impairment of renal function, who in addition have low levels of secretion of renin and aldosterone. These patients with so-called hyporeninemic hypoaldosteronism are usually in the older age group and commonly have diabetes in addition to mild renal insufficiency. When such individuals receive NSAID's, a severe hyperkalemia may develop, which is disproportionate to any concomitant worsening of glomerular filtration. The details of the pathophysiologic process remain to be clarified in their entirety, and the patient population at risk is not homogeneous. However, it appears that the basic underlying mechanism is removal of the stimulation to renin secretion provided by the products of the cyclo-oxygenase system. The reduction in renin secretion results sequentially in lower angiotensin II production, less stimulation of aldosterone secretion by angiotensin II, and loss of aldosterone-mediated potassium secretion by the renal tubules. As in the case of NSAID-induced renal insufficiency, the hyperkalemia resolves when the inhibitor of prostaglandin synthesis is removed.

4.3. Renal insufficiency caused by inhibition of the renin-angiotensin system

As described earlier in this chapter, autoregulation to preserve filtration at low renal perfusion pressure depends in large part upon increased resistance to blood flow in the efferent arteriole. The example described was the reduction in GFR, with increased total renal blood flow, which follows administration of a competitive antagonist of angiotensin II to dogs which were made hypotensive [23]. This study suggested that the vasoconstrictor effect of angiotensin II on the efferent arteriole is required to preserve glomerular filtration.

The physiological effects of angiotensin II can also be blocked by administration of inhibitors of the enzymatic action of converting enzyme, which converts angiotensin I to angiotensin II. Following the discovery that certain snake venoms can block converting enzyme activity, synthetic substances were produced for both parenteral and oral administration. These drugs show promise for treating hypertension, especially those types of hypertension associated with increased renal renin secretion. One of these substances, captopril, is now marketed for oral administration in the treatment of hypertension.

The best-understood and most-studied type of hypertension caused by increased renin secretion is that caused by renal artery stenosis. This form of hypertension was originally produced in dogs with experimental renal artery stenosis by Goldblatt, and is commonly referred to as 'Goldblatt hypertension'. The clinical counterpart occurs when blood flow through the renal arteries is impaired, usually by arteriosclerosis or fibrous dysplasia.

The hypertension which results from renal artery stenosis has proven responsive to the converting enzyme inhibitor (CEI), captopril. However, Hricik *et al.* have recently reported eleven patients with severe hypertension and renal artery stenosis who developed renal insufficiency while taking captopril [29]. Seven of these patients had bilateral renal artery stenosis, and the other four had a solitary kidney whose artery had a stenosis. Thus, all of the functioning kidney tissue in each of these patients was subject to reduced perfusion through a stenotic artery. These investigators tested whether the blood pressure reduction produced by captopril caused the renal insufficiency and found that an equal degree of blood pressure reduction with other drugs caused no decrease in renal function. There was no evidence of allergic reaction to the captopril, the urinary sediment showed no evidence of nephritis, and when the captopril was discontinued the renal function of all of the patients recovered. One patient was treated with another converting enzyme inhibitor, MK-421, and showed a reversible decline in renal function similar to that seen during captopril therapy.

A similar reversible decline in renal function during captopril therapy was reported in four renal

transplant recipients by Curtis *et al.* [30]. All of these patients had stenosis of the artery supplying the transplanted kidney. The degree of renal dysfunction was significant, with the average serum creatinine increasing three-fold from a normal value. Similar degrees of blood pressure reduction with other antihypertensive medications did not reduce renal function as did captopril, and when two of the patients were subsequently placed again on captopril the serum creatinine again rose. Five other hypertensive renal transplant recipients who were known not to have renal artery stenosis were treated with captopril and responded with blood pressure reduction equal to that of the patients with renal artery stenosis, but showed no change in renal function.

The conclusion reached from these observations is that the renin angiotensin system plays an important role in preservation of glomerular filtration in states of low renal arterial perfusion pressure. Interruption of this system, by blocking the generation of angiotensin II with a converting enzyme inhibitor for example, results in a significant reduction in glomerular filtration rate [31]. In patients with stenosis of the arteries supplying all of their functioning renal tissue this may result in serious renal insufficiency.

5. Renal insufficiency in the hepatorenal syndrome

5.1. Definition

The term 'hepatorenal syndrome' has suffered since its inception over 50 years ago because of the vague nature of the liver and kidney failure to which it was assigned. The term was originally coined by Helwig and Schutz to designate the unexplained renal failure following biliary tract surgery. More recently experts in the field have agreed that the hepatorenal syndrome (HRS) may be defined as 'incompletely explained renal failure in patients with liver disease in the absence of clinical, laboratory, or anatomic evidence of other known causes of renal failure' [32]. The entity is usually irreversible and carries a grave prognosis, although spontaneous recovery has been reported in isolated cases. Clinical observations regarding the 'functional' nature of the renal failure suggest that the kidneys involved in HRS are capable of normal function when the appropriate changes in the metabolic mileu are achieved. Figure 2 depicts the clinical course of a kidney from a patient with HRS that has been successfully transplanted into a patient with a normal liver [33]. Conversely, resumption of normal renal function in a patient with HRS who underwent a successful liver transplantation has been reported. It is the elusive nature of this 'functional' renal failure which has challenged clinicians and physiologists to determine its underlying pathophysiology.

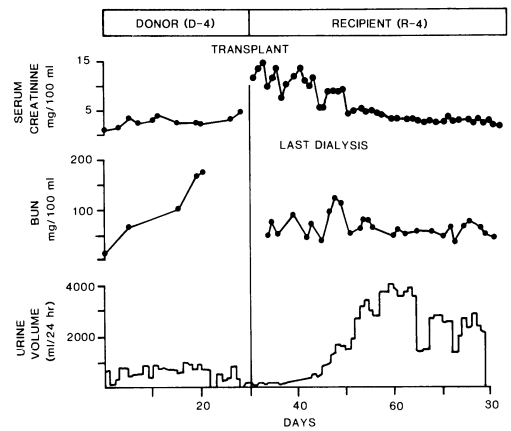

Fig. 2. Clinical course of a kidney donor with hepatorenal syndrome prior to death and that of the recipient after renal transplantation.

5.2. Pathophysiology

The hallmark of the reduced glomerular filtration rate of the HRS is an intense renal vasoconstriction which leads to reduced renal blood flow [34]. This intense vasoconstriction is most marked in the renal cortex and results in a dramatic reduction in cortical blood flow with shunting of the flow to medullary vessels. It appears that the afferent glomerular arterioles are the major sites of renal cortical resistance since filtration fraction has been noted to be reduced or normal in various series. Larger renal arteries such as the interlobar and arcuate arteries are thought to participate in the disorder as renal angiography has documented spasm and tortuousity of these larger caliber vessels. In fact, HRS may well be characterized by vasomotor instability of the entire renovascular tree. Attempts to characterize renal blood flow and its intrarenal distribution using xenon washout techniques have proven disappointing with results yielding markedly abnormal minute-to-minute pertubations in renal flow and intrarenal distribution [34]. The results from these xenon washout studies coupled with the observation that the spasm seen on renal angiography disappears on subsequent post-mortem angiography, suggests that the intense renal vasoconstriction is highly variable and perhaps 'functional' in nature. The position is further supported in that post-mortem pathologic examination of these vessels reveals no abnormalities. Clinically this view is further strengthened

by the observations cited above in which kidney function returns to normal when the kidney is placed in an environment in which liver function is normal.

Despite the intense renal vasoconstriction which is the hallmark of HRS, systemic hemodynamic parameters are usually characterized with increased cardiac output, lowered peripheral resistance, and mildly depressed mean arterial pressure. Clinical studies in decompensated cirrhosis without renal insufficiency demonstrate a high cardiac output, systemic vascular resistance which is normal or low, and blood pressure that is frequently mildly depressed [35]. The etiology of the elevated cardiac output and diminished peripheral resistance seen in decompensated cirrhosis is not clear, yet these findings have been attributed to A-V shunts demonstrated in the skin and lung, as well as peripheral vasodilatation secondary to liver failure per se. The mechanisms underlying this peripheral, as well as splanchnic, vasodilatation seen during the course of hepatic cirrhosis remain a subject of much debate. Since the systemic and renal hemodynamics appear reversible when derangements of liver function are corrected, it is felt that these mechanisms may be humoral or neural in nature. A more complete synopsis of this controversy can be found in the following section on pathogenesis. A vital piece of information required to interpret the theories regarding the intense renal vasoconstriction and sodium avidity is measurement of the plasma volume of the subject. Although the available techniques for measuring plasma volume can sometimes be insensitive to small changes, most studies report that plasma volume in patients with decompensated cirrhosis or the HRS is usually higher than normal [36]. However, these findings are subject to question concerning whether the increase in total plasma volume is adequate to explain the known increase in splanchnic blood volume secondary to splanchnic pooling with cirrhosis. Irrespective of this controversy, studies in subjects known to have HRS have been unable to document improvement in renal function with volume expansion. These findings suggest that there may be varying mechanisms operative during states of severe hepatic dysfunction which may lead to an increase in cardiac output and peripheral vasodilatation while simultaneously causing vasoconstriction in other vascular beds such as the kidney.

In Papper's review of his large series of patients, renal histology was normal or had only minimal changes without evidence of identifiable primary renal disease [32]. The pathologic picture of acute tubular necrosis is thought to be rare during the course of classical HRS. Acute tubular necrosis has been noted when the hepatic failure has been acute and fulminant, or when the patient with liver failure has been exposed to nephrotoxins or other renal insult.

5.3. Pathogenesis

The exact mechanisms underlying the development of HRS remain unknown at present. In general, two possibilities exist to explain the intense renal vasoconstriction and the systemic vasodilatation which are the hallmarks of HRS. The first theory offered contends that the renal findings are a 'physiological' normal response to the extra-renal hemodynamics. The second theory contends that humoral or neural factors occurring in liver failure result in the abnormalities of hemodynamic function. The pro's and con's of these theories will be briefly examined.

The former theory contends that the intense renal vasoconstriction is a physiological response due to the alterations in extra-renal hemodynamics. It is felt that the kidney perceives a reduction in 'effective' blood volume because of systemic vasodilatation alone or in combination with 'shunting' of blood away from vital organs such as the kidney, or by the pooling of blood in the splanchnic circulation as is known to occur with cirrhosis. This perception by the kidney that it is being underperfused results in stimulation of the renin-angiotensin-aldosterone and nervous systems which result in renal vasoconstriction and sodium avidity. Therefore, this theory maintains that renal vasoconstriction and sodium avidity are required to reexpand the reduced 'effective' blood volume to help perfuse vital organs. However, this hypothesis suffers in that a) measurements of blood volume have not been shown to be diminished, and b) volume expansion and systemic vasoconstrictor agents fail to correct the renal perfusion abnormalities. Hence, the validity of this proposal as the only mechanism operative in the development of HRS is brought into question.

An alternative hypothesis proposes that a putative circulating factor(s) which is produced by or inadequately destroyed by the failing liver is responsible for the systemic vasodilatation and simultaneous vasoconstriction in other vascular beds such as the renal circulation. Potential candidates under consideration include: false neurotransmitters, endotoxemia, jaundiced serum, vasoactive intestinal peptide (VIP), the kallikrein-kinin system, the renin-angiotensin system, and the renal prostaglandins.

Although evidence clearly implicating the aforementioned factors as the etiology of HRS remains unconvincing, several intriguing possibilities are

proposed. There have been several observations suggesting that conjugated (vs. unconjugated) hyperbilirubinemia results in an increased susceptibility to ischemia-induced renal dysfunction. The experimental canine model of choledoco-caval anastomosis resulting in marked conjugated hyperbilirubinemia with otherwise normal liver function results in a significant decrease in mean arterial pressure and peripheral resistance with no significant change in cardiac index [37]. These dogs had no significant decrease in GFR, but sodium avidity was noted. These findings suggest that conjugated hyperbilirubinemia does affect systemic and renal hemodynamics, but the application of these findings to HRS remains speculative. Other investigators speculate that a vasodilatory material, identified as ferritin, is increased in liver disease yet its role in HRS is questioned. Some propose that false neurotransmitters such as phenylethanolamine and octopamine are substituted for norepinephrine and dopamine resulting in mild systemic hypotension seen in HRS. Others feel that the renal vasoconstrictor endotoxins accumulate in cirrhosis from intestinal bacteria and are instrumental in the development of HRS. This proposal may warrant further study in that endotoxins are vasodilatory in some vascular beds while being renal vasoconstrictors. Other vasodilatory substances such as bradykinin and VIP are often found to be elevated in cirrhosis, and proponents speculate that the subsequent deficiency of these vasodilatory substances results in eventual genesis of HRS. However, evidence for these proposals as being pathogenetic for HRS remains unconvincing.

The role of the renin-angiotensin system in HRS has received a great deal of attention because of the elevated plasma renin activity documented in decompensated cirrhosis with and without renal dysfunction. In addition, measurement of renin substrate, which is usually produced by the normal liver and kidney, has been depressed and this has been implicated in HRS. It is claimed that the deficiency of substrate impairs the inhibitory feedback loop resulting in persistent renin secretion. Persistently elevated renin level within the kidney is thought to result in afferent renal constriction. Similarly, others implicate the secondary increase in angiotensin II in causing the intense renal vasoconstriction. However, angiotensin is not thought to cause constriction of the inter-lobular and arcuate arteries which are prominently involved in HRS. More likely, the activation of the renin-angiotensin system is secondary to the perceived decrease in 'effective' blood volume proposed in decompensated cirrhosis with ascites. These views are supported by the observations that infusion of dopamine is capable of increasing renal blood flow and suppressing renin activity in cirrhosis. Additionally, thereapeutic trials with saralasin, an angiotensin II antagonist, have failed to improve renal function in patients with HRS [38]. Additional therapeutic maneuvers such as the Leveen (peritoneovenous) shunt which increases cardiac output, measured plasma volume, and renal function also tends to suppress activation of the renin angiotensin system [38]. Hence, the majority of studies lend support to the hypothesis that the hyperreninemia seen both in cirrhosis and HRS is secondary to renal hypoperfusion, and thus not involved in the genesis of HRS.

More recently, attention has been focused on the role of renal prostaglandins in maintaining renal hemodynamics during cirrhosis and the pathogenetic role these substances may play in the development of HRS. An overview of the role of prostaglandins and their function in normal and abnormal kidneys can be found earlier in this chapter. Studies by Zipser *et al.* documented an increased level of urinary PGE in cirrhotic patients with ascities and normal renal function compared to control subjects [39]. Later studies by this group and by Boyer *et al.* demonstrated that the administration of non-steroidal anti-inflammatory drugs (NSAID's) such as indomethacin or ibuprofen resulted in a reduction of urinary PGE with a concomitant fall in creatinine clearance of approximately 50% [40, 41]. Observations by Zambraski and Dunn in the canine model of cirrhosis induced by chronic bile duct ligation added additional insight into the role of vasodilatory prostaglandins in maintaining GFR and renal blood flow during cirrhosis [42]. Urinary excretion rates of PGE_2, $PGF_{2\alpha}$, and a metabolite of PGI_2 (6k-$PGF_{1\alpha}$) were significantly increased following chronic bile duct ligation. The administration of indomethacin following chronic bile duct ligation reduced prostaglandin excretion by 65–90% and significantly decreased GFR and renal blood flow by greater than 50%. These changes were irrespective of plasma renin activity or the presence of ascites. These studies demonstrate that renal vasodilatory prostaglandin synthesis is increased following experimental cirrhosis and this increase in prostaglandin synthesis serves to maintain GFR and renal blood flow. Additional studies by Zipser *et al.* are even more intriguing in an attempt to relate renal prostaglandins to the development of HRS. Zipser and his group have documented significant reduction in the vasodilatory PGE in the urine of HRS patients compared with normal fluid-restricted control subjects, other groups of patients with cirrhosis and preserved

renal function, or patients with other categories of acute or chronic renal failure [43]. In addition to the reduction of urinary PGE, they also noted a significant elevation of urinary excretion of the vasoconstrictor thromboxane B_2, a marker of renal thromboxane A_2 production, in the HRS group compared to the others. They speculate that the increase in vasoconstrictor thromboxane A_2 with a decreased vasodilatory urinary PGE may play a pathogenic role in the development of HRS.

5.4. Clinical features and treatment

In general, patients with HRS have stigmata of advanced liver failure with the development of acute or subacute renal insufficiency occurring late in their course of liver disease [32]. The etiology of the underlying liver disease has been variable with no specific predilection for HRS to develop in any particular type of liver disease. There are no significant clinical nor laboratory parameters of the liver disease which appear predictive of those cirrhotics who will eventually develop HRS. Earlier reports suggested that the inability to excrete a free water load may have been predictive, yet this finding appears to be rather non-specific. Patients usually have signs of jaundice, ascites, and hepatic encephalopathy. However, there is no correlation of the degree of hyperbilirubinemia, ascites or encephalopathy with the development of the hepatorenal syndrome. There is often a mild reduction in blood pressure which also does not appear to correlate with the development of HRS. Some events such as GI hemorrhage, paracentesis, sepsis, and vigorous diuresis have been proposed as precipitating factors for HRS, but evidence for such claims is inconclusive.

Clinical laboratory studies confirm the presence of severe hepatic dysfunction. Often there are present signs of coagulopathy, markedly elevated bilirubin, and depressed serum albumin, but all these findings are not universal. In essence, the hospitalized patient appears to be slowly succumbing from the effects of liver failure, with azotemia developing late in his course. HRS is relatively uncommon as it was noted in only 24 of 350 patients dying of liver failure [32].

The urinary findings are characterized by marked oliguria in the later stages of the syndrome at a time when serum creatinine concentration is rising. Urinary sodium excretion is dramatically reduced, usually to less than 10 mEq per liter. Urinalysis discloses an acid pH and trace proteinuria with bile-stained granular and hyaline casts occasionally seen. The urine is usually concentrated relative to plasma. Patients with HRS exhibit a poor renal diluting ability with serum sodium concentration frequently found to be reduced. BUN and creatinine are elevated but usually not to the degree seen in equivalent states of 'terminal' renal failure. These parameters may poorly reflect the degree of renal dysfunction for several reasons. The blood urea nitrogen may be less elevated because of the poor dietary protein intake secondary to anorexia, as well as decreased hepatic synthesis of urea. Likewise, serum creatinine may not be as elevated for a given glomerular filtration rate because of reduced muscle mass. Quantitation of urinary lysozymes as markers of tubular dysfunction are normal contrasted with levels in acute tubular necrosis. The urinalysis and low urine sodium values are quite helpful in distinguishing HRS from ATN, yet a diagnostic dilemma exists differentiating HRS from prerenal azotemia in a patient with liver failure. In essence, the diagnosis of HRS is a diagnosis of exclusion in that the patient with HRS does not respond to volume expansion.

The prognosis for HRS remains grim with most patients dying within several days to several weeks after the diagnosis is made. Spontaneous recovery of renal function has been reported but is rare.

Given the dire prognosis of HRS, the clinician's first task is to exclude reversible causes of renal insufficiency such as urinary tract obstruction, septic shock, and exposure to nephrotoxins. In order to differentiate HRS from pre-renal axotemia clinically, the patient is usually hydrated with colloids or crystaloids to insure that vascular volume is adequate. If a renal insult other than HRS is identified, appropriate maneuvers aimed at the correction of the underlying disease are instituted and appropriate supportive measures and dialysis are offered until kidney function returns. However, if the diagnosis of HRS is readily apparent, therapeutic interventions including dialysis have not proven beneficial and the prognosis remains grim.

Numerous therapeutic interventions have been proposed for treatment of HRS and the reader is referred to the excellent review of Levenson *et al.* for a more complete synopsis of this topic [44]. Since the pathophysiology of HRS appears to be multi-factorial, therapies have been directed at the various abnormalities of renal function and hemodynamics which have been documented. However, there have been no controlled studies which demonstrate benefit on the outcome of HRS with administration of systemic vasoconstrictors nor intra-renal infusion of renal vasodilators. Infusion of PGE_2 and PGA_1 into patients with HRS have not produced a sustained improvement in renal function. Similarly, angioten-

sin II antagonists have been unsuccessful in improving renal function.

Several maneuvers have been attempted to improve the systemic and renal hemodynamics by expanding the vascular volume with the patient's own ascites. Improvement seen with paracentesis and removal of ascitic fluid has proven transient. The use of the peritoneovenous LeVeen shunt in returning ascitic fluid to the intravascular space for the management of HRS remains controversial. Recent reports on LeVeen shunt in HRS have demonstrated an increase in urine flow and sodium excretion with a subsequent increase in GFR [38]. However, these and other published reports suffer from the fact that there have not been controlled, randomized studies. Use of this type of therapy requires further study in which the potential benefits of the shunt are balanced against some of its known complications such as infection and disseminated intravascular coagulation. It appears that long-term controlled studies of the LeVeen shunt are warranted to evaluate the early reports of success. At present, therapy with the LeVeen shunt is being eagerly embraced by some because of the dismal results with other forms of therapy. Additional therapeutic attempts including steroids and immunosuppression, exchange transfusions, hemoperfusion, and cross-circulation experiments have likewise proven not to be beneficial. A prospective controlled examination of survival and complications with the LeVeen shunt is in order to assure that we are not just changing the mode of death for these patients from renal failure to deaths of sepsis and hemorrhage.

References

1. Bennett WM, Plamp C, Porter GA: Drug-related syndromes in clinical nephrology. Ann Int Med 87(5): 582–590, 1977.
2. Smith CR, Lipsky JJ, Laskin OL, Hellman DB, Mellits ED, Longstreth J, Leitman PS: Double-blind comparison of the nephrotoxicity and auditory toxicity of gentamycin and tobramycin. N Eng J Med 302(20): 1106–1109, 1980.
3. Bennett WM, Plamp CE, Gilbert DN, Parker RA, Porter GA: The influence of dosage regimen on experimental gentamycin nephrotoxicity: Dissociation of peak serum levels from renal failure. J Inf Dis 140(4): 576–580, 1979.
4. Bobrow SN, Jaffe E, Young RL: Anuria and acute tubular necrosis associated with gentamycin and cephalothin. JAMA 222(12): 1546–1547, 1972.
5. Plamp CE, Reger K, Bennett WM, McClung MR, Porter GA: Vasopressin resistant polyuria in gentamycin nephrotoxicity. Clin Res 26, 151A, 1978.
6. Houghton DC, Hartnett MN, Campbell-Boswell M, Porter GA, Bennett WM: A light and electron microscopic analysis of gentamycin nephrotoxicity in rats. Am J Pathol 82(3): 589–599, 1976.
7. Kosek JC, Mazze RI, Cousins MJ: Nephrotoxicity of gentamycin. Lab Invest 30(1): 48–57, 1974.
8. Kaloyanides GJ, Pastoriza-Munoze: Aminoglycoside nephrotoxicity. Kidney Int 18(5): 571–582, 1980.
9. Gilbert DM, Houghton DC, Bennett WM, Plamp CE, Reger K, Porter GA: Reversibility of gentamycin nephrotoxicity in rats: Recovery during continued drug administration. Proc Soc Exp Biol Med 160(1): 99–103, 1979.
10. Elliott WL and Bennett WM: Acquired gentamycin insensitivity: Rate of functional recovery with continued drug administration. Clin Res 29: 461A, 1981.
11. Baylis C: The mechanism of the decline in glomerular filtration rate in gentamycin-induced acute renal failure in the rat. J Antimicrob Chemother 6(3): 381–388, 1980.
12. Whelton A, Carter GC, Craig TJ, Bryant HA, Herbst DV, Walker WGC: Comparison of the intrarenal disposition of tobramycin and gentamycin: Therapeutic and toxicologic answers. J Antimicrob Chemother 4 (Suppl A): 13–22, 1978.
13. Kumin GD: Clinical nephrotoxicity of tobramycin and gentamycin: A prospective study. JAMA 244(16): 1808–1810, 1980.
14. Fong IW, Fenton RS, Bird R: Comparative toxicity of gentamycin versus tobramycin: A randomized clinical prospective study. J Antimicrob Chemother 7(1): 81–88, 1981.
15. Szot RJ, Tabachnick IIA. Animal studies with netilmycin. Clin Trials J 17(4): 318–324, 1980.
16. Lerner AM, Cone LA, Jansen W, Regis MP, Blair DC, Wright GE, Lorber RR: Randomized clinical trial of the comparative efficacy, auditory toxicity and nephrotoxicity of tobramycin and netilmycin. Lancet 1: 1123–1125, 1983.
17. Linton AL, Clark WF, Driedger AA, Turnbull DI, Lindsey RM: Acute interstitial nephritis due to drugs: Review of the literature with a report of nine cases. Ann Int Med 93(5): 735–741, 1980.
18. Galpin JE, Shinaberger JH, Stanley TM, Blumenkrantz MJ, Bayer AS, Friedman GS, Montgomerie JZ, Guze LB, Colburn JW, Glassock RJ: Acute interstitial nephritis due to methicillin. Am J Med 65(5): 756–765, 1978.
19. Abraham PA and Keane WF: Glomerular and interstitial disease induced by nonsteroidal anti-inflammatory drugs. Am J Nephrol 4: 1–6, 1984.
20. Jackson TE, Guyton AC, Hall JE: Transient response of glomerular filtration rate and renal blood flow to step changes in arterial pressure. Am J Physiol 233(5): F396–F402, 1977.
21. Dunn MJ: Renal prostaglandins. In: Renal Endocrinology, Dunn MJ (ed). Baltimore/London, Williams and Wilkins, 1983, pp 1–74.
22. Scharschmidt LA, Dunn MJ: Prostaglandin synthesis by rat glomerular mesangial cells in culture. J Clin Invest 71(6): 1756–1764, 1983.
23. Hall JE, Guyton AC, Jackson TE, Coleman TG, Lohmeier TE, Trippodo NC: Control of glomerular filtration rate by renin-angiotensin system. Am J Physiol 233(5): F366–F372, 1977.
24. Clive DM, Stoff JS: Renal syndromes associated with nonsteroidal antiinflammatory drugs. N Engl J Med 310(9): 563–572, 1984.
25. Kimberly RP, Plotz PH: Aspirin: induced depression of renal function. N Engl J Med 296(8): 418–424, 1977.
26. Kimberly RP, Gill JR Jr., Bowden RE, Keiser HR, Plotz PH: Elevated urinary prostaglandins and the effects of aspirin on renal function in lupus erythematosus. Ann Int Med 89(3): 336–341, 1978.
27. Kirschenbaum MA, Serros ER: Effect of prostaglandin inhibition on glomerular filtration rate in normal and uremic rabbits. Prostaglandins 22(2): 245–254, 1981.
28. Ciabattoni G, Cinotti GA, Pierucci A, Simonetti BM, Manzi M, Pugliese F, Barsotti P, Pecci G, Taggi F, Patrono C: Effects of sulindac and ibuprofen in patients with chronic glomerular disease. Evidence for the dependence of renal function on prostacyclin. N Engl J Med 310(5): 279–283, 1984.
29. Hricik DE, Browning PJ, Kopelman R, Goorno WE, Madias NE, Dzau VJ: Captopril-induced functional renal insufficiency in patients with bilateral renal-artery stenoses or renal-artery stenosis in a solitary kidney. N Engl J Med 308(7): 373–376, 1983.
30. Curtis JJ, Luke RG, Whelchel JD, Diethelm AG, Jones P, Duston HP: Inhibition of angiotensin-converting enzyme in renal-transplant recipients with hypertension. N Engl J Med 308(7): 377–381, 1983.
31. Blythe WB: Captopril and renal autoregulation. N Engl J Med 308(7): 390–391, 1983.
32. Papper S: Hepatorenal syndrome. In: The Kidney and Liver Disease. Second Edition, Epstein M (ed). New York, Elsevier Biomedical, 1983, pp 87–106.
33. Koppel MH, Coburn JW, Mims MM et al.: Transplantation of cadaveric kidneys from patients with hepatorenal syndrome. Evidence

for the functional nature of renal failure in advanced liver disease. N Engl J Med 280(25): 1367–1371, 1969.
34. Epstein M, Beck DP, Hollenberg NK et al.: Renal failure in the patient with cirrhosis. The role of active vasoconstriction. Am J Med 49(8): 175–185, 1970.
35. Baldus WP, Feichter RN, Summerskill WHJ: The kidney in cirrhosis. I. Clinical and biochemical features of azotemia in hepatic failure. Ann Intern Med 60(3): 353–365, 1964.
36. Lieberman FL, Ito S, Reynolds TB: Effective plasma volume in cirrhosis with ascites. Evidence that a decreased value does not account for renal sodium retention, a spontaneous reduction in glomerular filtration rate (GFR) and a fall in GFR during drug-induced diuresis: J Clin Invest 48(6): 975–981, 1969.
37. Alon U, Berant M, Mordechovitz D, Hashmonai M, Better OS: Effect of isolated cholaemia on systemic haemodynamics and kidney function in conscious dogs. Clin Sci 63(1): 59–64, 1982.
38. Schroeder ET, Anderson GH, Smylyan H: Effects of a portacaval or peritoneovenous shunt on renin in the hepatorenal syndrome. Kidney Int 15(1): 54–61, 1979.
39. Zipser RD, Hoefs JC, Speckart PF, et al.: Prostaglandins: Modulators of renal function and pressor resistance in chronic liver disease. J Clin Endocrinol Metab 48(6): 895–900, 1979.
40. Boyer TD, Zia P, Reynolds TB: Effect of indomethacin and prostaglandin A_1 on renal function and plasma renin activity in alcoholic liver disease. Gastroenterology 77(2): 215–222, 1979.
41. Mirouz D, Zipser RD, Reynolds TB: Effect of inhibitors of prostaglandin synthesis on induced diuresis in cirrhosis. Hepatology 3(1): 50–55, 1983.
42. Zambraski EJ, Dunn MJ: Importance of renal prostaglandins in control of renal function after chronic ligation of the common bile duct in dogs. J Lab Clin Med 103(4): 549–559, 1984.
43. Zipser RD, Radvan GH, Kronborg IJ, et al.: Urinary thromboxane B_2 and prostaglandin E_2 in the hepatorenal syndrome: Evidence for increased vascoconstrictor and decreased vasodilator factors. Gastroenterology 84(4): 697–703, 1983.
44. Levenson DJ, Skorecki KL, Narins RG: Acute renal failure associated with hepatobiliary disease. In: Acute Renal Failure. Brenner BM, Lazarus JM (eds). Philadelphia, WB Saunders, 1983, pp 482–491.

CHAPTER 15

Surgical aspects of nephrology

KENNETH A. KROPP

1. Introduction

The nephrologist is intimately involved in the diagnosis and treatment of renal parenchymal disease. The surgical aspects of nephrology entail diagnostic studies to rule out correctible causes of renal failure and surgical procedures designed to preserve renal function or correct the ravages of chronic renal failure through transplantation.

1.1. Renal biopsy

Renal biopsy has become an important diagnostic and prognostic tool for a variety of renal diseases. Whenever possible the biopsy should be done by the percutaneous technique. There are specific contraindications to percutaneous needle biopsy such as a solitary kidney, an ectopic kidney, small contractile kidney, an uncooperative patient, severe hypertension, marked obesity or a coagulopathy. In these instances it is probably safer to perform an open biopsy.

The posterior lumbar approach to the kidney represents an ideal incision for obtaining renal tissue. Not only is exposure more than adequate but division of only one muscle layer is required. The patient is usually placed in the prone position on the operating table following induction of anesthesia on the operating room cart. Both the surgeon and the anesthesiologist must be aware that this position creates significant problems because the body weight against the abdominal wall limits respiratory excursion, and may impede venous return from the legs [1]. Accordingly the patient must be placed on parallel lateral supports which will allow the anterior abdominal wall to hang above the table top rather than resting on it. Slight flexion of the table will increase the distance between the twelfth rib and the posterior iliac crest.

The relationship of the twelfth rib to the kidney is determined by the intravenous urogram. The twelfth rib and lateral border of the sacrospinal muscles are identified by palpation. The incision is begun just medial to the lateral border of the sacrospinalis, one centimeter beneath and parallel to the twelfth rib and carried laterally for about 4–6 cm. This length incision is more than adequate to obtain renal tissue from even the most obese patient. The lateral edge of the superficial layer of the lumbodorsal fascia overlying the sacrospinalis muscle is incised. The muscle fibers of the latissimus dorsi m. are incised to expose the fused layers of the lumbodorsal fascia. This fascia is incised and the 12th neurovascular bundle identified and protected. The pararenal fat is retracted downward and laterally and Gerota's fascia identified. Using a gauze sponge this fascial layer is also retracted downward and laterally and then opened to expose the renal surface. A 1.5 cm elipse of renal tissue 1.0 cm in depth is cut from the kidney surface and the gloved thumb or finger used to gently tamponade the biopsy site. After fife minutes bleeding will be controlled and removal of the gloved finger or thumb will not dislocate the well formed clot. No drains are used and the wound is reapproximated in layers. This biopsy technique provides more than enough tissue for light microscopy, EM and immunofluorescence. We have used this technique in well over 400 renal biopsies with minimal morbidity.

2. Obstructive uropathy

The nephrologist is responsible for determining that any given patient with newly diagnosed renal failure is not suffering from an obstructive lesion. This is done with the help of urologic and radiologic consultation. We will review the diagnosis and surgical management of the more common lesions causing impairment of renal function through obstruction.

Obstructive ureteral lesions causing renal parenchymal damage include scars, kinks, bands, aber-

L.J.A. DiDio and P.M. Motta (eds), Basic, Clinical, and Surgical Nephrology. ISBN 0-89838-689-5.

rant vessels, tumor, calculi and iatrogrenic injury. The importance of a carefully planned urologic work up cannot be over estimated. Once the cause and site of the obstruction is identified, urologic manipulation of ureteral catheters, stone baskets and placement of ureteral stents can be accomplished and the obstruction relieved. Permanent corrective urologic surgical procedures can be planned at a later date if endoscopic manipulation is unsuccessful.

2.1. Percutaneous nephrostomy

Ever since Goodwin [2] in 1955 described percutaneous access to the upper urinary tract, percutaneous nephrostomy has been gradually replacing operative nephrostomy as the procedure of choice for temporary proximal urinary diversion. This procedure is carried out in an operating suite equipped with fluoroscopy or in the radiology department. Patient preparation should include an IV for fluids, premedication and indwelling foley catheter. Choosing the optimal point of entry into the collection system is dictated by the pathology.

The patient is placed in the prone position and the pyelocalyceal system visualized by intravenous contrast or thin needle antegrade pyelography. We use the Cope percutaneous set up which includes a 22 gauge needle and a .038 angiographic guidewire. Once the tract is dilated with the stiff Teflon dilators, the pigtail nephrostomy tube is inserted. This initial placement of the nephrostomy tube allows numerous procedures to be carried out, including introduction of various stents and a more permanent percutaneous nephrostomy tube.

2.2. Obstructing urinary calculi

One of the commonest correctible causes of renal damage from obstruction is calculus located at the ureteropelvice junction, or further down the ureter. The selection of a surgical incision for removal of obstructive renal and ureteral calculi requires careful consideration of numerous factors. The primary goals of surgical therapy for renal and ureteral calculi include the following: (1) complete removal of all stones with the least amount of surgical trauma to the kidney, ureter and patient; (2) preservation of normal preoperative renal anatomy; (3) restoration toward normal of abnormal preoperative renal anatomy secondary to obstruction; (4) correction, if possible, of abnormalities of the collecting structures contributing to the formation of stones; (5) primary healing; and (6) minimal postoperative discomfort. These goals plus patient anatomy should dictate the selection of the appropriate surgical approach.

2.3. Preoperative considerations

2.3.1. X-rays

An intravenous urogram of good quality is one of the most valuable tools the urologic surgeon has in deciding on the appropriate surgical approach to a calculus. The intravenous pyelogram provides a rough assessment of renal function, position, size, and number of stones, but also the position of the renal pelvis in relation to the lumbar spine and ribs. Precontrast tomographic cuts of the kidney are extremely helpful in assessing the exact number and position of stones. For radiolucent calculi, echograms, CT scans, and retrograde pyelograms are helpful in this overall assessment of size, position, and number.

In all patients undergoing surgical stone removal, an immediate preoperative film with the patient in the exact position on the operative table is mandatory. Almost every surgeon who has operated on the patient with stones has experienced frustration of being unable to find a stone that had been localized preoperatively at a particular site in the urinary tract. Stones that appear to be stationary can, and do, move. The experienced surgeon realizes this and would not make the incision without X-ray localization of the stone.

2.3.2. Infection

In patients with urinary tract infection and stone, it is frequently important to know whether the infection is coming from the kidney containing the stone. Exact identification of the bacteria and their antibiotic sensitivity spectra are important preoperative facts. The amount of function of the kidney also is an important fact in terms of being able to tailor antibiotic doses to achieve desired concentrations in the urine surrounding the stone. Preoperative renal infection associated with stones is usually best treated for 5 to 7 days with high doses of antibiotics prior to surgery.

2.3.3. Probability of stone passage

It is useful to have some idea of the probability of any particular stone passing spontaneously. In 1956 Olsson [3] analyzed 541 cases of ureteral calculi and made observations that are summarized in Table 1. This information allows the surgeon to make a more objective statement about the chance of passage of any particular stone and the decision regarding surgery. However, the experienced urologic surgeon knows that the probability of stone passage is inexact

Table 1. Spontaneous passage of ureteral stones.[a]

Size of stone (mm)	Position (%)	
	Upper half	Lower half
<4	81	93
4–6	52	53
>6	4	22

[a] The percentage of stones that passed spontaneously or migrated from the upper half to the lower half of the ureter. The position and size determined on the urogram obtained at the time of initial presentation.

and that almost any stone of any size can pass. For that reason one should always allow adequate time for spontaneous passage.

2.3.4. Equipment

It is important to have available in the operating suite all possible necessary instruments and equipment for the removal of stones. The surgeon should be familiar with a system for intraoperative cooling of the kidney including preparation of an iced slush electrolyte solution, a plentiful supply of cold Ringer's lactate, sterile IV tubing and suction catheters, and a thorough knowledge of the techniques used. The formulation for making coagulum should be included in the surgeon's operative book. The various types of stone forceps, vascular bulldog clamps, and vessel loops should be selected and a dye for injection available to outline renal segmental anatomy. A technique for intraoperative X-ray localization of calculi should be worked out and kept in the surgeon's write-up. Some additional instruments are not always available in every operating room, such as a pulsatile water pic for adequate irrigation of the calices and renal pelvis, rigid and flexible nephroscopes, and ultrasonic equipment, all of which can be extremely helpful. Advance planning and preparation will make the procedure smoother and quicker and may spell the difference between success and failure.

2.4. Surgical exposures for renal surgery

Renal calculus surgery presents certain problems for the urologist. The kidneys can hardly be considered abdominal organs, and in most stone operations, the surgeon would like to avoid entering the pleural or peritoneal cavity. Accordingly he usually chooses the lateral flank approach in the hope of avoiding both. This incision necessitates dividing the great muscles of the flank, avoiding intercostal nerves, vessels, pleura, and peritoneum, and requires vigorous retraction with self-retaining retractors to enlarge the spaces between the ribs and iliac crest. Despite all of these efforts, the surgeon frequently finds that he has produced adequate exposure of only the lower renal pole. The other theoretical disadvantages to the flank approach include the disproportionately large incision relative to the small pathologic process and approaching from the lateral aspect when important vascular and pelvic structures are medial. For this reason, many are now advocating the posterior approach, the advantage of which will be described later.

All the standard surgical approaches to renal and ureteral calculus surgery have been well described and beautifully illustrated in several textbooks, including Campbell's Urology [4], Operative Urology [5], and Urologic Surgery [6]. The reader is referred to these basic texts for exact anatomic details. Below are practical observations, ideas, and suggestions that the author has found useful in performing surgery for renal and ureteral calculi.

2.5. The basic approaches to renal calculus surgery

The basic approaches to the kidney include anterior (extra- or transperitoneal), lateral (supra- or subcostal), and posterior (prone or lateral decubitus). We will discuss the indications, positioning techniques, and disadvantages of each approach.

2.5.1. The anterior approach

The anterior (trans- or extraperitoneal) approach to the kidney can be used in selected individuals who have spinal diseases or deformaties that preclude the use of the flank position. This approach can be appropriate for patients who would not tolerate the flank position because of blood pressure problems that occur during positioning. It also can be selected when previous surgical procedures have been done through the flank and one wants to avoid the anticipated considerable amount of scarring. It also can be used for simultaneous removal of bilateral renal calculi. However, the anterior approach is generally not the incision of choice for stone surgery.

The patient is positioned on the operating table in the supine position. The thoracic cage and ipsilateral flank are elevated with a pillow, foam rubber, or other appropriate positioning device. This lateral tilt is helpful because it naturally 'retracts' the peritoneal contents away from the side of the surgery. The incision is usually subcostal beginning contralateral to the midline two finger breadths below the costal margin. By beginning the deep dissection laterally, one can avoid entering the peritoneal cavity. This allows retraction of the colon and exposure of

the hilar structures. The Buckwalter self-retaining retractor is extremely helpful in maintaining exposure during the surgical procedure. The extraperitoneal approach allows any postoperative urinary leakage to drain laterally and away from the peritoneal cavity.

When previous surgery has created dense scarring it is best to go directly into the peritoneal cavity and begin the approach to the hilum by reflecting the colon medially. However, we have found that sooner or later one gets back to the dense scarring that we have been trying to avoid by the intraperitoneal approach. The anterior incision can be modified slightly by placing the patient in a steeper anterolateral position and beginning the incision over the bed of the eleventh rib. This incision then extends downward and anterior, paralleling the intercostal nerves to the lateral border of the rectus muscle. This provides excellent exposure and can be done in an extraperitoneal position.

A major advantage of the anterior approach is that intraoperative X-rays are extremely easy when compared to those done with the patient in the lateral position. All of these anterior approaches, however, suffer from the problems inherent in normal hilar anatomy, namely, the blood vessels are anterior to the renal pelvis and this means the entire kidney usually must be mobilized before a pyelotomy incision can be made.

2.5.2. The lateral approach

The lateral approach to the kidney is, by far, the commonest incision employed by the urologic renal surgeon. This includes the classic subcostal incision, a twelfth rib resection, an eleventh intercostal incision, a dorsolumbar flap, and rarely the combined thoracoabdominal incision. Neither the peritoneal nor the thoracic cavity need to be entered.

All lateral approaches require that the patient be placed on the operating table in the flexed lateral decubitus position, usually with the upper leg straight and the lower leg flexed at the hip and knee. The iliac crest is positioned over a fulcrum (the kidney rest) and the table flexed to increase the space between the rib cage and the iliac crest (Fig. 1). There is considerable debate about the best position of the patient in relation to the kidney rest. Flock and Culp advocate a posture that allows the kidney rest to strike just above the iliac crest [7]. Smith and Litton recommend positioning the twelfth rib over the kidney rest [4]. Grayhack and Graham recommend that the kidney rest be placed directly under the iliac crest [6].

For the convenience of the surgeon, the patient is usually placed on the side of the table closest to the operator. Once the patient's iliac crest has been positioned over the kidney rest, then with frequent blood pressure checks the kidney rest is elevated slowly to maximum height. The table is then flexed

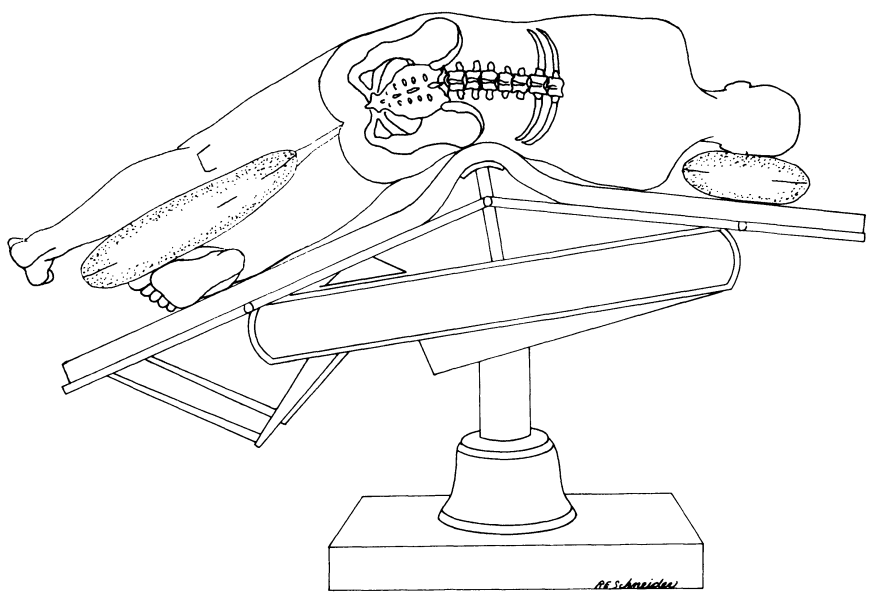

Fig. 1. Flexed lateral decubitus position. Note that the kidney rest is positioned beneath the iliac crest. (Courtesy of Martin, J.T. (1978). Positioning in Anesthesia and Surgery. Philadelphia, W.B. Saunders Co.).

until the muscles of the flank have become taut. Nothing further will be gained by increased flexion of the table. A pillow is placed between the legs and a roll underneath the axilla. The patient is then taped to the table with broad adhesive tape. Care must be taken to avoid placing these tapes too tightly because one can cause compression necrosis of the femoral head. The patient's head should also be adequately supported by a pillow and the arms placed in a well-supported and padded natural position to prevent strain on the back and shoulders.

Because the subsequent breaking of the table with elevation of the kidney rest creates severe skeletal stresses and ventilatory restrictions, these should be kept in mind when the patient is placed into the flank position. A thorough discussion of anesthesia considerations in the flexed lateral decubitus position can be found in *Positioning in anesthesia and surgery* [8].

In conformance with our goals for renal calculus surgery, the wound should be opened carefully with attention to the position of the intercostal nerves and vessels. Usually, anterior cutaneous branches must be divided in the course of the operative exposure. The dissection of the renal pelvis and hilar structures should be as gentle as possible. For branched or multiple calculi, the entire kidney usually must be freed and hilar structures dissected completely, including isolation of the renal artery and vein. Care should always be taken to preserve fat, especially the perirenal fat located posteriorly. If this posterior perirenal fat can be developed as a leaf and preserved, it can then be positioned posterior to the renal pelvis at the time of closure. Fine suture material should be selected for suturing the renal pelvis. We use 5-0 or 6-0 chromic.

Because it is advantagenous to have no urine draining from the kidney in the postoperative period, we generally test the anastomosis for major leaks by saline injection prior to final closure. Drains must be placed accurately so that any urinary drainage can have easy egress from the flank. We prefer the soft Penrose drain over the Hemovac because of its greater reliability, but have been pleased with the use of the soft Jackson-Pratt sump drain when we know that we will have considerable urinary leakage.

2.5.3. The posterior approach

Our interest in the posterior approach to the kidney began when performing open renal biopsies and bilateral nephrectomies for patients with chronic renal diseases [9]. As we became more familar with this approach, we extended the indications to include renal pelvic and upper ureteral calculus surgery and repair of ureteropelvic junction obstruction. We believe the posterior lumbar approach to the kidney represents an ideal incision for many pathologic processes. The advantages of this incision include the following: (1) minimal amount of muscle tissue is destroyed, and therefore the procedure is metabolically less traumatic; (2) both kidneys can be operated on simultaneously without repositioning the patient; (3) no major body cavity must be entered; (4) it constitutes the shortest route from skin to renal structures; (5) postoperative discomfort is minimal; and (6) drainage from the area is dependent with the patient in the supine position.

Positioning. It is important to position the patient accurately for performing this posterior surgery. It can be done in either the prone or the lateral position. We prefer the prone position, and therefore the patient is anesthetized on the operating room cart before being transferred to the operating table. It is essential that a device be placed on the operating table that will provide lateral support and allow the abdomen to lie between the two lateral supporting stuctures. We utilize any of the following: two operating room sheets rolled and secured with Kerlix gauge and then padded with foam rubber, the Vacpac padded with foam rubber, or the Wilson convex adjustable spinal frame.

Once the patient is placed in the prone position, the surgeon must check to make sure that a hand can be passed between the table top and the abdomen. This assures that no compression of the vena cava will take place. The patient is positioned so that slight flexion of the table will increase the distance between the twelfth rib and the posterior iliac crest. When the patient is placed in the lateral position, the axillary roll should be utilized and gentle taping accomplished. A slight amount of flexion may also be required.

With the patient in the prone position, X-ray cassettes can be located beneath the patient prior to the incision. Depending on the location of the renal pelvis and the calculi, either a vertical incision parallel to the lateral border of the paraspinal muscles or a transverse incision paralleling the rib casge is made. The secret to exposure of the renal hilum is in retraction, and this cannot be overemphasized. Once the perirenal fat is identified, the kidney is mobilized using gauze sponges and downward and lateral traction, prior to opening Gerota's fascia. Once the kidney has been retracted downward and laterally, Gerota's fascia can be opened as high as possible, either at or above the level of the renal pelvis. The dissection then proceeds with exposure of the renal

pelvis and upper ureter. The sinus renalis is opened, and vein retractors are used to maintain lateral traction on the kidney. As in all other renal surgery, the perirenal fat is positioned at closure so that the renal pelvis will not become adherent to the psoas and quadratus lumborum musclature posteriorly.

At this time, the posterior approach is our incision of choice for renal pelvic and upper ureter calculi because of its ease and speed of execution and the minimal postoperative discomfort experienced by the patient.

2.6. Surgical exposure of ureteral calculi

The surgical exposure of ureteral calculi depends upon the location of the calculus. A knowledge of three basic surgical exposures is all that is necessary for ureterolithotomy. For stones above the iliac vessels, any of the approaches for renal calculus surgery can be used. For stones located between the iliac vessels and the juxtavesical ureter, we prefer the incision that we use for renal transplantation. This incision allows for wide and maximal exposure of the pelvic ureter.

The patient is positioned on the operating table with the ipsilateral hip elevated with either a soft pillow or sand bag protected with foam rubber. This allows the intraperitoneal contents to fall away from the surgical area. The gentle 'S' incision is begun on the contralateral side of the midline two finger breadths above the pubic symphysis extending lateral, parallel to the inguinal ligament, upward and medial to the anterior superior spine, and outward toward the tip of the eleventh rib. The ipsilateral rectus muscle is divided using a Bovie knife, and the inferior epigastric vessels are doubly ligated. External, internal, and transversus abdominis musculature are divided with the Bovie, transversalis fascia incised, and the retroperitoneal space entered by retracting the peritoneal envelope medially. With this retraction, the entire ureter from the pelvic brim to the bladder is exposed in its entirety. A ureterotomy is then made over the exposed stone and then closed with interrupted sutures.

All too often we have attempted to do lower ureteral calculus surgery through a much smaller and limited incision. However, the ease with which this incision can be made and the tremendous exposure that it affords lead to accurate ureteral lithotomy and a smooth convalescent postoperative course.

For stones lodged in the juxtavesical and intramural ureter, we prefer to open the bladder through either a midline or transverse suprapubic incision. The ureter is then dissected from its attachments to the ureteral hiatus just the same as that dissection done for ureteral reimplantation. Once the ureter has been dissected and advanced into the bladder, the stone is palpated in the ureter, a ureterotomy made, and the stone removed. Ureterotomy is then closed and the ureter allowed to retract back into the ureteral hiatus and, if necessary, additional submucosal ureteral length attained by developing a submucosal tunnel. The ureter is then resutured to the bladder. I have struggled and have watched residents struggle for exposure when doing lower ureteral surgery through an extravesical approach, and I am convinced that the simplest way to do this type of surgery is to dissect the ureter from within the bladder.

2.7. Ureteropelvic junction obstruction

The second commonest benign cause of impairment of renal function through obstruction is 'congenital' ureteropelvic junction obstruction. Anatomically, the obstruction may be caused by intrinsic ureteral narrowing, angulation by crossing vessels or bands, or adhesions between the ureter and renal pelvis causing angulation. More often than not, no anatomic cause can be demonstrated but a functional obstruction exists because of the failure to develop an adequate sized ureteral cone.

Excretory urography with delayed images will suggest the diagnosis in most instances. Seldom, if ever, will contrast media be present in the ureter. Ultrasound will usually confirm the diagnosis and occasionally retrograde pyelograms are needed to delineate the exact anatomic arrangement and relationship of the renal pelvis and ureter. In doubtful cases either antegrade perfusion studies [10] or the diuretic renogram [11] can confirm the diagnosis of obstruction.

Not all diagnosed ureteropelvic junction obstructions in adults need to be treated. In many instances the obstruction has stabilized and is not progressive. However, in children once the diagnosis is established surgical treatment should be instituted.

The main indications for surgical treatment of ureteropelvic junction obstruction are documented progressive loss of renal function, persistent or recurrent pain, presence of infection, or presence of renal calculi. Although a number of procedures have been employed in the past, the most widely used today is the dismembered pyeloplasty. In this operation the obstructing area at the ureteropelvic junction is excised and the spatulated end of the ureter is reanastomosed end to side with the renal pelvis after excision of excessive renal pelvic tissue. The choice

of the incision, and other surgical techniques have already been outlined in the section on stone surgery and need not be reiterated here.

2.8. Malignant ureteral obstruction

The natural history of most pelvic malignancies is eventual death in uremia from bilateral ureteral obstruction. Internal ureteral stenting has become an effective way to bypass ureteral obstructions and reverse renal failure from obstruction. As chemotherapy for various pelvic malignancies becomes more effective, the indications and need for ureteral stenting will broaden.

The ureteral stents are usually placed by retrograde passage through the cystoscope but can also be passed antegrade after percutaneous puncture. The newer double J sialastic ureteral stents appear to be better tolerated and associated with fewer complications. We recently reviewed complications associated with ureteral stents in 89 patients. Eighteen patients experienced minor complication but generally the stents were well tolerated.

2.9. Bladder neck obstruction

The commonest site of obstructive uropathy leading to renal failure is at the bladder neck. Bladder neck obstruction in the adult is secondary to either benign prostatic hyperplasia or adenocarcinoma of the prostate in the vast majority of instances. Bladder neck obstruction can be temporarily relieved by urethral catheterization. This provides immediate relief of symptoms and allows almost immediate recovery of renal function. Once renal function has improved additional diagnostic studies such as intravenous urography, cystoscopy and biopsy can be performed. Definitive surgical procedures directed at permanent relief of the bladder neck obstruction can be performed on an elective basis.

Bladder neck obstruction in female children is rare and usually secondary to neurogenic causes. In male children the commonest cause of bladder neck obstruction leading to impaired renal function is the presence of posterior urethral valves. Diagnosis is made definitively by a *voiding* cystourethrogram. A further discussion of management of these lesions is beyong the scope of this chapter.

3. Surgical aspects of renal failure

3.1. Dialysis access

The nephrologist faced with the patient with chronic renal failure needs to plan for permanent dialysis access.

3.2. Hemodialysis

A smooth venous loop arteriovenous fistula using the patient's own vessels is the preferred method of management. This is usually constructed at the wrist by mobilizing the cephalic vein and radial artery and performing and end to side anastomosis using 6-0 or 7-0 polypropylene sutures. Less desireable is a fistula constructed at the antecubital fossa using either the median cubital vein or the distal cephalic vein anastomosed end to side with the brachial artery.

3.3. Peritoneal dialysis

For chronic peritoneal dialysis a Toronto-Western Hospital or Tenchkoff catheter should be placed in the lower abdomen to the left of the midline. Placement of the catheter on the left side will allow a cleaner access to the right lower quadrant should renal transplantation be considered in the future.

For a complete and excellent coverage of dialysis access surgery the reader is referred to the chapter by Barry [12].

4. End stage renal disease (ESRD)

Most urologists do not have any direct involvement in a renal transplant program. However, with the large number of end-stage renal disease patients and the broad geographic distribution of dialysis facilities, it is imperative that the practicing urologist be knowledgeable about renal transplantation. Most new patients with recently diagnosed end-stage renal disease will require urologic consultation and during the course of the end-stage renal disease patient's illness, the urologist may become involved in their case. We will attempt to review current information relative to the diagnostic work-up, donor and recipient evaluation, living and cadaver donor nephrectomy and other important current trends in the field of renal transplantation.

4.1. Renal biopsy

The usefulness of renal biopsy in the management of

end-stage renal disease patients is controversial. We examined the role of renal biopsy in end-stage renal failure and found a 48% diagnostic error when the clinical diagnosis was compared to the histologic diagnosis [13]. In spite of this and other similar reports there seems to be little enthusiasm in 1985 for documenting the type of renal disease by biopsy in these patients. When a biopsy is indicated, it generally can be done by the nephrologist utilizing the percutaneous needle technique. There are contraindications to closed needle biopsy of the kidney including a solitary kidney, active upper tract infection, a bleeding diathesis, an ectopic kidney and uncontrolled hypertension. When these patients become candidates for open biopsy we perform the biopsy under general anesthesia with the patient in the prone position. The biopsy is done through a small posterior incision about 3 cm in length and adequate tissue is easily obtained.

We have developed a practical approach to renal biopsy in uncooperative children and those where needle biopsy on the ward has been unsuccessful. With the patient under general anesthesia in the prone position on the operating table, a needle biopsy is attempted by the nephrologist. If no tissue is obtained or is inadequate, then the urologist proceeds with open biopsy. This plan insures that an adequate tissue sample will be obtained at the time of the procedure.

4.2. Screening the renal failure patient for reversible obstructive uropathy

The majority of patients with end stage renal disease who are candidates for transplantation do not have obstructive uropathy [14]. However, it is important to establish that obstruction does not exist in patients admitted with renal failure of unknown etiology. Arafa [15] reported finding 20 patients with bilateral hydronephrosis in 92 patients with renal failure. An infusion intravenous urogram done shortly after dialysis may give enough information in the renal failure patient to allow accurate assessment of the upper urinary tract. If not, the least invasive way to rule out obstructive uropathy is renal ultrasound Ellenbagen [16] and more recently Arafa [15] have recorded the accuracy of ultrasound in detecting hydronephrosis in the non-functioning kidney. The latter authors reported an accuracy of 98.1% in patients with obstruction. However, they did not confirm their ultrasound diagnosis in each case by either retrograde pyelography or surgery. It is difficult to exclude hydronephrosis by ultrasound in patients who are dehydrated and/or in those with pelvic stones. We recently saw a 45 y/o female with 'chronic renal failure' whose sonogram failed to show pelviocalyceal dilatation but retrograde studies were compatible with retroperitoneal fibrosis. Placement of bilateral ureteral stents completely reversed the renal failure. I would continue to recommend bilateral retrograde pyelograms in those patients with 'indeterminate' echograms and where obstruction cannot be completely ruled out by non-invasive means.

4.3. Pretransplant recipient urological evaluation

Most transplant recipients should have the lower urinary tract evaluated by a urologist prior to transplantation. Kabler and Cerny [17] found significant urinary tract abnormalities uncovered at the time of pretransplant evaluation in 28 of 112 patients (25%). The urologic evaluation should include a careful history of previous infections or abnormal voiding symptoms, examination of the external genitalia, and digital prostatic examination in males. We include a microscopic examination of expressed prostatic fluid and, where possible, a two glass urinalysis. Catheterization for residual urine followed by a voiding cystourethrogram is done in most patients. All diabetic patients and those suspected of having a neurogenic bladder also require a urodynamic evaluation.

In the patient with known or suspected lower urinary tract abnormalities a cystoscopic examination should be performed. Abnormalities such as bladder neck obstruction, massive reflux or bladder diverticula which predispose to residual urine and infection should be corrected [18]. Minor degrees of vesicoureteral reflux (grade 1–3) are frequently seen. We have elected not to treat this with reimplantation unless there is a history of recurrent urinary tract infection.

It has been our policy to recommend cystoscopy in all renal transplant candidates and have found two unsuspected transitional cell carcinomas, plus a number of other urologic abnormalities similar to those outlined by Kabler [17].

5. Pretransplant recipient urologic surgery

The renal transplant patient candidate may require surgical correction of abnormalities uncovered during the course of the evaluation. Our philosophy is that disease identification and correction prior to transplantation is preferrable to post-renal transplant recognition of problems. Correcting problems

before the patient is placed on steriods and other immunosuppressive drugs which may interfere with wound healing seems to be a rational course of action.

5.1. Nephrectomy

Indications for pretransplant bilateral nephrectomy include poorly controlled renin mediated hypertension, active upper urinary tract infection, grade V vesicoureteral reflux and Goodposture's syndrome [19]. For removal of the small end stage kidney we and others [20] prefer bilateral posterior incisions with the patient prone on the operating table. Freed [21] reported no mortalities and only three wound complications (2 hematomas, 1 abscess) in 135 patients undergoing bilateral nephrectomy through a posterior incision. Novick [22] reports no mortality and only one superficial wound infection using the posterior approach in 45 patients requiring bilateral nephrectomy. This is in contrast to the report by Yarimizu [23] from the same institution of a mortality rate of 11.1% in patients over 50 years of age undergoing transperitoneal nephrectomies. It is difficult to justify any surgical approach other than the posterior approach in removing small end-stage kidneys.

Patients with polycystic renal disease may require bilateral nephrectomy because of recurrent bleeding, persistent infection or severe hypertension. The nephrectomies are best done as a staged procedure because of the potential for heavy blood loss and the necessity of preserving adrenal tissue at least on one side.

In each patient being considered for bilateral nephrectomy, the risks of the procedure must be weighed against the advantages of retained kidneys. Generally dialysis patients with their own kidneys require fewer blood transfusions and able to have a more liberal intake of fluids.

We recommend performing the bilateral nephrectomy prior to rather than at the time of the transplant operation. Turner [24] has recently suggested that the previous practice of concomitant bilateral nephrectomy and transplantation, which has generally been abandoned, be reviewed. However, examination of the data supplied by these authors reinforced our philosophy of asynchronous bilateral nephrectomy and renal transplantation.

5.2. Urinary diversion and transplantation

Some end-stage renal disease patients will require or have had a urinary diversion. There are several questions which need to be addressed, namely; do the native kidneys need to be removed; is the defunctionalized bladder useable; when and what kind of a conduit should be constructed for the renal transplant? In the ESRD patient with an established cutaneous diversion, loop cultures will usually be positive even though the patient has no clinical evidence of a urinary tract infecton. Peters [18] and Confer [19] recommend bilateral nephroureterectomy. I am not aware of any patient with a urinary diversion who has not had bilateral nephrectomy before transplantation. Marshall [25] reports a 35 y/o who was diverted at age 15, found to have a normal functioning bladder after valve fulguration, but who has not been transplanted because he refuses bilateral nephrectomy. We are presently seeing a 17 y/o with a cutaneous ureterostomy who wants to be transplanted before dialysis with his native kidneys in situ. In the patient with an end ureterostomy Levitt [26] and Santiago-Delphin *et al.* [27] have reported leaving the distal ureteral stump attached to the skin at the time of nephrectomy and utilizing the stump as a conduit for receiving the transplant ureter.

The ESRD patient with a urinary diversion and an intact bladder may prove to have satisfactory bladder for renal transplantation. Urological evaluation must be individualized but usually includes cystogram, cystoscopy and cystometrics. The questions to be answered are: 1) can the bladder act as an effective storage organ; 2) can it empty satisfactorily, and 3) can continence be maintained? Most now agree that the most successful maneuver in this evaluation process is placement of a small suprapubic cystocath [25, 28, 29]. An initial small capacity bladder can usually be cycled over a short period of time and allow a decision to be made regarding capacity. In patients who demonstrate adequate capacity but cannot empty satisfactorily intermittent self-catheterization after transplantation has proven succesful [25, 30, 31] and probably preferrable to transplantation into a bowel conduit.

6. Living donor evaluation and management

Potential living donors are selected from the immediate family on the basis of histocompatibility testing. Obviously the donor must be in perfect health and have excellent kidney function. There should be no question about their willingness to donate. Confer and Banowsky [19] have recently outlined the necessary work-up. The final step in the evaluation of the living donor is angiography to assess renal vascular anatomy. Hopefully in the future

this invasive procedure may be replaced by digital subtraction angiography [32]. At the present time there are no studies on the accuracy of digital subtraction angiography in the evaluation of renal donors. Buonocore [33] has reported an accuracy of only 71% when compared to conventional angiography of the renal vessels. This degree of inaccuracy is presently unacceptable in planning a nephrectomy on a living donor.

The chosen renal donor is admitted to the hospital the night before the transplant. IV hydration is started after the evening meal. We infuse 5% D/l/3 N.S. at a rate of 250 ml/hr to 6:00 a.m., then increase this to 500 ml/hr from then until nephrectomy. No prophylactic antibiotics are given. We find it useful to give 25 mg Thorazine at the time of incision to help block renal vasospasms which occur during the dissection of the renal vasculature. Whenever possible we remove the left kidney because of the longer renal vein.

The preferred incision for living donor nephrectomy has been discussed by several authors [26, 34–37]. Ruiz [34] reported on 171 transperitoneal living donor nephrectomies done at the Cleveland Clinic and compared their results to 1022 extraperitoneal nephrectomies previously reported. Their 3.5% major complication rate compared favorably to those previously reported. Connor *et al.* [35] compared the morbidity of the standard flank incision to the anterior extraperitoneal approach in 36 patients. The two groups had fairly similar risk factors and postoperative morbidity except the anterior extraperitoneal group had a higher incidence of atelectasis, 10/23 (43.7%), vs 2/13 (15.4%) and a higher blood loss (1–3 units) 7/23 (30.4%) vs 1/13 (7.7%). They concluded that for patients whose anatomy or physiology precluded a flank approach, the anterior extraperitoneal exposure was a safe and effective alternative.

We agree with Lawson [38] that the extraperitoneal flank approach is the safest for the donor, but occasionally utilize the anterior transperitoneal approach when removing the right kidney. This allows us to free the left renal vein-vena caval junction for access to the takeoff of the right renal artery so that the artery can be removed in its entirety.

6.1. Cadaver donor nephrectomy

Many urologists are involved in the retrieval of cadaver kidneys. It is imperative that adequate hydration be maintained once the patient has been pronounced as brain-dead. We frequently see patients with a high serum sodium (>160/mEq/L) which results from inappropriate fluid replacement with an electrolyte solution rather than dextrose and water. When this or other electrolyte abnormalities have been corrected, and a diuresis established, the donor is transferred to the operating room. Our goal in cadaver donor nephrectomy includes en-block removal of both kidneys, aorta and vena cava. We prefer to maintain cardiac action until the kidneys have been removed. The cadaver donor nephrectomy is not an easy operation and cannot be done in a hurried manner. This requires extensive bowel mobilization and exposure of the aorta above the superior mesenteric artery. One should not attempt to place a clamp on the aorta below the superior mesenteric artery because the takeoff of both renal arteries arises only 1–2 mm caudal. Of course a long segment of ureter must be obtained for anastomosis to the bladder.

We give 25 mg of Thorazine when the patient is brought into the operating room and continue to maintain the diuresis with 500–1000 cc of fluid per hour. If the diuresis is less than 2 ml/min we give lasix 40–100 mg. Two suction units are available prior to start of the procedure. Through both a midline and bilateral subcostal incision, the entire abdomen is opened and the abdominal wall flaps are secured to the operative sheets with towel clips. With this type of exposure, only one assistant and no self-retaining retractors are needed. The retroperitoneum is exposed by complete mobilization of the right colon, cecum, and small bowel. We dissect the right kidney from its peri-renal fat leaving some of the fat attached to the kidney. The ureter on the right is dissected down to below the pelvic brim and the ureter amputated and a specimen collected for culture. We expose the left kidney by an incision in the left pericolic gutter and the mobilization of the splenic fluture. This requires clamping the vessel within the splenocolic ligament. The left kidney and adrenal are dissected out together and the ureter freed to the pelvic brim. The mesentery of the descending colon is opened widely so that the kidney can be brought through this mesenteric window. This requires division of the inferior mesenteric vein. When this has been completed, the aorta is mobilized to the level of the celiac axis superiorly. The superior mesenteric artery is freed for about 2 cm so that this can be subsequently divided. Once the superior mesenteric artery has been mobilized, the diaphragmatic slips which come down and encase the aorta at this point must be divided so that a vascular clamp can be placed on the proximal aorta. The vena cava is dissected both above and below the renal veins and completely freed from its surround-

ing attachments. When these preparations have been completed the patient is given 50–100 mg of Regetine, 10,000 units of Heparin and 100 mg of Lasix. Following the administration of Regitine, the superior mesenteric artery is ligated and divided and the aorta cross-clamped just below the celiac artery. The vena cava is then opened and the two surgical suctions placed within the vena cava and the patient exsanguinated. The vena cava is clamped above and below the entrance of the renal veins and a segment of cava removed. The aorta is divided above the superior mesenteric artery. With gentle upward traction, the lumbar arteries are divided and the aorta, vena cava, and both kidneys removed as a complex. It is very easy to injure the right renal artery if it has not been completedly dissected from its surrounding tissue at the time of this posterior dissection. We therefore, usually adhere to the principle of removing all periaortic tissue ventral to the anterior spinal ligament. This insures that we do not injure the right renal artery. We usually perfuse the ostia of the renal arteries with either chilled Urocollins or Ringers lactate through the open end of the aorta. When renal flushing has been completed (at least 300 ml flush/kidney) the small lumbar arteries are hemoclipped, the aortic cannula secured and the proximal aorta closed. The kidneys are then placed on pulsatile perfusion. Twenty to thirty lymph nodes and the spleen are removed for tissue typing.

If heart-beating cadaver nephrectomy is not performed we will mobilize the common iliac artery and pass a #16 Foley catheter to the level of the renal arteries. The Foley balloon is inflated and then an aortic clamp placed above the superior mesenteric artery and a second clamp placed on the superior mesenteric artery. When the respirator is stopped we begin flushing the aorta with chilled Urocollins. This very effectively cools the kidneys *in situ* then one can proceed with the dissection in an unhurried manner with essentially no warm ischemia time.

6.2. Transplant recipient management

The transplant operative technique has become so standardized that it does not need to be discussed at great length. Whenever possible the kidney should be placed on the right side utilizing the right internal iliac artery and right common iliac vein. A variety of techniques have been used for implanting the ureter into the urinary bladder and all seem to be successful. Antibiotics are started before the transplant operation and continued in the postoperative period. Wound drainage is not recommended. Postoperative management is made easier by immediate graft function. The accurate diagnosis of rejection continues to be primarily an art rather than a science. Cosimi [39] initially reported the usefulness of weekly T-cell subset monitoring in diagnosing rejection. We have been utilizing this technique on a daily basis and have not found it to be accurate enough to base antirejection therapy on its results.

6.3. Transplant nephrectomy

Renal transplant nephrectomy can be a most difficult operation and best done by the urologist or transplant surgeon who performed the transplant. The rejection reaction has usually caused a considerable amount of reaction around the kidney and the kidney is frequently, intimately adherent to the external iliac artery and vein. These vessels must be completely freed so that the hypogastric artery can be ligated and the renal vein removed. I have seen the external iliac artery mistakenly clamped and divided because it was erroneously identified as the renal artery. I would recommend that the transplant nephrectomy be done at the transplant center by the transplant surgeon.

6.4. New concepts in renal transplantation

Until recently all kidney transplantation has been between ABO compatible donor and recipient. However, there have recently been several centers that have reported the removal of circulating anti-A or anti-B antibodies by plasmaphoresis 12–24 hours before the transplant and then transplanting an ABO mismatch. This is not generally done in most centers. The usefulness of HLA matching has come under some question. The matching of class 1 HLA antigens has added little or nothing to the survival of cadaveric organ transplants in the United States. Class 2 antigens which include the DR antigen have been reported to be more accurate predictors of cadaver organ survival. Some have reported a 10–20% increase in success when no DR mismatches have been present in the donor-recipient combination. Negative crossmatches still are considered a 'must' in most transplant centers.

The liberal use of blood transfusions has recently been shown to be effective in selecting those recipients who will have a favorable result following transplantation. The exact mechanism of how blood transfusions confer this beneficial effect upon the recipient is not known at the present time. The use of donor specific transfusions as recommended by Salvatierra [40] has resulted in markedly improved graft survival for those patients who are MLC positive.

With the availability of Cyclosporine for clinical transplantation the role of random transfusions has come under question. Some have suggested we avoid random third party transfusions since 30% or more of patients will be sensitized which in time would reduce the possibility of readily identifying a compatible cadaver kidney by direct crossmatch testing.

Cyclosporine acts mainly on thymus derived lymphocytes that are responsible for the rejection reaction. It apparently leaves other elements of the immune system intact. There are fewer side-effects from Cyclosporine with reduced Prednisone doses than with the use of Azothioprine and high doses of Prednisone. Cyclosporine seems to be especially effective during the inductive phase of the rejection response but by the third to sixth post-transplant month, there is probably no advantage of Cyclosporine over Imuran. Because Cyclosporine costs above 15–20 times more than Azothioprine and Prednisone, many centers are switching their patients to Imuran after 6 months.

Immunologic monitoring has long been felt to be beneficial in predicting early graft rejection. The use of monoclonal antibodies against an array of human T and B cell lymphocyte antigens has sparked a great deal of interest in the area. These monoclonal antibody ratios change at the time of rejection and this might be used as a predictor of early rejection. There have also been reports that the monoclonal antibodies can effectively reverse an initial rejection reaction.

7. Concluding remarks

The management of many patients with nephrologic problems requires a team approach; internist and urologist working together to provide better patient care. I have attempted to review the areas of nephrology where surgical diagnostic and therapeutic tools are employed. I am sure a few areas have been covered in more detail than necessary, some covered only cursorily and many neglected entirely. However, it is my hope that the information provided will be useful to the practitioner caring for patients with renal disease.

References

1. Smith RH: In: Martin TJ (ed), Positioning in Anesthesia and Surgery. Philadelphia, WB Saunders, 1978, pp 32–43.
2. Goodwin WE, Casey WC, Woolf W: Percutaneous trocar (needle) nephrostomy in hydronephrosis. J Am Med Assoc 157: 891–894, 1955.
3. Olsson O: Encyclopedia of Medical Radiology: Roentgen Diagnosis of the Urogenital System. New York, Springer-Verlag, 1973.
4. Lytton B: Surgery of the kidney. In: Harrison JH, Gittes RF, Perlmutter AD et al. (eds), Campbell's Urology. Edition 4. Philadelphia, WB Saunders, 1979 (4th ed), pp 1993–2046.
5. Stewart BH: Operative Urology. Baltimore, Williams & Wilkins 1975.
6. Grayhack JT, Graham J: Renal surgery. In: Glenn JF (ed), Urologic Surgery. Philadelphia, JB Lippincott, 1975, pp 48–72.
7. Flocks R, Culp D: Surgical Urology. Chicago, Yearbook Medical Publishers, 1967.
8. Martin JT: Positioning in Anesthesia and Surgery. Philadelphia, WB Saunders, 1978.
9. Kropp K: Posterior approach to the kidney. Surg Clin North Am 51: 251–256, 1971.
10. Whitaker RH: Clinical assessment of pelvic and ureteral function. Urology 12: 146–150, 1978.
11. Koff SA, Thrall JA, Keyes JW Jr: Diuretic radionuclide urography: a non-invasive method for evaluating nephroureteral dilatation. J Urol 122: 451–454, 1979.
12. Barry JM: In: Glenn JF (ed). Urologic Surgery. Philadelphia, Toronto, JB Lippincott, 1983 (3rd ed), pp 315–327.
13. Kropp KA, Shapiro RS, Jhunjhunwala JS: Role of renal biopsy in end stage renal failure. Urology 12: 631–634, 1978.
14. Barry JM, Craig DH, Fischer SM, Fucha EF, Lawson RK, Bennett WM: An analysis of 100 primary cadaver kidney transplants. J Urol 124: 783–786, 1980.
15. Arafa NM, Fathi MM, Safwat M, Moro H, Torky H, Kenawi M, Abdel-Wahab M: Accuracy of ultrasound in the diagnosis of nonfunctioning kidneys. J Urol 128: 1165–1169, 1982.
16. Ellenbagen PH, Scheible FW, Talner LB, Leopold GR: Sensitivity of gray scale ultrasound in detecting urinary tract obstruction. Am J Roentgen 130: 131–133, 1978.
17. Kabler RL, Cerny JC: Pre-transplant urologic investigation and treatment of end stage renal disease. J Urol 129: 475–478, 1983.
18. Peters PC: The management of renal transplant recipients with abnormal lower urinary tract-reconstruction versus diversion. Urol Clin N Amer 3: 685–690, 1976.
19. Confer DJ, Banowsky LH: The urological evaluation and management of renal transplant donors and recipients. J Urol 124: 305–310, 1980.
20. Novick AC, Brown WE, Magnusson M, Stowe N: Current status of renal transplantation at the Cleveland Clinic. J Urol 122: 433–437, 1979.
21. Freed SZ: Bilateral nephrectomy in transplant recipients. Urology Suppl 10: 16–21, 1977.
22. Novick AC: Posterior surgical approach to the kidney and ureter. J Urol 124: 192–195, 1980.
23. Yarimizu SN, Susan LP, Straffon RA, Stewart BH, Magnusson MO, Nahamoto SS: Mortality and morbidity in pretransplant bilateral nephrectomy. Urology 12: 55–58, 1978.
24. Turner BI, Richie RE, Johnson HK, McDonell RC Jr, Tallent MB, Niblack GD: Bilateral nephrectomy concomitantly with renal transplantation. J Urol 130: 240–242, 1983.
25. Marshall FF, Smolev JK, Spees EK, Jaffs RD, Burdick JF: The urological evaluation and management of patients with congenital lower urinary tract anomalies prior to renal transplantation. J Urol 127: 1078–1081, 1982.
26. Levitt SB, Caherwal D, Kogan SJ, Rowas NA, Hardy MA: Use of preexisting ureterocutaneous anastomosis as conduit in renal transplantation. Urology 13: 377–382, 1979.
27. Santiago-Delphin EA, Acosta-Otera A, Vazquez-Lugo A: Ureteral implantation in kidney transplantation. The use of a mature end ureterostomy. J Urol 124: 513–514, 1980.
28. Firlit CF: Use of defunctionalized bladders in pediatric renal transplants. J Urol 116: 634–637, 1976.
29. Allen TD: Undiverting the ileal conduit. J Urol 124: 519–521, 1980.
30. Steinmuller DR: Evaluation and selection of candidates for renal transplantation. Urol Clin N Amer 10: 217–229, 1983.
31. Stanley OH, Chambers TL, Pentlow BD: Renal transplantation in children with occult neurogenic bladders drained by intermittent self-catheterization. Brit Med J 286: 1775–1776, 1983.
32. Lalli AF: Potential applications of digital angiography in G.U. imaging. Urol Radiol 4: 165–170, 1982.
33. Buonocore E, Meaney TF, Borkowski GP, Paylick W, Gallagher J: Digital subtraction angiography of the abdominal aorta and renal

arteries. Comparison with conventional aortography. Radiology 139: 281–286, 1981.
34. Ruiz R, Novick AC, Braun WE, Montagae DK, Stewart BH: Transperitoneal live donor nephrectomy. J Urol 123: 819–821, 1980.
35. Connor WT, Van Buren CT, Floyd M, Kahan BD: Anterior extraperitoneal donor nephrectomy. J Urol 126: 443–447, 1981.
36. DeMarco T, Amin M, Hardy JI: Living donor nephrectomy: factors influencing morbidity. J Urol 127: 1082–1083, 1982.
37. Weinstein SH, Navarre Jr RJ, Loening SA, Corry RJ: Experience with live donor nephrectomy. J Urol 124: 321–323, 1980.
38. Lawson RK: Editorial comment. J Urol 127: 1083–1085, 1982.
39. Cosimi AB, Colvin RB, Burton RC, Rubin RH, Goldstein G, Kung PC, Hansen WP, Delmonico FL, Russell PS: Use of monoclonal antibodies to T-cell subsets for immunologic monitoring and treatment in recipients of renal allografts. N Eng J Med 305: 308–314, 1981.
40. Salvatierra O, Iwaki Y, Vincenti F et al.: Update of the University of California at San Francisco experience with donor-specific blood transfusions. Transplant Proc 14: 363–366, 1982.

Index